AGGREGATION DYNAMICS OF LITHIUM DIISOPROPYLAMIDE AND THEIR MECHANISTIC INFLUENCE ON REACTIVITY

A Dissertation

Presented to the Faculty of the Graduate School

of Cornell University

In Partial Fulfillment of the Requirements for the Degree of

Doctor of Philosophy

by

Alexander Chris Hoepker

May 2011

© 2011 Alexander Chris Hoepker

AGGREGATION DYNAMICS OF LITHIUM DIISOPROPYLAMIDE AND THEIR MECHANISTIC INFLUENCE ON REACTIVITY

Alexander Chris Hoepker, Ph.D.
Cornell University 2011

Lithium diisopropylamide (LDA) is the premier base in organic chemistry ever since its development in 1950 by Hammel and Levine. In a comprehensive survey of reagents in approximately 500 natural product syntheses, LDA emerged at the top attesting to its wide range of synthetic applications and efficacy. Significant efforts to the understanding of its complex coordination chemistry and affiliated mode of reactivity has led to a review by Collum that painted a seemingly coherent and general picture of LDA-mediated reactions. This mechanistic view, however, was gleaned under conditions in which LDA aggregate equilibria proceeded very quickly compared to the rate of the reaction. The kinetics of LDA aggregation, therefore, were inconsequential and hidden to the investigator. While shifting the focus to more reactive substrates that required a reduction in temperature to -78 °C to maintain convenient time scales for monitoring reaction rates, something odd happened. Instead of conventional first-order substrate decays that had been observed for almost twenty years, we began to observe nonstandard curvatures with evidence of substrate-independent rates, autocatalysis and lithium salt catalysis. The mechanistic intricacy was eventually traced to one common culprit: the rate of LDA aggregation at -78 °C in tetrahydrofuran (THF) had become rate-limiting with the rate of

substrate reaction now being post-rate-limiting. The work described herein presents three experimental accounts that peer into the mechanism of three LDA-aggregation limited reactions: LDA-mediated ortholithiations of fluoro- and trifluoromethyl arenes and the 1,4-addition to unsaturated esters. Although the studies are internally consistent, a chaotic mechanistic picture emerged that appeared to lack coherency. A theoretical treatise of LDA aggregation concludes this work in an attempt to comprehend the source of this complexity and garner a more general understanding. Dozens of reactive forms of LDA emerged as part of a potential energy surface that began to explain our experimental findings. Despite significant advances, we have only scratched the surface of the mechanistic diversity of LDA aggregation. The kinetic tools and knowledge, however, are now in place to peer ever deeper into this mechanistic extravaganza.

BIOGRAPHICAL SKETCH

The author was born on February 9th, 1982 in Chur, Switzerland and was raised in Planken, Liechtenstein. After completing kindergarten and grade school in the small mountain town of Planken, he attended the *Liechtensteinisches Gymnasium* in Vaduz and completed his *Matura* in 2001. The same year he moved to Davis, CA to begin his study of chemistry where he soon became immersed in research under the guidance of Dr. Tadeusz Molinski. The work involved the isolation and characterization of pharmacologically intriguing natural products from marine sponges and a methodological study of the phase-transfer catalyzed cyclopropanation of methylacrylate. The author graduated summa cum laude with a B.S in chemistry in 2005 and subsequently began graduate studies at Cornell University. He joined the research group of David. B. Collum to study LDA mediated ortholithiations and LDA aggregation kinetics. He graduated with a M.S. in 2007 and Ph.D. in May 2011. He will continue his academic work as a postdoctoral fellow with Dr. Axel Brunger at Stanford University studying the molecular mechanism of synaptic neurotransmission.

This work is dedicated to my parents Waltraud and Chris

ACKNOWLEDGMENTS

I would like to begin by thanking Professor David Collum for providing me the opportunity to work in his laboratory. He was exceedingly supportive during the many years and guided me through many hard times with unmatched energy and vitality. He allowed me to explore ideas independently and was always open for discussions out of which so many ideas and research directions emerged. I express my gratitude towards Professor Geoffrey Coates and Professor Peng Chen for serving on my special committee. I would also like to thank Professor Melissa Hines for her tremendous help in developing a data analysis package written in *Igor Pro* which provided a framework for much of my kinetic analyses.

This work would not have been possible without the help and guidance of Dr. Kanwal Singh who sparked my interest in the field of reaction kinetics. I am grateful to Dr. Yun Ma for her endless energy and enthusiasm that brought a human element to the laboratory. I am indebted to past members of the Collum group who made my time at Cornell fun. I would like to thank Dr. Jason Riggs, Dr. Antonio Ramirez, Dr. Lekha Gupta and Dr. Jocelyn Gruver. I would like to acknowledge Marc Faggin with whom I worked in the development of a numerical integration-based curve fitting macro that made the analysis of complex reaction kinetics possible and greatly enriched many of our projects. He is not only a great programmer, but also a really nice guy to work with.

The facility and staff members of the Chemistry department, David Neish, David Wise, Michael Hint and Anthony Condo, have offered great support. In particular, I would like to thank Dr. Ivan Keresztes for immersing me in the field of nuclear magnetic resonance spectroscopy. He is a great

teacher in theoretical as well as practical aspects. A big thanks to Attilio Falco for his work on keeping our computational nodes humming. The computational work has become a major part of my graduate work.

I want to express my deepest gratitude to my girlfriend Meredith, who has given me much joy and love and has introduced me to a way of life I could have never seen without her. Finally, I would like to express my deepest gratitude to my family. My father Chris was always a role model for me throughout my life. I admire his love for knowledge, depth and detail. He has shaped my interests and influenced me in ways for which I will be forever grateful. My mother Waltraud has been eternally supportive throughout my years with an open ear for my joys and sorrows. I admire her liveliness and humor as well as her sense for civil involvement and determinacy. Lastly I would like to thank my brothers Nikolas and Robert who have been my companions and made my life that much fuller and richer.

TABLE OF CONTENTS

Biographical Sketch	iii
Dedication	iv
Acknowledgements	v
Table of Contents	vii
List of Figures	viii
List of Tables	xxii
Chapter 1: Autocatalysis in Lithium Diisopropylamide-Mediated Ortholithiations.	1
Chapter 2: 1,4-Addition of Lithium Diisopropylamide to Unsaturated Esters: Role of Rate-Limiting Deaggregation, Autocatalysis, Lithium Chloride Catalysis and Other Mixed Aggregation Effects.	124
Chapter 3: Regioselective Lithium Diisopropylamide-Mediated Ortholithiation of 1-Chloro-3-(trifluoromethyl)benzene: Role of Autocatalysis, Lithium Chloride Catalysis, and Reversibility.	224
Chapter 4: Computational Studies of Lithium Diisopropylamide Deaggregation.	398

LIST OF FIGURES

Chapter 1

Figure 1.1. Reaction of 0.10 M carbamate **1** with 0.10 M LDA at -78 °C in neat THF as monitored by ^{19}F NMR spectroscopy. 3

Figure 1.2. Reaction of 0.010 M carbamate **1** with 0.10 M LDA at -78 °C in neat THF as monitored by ^{19}F NMR spectroscopy. 4

Figure 1.3. ^{6}Li NMR spectrum of 0.10 M [^{6}Li,^{15}N]LDA at -90 °C with (A) 0.050 M **1**; (B) 0.10 M **1**; (C) 0.10 M **1** at -90 °C after warming at -40 °C for 60 minutes. 8

Figure 1.4. ^{19}F NMR spectrum of 0.10 M LDA with 0.10 M **1** at -78 °C. 9

Figure 1.5. Theoretical depiction of substrate dependence for a zeroth-order reaction. 12

Figure 1.6. Plot showing IR absorbance of **1** (1721 cm^{-1}) versus time for different initial concentrations of carbamate **1**. 13

Figure 1.7. Plot of Δ[**1**]/Δt (from Figure 1.6) versus [**1**] for the ortholithiation of **1** with 0.10 M LDA in 12.2 M THF/hexane cosolvent at -78 °C. 13

Figure 1.8. Absorbance versus time for the reaction of (0.004 M) **1-*d*$_1$** with (0.10 M) LDA in 12.2 M THF/hexane cosolvent at -78 °C. (**1-*d*$_1$**, 1721 cm^{-1}; **2 + 4**, 1660 cm^{-1}). 15

Figure 1.9. Concentrations versus time for the reaction of 0.0074 M **1** with 0.10 M LDA in 12.2 M THF at -78 °C monitored by ^{19}F NMR spectroscopy. 16

Figure 1.10. Concentrations versus time for the reaction of 0.0074 M **1** with 0.10 M LDA in 4.9 M THF at -78 °C monitored by ^{19}F NMR spectroscopy. 17

Figure 1.11. Concentrations versus time for the reaction of 0.01 M **1** with 0.40 M LDA in 12.2 M THF at -100 °C monitored by ^{19}F NMR spectroscopy. 18

Figure 1.12. Plot of initial rates versus [LDA] for the lithiation of carbamate **1** (0.0074 M) in 12.2 M THF at -78 °C. 19

Figure 1.13. Plot of initial rates versus [THF] for the lithiation of carbamate **1** (0.004 M) in 0.1 M LDA using hexanes as cosolvent at -78 °C. 20

Figure 1.14. Plot of k_{obsd} versus [LDA] for the condensation of LDA with aryllithium **2** (0.0074 M) in 12.2 M THF at -78 °C. 21

Figure 1.15. Plot of k_{obsd} versus [THF] for the condensation of LDA with aryllithium **2** (0.0074 M) and 0.1 M LDA at -78 °C. 22

Figure 1.16. Influence of autocatalysis on the LDA-mediated metalation of carbamate **1** as described in eqs 9-12. 31

Figure A1.1. ^{13}C and ^{1}H NMR spectra of **1**. 38

Figure A1.2. ^{13}C and ^{1}H NMR spectra of **1**. 39

Figure A1.3. ^{13}C and ^{1}H NMR spectra of **1-***d*. 40

Figure A1.4. ^{6}Li and ^{15}N NMR spectra of 0.10 M [^{6}Li,^{15}N]LDA with 0.033 M **1** in 0.62 M THF/pentane at -90 °C after aging at -78 °C for 60 min. 41

Figure A1.5. ^{6}Li and ^{15}N NMR spectra of 0.10 M [^{6}Li,^{15}N]LDA with 0.05 M **1** in 0.62 M THF/pentane at -90 °C after aging at -78 °C for 60 min. 42

Figure A1.6. ^{6}Li NMR spectra of 0.10 M [^{6}Li,^{15}N]LDA with 0.05 M **1** in 11.1 M THF/pentane at -90 °C. 43

Figure A1.7. ^{6}Li NMR spectra of 0.10 M [^{6}Li,^{15}N]LDA with 0.10 M **1** in 11.1 M THF/pentane at -90 °C. 44

Figure A1.8. Plot of [**4**]/[**5**] versus [LDA] in 12.2 M THF at -90 °C. 45

Figure A1.9. Plot of [**4**]/[**2**] versus [LDA] in 12.2 M THF at -90 °C. 46

Figure A1.10. Plot of [**4**]/[**5**] versus [THF] in hexanes and 0.05 M LDA at -90 °C. 47

Figure A1.11. Plot of [**4**]/[**2**] versus [THF] in hexanes and 0.05 M LDA at -90 °C. 48

Figure A1.12. ^{19}F NMR spectra of 0.01 M **1** in 11.1 M THF/pentane at various LDA concentrations at -78 °C. 49

Figure A1.13. ^{19}F NMR spectra of 0.010 M **1** in 11.1 M THF/pentane at various temperatures. 50

Figure A1.14. ^{13}C NMR spectrum of 0.40 M [^{6}Li]LDA with 0.33 equiv **1** in 3.1 M THF/pentane at -90 °C. 51

Figure A1.15. Representative IR plot for the ortholithiation of **1.** 52

Figure A1.16. Representative IR plot for the second injection of **1**. 53

Figure A1.17. Plot of absorbance versus time for the ortholithiation of **1** (0.004 M) by 0.10 M LDA in THF/hexane at -78 °C. 54

Figure A1.18. Plot of absorbance versus time for the ortholithiation of **1-***d* (0.004 M) by 0.10 M LDA in THF/hexane at -78 °C. 55

Figure A1.19. Plot of Δ[**1**]/Δt versus [**1**] for the ortholithiation of **1** by 0.10 M LDA in 12.2 M THF /hexanes at -78 °C. 56

Figure A1.20. Plot of k_{obsd} versus [LDA] for the ortholithiation of **1** (0.0074 M) in 12.2 M THF at -78 °C. 57

Figure A1.21. Plot of Δ[**1**]/Δt versus [THF] in hexanes for the ortholithiation of **1** (0.004 M) by 0.10 M LDA at -78 °C. 58

Figure A1.22. Plot of Δ[**1-***d*]/Δt versus [THF] in hexanes for the ortholithiation of **1-***d* (0.004 M) by 0.10 M LDA at -78 °C. 59

Figure A1.23. Plot of k_{obsd} versus [LDA] for the condensation of **2** and **3** in 12.2 M THF at -78 °C. 60

Figure A1.24. Plot of k_{obsd} versus [THF] for the condensation of **2** and **3** (0.10 M) at -78 °C. 61

Figure A1.25. Parametric fit to the ^{19}F NMR spectroscopy derived concentration versus time profile of 0.10 M LDA, 0.0074 M **1**, 12.2 M THF at -78 °C. 62

Figure A1.26. Global parametric fit to the ^{19}F NMR spectroscopy derived concentration versus time profile of 0.0074 M **1** in 12.2 M THF at -78 °C. 63

Figure A1.27. Parametric fit to the ^{19}F NMR spectroscopy derived concentration versus time profile of 0.10 M LDA, 0.0074 M **1**-*d*, 12.2 M THF at -78 °C. (A) First injection; (B) Second injection. 67

Figure A1.28. Parametric fit to the ^{19}F NMR spectroscopy derived concentration versus time profile of 0.10 M LDA, 0.0074 M **1**, 7.4 M THF/pentane at -78 °C. 69

Figure A1.29. Parametric fit to the ^{19}F NMR spectroscopy derived concentration versus time profile of 0.10 M LDA, 0.0074 M **1**, 4.9 M THF/pentane at -78 °C. 69

Figure A1.30. Parametric fit to the ^{19}F NMR spectroscopy derived concentration versus time profile of 0.10 M LDA, 0.0074 M **1**, 2.5 M THF/pentane at -78 °C. 70

Figure A1.31. Plot of concentration versus time by ^{19}F NMR spectroscopy of 0.10 M **1**, 0.10 M LDA, 12.2 M THF at -78 °C. 71

Figure A1.32. Parametric fit to the ^{19}F NMR spectroscopy derived concentration versus time profile of 0.40 M LDA, 0.010 M carbamate in 12.2 M THF at -100 °C. 72

Figure A1.33. Plot of intensity versus time by ^{19}F NMR spectroscopy of 0.20 M LDA, 0.01 M **1**, 5.0 M THF/pentane at -90 °C. 75

Figure A1.34. Plot of intensity versus time by ^{19}F NMR spectroscopy of 0.10 M LDA, 1.9 M *t*-BuOMe/cyclopentane at -78 °C. 76

Figure A1.35. Parametric fit to the ^{19}F NMR spectroscopy derived concentration versus time profile of 0.0074 M **1**, 0.10 M LDA, 5.0 M 2-methyltetrahydrofuran/hexanes at -78 °C. 87

Figure A1.36. Parametric fit to the ^{19}F NMR spectroscopy derived concentration versus time profile of 0.0074 M **1**, 0.10 M LDA, 5.0 M tetrahydropyran/pentane at -78 °C. 78

Figure A1.37. Plot of intensity versus time by ^{19}F NMR spectroscopy of 0.0074 M **1**, 0.10 M LDA, 4.1 M 2,2-dimethyltetrahydrofuran/pentane at -78 °C. 79

Figure A1.38. Plot of intensity versus time by ^{19}F NMR spectroscopy of 0.0074 M **1**, 0.10 M LDA, 4.1 M 2,5-dimethyltetrahydrofuran/pentane at -78 °C. 80

Figure A1.39 Plot of intensity versus time by ^{19}F NMR spectroscopy of 0.0074 M **1**-*d*, 0.10 M LDA, 0.5 M DMPU/THF at -78 °C. 81

Figure A1.40. Plot of intensity versus time by ^{19}F NMR spectroscopy of 0.0074 M **1**, 0.10 M LDA, 5.1 M dimethylethylamine (DMEA)/toluene at -78 °C. 82

Figure A1.41. Plot of intensity versus time by ^{19}F NMR spectroscopy of 0.0074 M **1**, 0.10 M LDA, 5.0 M oxetane/hexanes at -100 °C. 83

Figure A1.42. Plot of intensity versus time by ^{19}F NMR spectroscopy of 0.0074 M **1**, 0.10 M LDA, 1.4 M TMEDA/THF at -78 °C. 84

Figure A1.43. Relative free energies of solvation (ΔG, kcal/mol) at -78 °C. S = Me_2O. 86

Figure A1.44. Relative free energies of solvation (ΔG, kcal/mol) at -78 °C. S = Me_2O. 87

Figure A1.45. Relative free energies (ΔG, kcal/mol) at -78 °C. S = Me_2O of transition structures for the post-rate-limiting deprotonation of arene A9. 88

Figure A1.46. Relative free energy (ΔG, kcal/mol) at -78 °C. S = Me_2O. Free energy of activation for the deprotonation of arene **A9**. 89

Figure A1.47. ORTEP of **1**. 107

Chapter 2

Figure 2.1. Plot of IR absorbance vs time in THF (6.10 M) for 1,4-addition of ester **1** (0.004 M) with LDA (0.10 M) at -78 °C in the presence of various amounts of LiCl. 127

Figure 2.2. Representative ^6Li NMR spectrum of a 60:40 mixture of [^{6}Li]**5** and[^{6}Li]**3**. 129

Figure 2.3. Plot of the relative integrations of [^{6}Li]**3**, [^{6}Li]**4**, and [^{6}Li]**5** vs the mole fraction of LDA. 130

Figure 2.4. Plot showing IR absorbance of ester **1** vs time for the 1,4-addition of ester **1** (0.10 M) with LDA (0.10 M) in neat THF at -78 °C. 133

Figure 2.5. Time-dependent concentrations measured by ^{6}Li NMR spectroscopy using 0.05 M **3** (0.10 N) and 0.05 M **1** in 6.1 M THF at -78 °C. 134

Figure 2.6. Time-dependent concentrations measured by ^{6}Li NMR spectroscopy using 0.05 M **3** (0.10 N) and 0.025 M **1** in 6.1 M THF at -78 °C. 135

Figure 2.7. Time-dependent concentrations measured by ^{6}Li NMR spectroscopy using 0.05 M **3** (0.10 N) and 0.05 M ester **12** in 6.1 M THF at -78 °C. 136

Figure 2.8. Time-dependent concentrations measured by ^{6}Li NMR spectroscopy using 0.05 M **3** (0.10 N) and 0.10 M **12** in 6.1 M THF at -78 °C. 137

Figure 2.9. Plots of IR absorbance of ester **1** vs time for selected initial concentrations of **1**. 138

Figure 2.10. Plot of initial rate vs [**1**] in THF (6.1 M) for the 1,4-addition of ester **1** with LDA (0.10 M) at -78 °C. 139

Figure 2.11. Plot of initial rate vs [LDA] in THF (6.1 M) for the 1,4-addition of ester **1** (0.004 M) at -78 °C. 139

Figure 2.12. Plot of initial rate vs [THF] in hexane cosolvent for the 1,4-addition of ester **1** (0.004 M) with LDA (0.10 M) at -78 °C. 140

Figure 2.13. Plot of initial rate versus mole fraction of enolate (X_{ROLi}) for the serial injection of 10 aliquots of ester **1** (10 mol % each relative to LDA) into 0.10 M LDA in 6.1 M THF/hexane cosolvent at -78 °C. 143

Figure 2.14. Plot of initial rate vs [LDA] for the condensation of LDA dimer **3** with enolate dimer **5a** (0.025 M) in THF (6.10 M) at -78 °C. 144

Figure 2.15. Plot of initial rate vs the concentration of enolate **5** for the condensation of LDA dimer **3** (0.10 M) with enolate dimer **5a** in THF (6.10 M) at -78 °C. 145

Figure 2.16. Plot of initial rate vs [LiCl] in THF (6.1 M) for the 1,4-addition of ester **1** (0.004 M) with LDA (0.10 M) at -78 °C. 146

Figure 2.17. Plot of k_{obsd} vs [LDA] in THF (6.10 M) for the 1,4-addition of ester **1** (0.004 M) in the presence of 1 mol % LiCl at -78 °C. 148

Figure 2.18. Plot of k_{obsd} vs [THF] in hexane cosolvent for the 1,4-addition of ester **1** (0.004 M) with LDA (0.10 M) in the presence of 1.0 mol % LiCl at -78 °C. 148

Figure 2.19. Plots of ester concentration vs time for the uncatalyzed 1,4-addition of LDA (0.10 M) to a mixture of esters **1** and **12** (0.005 M each) in THF (6.10 M) at -78 °C. 153

Figure A2.1. ^{6}Li NMR spectra of LDA with 0.50 equiv ester **1** in THF after aging at -55 °C for 60 min: (A) 0.10 M [^{6}Li]LDA; (B) 0.10 M [^{6}Li,^{15}N]LDA. 172

Figure A2.2. ^{15}N NMR spectra of 0.10 M [^{6}Li,^{15}N]LDA with ester **1** in THF after aging at -55 °C for 60 min. 173

Figure A2.3. (A) Representative ^{6}Li NMR spectrum of a 60:40 mixture of [^{6}Li]**5** and[^{6}Li]**3** showing homodimers (A_2 and E_2) and mixed dimer [^{6}Li]**4** (AE). 174

Figure A2.4. ^{6}Li NMR spectra of [^{6}Li]LDA (0.10 M) with [^{6}Li]LiCl in 12.2 M THF at -110 °C. 175

Figure A2.5. Plot showing IR absorbance of ester **1** vs time for the 1,4-addition of ester **1** (0.10 M) with LDA (0.10 M) at -78 °C. 176

Figure 2.6. Plots of IR absorbance of ester **1** vs time for selected initial concentrations of **1**. 177

Figure A2.7. Plot of initial rates vs [**1**] for the 1,4-addition of LDA (0.10 M) to ester **1** in THF (6.10 M) at -78 °C. 178

Figure A2.8. Plot of initial slopes vs [LDA] in THF (6.10 M) for the 1,4-addition of ester **1** (0.004 M) at -78 °C. 179

Figure A2.9. Plot of initial slopes vs [THF] for the 1,4-addition of LDA (0.10 M) to ester **1** (0.004 M) in hexane at -78 °C. 180

Figure A2.10. Plot of initial slopes vs [LDA] for the condensation of LDA dimer **3** (0.10 M) with enolate dimer **5a** (0.025M) in THF (6.10 M) at -78 °C. 181

Figure A2.11. Plot of initial slopes vs the concentration of enolate **5** for the condensation of LDA dimer **3** (0.10 M) with enolate dimer **5a** (0.025M) in THF (6.10 M) at -78 °C. 182

Figure A2.12. Plot of initial slopes vs [THF] for the 1,4-addition of LDA (0.10 M) to enolate **3** (0.01M) in hexane at -78 °C. 183

Figure A2.13. Parametric fit to eqs 17-22 of the time-dependent concentrations measured by ^{6}Li NMR spectroscopy using 0.05 M **3** (0.10 *normal*), 0.05 M **1** in 6.1 M THF at -78 °C. 184

Figure A2.14. Parametric fit to eqs 17-22 of the time-dependent concentrations measured by ^{6}Li NMR spectroscopy using 0.05 M **3** (0.10 *normal*), 0.025 M **1** in 6.1 M THF at -78 °C. 185

Figure A2.15. Parametric fit to eqs 17-22 of the time-dependent concentrations measured by ^{6}Li NMR spectroscopy using 0.05 M **3**(0.10 N), 0.05 M **12** in 6.1 M THF at -78 °C. 186

Figure A2.16. Parametric fit to eqs 17-22 of the time-dependent concentrations measured by ^{6}Li NMR spectroscopy using 0.05 M **3** (0.10 *normal*), 0.10 M **12** in 6.1 M THF at -78 °C. 187

Figure A2.17. Plot of initial rate (y_1) versus X_{ROLi} for the serial injection of ten aliquots of ester **1 (**0.01 M final concentrations) to 0.10 M LDA in 6.1 M THF/hexanes co-solvent at -78 °C. 188

Figure A2.18. Plot of initial rate (y_1) versus X_{ROLi} for the serial injection of ten aliquots of ester **1** (0.01 M final concentrations) to 0.10 M LDA in 6.1 M THF/hexanes co-solvent at -78 °C. 189

Figure A2.19. Plot showing IR absorbance of ester **1** vs time for the 1,4-addition of LDA (0.10 M) to equimolar ester **1** (0.10 M) in THF (6.10 M) with hexane cosolvent at -78 °C containing 1.0 mol % LiCl. 190

Figure A2.20. Plot of IR absorbance vs time in THF (6.10 M) for the 1,4-addition of LDA (0.10 M) to ester **1** (00M) at -78 °C in the presence of LiCl. 191

Figure A2.21. Plot of initial rates vs [LiCl] for the 1,4-addition of LDA (0.10 M) to ester **1** (0.004 M) in THF (6.1 M) at -78 °C. 192

Figure A2.22. Plot of k_{obsd} vs [LiCl] for the 1,4-addition of LDA (0.10 M) to ester **1** (0.004 M) in THF (6.10 M) at -78 °C. 193

Figure A2.23. Plot of k_{obsd} vs [LDA] for the 1,4-addition of in LDA (0.10 M) ester **1** (0.004 M) with LDA (0.10 M) in [THF] in hexane cosolvent at -78 °C. 194

Figure A2.24. Plot of k_{obsd} vs [THF] in hexane cosolvent for the 1,4-additionof [LDA] (0.10 M) to ester **1** (0.004 M) in the presence of 1% LiCl at -78 °C. 195

Figure A2.25. Plot of concentration vs time for the uncatalyzed 1,4-addition of a mixture of esters **1** and **12** (0.05 M each) to LDA (0.10 M) in THF (6.10 M) at -78 °C. 196

Figure A2.26. Plot of concentration vs time for the uncatalyzed 1,4-addition of a mixture of esters **1** and **12** (0.005 M each) to LDA (0.10 M) in THF (6.10 M) at -78 °C. 197

Figure A2.27. Plot of concentration vs time for the LiCl catalyzed (1.0 mol %) 1,4-addition of LDA (0.10 M) to a mixture of esters **1** and **12** (0.05 M each) to LDA in THF (6.10 M) at -78 °C. 198

Figure A2.28. Plot of concentration vs time for the 1,4-addition of LDA (0.10 M) to a mixture of esters **1** and **12** (0.05 M each) to LDA (0.10 M) in THF (6.10 M) at -78 °C in the presence of lithium enolate **5** (50.0 mol %). 199

Figure A2.29. Plot of initial rate vs [LDA] in THF (6.10 M) on serially injecting ester **1** and (0.014 M) in LDA (0.10 M) in presence of 1.0% LiCl at -78 °C. 200

Figure A2.30. Derivation of expression for fitting LiCl saturation curve. 201

Figure A2.31. Derivation of expression for fitting incremental addition curves depicted in Figures 2.9 and 2.10. 202

Chapter 3

Figure 3.1. Representative plots of concentration versus time monitored by ^{19}F NMR spectroscopy for the ortholithiation of **1** and formation of **2** and **3** by LDA (0.10 M) in THF (12.2 M) at –60 °C. The curves represent best-fit numerical integrations as described below. 227

Figure 3.2. Ortholithiation of **1** (0.010 M) with LDA (0.10 M) in THF (12.2 M) at –78 °C monitored by IR spectroscopy (1325 cm^{-1}) with injection of 1.0 mol % LiCl. 228

Figure 3.3. Plot of initial rate vs [**1**] (initial arene concentration) for the ortholithiation of **1** with LDA (0.10 M) in THF (12.2 M) at –78 °C. 232

Figure 3.4. Plot of initial rate versus [THF] for the ortholithiation of **1** (0.050 M) by LDA (0.10 M) at –78 °C. 232

Figure 3.5. Plot of initial rate versus [LDA] in THF (12.2 M) for the ortholithiation of **1** (0.050 M) at –78 °C. 233

Figure 3.6. Competitive ortholithiation of **1** (0.050 M) and **1**-2,6-d_2 (0.050 M) with LDA (0.10 M) in THF (12.2 M) at –78 °C. 237

Figure 3.7. Plot of initial rate versus [**1**-2,6-d_2] for the ortholithiation of **1**-2,6-d_2 by 0.10 M LDA in 12.2 M THF at -78 °C. 238

Figure 3.8. Ratio of relative initial rates of formation of **2** and **3**, $(\Delta\mathbf{2}/\Delta t)/(\Delta\mathbf{3}/\Delta t)$, versus [THF] for the ortholithiation of **1** (0.050 M) by LDA (0.10 M) at –65 °C. 240

Figure 3.9. Plot of k_{obsd} versus [LDA] in THF (12.2 M) for the ortholithiation of **1**-2,6-d_2 (0.002 M) at –65 °C. 241

Figure 3.10. Plot of k_{obsd} versus [THF] in hexanes for the ortholithiation of **1**-2,6-d_2 (0.002 M) by LDA (0.05 M) at –65 °C. 242

Figure 3.11. DFT computations [MP2/6–31G(d)//B3LYP/6–31G(d)] of dimer-based transition structures for the metalation of **1**. 244

Figure 3.12. Representative plot of the IR absorbance of **1** (0.005 M) versus time for the ortholithiation by LDA (0.10 M) in 12.2 M THF in the presence of 5 mol% LiCl at –78 °C. 245

Figure 3.13. Plot of initial rate versus [LiCl] for the ortholithiation of **1** (0.074 M) by 0.10 M LDA in 12.2 M THF at –78 °C. 246

Figure 3.14. Plot of initial rate versus [LDA] in THF (12.2 M) for the ortholithiation of **1** (0.075 M) in the presence of 5 mol% LiCl at –78 °C. 247

Figure 3.15. Plot of initial rate versus [THF] in hexanes (curve A) and 2,5-dimethyl-tetrahydrofuran (curve B) cosolvent for the ortholithiation of **1** (0.075 M) by LDA (0.10 M) in the presence of 5 mol% LiCl at –78 °C. 248

Figure 3.16. Plot of relative initial rate versus [THF] in 2,5-dimethyl-tetrahydro-furan cosolvent for the ortholithiation of **1** (0.050 M) by LDA (0.10 M) in the presence of 5 mol% LiCl at –78 °C. 249

Figure 3.17. DFT computations [MP2/6–31G(d)//B3LYP/6–31G(d)] of monomer-based transition structures for the metalation of **1**. 250

Figure 3.18. Representative plot showing absorbance of arene **1** vs time for the ortholithiation of **1** (0.010 M) with LDA (0.10 M) in THF (12.20 M) at –78 °C. 252

Figure 3.19. Plot of initial rate versus aryllithium [**2**-6-*d*] for the ortholithiation of **1** (0.075 M) by 0.10 M LDA in 12.2 M THF at –78 °C. 252

Figure 3.20. Representative plot of absorbance of **3** (0.050 M, 1154 cm^{-1}) versus time for isomerization by *i*-Pr_2NH (0.31 M) in 12.2 M THF at –78 °C. 254

Figure 3.21. Plot of k_{obsd} vs [*i*-Pr_2NH] for the isomerization of **3** (0.050 M) to **2** in 12.2 M THF at –78 °C. 254

Figure A3.1. ^{19}F NMR spectrum of LDA (0.10 M) with **1** (0.05 M) in 12.2 M THF after aging for 10 minutes at - 90 °C. 279

Figure A3.2. ^{6}Li NMR spectrum of [^{6}Li,^{15}N]LDA (0.10 M) and **1** (0.05 M) in neat THF recorded at -90 °C. 279

Figure A3.3. $^{13}C\{^{1}H\}$ NMR spectrum of **2** generated from **1** (0.20 M) with [^{6}Li]LDA (0.30 M) in 12.2 M THF-d_8 at -105 °C. 280

Figure A3.4. $^{13}C\{^{19}F\}$ NMR spectrum of **2** generated from **1** (0.20 M) with [^{6}Li]LDA (0.30 M) in 12.2 M THF-d_8 at -105 °C. 281

Figure A3.5. $^{13}C\{^{19}F\}$ NMR spectrum of **3** generated from **1** (0.15 M) with [^{6}Li,^{15}N]LiTMP (0.20 M) in 12.2 M THF-d_8 at -90 °C. 282

Figure A3.6. ^{1}H and ^{13}C NMR spectra of **1**-h_2 in $CDCl_3$ and THF-d_8. 283

Figure A3.7. ^{1}H and ^{13}C NMR spectra of **1**-2-d_1 in $CDCl_3$. 284

Figure A3.8. ^{1}H and ^{13}C NMR spectra of **1**-2-d_1 in $CDCl_3$. 285

Figure A3.9. ^{1}H and ^{13}C NMR spectra of **1**-6-d_1 in $CDCl_3$. 286

Figure A3.10. ^{1}H and ^{13}C NMR spectra of **1**-6-d_1 in $CDCl_3$. 287

Figure A3.11. ^{1}H NMR spectra of **1**-6-d_1 in $CDCl_3$. 288

Figure A3.12. ^{1}H and ^{13}C NMR spectra of **1**-2,6-d_2 in $CDCl_3$. 289

Figure A3.13. Representative in situ IR trace for the ortholithiation of **1** (0.05 M) by LDA (0.10 M) in THF at -78 °C. 290

Figure A3.14. Time-dependent concentrations measured by ^{19}F NMR spectroscopy using 0.05 M **4** (0.10 N) and **1**in 12.2 M THF at -65 °C. 291

Figure A3.15. Representative plot showing absorbance of arene **1** vs time for the ortholithiation of **1** (0.010 M) with LDA (0.10 M) in THF (12.20 M) at –78 °C. 296

Figure A3.16. Ortholithiation of **1** (0.010 M) with LDA (0.10 M) in THF (12.2 M) at –78 °C with injection of 1.0 mol% LiCl. 296

Figure A3.17 Competitive ortholithiation of **1** (0.050 M) and **1**-2,6-d_2 (0.050 M) with LDA (0.10 M) in THF (12.2 M) at –78 °C. 297

Figure A3.18. Plot of initial rate versus [**1**-2,6-d_2] for the ortholithiation of **1**-2,6-d_2 by 0.10 M LDA in 12.2 M THF at -78 °C. 298

Figure A3.19. Plot of **2/3** versus time for the ortholithiation of **1** by LDA in THF (12.2 M) at -65 °C. 299

Figure A3.20. Representative IR plot for the equilibration of **3** (1151 cm^{-1}) to **2** (1306 cm^{-1}). 303

Figure A3.21. Plot of initial rate vs [**1**] (initial arene concentration) for the ortholithiation of **1** with LDA (0.10 M) in THF (12.2 M) at –78 °C. 304

Figure A3.22. Plot of initial rate versus [LDA] in THF (12.2 M) for the ortholithiation of **1** (0.050 M) at –78 °C. 305

Figure A3.23. Plot of initial rate versus [THF] for the ortholithiation of **1** (0.050 M) by LDA (0.10 M) at –78 °C. 306

Figure A3.24. Ratio of relative initial rates of formation of **2** and **3**, $(\Delta\mathbf{2}/\Delta t)/(\Delta\mathbf{3}/\Delta t)$, versus [THF] for the ortholithiation of **1** (0.050 M) by LDA (0.10 M) at –65 °C. 307

Figure A3.25. Plot of k_{obsd} versus [LDA] in THF (12.2 M) for the ortholithiation of **1**-2,6-d_2 (0.002 M) at –65 °C. 309

Figure A3.26. Plot of k_{obsd} versus [THF] in hexanes for the ortholithiation of **1**-2,6-d_2 (0.002 M) by LDA (0.05 M) at –65 °C. 310

Figure A3.27. Representative plot of **1** (0.005 M) versus time for the

ortholithiation by LDA (0.10 M) in 12.2 M THF in the presence of 5 mol% LiCl at -90 °C. 311

Figure A3.28. Plot of initial rate versus [LiCl] for the ortholithiation of **1** (0.074 M) by 0.10 M LDA in 12.2 M THF at –78 °C. 312

Figure A3.29. Plot of initial rate versus [LDA] in THF (12.2 M) for the ortholithiation of **1** (0.075 M) in the presence of 5 mol% LiCl at –78 °C. 313

Figure A3.30. Plot of initial rate versus [THF] in hexanes (curve A) and 2,5-dimethyl-tetrahydrofuran (Me_2-THF) (curve B) cosolvent for the ortholithiation of **1** (0.075 M) by LDA (0.10 M) in the presence of 5 mol% LiCl at –78 °C. 314

Figure A3.31. Plot of relative initial rate versus [THF] in 2,5-dimethyltetrahydrofuran cosolvent for the ortholithiation of **1** (0.050 M) by LDA (0.10 M) in the presence of 5 mol% LiCl at –78 °C. 315

Figure A3.32. Plot of k_{obsd} versus [*i*-Pr_2NH] for the isomerization of **3** (0.050 M) to **2** in 12.2 M THF at –78 °C. 316

Figure A3.33. Plot of k_{obsd} versus [THF] for the isomerization of **3** (0.050 M) to **2** in 12.2 M THF at –78 °C. 317

Figure A3.34. Plot of initial rate versus arylithium [**2**-6-*d*] for the ortholithiation of **1** (0.075 M) by 0.10 M LDA in 12.2 M THF at –78 °C. 318

Figure A3.35. Plot of the equilibrium constant (K_{eq}) versus total concentration of lithium titer LiX_T. 320

Figure A3.36. Relative free energies for the solvation(ΔG, kcal/mol) of **2**, **3**, and 4-lithio-1-chloro-3-(trifluoromethyl)benzene at -78 °C. 324

Figure A3.37. DFT computations [MP2/6–31G(d)//B3LYP/6–31G(d)] of monomer-based transition structures for the metalation of **1**. 325

Figure A3.38. DFT computations [MP2/6–31G(d)//B3LYP/6–31G(d)] of dimer-based transition structures for the metalation of **1**. 326

Figure A3.39. Relative free energies (ΔG, kcal/mol) at -78 °C for the solvation of (A) THF-tetrasolvated lithium ion and (B) THF-hexasolvated LiCl triple ion. 327

Figure A3.40. Relative free energies (ΔG, kcal/mol) at -78 °C of (A) dimeric LiCl and relative free energy of monomeric and dimeric LiCl at -78 °C. 328

Figure A3.41. Reaction scheme showing LiCl deaggregating THF-disolvated closed dimer. Free energies are given in kcal/mol at -78 °C. 329

Chapter 4

Figure 4.1. Artist's rendition of the influence of lithium chloride on metalation rate plotted versus the rate of the corresponding uncatalyzed metalation. 418

LIST OF TABLES

Table A1.1. Optimized geometry at B3LYP level of theory with 6-31G(d) basis set, free energy (G, Hartrees), and cartesian coordinates (X, Y, Z). 90

Table A1.2. Crystal data and structure refinement for **1**. 108

Table A1.3. Atomic coordinates (x 10^4) and equivalent isotropic displacement parameters ($Å^2$x 10^3) for **1**. 109

Table A1.4. Bond lengths [Å] and angles [°] for **1**. 110

Table A1.5. Symmetry transformations used to generate equivalent atoms: Anisotropic displacement parameters ($Å^2$x 10^3) for **1**. 112

Table A1.6. Hydrogen coordinates (x 10^4) and isotropic displacement parameters ($Å^2$x 10 ^{3}) for **1**. 113

Chapter 2

Table A2.1. Optimized geometry, free energy (G, Hartrees), and cartesian coordinates (X, Y, Z). 203

Chapter 3

Table A3.1. Relative initial rates for formation of **2** and **3** for the ortholithiation of **1**, **1**-2-*d*, **1**-6-*d* and **1**-2,6-d_2 (0.05 M each) by LDA (0.10 M) in THF (12.2 M) at -78 °C. 300

Table A3.2. Table showing the relative initial rates for formation of **2** and **3** with various lithium salts (0.020 M) for the ortholithiation of **1** (0.050 M) by LDA (0.10 M) in 12.2 M THF at -90 °C. 301

Table A3.3. Table showing regioselectivity at equilibrium for the ortholithiation of **1** by *sec*-BuLi (0.11 M) and *n*-BuLi (0.11 M) in 12.2 M THF at -90 °C. 302

Table A3.4. Table of relative initial rate versus [LDA] for the ortholithiation of **1** (0.050 M) by LDA (0.10 M) at -65 °C. 308

Table A3.5. Optimized geometries at B3LYP level of theory with 6-31G(d) basis set for the serial solvation of **2**, **3**, and 4-lithio-1-chloro-3-(trifluoromethyl)benzene at -78 °C. 330

Table A3.6. Optimized geometries of reactants and monomer-based transition structures at B3LYP level of theory with 6-31G(d) basis set for the ortholithiation of **1** at -78 °C. 337

Table A3.7. Optimized geometries of reactants and dimer-based transition structures at B3LYP level of theory with 6-31G(d) basis set for the ortholithiation of **1** at -78 °C. 348

Table A3.8. Optimized geometries at the B3LYP level of theory with 6-31G(d) basis set of lithium ions, LiCl aggregates, LiCl triple ions, LiCl- LDA mixedaggregates and LiCl-LDA triple ions at -78 °C. 360

Chapter 4

Table A4.1. Optimized geometries at the B3LYP level of theory with 6-31G(d) basis set of THF disolvated and trisolvated LDA aggregates including closed and open dimers as well as monomers at -78 °C. 422

Table A4.2. Optimized geometries at the B3LYP level of theory with 6-31G(d) basis set of THF disolvated LDA open dimers at -78 °C. 442

Table A4.3. Optimized geometries at the B3LYP level of theory with 6-31G(d) basis set of THF trisolvated LDA open dimers at -78 °C. 455

CHAPTER 1

AUTOCATALYSIS IN LITHIUM DIISOPROPYLAMIDE-MEDIATED ORTHOLITHIATIONS

AUTOCATALYSIS IN LITHIUM DIISOPROPYLAMIDE-MEDIATED ORTHOLITHIATIONS

Abstract

Ortholithiation of 3-fluorophenyl-*N,N*-diisopropyl carbamate by lithium diisopropylamide (LDA) in THF at -78 °C affords unusual rate behavior including linear decays of the carbamate, delayed formation of LDA-aryllithium mixed dimers, and evidence of autocatalysis. A mechanistic model in conjunction with numeric integration methods accounts for the time-dependent changes in concentration. The two critical rate-limiting steps in the model entail (1) an LDA dimer-based metalation of arylcarbamate, and (2) A rate-limiting condensation of the resulting aryllithium with the LDA dimer to form two isomeric LDA-ArLi mixed dimers. One isomer is elicits a highly efficient (post-rate-limiting) metalation of aryl carbamate, in turn, regenerating aryllithium. The prevalence and implications of such autocatalysis are discussed.

Introduction

Lithium diisopropylamide (LDA) is often the reagent of choice for reactions requiring a strong base.[1] The central importance of LDA motivated us to examine how solvation and aggregation influence its reactivity.[2] Studies spanning two decades have documented more than a dozen mechanisms that differ in solvation and aggregation at the rate-limiting transition structures. Recent studies of the LDA-mediated ortholithiation of aryl carbamates[3,4] underscore the potential complexity by revealing both monomer and dimer-

based pathways. A pronounced autoinhibition was traced to intervening mixed aggregates, which are often observed in reactions of LDA.[5]

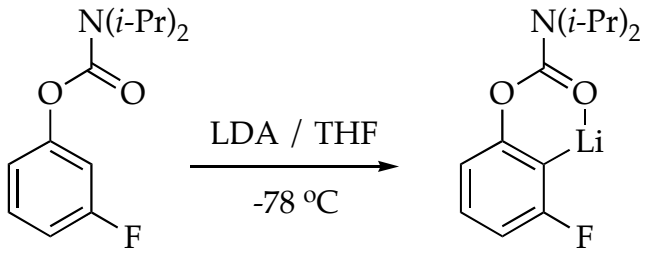

1 **2** (1)

LDA-mediated metalation aryl carbamate **1**, the most reactive of all carbamates we had studied to date,[ref] displayed two perplexing behaviors. First, treating carbamate **1** with 1.0 equiv of LDA in neat THF at -78 °C--conditions used for many LDA-mediated reactions--affords aryllithium monomer **2** to the exclusion of mixed aggregates. The concentration of **1** also follows a first-order decay to a reasonable approximation (Figure 1.1); a second-order fit (dashed line) is clearly inferior.

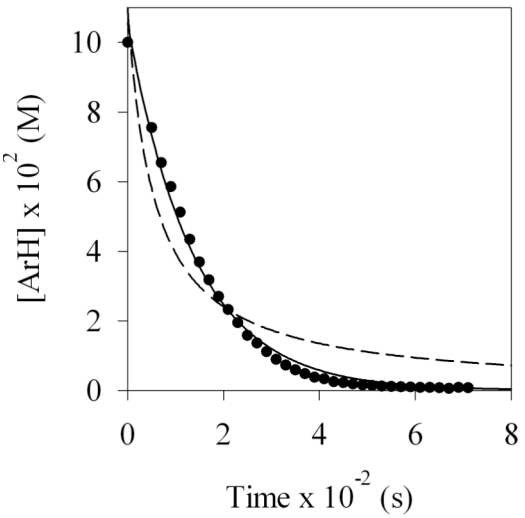

Figure 1.1. Reaction of 0.10 M carbamate **1** with 0.10 M LDA at -78 °C in neat THF as monitored by ^{19}F NMR spectroscopy. The solid and dashed lines represent least squares fits to first and second order decays, respectively.

Thus, on first inspection, we appeared to have discovered the most outwardly simple LDA-mediated reaction reported to date. Something was wrong, however: This inherently bimolecular reaction should *not* be first order, regardless of whether the rate-limiting transition structure is based on an LDA monomer or dimer. The second strange observation appeared when a large excess of LDA was used. The large excess--so-called pseudo-first-order conditions--usually forces a higher-order reaction to behave as if it is first order (thus the name). When such pseudo-first-order conditions are used we observe a linear decay of **1** (Figure 1.2). The decay is clearly *not* first order in carbamate **1**, appearing instead to be *zeroth*-order.

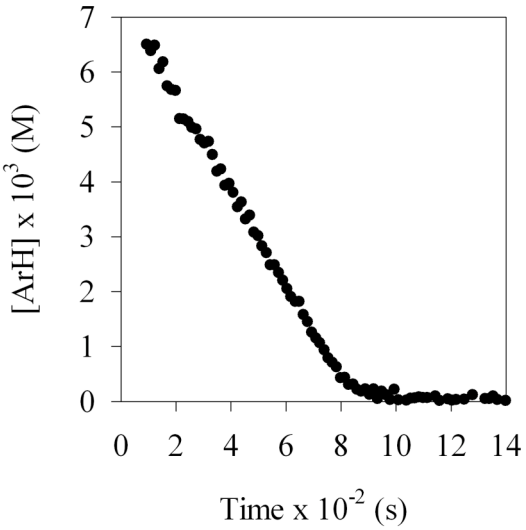

Figure 1.2. Reaction of 0.010 M carbamate **1** with 0.10 M LDA at -78 °C in neat THF as monitored by ^{19}F NMR spectroscopy.

We describe herein structural and rate studies showing that numerous deviant rate behaviors for the ortholithiation of **1** stem from mixed aggregates

and autocatalysis[6,7] as summarized generically in Scheme 1.[5-11] *It is the most mechanistically complex reaction of LDA reported to date.* Autocatalysis results from intervening LDA-ArLi mixed dimers **4** and **5**. Although metalation of arene **1** by minor isomer **5** (Step III) is an important step in this unusual autocatalysis, the condensation of aryllithium **2** with LDA dimer **3** (Step IV) is rate limiting. Mounting evidence suggests that autocatalysis may be prevalent in LDA/THF-mediated reactions at -78 °C.

Scheme 1

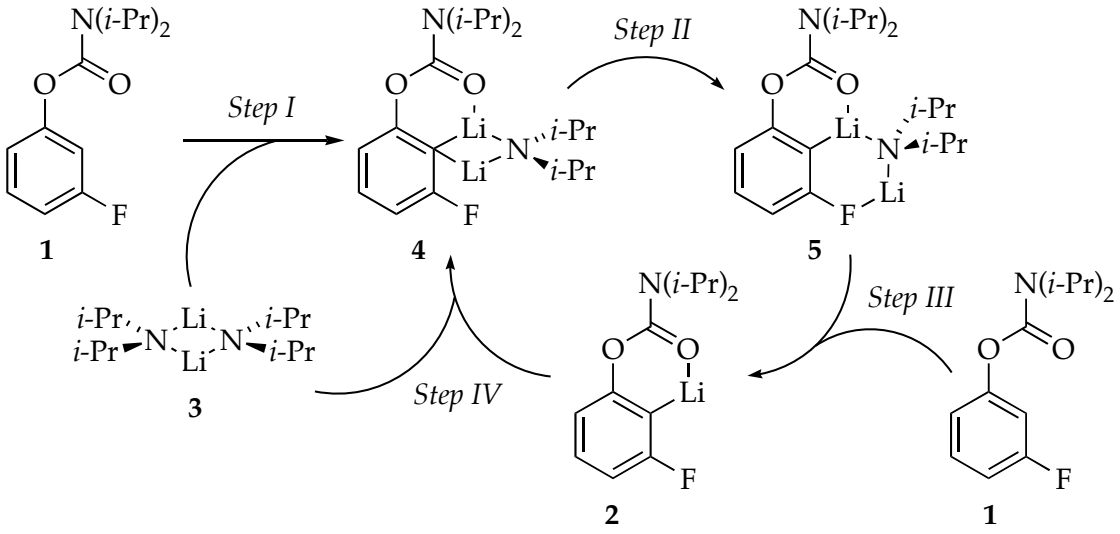

Results

General Methods. LDA, [^{6}Li]LDA, and [^{6}Li,^{15}N]LDA were purified as white crystalline solids.[12] The structural assignments derive from routine ^{6}Li, ^{13}C, and ^{15}N NMR spectroscopic methods.[9,13]

Rate studies were carried out using in situ IR spectroscopy[14] and ^{19}F NMR spectroscopy[15] following standard protocols. The results from the two forms of spectroscopy are fully consistent. Unless stated otherwise, pseudo-

first-order conditions were established by maintaining the concentration of carbamate **1** at 0.004-0.008 M. LDA and THF were maintained at high yet adjustable concentrations using hexane as the cosolvent.[16] Although pseudo-first-order conditions are used routinely to preclude the effects of mixed aggregation and other conversion-dependent effects,[2,8b,11] mixed aggregation effects are pronounced under all conditions used to lithiate carbamate **1**.[17,18] IR spectroscopic analysis of the lithiation of carbamate **1** with $\geq$1.0 equiv of LDA in THF reveals that the reaction proceeds to full conversion. Under no conditions do we observe carbamate-LDA complexation. Time-dependent concentrations measured by ^{19}F NMR spectroscopy are fit to a mechanistic model (see Discussion) expressed by a set of differential equations (see Experimental) using numeric integration, yielding functions describing concentration versus time for multiple species.

Density functional theory (DFT) computations were carried out at the B3LYP/6-31G(d) level.[19] The isopropyl moieties of carbamate **1** were approximated with methyl groups, and THF was modeled using Me_2O. Free energies are reported in kcal/mol at -78 °C. The computational results are described sparingly in appropriate contexts below; additional results are archived in supporting information, including some calculations using LDA rather than Me_2NLi.

Solution Structures. In this section we focus only on structure; the time-dependent aggregate concentrations are examined extensively in subsequent sections. ^{6}Li and ^{15}N NMR spectroscopic studies using 2.0 equiv [^{6}Li,^{15}N]LDA reveal aryllithium **2**, LDA dimer **3**, and mixed dimer **4** (Figure 1.3).[13,20] An additional species (ca. 3%), putative mixed dimer **5**, was detected using ^{19}F NMR spectroscopy (below) but was not observed in the ^{6}Li spectra.

Aryllithium **2** shows no ^{15}N coupling, consistent with the absence of an LDA fragment. Limited solubility prevented ^{13}C NMR spectroscopic analysis of the ^{6}Li-^{13}C coupling, but analogous aryllithiums with ortho fluoro moieties[21] or other potentially coordinating ortho substituents are monomeric.[22] Computional studies show minima for mono- and disolvated aryllithium monomer and suggest that disolvated monomer is preferred. Mixed dimer **4** is easily assigned from ^{6}Li-^{13}C and ^{6}Li-^{15}N coupling patterns as described previously.[5a]

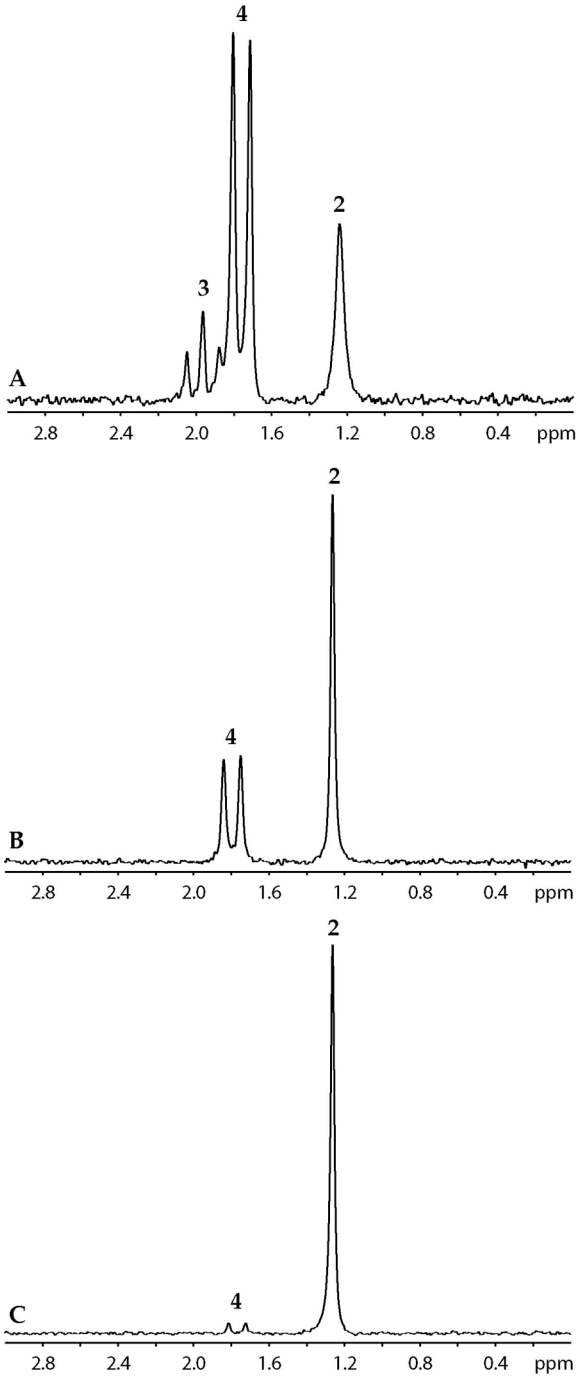

Figure 1.3. ^{6}Li NMR spectrum of 0.10 M [^{6}Li,^{15}N]LDA at -90 °C with (A) 0.050 M **1**; (B) 0.10 M **1**; (C) 0.10 M **1** at -90 °C after warming at -40 °C for 60 minutes.

3

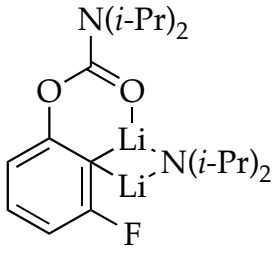

4

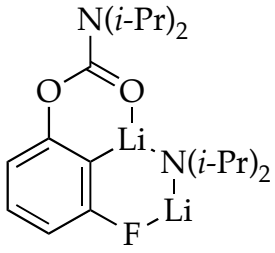

5

Monitoring ortholithiations of **1** using ^{6}Li and ^{19}F NMR spectroscopies allowed us to assign ^{19}F resonances to aryllithium monomer **2** and mixed dimer **4**; a representative spectrum is shown in Figure 1.4. We also observe an additional species (**5** in Figure 1.4) initially suspected to be a mixed trimer akin to those characterized previously.[5,8,10] The ratio of **4** and **5**, however, is invariant with large changes in ArLi, LDA, and THF concentrations (see supporting information). Thus, **4** and **5** are *isomers*.

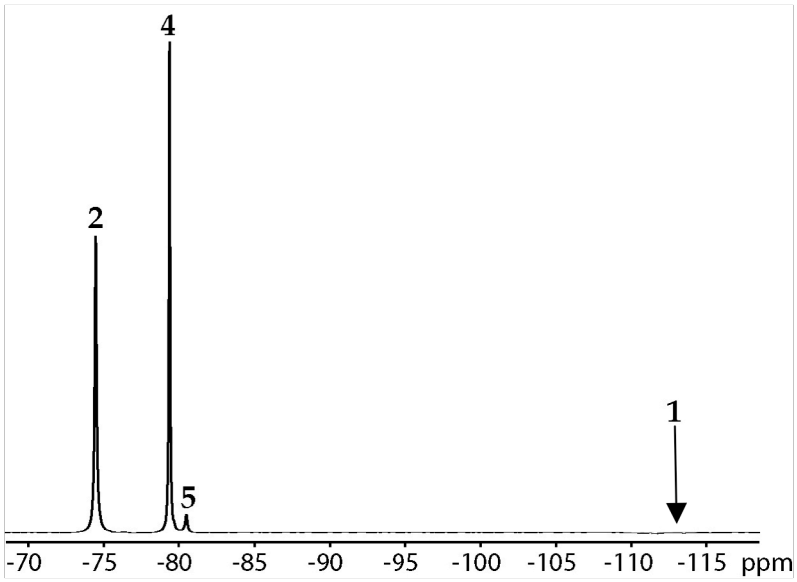

Figure 1.4. ^{19}F NMR spectrum of 0.10 M LDA with 0.10 M **1** at -78 °C.

Computations were used to investigate the solvation of **4** and the more elusive gross structure and solvation of **5** (Scheme 2). Serial solvation shows minima for mono- and disolvated mixed dimers **6**-**9**. Trisolvates failed to minimize, resulting in desolvation in each attempt. Mono- and disolvated dimers **6** and **7** are isoenergetic whereas **8** and **9** are significantly less stable. Dimer **7**, bearing a C-Li-N-Li connectivity characteristic of open dimers[23,24] but with an unusual Li-F interaction, is the only detectable structure bearing two solvents coordinated to the lithium distal to the carbamoyl moiety. No minimum was found corresponding to the analog of **7** with a single solvent on the distal lithium.

Experimental data show that **4** and **5** are isomeric, whereas computations suggest such closed and ring-expanded forms prefer different solvation numbers. We are convinced by the experimental data and, given the approximations used, are comfortable offering **9** and **7** as computational models of isomeric mixed dimers **4** and **5** (respectively). The unusual structural features in **7** reappear in calculated transition structures (vide infra) and in mechanistic discussions.

Scheme 2

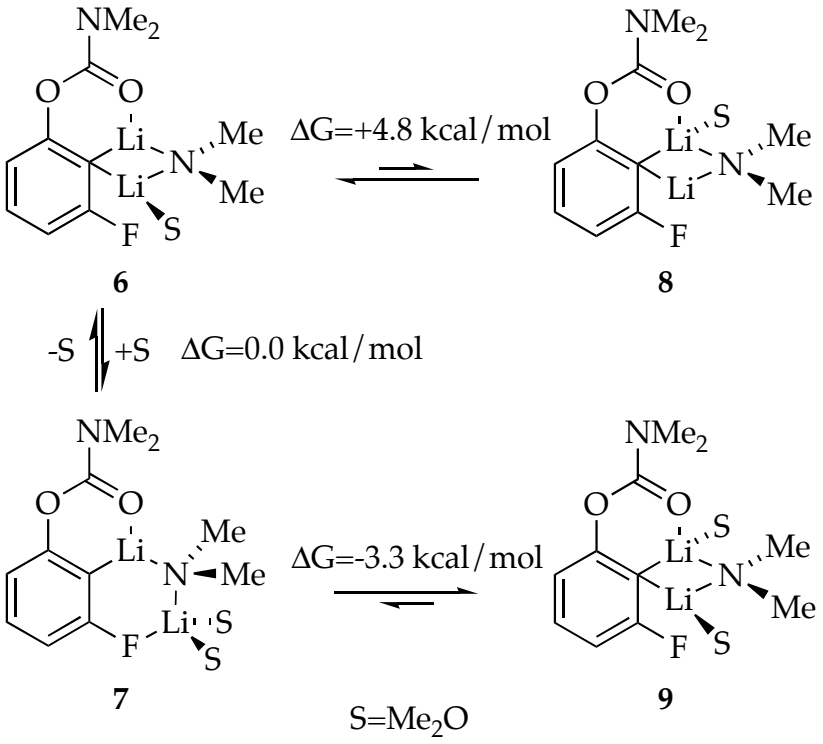

Linear Decays. In theory, the linear decay for the ortholithiation of **1** (illustrated in Figure 1.2) could arise if an aggregation event such as a deaggregation is rate limiting (eqs 2 and 3).[25] The rate of ortholithiation would be dictated by the rate at which monomer is formed[26] and independent of the initial substrate concentration (Figure 1.5).

$$\underset{\mathbf{3}}{(i\text{-Pr}_2\text{NLi})_2} \underset{slow}{\overset{slow}{\rightleftharpoons}} 2\ i\text{-Pr}_2\text{NLi} \qquad (2)$$

$$i\text{-Pr}_2\text{NLi} + \underset{\mathbf{1}}{\text{ArH}} \xrightarrow{fast} [(i\text{-Pr}_2\text{NLi})(\text{ArH})]^{\ddagger} \qquad (3)$$

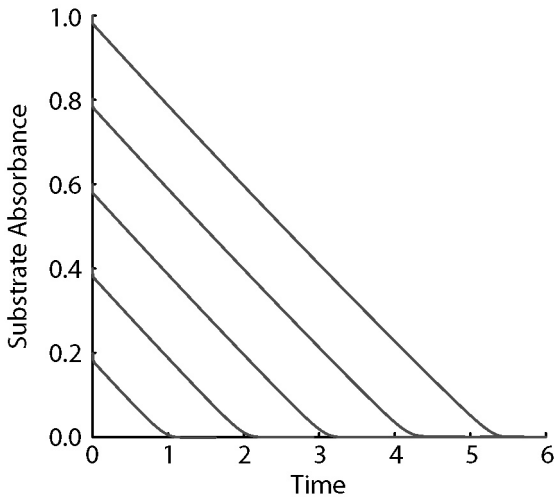

Figure 1.5. Theoretical depiction of substrate dependence for a zeroth-order reaction.

In practice, the scenario in eqs 2 and 3 did not withstand scrutiny. Figure 1.6 reveals reaction rates that depend markedly on the initial concentration of the carbamate. The nearly coincident *x*-intercepts in Figure 1.6 are strikingly similar to those in plots of initial rates arising from a first-order reaction.[26] A plot of the slopes from Figure 1.6 versus initial substrate concentration (Figure 1.7) illustrates the concentration-dependent rates. The highest substrate concentrations in Figure 1.6 far exceed those necessary to preserve pseudo-first-order conditions, yet the linearities persist.

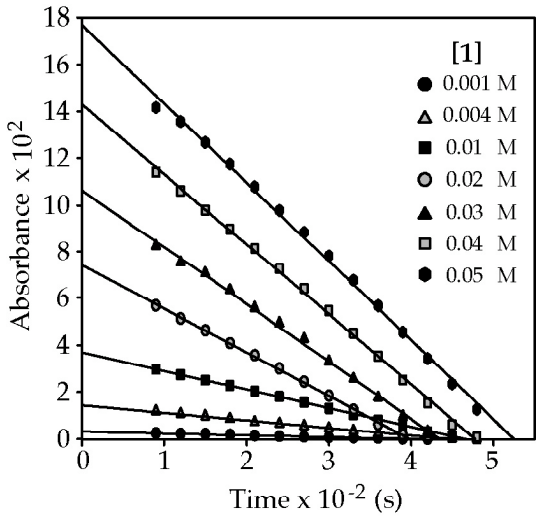

Figure 1.6. Plot showing IR absorbance of **1** (1721 cm^{-1}) versus time for different initial concentrations of carbamate **1**.

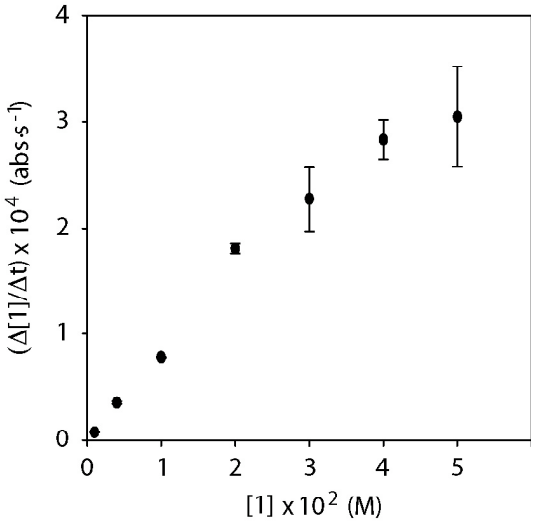

Figure 1.7. Plot of Δ[**1**]/Δt (from Figure 1.6) versus [**1**] for the ortholithiation of **1** with 0.10 M LDA in 12.2 M THF/hexane cosolvent at -78 °C

These results present a paradox. The linearities suggest zeroth-order substrate dependencies, but the substrate concentration-dependent slopes are akin to those for first-order substrate dependencies. Autocatalysis is the culprit.[27]

Evidence of Autocatalysis. We routinely carry out rate studies under pseudo-first-order conditions in which the substrate is kept at low concentration. By allowing no more than a 5% accumulation of new lithium salts one usually precludes autoinhibition and autocatalysis that can arise from the intervention of mixed aggregates.[2] The successful exclusion of such mixed aggregation effects is demonstrated by a simple control experiment: on completion of a reaction, injection of a second small aliquot of substrate provides a decay and a second value for k_{obsd} that is unchanged ($\pm$10%). By inference, the products of the reaction do not influence the rate or mechanism.

One might expect a second aliquot of **1** would afford an analogous linear decay that is superimposable on the first ($\pm$10%.) Experimentally, however, serial injection of two aliquots of carbamate **1** to a large excess of LDA in THF at -78 °C reveals a linear decay in the first and an almost instantaneous reaction in the second. Significant accelerations in the second aliquot are observable under many conditions studied, suggesting to us that the linear decays in Figure 1.6 derive, at least in part, from the superposition of autocatalysis on a normal (first-order) decay.[6] Pronounced mechanistic changes likely derive from LDA-aryllithium mixed aggregates.[28]

Autocatalysis emerged in a more conventional form[6,7] with minor changes in the reaction conditions. By example, sigmoidal curvature (anomalous acceleration) is observed at low THF concentration using hexane as a cosolvent.[29] Similar sigmoidal decays are observed for the lithiation of **1-*d*$_1$** (Figure 1.8). A second aliquot of **1-*d*$_1$** is consumed nearly instantaneously. Comparing the initial rates (slopes at early conversion) of **1** and **1-*d*$_1$** affords a small kinetic isotope effect (k_H/k_D = 2-3). Ortholithiations, including LDA-

mediated ortholithiations of structurally related carbamates,[5] display isotope effects covering a wide range (k_H/k_D = 3 to >20).[30,31] The high reactivity of the LDA-ArLi mixed aggregates--an essential component of autocatalysis--correlates with the delayed onset on mixed aggregation as shown below.

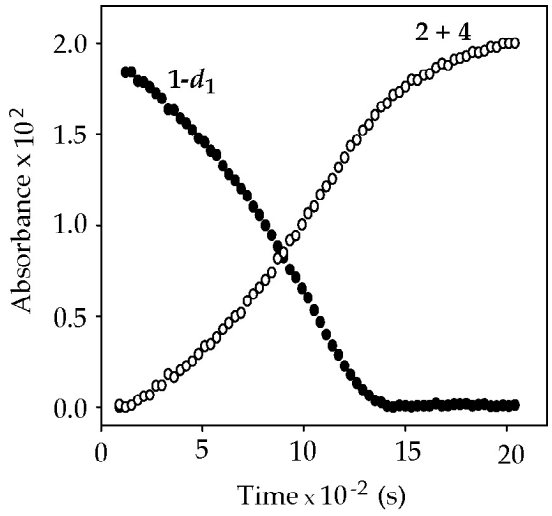

Figure 1.8. Absorbance versus time for the reaction of (0.004 M) **1-*d*$_1$** with (0.10 M) LDA in 12.2 M THF/hexane cosolvent at -78 °C. (**1-*d*$_1$**, 1721 cm^{-1}; **2 + 4**, 1660 cm^{-1}).

Delayed Mixed Aggregation. Monitoring ortholithiations of **1** using ^{19}F NMR spectroscopy reveals very odd time-dependent changes in concentrations illustrated emblematically in Figures 1.9-1.11. The origins of the functions drawn through the data are described in the discussion. Several qualitative observations and control experiments are immediately noteworthy.

The linear loss of carbamate **1** in Figure 1.9 correlates quantitatively with appearance of aryllithium monomer **2**. Oddly, mixed dimers **4** and **5** appear after the ortholithiation of **1** is complete and quite slowly: *Aggregates are not completely equilibrated on the time scale of the ortholithiation.*[25] At low THF concentrations (Figure 1.10), the mixed dimers begin to appear before the

metalation of **1** is complete. The inflection point in the formation of mixed dimer **4**--the point of maximum rate--correlates with the maximum concentration of aryllithium **2**, suggesting that **2** is a key precursor to **4**.[32] Importantly, the ratio of **4** and **5** remains constant at the equilibrium value throughout the reaction coordinate, indicating that **4** and **5** exchange rapidly on the time scale of the metalation.

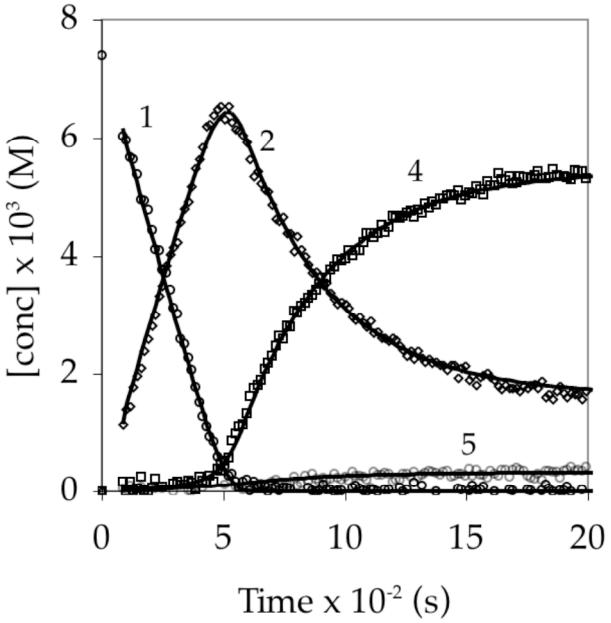

Figure 1.9. Concentrations versus time for the reaction of 0.0074 M **1** with 0.10 M LDA in 12.2 M THF at -78 °C monitored by ^{19}F NMR spectroscopy. The functions result from a least squares fit to the model outline in eqs 9-12 and described mathematically by eqs 16-20.

Mixed dimers appeared to be the probable source of autocatalysis. Indeed, injecting carbamate **1** directly into solutions containing LDA dimer **3** and mixed dimers **4** and **5** within the NMR probe.[25] ^{19}F NMR spectroscopic analysis showed that both **4** and **5** disappear in seconds with concomitant appearance of aryllithium monomer **2** (Step III, Scheme 1). The much slower

condensation of aryllithium **2** with LDA to regenerate the mixed dimers (Step IV, Scheme 1) occurs subsequently.

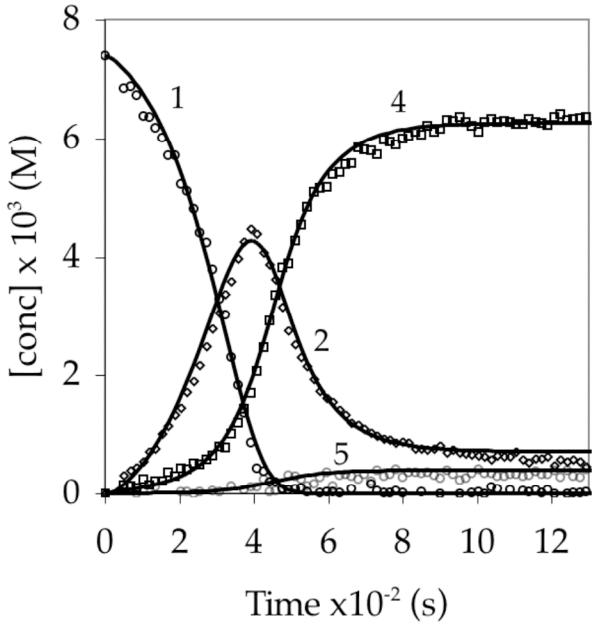

Figure 1.10. Concentrations versus time for the reaction of 0.0074 M **1** with 0.10 M LDA in 4.9 M THF at -78 °C monitored by ^{19}F NMR spectroscopy. The functions result from a least squares fit to the model outline in eqs 9-12 and described mathematically by eqs 16-20.

Temperature Effects. Ortholithiation at -100 °C (Figure 1.11) causes mixed dimer **4** to build to an appreciable and relatively constant concentration whereas mixed dimer **5** does not. The ratio of **4** and **5** is also *not* constant and is markedly perturbed from its equilibrium value until the carbamate is consumed. *The isomerization of **4** and **5** is slow on the time scale of the metalation at -100 °C.* This temperature effect proves to be important in showing that **5** is the key reactive form (vide infra).

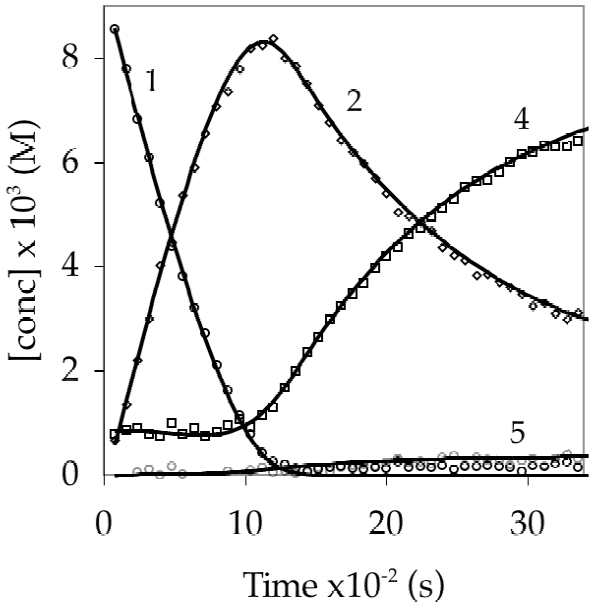

Figure 1.11. Concentrations versus time for the reaction of 0.01 M **1** with 0.40 M LDA in 12.2 M THF at -100 °C monitored by ^{19}F NMR spectroscopy. The functions result from a least squares fit to the model outline in eqs 9-12 and described mathematically by eqs 16-20.

Reaction of LDA Dimer with ArH. The first stage in teasing apart the overall mechanism is to investigate key steps individually. The method of initial rates offers insight into the reaction of LDA and carbamate **1** before the onset of autocatalysis (Step I, Scheme 1). (By virtue of the linearities illustrated in Figure 1.6, the slopes and initial rates are equivalent.) Using ^{19}F NMR spectroscopic data we showed a first order in LDA (Figure 1.12) and zeroth order in THF (Figure 1.13). The idealized rate law[33] in eq 4, in conjunction with the assignment of LDA dimer **3** as a disolvate,[2,9a] is consistent with the generic mechanism in eq 5. Open-dimer-based transition structure **10** is shown to be plausible by computation.[8] Analogous open-dimer-based transition structures have been implicated on many occasions.[23]

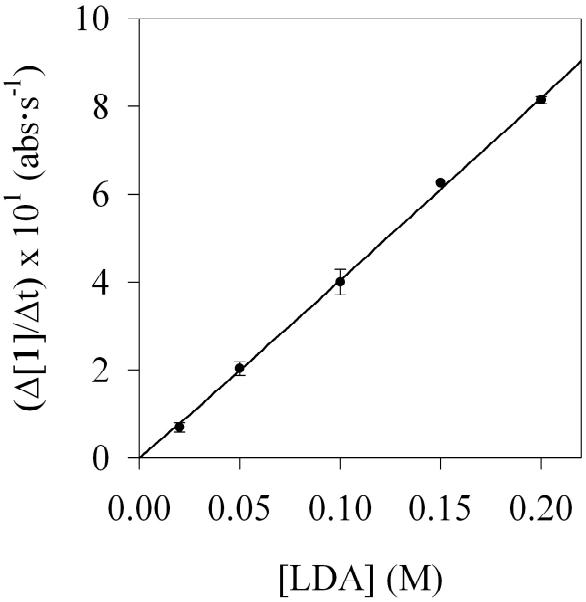

Figure 1.12. Plot of initial rates versus [LDA] for the lithiation of carbamate **1** (0.0074 M) in 12.2 M THF at -78 °C. The curve depicts the result of an unweighted least-squares fit to *rate* = k[LDA]^n (k = (4.2 ± 0.2) x 10^1; n = 1.02 ± 0.03).

$$-d[\mathrm{ArH}]/dt = k'[\mathrm{LDA}][\mathrm{THF}]^0[\mathrm{ArH}] \tag{4}$$

$$\underset{\mathbf{3}}{(i\text{-Pr}_2\mathrm{NLi})_2(\mathrm{THF})_2} + \underset{\mathbf{1}}{\mathrm{ArH}} \xrightarrow{k'} \underset{\mathbf{10}}{[(i\text{-Pr}_2\mathrm{NLi})_2(\mathrm{ArH})(\mathrm{THF})_2]^{\ddagger}} \tag{5}$$

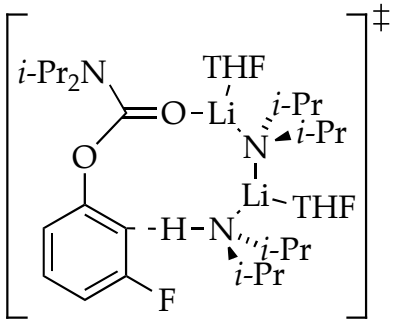

10

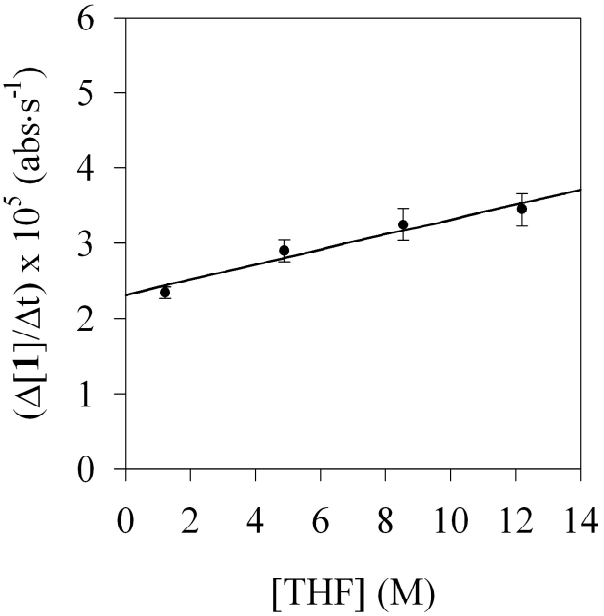

Figure 1.13. Plot of initial rates versus [THF] for the lithiation of carbamate **1** (0.004 M) in 0.1 M LDA using hexanes as cosolvent at -78 °C. The curve depicts the result of an unweighted least-squares fit to *rate* = k[THF] + k' (k = (1.0 ± 0.2) x 10^{-6}; k' = 2.3 ± 0.1) x 10^{-5}).

Reaction of LDA Dimer with ArLi. After substrate **1** is consumed, the loss of aryllithium **2** via condensation with LDA dimer **3** to form mixed dimer **4** (Step IV, Scheme 1) follows clean pseudo-first-order behavior. Analogous reactivity was observed by adding a solution of LDA dimer **3** to aryllithium monomer **2**. Monitoring the pseudo-first-order rate constants as a function of LDA and THF concentrations (Figures 1.14 and 1.15) shows that the condensation is first order in LDA and an inverse first order in THF.[34] The idealized rate law (eq 6) is consistent with a rate-limiting transition structure of stoichiometry [(*i*-$Pr_2NLi)_2$(ArLi)]‡ (eq 7).[35] (The THF ligands are not included because the solvation number of ArLi **2** was studied only computationally, but disolvation seems likely.) This slow aggregation event is important in the formulation of an overall mechanistic hypothesis. Although we cannot even hazard a guess as to what transition structure **11** might look

like, the relationship of transition structures **10** and **11** may be important (vide infra).

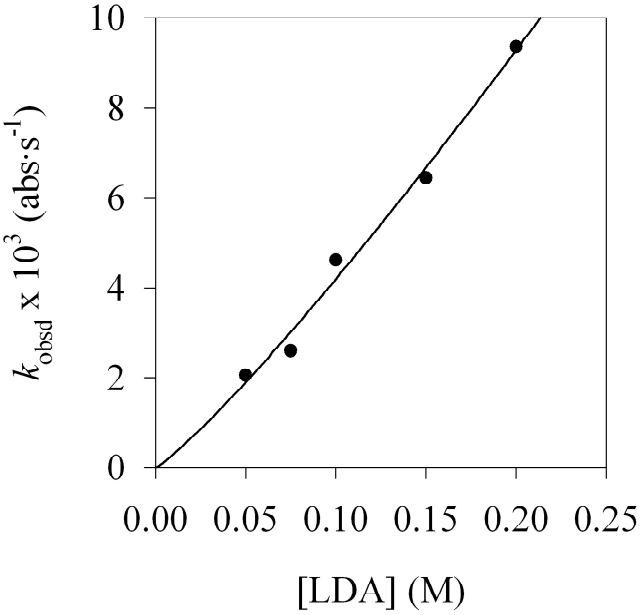

Figure 1.14. Plot of k_{obsd} versus [LDA] for the condensation of LDA with aryllithium **2** (0.0074 M) in 12.2 M THF at -78 °C. The curve depicts the result of an unweighted least-squares fit to $k_{obsd} = k[\text{LDA}]^n + c$ ($k = (60 \pm 10)$; $n = 1.1 \pm 0.1$).

$$-d[\text{ArLi}]/dt = k'[\text{LDA}][\text{ArLi}][\text{THF}]^{-1} \quad (6)$$

$$\underset{\mathbf{3}}{(i\text{-Pr}_2\text{NLi})_2} + \underset{\mathbf{2}}{\text{ArLi}} \xrightarrow{k'} \underset{\mathbf{11}}{[(i\text{-Pr}_2\text{NLi})_2(\text{ArLi})]^{\ddagger}} \quad (7)$$

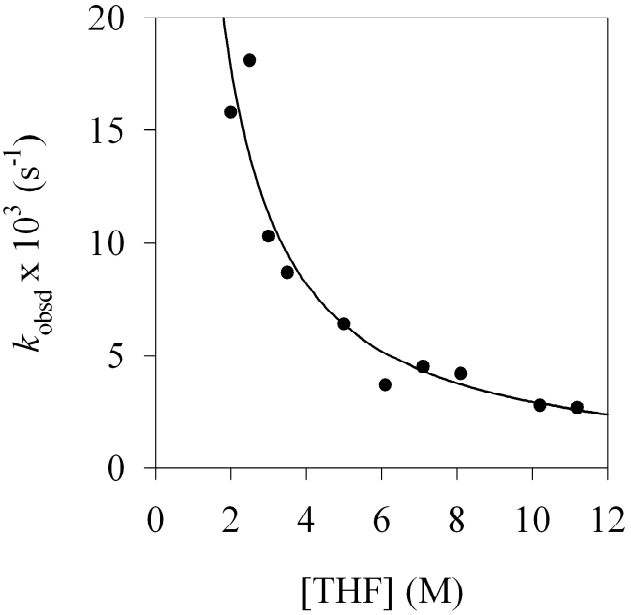

Figure 1.15. Plot of k_{obsd} versus [THF] for the condensation of LDA with aryllithium **2** (0.0074 M) and 0.1 M LDA at -78 °C. The curve depicts the result of an unweighted least-squares fit to $k_{obsd} = k[\text{THF}]^n$ ($k = (39 \pm 7)$; $n = -1.1 \pm 0.2$).

Reaction of Mixed Dimers with ArH. The reaction of arene **1** with the mixed dimers (Step III, Scheme 1) was too fast to obtain useful rate data as evidenced by the nearly instantaneous reaction when a carbamate **1** is added to a solution of **4** and **5**. DFT computations, however, provide insights that we find quite provocative. Given the circumstantial evidence supporting disolvation of **4** and **5**, we focused our computations on transition structures bearing the carbamate carbonyl moiety and one or two solvents. The transition structures bearing only one solvent proved to be much more stable computationally. (We have no experimental evidence to support either solvation number.) The results focusing on monosolvated transition structures **12** and **13** are illustrated in Scheme 3.

Scheme 3

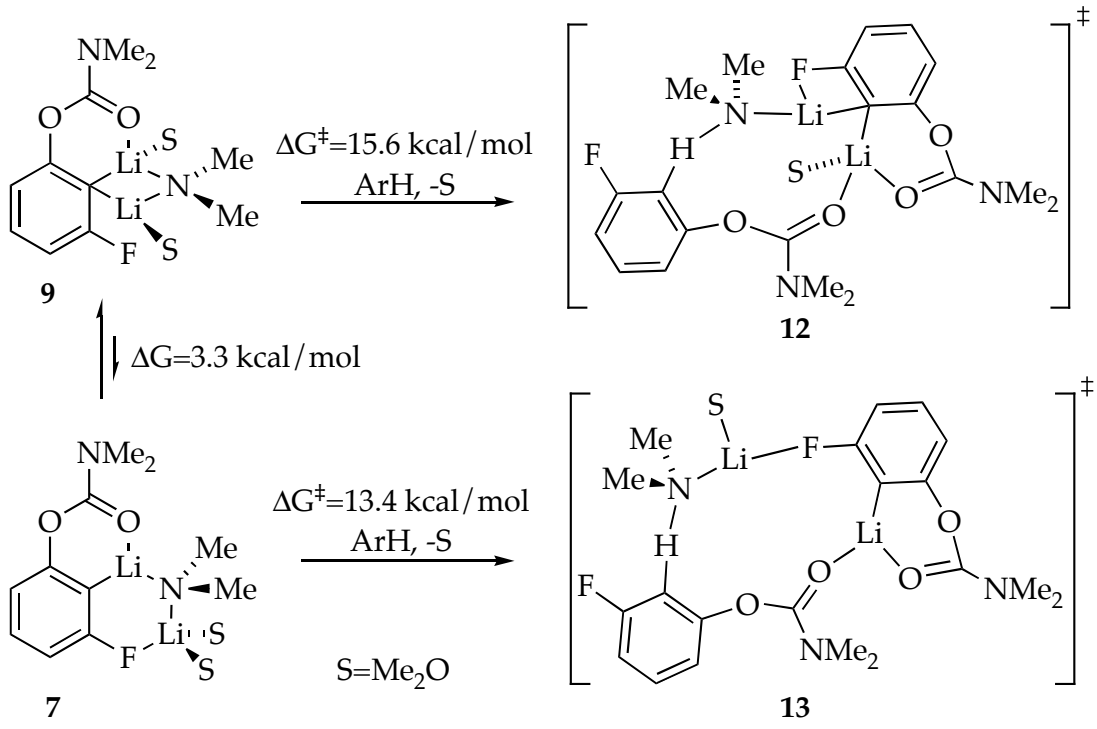

We believe the most logical scenario to explain the data at -100 °C is that **5** reacts directly with carbamate **1** (modeled by the conversion of **7** to **13**) and that **4** reacts by a rate-limiting conversion to **5** (modeled by the conversion of **9** to **7**). We not that the lack of Li-C-Li contacts in **7** and **13** is intriguing.

Discussion

We have described rate studies of the LDA-mediated metalation of carbamate **1** (eq 1). A host of observations that are unusual when placed in the context of previous mechanistic studies point to the importance of autocatalysis in which the resulting ArLi forms highly reactive mixed aggregates (Scheme 1). A summary of the key observations is followed by a detailed discussion of a mechanistic model depicted generically in Scheme 1.

Strange Rate Behavior. Ortholithiation of carbamate **1** under standard conditions--equimolar LDA in THF at -78 °C--shows a notable simplicity exemplified by an apparent first-order decay (Figure 1.1) and an absence of mixed aggregates. Surprisingly, metalations using >2.0 equiv of LDA display unusual linear decays of carbamate **1** to full conversion (Figure 1.2). Linear decays of substrate versus time typically stem from zeroth-order dependencies on substrate that occur because the substrate is *not* involved in the rate-limiting step.[7c] The carbamate concentration dependence of the decays in Figure 1.6, however, suggests a first-order dependence on carbamate **1**. The two conclusions seem paradoxical. Indeed, the downwardly curving (sigmoidal) decays observed when using deuterated carbamate **1** (Figure 1.8) or low THF concentrations suggest autocatalysis is the culprit,[29] and the high reactivities of LDA-ArLi mixed dimers are supportive.

^{19}F NMR spectroscopy offers a vivid picture of the odd time-dependent aggregate concentrations (Figures 1.9-1.11). The linear disappearance of carbamate **1** in Figure 1.9 correlates quantitatively with an analogous linear formation of aryllithium monomer **2**. Mixed dimer **4** and traces of isomeric mixed dimer **5** eventually appear, but only after the ortholithiation is complete. (Depiction of **5** as a fluorine-chelated open dimer[23,24] derives from computational rather than spectroscopic data.) This delayed mixed aggregation was difficult to understand at the outset.

Reducing the THF concentration (Figure 1.10) causes aryllithium **2** to reach a lower maximum concentration and makes aggregates **4** and **5** visible before the carbamate has been fully consumed. Lowering the reaction temperature to -100 °C produces several notable changes including a measurable and surprisingly constant concentration of mixed dimer **4** but not

5 (Figure 1.11). The deviation of isomeric mixed dimers **4** and **5** from their equilibrium ratio is significant.

Mechanistic Model. It is an understatement to say that the conventional mechanisms for LDA-mediated reactions[2] fail to account for the results summarized above. Many unconventional models were considered and also found wanting. We offer a single model described by eqs 9-12 (referred to as simply "the model") based on the four steps summarized in Scheme 1.

LDA Dimer-Based Metalation* (*Step I)

$$\underset{\mathbf{3}}{(i\text{-Pr}_2\text{NLi})_2} + \underset{\mathbf{1}}{\text{ArH}} \xrightarrow{k_1} \underset{\mathbf{4}}{(i\text{-Pr}_2\text{NLi})(\text{ArLi})} + i\text{-Pr}_2\text{NH} \tag{9}$$

Mixed Dimer Isomerization (Step II)

$$\underset{\mathbf{4}}{(i\text{-Pr}_2\text{NLi})(\text{ArLi})} \underset{k_{-2}}{\overset{k_2}{\rightleftharpoons}} \underset{\mathbf{5}}{(i\text{-Pr}_2\text{NLi})(\text{ArLi})^*} \tag{10}$$

Mixed Dimer-Based Metalation (Step III)

$$\underset{\mathbf{5}}{(i\text{-Pr}_2\text{NLi})(\text{ArLi})^*} + \underset{\mathbf{1}}{\text{ArH}} \xrightarrow{k_3} \underset{\mathbf{2}}{2\ \text{ArLi}} + i\text{-Pr}_2\text{NH} \tag{11}$$

LDA-ArLi Condensation (Step IV)

$$\underset{\mathbf{3}}{(i\text{-Pr}_2\text{NLi})_2} + \underset{\mathbf{2}}{\text{ArLi}} \underset{k_{-4}}{\overset{k_4}{\rightleftharpoons}} \underset{\mathbf{4}}{(i\text{-Pr}_2\text{NLi})(\text{ArLi})} + 1/2\ \underset{\mathbf{3}}{(i\text{-Pr}_2\text{NLi})_2} \tag{12}$$

A discussion of the model is prefaced by a few essential points. First, we used standard kinetic methods to measure the full rate laws for the key rate-limiting steps (eqs 9 and 12). The THF dependencies were also measured,

but they add more complexity than clarity. Thus, we exclude them from the discussion and simply note that the model is consistent with data acquired at all THF concentrations. Similarly, the differential equations used in the numeric integrations add little to the discussion; they are presented and discussed in the experimental section.

Second, models containing large numbers of differential equations and adjustable parameters are said to be "sloppy" if they are highly under determined.[36] Can't *any* model with such a plethora of adjustable parameters fit the data? Can the model "fit an elephant and make it wag its tail"?[37] The answer is no (for the first question, at least). The model is *not* sloppy. The adjustable parameters corresponding to the six rate constants are well defined. Moreover, many other models that were poked and prodded included provisions for autocatalysis, linear (or sigmoidal) decays, or delayed mixed aggregate formation but failed to account for *all* behaviors. The model has one compelling strength when compared with all other models that we considered and dismissed: *It fits the data in every instance*. The numeric integrations illustrated in Figures 1.9-1.11 are emblematic of the quality of the fits.

To facilitate the discussion, the model is described as four discrete steps, and the origins of each as well as the portions of the model that are negotiable are discussed. To minimize confusion we also note at the outset that, although facile mixed dimer-based lithiation of carbamate **1** is necessary, the condensation of ArLi with LDA dimer in eq 12--an aggregation event, not a metalation[25]--is the key rate-limiting step in the autocatalysis.

LDA Dimer-Based Metalation. The first stage of the metalation of carbamate **1** (Scheme 1, Step I)--the reaction before the appearance of lithium salt products--was shown using standard methods to be LDA dimer-based as

described by eq 9 and represented by transition structure **10**. Temperature dependencies (discussed below) are only consistent with mixed dimer **4** as the first-formed product and isomer **5** as the key reactive form.

Mixed Dimer Isomerization. Eq 10 represents the exchange between cyclic dimer **4** and open dimer **5** (Scheme 1, Step II). Several experiments showed that at -78 °C **4** and **5** interconvert rapidly on the time scales that they are formed or consumed. By contrast, at -100 °C the rate of exchange becomes slow relative to the rate of mixed dimer-based metalations, which allows us--actually forces us--to distinguish which dimer is the reactive form (vide infra).

Mixed Dimer-Based Metalation. It almost goes without saying that an autocatalytic organolithium reaction involves highly reactive mixed aggregates as described by eq 11 (Scheme 1, Step III). Spectroscopic studies using rapid-injection methods[25a,b] confirm that the resulting mixed dimers react almost instantaneously at -78 °C. In some sense, this mixed dimer-based metalation is of lesser consequence to the model than one might suspect because it is a post-rate-limiting step. Their high reactivities, however, explain two empirical observations: (1) the delayed appearance of the mixed dimers **4** and **5**, and (2) the highly temperature sensitive concentration dependencies. Both are discussed below.

LDA-ArLi Condensation. The rate-limiting step in the autocatalysis is the condensation of aryllithium **2** with LDA dimer **3** (Scheme 1, Step IV) which proceeds via an LDA dimer-based mechanism.[35] The reaction coordinate is likely to be more complex than described by eq 12, however, in that the first-formed product is logically some form of (*i*-$Pr_2NLi)_2$(ArLi) trimer. Whether the putative trimer is akin to previously characterized cyclic trimers

is unknown,[5,9] but it is too fleeting to detect spectroscopically and is not germane to the numeric integrations.

Origins of Delayed Mixed Aggregation. Following an organolithium reaction using NMR spectroscopy reveals that the starting organolithium aggregates are replaced by new product-derived mixed and homoaggregates.[5] The aggregate distributions change as the reaction proceeds, but equilibrium populations are maintained[38] *provided that aggregate exchange is rapid on the time scales of the reaction.* This is not the case in the metalation of carbamate **1**. Mixed aggregates **4** and **5** appear only after carbamate **1** is consumed. The rapid metalation in eq 11 accounts for the delayed appearance of the mixed dimers; the mixed dimers do indeed form but are consumed rapidly by carbamate **1** as they form.

Relative Mixed Dimer Reactivities. Unraveling the relative importance of isomeric mixed dimers **4** and **5** was particularly challenging. It was *very* tempting at the outset to ignore dimer **5** altogether given that **5** forms in low concentrations (≈3%). Although **5** was confirmed to be an isomer of **4**, its three-dimensional structure was assigned using exclusively DFT computations. Moreover, using data collected at -78 °C, conditions under which **4** and **5** equilibrate rapidly on the time scales of the metalation, it is not constructive to consider which is the so-called reactive form; **4** and **5** simply represent two resting states. At -100 °C, however, ***4*** *and* ***5*** *interconvert slowly on the time scale of the metalation.* Under these conditions it is valid to consider the relative reactivities of **4** and **5** toward arene **1**.

The model described in eqs 9-12 that is based on metalations by mixed dimer **5** fits the data, whereas alternative models based on the reaction of **4** do not. The alternative models fail to include provisions for the elevated and

constant concentration of **4** during the consumption of carbamate at -100 °C (Figure 1.11). When the model presented is expanded to include provisions for reaction of both **4** *and* **5**, the fit suggests <1% contribution from a **4**-based metalation.

The most logical scenario that is fully consistent with the data is that **4** isomerizes to **5** and dimer **5** subsequently reacts with carbamate **1** (see Scheme 1). The isomerization is fast relative to the metalation at -78 °C, whereas the isomerization becomes rate limiting at -100 °C. It was in this context that we wondered whether the transition structure for the metalation may show a ring expanded motif similar to that of **5** rather than a more conventional closed form with a Li-C-Li contact as in **4**.

Computational studies of the mixed dimer-based metalation are summarized in Scheme 3. Dimers **4** and **5** are represented by simplified reactants **9** and **7**, respectively. Transition structures **12** and **13** are analogous to **9** and **7** in that conventional Li-C-Li contacts in **9** and **12** are absent in **7** and **13**. Curiously, the calculated activation energies are also qualitatively consistent with experiment. Most significant, the computations suggest that the ring expanded motif is relatively unfavorable in reactant **7** yet stabilizing in transition structure **13**.

Origins of Linear Decays. The model reproduces the linear decays by superimposing a downward curvature from autocatalysis on the normal upward curvature resulting from loss of substrate.[27] That is not to say, however, that it is obvious *why* the model is successful or why the linearities persist over a wide range of initial LDA concentrations. This coincidence requires elaboration as follows.

Using some abstraction we can distill the model to its simplest components. In the absence of autocatalysis, the metalation proceeds via an LDA dimer-based mechanism (eq 9). Let us recast this as eq 13 and the affiliated rate constant as k_{init}. Similarly, the autocatalytic pathway occurs via an LDA dimer-based rate-limiting condensation with ArLi. The autocatalysis simplifies to eq 14 with a rate constant denoted as k_{cat}.

$$(i\text{-Pr}_2\text{NLi})_2 + \text{ArH} \xrightarrow{k_{init}} \text{product} \qquad (13)$$

$$(i\text{-Pr}_2\text{NLi})_2 + \text{ArLi} \xrightarrow{k_{cat}} \text{product} \qquad (14)$$

If only the uncatalyzed ortholithiation in eq 13 is operative, the reaction will follow a normal exponential decay (Figure 1.16, curve A). At 50% conversion of ArH, the reaction rate (the tangent to the curve A) would be 50% of the initial rate. For autocatalysis to straighten curve A to perfect linearity (curve B), the deceleration caused by the depletion of ArH must be precisely offset by the acceleration caused by the buildup of ArLi (eq 14). *Linearity is observed when* $k_{init} = k_{cat}$. Indeed, inspection of Figure 1.9 shows that the instantaneous slopes for the loss of carbamate **1** at early conversion and the loss of aryllithium monomer **2** (the initial slope to the right of its apex) are equal.

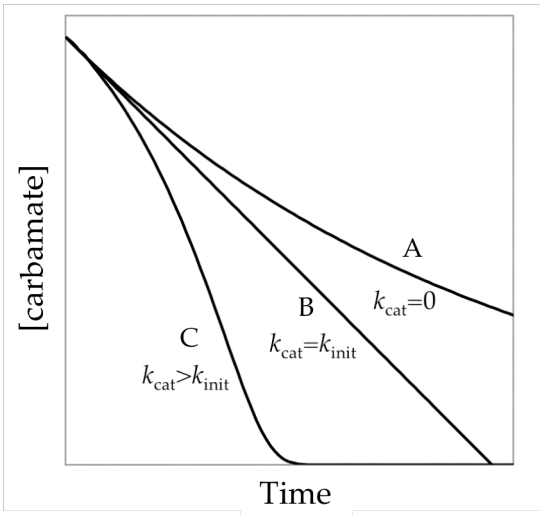

Figure 1.16. Influence of autocatalysis on the LDA-mediated metalation of carbamate **1** as described in eqs 9-12.

Is it a coincidence that the rates of the uncatalyzed and the catalyzed ortholithiation are equal? On one level, yes. Decreasing the THF concentration or introducing orthodeuteration results in sigmoidal behavior consistent with a relatively higher rate for the catalyzed process (Figure 1.16, curve C). (k_{init} is isotopically sensitive whereas k_{cat} is not.) Nonetheless, through the reductionist approach described by eqs 13 and 14, one can see haunting similarities. Is there a common reactive intermediate such as an LDA open dimer[23] that reacts with ArH or ArLi (eq 15) with nearly equal efficacy? Although it is unclear why the ArH and ArLi react so similarly (and certainly further speculation is getting excessive), we wonder whether the Lewis basic[39] fluoro moieties are important.

$$(i\text{-Pr}_2\text{NLi})_2 \rightleftharpoons (i\text{-Pr}_2\text{NLi})_2^* \xrightarrow[\text{rate limiting}]{\text{ArH or ArLi}} \text{products} \qquad (15)$$

Conclusion

LDA continues to harbor mysteries and offer insights into how aggregation and solvation influence organolithium reactivity. The LDA-mediated ortholithiation delineated in eq 1 revealed linear and sigmoidal decays--evidence of autocatalysis--and exceptional reactivities of mixed aggregates that are unexpected in the context of previously studied LDA-mediated metalations.[2] The model presented, although somewhat flexible in detail and vulnerable to revision, nicely accounts for the odd observations. Taking a wider view, these results are not merely curiosities. As we peer into the past, we are reminded of LDA-mediated enolizations in THF at -78 °C[10c,40,41] in which LDA-lithium enolate mixed aggregates markedly altered *E*/*Z* selectivities.[42] We can also offer a peek into the future. Ongoing studies are uncovering many ortholithiations that are autocatalytic. Both the similarities and substrate-dependent differences are striking. We have also discovered that Michael additions to unsaturated esters, imine metalations, and ester enolizations display such anomalous behavior.[43] All of these reactions share a common denominator: They are effected using LDA in THF at -78 °C. This is exciting from a mechanistic perspective. The prevalence of the autocatalysis, however, is also disquieting given the importance of this particular base-solvent-temperature combination in organic chemistry.

Experimental Section

Reagents and Solvents. THF, hexane, and pentane were distilled from blue or purple solutions containing sodium benzophenone ketyl. The hydrocarbon stills contained 1% tetraglyme to dissolve the ketyl. LDA was prepared from *n*-BuLi and subsequently rescrystallized.[12] The purified LDA

was shown by both potentiometry[44] and ion chromatography[45] to contain ≤0.02% LiCl. Air- and moisture-sensitive materials were manipulated under argon or nitrogen using standard glove box, vacuum line, and syringe techniques. Solutions of *n*-BuLi and LDA were titrated for active base using a literature method.[46]

NMR Spectroscopic Analyses. All NMR tubes were prepared using stock solutions and sealed under partial vacuum. Standard ^{6}Li, ^{13}C, ^{15}N, and ^{19}F NMR spectra were recorded on a 500 MHz spectrometer at 73.57, 125.79, 50.66 and 470.35 MHz (respectively). The ^{6}Li, ^{13}C, ^{15}N, and ^{19}F resonances are referenced to 0.30 M [^{6}Li]LiCl/MeOH at -90 °C (0.0 ppm), the CH_2O resonance of THF at -90 °C (67.57 ppm), neat Me_2NEt at -90 °C (25.7 ppm), and C_6H_5F in neat THF at -78 °C (-113.15 ppm), respectively.

IR Spectroscopic Analyses. Spectra were recorded using an in situ IR spectrometer fitted with a 30-bounce, silicon-tipped probe. The spectra were acquired in 16 scans at a gain of 1 and a resolution of 8 cm^{-1}. A representative reaction was carried out as follows: The IR probe was inserted through a nylon adapter and FETFE O-ring seal into an oven-dried, cylindrical flask fitted with a magnetic stir bar and a T-joint. The T-joint was capped by a septum for injections. Following evacuation under full vacuum and flushing with N_2, the flask was charged with a solution of LDA (108.2 mg, 1.01 mmol) in THF (10.0 mL) and cooled in a freshly prepared dry ice/acetone cooling bath. (Condensation of moisture adversely affects temperature consistency.) After recording a background spectrum, carbamate **1** was added to the LDA/THF mixture at -78 °C from a dilute stock solution (100 μL, 0.404 M) with stirring. IR spectra were recorded over the course of the reaction. To

account for mixing and temperature equilibration, spectra recorded in the first 1.5 min were discarded. All reactions were monitored to >5 half-lives.

Rate Studies Using ^{19}F NMR Spectroscopy. The rates of metalation and mixed aggregation were monitored using ^{19}F NMR spectroscopy. Spectroscopic samples were prepared using either standard methods described previously or by injecting carbamate **1** via 25 μm ID flexible capillary tubing directly into the solution of LDA at -78 °C in the NMR probe.[25a,b] The methyl ^{1}H resonances on the magnetically inequivalent *i*-propyl groups on carbamate **1** coalesce on warming above -70 °C as described previously. Monitoring the decoalescence to give two distinct resonances showed that the temperature equilibration occurs in <30 s. T1 relaxation times were determined for all species, and the delay between scans was set to > 5 x T1 to ensure accurate integrations.

The condensation of **2** with LDA to form mixed aggregates **4** and **5** was easily monitored in situ because the condensation occurs only after **1** is consumed. Loss of **2** followed clean exponential decays, and formation of **4** correlated quantitatively. Results obtained from fitting the decay of **2** [$A = A_0\exp(-k_{obsd}t) + C$] or formation of **4**{$A = A_0[1 - \exp(-k_{obsd}t)]$} afforded equivalent first-order rate constants ($\pm$10 %).

Numeric Integrations. The proposed mechanism (eqs 9-12) can be expressed as a series of differential equations as follows:

$$d[\mathrm{ArH}]/dt = -k_1[\mathrm{ArH}][\mathrm{A_2}] - k_3[\mathrm{A{\cdot}ArLi^*}][\mathrm{ArH}] \quad (16)$$

$$d[\mathrm{ArLi}]/dt = -k_4[\mathrm{ArLi}][\mathrm{A_2}] + k_{-4}[\mathrm{A{\cdot}ArLi}][\mathrm{A_2}]^{0.5} + 2k_3[\mathrm{A{\cdot}ArLi^*}][\mathrm{ArH}] \quad (17)$$

$$d[\mathrm{A{\cdot}ArLi}]/dt = k_1[\mathrm{ArH}][\mathrm{A_2}] - k_2[\mathrm{A{\cdot}ArLi}] + k_{-2}[\mathrm{A{\cdot}ArLi^*}] + k_4[\mathrm{ArLi}][\mathrm{A_2}] - k_{-4}[\mathrm{A{\cdot}ArLi}][\mathrm{A_2}]^{0.5} \quad (18)$$

$$d[A\cdot ArLi^*]/dt = k_2[A\cdot ArLi] - k_{-2}[A\cdot ArLi^*] - k_3[A\cdot ArLi^*][ArH] \quad (19)$$

$$[A_2] = [A_2(init)] - 0.5[ArLi] - [A\cdot ArLi] - [A\cdot ArLi^*] \quad (20)$$

where A_2 is LDA dimer **3**, ArH is arene **1**, ArLi is monomer **2**, A·ArLi is mixed dimer **4**, A·ArLi* is mixed dimer **5**, and $[A_2(init)]$ is the initial concentration of LDA.

The time-dependent concentration plots obtained by ^{19}F NMR spectroscopy are fit to a mechanistic model expressed by a set of differential equations. The curve fitting operation minimizes chi-square in searching for the coefficient values (rate constants). The Levenberg-Marquardt algorithm[47] is used for the chi-square minimization and is a form of nonlinear, least-squares fitting. The fitting procedure implements numeric integration based on the backward differentiation formula (BDF)[48] to solve the differential equations, yielding functions describing concentration versus time.

The results from the fits are as follows. From a single run, the rate constant for the LDA dimer-based metalation (k_1 in eq 9) can be uniquely determined. The equilibrium constant for the exchange of mixed dimers **4** and **5** (k_2/k_{-2}) is also well defined, yet only a lower limit can be established for the individual values of k_2 and k_{-2} (k_2, $k_{-2}>10\cdot k_1$). The rate constant corresponding to metalation of carbamate **1** by mixed dimer **5** (k_3 in eq 11) has a lower boundary ($>10^5\cdot k_1$). The k_4/k_{-4} ratio corresponding to the monomer-mixed dimer equilibrium (eq 12) is well defined as are the separate values of k_4 and k_{-4}. By carrying out a global fit of multiple data sets, the quality of the individual fits are decreased somewhat as expected for a reaction that is sensitive to initial conditions. We find, however, that best-fit values of the rate constants from the global fit do not differ much from the individual fits.

The data recorded at -100 °C offer insights into the relative rate constants unavailable at -78 °C (vide infra). The individual values of k_2 and k_{-2} become well defined, which ultimately leads to the conclusion that LDA dimer-mediated metalation affords **4** and the mixed dimer-mediated metalation proceeds via **5** as described in the discussion.

APPENDIX ONE

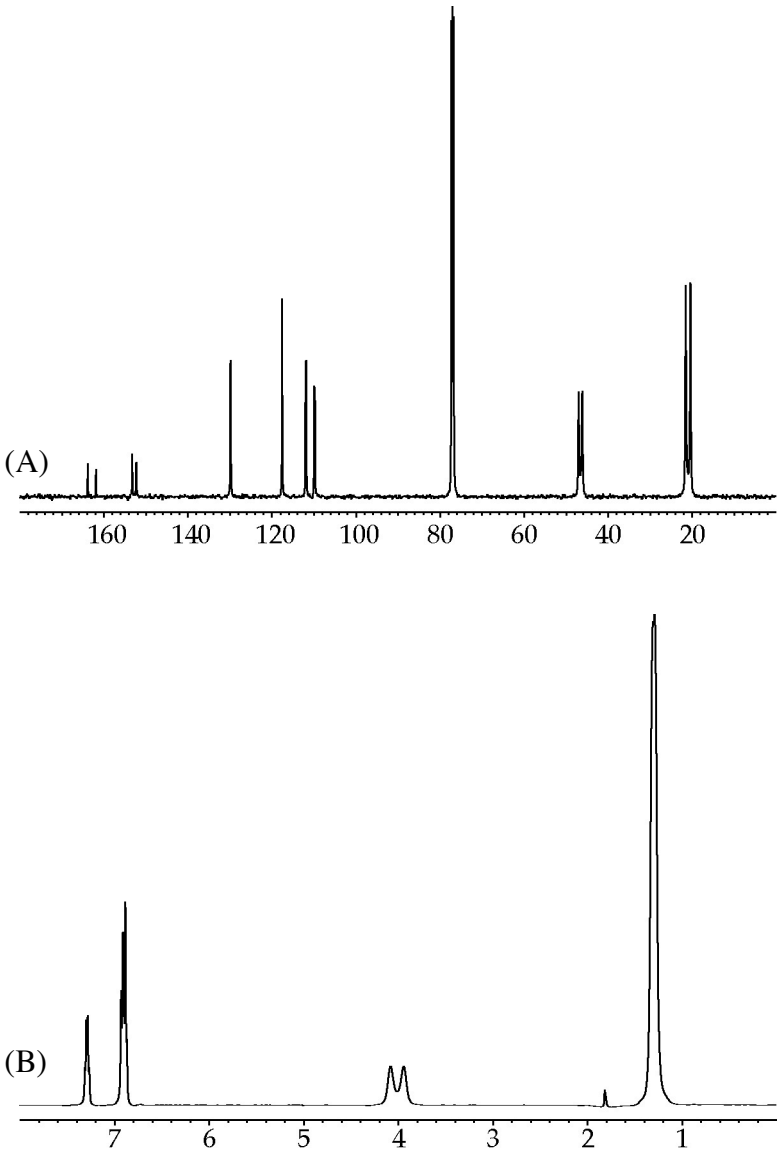

Figure A1.1. ^{13}C and ^{1}H NMR spectra of **1**. (A) ^{13}C NMR spectrum, 125 MHz, $CDCl_3$: δ 163.1 (d, J = 246.3 Hz), 153.5, 152.5 (d, J = 11.1 Hz), 130.1 (d, J = 9.6 Hz), 117.8 (d, J = 3.0 Hz), 112.1 (d, J = 21.2 Hz), 110.1 (d, J = 24.2 Hz), 47.2, 46.3, 21.8, 20.6; (B) ^{1}H NMR spectrum, 500 MHz, $CDCl_3$: δ 7.28 (m, 1H), 6.89 (m, 3H), 4.07 (s, 1H), 3.92 (s, 1H), 1.30 (br s, 6H), 1.27 (br s, 6H).

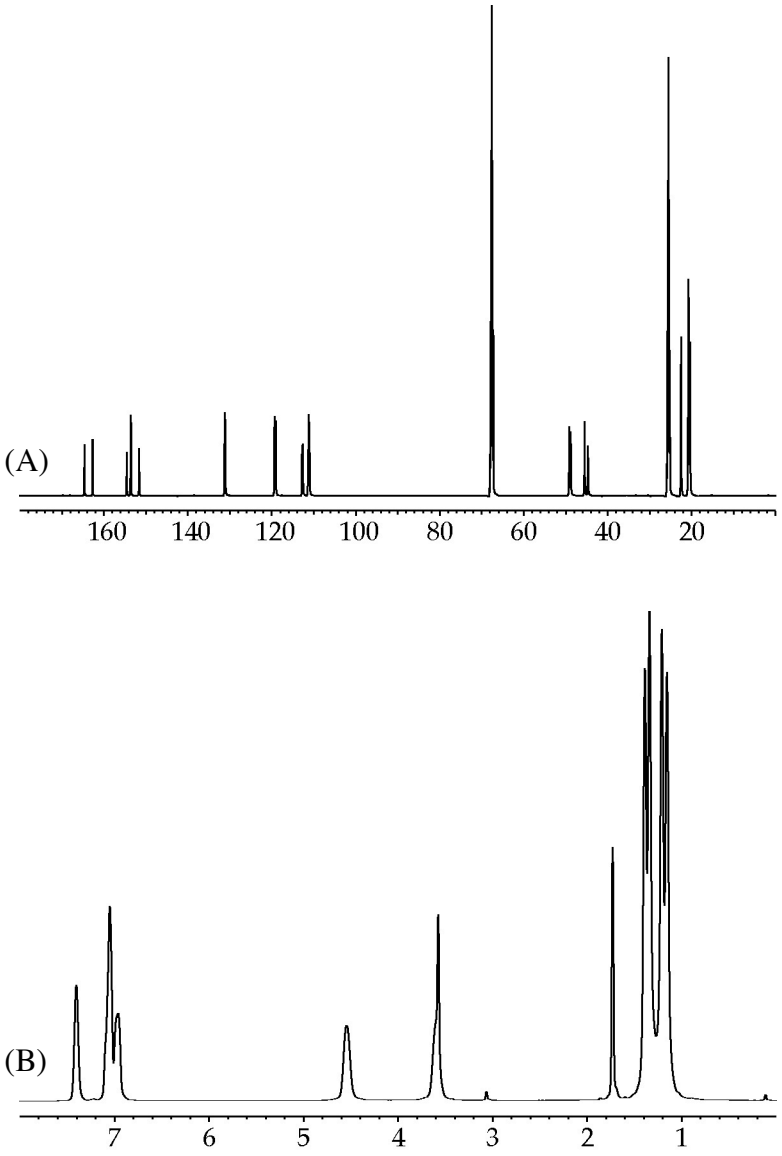

Figure A1.2. ^{13}C and ^{1}H NMR spectra of **1** at -90 °C. (A) ^{13}C NMR spectrum, 125 MHz, THF-d_8: δ 163.6 (d, J = 244.7 Hz), 154.5, 153.5 (d, J = 11.3 Hz), 151.5, 131.2 (d, J = 10.1 Hz), 131.0 (d, J = 10,1 Hz), 119.1 (d, J = 37.9 Hz), 112.6 (d, J = 20.2 Hz), 112.5 (d, J = 19.3 Hz), 111.2 (d, J = 24.9 Hz), 111.0 (d, J = 26.1 Hz), 49.1, 48.7, 45.4, 44.6, 22.4, 20.7, 20.6, 20.3; (B) ^{1}H NMR spectrum, 500 MHz, THF-d_8: δ 7.40 (br s, 1H), 7.05 (br s, 2H), 6.97 (br s, 1H), 4.54 (s, 1H), 3.59 (s, 1H), 1.39 (s, 3H), 1.34 (s, 3H), 1.21 (s, 3H), 1.16 (s, 3H), (Reference: 1H (CH_2O, THF, 3.58 ppm); ^{13}C (CH_2O, THF, 67.57 ppm).

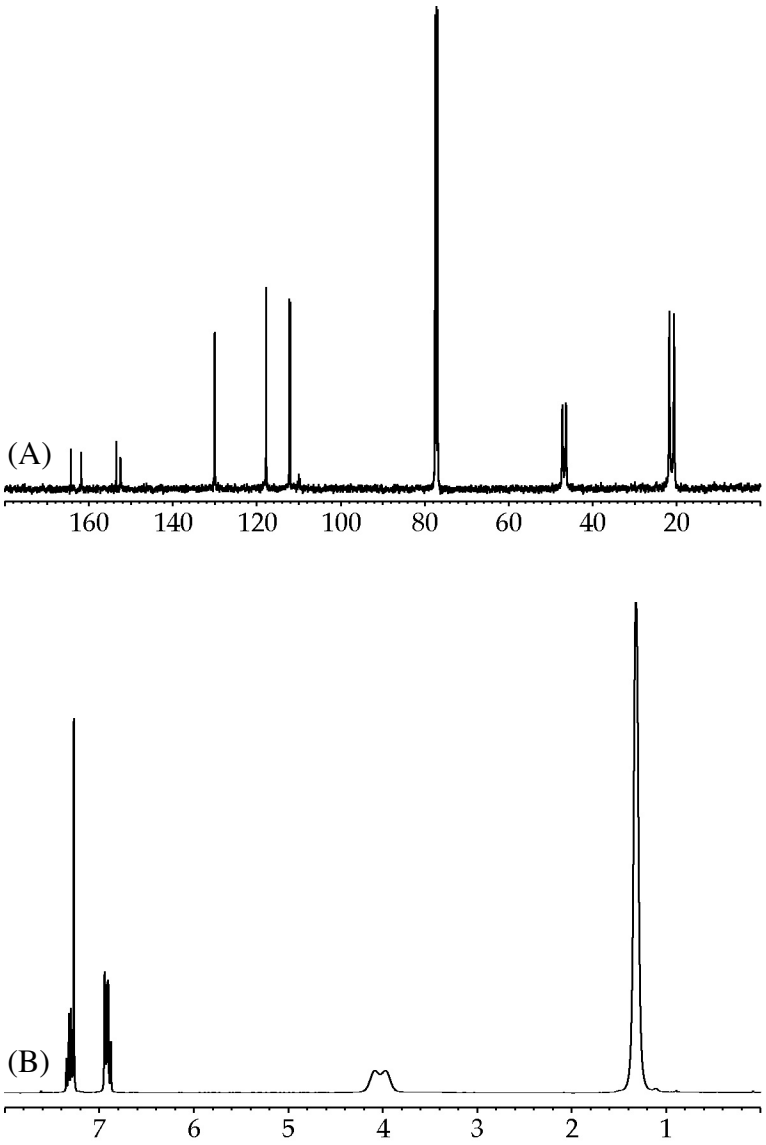

Figure A1.3. ^{13}C and ^{1}H NMR spectra of **1-*d*$_1$**. (A) ^{13}C NMR spectrum, 125 MHz, $CDCl_3$: δ 163.0 (d, J = 246.4 Hz), 153.5, 152.4 (d, J = 10.9 Hz), 130.0 (d, J = 9.4 Hz), 117.8 (d, J = 2.4 Hz), 112.1 (d, J = 21.0 Hz), 109.9 (t, J = 24.3 Hz), 47.2, 46.3, 21.7, 20.6; (B) ^{1}H NMR spectrum, 500 MHz, $CDCl_3$: δ 7.30 (m, 1H), 6.91 (m, 2H), 4.09 (s, 1H), 3.95 (s, 1H), 1.31 (br s, 12H).

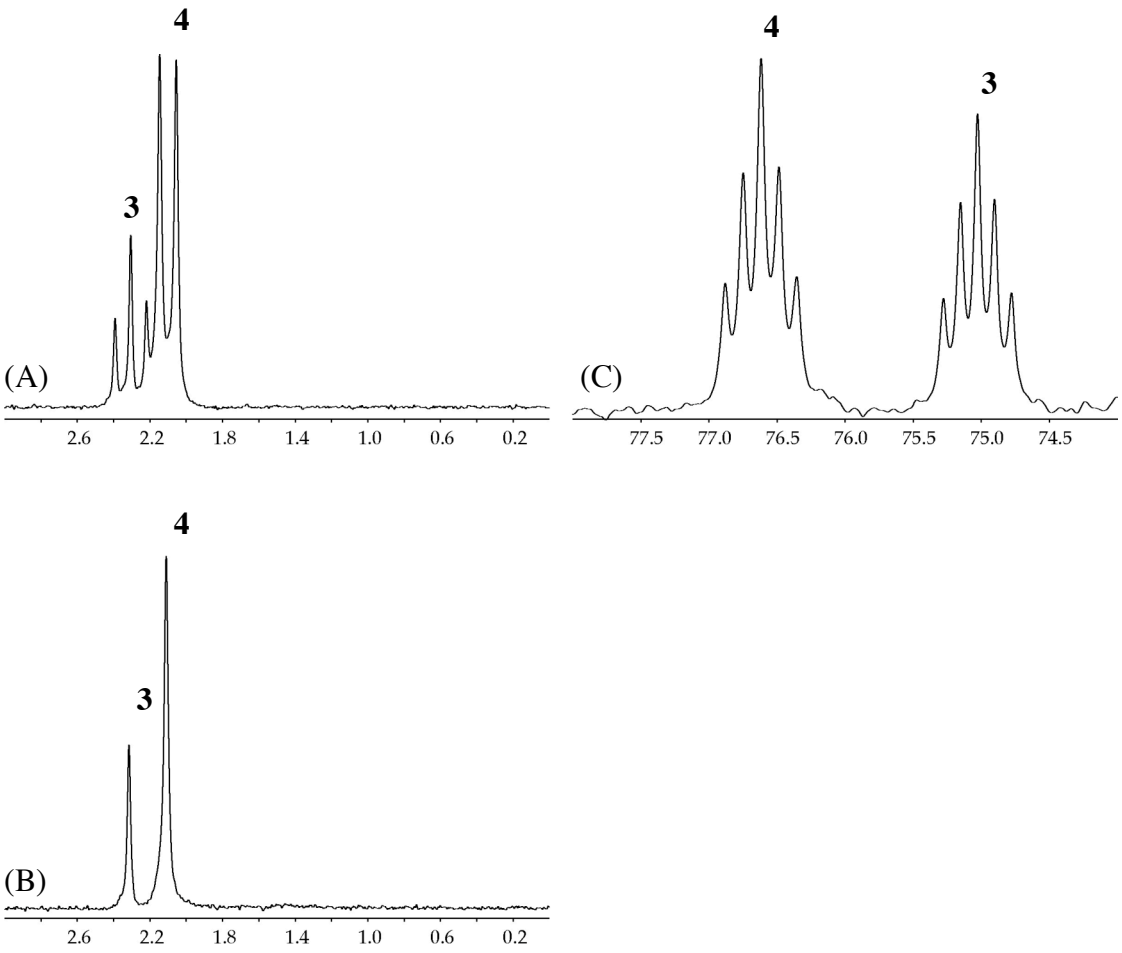

Figure A1.4. ^{6}Li and ^{15}N NMR spectra of 0.10 M [^{6}Li,^{15}N]LDA with 0.033 M **1** in 0.62 M THF/pentane at -90 °C after aging at -78 °C for 60 min: **(A)** ^{6}Li spectrum; **(B)** ^{6}Li{^{15}N} spectrum; **(C)** ^{15}N spectrum.

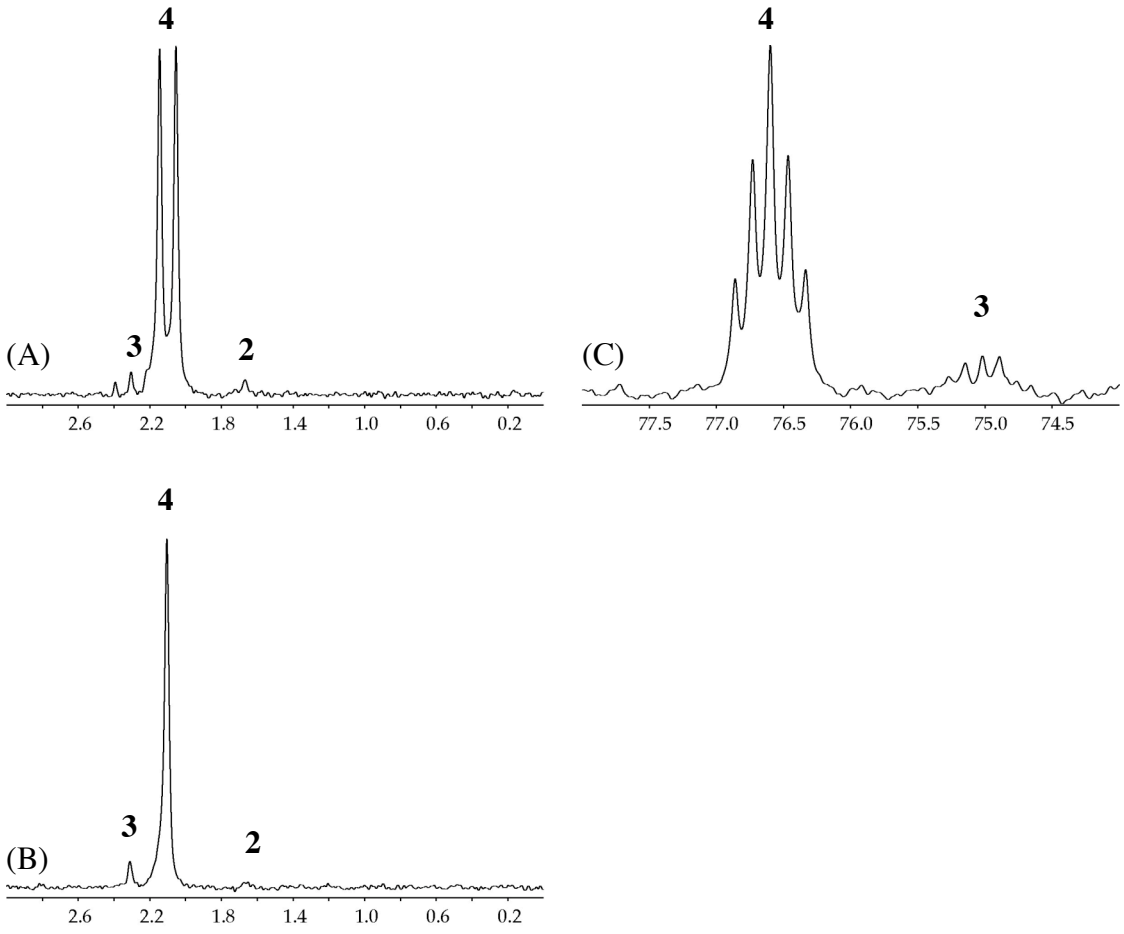

Figure A1.5. ^{6}Li and ^{15}N NMR spectra of 0.10 M [^{6}Li,^{15}N]LDA with 0.05 M **1** in 0.62 M THF/pentane at -90 °C after aging at -78 °C for 60 min: **(A)** ^{6}Li spectrum; **(B)** ^{6}Li{^{15}N} spectrum; **(C)** ^{15}N spectrum.

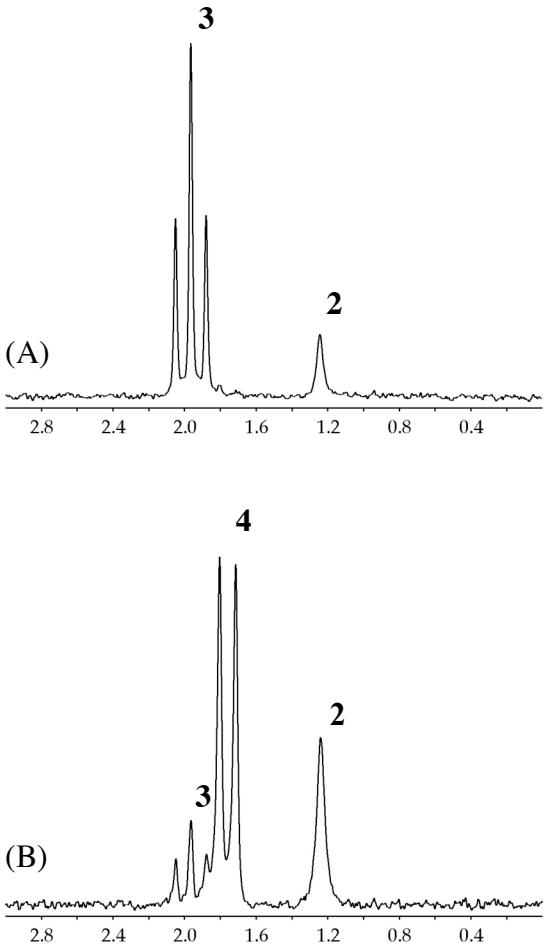

Figure A1.6. ^{6}Li NMR spectra of 0.10 M [^{6}Li,^{15}N]LDA with 0.05 M **1** in 11.1 M THF/pentane at -90 °C: **(**A**)** ^{6}Li spectrum after aging at -78 °C for 5 min; **(**B**)** ^{6}Li spectrum after aging at -78 °C for 30 min.

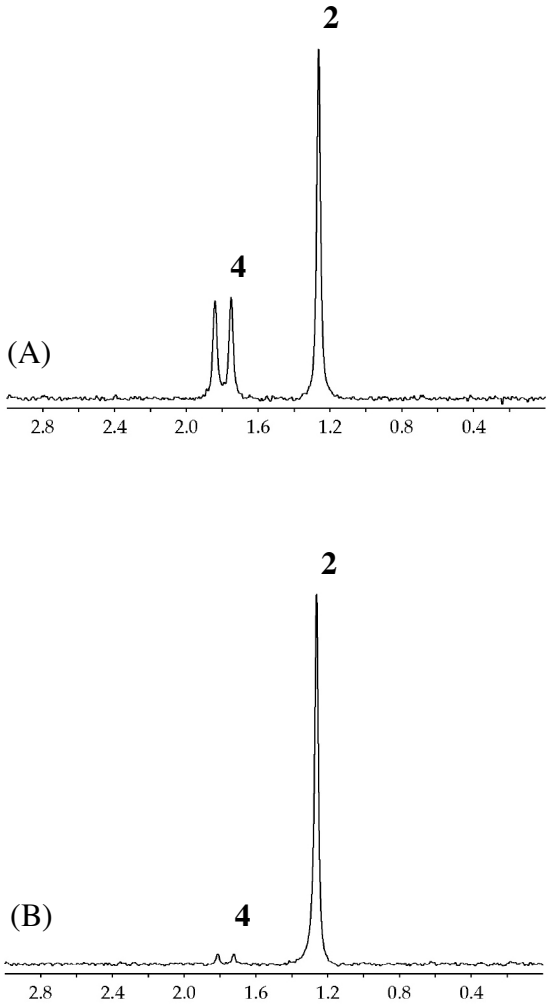

Figure A1.7. ^{6}Li NMR spectra of 0.10 M [^{6}Li,^{15}N]LDA with 0.10 M **1** in 11.1 M THF/pentane at -90 °C: **(A)** ^{6}Li spectrum after aging at -78 °C for 60 min; **(B)** ^{6}Li spectrum after aging at -40 °C for 60 min.

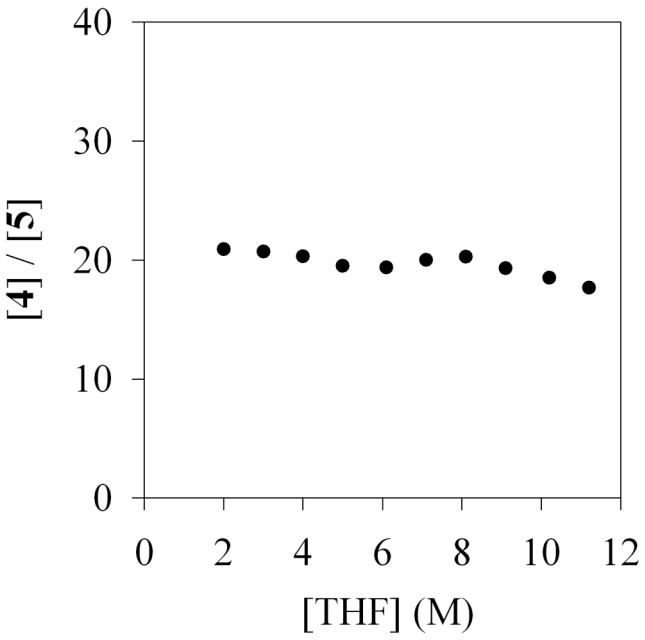

Figure A1.8. Plot of [**4**]/[**5**] versus [LDA] in 12.2 M THF at -90 °C.

[LDA] (M)	[**4**]/[**5**]
0.010	17.85
0.015	17.86
0.020	17.48
0.025	17.73
0.030	17.07
0.035	17.47
0.040	15.40

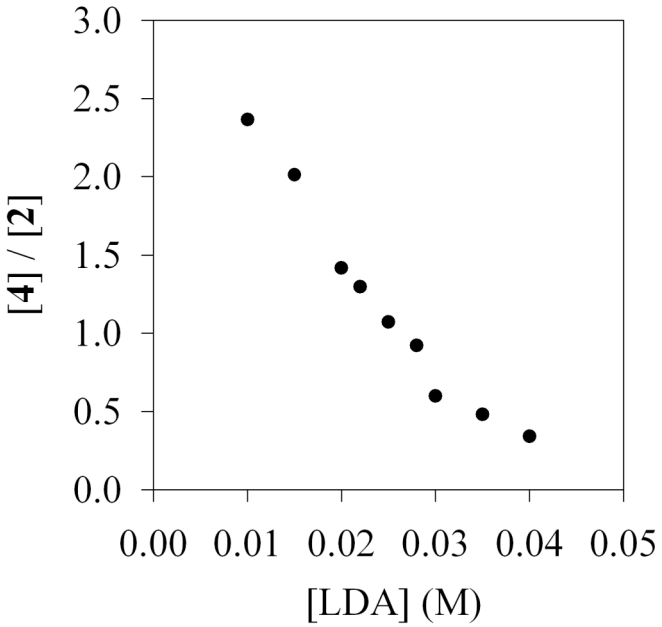

Figure A1.9. Plot of [**4**]/[**2**] versus [LDA] in 12.2 M THF at -90 °C.

[LDA] (M)	[**4**]/[**2**]
0.010	2.36
0.015	2.01
0.020	1.41
0.022	1.30
0.025	1.07
0.028	0.92
0.030	0.60
0.035	0.48
0.040	0.34

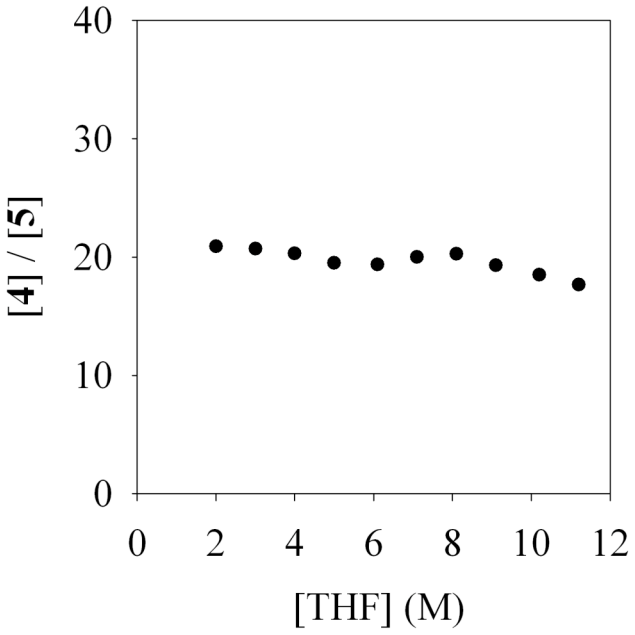

Figure A1.10. Plot of [**4**]/[**5**] versus [THF] in hexanes and 0.05 M LDA at -90 °C.

[THF] (M)	[**4**]/[**5**]
2.0	20.89
3.0	20.69
4.0	20.29
5.0	19.48
6.1	19.35
7.1	19.99
8.1	20.24
9.1	19.26
10.2	18.49
11.2	17.64

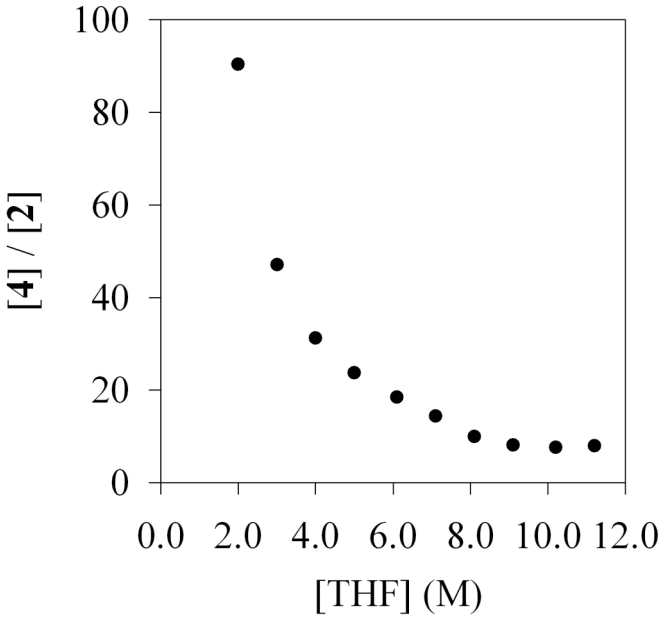

Figure A1.11. Plot of [**4**]/[**2**] versus [THF] in hexanes and 0.05 M LDA at -90 °C.

[THF] (M)	[**4**]/[**2**]
2.0	90.32
3.0	47.01
4.0	31.22
5.0	23.68
6.1	18.41
7.1	14.39
8.1	9.92
9.1	8.09
10.2	7.58
11.2	7.94

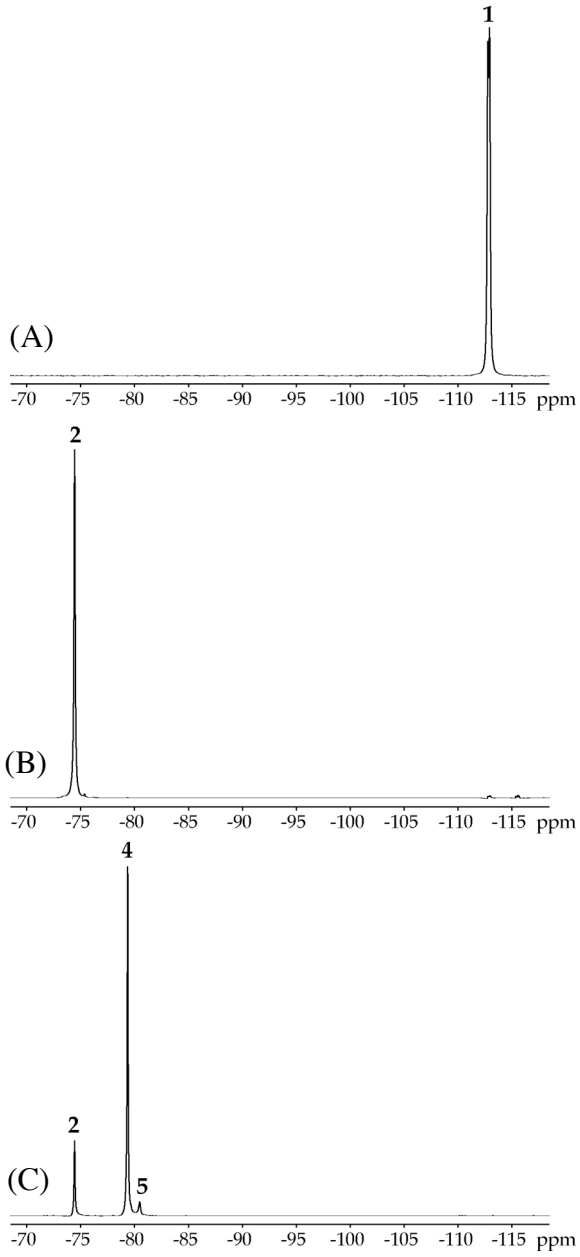

Figure A1.12. ^{19}F NMR spectra of 0.01 M **1** in 11.1 M THF/pentane at various LDA concentrations at -78 °C: **(**A**)** 0.010 M **1**, 0.0 M LDA; **(**B**)** 0.10 M **1**, 0.10 M LDA, after aging at -40 °C for 60 min; **(**C**)** 0.025 M **1**, 0.10 M LDA, after aging at -78 °C for 60 min.

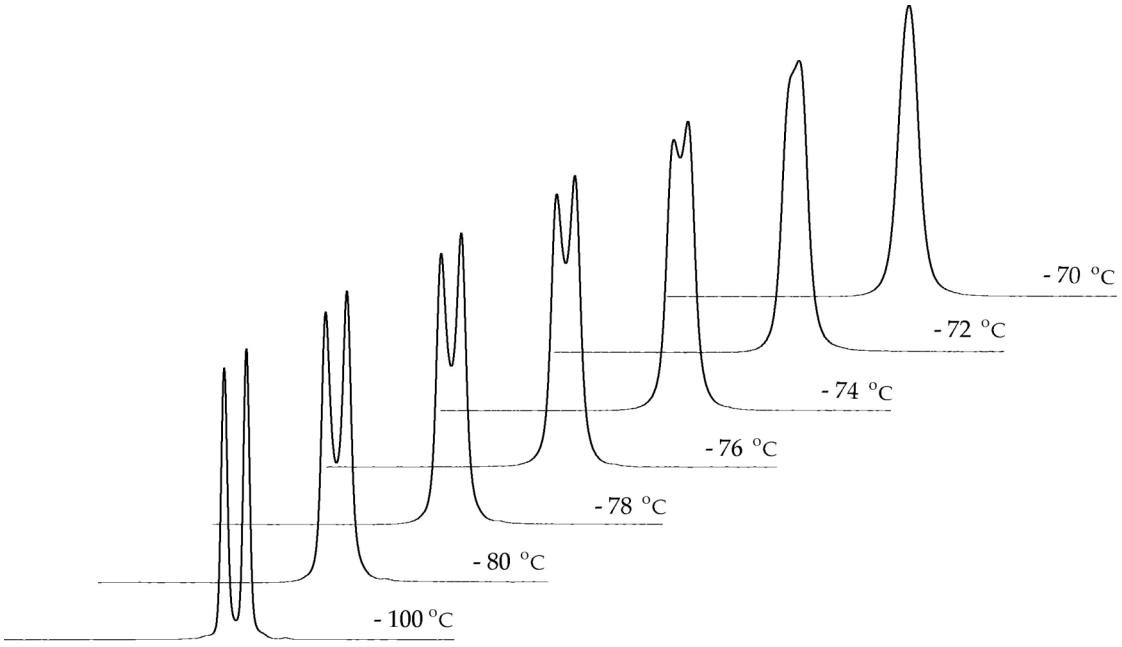

Figure A1.13. ^{19}F NMR spectra of 0.010 M **1** in 11.1 M THF/pentane at various temperatures using the approximation that $k_{exchange} = 2.22\ (\Delta\nu)$ at the coalescence temperature (T_c = -72 °C) where $\Delta\nu$ = 93.3 Hz (at -100 °C in the slow exchange limit), $\Delta G^{\neq}$ = 9.5 kcal/mol as calculated using the Eyring equation[1]).

Carbamate **1** and structurally related diisopropylamine-derived carbamates and carboxamides[2] display distinct conformational properties that are not observed in less sterically congested analogues. Carbamate **1** affords normal NMR spectra at ambient temperature. On cooling the sample below -70 °C, the single ^{19}F resonance (-113.1 ppm) appears as a pair of resonances in equal proportions. Similarly in the ^{13}C NMR spectrum, two methyne resonances of the diisopropyl moiety are observed at ambient temperatures whereas four are observed at <-90 °C. One can explain these results by a assuming a slow conformer exchange.

[1] (a) Jackman, L. M.; Cotton, F. A. eds. "Dynamic Nuclear Magnetic Resonance Spectroscopy", Academic Press, New York, NY, 1975. (b) Gasparro, F. P.; Kolodny, N. H. *J. Chem. Educ.* **1977**, *54*, 258.
[2] For leading references to conformational studies of acylated diisopropylamido framgments, see (a) Stewart, W. E.; Siddall, T. H. III. *Chem. Rev.* **1970**, *70*, 517. (b) Lidén, A.; Roussel, C.; Liljefors, T.; Chano, M.; Carter, R. E.; Metzger, J.; Sandström, J. *J. Am. Chem. Soc.* **1976**, *98*, 2853.

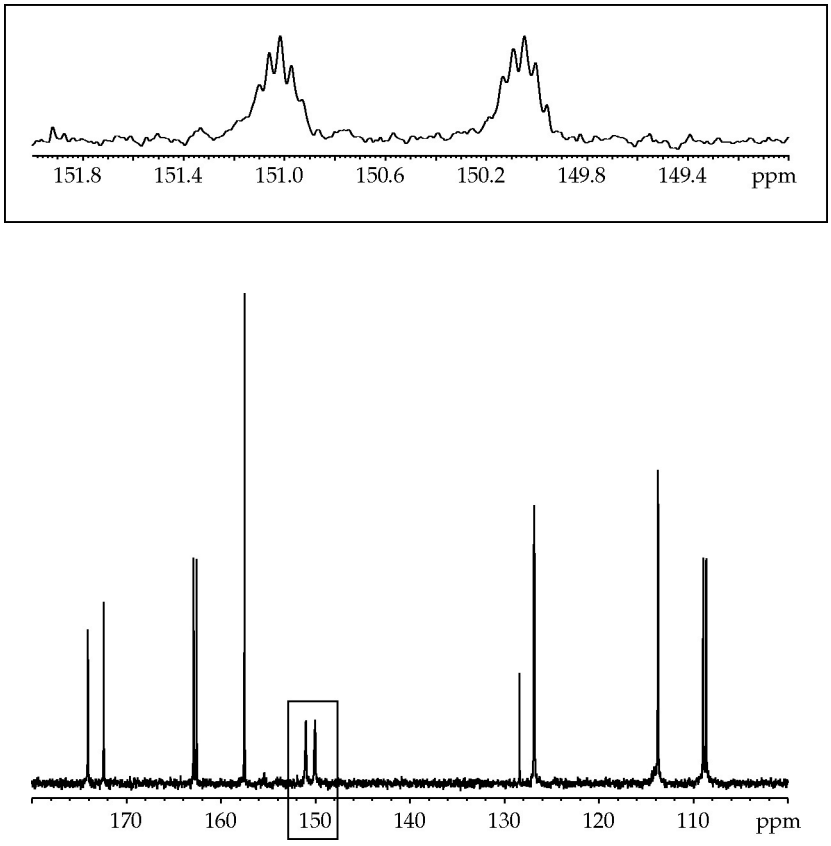

Figure A1.14. ^{13}C NMR spectrum of 0.40 M [^{6}Li]LDA with 0.33 equiv **1** in 3.1 M THF/pentane at -90 °C (δ ^{13}C = 150.5 ppm, $J_{C\text{-}F}$ = 121.7 Hz, $J_{C\text{-}Li}$ = 5.6 Hz).

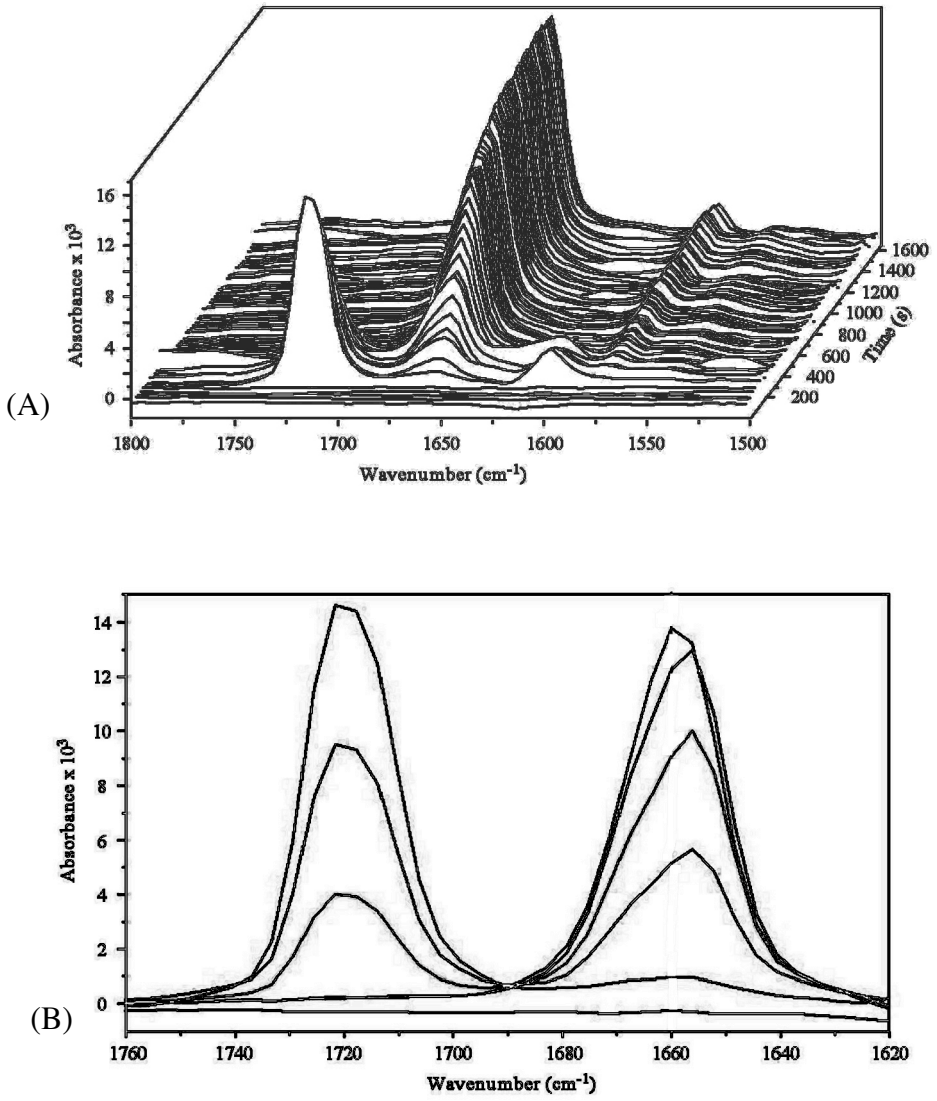

Figure A1.15. **(**A**)** Representative IR plot for the ortholithiation of **1** (0.004 M) by 0.10 M LDA in 12.2 M THF at -78 °C (**1**: 1721 cm^{-1}, **2 + 4**: 1660 cm^{-1}); **(B)** Cross-section of the plot in Figure 15A. The peak shift around 1660 cm^{-1} indicates product equilibration between **2** and **4**, as independently determined by ^{19}F NMR spectroscopy.

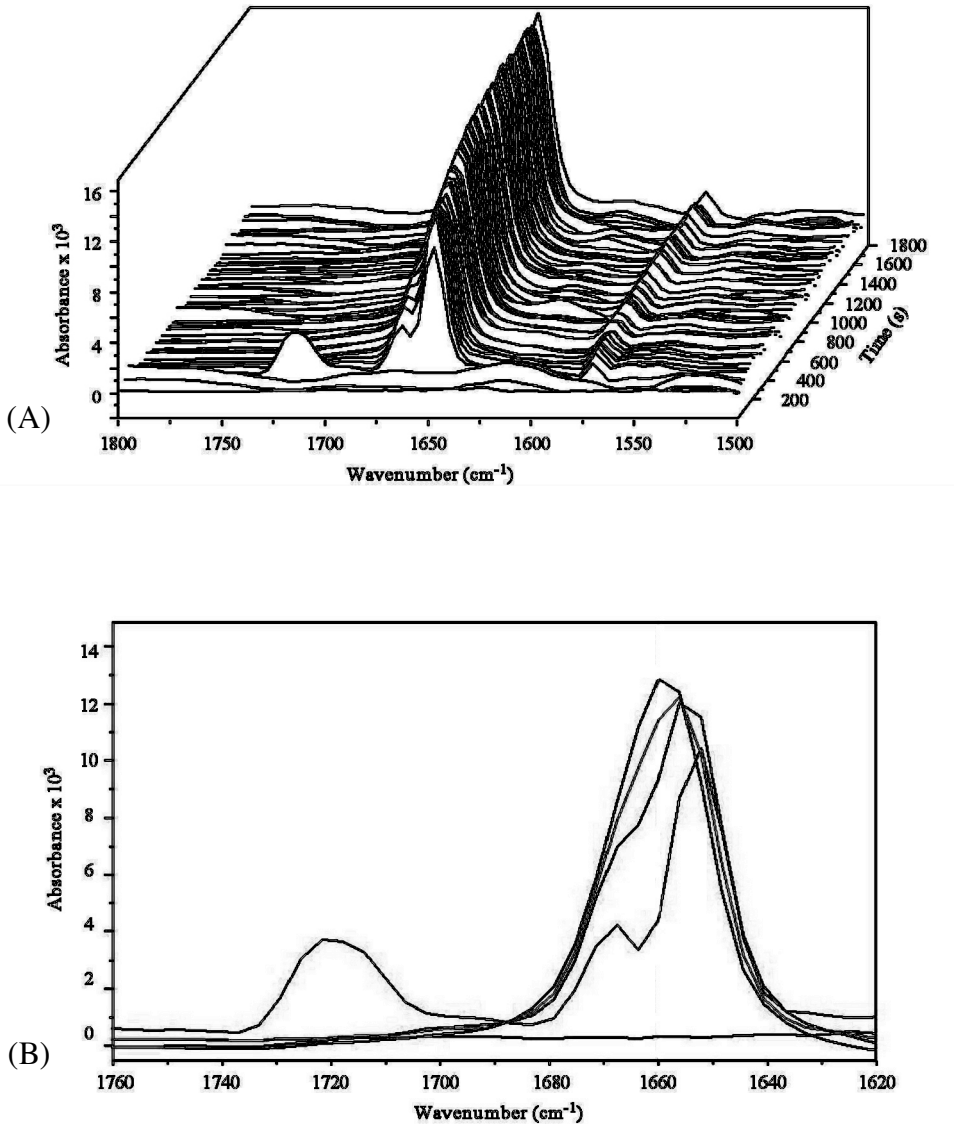

Figure A1.16. (A) Representative IR plot for the second injection of **1** (0.004 M) by 0.10 M LDA in 12.2 M THF/hexanes at -78 °C after zeroing the baseline of the reaction in Figure 16A. Note nearly instantaneous consumption of **1**. (**1**: 1721 cm^{-1}, **2 + 4**: 1660 cm^{-1}); (B) Cross-section of the plot in Figure 16A.

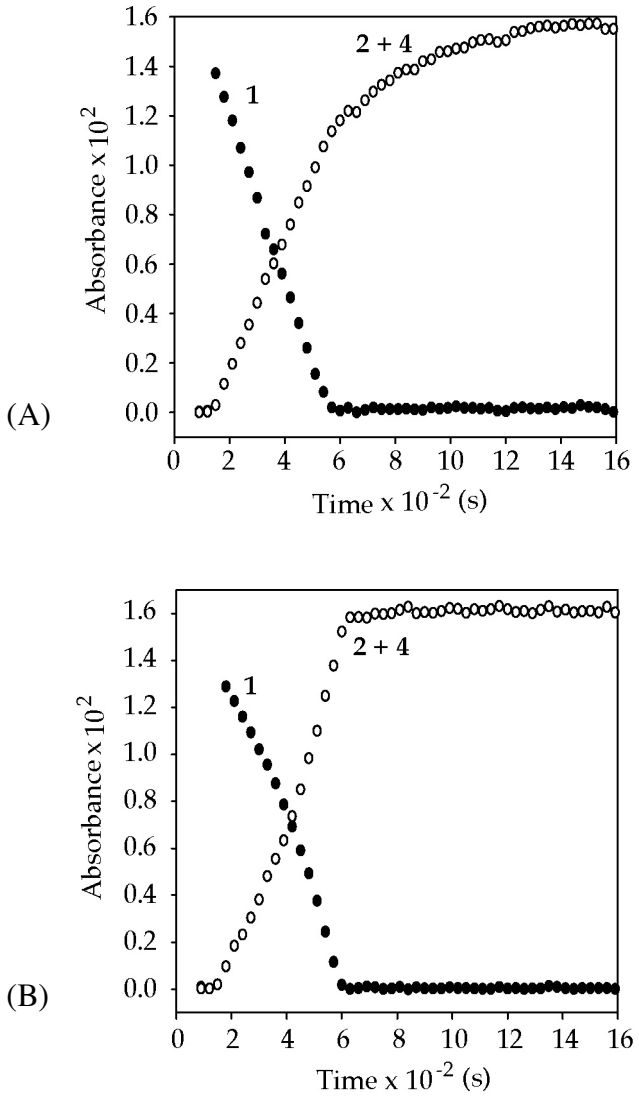

Figure A1.17. Plot of absorbance versus time for the ortholithiation of **1** (0.004 M) by 0.10 M LDA in THF/hexane at -78 °C: (A) 12.2 M THF; (B) 1.23 M THF. (**1**: 1721 cm^{-1}, **2 + 4**: 1660 cm^{-1}. Product (**2** + **4**) growth continues after consumption of **1** in Figure 17A and not in 17B.

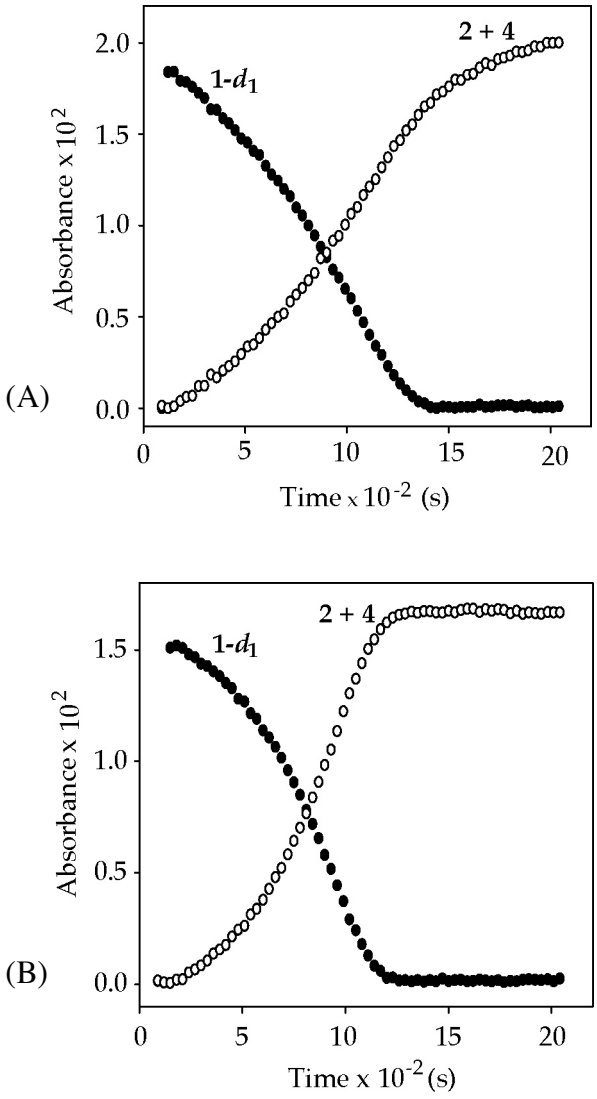

Figure A1.18. Plot of absorbance versus time for the ortholithiation of **1-d_1** (0.004 M) by 0.10 M LDA in THF/hexane at -78 °C: (A) 12.2 M THF (B) 1.23 M THF. (**1-d_1**: 1721 cm^{-1}, **2 + 4**: 1660 cm^{-1}).

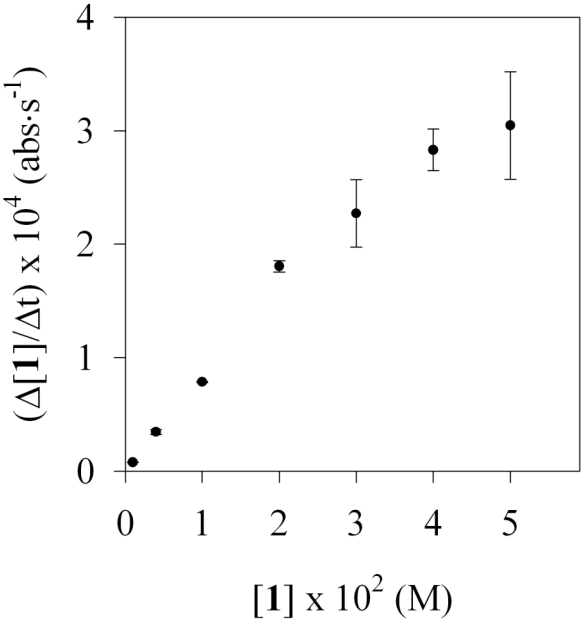

Figure A1.19. Plot of Δ[**1**]/Δt versus [**1**] for the ortholithiation of **1** by 0.10 M LDA in 12.2 M THF /hexanes at -78 ºC.

[**1a**] (M)	(Δ[**1**]/Δt) 1 (abs·s^{-1})	(Δ[**1**]/Δt) 2 (abs·s^{-1})
0.001	0.0000079 ± 1E-7	0.0000075 ± 1E-7
0.004	0.000036 ± 1E-6	0.000033 ± 1E-6
0.010	0.0000789 ± 9E-7	0.000078 ± 1E-6
0.020	0.000184 ± 3E-6	0.000177 ± 2E-6
0.030	0.000248 ± 4E-6	0.000206 ± 2E-6
0.040	0.000270 ± 3E-6	0.000296 ± 6E-6
0.050	0.000338 ± 4E-6	0.000271 ± 3E-6

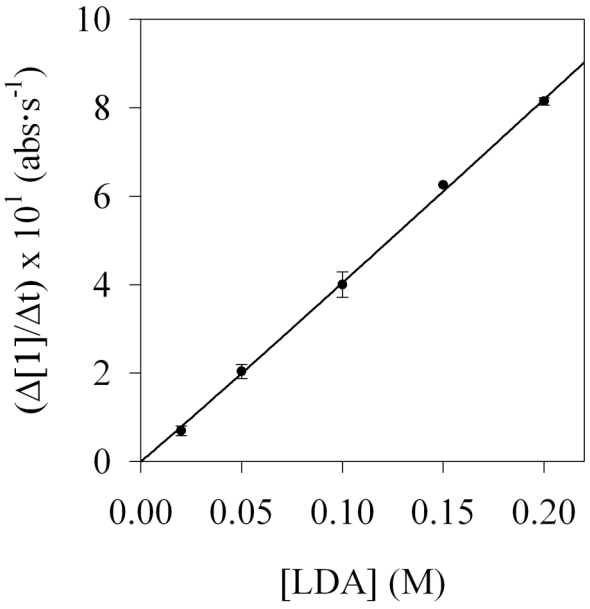

Figure A1.20. Plot of k_{obsd} versus [LDA] for the ortholithiation of **1** (0.0074 M) in 12.2 M THF at -78 °C. The curve depicts an unweighted least-squares fit to $k_{obsd} = k[\text{LDA}]^n$. ($k = (4.2 \pm 0.2) \times 10^1$, $n = (1.02 \pm 0.03)$.

[LDA] (M)	k_{obsd} 1 (abs·s^{-1})	k_{obsd} 2 (abs·s^{-1})
0.02	0.6160 E-5± 5E-8	0.7714E-5 ± 2E-8
0.05	1.921E-5 ± 1E-7	2.148E-5 ± 7E-8
0.10	6.796E-5 ± 5E-7	4.198E-5 ± 3E-7
0.15	6.252E-5 ± 6E-7	--
0.20	8.082E-5 ± 3E-7	8.205E-5 ± 5E-7

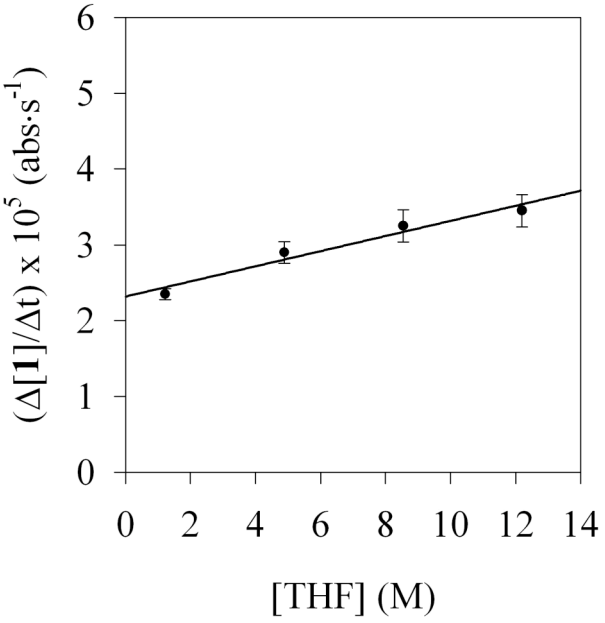

Figure A1.21. Plot of $\Delta[\mathbf{1}]/\Delta t$ versus [THF] in hexanes for the ortholithiation of **1** (0.004 M) by 0.10 M LDA at -78 °C. The curve depicts an unweighted least-squares fit to $\Delta[\mathbf{1}]/\Delta t = k[\text{THF}] + k'$ ($k = (1.0 \pm 0.2) \times 10^{-6}$, $k' = (2.3 \pm 0.1) \times 10^{-5}$).

[THF] (M)	$(\Delta[\mathbf{1}]/\Delta t)$ 1 (abs·s^{-1})	$(\Delta[\mathbf{1}]/\Delta t)$ 2 (abs·s^{-1})
1.22	0.000024 ± 1E-6	0.000023 ± 1E-6
4.88	0.000028 ± 2E-6	0.000030 ± 2E-6
8.54	0.000031 ± 1E-6	0.000034 ± 2E-6
12.2	0.000036 ± 1E-6	0.000033 ± 1E-6

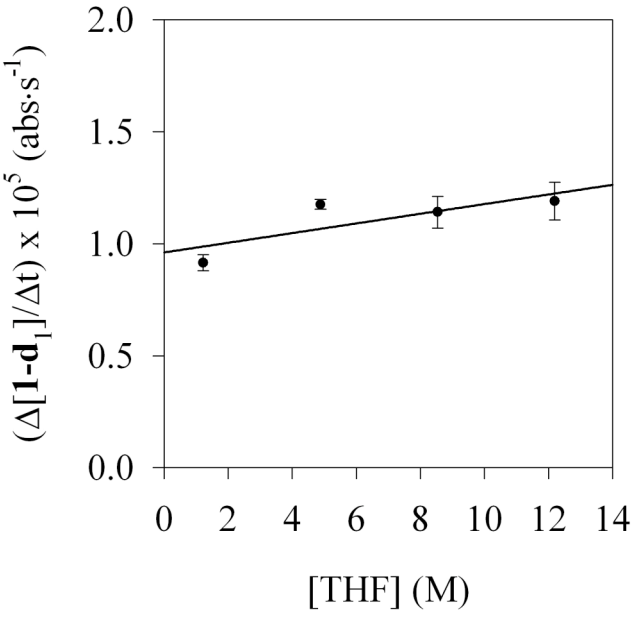

Figure A1.22. Plot of $\Delta[\mathbf{1}\text{-}d_1]/\Delta t$ versus [THF] in hexanes for the ortholithiation of **1-*d*$_1$** (0.004 M) by 0.10 M LDA at -78 °C. The curve depicts an unweighted least-squares fit to $\Delta[\mathbf{1}\text{-}d_1]/\Delta t = k[\text{THF}] + k'$ ($k = (2.2 \pm 0.8) \times 10^{-7}$, $k' = (9.6 \pm 0.6) \times 10^{-6}$).

[THF] (M)	$(\Delta[\mathbf{1}\text{-}d_1]/\Delta t)$ 1 (abs·s^{-1})	$(\Delta[\mathbf{1}\text{-}d_1]/\Delta t)$ 2 (abs·s^{-1})
1.22	0.0000089 ± 5E-7	0.0000094 ± 4E-7
4.88	0.0000119 ± 2E-7	0.0000116 ± 1E-7
8.54	0.0000109 ± 3E-7	0.0000119 ± 1E-7
12.2	0.0000113 ± 1E-7	0.0000125 ± 2E-7

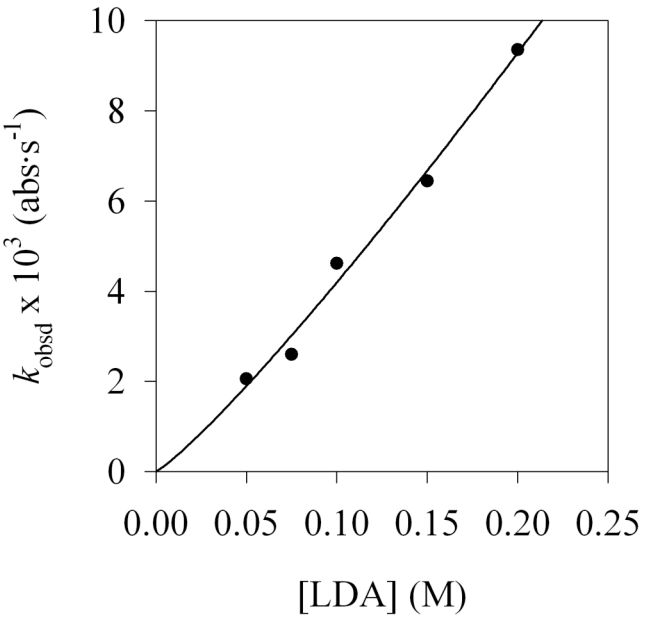

Figure A1.23. Plot of k_{obsd} versus [LDA] for the condensation of **2** and **3** in 12.2 M THF at -78 °C. The curve depicts an unweighted least-squares fit to $k_{obsd} = k[\text{LDA}]^n$ ($k = (60 \pm 10)$, $n = (1.1 \pm 0.1)$. Individual rates were obtained by fitting the exponential decay to the expression: $y = y_0 + ae^{-kt}$.

[LDA] (M)	k_{obsd} (abs·s^{-1})
0.05	0.002055 ± 5E-5
0.075	0.002598 ± 6E-5
0.10	0.004614 ± 9E-5
0.15	0.006440 ± 1E-4
0.20	0.009347 ± 3E-4

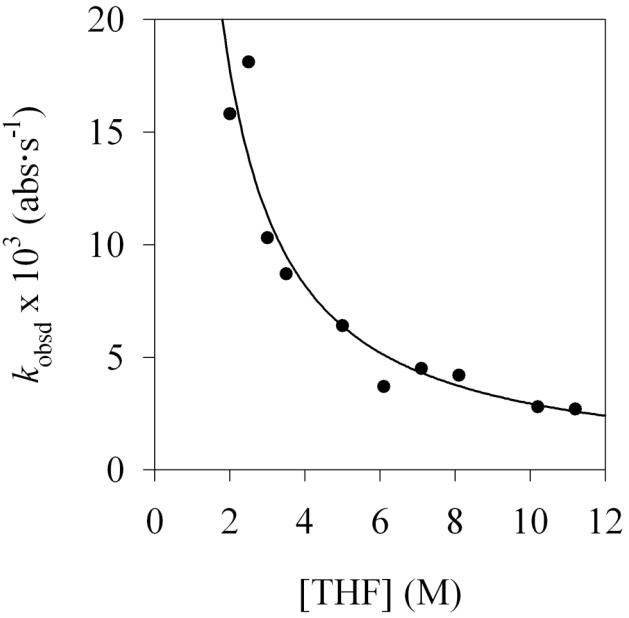

Figure A1.24. Plot of k_{obsd} versus [THF] for the condensation of **2** and **3** (0.10 M) at -78 °C. The curve depicts an unweighted least-squares fit to $k_{obsd} = k[\text{THF}]^n$ (k = (39 $\pm$ 7), n = (-1.1 $\pm$ 0.2). Individual rates were obtained by fitting the exponential decay to the expression: $y = y_0 + ae^{-kt}$.

[THF] (M)	k_{obsd} (abs·s^{-1})
2.0	0.01584 $\pm$ 3.34E-3
2.5	0.01812 $\pm$ 2.85E-3
3.0	0.01031 $\pm$ 8.2E-4
3.5	0.008737 $\pm$ 5.6E-4
5.0	0.006421 $\pm$ 2.3E-4
6.1	0.003681 $\pm$ 2.8E-4
7.1	0.004487 $\pm$ 1.1E-4
8.1	0.004163 $\pm$ 7E-5
10.2	0.002809 $\pm$ 7E-5
11.2	0.002683 $\pm$ 1.4E-4

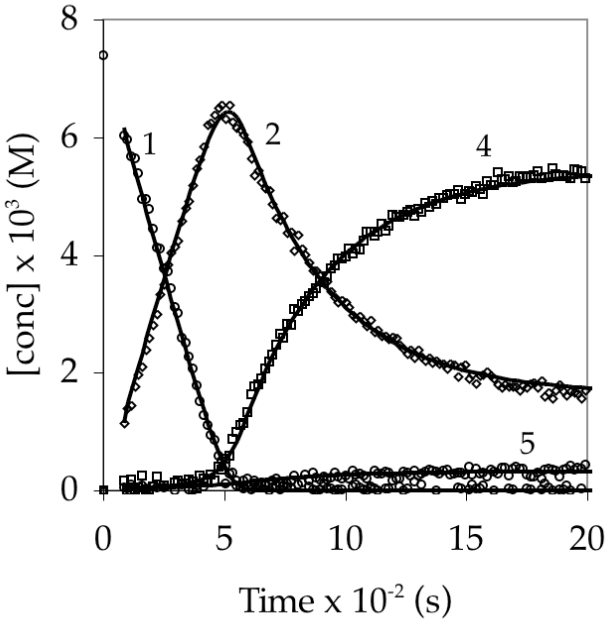

Figure A1.25. Parametric fit to the ^{19}F NMR spectroscopy derived concentration versus time profile of 0.10 M LDA, 0.0074 M **1**, 12.2 M THF at -78 °C.

$k_1 = 0.020495 \pm 0.000728$
$k_2 = 0.09695 \pm 0.0275$
$k_{-2} = 1.4131 \pm 0.456$
$k_3 = 828.12 \pm 86.4$
$k_4 = 0.0461 \pm 0.000664$
$k_{-4} = 0.0027294 \pm 9.36e\text{-}005$

	k_1	k_2	k_{-2}	k_3	k_4	k_{-4}
k_1	1.00	-0.76	-0.74	0.11	-0.87	-0.63
k_2	-0.76	1.00	0.99	-0.41	0.58	0.41
k_{-2}	-0.74	0.99	1.00	-0.37	0.55	0.41
k_3	0.11	-0.41	-0.37	1.00	-0.20	-0.15
k_4	-0.87	0.58	0.55	-0.20	1.00	0.82
k_{-4}	-0.63	0.41	0.41	-0.15	0.82	1.00

Shown are best estimates of rate constants with 95% confidence intervals and a covariance matrix describing the magnitude of correlation between the parameters. The parameters exhibit low correlations except for the rate constants describing mixed aggregate equilibration (k_2, k_{-2}). The values of k_2 and k_{-2} are lower bounds and can be higher provided that their ratio remains constant.

Figure A1.26. Global parametric fit to the ^{19}F NMR spectroscopy derived concentration versus time profile of 0.0074 M **1** in 12.2 M THF at -78 °C with (A) 0.05 M LDA, (B) 0.10 M LDA, (C) 0.15 M LDA and (D) 0.20 M LDA. The four traces are fit simultaneously with a global fitting routine.

Figure A1.26 (Continued).

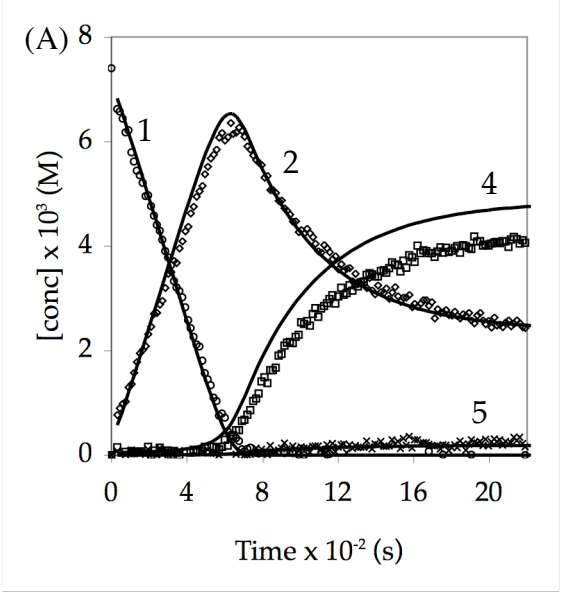

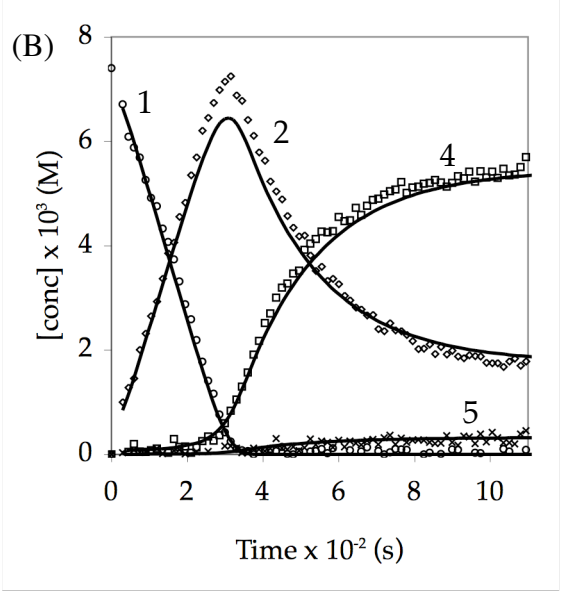

Figure A1.26 (Continued).

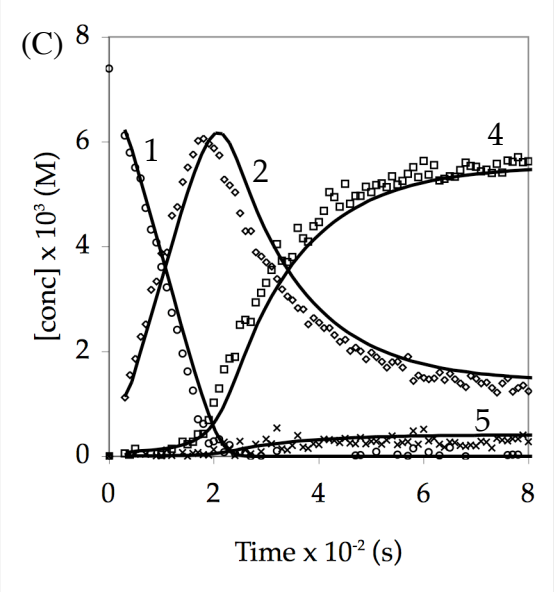

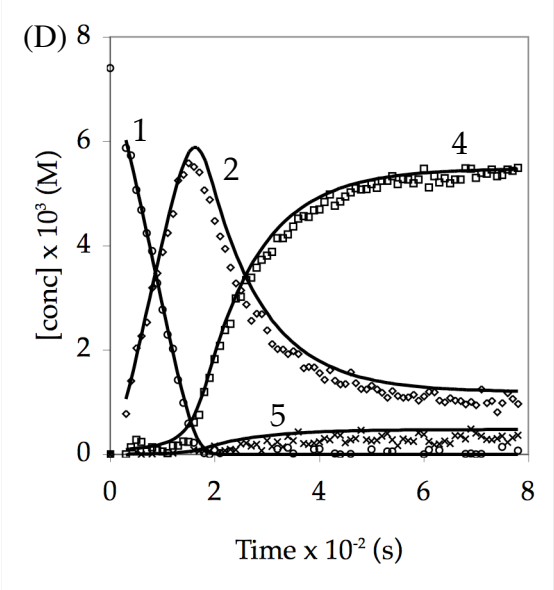

Figure A1.26 (Continued).

		k_1	k_2	k_{-2}	k_3	k_4	k_{-4}
$k_1 = 0.021785 \pm 0.000869$	k_1	1.00	0.03	0.07	-0.21	-0.81	-0.55
$k_2 = 0.47672 \pm 0.0898$	k_2	0.03	1.00	0.92	-0.44	0.03	-0.08
$k_{-2} = 7.7405 \pm 1.5$	k_{-2}	0.07	0.92	1.00	-0.25	0.00	-0.02
$k_3 = 584.99 \pm 69.9$	k_3	-0.21	-0.44	-0.25	1.00	0.09	0.21
$k_4 = 0.056128 \pm 0.00101$	k_4	-0.81	0.03	0.00	0.09	1.00	0.78
$k_{-4} = 0.0037294 \pm 0.000165$	k_{-4}	-0.55	-0.08	-0.02	0.21	0.78	1.00

Shown are best estimates of rate constants with 95% confidence intervals and a covariance matrix describing the magnitude of correlation between the parameters. All parameters exhibit low correlations except for the rate constants describing mixed aggregate equilibration (k_2, k_{-2}). The global fit does not yield an improvement in the magnitude of the correlations as compared to individual fits. However, the global fit to a series of LDA concentrations does support the model and indicates that it correctly predicts the LDA dependence of the proposed mechanism.

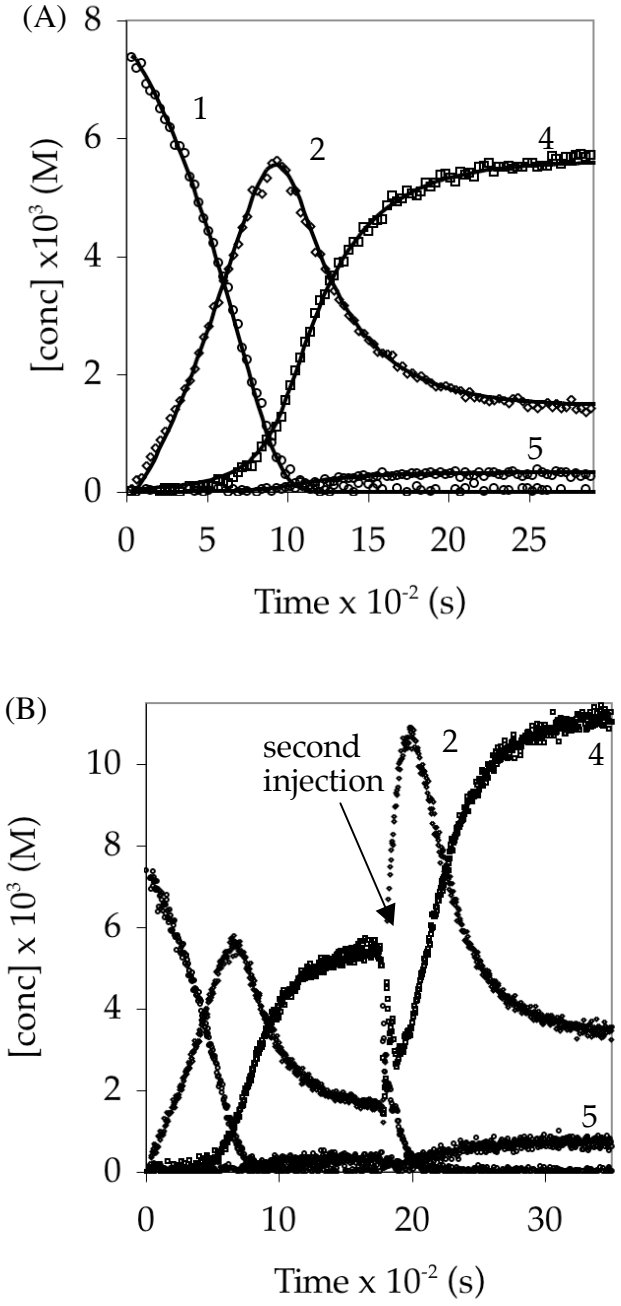

Figure A1.27. Parametric fit to the ^{19}F NMR spectroscopy derived concentration versus time profile of 0.10 M LDA, 0.0074 M **1**-d_1, 12.2 M THF at -78 °C. (A) First injection; (B) Second injection.

Figure A1.27 (Continued).

$k_1 = 0.0066199 \pm 0.000119$
$k_2 = 0.34666 \pm 0.0503$
$k_{-2} = 6.0123 \pm 0.914$
$k_3 = 152.01 \pm 9.48$
$k_4 = 0.049395 \pm 0.000435$
$k_{-4} = 0.002603 \pm 6.82e\text{-}005$

	k_1	k_2	k_{-2}	k_3	k_4	k_{-4}
k_1	1.00	-0.51	-0.52	0.03	-0.42	-0.04
k_2	-0.51	1.00	0.95	-0.60	-0.26	-0.57
k_{-2}	-0.52	0.95	1.00	-0.40	-0.30	-0.54
k_3	0.03	-0.60	-0.40	1.00	0.01	0.34
k_4	-0.42	-0.26	-0.30	0.01	1.00	0.72
k_{-4}	-0.04	-0.57	-0.54	0.34	0.72	1.00

Shown are best estimates of rate constants with 95% confidence intervals and a covariance matrix describing the magnitude of correlation between the parameters. All parameters exhibit low correlations except for the rate constants describing mixed aggregate equilibration (k_2, k_{-2}). The kinetic isotope effect is calculated as KIE = k_{1h}/k_{1d}= 3.0. The value matches the kinetic isotope effect measured by in situ IR by an initial rates method.

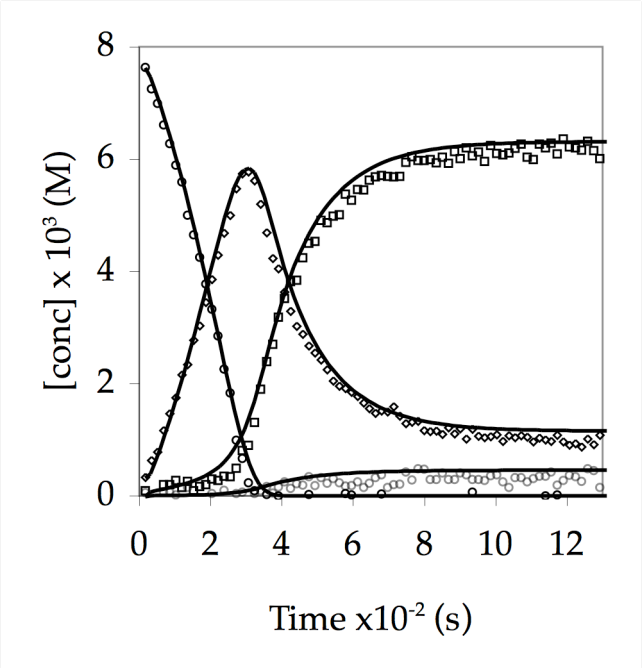

Figure A1.28. Parametric fit to the ^{19}F NMR spectroscopy derived concentration versus time profile of 0.10 M LDA, 0.0074 M **1**, 7.4 M THF/pentane at -78 °C.

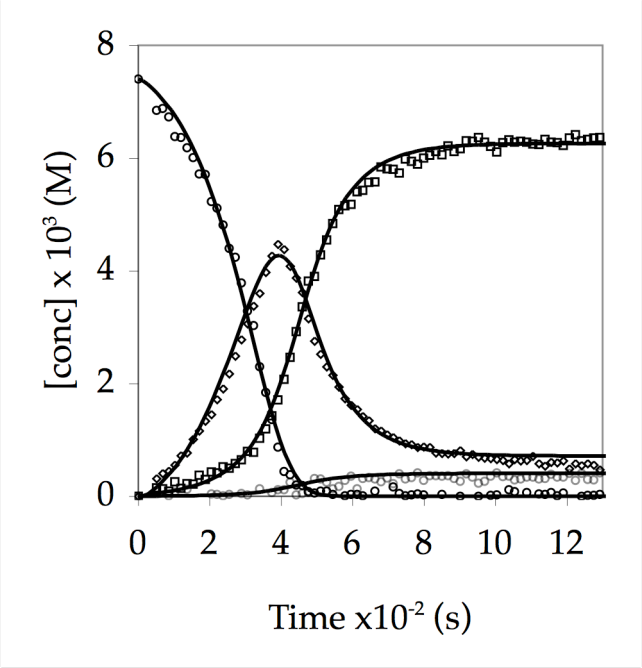

Figure A1.29. Parametric fit to the ^{19}F NMR spectroscopy derived concentration versus time profile of 0.10 M LDA, 0.0074 M **1**, 4.9 M THF/pentane at -78 °C.

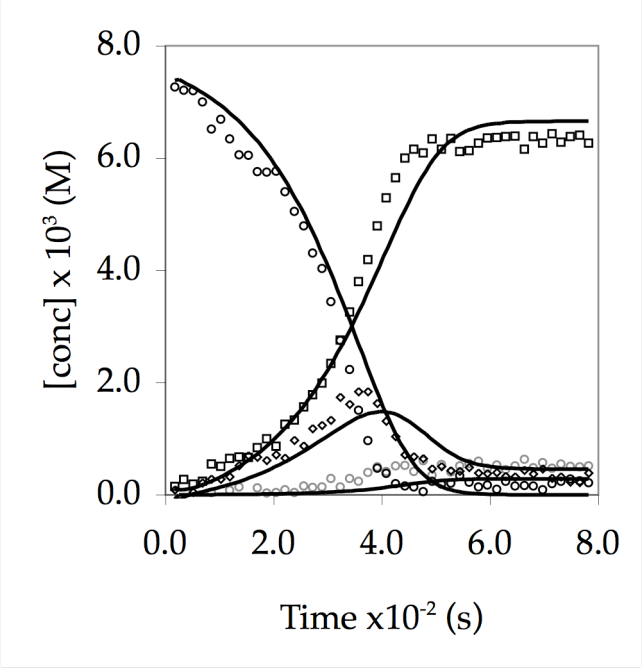

Figure A1.30. Parametric fit to the ^{19}F NMR spectroscopy derived concentration versus time profile of 0.10 M LDA, 0.0074 M **1**, 2.5 M THF/pentane at -78 °C.

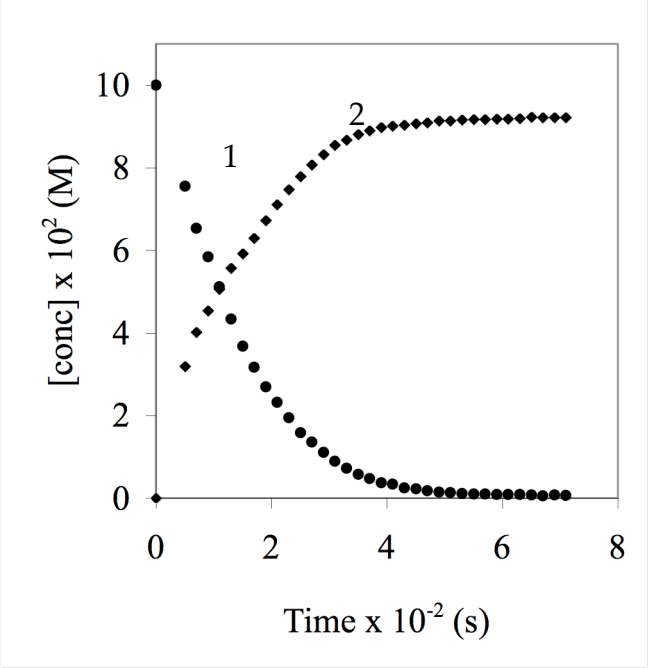

Figure A1.31. Plot of concentration versus time by ^{19}F NMR spectroscopy of 0.10 M **1**, 0.10 M LDA, 12.2 M THF at -78 °C.

Under stoichiometric conditions, **1** is converted quantitatively to aryllithium monomer **2.** No mixed aggregates are observed because they are rapidly consumed by **1**. Once the starting material has reacted there is no excess LDA and **2** cannot form mixed aggregates **4** and **5**. The decay in **1** fits a first order exponential function and does not fit a second order function.

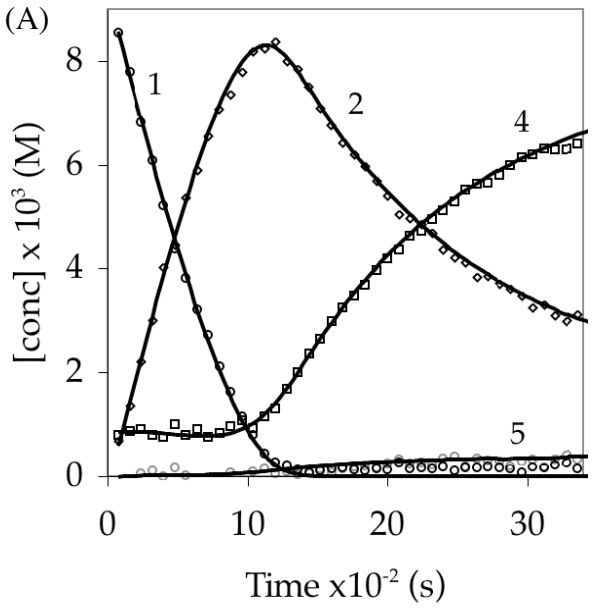

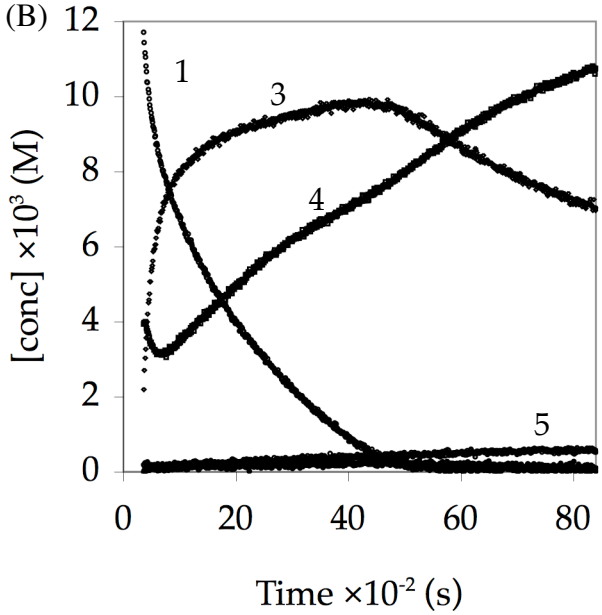

Figure A1.32. Parametric fit to the ^{19}F NMR spectroscopy derived concentration versus time profile of 0.40 M LDA, 0.010 M carbamate in 12.2 M THF at -100 °C. (A) First injection; (B) Second injection of 0.010 M carbamate.

Figure A1.32 (Continued).

$k_1 = 0.0032963 \pm 6.09e\text{-}005$
$k_2 = 0.0080387 \pm 0.000479$
$k_{-2} = 0.13174 \pm 0.0129$
$k_3 = 159.4 \pm 12.4$
$k_4 = 0.0033048 \pm 5.55e\text{-}005$
$k_{-4} = 0.00032168 \pm 3.11e\text{-}005$

	k_1	k_2	k_{-2}	k_3	k_4	k_{-4}
k_1	1.00	-0.64	-0.33	0.17	-0.81	-0.59
k_2	-0.64	1.00	0.79	-0.57	0.48	0.38
k_{-2}	-0.33	0.79	1.00	-0.41	0.22	0.22
k_3	0.17	-0.57	-0.41	1.00	-0.05	-0.08
k_4	-0.81	0.48	0.22	-0.05	1.00	0.90
k_{-4}	-0.59	0.38	0.22	-0.08	0.90	1.00

Shown are best estimates of rate constants with 95% confidence intervals and a covariance matrix describing the magnitude of correlation between the parameters. The correlation between k_2 and k_{-2} has decreased and now allows one to determine their values individually. This permits one to distinguish the reactivity of mixed dimers **4** and **5** (vide infra). The distinct reactivity at -100 °C also allows to exclude the possibility of forming aryllithium monomer **2** in the initiation step.

Solvent effects on the ortholithiation of carbamate **1**

Interesting solvent effects were observed and are summarized in the following figures (Figures A1.33–A1.42). Systems in 2-methyltetrahydrofuran, tetrahydropyran and oxetane behaved similarly to the reaction in THF. These concentration versus time profiles were fit to the established model in THF. Structural assignments were made based on a ^{19}F NMR chemical shift analogy to the parent system in THF. The assignments are therefore tentative.

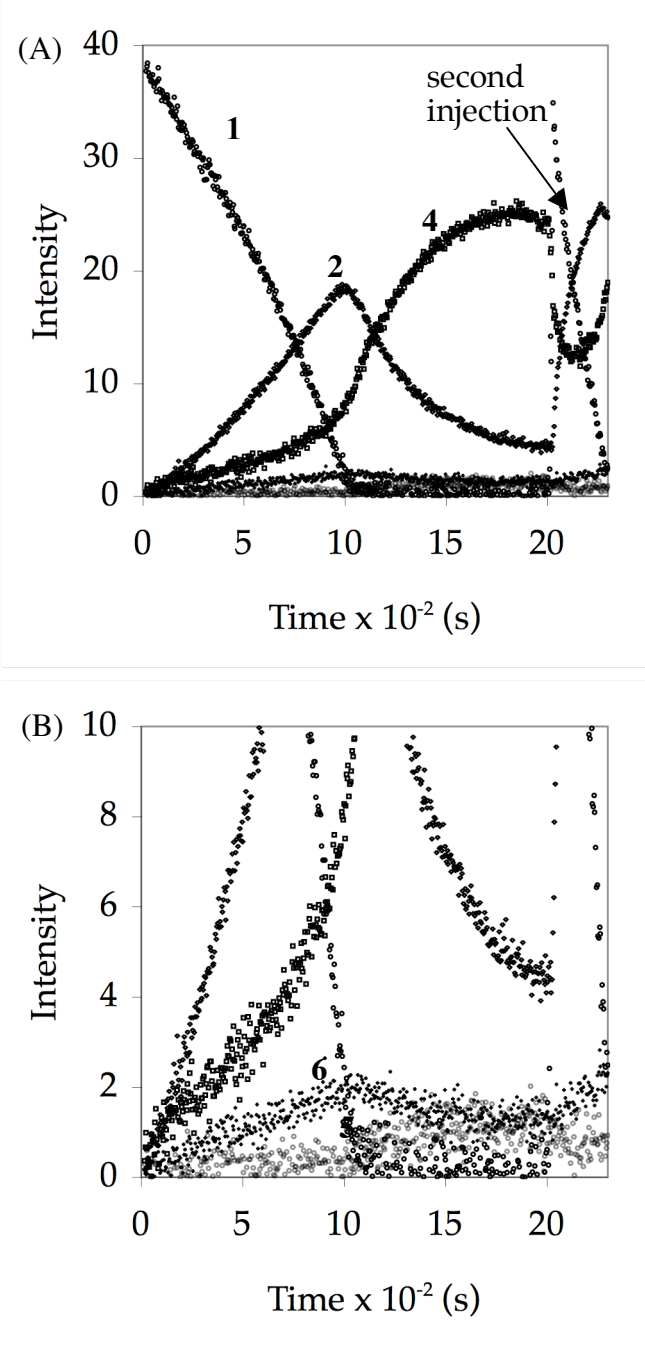

Figure A1.33. Plot of intensity versus time by ^{19}F NMR spectroscopy of 0.20 M LDA, 0.01 M **1**, 5.0 M THF/pentane at -90 °C. (A) Trace including double injection; (B) Expansion of Figure 33A.

Pentane cosolvent at < 8.0 M THF gives rise to an additional lithium aggregate (**6**) (hexanes were used in all kinetic experiments). It appears as two 1:1 resonances at -77.5 and -77.7 ppm in the ^{19}F NMR spectrum. It is not observable with hexanes as cosolvent down to 1.0 M THF.

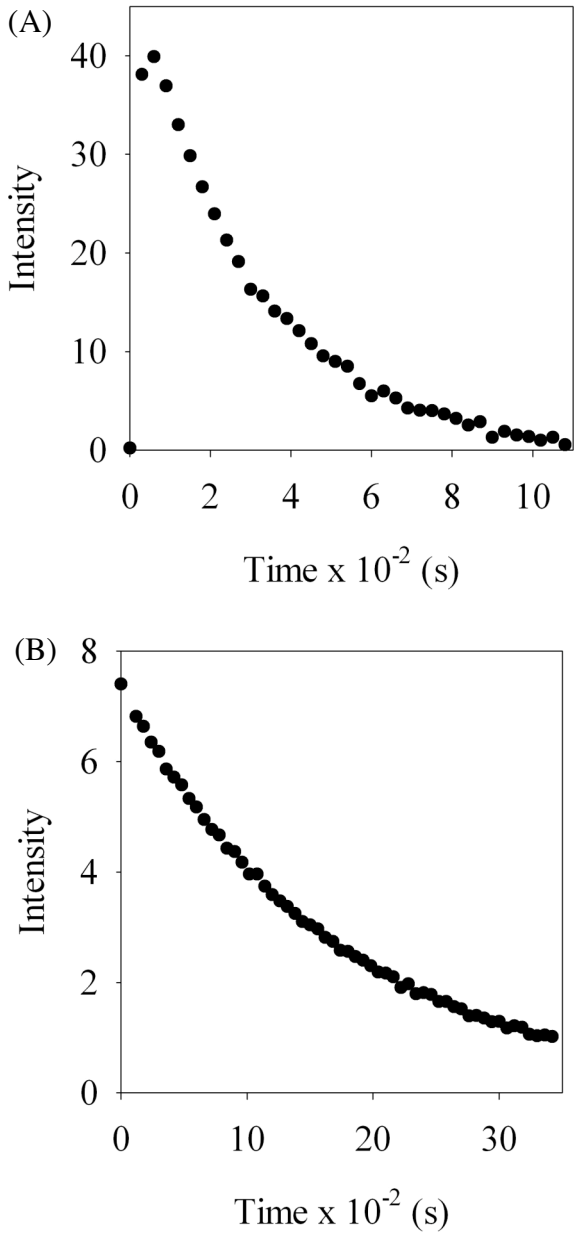

Figure A1.34. Plot of intensity versus time by ^{19}F NMR spectroscopy of 0.10 M LDA, 1.9 M *t*-BuOMe/cyclopentane at -78 °C. (A) 0.0074 M **1**, k_{obsd}= 3.4 ±0.1 (×10^{-3}) s^{-1}; (B) 0.0074 M **1**-***d*$_1$**, k_{obsd}= 0.56 ±0.02 (×10^{-3}) s^{-1}; KIE=6.1.

Studies by ReactIR show that **1** in 1.9 M *t*-BuOMe/cyclopentane appears as a precomplex with a 30 cm^{-1} downward shift in the IR spectrum. The reaction is zeroth order in LDA. The ^{19}F NMR resonance of **1** (-113.1 ppm) shifts by 2.4 ppm upfield to -110.7 ppm upon complexation with LDA.

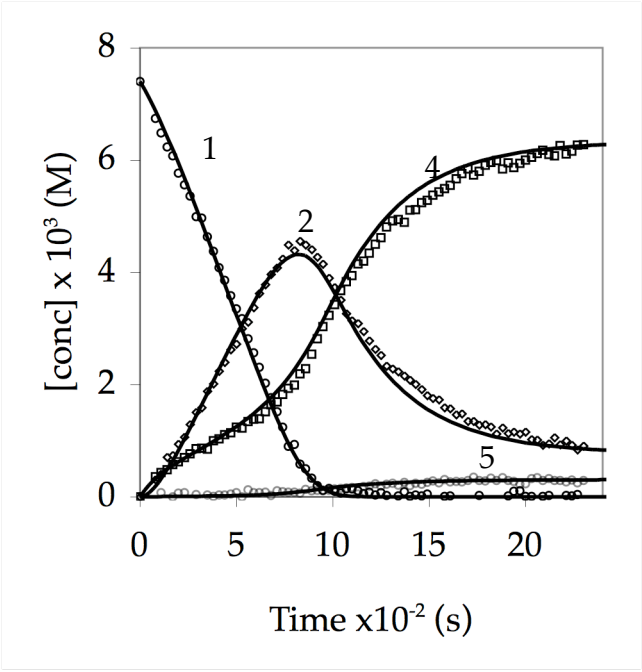

Figure A1.35. Parametric fit to the ^{19}F NMR spectroscopy derived concentration versus time profile of 0.0074 M **1**, 0.10 M LDA, 5.0 M 2-methyltetrahydrofuran/hexanes at -78 °C.

The reaction in 2-methyltetrahydrofuran is similar to the parent system in THF. Strikingly though, mixed dimer **4** does not exhibit a delayed onset whereas mixed dimer **5** does. Species **4** does not maintain a steady state concentration but instead builds up as **1** is decaying. The following chemical shifts were observed: **1** (-113.1 ppm), **2** (-74.5 ppm), **4** (-79.8 ppm), **5** (-80.1 ppm).

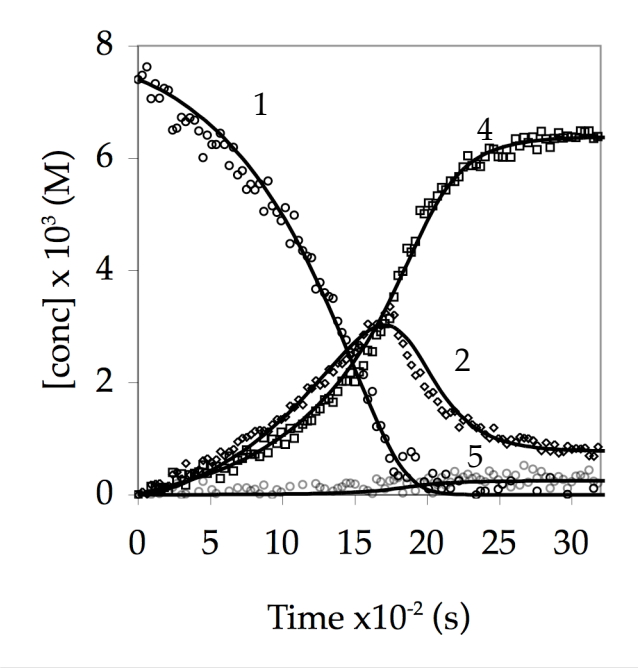

Figure A1.36. Parametric fit to the ^{19}F NMR spectroscopy derived concentration versus time profile of 0.0074 M **1**, 0.10 M LDA, 5.0 M tetrahydropyran/pentane at -78 °C.

The reaction in tetrahydropyran (THP) is similar to the reaction in THF. Strikingly as in the case of 2-methyltetrahydrofuran, mixed dimer **4** does not exhibit a delayed onset whereas mixed dimer **5** does. In addition, the decay in **1** is sigmoidal. This is an indication that the rate of the autocatalytic step has been accelerated relative to the initiation rate when switching from THF to THP.

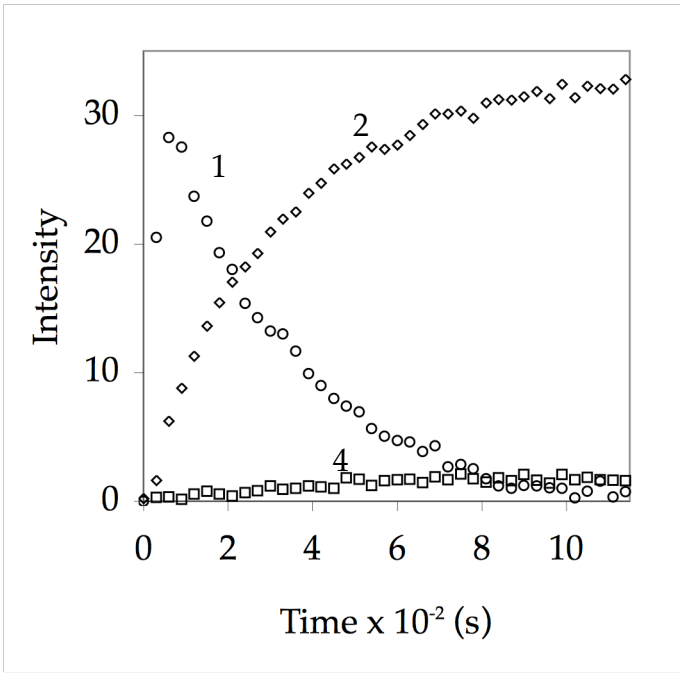

Figure A1.37. Plot of intensity versus time by ^{19}F NMR spectroscopy of 0.0074 M **1**, 0.10 M LDA, 4.1 M 2,2-dimethyltetrahydrofuran/pentane at -78 °C. The following chemical shifts were observed: **1** (-113.1 ppm), **2** (-74.9 ppm), **4** (-79.1 ppm). Small amounts of a supposed precomplex was observed at -112.0 ppm.

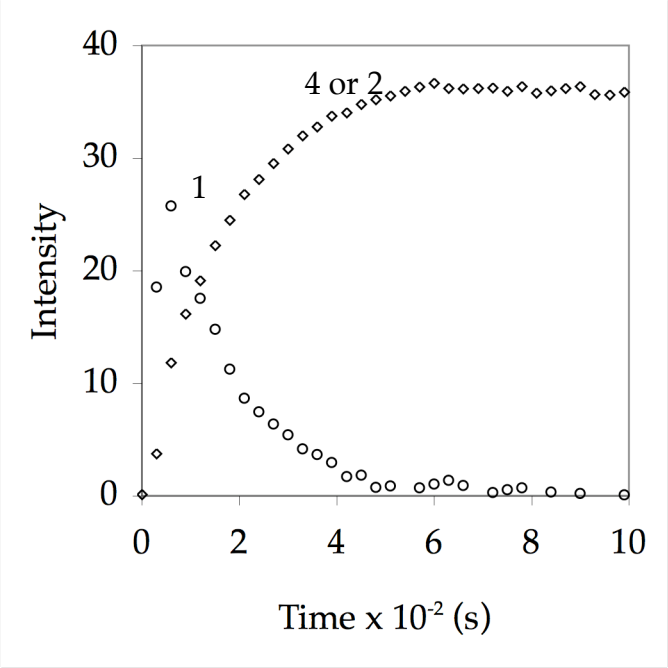

Figure A1.38. Plot of intensity versus time by ^{19}F NMR spectroscopy of 0.0074 M **1**, 0.10 M LDA, 4.1 M 2,5-dimethyltetrahydrofuran/pentane at -78 °C. The following chemical shifts were observed: **1** (-113.1 ppm), **4** or **2** (-80.4 ppm). It is unclear whether the product is **2** or **4**.

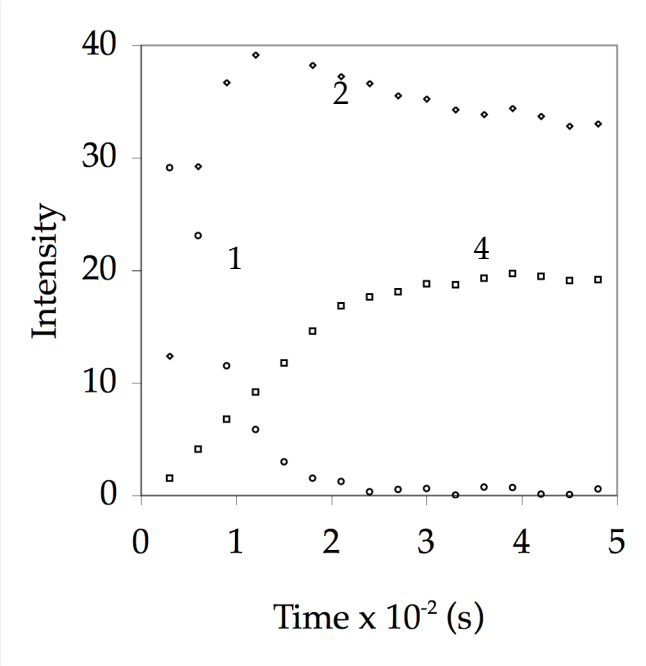

Figure A1.39 Plot of intensity versus time by ^{19}F NMR spectroscopy of 0.0074 M **1**-d_1, 0.10 M LDA, 0.5 M DMPU/THF at -78 °C. (DMPU = 1,3-Dimethyl-3,4,5,6-tetrahydro-2(1*H*)-pyrimidinone)

The reaction with >0.50 M DMPU is intractably fast at -78 °C. It was also necessary to use the deuterated starting material to further slow down the rate. It is noteworthy that addition of 0.50 M DMPU will stabilize the ground state. The rate increase must therefore derive either from a relative transition state stabilization or an enhancement of mixed aggregate reactivity. The following chemical shifts were observed: **1**-d_1 (-114.1 ppm), **2** (-75.1 ppm), **4** (-78.3 ppm).

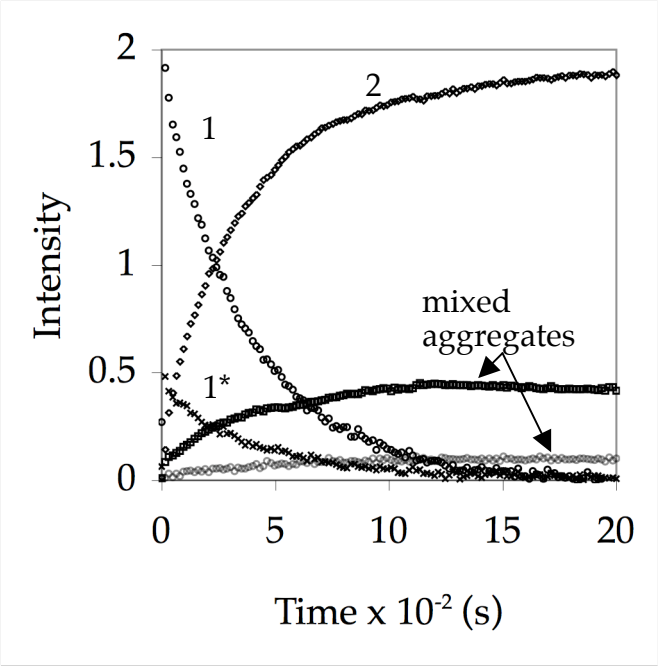

Figure A1.40. Plot of intensity versus time by ^{19}F NMR spectroscopy of 0.0074 M **1**, 0.10 M LDA, 5.1 M dimethylethylamine (DMEA)/toluene at -78 °C.

At 5.1 M DMEA, carbamate **1** is a mixture of its free and precomplexed form (**1**/**1***= 4:1 ratio, respectively). Three lithiated products are observed. The major species in solution is an aryllithium monomer or a homoaggregate (**2**) as evident from its singlet in the ^{6}Li NMR spectrum. The other products are likely to be mixed aggregates. The following chemical shifts were observed: **1** (-112.3 ppm), **1*** (-112.3 ppm), **2** (-73.6 ppm) and mixed aggregates at -76.1 ppm (major) and -76.7 ppm (minor).

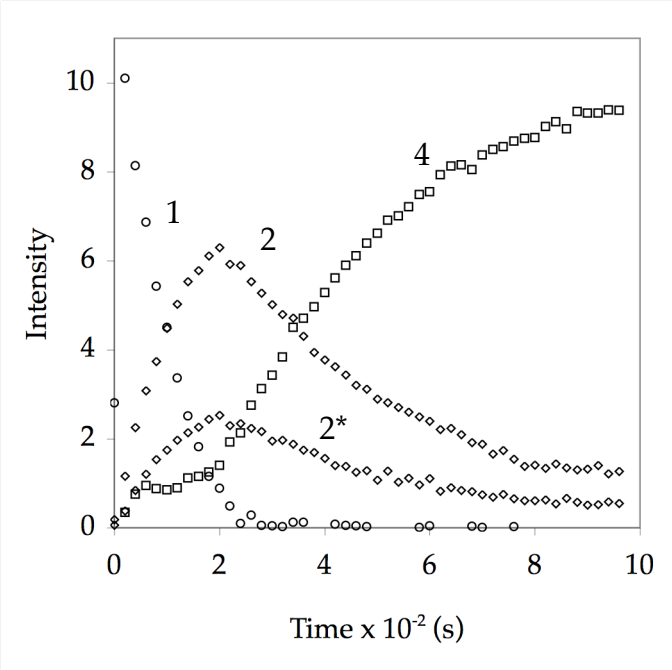

Figure A1.41. Plot of intensity versus time by ^{19}F NMR spectroscopy of 0.0074 M **1**, 0.10 M LDA, 5.0 M oxetane/hexanes at -100 °C.

The reaction is too fast to monitor at -78 °C and needed to be cooled to -100 °C. There are three other mixed aggregates at low concentrations that are not shown in the above plot. It is not clear whether these are distinct lithium aggregates or conformers. In THF at -100 °C, mixed dimer **4** initially grows in to a steady concentration until **1** is consumed. It appears that this 'plateau' arises from a delicate balance between the rates of consumption and formation of **4**. If the rate of consumption is greater we arrive at cases as in THF at -78 °C where **4** never appears observably. On the contrary, if the rate of formation is greater, we arrive at cases as in Me-THF and THP where **4** increases steadily. Only in oxetane and THF at -100 °C is this balance ('plateau') satisfied. The following chemical shifts were observed: **1** (doublet at -112.6 ppm), **2** (-74.7 ppm), **2*** (-75.1 ppm), **4** (-76.8 ppm) and minor peaks at -75.6, -77.5 and -77.9 ppm. Species **2** and **2*** preserve a constant ratio and are therefore either conformers of the same aryllithium or rapidly equilibrating lithium aggregates.

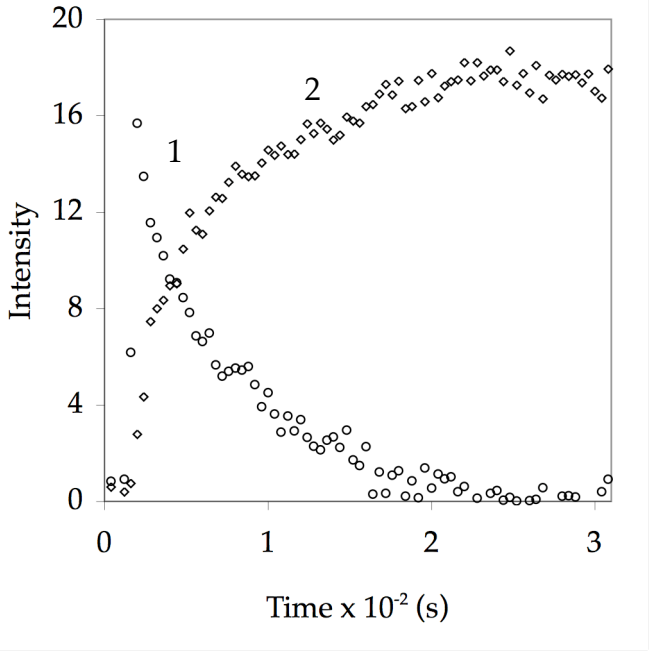

Figure A1.42. Plot of intensity versus time by ^{19}F NMR spectroscopy of 0.0074 M **1**, 0.10 M LDA, 1.4 M TMEDA/THF at -78 °C (TMEDA = tetramethylethylenediamine).

The reaction is too fast to monitor at >2.0 M TMEDA in THF. As THF concentration is increased the reaction gradually shifts to the profile shown in Figure 25. It is striking that a small amount of TMEDA in THF so dramatically alters the course of the reaction. Because LDA remains solvated by THF and because there are no detectable mixed aggregates present it is likely that TMEDA selectively stabilizes the transition state. The initial rate of decay in **1** is accelerated 300 fold relative to the parent system in THF. The following chemical shifts were observed: **1** (-113.1 ppm) and two peaks with a 10:7 ratio at -74.7 and -75.0 ppm. It is likley that the peaks represent two conformations of the of an aryllithium monomer **2**. Even though conformer of the diisopropyl moiety have only been seen in THF at -78 °C for **1**, such conformers may arise for the lithiated species in different solvents as well.

Model:

Initiation

$$\underset{\mathbf{3}}{(i\text{-}Pr_2NLi)_2} + \underset{\mathbf{1}}{ArH} \xrightarrow{k_1} \underset{\mathbf{4}}{(i\text{-}Pr_2NLi)(ArLi)} + i\text{-}Pr_2NH \quad (1)$$

Mixed Aggregate Exchange

$$\underset{\mathbf{4}}{(i\text{-}Pr_2NLi)(ArLi)} \underset{k_{-2}}{\overset{k_2}{\rightleftharpoons}} \underset{\mathbf{5}}{(i\text{-}Pr_2NLi)(ArLi)^*} \quad (2)$$

Autocatalysis

$$\underset{\mathbf{5}}{(i\text{-}Pr_2NLi)(ArLi)^*} + \underset{\mathbf{1}}{ArH} \xrightarrow{k_3} \underset{\mathbf{2}}{2\ ArLi} + i\text{-}Pr_2NH \quad (3)$$

$$\underset{\mathbf{3}}{(i\text{-}Pr_2NLi)_2} + \underset{\mathbf{2}}{ArLi} \underset{k_{-4}}{\overset{k_4}{\rightleftharpoons}} \underset{\mathbf{4}}{(i\text{-}Pr_2NLi)(ArLi)} + 0.5\underset{\mathbf{3}}{(i\text{-}Pr_2NLi)_2} \quad (4)$$

The model is described by the following differential equations [5]

$$d[ArH]/dt = -k_1[ArH][A_2] - k_3[A{\cdot}ArLi^*][ArH]$$

$$d[ArLi]/dt = -k_4[ArLi][A_2] + k_{-4}[A{\cdot}ArLi][A_2]^{0.5} + 2k_3[A{\cdot}ArLi^*][ArH]$$

$$d[A{\cdot}ArLi^*]/dt = k_2[A{\cdot}ArLi] - k_{-2}[A{\cdot}ArLi^*] - k_3[A{\cdot}ArLi^*][ArH]$$

$$d[A{\cdot}ArLi]/dt = k_1[ArH][A_2] - k_2[A{\cdot}ArLi] + k_{-2}[A{\cdot}ArLi^*] + k_4[ArLi][A_2] - k_{-4}[A{\cdot}ArLi][A_2]^{0.5}$$

$$A_2 = [A_2(init)] - 0.5[ArLi] - [A_2{\cdot}ArLi] - [A_2{\cdot}ArLi^*]$$

where,

ArH = **1** A·ArLi = **4**
ArLi = **2** A·ArLi* = **5**
A_2 = **3** $[A_2(init)]$ = initial concentration of LDA

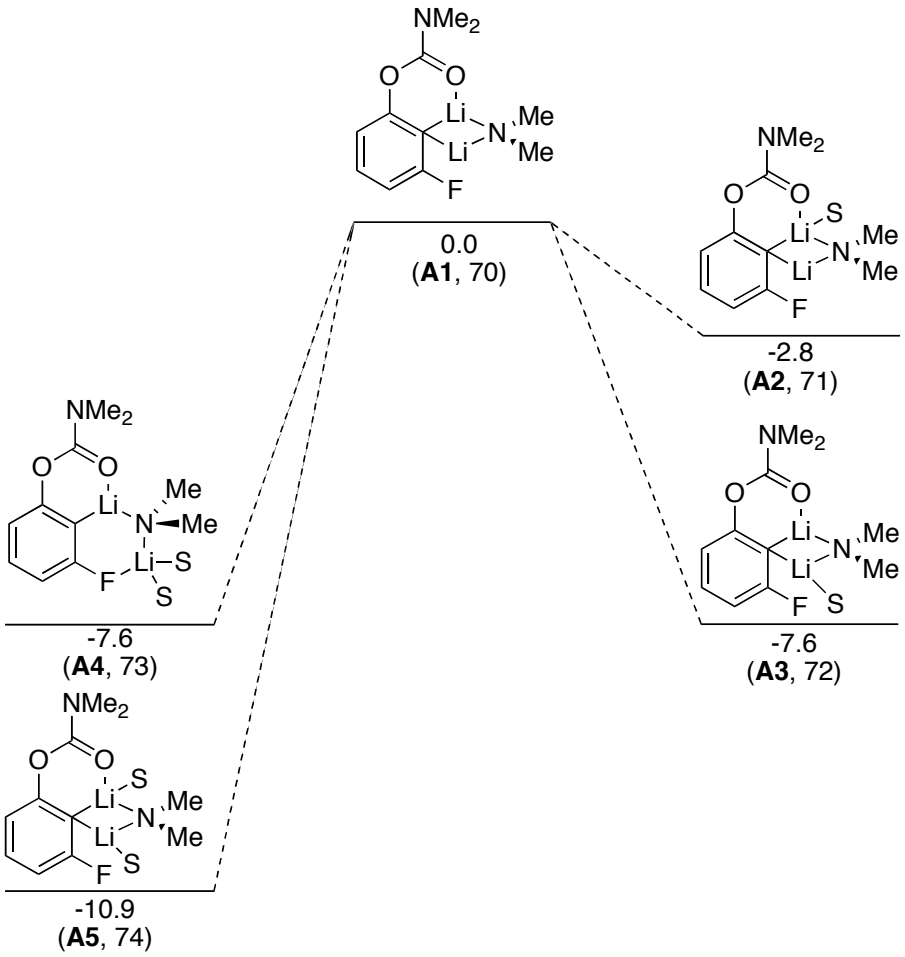

Figure A1.43. Relative free energies of solvation (ΔG, kcal/mol) at -78 °C. S = Me_2O.

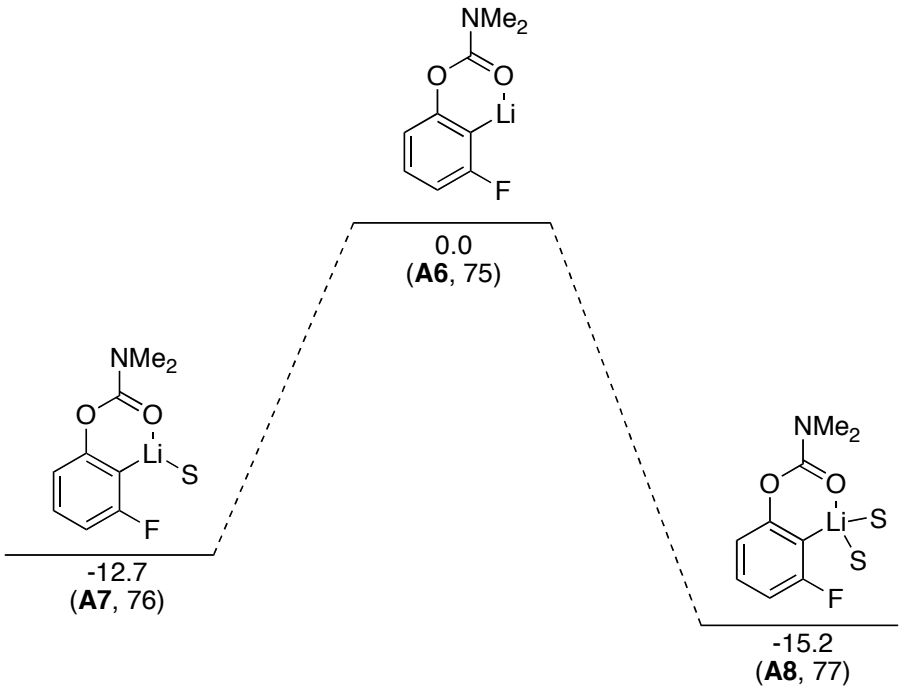

Figure A1.44. Relative free energies of solvation (ΔG, kcal/mol) at -78 °C. S = Me_2O.

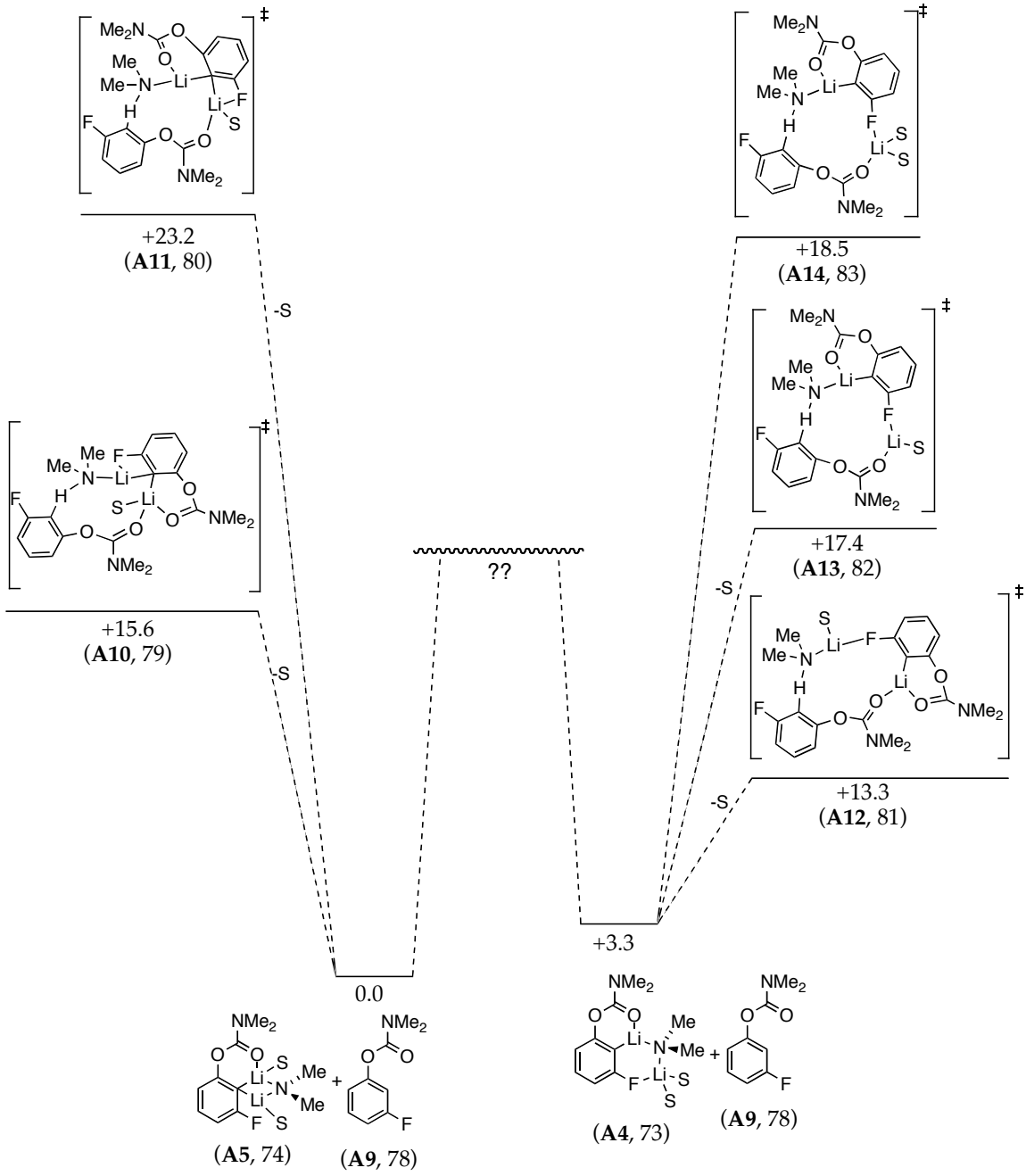

Figure A1.45. Relative free energies (ΔG, kcal/mol) at -78 °C. S = Me_2O. Transition structures for the post-rate-limiting deprotonation of arene **A9** by mixed dimers **A4** and **A5**. Free energies of activation are reported relative to the ground state energy of closed mixed dimer **A5** and arene **A9**. The left-hand transition structures exhibit a closed mixed dimer motif akin to **A5** whereas the right-hand transition structures exhibit an open dimer motif akin to **A4**.

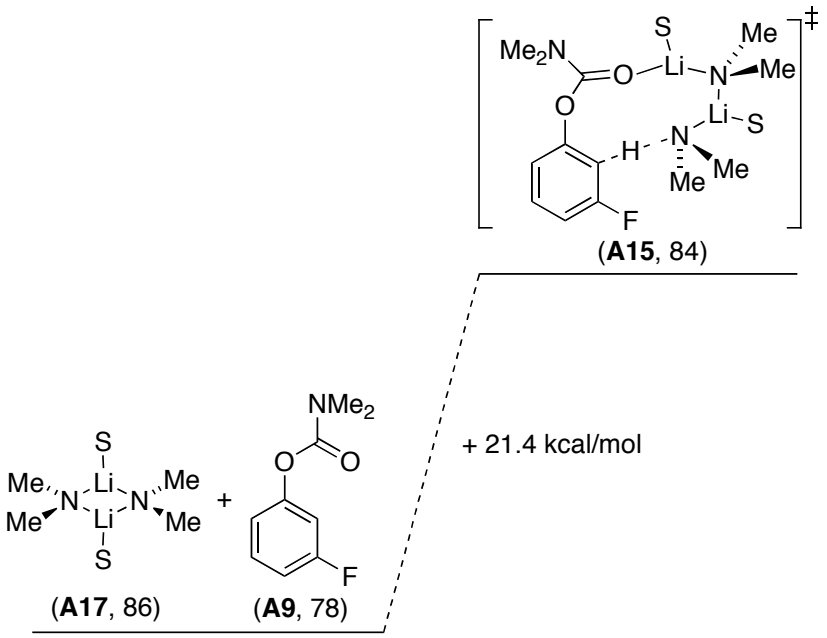

Figure A1.46. Relative free energy (ΔG, kcal/mol) at -78 °C. S = Me_2O. Free energy of activation for the deprotonation of arene **A9** leading to disolvated open dimer transition state **A15**.

Table A1.1. Optimized geometry at B3LYP level of theory with 6-31G(d) basis set, free energy (G, Hartrees), and cartesian coordinates (X, Y, Z).

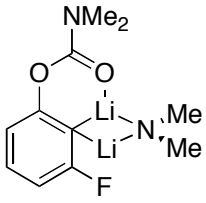

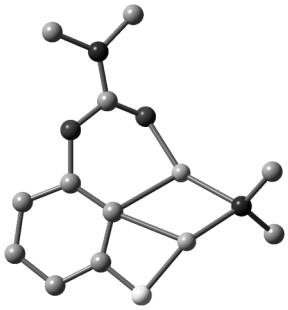

A1
G = -802.924566
(-78 °C)

Atom	X	Y	Z	Atom	X	Y	Z
Li	-0.624833	-1.264982	-0.498977	C	0.323528	1.510318	0.050073
C	-0.871734	0.820380	0.261375	O	1.604128	0.905222	0.218154
C	-1.948328	1.680260	0.159169	C	1.932116	-0.310103	-0.245768
F	-3.227229	1.079954	0.386587	O	1.177363	-1.056834	-0.886935
Li	-2.475195	-0.610438	0.852900	N	3.210726	-0.649116	0.058405
N	-2.164200	-2.336329	0.106435	C	3.753728	-1.913370	-0.420900
C	-3.129199	-2.808543	-0.874934	H	2.954214	-2.505743	-0.861142
H	-2.717933	-3.584660	-1.555059	H	4.531028	-1.736518	-1.175921
H	-4.032987	-3.262983	-0.417669	H	4.200352	-2.464817	0.414746
H	-3.475326	-1.979021	-1.510521	C	4.146801	0.238888	0.736967
C	-1.742229	-3.456690	0.933123	H	3.617760	1.084263	1.169355
H	-2.577592	-3.933625	1.487666	H	4.654790	-0.313205	1.535995
H	-1.266463	-4.275838	0.352241	H	4.907404	0.608949	0.036174
H	-1.007531	-3.130346	1.686519	H	1.408924	3.321532	-0.390750
C	-1.973935	3.038956	-0.108881	H	-0.669660	4.702647	-0.540916
C	-0.731081	3.641031	-0.320638	H	-2.904311	3.595664	-0.150377
C	0.431142	2.874105	-0.240424				

Table A1.1 (Continued).

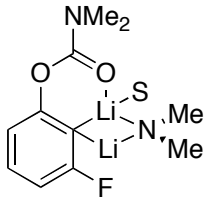

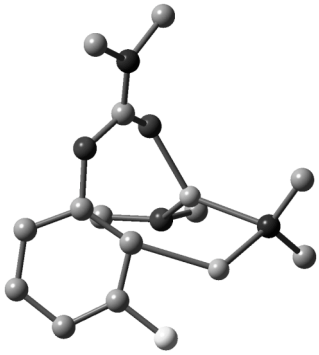

A2
G = -957.888979
(-78 °C)
S=Me_2O

Atom	X	Y	Z	Atom	X	Y	Z
Li	1.538805	-0.183019	-1.981520	C	-4.415377	-0.094867	-0.575358
N	1.666073	-1.961363	-1.314191	H	-4.064784	0.842440	-1.000513
Li	0.703742	-0.995534	0.177978	H	-4.904155	-0.684352	-1.359537
O	-1.138232	-0.959785	0.707347	H	-5.156415	0.119532	0.207124
C	-2.070747	-0.314963	0.213174	O	1.727461	-0.704333	1.875039
O	-2.017298	0.993112	-0.100623	C	2.378951	-1.794743	2.515117
C	-0.781402	1.691704	-0.201734	H	3.275037	-1.449512	3.049625
C	0.309780	1.141830	-0.868215	H	1.704690	-2.289451	3.229341
C	1.346826	2.046645	-0.956040	H	2.670543	-2.498200	1.734073
C	1.418322	3.346949	-0.478971	C	1.311681	0.302851	2.790907
C	0.281950	3.812040	0.190776	H	0.834292	1.091164	2.207850
C	-0.833047	2.982323	0.334515	H	0.595122	-0.101965	3.519418
H	-1.729852	3.330268	0.838847	H	2.178490	0.713942	3.326925
H	0.263044	4.821124	0.592492	C	2.976393	-2.540671	-1.090115
H	2.300014	3.963745	-0.620978	H	2.961902	-3.416003	-0.400280
F	2.492102	1.564152	-1.650048	H	3.460281	-2.916666	-2.017237
N	-3.293393	-0.852451	-0.036562	H	3.660271	-1.798557	-0.651468
C	-3.571078	-2.224216	0.364554	C	0.799713	-2.970133	-1.901016
H	-2.652128	-2.686367	0.719573	H	-0.201730	-2.555497	-2.095025
H	-4.323585	-2.247190	1.164337	H	0.658437	-3.861545	-1.249703
H	-3.957052	-2.791467	-0.490700	H	1.175032	-3.370897	-2.867507

Table A1.1 (Continued).

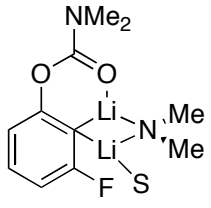

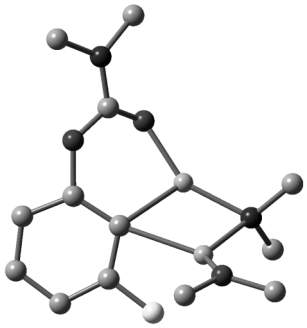

A3
G = -957.896696
(-78 °C)
S=Me_2O

Atom	X	Y	Z	Atom	X	Y	Z
Li	0.101372	-1.069732	-1.126766	H	-5.071450	-0.597213	1.431387
C	-0.067547	0.949959	-0.298910	H	-3.994617	-1.967080	1.012527
C	-0.962323	1.924352	-0.700360	C	-0.739622	3.275286	-0.926535
F	-2.296339	1.484919	-0.886546	C	0.570625	3.724325	-0.741736
Li	-1.957887	-0.336946	-0.057821	C	1.561041	2.825436	-0.344469
N	-1.637778	-1.958306	-1.104837	C	1.208406	1.488275	-0.138102
C	-2.376859	-2.044231	-2.352318	O	2.301321	0.716700	0.362837
H	-1.955034	-2.783345	-3.067929	C	2.579751	-0.526964	-0.057088
H	-3.439949	-2.344589	-2.215530	O	1.961910	-1.138995	-0.940209
H	-2.386504	-1.071217	-2.866779	N	3.645219	-1.063596	0.594456
C	-1.649870	-3.256977	-0.459562	C	4.132258	-2.381291	0.210338
H	-2.673954	-3.626942	-0.220716	H	3.422147	-2.842007	-0.473437
H	-1.190973	-4.063088	-1.072976	H	5.110677	-2.303663	-0.282643
H	-1.096350	-3.225813	0.492188	H	4.242432	-3.009494	1.102142
O	-3.015895	-0.282617	1.583646	C	4.448271	-0.337308	1.569538
C	-3.073652	0.854766	2.437046	H	3.930954	0.565434	1.884495
H	-2.159467	1.426907	2.268708	H	4.621068	-0.975677	2.443750
H	-3.947295	1.478026	2.201503	H	5.423988	-0.064186	1.144575
H	-3.124546	0.543563	3.489486	H	2.586099	3.150245	-0.192576
C	-4.151413	-1.134775	1.700562	H	0.817529	4.769231	-0.906273
H	-4.242596	-1.515850	2.726833	H	-1.540735	3.940030	-1.234024

Table A1.1 (Continued).

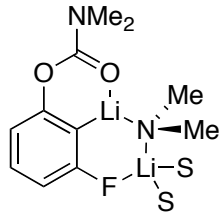

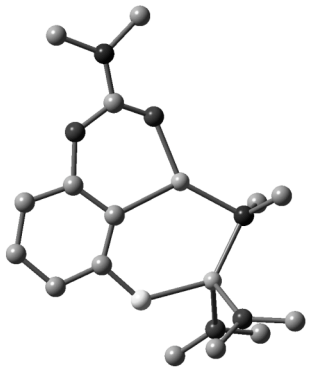

A4
G = -1112.856618
(-78 °C)
S=Me_2O

Atom	X	Y	Z	Atom	X	Y	Z
Li	-2.139629	-0.301924	0.033013	H	3.943651	-3.084066	-0.125256
F	-1.481740	1.619872	0.001697	H	5.454959	-2.717069	-0.996261
C	-0.103922	2.004807	-0.025467	H	5.475737	-2.914383	0.772766
C	0.820035	0.989392	0.013171	C	5.774750	-0.260664	0.263276
Li	0.545906	-1.050824	-0.148863	H	5.464729	0.736568	0.565154
N	-1.184801	-2.018456	-0.153130	H	6.431878	-0.680084	1.034027
C	-1.302077	-2.762453	-1.393663	H	6.346569	-0.189807	-0.673200
H	-0.457756	-3.465817	-1.574411	O	-3.176023	-0.088777	1.770866
H	-2.217109	-3.396255	-1.450311	C	-3.950951	-1.158419	2.294568
H	-1.335686	-2.078389	-2.254973	H	-3.741396	-2.035709	1.681426
C	-1.146525	-2.961173	0.949221	H	-3.670111	-1.370138	3.335854
H	-2.058432	-3.598725	1.026152	H	-5.024011	-0.919919	2.255564
H	-0.301656	-3.684792	0.890167	C	-3.319876	1.114060	2.515572
H	-1.045767	-2.432710	1.909231	H	-2.682931	1.857673	2.037918
O	2.389800	-1.423671	-0.278066	H	-3.000642	0.966159	3.556866
C	3.338872	-0.659673	-0.066605	H	-4.364825	1.457056	2.507209
O	3.287705	0.676127	0.024453	O	-3.497466	0.035579	-1.469338
C	2.115517	1.493254	-0.030195	C	-4.346249	-1.018961	-1.901243
C	2.460280	2.849150	-0.099839	H	-4.155775	-1.871370	-1.247788
C	1.436953	3.795195	-0.128479	H	-5.403009	-0.721948	-1.832841
C	0.103280	3.375289	-0.090083	H	-4.120032	-1.304461	-2.937874
H	-0.721894	4.081137	-0.111191	C	-3.604399	1.197834	-2.281176
H	1.674813	4.853975	-0.180496	H	-3.339743	0.970491	-3.323607
H	3.503352	3.151244	-0.129209	H	-4.626711	1.602205	-2.252465
N	4.612814	-1.123212	0.105286	H	-2.905828	1.929159	-1.876166
C	4.885353	-2.541472	-0.072794				

Table A1.1 (Continued).

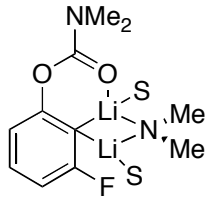

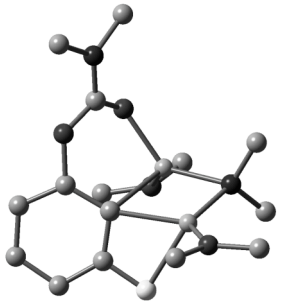

A5
G = -1112.861835
(-78 °C)
S=Me_2O

Atom	X	Y	Z
Li	1.880224	-0.378052	0.092888
Li	-0.121979	0.612900	1.175384
N	1.528840	-0.139946	2.000493
C	2.423041	0.720832	2.744092
H	2.609775	1.655555	2.195340
H	2.035917	1.009056	3.749945
H	3.418817	0.262848	2.950252
C	1.297489	-1.349824	2.762249
H	2.225575	-1.927677	2.984604
H	0.831068	-1.168328	3.757821
H	0.625493	-2.030802	2.216756
O	-1.881990	-0.174026	0.971351
C	-2.255949	-0.928194	0.066676
O	-2.005866	-0.741818	-1.242436
C	-1.061093	0.233434	-1.681736
C	0.206961	0.306319	-1.113323
C	0.991496	1.248137	-1.753254
F	2.295085	1.386249	-1.249614
C	0.656929	2.060362	-2.830646
C	-0.639587	1.920394	-3.335894
C	-1.516850	0.998362	-2.759331
H	-2.526348	0.868512	-3.138788
H	-0.963582	2.525553	-4.178133
H	1.367771	2.763246	-3.254508
N	-3.007202	-2.039870	0.294560
C	-3.459998	-2.332414	1.646478
H	-2.951639	-1.671113	2.345498
H	-4.545777	-2.187230	1.733220
H	-3.229455	-3.374511	1.897291
C	-3.525743	-2.896978	-0.762376
H	-3.038115	-2.664343	-1.705940
H	-3.334168	-3.946183	-0.507849
H	-4.610754	-2.763969	-0.875965
O	-0.475268	2.549401	1.583356
C	-0.675914	2.863779	2.955436
H	-0.433151	3.918068	3.150321
H	-1.717579	2.674995	3.254265
H	-0.004606	2.224331	3.530613
C	-1.290620	3.325546	0.713865
H	-1.049467	3.024524	-0.306421
H	-2.356856	3.144174	0.909661
H	-1.076529	4.396224	0.841607
O	3.129770	-1.701620	-0.605805
C	3.111519	-2.231079	-1.924558
H	2.284756	-1.748247	-2.448751
H	4.055255	-2.015960	-2.444811
H	2.950382	-3.318370	-1.904191
C	4.152799	-2.250694	0.216376
H	4.025866	-3.337295	0.320958
H	5.145301	-2.042117	-0.207126
H	4.060030	-1.776399	1.194627

Table A1.1 (Continued).

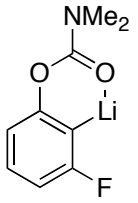

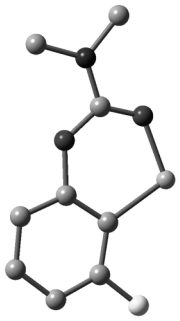

A6
G = -660.832717
(-78 °C)

Atom	X	Y	Z
C	-4.050422	-0.810708	0.018894
N	-2.916883	0.100402	-0.039833
C	-1.646760	-0.389793	0.001582
O	-0.735550	0.577240	0.012614
C	0.702804	0.459376	0.007660
C	1.378924	-0.751982	-0.006539
Li	0.220158	-2.346082	0.009898
O	-1.433154	-1.619433	0.023610
C	2.758669	-0.586646	-0.009757
F	3.533728	-1.718387	-0.022388
C	3.442592	0.624793	-0.000278
C	2.683796	1.799088	0.014527
C	1.292784	1.728781	0.018752
H	0.681193	2.626149	0.030590
H	3.177638	2.766977	0.022533
H	4.528269	0.646987	-0.003890
C	-3.239146	1.521228	-0.028479
H	-2.343606	2.110964	-0.204772
H	-3.971356	1.733765	-0.816522
H	-3.677429	1.811749	0.935945
H	-3.691487	-1.836878	-0.018726
H	-4.617623	-0.658480	0.946897
H	-4.721258	-0.627605	-0.829397

Table A1.1 (Continued).

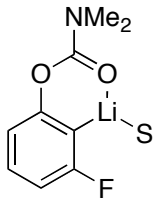

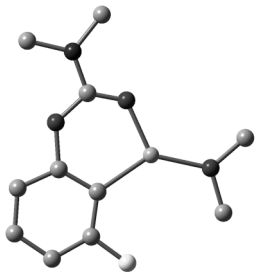

A7
G = -815.812997
(-78 °C)
S=Me_2O

Atom	X	Y	Z	Atom	X	Y	Z
C	3.665407	2.087935	0.010268	H	-2.371550	4.347358	0.960941
N	3.196836	0.713732	-0.072842	C	-1.945166	-1.759068	-0.041667
C	1.858108	0.448421	-0.001814	F	-3.223054	-1.229492	-0.094658
O	1.616280	-0.859669	0.021783	C	-1.877662	-3.147277	0.009208
C	0.340245	-1.531991	0.016297	C	-0.607433	-3.728926	0.067420
C	-0.878161	-0.871934	-0.042226	C	0.525681	-2.918842	0.071701
Li	-0.808469	1.135769	-0.022358	H	1.524027	-3.344600	0.116503
O	1.020616	1.366856	0.032510	H	-0.503079	-4.809827	0.108628
O	-2.137813	2.512625	0.005879	H	-2.781987	-3.748757	0.004145
C	-3.517188	2.134131	0.003650	C	4.225882	-0.316391	-0.047703
H	-4.023883	2.550039	-0.877589	H	3.795670	-1.282663	-0.298280
H	-3.544198	1.044156	-0.026981	H	5.001671	-0.067516	-0.781195
H	-4.012560	2.499290	0.913372	H	4.697649	-0.380473	0.943083
C	-1.932189	3.917832	0.050132	H	2.814222	2.762224	-0.056342
H	-0.853131	4.086842	0.051719	H	4.192388	2.263886	0.958563
H	-2.378233	4.404748	-0.827966	H	4.360241	2.295476	-0.812685

Table A1.1 (Continued).

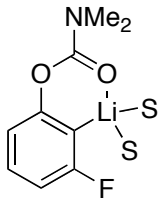

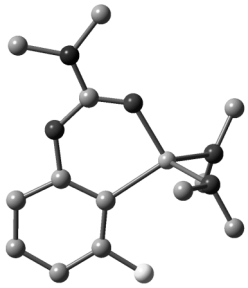

A8
G = -970.776834
(-78 °C)
S=Me_2O

Atom	X	Y	Z
Li	-0.679154	-0.966331	0.065571
C	-0.583232	1.086798	-0.000816
C	-1.615081	2.010361	-0.041095
F	-2.914226	1.515068	0.033591
C	-1.509014	3.392014	-0.159487
C	-0.220054	3.927614	-0.250246
C	0.885292	3.079426	-0.222582
C	0.654712	1.703212	-0.099819
O	1.904578	0.986015	-0.081619
C	2.081855	-0.333696	-0.020423
O	1.203993	-1.208978	-0.007913
N	3.411608	-0.657794	0.040554
C	3.809766	-2.055204	-0.007990
H	2.935430	-2.683056	0.152061
H	4.258848	-2.304571	-0.980317
H	4.551997	-2.256954	0.773869
C	4.485356	0.319119	-0.068485
H	4.111635	1.313964	0.160265
H	5.279300	0.062021	0.642543
H	4.918866	0.323910	-1.079101
H	1.896913	3.469293	-0.294248
H	-0.079640	5.001265	-0.343325
H	-2.393411	4.022512	-0.179768
O	-1.742115	-1.876755	-1.373794
C	-1.235574	-3.027579	-2.032935
H	-2.056753	-3.656572	-2.405615
H	-0.588518	-2.747454	-2.876369
H	-0.651684	-3.588689	-1.300137
C	-2.517227	-1.037504	-2.229675
H	-2.833119	-0.182319	-1.632139
H	-1.915463	-0.688961	-3.080227
H	-3.393092	-1.584839	-2.606602
O	-1.488737	-1.753750	1.743068
C	-0.832385	-1.225949	2.892809
H	-1.210551	-1.708686	3.805190
H	0.231184	-1.443435	2.777479
H	-0.976777	-0.139780	2.961147
C	-2.897122	-1.521137	1.772008
H	-3.315597	-2.027099	0.900290
H	-3.336153	-1.942182	2.687301
H	-3.114680	-0.447537	1.709269

Table A1.1 (Continued).

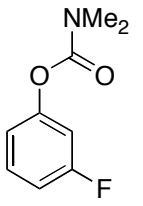

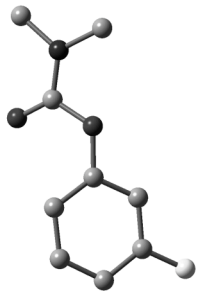

A9
G = -653.870377
(-78 °C)

Atom	X	Y	Z
C	-2.385163	1.644281	0.480605
C	-1.028254	1.322421	0.528044
C	-0.636544	0.022115	0.203143
C	-1.572098	-0.948119	-0.154763
C	-2.913428	-0.588360	-0.182096
C	-3.346010	0.695231	0.127355
F	-3.823469	-1.524927	-0.524631
O	0.675330	-0.423564	0.300089
C	1.709565	0.344587	-0.199865
O	1.551540	1.404106	-0.774601
N	2.910978	-0.253860	0.044331
C	3.084100	-1.544887	0.693488
C	4.117312	0.380955	-0.464035
H	-2.698880	2.654655	0.726342
H	-0.287744	2.065132	0.792055
H	-1.262163	-1.956625	-0.402632
H	-4.403688	0.932154	0.089851
H	3.464906	-2.289277	-0.019611
H	3.810881	-1.452879	1.510586
H	2.138108	-1.893876	1.099536
H	3.851159	1.336011	-0.914046
H	4.830631	0.547011	0.353261
H	4.599332	-0.254619	-1.219142

Table A1.1 (Continued).

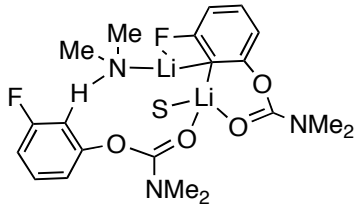

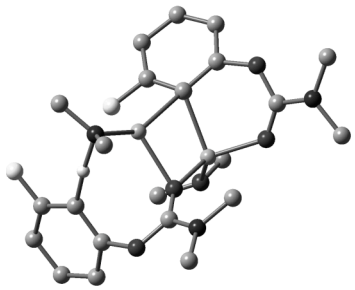

A10
G = -1611.747433
(-78 °C)
S=Me_2O

Atom	X	Y	Z	Atom	X	Y	Z
Li	-0.982916	0.069237	-1.045221	H	-4.735432	3.560401	-0.214930
O	0.489335	1.094149	-0.303090	C	-5.662755	1.267694	0.987459
C	1.167285	2.140222	-0.220919	H	-6.601569	0.982466	0.492960
O	2.484168	2.190700	-0.412807	H	-5.379760	0.488533	1.691110
C	3.243811	0.988811	-0.613460	H	-5.831511	2.201438	1.535088
C	3.315935	0.051995	0.404318	C	-3.454331	-2.865359	0.607454
C	4.146759	-1.019038	0.099569	C	-2.655180	-4.005693	0.703373
C	4.873028	-1.162321	-1.081779	C	-1.262771	-3.883878	0.687125
C	4.761590	-0.163858	-2.052148	C	-0.757531	-2.596213	0.565368
C	3.932276	0.936752	-1.825653	F	0.638519	-2.471838	0.551559
H	3.829106	1.732004	-2.558386	H	-0.606307	-4.744406	0.769214
H	5.320459	-0.241612	-2.980696	H	-3.115260	-4.985299	0.796402
H	5.508614	-2.030629	-1.228485	H	-4.537968	-2.934383	0.625098
F	4.272257	-2.019059	1.018312	N	1.658072	0.052566	2.579456
N	0.623375	3.349872	0.049115	C	2.066884	-1.032191	3.459743
C	1.431999	4.543598	0.285026	H	2.158348	-1.963092	2.886679
H	0.967679	5.396456	-0.221699	H	3.048260	-0.846936	3.940787
H	1.491655	4.762908	1.358965	H	1.343884	-1.211664	4.276978
H	2.436532	4.397212	-0.103305	C	1.677539	1.313113	3.293850
C	-0.790147	3.453478	0.391170	H	0.938103	1.354822	4.116110
H	-1.342247	2.614191	-0.027855	H	2.663216	1.538756	3.750935
H	-0.929629	3.467039	1.480501	H	1.442889	2.145695	2.612598
H	-1.185875	4.386143	-0.024163	O	-0.431937	-0.810187	-2.729097
Li	0.445000	-0.396247	1.137625	C	-1.422625	-1.651002	-3.314486
C	-1.452778	-1.403123	0.471651	H	-1.193739	-1.831659	-4.373604
C	-2.826653	-1.620972	0.499568	H	-1.480166	-2.610927	-2.783911
O	-3.764125	-0.540378	0.508188	H	-2.377086	-1.128548	-3.229141
C	-3.638204	0.550203	-0.256134	C	0.876028	-1.387455	-2.787776
O	-2.770558	0.722877	-1.127447	H	0.907055	-2.332419	-2.231145
N	-4.598592	1.476166	0.012213	H	1.162739	-1.564934	-3.832906
C	-4.722500	2.654810	-0.833381	H	1.565331	-0.676218	-2.332802
H	-3.880399	2.694898	-1.521528	H	2.565551	0.095598	1.543904
H	-5.656726	2.618316	-1.409915				

Table A1.1 (Continued).

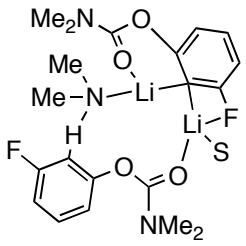

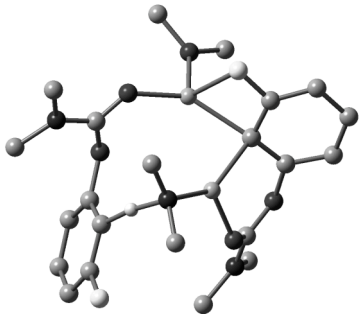

A11
G = -1611.735290
(-78 °C)
S=Me_2O

Atom	X	Y	Z	Atom	X	Y	Z
Li	-1.321363	-1.747387	-0.313956	C	-1.535831	4.021621	-2.193091
O	0.320680	-2.663494	-0.176337	H	-4.846744	2.404403	0.558302
C	1.443795	-2.232624	-0.490336	H	-6.122799	0.592058	1.719466
O	1.502108	-1.127200	-1.266912	H	-5.030233	-1.652158	2.063418
C	2.385697	-0.032233	-1.012581	H	0.877064	3.897978	0.189259
C	2.624460	0.393034	0.288261	H	1.177278	3.842269	-1.561596
C	3.482769	1.487743	0.348433	H	0.444613	5.297183	-0.832532
C	4.055742	2.131027	-0.747278	H	-1.562601	5.114912	-2.273585
C	3.745019	1.658560	-2.024411	H	-1.014883	3.624056	-3.074526
C	2.900535	0.557472	-2.169736	H	-2.554042	3.640291	-2.178833
F	3.793475	1.995586	1.575033	H	4.461005	-1.915372	0.031261
N	2.583870	-2.878952	-0.169988	H	4.457752	-3.472773	-0.844074
C	2.537259	-3.999168	0.766401	H	3.834442	-2.008400	-1.626936
C	3.909342	-2.539178	-0.680075	H	1.514695	-4.145720	1.105342
O	-2.205063	-2.459423	-1.920809	H	2.892966	-4.912604	0.273865
C	-1.882846	-3.750620	-2.425102	H	3.179834	-3.787643	1.628526
C	-3.346593	-1.882030	-2.544861	H	1.886211	0.075857	1.370988
C	-2.411794	-0.035663	0.478884	H	2.647758	0.159098	-3.148349
Li	-0.514306	0.579214	1.483723	H	4.169566	2.138460	-2.902173
N	1.022255	-0.041176	2.479385	H	4.719951	2.976660	-0.595626
C	1.183552	-1.370806	3.039028	H	0.651088	-1.493614	4.000528
C	1.505833	0.950873	3.434510	H	0.781305	-2.124915	2.352431
O	-0.683010	2.372066	0.916285	H	2.245783	-1.629650	3.242680
C	-1.300121	2.716090	-0.097724	H	1.407889	1.959831	3.014848
O	-2.514910	2.234503	-0.438542	H	0.939469	0.926449	4.383749
C	-3.093644	1.171596	0.307647	H	2.572742	0.812666	3.696364
C	-4.398456	1.431096	0.733805	H	-0.999066	-4.088424	-1.882223
C	-5.107015	0.414243	1.378087	H	-2.713107	-4.451365	-2.259721
C	-4.510241	-0.833112	1.576668	H	-1.661616	-3.701699	-3.500352
C	-3.206705	-0.971479	1.117863	H	-4.234312	-2.511077	-2.391647
F	-2.628117	-2.245819	1.263227	H	-3.503885	-0.908244	-2.079379
N	-0.839571	3.644045	-0.971141	H	-3.173966	-1.757689	-3.622915
C	0.494294	4.203017	-0.782307				

Table A1.1 (Continued).

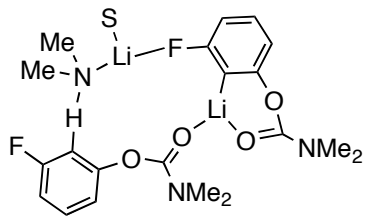

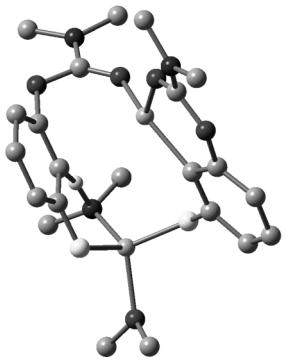

A12
G = -1611.750819
(-78 °C)
S=Me_2O

Atom	X	Y	Z	Atom	X	Y	Z
Li	0.999573	0.610510	-0.627879	H	6.086156	1.855696	-0.177271
O	0.191034	2.263591	-1.135255	C	5.973882	-0.832972	0.519235
C	-0.446730	3.173712	-0.599983	H	5.539042	-1.829227	0.541611
O	-0.704981	3.230254	0.728853	H	6.709444	-0.781731	-0.296551
C	-0.470694	2.060544	1.491656	H	6.498270	-0.650198	1.464312
C	-1.194165	0.909200	1.205325	C	2.635347	-3.384945	-1.228417
C	-0.891649	-0.150509	2.035097	C	1.589727	-4.192009	-1.670837
C	0.003370	-0.143514	3.095139	C	0.295859	-3.665768	-1.739806
C	0.676516	1.056732	3.344253	C	0.148629	-2.340345	-1.352743
C	0.451630	2.172148	2.532629	F	-1.191709	-1.860382	-1.438850
H	0.975598	3.108006	2.702208	Li	-2.468638	-1.446791	-0.101181
H	1.385179	1.118351	4.165034	N	-3.325499	0.292769	-0.380637
H	0.172643	-1.031977	3.695218	C	-4.486162	0.757885	0.351986
F	-1.556018	-1.355760	1.772089	H	-4.445547	0.403411	1.392756
H	-2.194628	0.730250	0.353053	H	-4.564429	1.865291	0.390511
N	-0.929968	4.246015	-1.271827	H	-5.444795	0.403728	-0.076953
C	-0.729385	4.338993	-2.711272	C	-3.304872	0.862491	-1.714541
H	-0.052398	3.549117	-3.030861	H	-4.163501	0.540357	-2.335493
H	-1.685778	4.230305	-3.238632	H	-3.333417	1.974725	-1.712379
H	-0.299783	5.316064	-2.963575	H	-2.390791	0.559043	-2.240814
C	-1.768001	5.272966	-0.667010	O	-3.441493	-3.133063	0.247004
H	-1.827589	5.123614	0.408078	C	-4.812763	-3.063456	0.622377
H	-1.344138	6.264029	-0.870977	H	-5.206357	-2.132614	0.211828
H	-2.779775	5.234768	-1.091259	H	-5.368618	-3.916988	0.210436
C	1.102368	-1.450780	-0.912555	H	-4.918760	-3.057599	1.716486
C	2.354196	-2.059885	-0.870223	C	-2.783875	-4.293840	0.742711
O	3.541000	-1.409902	-0.407221	H	-2.798904	-4.313085	1.841388
C	3.695053	-0.102136	-0.167064	H	-3.266850	-5.203061	0.358859
O	2.863673	0.788922	-0.372825	H	-1.751230	-4.254840	0.390860
N	4.930181	0.168145	0.353200	H	-0.546895	-4.253044	-2.092571
C	5.328085	1.552075	0.558711	H	1.778947	-5.221408	-1.962049
H	4.455268	2.193954	0.457210	H	3.649933	-3.767276	-1.161922
H	5.755378	1.670030	1.561874				

Table A1.1 (Continued).

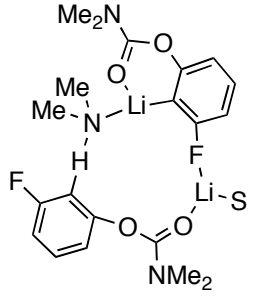

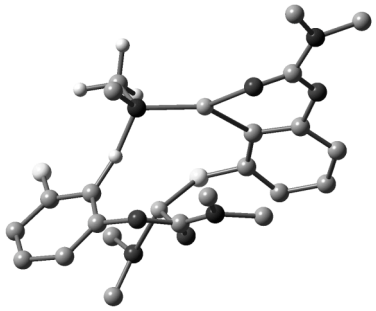

A13
G = -1611.744505
(-78 °C)
S=Me_2O

Atom	X	Y	Z
C	0.564709	-0.712537	-3.126678
N	0.305432	-1.310002	-1.822236
Li	-1.322245	-0.545890	-1.066903
C	-1.836095	1.392537	-0.525336
C	-3.098557	1.623133	0.009376
O	-4.183099	0.701077	-0.149614
C	-4.045017	-0.608511	-0.400433
O	-2.983134	-1.247162	-0.380425
N	-5.243651	-1.202445	-0.667666
C	-5.298498	-2.636312	-0.907713
H	-4.286746	-3.036577	-0.923444
H	-5.876610	-3.137274	-0.119195
H	-5.784080	-2.837142	-1.870809
C	-6.521185	-0.503964	-0.665619
H	-7.048047	-0.695542	-1.608703
H	-7.154262	-0.860748	0.158538
H	-6.363811	0.565861	-0.557046
C	-3.501090	2.773641	0.696293
C	-2.570186	3.798156	0.872832
C	-1.272971	3.650718	0.370642
C	-1.005425	2.457472	-0.285345
F	0.346210	2.338476	-0.761105
Li	1.584505	1.161305	0.040247
O	1.090511	0.338606	1.663404
C	0.846702	-0.862163	1.853206
O	1.705175	-1.854340	1.516290
C	2.850684	-1.536617	0.754950
C	2.703696	-0.923119	-0.489355
C	3.900106	-0.725801	-1.169341
C	5.155095	-1.103195	-0.697451
C	5.228390	-1.726681	0.550253
C	4.068499	-1.938515	1.298648
H	4.100591	-2.414836	2.273597
H	6.191169	-2.042205	0.942146
H	6.040651	-0.920723	-1.298575
F	3.859559	-0.090618	-2.376807
N	-0.273704	-1.316042	2.449133
C	-0.594145	-2.730306	2.609818
H	-1.477394	-2.978981	2.009434
H	0.242424	-3.345825	2.289119
H	-0.815104	-2.939162	3.663710
C	-1.305906	-0.372669	2.868100
H	-2.220358	-0.547478	2.292140
H	-1.517556	-0.510280	3.935559
H	-0.963926	0.643807	2.687573
O	3.089978	2.417227	0.129795
C	4.145422	2.192943	1.061745
H	4.922654	1.554114	0.624094
H	4.585021	3.149305	1.375259
H	3.704110	1.690580	1.923981
C	3.525399	3.068766	-1.063189
H	3.997168	4.030517	-0.821777
H	4.231143	2.435980	-1.615278
H	2.635412	3.243565	-1.670020
H	-0.519480	4.423878	0.486908
H	-2.852366	4.707095	1.396658
H	-4.515336	2.865306	1.074870
C	0.402683	-2.757466	-1.927993
H	-0.327122	-3.189391	-2.641433
H	1.401715	-3.105953	-2.267008
H	0.216131	-3.225084	-0.950680
H	0.464384	0.380581	-3.068174
H	1.582615	-0.929092	-3.510570
H	-0.139221	-1.060644	-3.909015
H	1.581696	-0.951520	-1.055359

Table A1.1 (Continued).

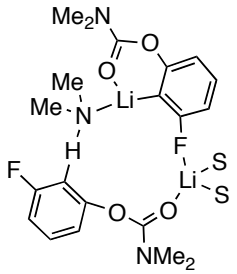

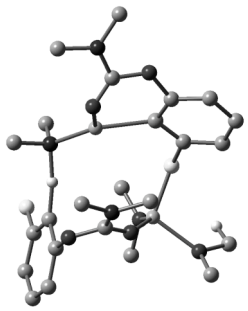

A14
G = -1766.702728
(-78 °C)
S=Me_2O

Atom	X	Y	Z	Atom	X	Y	Z
Li	1.743046	1.541289	-0.166678	H	-6.087829	-2.927402	0.974526
O	1.274767	0.701012	1.443227	H	-5.843922	-3.371633	-0.731529
C	0.733729	-0.264780	2.007190	C	-6.642282	-0.774039	-0.691389
N	-0.457241	-0.186180	2.642251	H	-7.053714	-1.331144	-1.542478
C	-1.176857	1.079068	2.707714	H	-7.375645	-0.806828	0.125931
H	-2.131270	0.996507	2.178449	H	-6.482489	0.259500	-0.986987
H	-1.367856	1.340268	3.756687	N	-0.234429	-2.354434	-1.142640
H	-0.584347	1.860361	2.237725	C	0.005525	-2.476815	-2.576115
C	-1.138895	-1.335730	3.230693	H	0.197162	-1.486816	-3.012810
H	-0.514845	-2.221972	3.150045	H	0.880220	-3.113564	-2.813812
H	-1.350280	-1.136991	4.289086	H	-0.857416	-2.908794	-3.117820
H	-2.083816	-1.508035	2.703043	C	-0.551607	-3.665567	-0.592420
O	1.292902	-1.481603	2.091977	H	-1.464975	-4.106648	-1.034270
C	2.440521	-1.778551	1.296649	H	0.259768	-4.406516	-0.746384
C	2.256021	-2.044128	-0.053197	H	-0.716089	-3.590115	0.491266
C	3.424671	-2.431636	-0.692594	H	-4.710623	3.016550	-0.040311
C	4.675449	-2.558898	-0.090632	H	-3.044190	4.880127	-0.190424
C	4.780078	-2.273948	1.273472	H	-0.664716	4.336685	-0.813383
C	3.649195	-1.871184	1.986172	O	3.046982	1.240311	-1.631254
H	3.696276	-1.653524	3.049329	C	4.440209	1.131516	-1.350536
H	5.737616	-2.369444	1.778105	H	4.626001	1.702342	-0.438260
H	5.532429	-2.885778	-0.672878	H	4.727896	0.085593	-1.194485
F	3.370515	-2.701695	-2.039562	H	5.030371	1.556581	-2.174897
F	0.252872	1.989983	-1.282918	C	2.669996	0.552631	-2.830500
C	-1.121021	2.223169	-0.953976	H	1.593056	0.682787	-2.938741
C	-1.419145	3.560432	-0.723320	H	3.185717	0.996727	-3.693458
C	-2.742216	3.854291	-0.382074	H	2.910193	-0.512353	-2.758864
C	-3.673685	2.819647	-0.297567	O	2.523886	3.279566	0.482055
C	-3.245074	1.514736	-0.564889	C	2.441199	3.699381	1.839865
C	-1.950798	1.128093	-0.910111	H	2.232092	2.807243	2.430344
Li	-1.497674	-0.923391	-0.707180	H	3.389464	4.151475	2.162383
O	-3.168247	-1.230075	0.245099	H	1.631723	4.430931	1.973276
C	-4.209474	-0.696193	-0.159264	C	2.755801	4.353748	-0.420908
O	-4.335221	0.589332	-0.524596	H	2.815592	3.919249	-1.419687
N	-5.385562	-1.375649	-0.268931	H	1.934728	5.083281	-0.381286
C	-5.438674	-2.782313	0.100309	H	3.699294	4.864532	-0.182420
H	-4.434313	-3.130065	0.333750	H	1.026204	-2.103495	-0.607138

Table A1.1 (Continued).

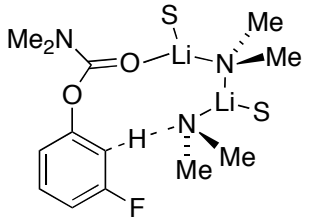

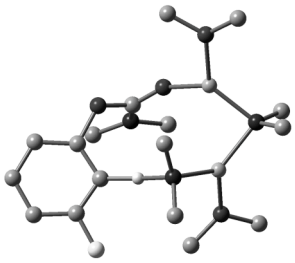

A15
G = -1247.905576
(-78 °C)
S=Me_2O
See pg S69

Atom	X	Y	Z	Atom	X	Y	Z
C	-4.597855	-0.432083	-1.063330	H	0.977044	0.414029	2.697038
C	-4.607581	-1.712094	-0.503362	H	-0.476131	1.256072	3.291076
C	-3.444745	-2.233715	0.065548	H	0.209083	-0.103771	4.217827
C	-2.290570	-1.449118	0.038822	H	-2.177145	-0.731798	4.020502
C	-2.189830	-0.190360	-0.542405	H	-2.834422	0.014311	2.537269
C	-3.394535	0.267480	-1.062174	H	-2.596922	-1.742981	2.624618
F	-3.404718	1.515593	-1.628318	H	-0.234598	-0.955136	-3.037196
O	-1.138714	-2.047064	0.638482	H	1.436825	-0.367651	-2.975350
C	-0.299246	-1.301118	1.394072	H	0.733064	-1.241939	-1.589765
N	-0.816326	-0.635148	2.451557	H	-0.774456	2.580302	-2.395152
C	-2.188667	-0.780672	2.926523	H	0.396242	1.894333	-3.538997
C	0.025476	0.284936	3.207981	H	-1.233650	1.207153	-3.413666
O	0.915560	-1.325007	1.151811	H	3.388022	1.074898	-2.062303
Li	2.398435	-0.820431	0.108489	H	4.104754	2.451035	-1.194784
N	3.049527	1.018122	0.019750	H	4.879649	0.869234	-1.114411
C	3.880547	1.363136	-1.122160	H	3.143936	1.174699	2.122574
Li	1.215913	1.628048	-0.434855	H	4.728570	0.915079	1.364548
N	0.059858	0.745951	-1.763305	H	3.969966	2.503963	1.281395
C	0.520455	-0.495161	-2.367862	H	5.248270	-3.196620	-0.493276
C	-0.404347	1.638027	-2.819280	H	4.521527	-2.808903	-2.083318
O	0.338493	3.139843	0.494997	H	5.004878	-1.489681	-0.976163
C	-1.040193	3.483761	0.365008	H	1.655848	-3.559420	0.007651
C	1.119894	4.193043	1.047021	H	2.503592	-4.066299	-1.486714
C	3.742314	1.414068	1.230221	H	3.199427	-4.464928	0.115214
O	3.302846	-2.458300	-0.431246	H	-1.471147	3.704603	1.352059
C	4.592742	-2.498526	-1.031841	H	-1.159045	4.364909	-0.280470
C	2.631447	-3.716011	-0.453468	H	-1.553895	2.632345	-0.081232
H	-1.062824	0.348254	-1.013596	H	2.147582	3.832115	1.108961
H	-5.523221	-2.296986	-0.499432	H	1.078074	5.086674	0.408313
H	-3.430168	-3.219523	0.522128	H	0.761447	4.457045	2.052231
H	-5.489490	0.009577	-1.497865				

Table A1.1 (Continued).

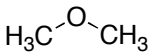

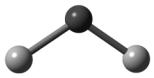

A16
G = -154.959965
(-78 °C)
See pg S66,67,68

Atom	X	Y	Z	Atom	X	Y	Z
O	-0.000002	-0.590096	0.000019	H	-1.231078	0.841249	-0.891928
C	1.170987	0.195373	-0.000004	H	1.232122	0.839832	0.892886
C	-1.170983	0.195373	0.000003	H	2.021832	-0.491270	0.000142
H	-2.021833	-0.491263	-0.002201	H	1.232128	0.839577	-0.893071
H	-1.233173	0.838164	0.894024				

Table A1.1 (Continued).

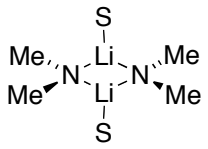

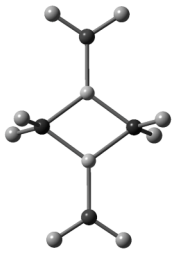

A17
G = -594.069311
(-78 °C)
S=Me_2O
See pg S69

Atom	X	Y	Z	Atom	X	Y	Z
N	-0.000649	1.589387	0.003319	H	4.444149	-1.235814	-0.932190
Li	-1.176636	-0.000012	-0.097348	H	-0.732842	-3.107130	-1.337374
Li	1.177294	0.000852	0.102285	H	1.020614	-3.108821	-1.132982
N	0.000692	-1.588611	0.003054	H	0.242525	-1.820982	-2.078905
O	-3.110978	-0.000835	-0.088970	H	-1.022193	3.107662	1.140457
O	3.111475	0.000403	0.084379	H	0.731236	3.107385	1.345242
C	3.885448	1.192440	0.011343	H	-0.243116	1.819717	2.085447
C	3.883735	-1.192812	0.012062	H	-0.734691	3.108634	-1.336048
C	0.134913	2.432935	-1.166776	H	0.242004	1.823917	-2.078285
C	-0.137300	2.430602	1.175038	H	1.018639	3.111461	-1.130712
C	-0.135087	-2.430971	1.173991	H	-4.585224	-1.252312	-0.863099
C	0.136335	-2.430962	-1.167926	H	-4.449062	-1.235266	0.922615
C	-3.884344	1.191814	-0.020739	H	-3.181288	-2.027104	-0.063311
C	-3.884231	-1.193467	-0.019058	H	-4.449252	1.234885	0.920844
H	3.183423	2.026686	0.058562	H	-3.181463	2.025447	-0.066048
H	4.446346	1.233824	-0.932697	H	-4.585319	1.249439	-0.864880
H	4.590033	1.250584	0.852423	H	-0.241535	-1.821014	2.084943
H	3.180515	-2.025986	0.060318	H	0.734114	-3.107076	1.343657
H	4.588608	-1.251189	0.852886	H	-1.019284	-3.108935	1.138825

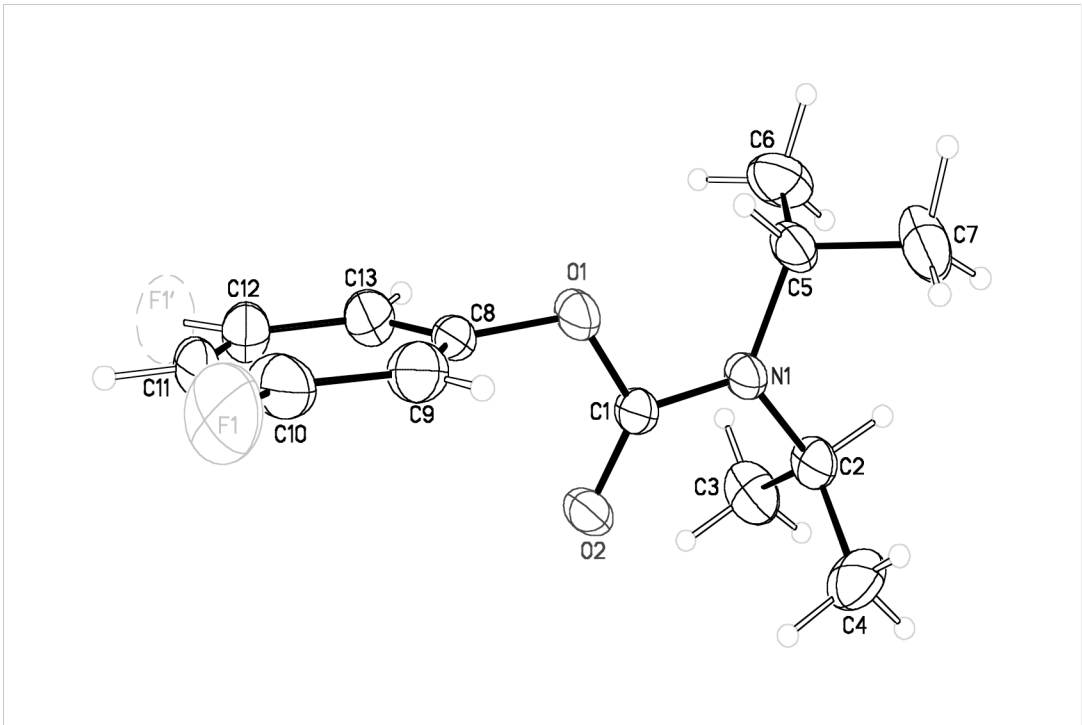

Figure A1.47. ORTEP of **1** revealing the orientation of the carbonyl group (C1-O2) relative to the *N,N*-diisopropyl groups (C2-C4 and C5-C7). The *meta* fluorine (F1) shows disorder between the two *meta* positions.

Table A1.2. Crystal data and structure refinement for **1**.

Identification code	**1**
Empirical formula	C13 H17 F N O2
Formula weight	238.28
Temperature	173(2) K
Wavelength	0.71073 Å
Crystal system	Monoclinic
Space group	P2(1)/c
Unit cell dimensions	a = 10.7977(4) Å α = 90°.
	b = 11.3149(5) Å β = 116.2230(10)°.
	c = 11.9339(5) Å γ = 90°.
Volume	1307.96(9) $Å^3$
Z	4
Density (calculated)	1.210 Mg/m^3
Absorption coefficient	0.091 mm^{-1}
F(000)	508
Crystal size	0.40 x 0.30 x 0.10 mm^3
Theta range for data collection	2.10 to 28.31°.
Index ranges	-14<=h<=11, -14<=k<=15, -15<=l<=15
Reflections collected	16281
Independent reflections	3231 [R(int) = 0.0298]
Completeness to theta = 28.31°	99.7 %
Absorption correction	Semi-empirical from equivalents
Max. and min. transmission	0.9910 and 0.9647
Refinement method	Full-matrix least-squares on F^2
Data / restraints / parameters	3231 / 0 / 232
Goodness-of-fit on F^2	1.058
Final R indices [I>2sigma(I)]	R1 = 0.0415, wR2 = 0.1163
R indices (all data)	R1 = 0.0612, wR2 = 0.1267
Largest diff. peak and hole	0.184 and -0.233 $e.Å^{-3}$

Table A1.3. Atomic coordinates (x 10^4) and equivalent isotropic displacement parameters ($Å^2$x 10^3) for **1**. U(eq) is defined as one third of the trace of the orthogonalized U^{ij} tensor.

	x	y	z	U(eq)
F(1)	1435(2)	317(1)	4340(2)	101(1)
F(1')	-433(4)	851(3)	463(3)	99(1)
O(1)	2238(1)	3971(1)	2884(1)	47(1)
O(2)	3982(1)	3358(1)	2471(1)	49(1)
N(1)	3750(1)	5307(1)	2820(1)	35(1)
C(1)	3398(1)	4167(1)	2698(1)	35(1)
C(2)	4960(1)	5677(1)	2626(1)	43(1)
C(3)	4806(2)	5384(1)	1335(2)	59(1)
C(4)	6297(2)	5214(2)	3645(2)	64(1)
C(5)	2902(1)	6241(1)	2996(1)	45(1)
C(6)	2073(2)	6884(2)	1780(2)	71(1)
C(7)	3752(2)	7083(2)	4039(2)	67(1)
C(8)	1722(1)	2825(1)	2694(1)	44(1)
C(9)	1974(2)	2129(1)	3709(2)	59(1)
C(10)	1349(2)	1022(1)	3470(2)	80(1)
C(11)	527(2)	618(1)	2292(2)	81(1)
C(12)	296(2)	1348(2)	1309(2)	76(1)
C(13)	880(2)	2458(1)	1492(2)	57(1)

Table A1.4. Bond lengths [Å] and angles [°] for **1**.

F(1)-C(10)	1.279(2)
F(1')-C(12)	1.118(3)
O(1)-C(1)	1.3827(13)
O(1)-C(8)	1.3906(13)
O(2)-C(1)	1.2086(13)
N(1)-C(1)	1.3348(13)
N(1)-C(5)	1.4725(14)
N(1)-C(2)	1.4838(14)
C(2)-C(3)	1.512(2)
C(2)-C(4)	1.512(2)
C(5)-C(6)	1.513(2)
C(5)-C(7)	1.513(2)
C(8)-C(9)	1.367(2)
C(8)-C(13)	1.380(2)
C(9)-C(10)	1.391(2)
C(10)-C(11)	1.368(3)
C(11)-C(12)	1.365(3)
C(12)-C(13)	1.379(2)
C(1)-O(1)-C(8)	116.72(8)
C(1)-N(1)-C(5)	122.98(9)
C(1)-N(1)-C(2)	118.89(9)
C(5)-N(1)-C(2)	117.75(9)
O(2)-C(1)-N(1)	127.24(10)
O(2)-C(1)-O(1)	120.95(9)
N(1)-C(1)-O(1)	111.80(9)
N(1)-C(2)-C(3)	112.93(11)
N(1)-C(2)-C(4)	111.77(11)
C(3)-C(2)-C(4)	112.29(13)
N(1)-C(5)-C(6)	110.45(11)
N(1)-C(5)-C(7)	112.33(12)
C(6)-C(5)-C(7)	111.91(13)
C(9)-C(8)-C(13)	121.97(13)

Table A1.4 (Continued).

C(9)-C(8)-O(1)	118.96(13)
C(13)-C(8)-O(1)	118.86(12)
C(8)-C(9)-C(10)	116.66(18)
F(1)-C(10)-C(11)	114.02(17)
F(1)-C(10)-C(9)	122.7(2)
C(11)-C(10)-C(9)	123.13(17)
C(12)-C(11)-C(10)	118.12(14)
F(1')-C(12)-C(11)	105.1(3)
F(1')-C(12)-C(13)	133.7(3)
C(11)-C(12)-C(13)	121.16(19)
C(12)-C(13)-C(8)	118.94(17)

Table A1.5. Symmetry transformations used to generate equivalent atoms: Anisotropic displacement parameters ($Å^2 x\ 10^3$) for **1**. The anisotropic displacement factor exponent takes the form: $-2\pi^2[\ h^2\ a^{*2}U^{11} + ... + 2\ h\ k\ a^*\ b^*\ U^{12}\ ]$.

	U^{11}	U^{22}	U^{33}	U^{23}	U^{13}	U^{12}
F(1)	101(1)	68(1)	126(1)	50(1)	43(1)	-8(1)
F(1')	92(2)	92(2)	99(2)	-59(2)	30(2)	-36(2)
O(1)	48(1)	27(1)	84(1)	-8(1)	45(1)	-7(1)
O(2)	48(1)	27(1)	88(1)	-1(1)	45(1)	1(1)
N(1)	38(1)	25(1)	50(1)	-1(1)	26(1)	-3(1)
C(1)	34(1)	28(1)	47(1)	1(1)	22(1)	-1(1)
C(2)	46(1)	31(1)	63(1)	1(1)	34(1)	-7(1)
C(3)	80(1)	45(1)	75(1)	0(1)	57(1)	-8(1)
C(4)	41(1)	61(1)	90(1)	6(1)	29(1)	-10(1)
C(5)	52(1)	27(1)	69(1)	-6(1)	39(1)	-3(1)
C(6)	70(1)	49(1)	93(1)	11(1)	35(1)	21(1)
C(7)	94(1)	46(1)	84(1)	-25(1)	60(1)	-21(1)
C(8)	36(1)	26(1)	81(1)	-3(1)	37(1)	-3(1)
C(9)	52(1)	44(1)	90(1)	12(1)	39(1)	1(1)
C(10)	75(1)	41(1)	151(2)	26(1)	76(1)	6(1)
C(11)	62(1)	35(1)	174(2)	-19(1)	78(1)	-14(1)
C(12)	58(1)	49(1)	138(2)	-33(1)	57(1)	-17(1)
C(13)	53(1)	43(1)	83(1)	-12(1)	38(1)	-6(1)

Table A1.6. Hydrogen coordinates (x 10^4) and isotropic displacement parameters ($Å^2$x 10^3) for **1**.

	x	y	z	U(eq)
H(2)	4972(12)	6536(12)	2701(11)	35(3)
H(3C)	3870(20)	5670(17)	677(18)	88(6)
H(3B)	4817(17)	4537(15)	1219(15)	66(4)
H(3A)	5532(19)	5766(15)	1197(16)	75(5)
H(4C)	6360(17)	4350(17)	3581(15)	70(5)
H(4A)	6330(20)	5409(17)	4461(19)	84(6)
H(4A)	7070(20)	5530(16)	3517(17)	87(6)
H(5)	2289(14)	5838(12)	3237(12)	44(3)
H(6C)	1470(20)	6320(20)	1120(20)	107(7)
H(6B)	2681(17)	7291(14)	1509(14)	58(4)
H(6A)	1463(19)	7461(17)	1909(16)	82(5)
H(7C)	4322(19)	6665(16)	4820(17)	80(6)
H(7B)	3060(20)	7622(19)	4160(18)	94(6)
H(7A)	4374(18)	7609(15)	3808(15)	71(5)
H(9)	2560(20)	2386(16)	4537(17)	81(6)
H(11)	130(20)	-150(20)	2173(19)	98(6)
H(13)	704(19)	3027(17)	767(18)	91(6)

REFERENCES

1. (a) Bakker, W. I. I.; Wong, P. L.; Snieckus, V. Lithium Diisopropylamide. In *e-EROS*; Paquette, L. A., Ed.; John Wiley: New York, 2001. (b) Clayden, J. "Organolithiums: Selectivity for Synthesis"; Baldwin, J. E., Williams, R. M., Eds.; Pergamon: New York, 2002.

2. For a review summarizing rate studies of LDA-mediated reactions: Collum, D. B.; McNeil, A. J.; Ramirez, A. *Angew. Chem., Int. Ed.* **2007**, *46*, 3002.

3. (a) Hartung, C. G.; Snieckus, V. in *Modern Arene Chemistry*, Astruc, D. (Ed.), Wiley-VCH, Weinheim, 2002; Chapter 10. (b) MacNeil, S. L.; Wilson, B. J.; Snieckus, V. *Org. Lett.* **2006**, *8*, 1133.

4. Reviews of ortholithiation: (a) Snieckus, V. *Chem. Rev.* **1990**, *90*, 879. (b) Gschwend, H. W.; Rodriguez, H. R. *Organic React.* **1979**, *26*, 1. Also, see ref 8.

5. (a) Sun, X.; Collum, D. B. *J. Am. Chem. Soc.* **2000**, *122*, 2459. (b) Ramirez, A.; Sun, X.; Collum, D. B. *J. Am. Chem. Soc.* **2006**, *128*, 10326.

6. Nudelman, N. S.; Velurtas, S.; Grela, M. A. *J. Phys. Org. Chem.* **2003**, *16*, 669. Alberts, A. H.; Wynberg, H. *J. Am. Chem. Soc.* **1989**, *111,* 7265. Alberts, A. H.; Wynberg, H. *J. Chem. Soc., Chem. Commun.* **1990**, 453. Xie, L; Saunders, W. H. *J. Am. Chem. Soc.* **1991**, *113,* 3123.

7. (a) Besson, C.; Finney, E. E.; Finke, R. G. *J. Am. Chem. Soc.* **2005,** *127,* 8179. (b) Besson, C.; Finney, E. E.; Finke, R. G. *Chem. Mater.* **2005,** *17,* 4925. (c) Huang, K. T.; Keszler, A.; Patel, N.; Patel, R. P.; Gladwin, M. T.; Kim-Shapiro, D. B.; Hogg, N. *J. Biol. Chem.* **2005**, *280*, 31126. (d) Huang, Z.; Shiva, S.; Kim-Shapiro, D. B.; Patel, R. P.; Ringwood, L. A.; Irby, C. E.; Huang, K. T.; Ho, C.; Hogg, N.; Schechter, A. N.; Gladwin, M. T. *J. Clin. Invest.* **2005**, *115*, 2099. (e) Tanj, S; Ohno, A; Sato, I; Soai, K *Org. Lett.* **2001**, *3*, 287. (f) Barrios-Kabderism, F.; Carrow, B. P.; Hartwig, *J. Am. Chem. Soc.* **2008**, *130*, 5842.

8. (a) Singh, K. J.; Collum, D. B. *J. Am. Chem. Soc.* **2006**, *128*, 13753. (b) Ma, Y.; Collum, D. B. *J. Am. Chem. Soc.* **2007**, *129*, 14818.

9. (a) Collum, D. B. *Acc. Chem. Res.* **1993**, *26*, 227. (b) Pratt, L.M. *Mini-Rev. Org. Chem.* **2004**, *1*, 209.

10. (a) Romesberg, F. E.; Collum, D. B. *J. Am. Chem. Soc.* **1994**, *116*, 9198. (b) Hall, P. L.; Gilchrist, J. H.; Harrison, A. T.; Fuller, D. J.; Collum, D. B. *J. Am. Chem. Soc.* **1991**, *113*, 9575. (c) Galiano-Roth, A. S.; Kim, Y.-J.; Gilchrist, J. H.; Harrison, A. T.; Fuller, D. J.; Collum, D. B. *J. Am. Chem. Soc.* **1991**, *113*, 5053. (d) Sun, C.; Williard, P. G. *J. Am. Chem. Soc.* **2000**, *122*, 7829.

11. (a) Depue, J. S.; Collum, D. B. *J. Am. Chem. Soc.* **1988**, *110*, 5524. (b) McNeil, A. J.; Toombes, G. E. S.; Gruner, S. M.; Lobkovsky, E.; Collum, D. B.; Chandramouli, S. V.; Vanasse, B. J.; Ayers, T. A. *J. Am. Chem. Soc.* **2004**, *126*, 16559.

12. Kim, Y.-J.; Bernstein, M. P.; Galiano-Roth, A. S.; Romesberg, F. E.; Fuller, D. J.; Harrison, A. T.; Collum, D. B.; Williard, P. G. *J. Org. Chem.* **1991**, *56*, 4435.

13. Spectral data: ^{6}Li NMR; **2** (δ1.27, s), **3** (δ1.97, t, *J* = 5.0 Hz), **4** (δ1.79, d, *J* = 5.3 Hz). ^{13}C NMR; **4** (δ150.5, dq, *J* = 121.7, 5.6 Hz). ^{15}N NMR; **3** (δ74.7, q, *J* = 5.0), **4** (δ76.4, q, *J* = 5.3). ^{19}F NMR; **1** (δ-113.0, -113.2), **2** (δ-74.5), **4** (δ-79.4), **5** (δ-80.5). ^{6}Li and ^{15}N NMR spectra were recorded in 11.1 M THF/pentane at -90 °C, ^{13}C NMR spectra were recorded in 3.1 M THF/pentane at -90 °C, ^{19}F NMR spectra were recorded in 11.1 M THF/pentane at -78 °C. All ^{19}F NMR resonances correspond to singlets.

14. Rein, A. J.; Donahue, S. M.; Pavlosky, M. A. *Curr. Opin. Drug Discov. Develop.* **2000**, *3*, 734.

15. ^{19}F NMR spectroscopy proved particularly useful in following the 1,2-additions to fluorinated quinazolinones. (a) Briggs, T. F.; Winemiller, M. D.; Collum, D. B.; Parsons, R. L., Jr.; Davulcu, A. K.; Harris, G. D.; Fortunak, J. D.; Confalone, P. N. *J. Am. Chem. Soc.* **2004**, *126*, 5427. (b) For a review of structural studies using ^{19}F NMR spectroscopy, see: Gakh, Y. G.; Gakh, A. A.; Gronenborn, A. M. *Magn. Reson. Chem.* **2000**, *38*, 551.

16. The concentration of LDA, although expressed in units of molarity, refers to the concentration of the monomer unit (normality).

17. Carbamate **1** and structurally related diisopropylamine-derived carbamates and carboxamides[18] display distinct conformational properties that

are not observed in less sterically congested analogues. Carbamate **1** affords normal NMR spectra at ambient temperature. On cooling the NMR probe below -70 °C, the single ^{19}F resonance (-113.1 ppm) appears as a pair of resonances (-113.2 and -113.0 ppm) in equal proportions. Similarly in the ^{13}C NMR spectrum, two methyne resonances of the diisopropyl moiety are observed at ambient temperatures whereas four are observed at $\leq$ -90 °C. One can explain these results by assuming a slow conformer exchange illustrated below and discussed previously.[18] A crystal structure of **1** affords the following structure displaying a highly typical orientation of the diisopropyl moiety.

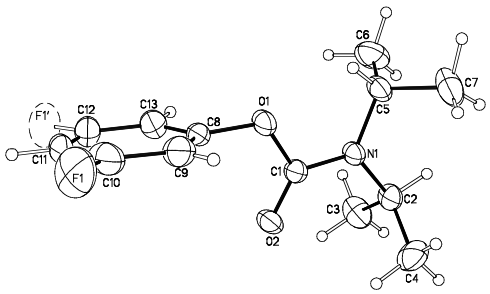

We have no evidence that conformation influences the mathematical form of the rate law described herein. To the contrary, the conformers are shown to maintain the equilibrium proportions throughout the course of the reaction.

18. For leading references to conformational studies of acylated diisopropylamido fragments, see: (a) Stewart, W. E.; Siddall, T. H., III. *Chem. Rev.* **1970**, *70*, 517. (b) Lidén, A.; Roussel, C.; Liljefors, T.; Chanon, M.; Carter, R. E.; Metzger, J.; Sandström, J. *J. Am. Chem. Soc.* **1976**, *98*, 2853.

19. Gaussian 03, Revision B.04, Frisch, M. J.; Trucks, G. W.; Schlegel, H. B.; Scuseria, G. E.; Robb, M. A.; Cheeseman, J. R.; Montgomery, Jr., J. A.; Vreven, T.; Kudin, K. N.; Burant, J. C.; Millam, J. M.; Iyengar, S. S.; Tomasi, J.; Barone, V.; Mennucci, B.; Cossi, M.; Scalmani, G.; Rega, N.; Petersson, G. A.; Nakatsuji, H.; Hada, M.; Ehara, M.; Toyota, K.; Fukuda, R.; Hasegawa, J.; Ishida, M.; Nakajima, T.; Honda, Y.; Kitao, O.; Nakai, H.; Klene, M.; Li, X.; Knox, J. E.; Hratchian, H. P.; Cross, J. B.; Bakken, V.; Adamo, C.; Jaramillo, J.; Gomperts, R.; Stratmann, R. E.; Yazyev, O.; Austin, A. J.; Cammi, R.; Pomelli, C.; Ochterski, J. W.; Ayala, P. Y.; Morokuma, K.; Voth, G. A.; Salvador, P.; Dannenberg, J. J.; Zakrzewski, V. G.; Dapprich, S.; Daniels, A. D.; Strain, M. C.; Farkas, O.; Malick, D. K.; Rabuck, A. D.; Raghavachari, K.; Foresman, J. B.; Ortiz, J. V.; Cui, Q.; Baboul, A. G.; Clifford, S.; Cioslowski, J.; Stefanov, B. B.; Liu, G.; Liashenko, A.; Piskorz, P.; Komaromi, I.; Martin, R. L.; Fox, D. J.; Keith, T.; Al-Laham, M. A.; Peng, C. Y.; Nanayakkara, A.; Challacombe, M.; Gill, P. M. W.; Johnson, B.; Chen, W.; Wong, M. W.; Gonzalez, C.; and Pople, J. A.; Gaussian, Inc., Wallingford CT, 2004.

20. The structurally analogous form derived from the *N*,*N*-dimethyl carbamate derivative[8] shows two resonances (1:1) at -130 °C, consistent with the presence of the chelate.

21. Ramirez, A.; Candler, J.; Bashore, C. G.; Wirtz, M. C.; Coe, J. W.; Collum, D. B. *J. Am. Chem. Soc.* **2004**, *126*, 14700.

22. (a) Stratakis, M.; Wang, P. G.; Streitwieser, A. *J. Org. Chem.* **1996**, *61*, 3145. (b) Reich, H. J.; Green, D. P.; Medina, M. A.; Goldenberg, W. S.;

Gudmundsson, B. Ö.; Dykstra, R. R.; Phillips, N. H. *J. Am. Chem. Soc.* **1998,** *120,* 7201.

23. Open dimers were first proposed for the isomerization of oxiranes to allylic alcohols by mixed metal bases: Mordini, A.; Rayana, E. B.; Margot, C.; Schlosser, M. *Tetrahedron* **1990**, *46*, 2401. For a bibliography of lithium amide open dimers, see ref 5b.

24. We have also detected an analogous open dimer-based transition structure bearing a chelated meta substituent for the Snieckus-Fries rearrangement of mixed dimer **9**.

25. For examples of reactions that are fast relative to the rates of aggregate-aggregate exchanges see: (a) McGarrity, J. F.; Ogle, C. A. *J. Am. Chem. Soc.* **1985**, *107*, 1810. (b) Jones, A. C.; Sanders, A. W.; Bevan, M. J.; Reich, H. J. *J. Am. Chem. Soc.* **2007**, *129*, 3492. (c) Thompson, A.; Corley, E. G.; Huntington, M. F.; Grabowski, E. J. J.; Remenar, J. F.; Collum, D. B. *J. Am. Chem. Soc*. **1998**, *120*, 2028.

26. (a) Espenson, J. H. *Chemical Kinetics and Reaction Mechanisms*, 2nd ed.; McGraw-Hill: New York, 1995; Chapter 2, p 44. Atkins, P. W.; Jones, L. L. *Chemical Principles: the Quest for Insight*, 2nd ed.; W H. Freeman: New York, 2002.

27. For other examples of odd linearities that may or may not have origins similar to those described herein, see: (a) Blackmond, D. G.; Ropic, M.;

Stefinovic, M. *Org. Proc. Res. Develop.* **2006**, *10*, 457. (b) Akao, A.; Nonoyama, N.; Mase, T.; Yasuda, N. *Org. Proc. Res. Develop.* **2006**, *10*, 1178. (c) Rowley, J. M.; Lobkovsky, E. B.; Coates, G. W. *J. Am. Chem. Soc.* **2007**, *129*, 4948. (d) Yin, C.-X.; Finke, R. G. *J. Am. Chem. Soc.* **2005**, *127*, 13988.

28. Addition of excess *i*-Pr_2NH to the metalation has no measurable effect on the rates or curvatures.

29. Sigmoidal curvature for the loss of aryl carbamate is also observed using tetrahydropyran and 2-methyltetrahydrofuran.

30. (a) Chadwick, S. T.; Rennels, R. A.; Rutherford, J. L.; Collum, D. B. *J. Am. Chem. Soc.* **2000,** *122,* 8640. (b) Anderson, D. R.; Faibish, N. C.; Beak, P. *J. Am. Chem. Soc.* **1999,** *121,* 7553.

31. (a) Dyke, A. M.; Gill, D. M.; Harvey, J. N.; Hester. A. J.; Lloyd-Jones, G. C.; Munoz, M. P.; Shepperson, I. R. *Angew. Chem., Int. Ed.* **2008**, *47*, 5067. (b) Metalation of carbamate **1** in *t*-BuOMe proceeds from an LDA-carbamate complex via a normal (first-order) disappearance and displays k_H/k_D = 3-4.

32. Hughes, E. *J. Chem. Educ.* **1989**, *66*, 46.

33. We define the idealized rate law as that obtained by rounding the observed reaction orders to the nearest rational order.

34. The rates rose with decreasing THF concentrations, although the high rates precluded a quantitative study. A seemingly analogous inverse THF dependence for the reaction of an aryllithium has been reported.[21]

35. The rate law provides the stoichiometry of the transition structure relative to that of the reactants: Edwards, J. O.; Greene, E. F.; Ross, J. *J. Chem. Educ.* **1968**, *45*, 381.

36. Brown, K. S.; Sethna, J. P. *Phys. Rev. E* **2003**, *68*, 021904.

37. A discussion and attribution of this famous aphorism is found in reference 36. Physicists, apparently with considerable free time, are reputed to have successfully drawn elephants using complex mathematics and numerous adjustable parameters.

38. (a) Casado, J.; Lopez-Quintela, M. A.; Lorenzo-Barral, F. M. *J. Chem. Educ.* **1986**, *63*, 450. (b) Alberty, R. A. *J. Chem. Educ.* **2004**, *81*, 1206. (c) Hammes, G. G. "Principles of Chemical Kinetics"; Academic Press: New York, 1978; pp 14-15.

39. Through-space Li-F interactions have been detected. (a) Stalke, D.; Klingebiel, U.; Sheldrick, G. M. *Chem. Ber.* **1988**, *121*, 1457. (b) Armstrong, D. R.; Khandelwal, A. H.; Kerr, L. C.; Peasey, S.; Raithby, P. R.; Shields, G. P.; Snaith, R.; Wright, D. S. *Chem. Commun.* **1998**, 1011. (c) Plenio, H.; Diodone, R. *J. Am. Chem. Soc.* **1996**, *118*, 356. (d) Henderson, K. W.; Dorigo, A. E.; Liu, Q.-Y.; Williard, P. G. *J. Am. Chem. Soc.* **1997**, *119*, 11855. (e) Kessar, S. V.; Singh, P.;

Singh. K. N.; Bharatam, P. V.; Sharma, A. K.; Lata, S.; Kaur, A. *Angew. Chem., Int. Ed.* **2008**, *47*, 4703.

40. For leading references and discussions of mixed aggregation effects, see: (a) Seebach, D. *Angew. Chem., Int. Ed. Engl.* **1988**, *27*, 1624. (b) Tchoubar, B.; Loupy, A. *Salt Effects in Organic and Organometallic Chemistry*; VCH: New York, 1992; Chapters 4, 5, and 7. (c) Briggs, T. F.; Winemiller, M. D.; Xiang, B.; Collum, D. B. *J. Org. Chem.* **2001**, *66*, 6291. (d) Caubère, P. *Chem. Rev.* **1993**, *93*, 2317.

41. Hall, P. L.; Gilchrist, J. H.; Collum, D. B. *J. Am. Chem. Soc.* **1991**, *113*, 9571.

42. Xie and Saunders also observed oddly variable isotope effects on the enolization. Xie, L.; Saunders, W. H., Jr. *J. Am. Chem. Soc.* **1991**, *113*, 3123.

43. Collum, D. B.; Singh, K.; Viciu, M.; Ramirez, A.; Yun, M. unpublished. (b) Hints of linear decays were noted in metalations of imines by LDA/THF at -78 °C: Liao, S.; Collum, D. B. *J. Am. Chem. Soc.* **2003**, *125*, 15114.

44. A. Evans, *Potentiometry and Ion-Selective Electrodes*. New York: Wiley, 1987.

45. Fuji, T. *Anal. Chem.* **1992**, *64*, 775.

46. Kofron, W. G.; Baclawski, L. M. *J. Org. Chem.* **1976**, *41*, 1879.

47. For an explanation of the Levenberg-Marquardt nonlinear least-squares optimization, see: Press, W. H.; Flannery, B. P.; Teukolsky, S. A.; Vetterling, V. T. *Numerical Recipes in C*, Cambridge University Press, London, 1988; Chapter 14.4.

48. Brown, P.N., Byrne, G. D.; Hindmarsh, A. C. *J. Sci. Stat. Comput.* **1989**, *10*, 1038.

49. *Gaussview*, Version 3.09, Dennington II, R.; Keith, T.; Millam, J.; Eppinett, K.; Hovell, W. L.; Gilliland, R.; Semichem, Inc.; Shawnee Mission, KS, 2003.

CHAPTER 2

1,4-ADDITION OF LITHIUM DIISOPROPYLAMIDE TO UNSATURATED ESTERS: ROLE OF RATE-LIMITING DEAGGREGATION, AUTOCATALYSIS, LITHIUM CHLORIDE CATALYSIS, AND OTHER MIXED AGGREGATE EFFECTS

1,4-Addition of Lithium Diisopropylamide to Unsaturated Esters: Role of Rate-Limiting Deaggregation, Autocatalysis, Lithium Chloride Catalysis, and Other Mixed Aggregation Effects

Abstract

Lithium diisopropylamide (LDA) in tetrahydrofuran at -78 °C undergoes 1,4-addition to an unsaturated ester via a rate-limiting deaggregation of LDA dimer followed by a post-rate-limiting reaction with the substrate. Muted autocatalysis is traced to a lithium enolate-mediated deaggregation of the LDA dimer and the intervention of LDA-lithium enolate mixed aggregates displaying higher reactivities than LDA. Striking accelerations are elicited by <1.0 mol % LiCl. Rate and mechanistic studies have revealed that the uncatalyzed and catalyzed pathways funnel through a common monosolvated-monomer-based intermediate. Four distinct classes of mixed aggregation effects are discussed.

Introduction

1,4-Additions of lithium amides have been reported on numerous occasions.[1-3] In one of the earliest reports, Schlessinger and co-workers found that attempted enolizations of unsaturated esters using lithium diisopropylamide (LDA) in tetrahydrofuran (THF) at -78 °C afforded β-amino esters instead.[1,4] They solved the problem by adding hexamethylphosphoramide (HMPA). Davies and co-workers, recognizing the medicinal importance of β-amino esters, developed highly enantioselective 1,4-additions of structurally analogous β-phenethylamine-derived lithium dialkylamides.[3]

Our interest was piqued by the 1,4-addition of LDA described in eq 1. Previous studies of the 1,4-addition in the presence of HMPA showed that addition occurs to the exclusion of enolization via highly solvated LDA dimers suggested to be triple ions.[5-7] When the reaction is carried out in the absence of HMPA under conditions that would be familiar to synthetic organic chemists (LDA/THF/-78 °C), strange decays are observed that are neither first- nor second-order (Figure 2.1, curve A). The near linearity of these decays seems more akin to a zeroth-order dependence on ester.[8,9] Moreover, traces of LiCl (<1 mol %) elicit a 70-fold acceleration accompanied by curvature that appears decidedly more normal (Figure 2.1, inset).

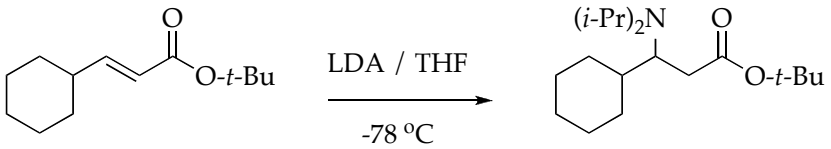

1 **2**

82% yield

(1)

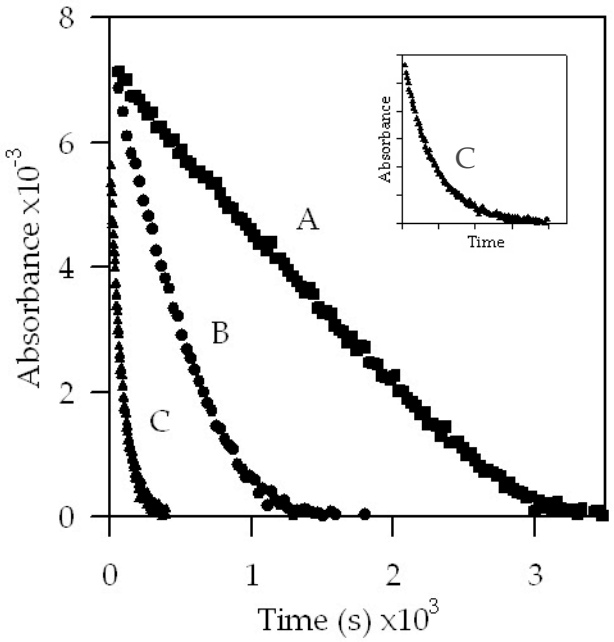

Figure 2.1. Plot of IR absorbance vs time in THF (6.10 M) for 1,4-addition of ester **1** (0.004 M) with LDA (0.10 M) at -78 °C in the presence of various amounts of LiCl: (A) no LiCl; (B) 0.01 mol % LiCl; (C) 0.4 mol % LiCl. The insert shows an expanded view of curve C.

We describe herein rate and mechanistic studies of the 1,4-addition in eq 1. The superposition of rate-limiting deaggregation, intervention of LDA-lithium enolate mixed aggregates, muted autocatalysis, and marked catalysis by LiCl present considerable mechanistic complexity.[10] Such overt complexity is exhilarating in a mechanistic context, yet the growing number of examples of such odd effects affiliated with LDA/THF/-78 ºC are troubling in light of the prevalence of these conditions in organic synthesis.[11,12] Furthermore, the LiCl catalysis, which is detectable using as little as 1.0 ppm LiCl, represents a mixed aggregation effect that is, to the best of our knowledge, undocumented.[13-15]

The Results describes strategies and tactics for specialists who wish to understand the details of the rate studies; the section culminates in a

mechanistic hypothesis that accounts for the disparate behaviors. Discussion section summarizes the results for a more general audience and describes how mixed aggregates influence the reactivity.

Results

Caveat: Purification of LDA. We previously showed by potentiometry[16] and ion chromatography[17] that recrystallized LDA[18] prepared from recrystallized *n*-BuLi[19] contains <0.02 mol % LiCl.[11,12] Accelerations of the 1,4-addition in eq 1 by as little as *0.001 mol % LiCl*, however, prompted us to modify a literature synthesis[20] of rigorously LiCl-free LDA from lithium metal, diisopropylamine, isoprene, and dimethylethylamine (DMEA). DMEA accelerates the reduction yet does not remain bound to the recrystallized LDA.[21] Despite taking these precautions, however, we observed some variability when stock solutions prepared from a common batch of LDA were used. Control experiments examining the influence of LDA aging, traces of H_2O and O_2, contaminants in solvents, joint greases, and even the specific researcher carrying out the work failed to uncover the source of this residual variability. The consequences were not large, although triplicate measurements proved necessary in some instances.

Solution Structures. Reaction of 2.0 equiv of LDA with unsaturated ester **1** in THF at -78 °C with slow warming to room temperature afforded β-amino ester **2** in 82% yield (eq 1).[5] Monitoring the reaction of [^{6}Li,^{15}N]LDA with ester **1** using ^{6}Li and ^{15}N NMR spectroscopy revealed the presence of LDA-lithium enolate mixed dimer **4** along with a concentration-independent pair of resonances in a nearly 1:1 ratio that was shown by the absence of ^{6}Li-^{15}N coupling to be attributable to enolate **5** (Figure 2.2). Although we were

tempted to presume that the two resonances derived from an *E*/*Z* mixture, we suspected that they were homochiral and heterochiral dimers **5a**. (The existence of chelation is depicted out of convenience; the typically small Li-N coupling anticipated for a Li-NR_3 interaction[22] was not observed.) By varying the proportions of LDA and lithium enolate and monitoring LDA homodimer **3**, mixed dimer **4**, and the enolate homoaggregates (an A_2-AE-E_n ensemble), we used the method of continuous variation (the method of Job[23]) to show that the enolate (E_n) is indeed a dimer (Figure 2.3). Detailed descriptions of this method for characterizing lithium enolates have been reported.[24] Although monomeric enolate was not observed, it is invoked as an intermediate. Density functional theory (DFT) computations at the B3LYP/6-31G(d) level of theory[25] suggested disolvated monomer **5b** as the fleetingly stable resting state.

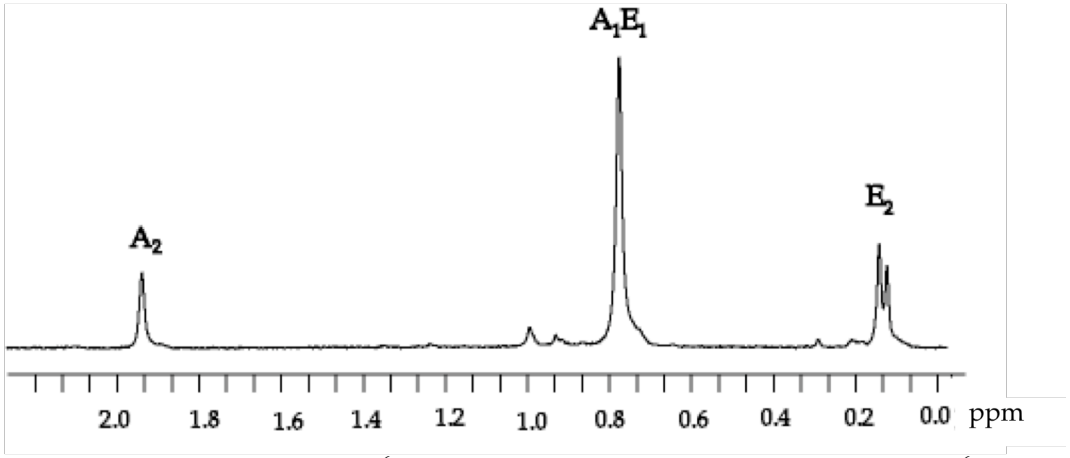

Figure 2.2. Representative ^{6}Li NMR spectrum of a 60:40 mixture of [^{6}Li]**5** and[^{6}Li]**3** showing resonances of the homodimers (A_2 and E_2) and the mixed dimer [^{6}Li]**4** (AE).

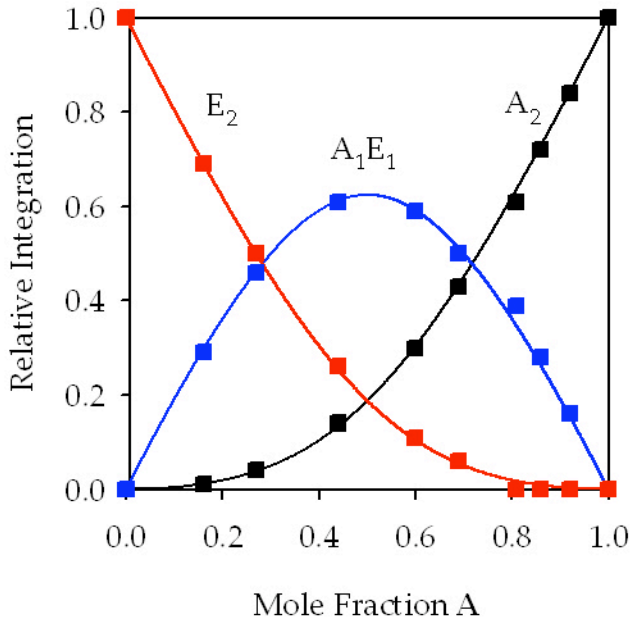

Figure 2.3. Plot of the relative integrations of [^{6}Li]**3**, [^{6}Li]**4**, and [^{6}Li]**5** vs the mole fraction of LDA (A). The curves were derived from a parametric fit as described previously.[24]

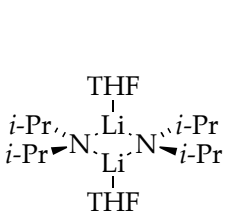

3

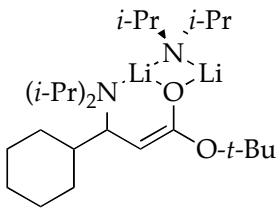

4

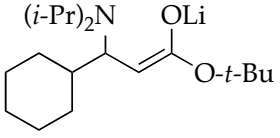

5

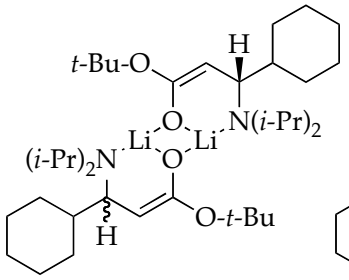

5a

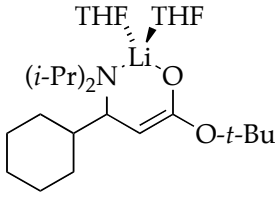

5b

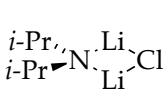

6

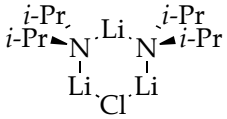

7

Catalysis by LiCl is discussed in light of the structures of LDA-LiCl mixed aggregates. Previous studies have shown that LiCl is dimeric in THF solution.[26,27] Mixtures of LDA with LiCl at the very low LiCl concentrations used in the rate studies described below (≤2 mol % LiCl) afford a LiCl-concentration-independent 1:8 mixture of **6** and **7** to the exclusion of free LiCl.[27,28]

Kinetics: General Protocols. LDA used in rate studies was prepared as described above. Exogenous LiCl was generated in situ from $Et_3N{\cdot}HCl$.[29] (The Et_3N byproduct is a poor ligand[21] that has no effect on LDA structure or reactivity.) The disappearance of ester **1** (1715 cm^{-1}) during the 1,4-additions was monitored using in situ IR spectroscopy.[30] Formation of lithium enolate **5** (1630 cm^{-1}) was correlated with the loss of **1**. It should be noted, however, that

the absorbance at 1630 cm^{-1} arises from the superposition of mixed and homoaggregated dimers **4** and **5a**, respectively. Using ^{6}Li NMR spectroscopy, we were able to show that this IR spectral simplicity belies a substantial underlying complexity (see below).[31]

Strange Curvatures. Monitoring additions of LDA to ester **1** by IR spectroscopy under pseudo-first-order conditions (excess LDA) showed a linear decay, suggesting a zeroth-order dependence on ester **1**. Equimolar mixtures of LDA and ester **1** (second-order conditions) afforded the decay depicted in Figure 2.4. If the linearity in Figure 2.1 derived solely from a zeroth-order dependence on ester **1**, this dependence in conjunction with a first-order dependence on LDA would cause the decay in Figure 2.4 to be first-order overall. The first-order fit in Figure 2.4 (dashed line) is poor, suggesting a persistent linearity stemming from autocatalysis (see below). (Previous studies of arylcarbamate lithiations revealed linear decays that were traced to straightening of first-order decays by autocatalysis.[11])

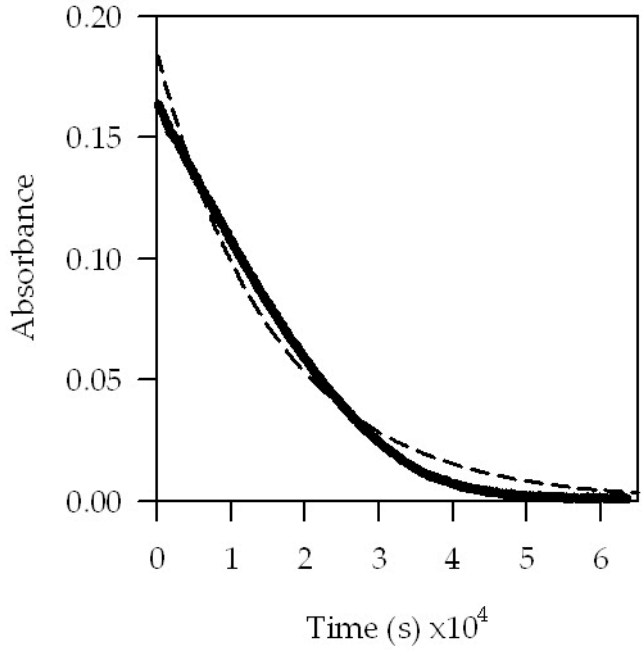

Figure 2.4. Plot showing IR absorbance of ester **1** vs time for the 1,4-addition of ester **1** (0.10 M) with LDA (0.10 M) in neat THF at -78 °C. The dashed line shows the poor first-order fit ($A = ae^{bt}$).

^{6}Li NMR spectroscopy allowed us to follow the loss of LDA dimer **3**, mixed dimer **4**, and enolate dimer **5a** (Figure 2.5). The concentrations of the aggregates also allowed us to calculate the concentration of the spectroscopically silent ester **1**. The calculated linear decay of ester **1** correlated well with the experimentally measured linear decay detected by IR spectroscopy. The curved loss of LDA dimer **3** (the noncorrelation with the ester) reflects the consumption of **3** by both metalation and formation of mixed dimer **4**. The time dependencies of **4** and **5a** (represented as A_2 and AE in Figures 2.5 and 2.6) clearly departed from conventional behavior. Minor changes in the initial concentration ester of ester **1** produced overt visual changes (Figure 2.6). Even more striking curvatures and discontinuities were observed when *n*-alkyl ester **12** was used (Figures 2.7 and 2.8). (Ester **12**, *n*-$C_7H_{15}CHCHCO_2$-*t*-Bu, was introduced in the context of the competition

studies described below.) The overshoot of the concentration of enolate dimer **5a'** relative to the final equilibrium value and the discontinuity in the mixed dimer concentration place significant constraints on a mechanistic model. The rate studies described below were employed to extract the critical details required in order to account for the strange time-dependent concentrations, and best-fit numerical integrations afforded the curves (see below).

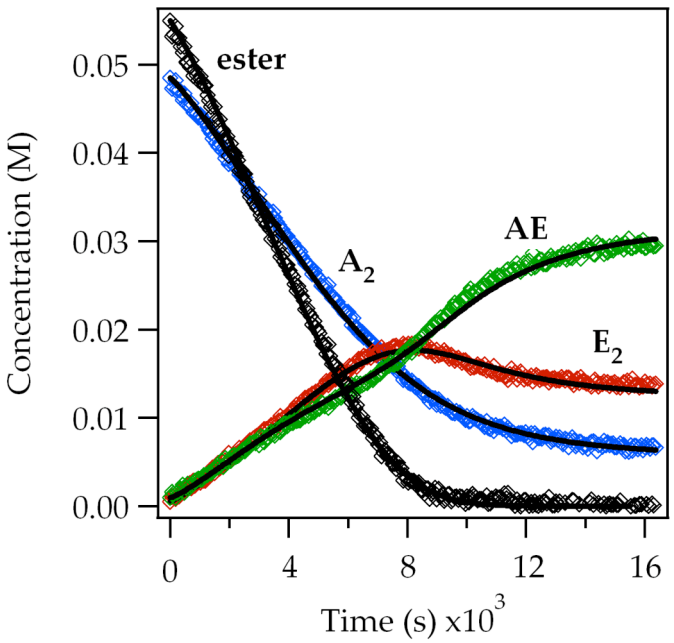

Figure 2.5. Time-dependent concentrations measured by ^{6}Li NMR spectroscopy using 0.05 M **3** (0.10 N) and 0.05 M **1** in 6.1 M THF at -78 °C. Legend: ester = **1**; A_2 = LDA dimer **3**; E_2 = enolate dimer **5a**; AE = enolate mixed dimer **4**. The curves represent a parametric fit to eqs 17-22 (described below). The best-fit values for the rate constants are listed in the Appendix.

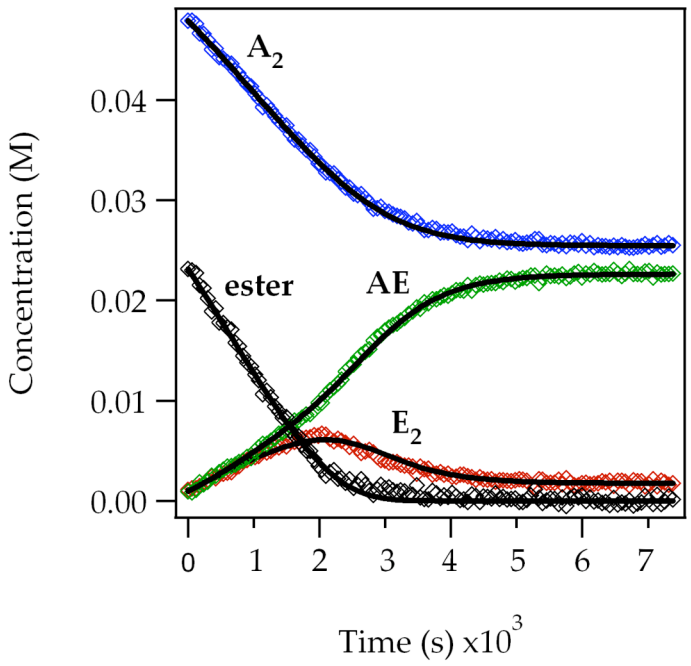

Figure 2.6. Time-dependent concentrations measured by ^{6}Li NMR spectroscopy using 0.05 M **3** (0.10 N) and 0.025 M **1** in 6.1 M THF at -78 °C. Legend: ester = **1**; A_2 = LDA dimer **3**; E_2 = enolate dimer **5a**; AE = enolate mixed dimer **4**. The curves represent a parametric fit to eqs 17-22 (described below). The best-fit values for the rate constants are listed in the Appendix.

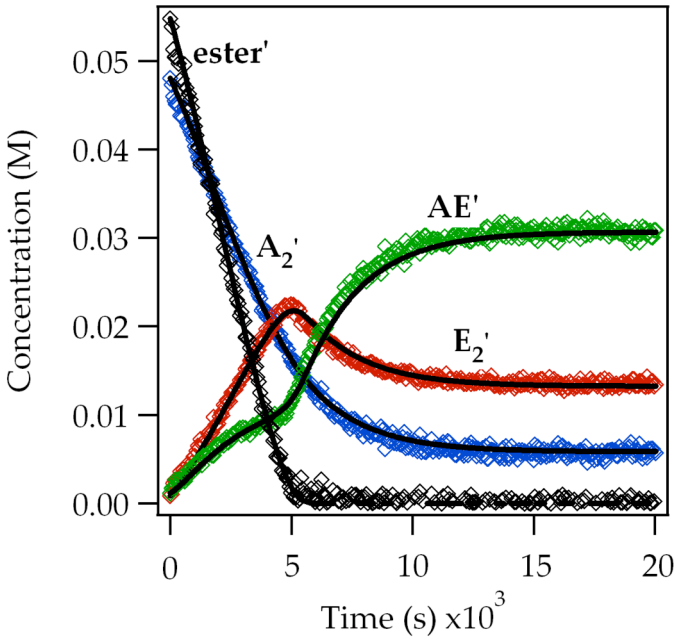

Figure 2.7. Time-dependent concentrations measured by ^{6}Li NMR spectroscopy using 0.05 M **3** (0.10 N) and 0.05 M ester **12** in 6.1 M THF at -78 °C. Legend: ester = **12**; A_2 = LDA dimer **3**; E_2' = enolate dimer of ester **12**; AE′ = enolate mixed dimer . The curves represent a parametric fit to eqs 17-22 (described below). The best-fit values for the rate constants are listed in the Appendix.

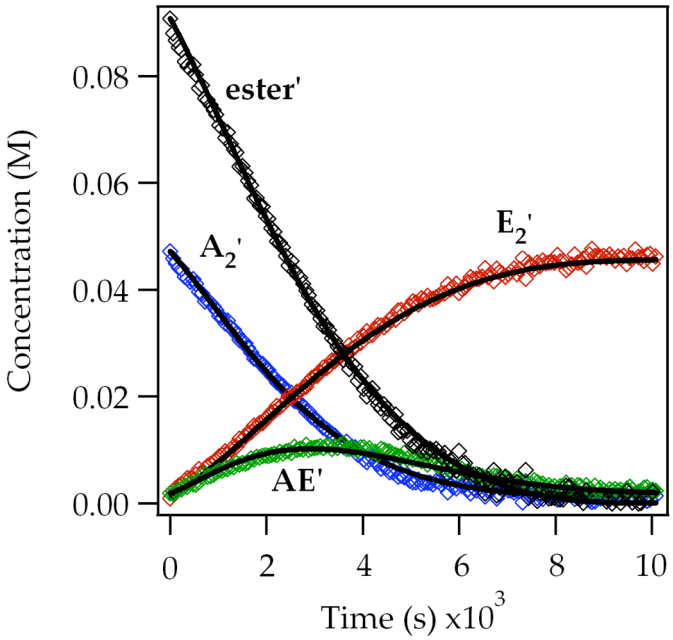

Figure 2.8. Time-dependent concentrations measured by ^{6}Li NMR spectroscopy using 0.05 M **3** (0.10 N) and 0.10 M **12** in 6.1 M THF at -78 °C. Legend: ester = **12**; A_2 = LDA dimer **3**; E_2' = enolate dimer of **12**; AE′ = enolate mixed dimer. The curves represent a parametric fit to eqs 17-22 (described below). The best-fit values for the rate constants are listed in the Appendix.

Kinetics: Uncatalyzed 1,4-Additions. The mechanism of the uncatalyzed 1,4-addition (i.e., the addition before the appearance of mixed dimers and the onset of autocatalysis) was examined by monitoring the rates at early conversion using IR spectroscopy. Plots of ester concentration versus time for different initial concentrations of ester **1** (Figure 2.9) showed linear, parallel decays consistent with a zeroth-order dependence on **1**, which was confirmed by a plot of the initial rates versus initial ester concentration (Figure 2.10). Plots of initial rate versus LDA concentration (Figure 2.11)[32] and THF concentration (Figure 2.12) revealed first-order dependencies in both instances. The idealized[33] rate law (given by eq 2) is consistent with a mechanism involving rate-limiting deaggregation (eq 3) followed by post-rate-

limiting reaction with ester **1**.[34] To describe some fairly complex mechanistic scenarios, we take the liberty of introducing the following shorthand: A = an LDA monomeric subunit and S = THF (e.g., A_2S_2 = **3**).

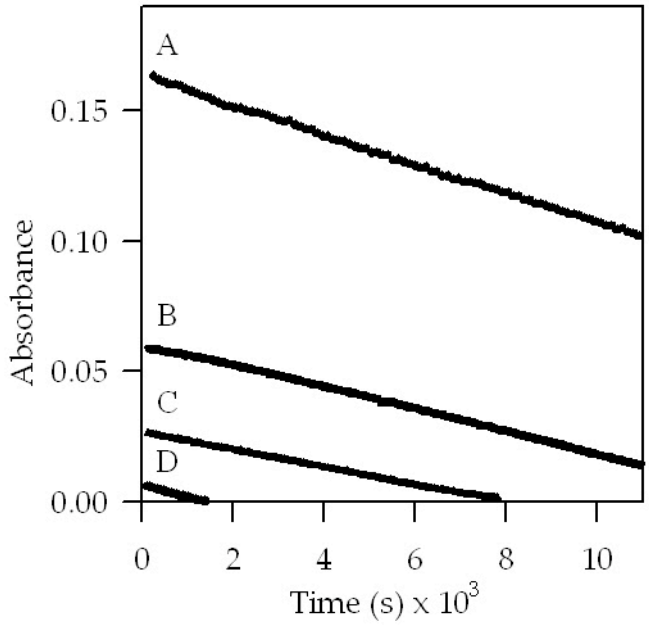

Figure 2.9. Plots of IR absorbance of ester **1** vs time for selected initial concentrations of **1**: (A) 0.10 M; (B) 0.050 M; (C) 0.025 M; (D) 0.004 M.

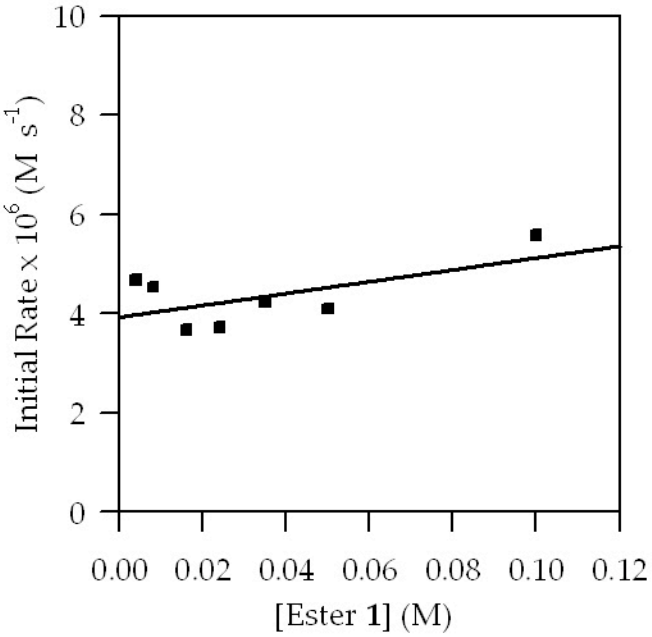

Figure 2.10. Plot of initial rate vs [**1**] in THF (6.1 M) for the 1,4-addition of ester **1** with LDA (0.10 M) at -78 °C. The curve depicts an unweighted least-squares fit to $y = k[\mathbf{1}] + k'$ [$k = (1.2 \pm 1) \times 10^{-5}$, $k' = (3.9 \pm 0.4) \times 10^{-6}$].

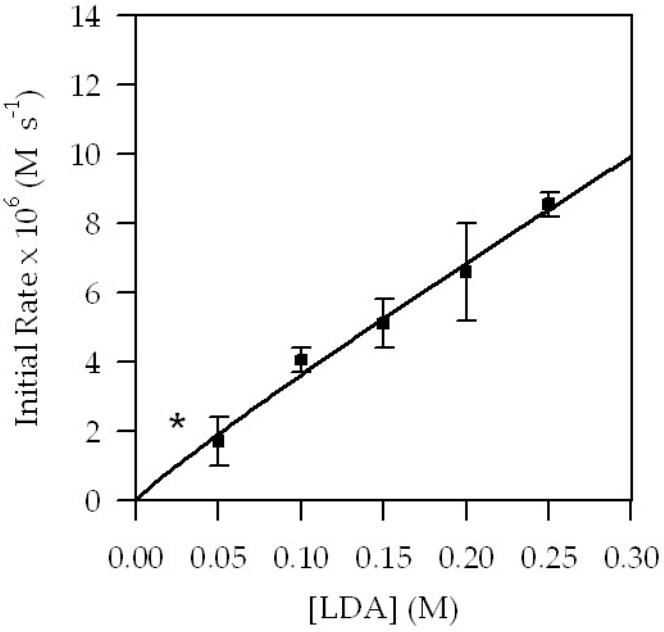

Figure 2.11. Plot of initial rate vs [LDA] in THF (6.1 M) for the 1,4-addition of ester **1** (0.004 M) at -78 °C. The curve depicts an unweighted least-squares fit to $y = k[\text{LDA}]^n$ [$k = (3.1 \pm 0.4) \times 10^{-5}$; $n = 0.92 \pm 0.03$].

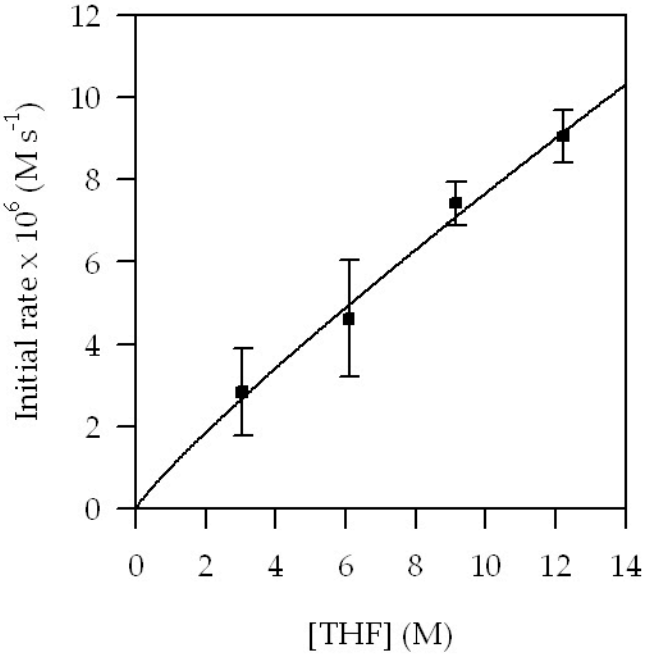

Figure 2.12. Plot of initial rate vs [THF] in hexane cosolvent for the 1,4-addition of ester **1** (0.004 M) with LDA (0.10 M) at -78 °C. The curve depicts an unweighted least-squares fit to $y = k[\mathrm{THF}]^n + k'$ [$k = (8.1 \pm 0.2) \times 10^{-7}$; $n = 0.95 \pm 0.03$; $k' = (4.05 \pm 0.04) \times 10^{-7}$].

$$-d[\mathbf{1}]/dt = k[A_2S_2][S] \quad (2)$$

$$A_2S_2 + S \xrightarrow{k} [A_2S_3]^{\ddagger} \quad (3)$$

DFT computations showed that trisolvated-dimer-based transition structures representing rate-limiting open dimer formation (**8**) and deaggregation (**9**) are both plausible (Scheme 1).[35] The dimer-based rate-limiting step does *not* attest to whether the post-rate-limiting 1,4-addition is monomer- or dimer-based, but strong support for a monomer-based 1,4-addition emerged from studies of catalysis (see below).

Scheme 1

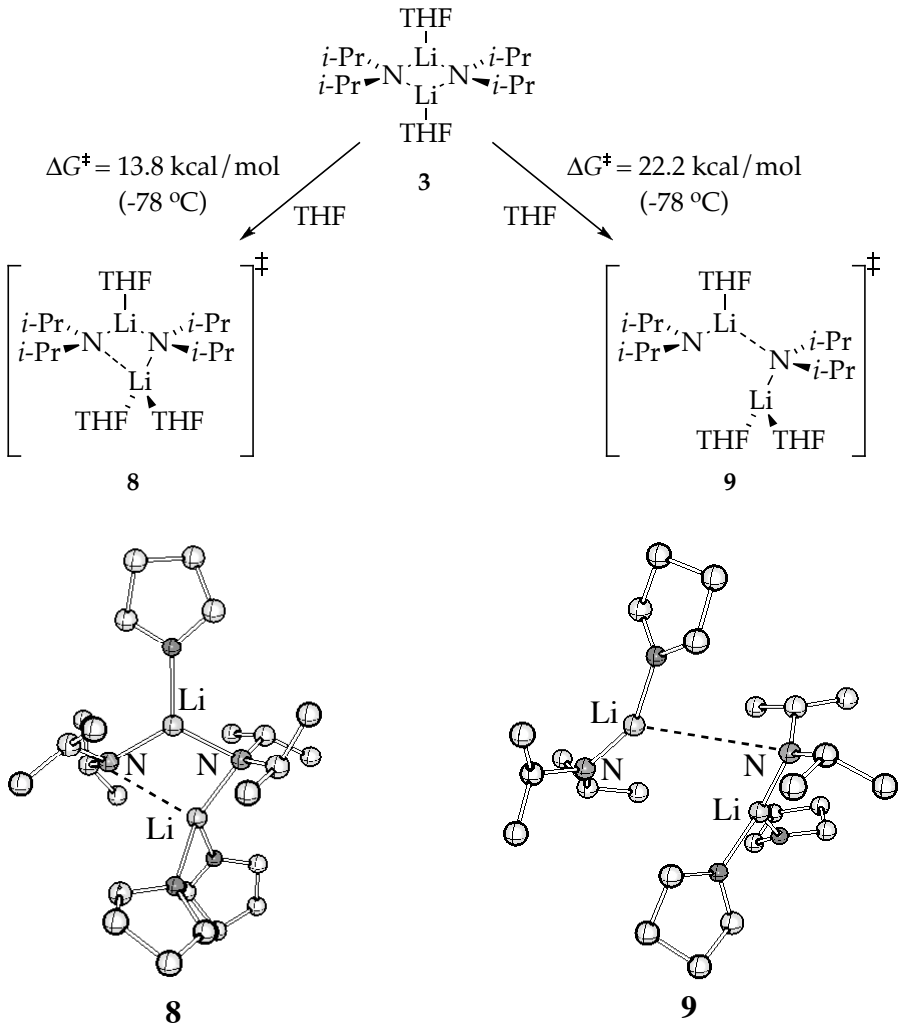

Autocatalysis. Product-derived acceleration—so-called autocatalysis—in its most extreme form manifests sigmoidal decays of substrate versus time[36,37] and should be most easily observed using equimolar mixtures of LDA and substrate. Figure 2.1 shows no sigmoid but does show a persistent linearity in the first two half-lives, suggesting muted autocatalysis. We developed a method for detecting low levels of mixed aggregation effects using serial substrate injections as follows.

In a routine control experiment, the IR baseline was zeroed at the end of a pseudo-first-order kinetic run, and a second aliquot of substrate was added. In the absence of autocatalysis, the rate for the second aliquot should have shown a minor decrease relative to the first aliquot because of the slight loss in LDA titer. In the 1,4-addition, however, the second aliquot afforded a measurably *higher* rate. This effect was amplified by serially injecting aliquots containing 10 mol % ester **1** until the LDA was completely consumed. The initial rate is plotted versus mole fraction of enolate **5** (X_{ROLi}) in Figure 2.13. The serial injections correspond to movement from left to right along the X_{ROLi}-axis.[23] Figure 2.13 differs from a standard plot of concentration versus time in that (1) the normal upward curvature resulting from substrate loss was factored out by adding substrate at constant concentrations and monitoring initial rates and (2) all aggregates were allowed to equilibrate between injections.

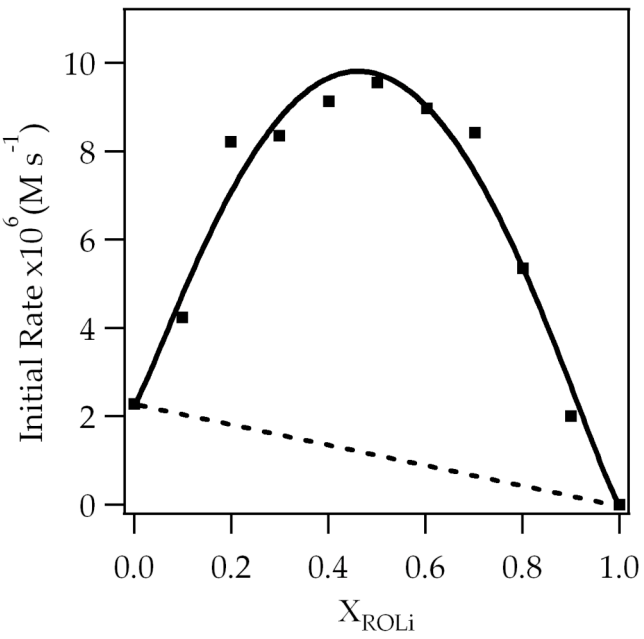

Figure 2.13. Plot of initial rate versus mole fraction of enolate (X_{ROLi}) for the serial injection of 10 aliquots of ester **1** (10 mol % each relative to LDA) into 0.10 M LDA in 6.1 M THF/hexane cosolvent at -78 °C. The dashed line depicts the theoretical behavior of the initial rate in the absence of autocatalysis, and the solid curve represents a nonlinear least-squares fit to eq 4.

$$-\Delta[\text{ester}_0]/\Delta t_0 = k[X_{ROLi}]^n[1 - X_{ROLi}]^m + k'[1 - X_{ROLi}]^{1.0} \quad (4)$$

The maximum at $X_{ROLi} = 0.5$ in Figure 2.13 suggests that a 1:1 LDA/enolate ratio is optimal.[23,24] The solid curve in Figure 2.13 corresponds to a nonlinear least-squares fit to eq 4 (see the Appendix). This behavior could arise either from a key condensation involving LDA dimer **3** and enolate dimer **5a** (affording the mathematically equivalent 2:2 stoichiometry) or from mixed dimer **4** maximized at $X_{ROLi} = 0.5$. There is, however, a telling paradox: Figure 2.13 suggests that a 1,4-addition from equimolar mixtures of LDA and ester **1** should be markedly faster at 50% conversion than at the start.

Nonetheless, there is no sigmoidal behavior in Figure 2.4; only a gentle straightening of the decay appears. (Perfect linearity arises when the autocatalysis precisely offsets the consumption of LDA.[11])

Using ^{6}Li NMR spectroscopy, we monitored the reaction of LDA dimer **3** and enolate dimer **5a** to give mixed dimer **4**. The reaction using 0.05 M each of **3** and **5a** revealed a half-life of 3000 s. First-order dependencies in **3** and **5a** (Figures 2.14 and 2.15) in conjunction with a zeroth-order THF dependence (see the Appendix) afforded the idealized[33] rate law given in eq 5. The associative mechanism suggests mixed-tetramer-based exchange.[38] We can imagine ladder-based intermediates (eq 6),[39,40] but monomeric LDA would not necessarily be formed during the exchange, and the role this exchange plays in the 1,4-addition is minor at best (see below).[41]

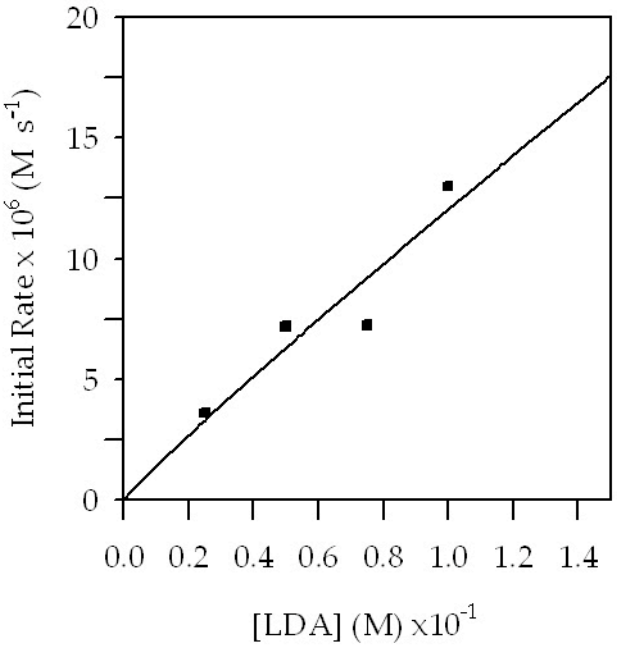

Figure 2.14. Plot of initial rate vs [LDA] for the condensation of LDA dimer **3** with enolate dimer **5a** (0.025 M) in THF (6.10 M) at -78 °C. The curve depicts an unweighted least-squares fit to $y = k[\mathrm{LDA}]^n$ [$k = (1.0 \pm 0.3) \times 10^{-4}$; $n = 0.93 \pm 0.24$].

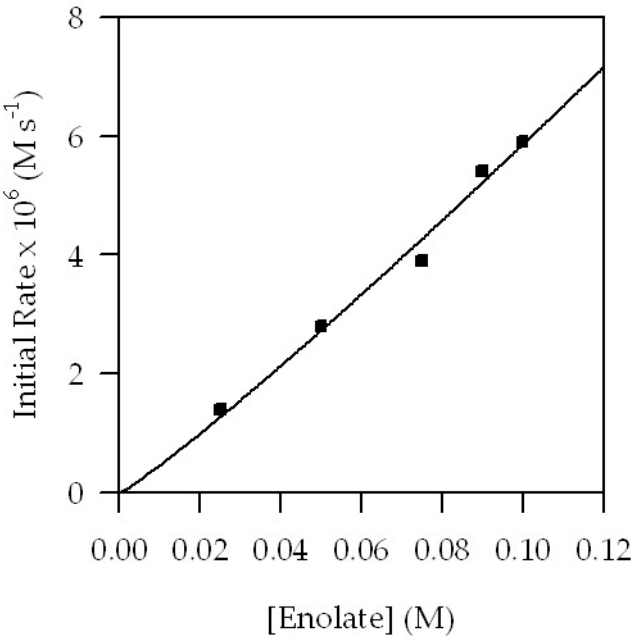

Figure 2.15. Plot of initial rate vs the concentration of enolate **5** for the condensation of LDA dimer **3** (0.10 M) with enolate dimer **5a** in THF (6.10 M) at -78 °C. The curve depicts an unweighted least-squares fit to $y = k[\text{enolate}]^n$ [$k = (7.4 \pm 0.3) \times 10^{-5}$; $n = 1.10 \pm 0.14$].

$$-d[\mathbf{1}]/dt = k[A_2S_2][E_2][S]^0 \qquad (5)$$

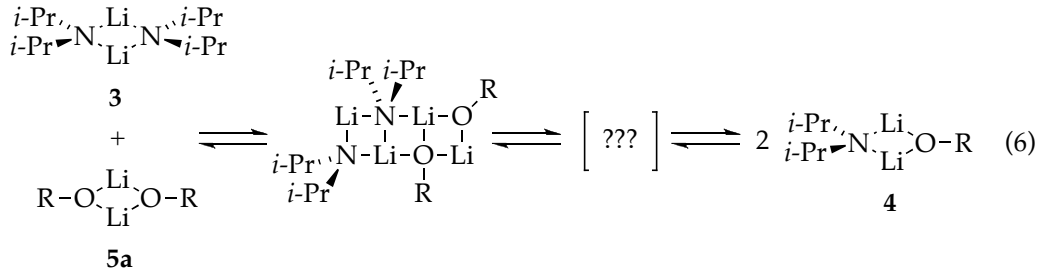

(6)

LiCl-Catalyzed 1,4-Additions. Very low concentrations of LiCl (<0.5 mol % relative to LDA) cause marked accelerations of the 1,4-addition and impart upward curvatures in plots of ester concentration versus time (Figure 2.1), which suggests that LiCl catalysis brings ester **1** into the rate law. The decays become cleanly first-order at >0.5 mol % LiCl under pseudo-first-order

conditions. Plotting the initial rate versus LiCl concentration revealed saturation kinetics with rates that plateau at >0.5 mol % LiCl (Figure 2.16).[42]

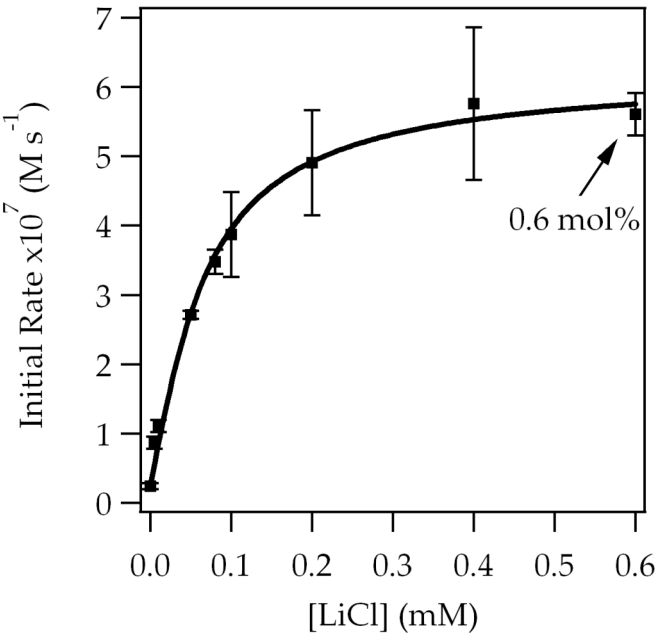

Figure 2.16. Plot of initial rate vs [LiCl] in THF (6.1 M) for the 1,4-addition of ester **1** (0.004 M) with LDA (0.10 M) at -78 °C. The 0.6 mol % notation is relative to the LDA concentration.

Saturation often arises when a bimolecular reaction at low concentration becomes unimolecular at higher concentrations because an observable complex is formed.[43] Enzymology offers a plethora of examples under the rubric of Michaelis-Menten kinetics.[44] Michaelis-Menten-like saturation behavior, however, would require ≥100 mol % LiCl, not a mere 0.5 mol %, to form observabe LDA-LiCl mixed aggregates **6** and **7** as the dominant species.[45]

Saturation kinetics can also be caused by a change in the rate-limiting step.[43] Indeed, our rate studies are consistent with a scenario in which LiCl catalyzes a dimer-monomer exchange (eq 7):

$$\tfrac{1}{2}\,A_2S_2 \underset{k_{-1}[LiCl_T]}{\overset{k_1[LiCl_T]}{\rightleftharpoons}} AS \qquad (7)$$

where $LiCl_T$=lithium chloride titer. The competition studies described below confirm this assertion. The mechanism at full saturation (1.0 mol % LiCl) was gleaned from plots showing a half-order LDA dependence (Figure 2.17) and zeroth-order THF dependence (Figure 2.18). The equilibrium approximation affords the idealized[33] rate law (given by eq 8), which implicates the monosolvated-monomer-based transition structure $[AS(ester)]^{‡}$ formed according to eq 9:[34]

$$-d[ester]/dt = (k_1/k_{-1})^{1/2}k_2[ester][S]^0[A_2S_2]^{1/2} \qquad (8)$$

$$AS + ester \xrightarrow{k_2} [AS(ester)]^{‡} \qquad (9)$$

where ester = **1**. Importantly, although LiCl catalyzes the deaggregation, it has no role in the product-determining 1,4-addition step (see eq 10 below).

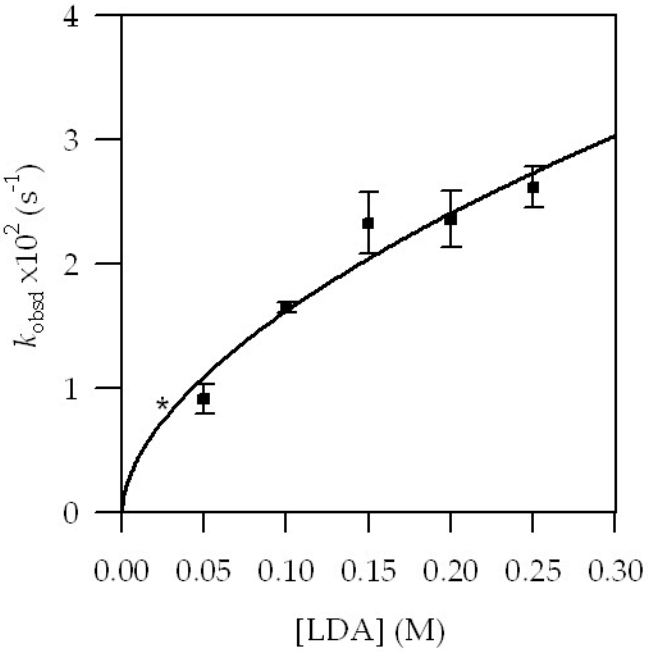

Figure 2.17. Plot of k_{obsd} vs [LDA] in THF (6.10 M) for the 1,4-addition of ester **1** (0.004 M) in the presence of 1 mol % LiCl at -78 °C. The curve depicts an unweighted least-squares fit to $y = k[LDA]^n$ [$k = (6.01 \pm 0.04) \times 10^{-2}$; $n = 0.57 \pm 0.08$]. The asterisk denotes a point that departed markedly from pseudo-first-order conditions and was not included in the fit.

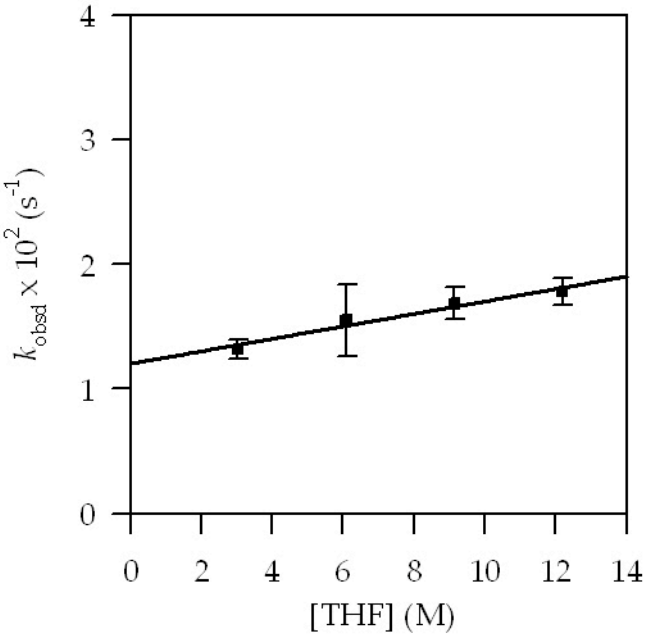

Figure 2.18. Plot of k_{obsd} vs [THF] in hexane cosolvent for the 1,4-addition of ester **1** (0.004 M) with LDA (0.10 M) in the presence of 1 mol % LiCl at -78 °C. The curve depicts an unweighted least-squares fit to $y = k[THF] + k'$ [$k = (5.0 \pm 0.01) \times 10^{-4}$; $k' = (1.2 \pm 0.1) \times 10^{-2}$].

We can now complete the mathematical analysis of the saturation curve in Figure 2.16. The transition from a rate-limiting deaggregation of dimer **3** in the absence of LiCl to a fully established pre-equilibrium at high $LiCl_T$ concentration precludes the equilibrium approximation. The time dependencies of the concentrations of ester **1** and LDA dimer and monomer are described by eqs 10-12, respectively:

$$-d[\text{ester}]/dt = -k_2[\text{ester}][\text{AS}] \quad (10)$$

$$-d[A_2S_2]/dt = k_1[LiCl_T][A_2S_2] - k_{-1}[LiCl_T][\text{AS}]^2 \quad (11)$$

$$-d[\text{AS}]/dt = -2k_1[LiCl_T][A_2S_2] + 2k_{-1}[LiCl_T][\text{AS}]^2 + k_2[\text{ester}][\text{AS}] \approx 0 \quad (12)$$

Solving for the concentration of monomer AS in eq 12 using the quadratic equation and substituting the result into eq 10 affords the rate law in eq 13:

$$-\frac{d[\text{ester}]}{dt} = \frac{k_2[\text{ester}]}{4k_{-1}[LiCl_T]}\left(\sqrt{k_2^2[\text{ester}]^2 + 16k_1k_{-1}[A_2S_2][LiCl_T]^2} - k_2[\text{ester}]\right) + c \quad (13)$$

where *c* corresponds to the low basal rate of uncatalyzed deaggregation. The quantity $-d[\text{ester}]/dt$ in eq 13 is equal to $-\Delta[\text{ester}]/\Delta t_{(t=0)}$ obtained by initial rates. The curve in Figure 2.16 corresponds to a fit to eq 13. Although eq 13 lacks the intuitive appeal of simple saturation functions, the rate reduces to *c* as $LiCl_T$ concentration approaches zero and to eq 9 at high $LiCl_T$ concentration.[46]

Since deaggregation is rate-limiting in the absence of LiCl (eq 3), it is logical that accelerating the deaggregation through LiCl catalysis would

accelerate the reaction. Why LiCl changes the rate-limiting step is less obvious. Inspection of the mechanism in eqs 7 and 8 shows that elevated LiCl concentrations (k_{-1}[$LiCl_T$] >> k_2[ester]) cause the reaggregation to become competitive with the 1,4-addition, eventually affording a fully established pre-equilibrium. Thus, it is formally the catalysis of the *reaggregation* of LDA monomer by LiCl that causes the 1,4-addition to become rate-limiting. Such reversibility is also required for a fractional-order dependence on LDA concentration to be observed.

The mechanism by which LiCl catalyzes the deaggregation of LDA is elusive, but a few comments are warranted. In LDA-LiCl mixtures containing low LiCl concentrations, LiCl exists exclusively as mixed aggregates **6** and **7** (1:8) to the exclusion of appreciable free LiCl.[27,28] Thus, an apparent first-order dependence on the total LiCl concentration at the lowest LiCl concentration[47] is tantamount to a first-order dependence on the mixed aggregates.

With the monosolvated-monomer-based stoichiometry established for the addition under full LiCl catalysis, we turned to DFT computations. Transition structure **10** is plausible (MP2-corrected $\Delta G^{\ddagger}$ = 16.3 kcal/mol at -78 °C), although the energy is large relative to the calculated barrier for the rate-limiting deaggregation (Scheme 1).

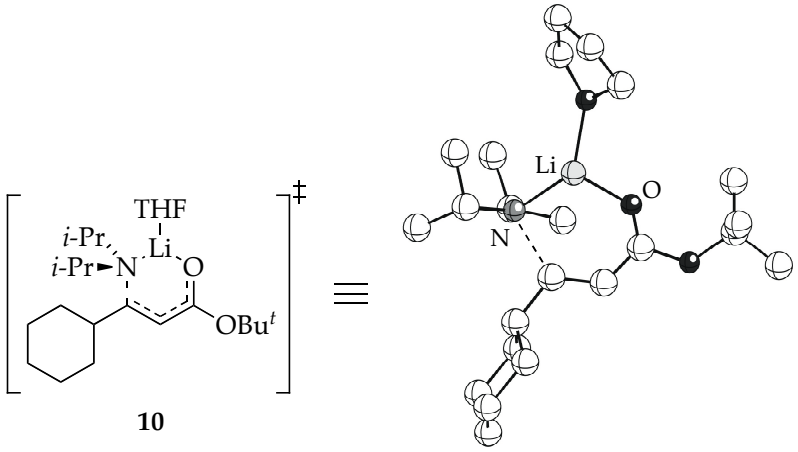

10

Competition Studies. We delineated three pathways for 1,4-addition that *may* share a common reactive intermediate: (1) uncatalyzed 1,4-addition with the key post-rate-limiting addition opaque to standard kinetic analysis; (2) autocatalyzed (enolate-mediated) deaggregation with the key 1,4-addition remaining post-rate-limiting; and (3) LiCl-catalyzed deaggregation with rate-limiting 1,4-addition (eqs 7 and 8), which was shown to proceed via LDA monomer **11**. (We have chosen to draw the fleeting monomer **11** as the computationally most stable trisolvate.[48]) Standard protocols for examining post-rate-limiting steps to probe for common (shared) intermediates usually entail comparing inter- and intramolecular isotope effects.[49] Showing that isotopic substitution affects the selectivity at a key branch point, but not the reaction rate, confirms that the isotopically sensitive step is post-rate-limiting. Since the 1,4-addition is poorly suited for isotopic labeling, we turned to a related approach using two structurally distinct substrates.

We established the reactivity of monomer **11** toward ester **1** and its *n*-alkyl analogue **12**[50] under conditions of fully saturated LiCl catalysis (eq 14). Whether in competition or in separate vessels, **12** displayed 7-fold greater

reactivity. (We used gas chromatography of serially quenched separate vessels to monitor mixtures of esters **1** and **12** for the competition experiments.) The 7:1 relative reactivity provides an important benchmark for monomer **11**.

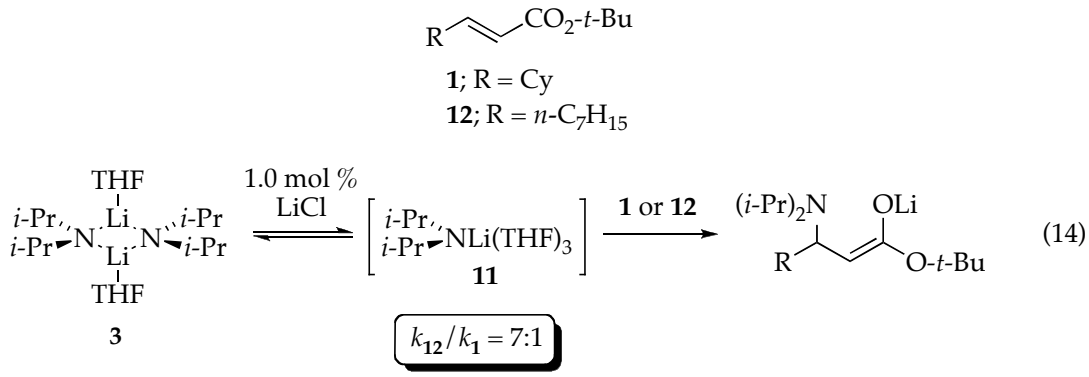

(14)

The uncatalyzed reaction of ester **1** with LDA involves a post-rate-limiting 1,4-addition: is the key intermediate in that case also monomer **11**? Ester **1** and *n*-alkyl analogue **12** underwent 1,4-additions at indistinguishable rates despite differing steric demands, as expected for a rate-limiting deaggregation and post-rate-limiting 1,4-addition. In contrast, reacting an equimolar mixture of **1** and **12** with 2.0 equiv of LDA revealed a 7-fold greater reactivity of **12** relative to **1** (eq 15), as expected if monomer **11** is the intermediate. We also observed that once **12** was fully consumed, ester **1** reacted at a rate comparable to that of **12** (Figure 2.19). Such biphasic kinetics would be expected for post-rate-limiting 1,4-additions.[51]

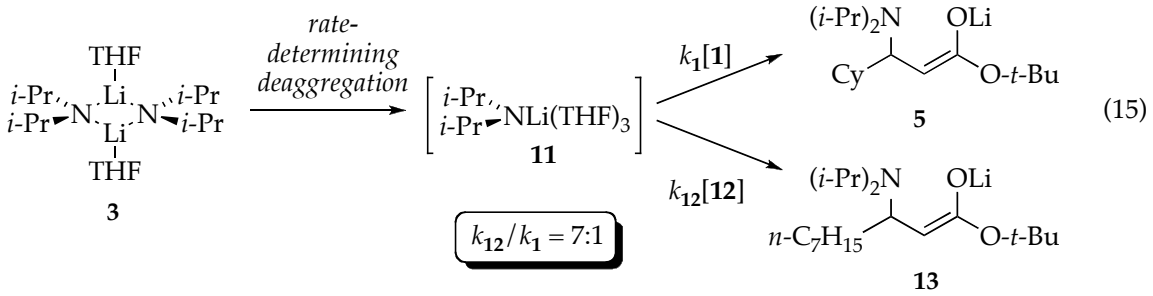

(15)

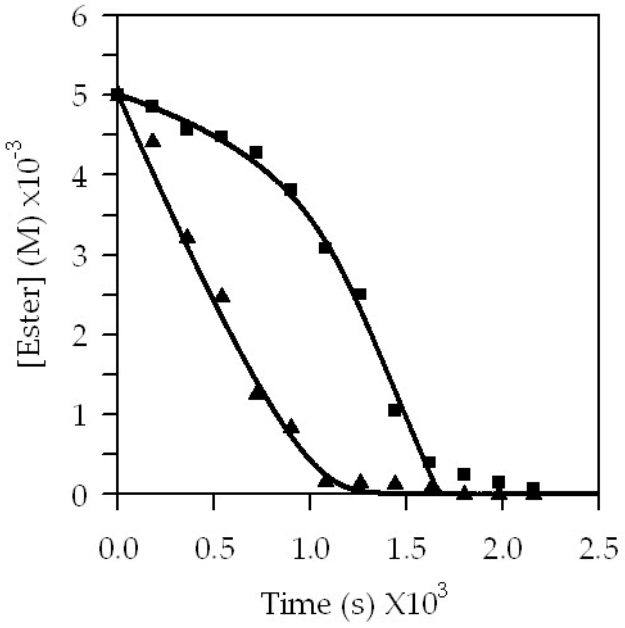

Figure 2.19. Plots of ester concentration vs time for the uncatalyzed 1,4-addition of LDA (0.10 M) to a mixture of esters **1** and **12** (0.005 M each) in THF (6.10 M) at -78 °C: (■) Ester **1**; (▲) Ester **12**. Results were analyzed by GC relative to a decane internal standard.

We suspected that the weak autocatalysis arises because ester enolate **5** is an inferior deaggregation catalyst in comparison with LiCl. A reaction was carried out to 50% conversion by adding 0.5 equiv of ester **1**—conditions to establish lithium enolate-induced acceleration—and subsequently treating the mixture with either **1** or **12** (separate reactions); the accelerations were indistinguishable for the two substrates. These results indicate that the formation of monomer **11** is still rate-limiting, as expected for a catalyst that is

poor compared with LiCl. In contrast, treating an analogous equimolar mixture of LDA and mixed dimer **4** with an equimolar mixture of esters **1** and **12** showed a relative reactivity of 7:1. This confirmed that the back-reaction in eq 15 (the reaggregation of LDA) is slow relative to the 1,4-addition (eq 16) and showed commonality of intermediate with in the uncatalyzed and LiCl-catalyzed 1,4-additions.

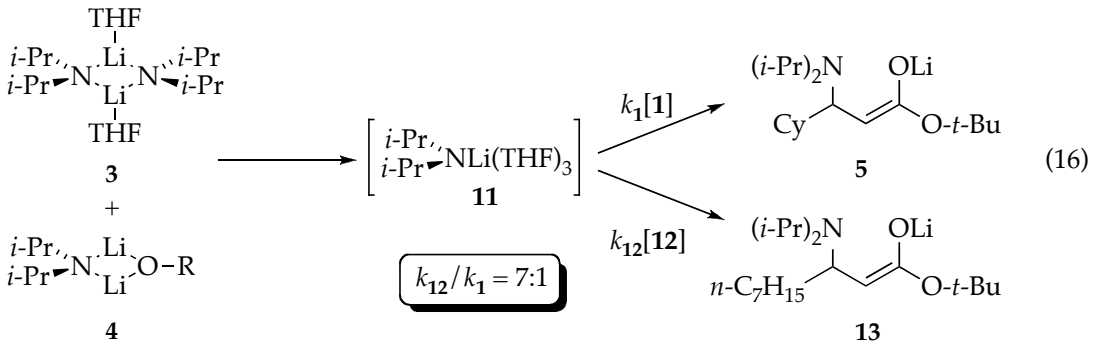

(16)

Mechanistic Hypothesis and Numerical Integrations.[52,53] The rate and mechanistic studies were pieced together to form the mechanistic hypothesis shown in Scheme 2 and described by the affiliated differential equations given in eqs 17-22. As mentioned previously, in these equations A stands for an LDA subunit and E stands for an enolate subunit. We have taken some liberties with the depiction of the model in Scheme 2 to optimize the visual presentation. Although the role of the solvent has been elucidated for a number of steps, it is not germane to the numerical fitting and has been omitted for clarity. We have depicted the critical autocatalytic step by affiliating k_3 and k_{-3} with fleeting the mixed trimer A_2E; this step is described numerically in the differential equations by means of the equilibrium $A_2 + E \rightleftharpoons A + AE$. The equilibria in Scheme 2 are unbalanced to minimize clutter.

However, the differential equations are all fully balanced to provide a valid mathematical description.

Scheme 2

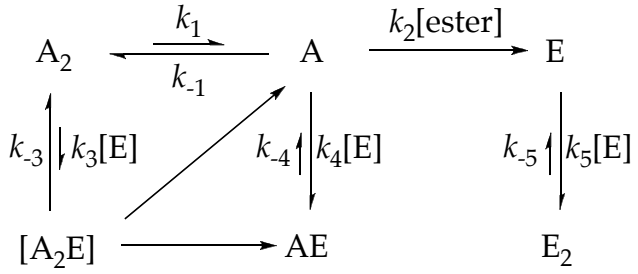

$$d[\text{ester}]/dt = k_2[\text{A}][\text{ester}] \tag{17}$$

$$d[\text{A}_2]/dt = -k_1[\text{A}_2] + k_{-1}[\text{A}]^2 - k_3[\text{A}_2][\text{E}] + k_{-3}[\text{A}][\text{AE}] \tag{18}$$

$$d[\text{A}]/dt = 2k_1[\text{A}_2] - 2k_{-1}[\text{A}]^2 - k_2[\text{A}][\text{ester}] + k_3[\text{A}_2][\text{E}] - k_{-3}[\text{A}][\text{AE}] - k_4[\text{A}][\text{E}] + k_{-4}[\text{AE}] \tag{19}$$

$$d[\text{AE}]/dt = k_3[\text{A}_2][\text{E}] - k_{-3}[\text{A}][\text{AE}] + k_4[\text{A}][\text{E}] - k_{-4}[\text{AE}] \tag{20}$$

$$d[\text{E}]/dt = k_2[\text{A}][\text{ester}] - k_3[\text{A}_2][\text{E}] + k_{-3}[\text{A}][\text{AE}] - k_4[\text{A}][\text{E}] + k_{-4}[\text{AE}] - 2k_5[\text{E}]^2 + 2k_{-5}[\text{E}_2] \tag{21}$$

$$d[\text{E}_2]/dt = k_5[\text{E}]^2 - k_{-5}[\text{E}_2] \tag{22}$$

It is nearly impossible to reproduce in prose how the model came into being, but we can describe the general strategy as well as the most critical constraints. We hasten to add at the outset that despite aphorisms proclaiming that anything can be fit given enough differential equations, our experience with complex systems containing a large number of restrictions and observables (see Figures 2.5-2.8) is quite the opposite. The model in Scheme 2 is the simplest model that fits the data, and many others failed to do so quite decisively.

First, a few comments about general tactics are warranted. The rate data placed significant constraints on the model. In other instances, seemingly reasonable hypotheses were excluded only through numerical simulations showing that key curvatures were not reproduced. Once the data in Figures 2.5-2.8 were qualitatively reproduced through numerical simulations, best-fit numerical integrations of eqs 17-22 afforded the functions displayed.

The key constraints imparted by the curvatures in Figures 2.5-2.8 include the following: (1) the linear decay of ester; (2) the two obvious discontinuities (most easily seen in Figure 2.8), namely, the maximum in enolate dimer (E_2) concentration and the marked change in rate of formation of the mixed dimer (AE) concentration, that coincide with the consumption of ester; (3) an overshoot in the concentration of E_2 relative to the equilibrium population; and (4) the coincident formation of AE and E_2 at the outset of the reaction (most easily observed in Figure 2.5), indicating that AE is *not* a requisite precursor to E_2 (or vice versa).[54]

The model was assembled as follows:

(1) Rate-limiting deaggregation of A_2 gives monomer A, which subsequently reacts in a post-rate-limiting step with ester to give enolate. This enolate necessarily forms as a monomer (E). Thus, the $A_2 \rightarrow A \rightarrow E$ sequence representing the top half of Scheme 2 was fully established by traditional kinetic methods.

(2) The fate of enolate monomer E was quite obviously a central issue. Self-condensation of E is one logical source of E_2 (the other logical source would be direct reaction of AE with ester). The condensation of A and E is an obvious source of the mixed dimer AE. A critical insight was that the

bifurcation of E to form E_2 and AE allows for their concurrent formation (with no induction period in either case).

(3) Two factors elicited the inclusion of the pathways involving the condensation of E with A_2 (via A_2E) to give the mixed dimer AE and monomer A. (To reiterate, this was modeled as a net conversion and does not connote a single-barrier pathway.) The most important factor was that the numerical simulations failed to reproduce the curvatures. *How* the simulations failed was key, in that the simulations kept suggesting a source of AE independent of the simple reaggregation of A and E. Of course, there was considerable experimental evidence of autocatalysis, which could only arise by accelerating the rate-limiting deaggregation of LDA dimer A_2.

(4) One might ask why the autocatalytic step is depicted as proceeding via A_2E rather than through a dimer-dimer condensation via A_2E_2. Again, the simple answer is that no amount of tinkering could force the curves to fit using an A_2E_2-based pathway. One could justify a provision for A_2E_2 *in addition to* A_2E on the basis of the kinetics of mixed aggregation described in eqs 5 and 6, but the improvement in the fit was statistically insignificant.

The components of the model in Scheme 2 are well founded by the rate and mechanistic studies. As can be seen from Figures 2.5-2.8, the best-fit numerical integrations to eqs 17-22 are exceptional.

Discussion

It is becoming evident that reactions of LDA in THF at -78 °C are mechanistically complex even by the standards of organolithium chemistry.[11,12] Nature could not have chosen a more inauspicious opportunity—a more synthetically relevant reagent under the most commonly used conditions—to insert confusion. The complexity stems from aggregate

exchanges that occur at rates comparable to those of reaction with substrate.[10] The result is that aggregation events can become rate-limiting, so LDA-containing aggregates are not at full equilibrium on the time scales of their reactions with substrates. The first detailed investigations of such phenomena focused on ortholithiations of fluorinated aryl carbamates.[11] The almost perfectly linear decays normally attributed to zeroth-order ester dependencies were traced to the superposition of a *first*-order ester dependence and autocatalysis. In the case of the 1,4-addition, seemingly analogous linear decays were traced to the superposition of a *zeroth*-order ester dependence and much less pronounced autocatalysis. A summary of the mechanism customized for mathematical treatment is provided in Scheme 2. The more structurally illuminating version with the full complement of intermediates and transition structures is summarized in Scheme 3. A compartmentalized summary follows.

Scheme 3

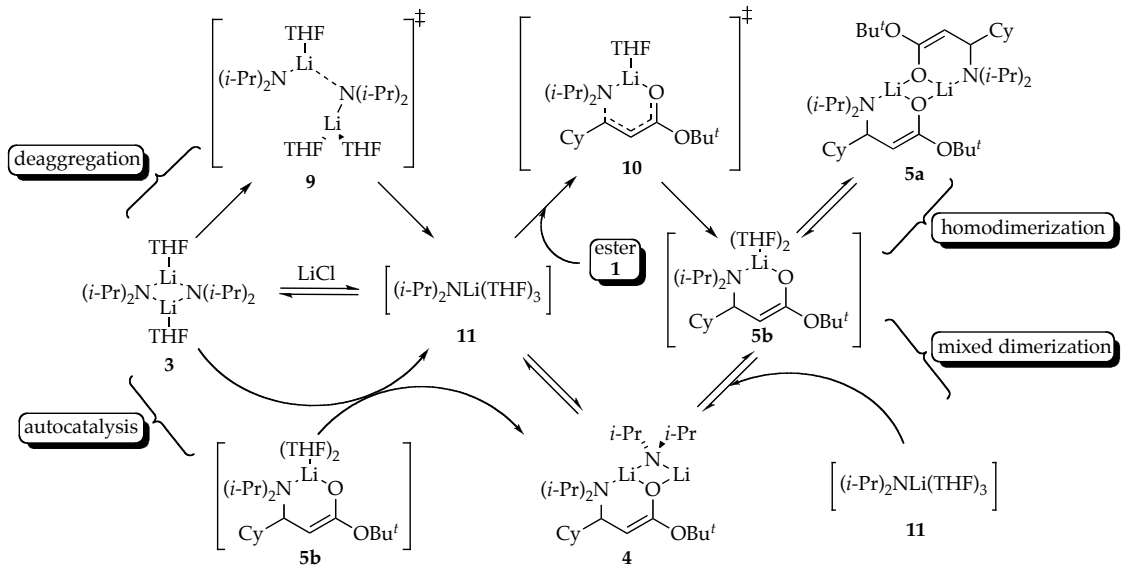

Rate-Limiting Deaggregation. Monitoring the initial rates of the uncatalyzed 1,4-addition to ester **1** revealed a true zeroth-order ester dependence: deaggregation of LDA is rate-limiting, and the 1,4-addition step is post-rate-limiting. The trisolvated-dimer-based deaggregation is either a partial deaggregation to form the open dimer[35] via transition structure **8** or a complete deaggregation to form the monomer via transition structure **9**. Computational studies indicate that **9** has the higher barrier. Even if the rate-limiting step involves formation of the open dimer via **8**, however, standard rate studies do not peer past the rate-limiting step to distinguish between monomer-based and dimer-based reactions with ester **1**. A combination of rate studies in the presence of LiCl and competition studies (both discussed below) support monomeric intermediate **11** and monosolvated-monomer-based transition structure **10**.

Autocatalysis. The rate-limiting deaggregation of dimer **3** that is dominant at the onset of 1,4-addition is overlaid by contributions from muted autocatalysis as the reaction progresses. It is very tempting to focus on mixed dimer **4** for an explanation, but that would be wrong. Neither the elevated concentration nor higher reactivity of mixed dimer **4** causes the autocatalysis. Mixed dimer **4** could react with ester **1** instantaneously, and this *still* would not constitute autocatalysis. An autocatalyst *must* catalyze the rate-limiting deaggregation of LDA. To understand autocatalysis, it is instructive to focus on the structurally simplified model in Scheme 2.

Autocatalysis stems from acceleration of the the rate-limiting deaggregation of LDA dimer, denoted as A_2. Notably, enolate homodimer E_2 is an ineffectual catalyst: it reacts with LDA dimer *very* slowly. The autocatalysis was traced to the reaction of enolate *monomer* E. When LDA

monomer A reacts with ester to form enolate monomer E, E can dimerize to form E_2 or react with an LDA monomer A to form the mixed dimer AE. Occasionally, however, E reacts with LDA dimer A_2 to form AE and monomer A. *This* is autocatalysis.

The data, however, seem paradoxical. The plot of the reaction rate versus time when equimolar LDA and ester were used (Figure 2.4) shows some straightening that hints at autocatalysis, but a marked sigmoidal decay characteristic of virulent autocatalysis is notably absent. In short, the reaction is *not* faster at 50% conversion. In contrast, however, incremental additions of ester **1** to LDA (Figure 2.13) showed a marked increase in rate with each increment, reaching a net 4-fold higher rate at 50% consumption of LDA and 50% formation of enolate. An analogous 4-fold autocatalysis certainly would have elicited a quite distinct sigmoidal curvature in Figure 2.4.

How do we reconcile these two contrasting views? The key to understanding Figure 2.13 is to note that under normal reaction conditions, the aggregates are *not* at full equilibrium, so the LDA-enolate mixed dimer AE remains well below its equilibrium concentration. In contrast, the incremental additions in Figure 2.13 allow full equilibration of the aggregates between increments. As a consequence, AE attains substantial equilibrium concentrations. When the subsequent increment of ester is added, the key LDA monomer is generated either from rate-limiting deaggregation of A_2 or by a more facile (and only partially rate-limiting) deaggregation of mixed dimer AE. The rate maximum in Figure 2.13 corresponds to the maximum concentration of the kinetically labile AE mixed dimer. Thus, an experiment initially intended to explicitly probe autocatalysis uncovered an altogether different mixed aggregation effect. We will return to these distinctions below.

LiCl Catalysis. The 1,4-addition of LDA to ester **1** is measurably accelerated by as little as 0.001 mol % LiCl (i.e., *1.0 ppm*). At the risk of stating the obvious, we note that this is remarkably efficient catalysis.[13] Readers might be unsurprised that this catalysis plagued the rate studies until we adapted protocols for preparing rigorously LiCl-free LDA from lithium metal.[20] (Ironically, the modified synthesis is also more convenient than our standard method.)

Lithium chloride accelerates the 1,4-addition by catalyzing the deaggregation of LDA, as summarized in eqs 7 and 8. Saturation behavior (Figure 2.16) with an onset of saturation at >0.5 mol % LiCl derives from a LiCl-catalyzed exchange of LDA dimers and monomers, resulting in a change from rate-limiting deaggregation to rate-limiting 1,4-addition. How LiCl catalyzes LDA deaggregation is still unclear and the subject of ongoing investigations. Nonetheless, the rate studies revealed a monosolvated monomer-based pathway for the addition, and the computational studies filled in the intimate details of transition structure **10**.

Competition Studies: Commonality of Intermediate. Competing esters **1** and **12** having different steric demands allowed us to probe the post-rate-limiting reactivity (eqs 14-16). These studies are tactically analogous to comparisons of inter- and intramolecular isotope effects.[50]

The substrate-dependent rates under LiCl catalysis showed that the 1,4-addition is rate-limiting. Ester **12** is 7-times more reactive than ester **1** toward monomer **11** (eq 14) both in separate reactions and in competition. Most importantly, this 7:1 preference serves as a benchmark for the monomer-based addition.

In the 1,4-addition under *uncatalyzed* conditions, where partial or total deaggregation is rate-limiting, the rates of 1,4-addition were identical for **1** and **12** when measured independently, confirming a post-rate-limiting addition. Using mixtures of **1** and **12** in competition, however, produced the same 7-fold higher reactivity of **12** (eq 15) characteristic of trapping of monomer **11**.

A competition was carried out using equimolar mixtures of LDA and lithium enolate **5** to examine the influence of mixed dimer **4** (eq 16). When compared independently, esters **1** and **12** showed identical reactivities, indicating that the deaggregations of **3** *and* **4** remain rate-limiting. In contrast, competition of **1** and **12** revealed the 7-fold greater reactivity of **12** characteristic of reaction with monomer **11**.

Do the 7:1 selectivities for the uncatalyzed, LiCl-catalyzed, and enolate-mediated additions *rigorously* show the commonality of intermediate **11** and transition structure **10**? In a word, no. The selectivities do, however, make for a compelling circumstantial case.

Mixed Aggregation Effects: Four Variants. Effects of lithium salts on organolithium reactivity—so-called mixed aggregation effects—were first documented decades ago.[14] Examples of mixed aggregation effects on rates and selectivities, whether LiX salts are added explicitly or formed in situ, are now legion.[13] Mechanistically well-defined examples, however, are quite rare by comparison.[15] We take this opportunity to discuss four distinct classes of mixed aggregation effects using LDA emblematically.

Case 1. Probably the most often cited and certainly the most intuitively simple salt effect derives from the direct reaction of mixed aggregates (such as **4**, **6**, and **7**) with substrate (eq 23). Because the steric and electronic properties

of LDA-LiX mixed aggregates are markedly different than those of homoaggregated LDA dimer **3**, and the LiX salt is assumed to be strategically located in the rate- and product-determining transition structures, it is easy to understand how LiX could markedly influence both the rate and selectivity. We have documented the direct reaction of LDA mixed dimers.[15] Although the mixed aggregates could be either fleetingly stable or observable quantitatively, inhibition by observable mixed aggregates is prevalent.[15,55] The critical requirement common to all examples in case 1, whether inhibiting or accelerating, is that the LiX salt remain intimately involved in the rate- or product-determining transition structure.

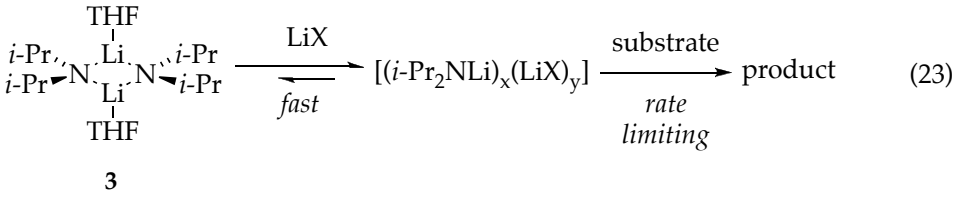

3 (23)

Case 2. Rate reductions are not the only consequence of inhibition. Imagine that a mixed aggregate forms quantitatively and shows no reactivity toward substrate (eq 24). The only available avenue of reaction is via free LDA. To the extent that the steady-state concentration of LDA is decreased to very low levels, representing a dilution of sorts, monomer-based pathways will be promoted relative to dimer-based pathways.[56] The influence of such a mass-action effect on the efficacies of the monomer- and dimer-based pathways is illustrated in eq 25.[15] Indeed, an LDA-dimer-based ester enolization was diverted by an intervening LDA-lithium enolate mixed dimer through both mixed-dimer-based *and* monomer-based pathways. To the

extent that LiX can divert a dimer-based pathway to a monomer-based pathway, an LiX-dependent change in selectivity could arise *without intimate association of LiX with the product-determining transition structure.*

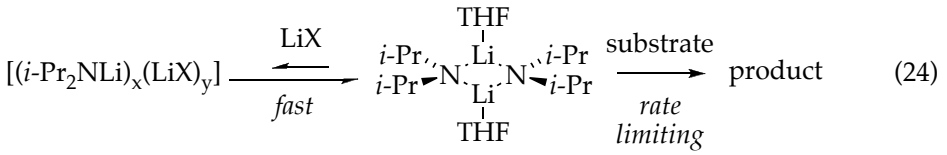

(24)

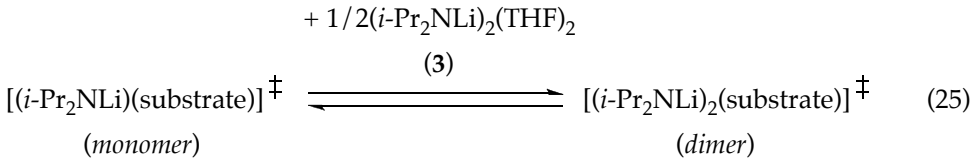

(25)

Case 3. The mixed aggregation effects described in this paper involve LiX-catalyzed deaggregation. We must point out that there is jargon in the literature that loosely refers to LDA-LiX mixed aggregates as deaggregated because the mixed aggregate contains only one LDA subunit. We find this usage to be unconstructive. In the case described herein, however, the role of LiX salts (LiCl and, to a much lesser extent, lithium enolate) is to catalyze the formation of true LDA monomer (eq 26). To the best of our knowledge, this catalysis is undocumented. It could be observed only for reactions in which deaggregation is either rate-limiting or precluded altogether by a high barrier (forcing the reaction to occur with the aggregated form). No catalysis by LiCl will be observed if all of the aggregation states are fully equilibrated on the time scale of the reaction without added catalyst. Of course, to the extent that a rate-limiting deaggregation is accelerated, the overall reaction will be accelerated also. If that catalysis affords the same intermediate as the

uncatalyzed deaggregation (monomer **11**), only faster, then the accelerations and even changes in the rate-limiting step will *not* be accompanied by changes in regio- or stereoselectivity. However, if the preferred pathway for the uncatalyzed reaction is *dimer*-based because of a prohibitively high barrier to deaggregation and LiX catalyzes monomer formation, the acceleration could be accompanied by a change in selectivity. We suspect that regioselective ortholithiations may be a fruitful place to look for such phenomena.

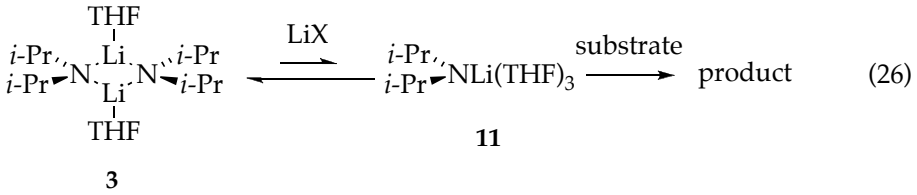

(26)

Case 4. In cases 1 and 2, we have implicitly assumed that the aggregate exchanges are fast relative to reactions with substrate. Under this criterion, mixed aggregation must necessarily inhibit a reaction according to the principle of detailed balance[56] unless the mixed aggregate can react with the substrate directly and rapidly. Case 4 addresses the consequences of mixed aggregation when aggregate exchanges are *not* at equilibrium during the course of the reaction. If, for example, deaggregations of LDA dimer **3** and mixed dimer **4** are rate-limiting (i.e., if reaction with LDA monomer is at least competitive with reaggregation, as the model in Scheme 2 suggests), the result would be a scenario in which facile deaggregation of mixed dimer **4** increases the rate that monomeric LDA is released and subsequently trapped. Formally, this is not autocatalysis because autocatalysis requires a provision for accelerating the deaggregation of LDA dimer **3**. Solutions containing

considerable concentrations of labile mixed dimer **4**, however, would show a higher reactivity than analogous solutions containing only LDA dimer **3**. This scenario accounts for 1,4-additions in the presence of enolate that are more rapid than would be predicted on the basis of the low levels of autocatalysis.

Conclusion

A number of consequences of the work described herein are clear. Because traces of LiCl may contaminate LDA, source and batch dependencies could become acute. Synthetic chemists carrying out LDA-mediated reactions in THF at -78 °C might notice enormous differences between commercial LDA (which tends to be LiCl-free) and LDA generated in situ from *n*-BuLi (which contains ample LiCl to catalyze exchanges). Indeed, this is the case for the 1,4-addition in eq 1. Adding traces of LiCl (in the form of Et_3NHCl) to commercial LDA equalizes the two protocols. Moreover, marked catalysis by traces of LiCl and inhibitions by molar excesses of LiCl suggest that the quantity of LiCl is important. We are reminded of LDA-mediated 3-pentanone enolizations, in which the *E*/*Z* selectivities are maximized using fractional-equivalent amounts of LiCl.[28] Could a composite of mixed aggregation effects be operative? We have long believed that deconvoluting the roles of LiCl in *E*-selective ketone enolizations would remain outside our grasp, but we are not so pessimistic now. We have also reported LiCl-accelerated ortholithiations in which traces of LiCl dramatically accelerated the rates but had *no* influence on regiocontrol because the regioisomers were fully equilibrated.[57] Some LDA-mediated ortholithiations are *not* at equilibrium,[58] however, and may display regioselectivities that *are* sensitive to traces of LiCl.

It is instructive to look forward. We have now reported two extensive studies of LDA-mediated reactions in which inordinate complexity rears its ugly head under conditions favored by synthetic chemists: LDA/THF/-78 °C. This is no bizarre coincidence: under these conditions, aggregation events occur with half-lives on the order of minutes. *Any* LDA/THF-mediated reaction that proceeds on a similar time scale at -78 °C will be subjected to potentially rate-limiting deaggregation and display a hypersensitivity to added lithium salts. Subtle changes in substrate reactivity and product (autocatalyst) structure could cause marked shifts in the relative efficacies of the competing steps and consequent baffling changes in rate behavior. Ongoing studies suggest that there may even be several rate-limiting LDA deaggregations (depending on the choice of substrate) and several variants of autocatalysis. We are becoming increasingly certain that many—possibly all—LDA/THF-mediated reactions carried out at -78 °C are influenced by the rates at which aggregates exchange.

We close with a caveat, but not one readers may expect. In the earliest studies of organolithium chemistry, when the role of mixed aggregates was beginning to surface, salt effects were often couched in a mechanistic context and language that were inadequate. Chastened by that experience and the daunting mechanistic and structural complexity, specialists often warn nonspecialists against invoking overly simplistic interpretations of salt effects on organolithium rates and selectivities. We admit some schadenfreude when uncovering complexity that undermines conventional mechanistic views, but it would be unfortunate if speculation (even unsubstantiated speculation) becomes stifled.

Experimental Section

Reagents and Solvents. THF and hexanes were distilled from blue or purple solutions containing sodium benzophenone ketyl. The hexanes contained 1% tetraglyme to dissolve the ketyl. Esters **1** and **12** were prepared via literature protocols.[22,50] Et_3NHCl was recrystallized from THF/2-propanol.

Preparation and Purification of LDA. Modifications of literature procedures[20] were used to prepare LDA as a LiCl-free and ligand-free solid as follows. A 250 mL Schlenk flask with an attached fine-mesh glass frit and a 250 mL receiving flask was charged with lithium shavings (1.11 g, 160 mmol), diisopropylamine (16.5 g, 160 mmol), and 80 mL of Me_2NEt. The flask was submerged in a bath at 25 °C and isoprene (5.44 g, 80 mmol) in 30 mL of dry Me_2NEt was added over 1.0 h via syringe pump. The solution was stirred for 1.0 h at 25 °C until the lithium dissolved. (The reaction became exothermic when isoprene was added too quickly, affording highly undesirable dark-yellow or purple solutions if the temperature exceeded 35 °C.) The nearly homogenous reaction mixture was filtered through a fine-mesh glass frit, and the solvent was removed under vacuum (~6 hr) to afford LDA as a white solid (16.0 g, 90% yield). With the aid of a glovebox, the LDA (8.0 g) was transferred to a 250 mL round-bottom flask fitted with a fine-mesh glass frit and a 250 mL pear-shaped receiving flask fitted with a sidearm/stopcock. The apparatus was attached to a vacuum line, and ~200 mL of hexanes was vacuum-transferred into the flask containing the solid LDA. The slurry was stirred at 63 °C (~2 h) to afford a pale-yellow solution of LDA that was subsequently filtered to remove any undissolved particles. The filtrate was transferred by cannula to a 250 ml round-bottom flask fitted with a coarse-mesh glass frit and a 250 ml receiving flask. The solution was cooled to -78 °C by incrementally

raising a dry ice/acetone bath in order to precipitate the LDA and was maintained at -78 °C overnight. The mother liquor was carefully removed by filtration, and the solid was washed three times with 10 mL of hexanes and then dried in vacuo for 6 h. The assembly was moved to the glovebox, where the LDA was collected as a white solid in 75-85% yield. The isolated material was spectroscopically indistinguishable from samples prepared previously.[18]

Synthesis of 2. Unsaturated ester **1** (0.63 g, 3.0 mmol) in 3.0 mL of THF was added to LDA (0.64 g, 6.0 mmol) in 15 mL of THF at -78 °C. The solution was stirred for 30 min and then warmed to room temperature with stirring for 1.0 h. The reaction was quenched with 10 mL of H_2O, and the mixture was extracted with diethyl ether (3 x 10 mL). The extracts were dried using Na_2SO_4, and the solvent was removed in vacuo. The residue was redissolved in CH_2Cl_2 (5 mL) and extracted with 4.0 M HCl (3 x 3 mL). The aqueous layer was neutralized with 10% NaOH and extracted with diethyl ether (3 x 5 mL). The combined organic layers were dried with $MgSO_4$, and the solvent was removed. Flash chromatography (30% ethyl acetate/hexane) afforded amino ester **2** (78-82% yield) having the spectral properties described previously.[5]

IR Spectroscopic Analyses. IR spectra were recorded using an in situ IR spectrometer fitted with a 30-bounce silicon-tipped probe. The spectra were acquired in 16 scans at a gain of 1 and a resolution of 4 cm^{-1}, and the absorbance at 1715 cm^{-1} was monitored over the course of the reaction. For the most rapid reactions, IR spectra were recorded every 3 s.

A representative reaction was carried out as follows: The IR probe was inserted through a nylon adapter and O-ring seal into an oven-dried, cylindrical flask fitted with a magnetic stir bar and a T-joint. The T-joint was capped by a septum for injections and a nitrogen line. After the flask was

evacuated under full vacuum, heated, and flushed with nitrogen, it was charged with LDA (107 mg, 1.00 mmol) in THF and cooled in a dry ice/acetone bath prepared from fresh acetone. LiCl (0.5 mol % relative to LDA) was added as a stock solution (0.50 mL) containing $Et_3N{\cdot}HCl$ (8.3 mg, 0.06 mmol) and LDA (13.5 mg, 0.12 mmol) in 5 mL of THF. After recording a background spectrum, we added ester **1** (0.005 mmol) with stirring.

NMR Spectroscopic Analyses. All of the NMR tubes were prepared using stock solutions and sealed under partial vacuum. Standard ^{6}Li, ^{13}C, and ^{15}N NMR spectra were recorded on a 500 MHz spectrometer at 73.57, 125.79, and 50.66 MHz, respectively. The ^{6}Li, ^{13}C, and ^{15}N resonances were referenced to 0.30 M [^{6}Li]LiCl/MeOH at -90 °C (0.0 ppm), the CH_2O resonance of THF at -90 °C (67.57 ppm), and neat Me_2NEt at -90 °C (25.7 ppm), respectively.

Numerical Integrations. The time-dependent concentration plots obtained using ^{6}Li NMR spectroscopy (Figures 2.5-2.8) were fit to a mechanistic model expressed by a set of differential equations. The curve fitting minimized χ^2 in searching for the coefficient values (rate constants). The Levenberg-Marquardt algorithm[52] used for the χ^2 minimization is a form of nonlinear, least-squares fitting. The fitting procedure implemented numerical integration based on the backward-differentiation formula[53] to solve the differential equations, yielding functions describing concentration versus time.

APPENDIX TWO

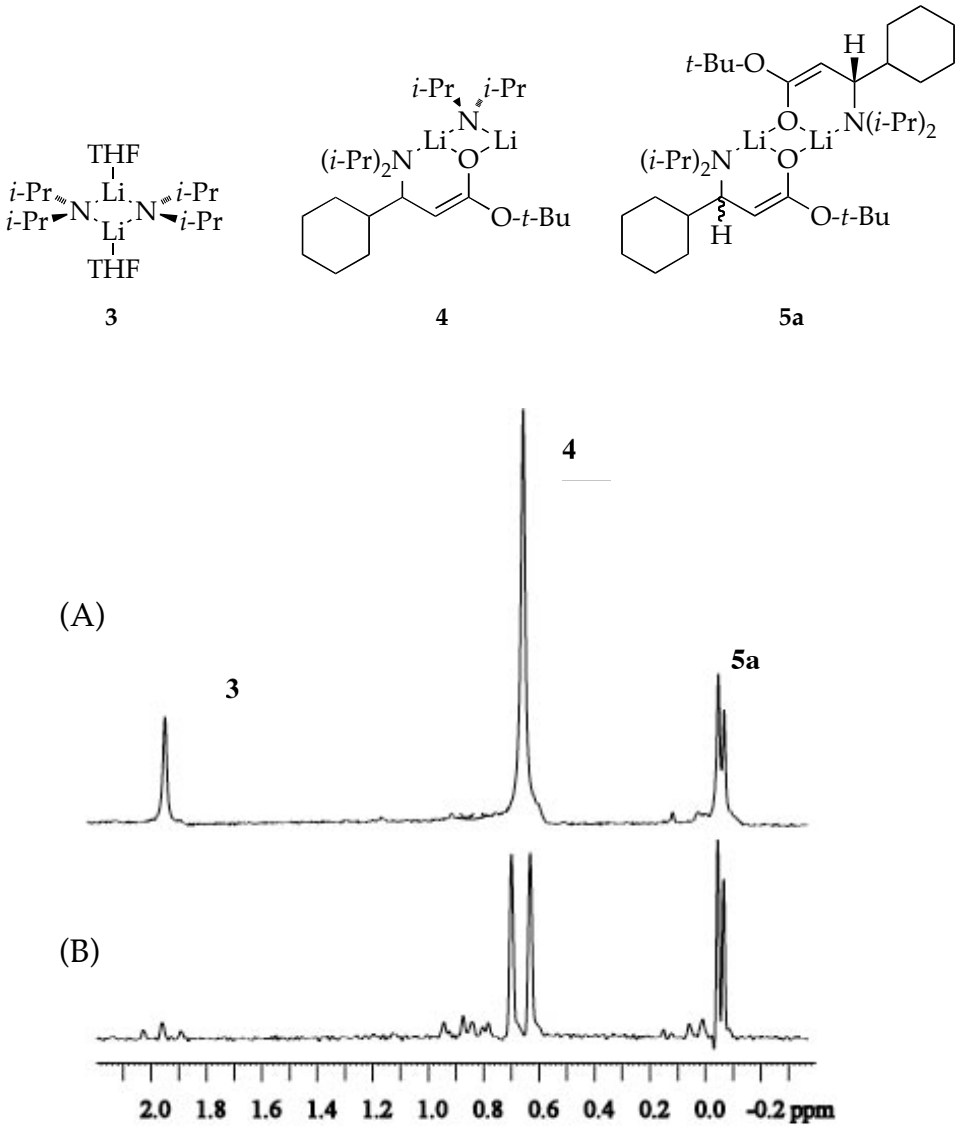

Figure A2.1. ^{6}Li NMR spectra of LDA with 0.50 equiv ester **1** in THF after aging at -55 °C for 60 min: (A) 0.10 M [^{6}Li]LDA; (B) 0.10 M [^{6}Li,^{15}N]LDA.

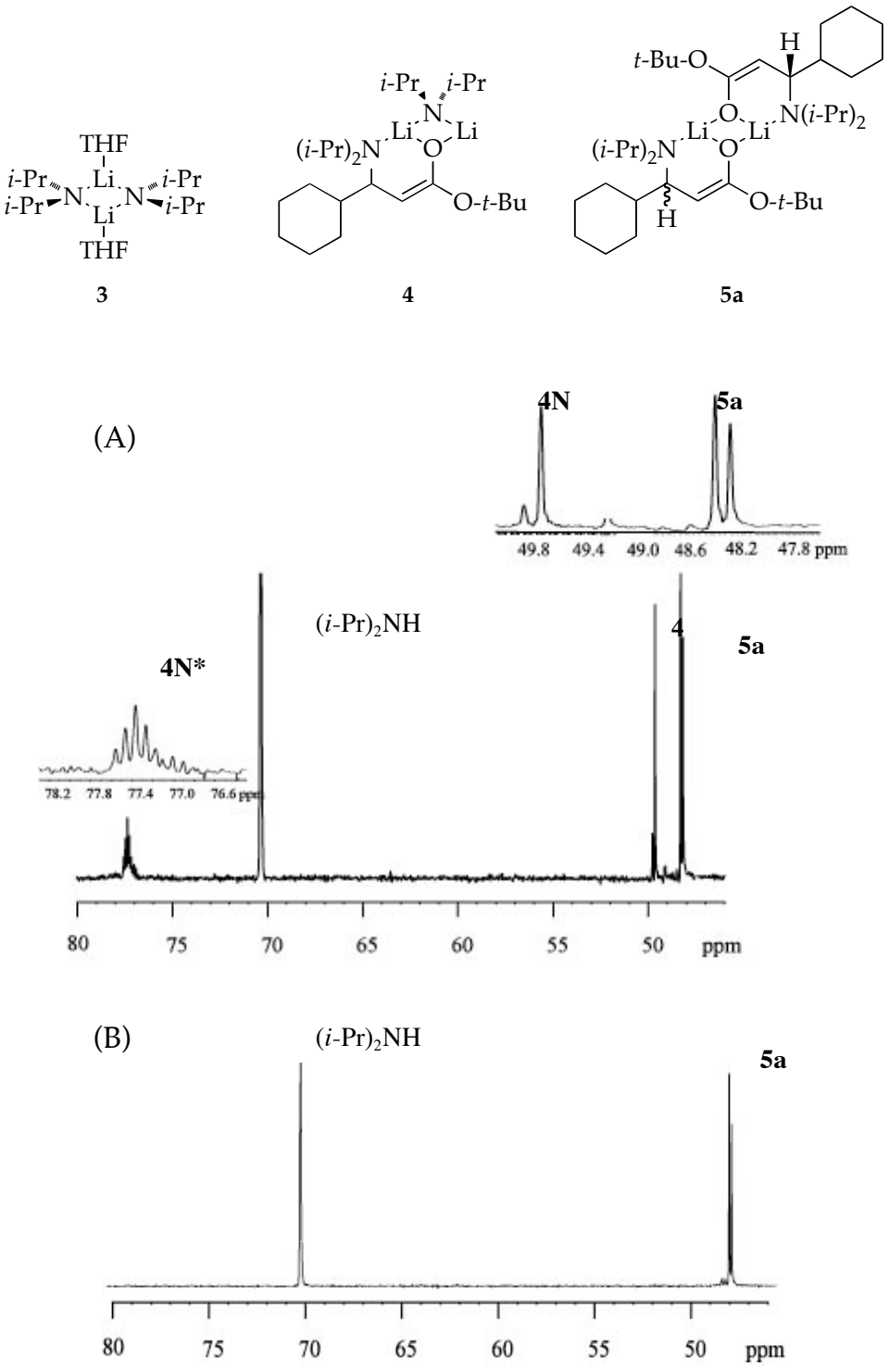

Figure A2.2. ^{15}N NMR spectra of 0.10 M [^{6}Li,^{15}N]LDA with ester **1** in THF after aging at -55 °C for 60 min: (A) 0.50 equiv ester **1**; (B) 0.90 equiv ester **1**.

(A)

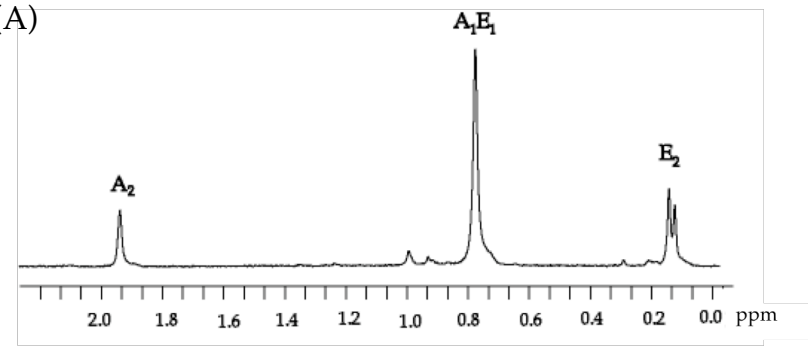

(B)

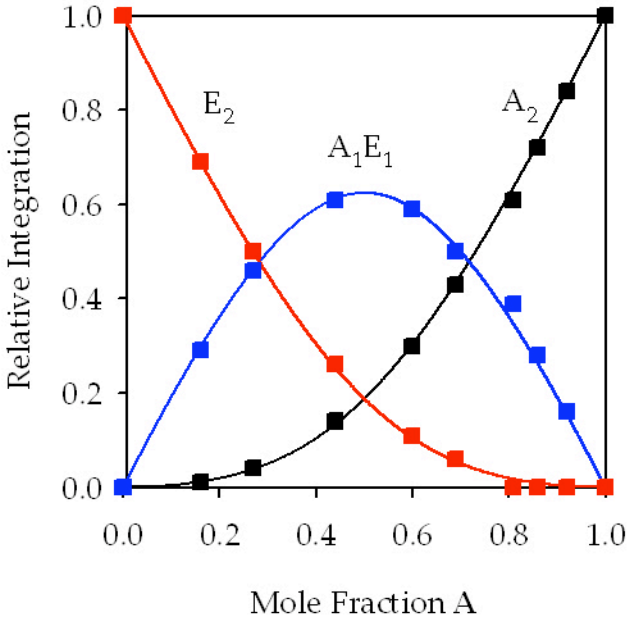

(C)

Calc. X_A	E_2	A_1E_1	A_2
1.00	0.00	0.00	1.00
0.84	0.16	0.00	0.92
0.72	0.28	0.00	0.86
0.61	0.39	0.00	0.81
0.43	0.50	0.06	0.69
0.30	0.59	0.11	0.60
0.14	0.61	0.26	0.44
0.04	0.46	0.50	0.27
0.01	0.29	0.69	0.16
0.00	0.00	0.00	1.00

Figure A2.3. (A) Representative ^{6}Li NMR spectrum of a 60:40 mixture of [^{6}Li]**5** and[^{6}Li]**3** showing homodimers (A_2 and E_2) and mixed dimer [^{6}Li]**4** (AE); (B) Plot of the relative integration vs the mole fraction of [^{6}Li]**3**, [^{6}Li]**4**, and [^{6}Li]**5**; (C) measured mole fractions of each aggregate.

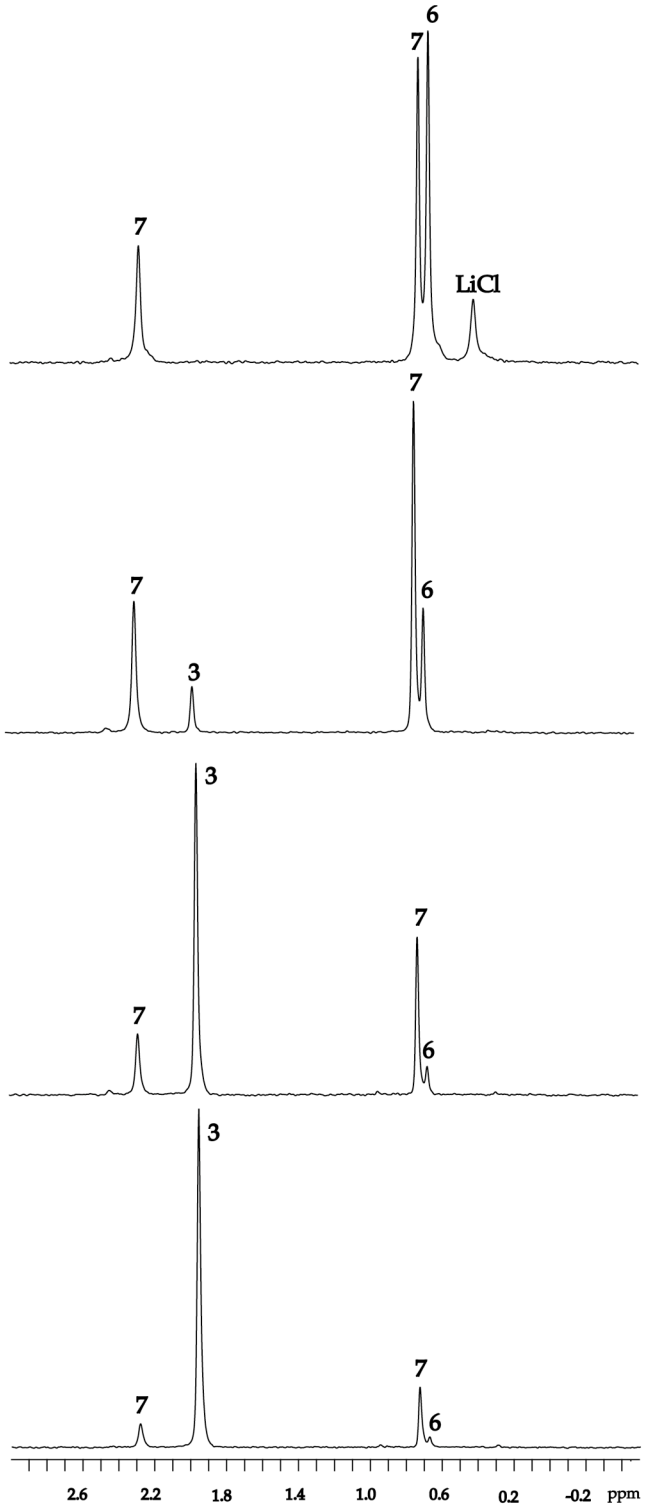

Figure A2.4. ^{6}Li NMR spectra of [^{6}Li]LDA (0.10 M) with [^{6}Li]LiCl in 12.2 M THF at -110 °C: (A) 0.05 M [^{6}Li]LiCl; (B) 0.025 M [^{6}Li]LiCl; (C) 0.01 M [^{6}Li]LiCl; (D) 0.005 M [^{6}Li]LiCl. LiCl has been characterized as a dimer in THF solution.

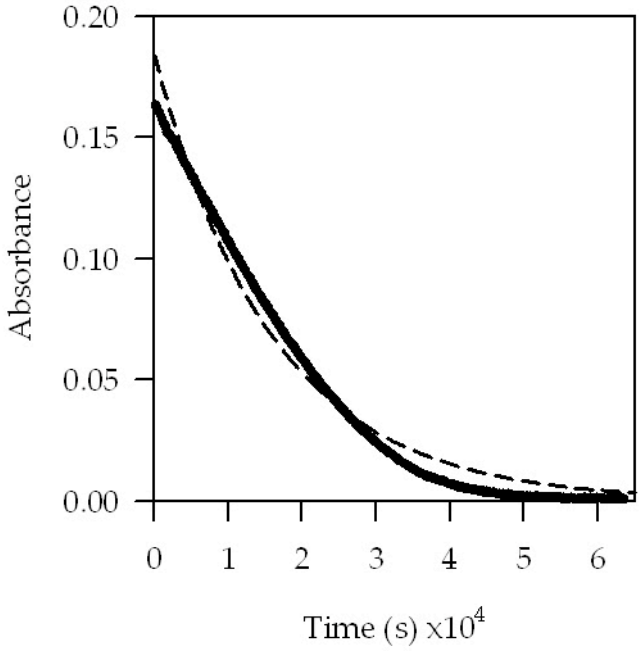

Figure A2.5. Plot showing IR absorbance of ester **1** vs time for the 1,4-addition of ester **1** (0.10 M) with LDA (0.10 M) at -78 °C. The dashed line shows the results of a first-order fit ($y = ae^{bx}$).

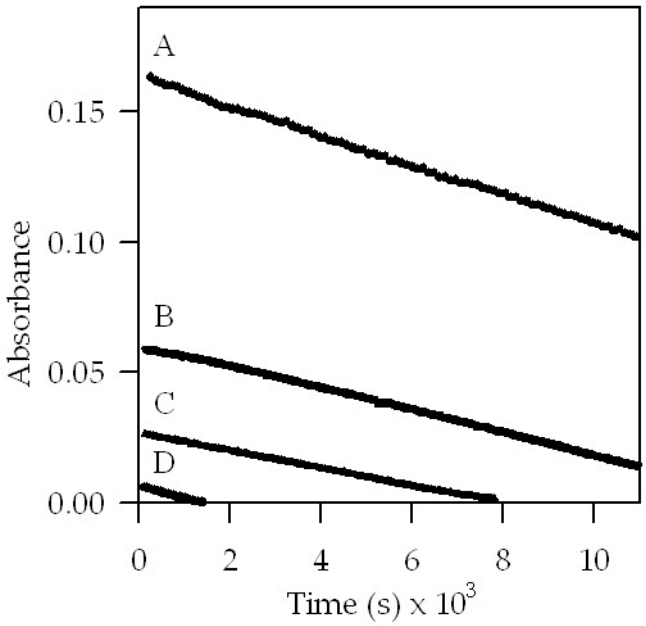

Figure 2.6. Plots of IR absorbance of ester **1** vs time for selected initial concentrations of **1**: (A) 0.10 M; (B) 0.050 M; (C) 0.025 M; (D) 0.004 M.

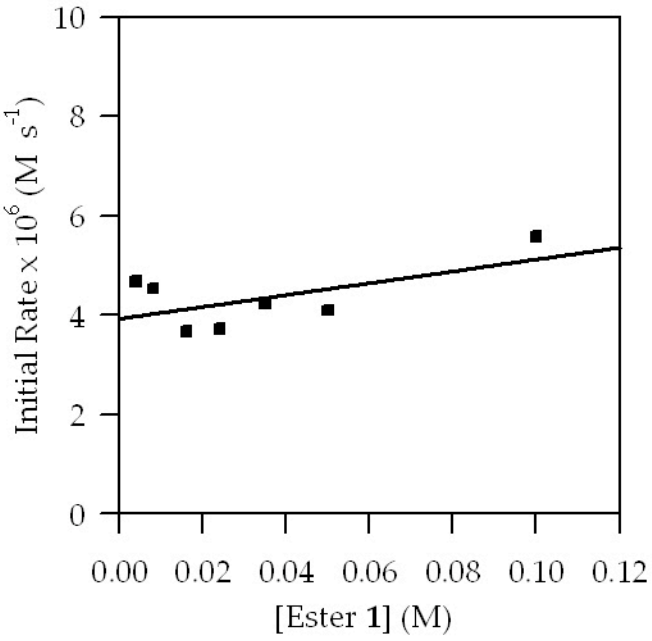

Figure A2.7. Plot of initial rates vs [**1**] for the 1,4-addition of LDA (0.10 M) to ester **1** in THF (6.10 M) at -78 °C. The curve depicts an unweighted least-squares fit to y = k[ester **1**] + k' (k = (1.2 $\pm$ 1) x 10^{-5}, k' = (3.9 $\pm$ 0.4) x 10^{-6}).

[**1**] (M)	y x 10^6 ($M^{-1}.s^{-1}$)
0.004	4.68 $\pm$ 1
0.008	4.54 $\pm$ 2
0.016	3.68 $\pm$ 1
0.024	3.72 $\pm$ 1
0.035	4.23 $\pm$ 2
0.050	4.10 $\pm$ 1
0.10	5.58 $\pm$ 3

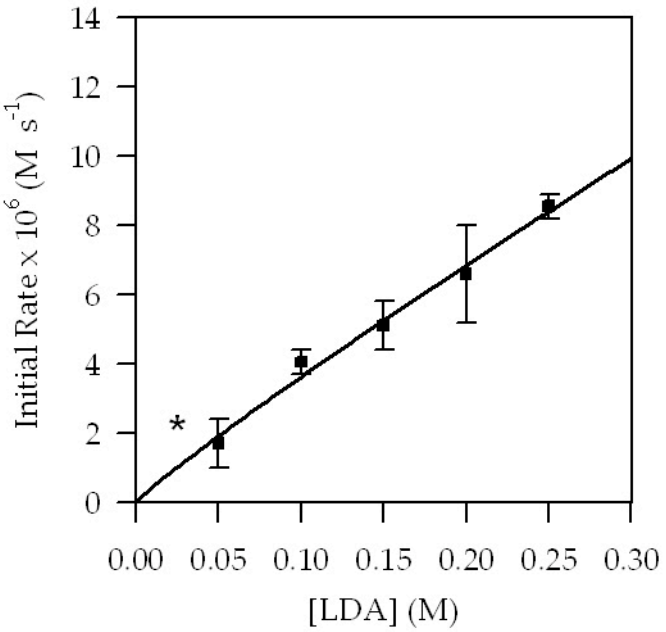

Figure A2.8. Plot of initial slopes vs [LDA] in THF (6.10 M) for the 1,4-addition of ester **1** (0.004 M) at -78 °C. The curve depicts an unweighted least-squares fit to $y = k[LDA]^n$ ($k = (3.1 \pm 0.4) \times 10^{-5}$, $n = 0.92 \pm 0.03$).

[LDA] (M)	$y_1 \times 10^6$ ($M^{-1}.s^{-1}$)	$y_2 \times 10^6$ ($M^{-1}.s^{-1}$)	$y_3 \times 10^6$ ($M^{-1}.s^{-1}$)
0.025	2.00 ± 0.03		
0.05	1.16 ± 0.01	2.21 ± 0.01	
0.10	3.88 ± 0.02	4.30 ± 2E-3	0.091 ± 2E-3
0.15	5.60 ± 0.02	4.61 ± 8E-3	0.209 ± 7E-3
0.20	7.57 ± 0.01	5.69 ± 8E-3	0.31 ± 1E-2
0.25	8.81 ± 0.03	8.25 ± 2E-2	

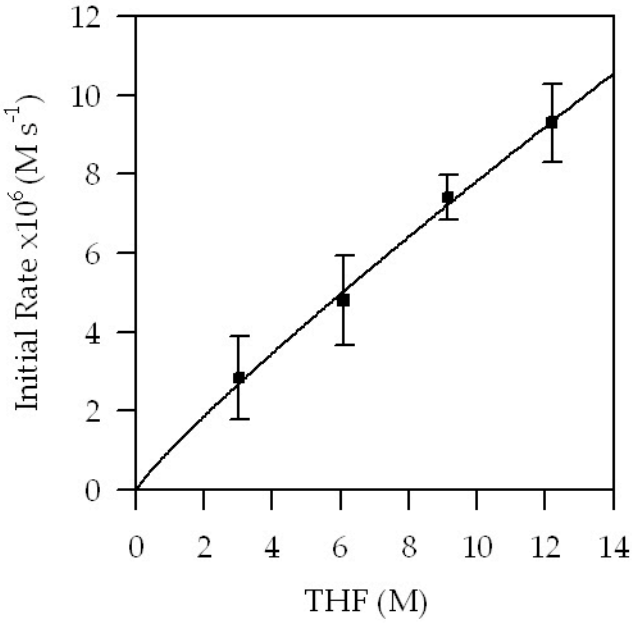

Figure A2.9. Plot of initial slopes vs [THF] for the 1,4-addition of LDA (0.10 M) to ester **1** (0.004 M) in hexane at -78 °C. The curve depicts an unweighted least squares fit to $y = k[LDA]^n + k'$ ($k = (8.1 \pm 0.2) \times 10^{-7}$, $n = 0.95 \pm 0.03$), $k' = (4.05 \pm 0.04) \times 10^{-7}$).

[THF] (M)	$y_1 \times 10^6$ ($M^{-1}.s^{-1}$)	$y_2 \times 10^6$ ($M^{-1}.s^{-1}$)
3.01	3.58 ± 0.03	2.09 ± 0.01
6.10	3.62 ± 0.02	5.62 ± 0.04
9.15	7.8 ± 0.05	7.05 ± 0.01
11.20	8.6 ± 0.04	9.5 ± 0.03

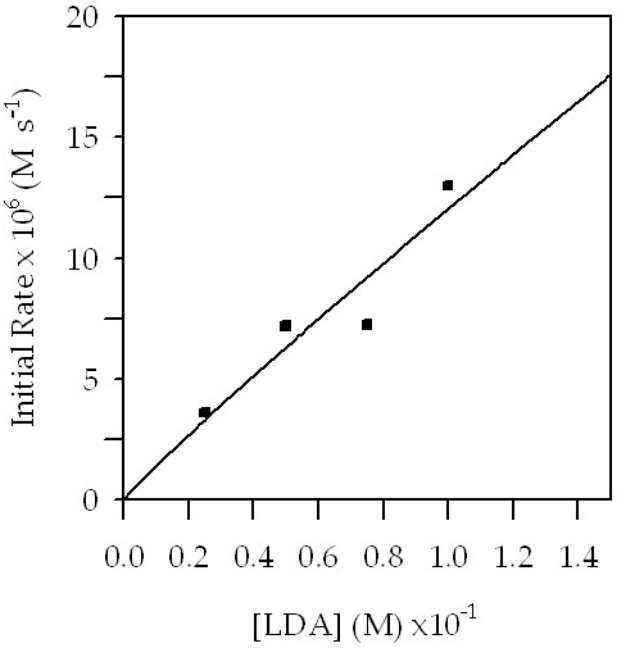

Figure A2.10. Plot of initial slopes vs [LDA] for the condensation of LDA dimer **3** (0.10 M) with enolate dimer **5a** (0.025M) in THF (6.10 M) at -78 °C. The curve depicts an unweighted least-squares fit to $y = k[\text{LDA}]^n$ ($k = (1.0 \pm 0.3) \times 10^{-4}$, $n = 0.93 \pm 0.24$).

[LDA] (M)	$y_1 \times 10^6$ ($M^{-1}.s^{-1}$)
0.025	0.36 ± 0.02
0.05	0.72 ± 0.01
0.75	0.73 ± 0.03
0.1	13.7 ± 0.1

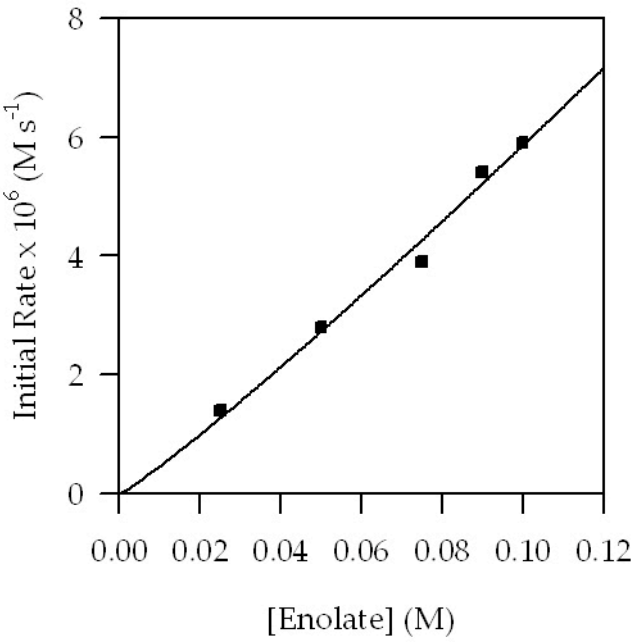

Figure A2.11. Plot of initial slopes vs the concentration of enolate **5** for the condensation of LDA dimer **3** (0.10 M) with enolate dimer **5a** (0.025M) in THF (6.10 M) at -78 °C. The curve depicts an unweighted least-squares fit to $y = k[\text{enolate}]^n$ ($k = (7.4 \pm 0.3) \times 10^{-5}$, $n = 1.10 \pm 0.14$).

[Enolate] (M)	$y_1 \times 10^6$ ($M^{-1}.s^{-1}$)
0.025	1.40 ± 0.02
0.050	2.82 ± 0.01
0.075	3.90 ± 0.03
0.090	5.41 ± 0.03
0.100	5.94 ± 0.02

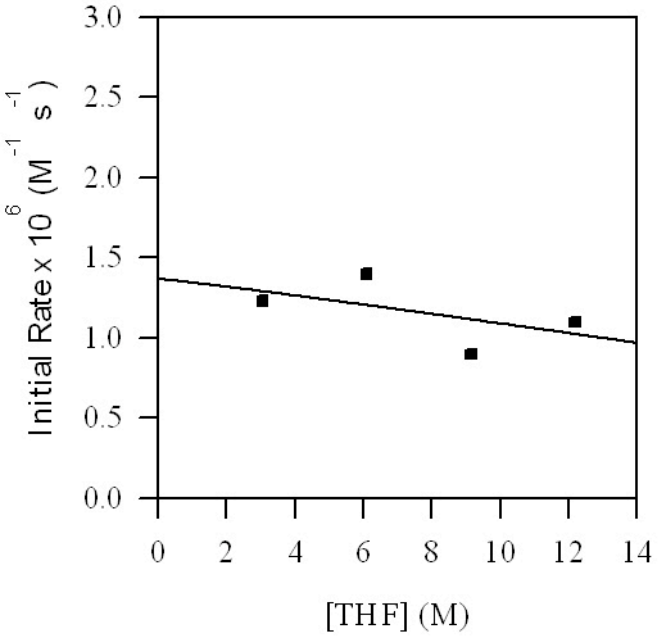

Figure A2.12. Plot of initial slopes vs [THF] for the 1,4-addition of LDA (0.10 M) to enolate **3** (0.01M) in hexane at -78 °C. The curve depicts an unweighted least squares fit to $y = k[THF] + k'$ ($k = (1.1 \pm 0.1) \times 10^{-7}$, $n = 0.95 \pm 0.03$), $k' = (-2{,}37 \pm 0.04) \times 10^{-9}$).

[THF] (M)	$y_1 \times 10^6$ ($M^{-1}.s^{-1}$)
3.05	1.23 ± 0.01
6.10	1.40 ± 0.01
9.15	0.92 ± 0.02
12.20	1.10 ± 0.03

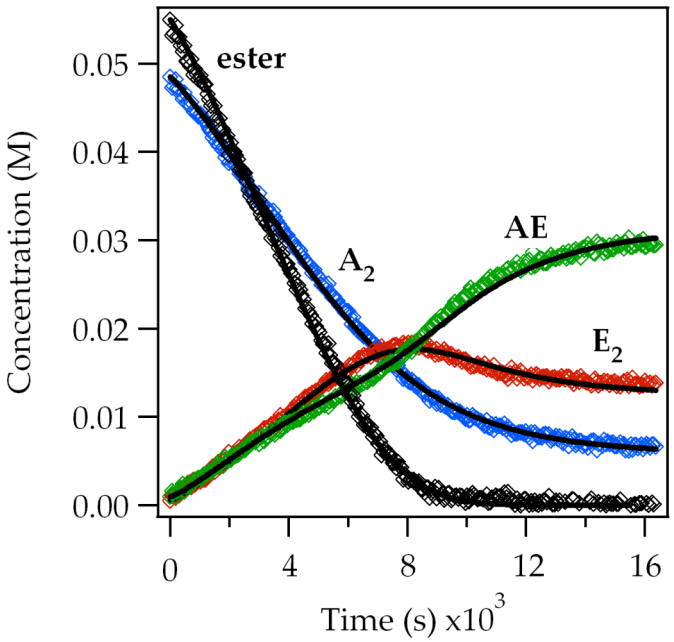

Figure A2.13. Parametric fit to eqs 17-22 of the time-dependent concentrations measured by ^{6}Li NMR spectroscopy using 0.05 M **3** (0.10 *normal*), 0.05 M **1** in 6.1 M THF at -78 °C. Ester = **1**; A_2 = LDA dimer **3**; E_2 = enolate dimer **5a**; AE = enolate mixed dimer **4**. Best-fit values of the rate constants (95% confidence) are as follows:

k_1 = 3.6914e-005 ± 9.5e-007
k_{-1} = 2190 ± 883
k_2 = 126.33 ± 14.4
k_3 = 0.19969 ± 0.0164
k_{-3} = 1.5147 ± 0.483
k_4 = 1318.1 ± 143
k_{-4} = 0.00038533 ± 1.67e-005
k_5 = 225.12 ± 80.7
k_{-5} = 0.0084579 ± 0.00324

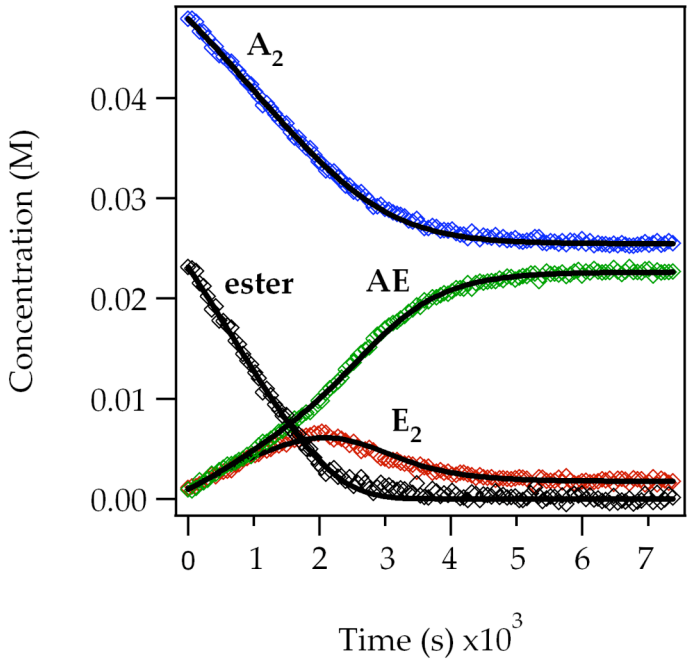

Figure A2.14. Parametric fit to eqs 17-22 of the time-dependent concentrations measured by ^{6}Li NMR spectroscopy using 0.05 M **3** (0.10 *normal*), 0.025 M **1** in 6.1 M THF at -78 °C. Ester = **1**; A_2 = LDA dimer **3**; E_2 = enolate dimer **5a**; AE = enolate mixed dimer **4**. Best-fit values of the rate constants (95% confidence) are as follows:

k_1 = 7.8377e-005 ± 2.98e-006
k_{-1} = 547.7 ± 212
k_2 = 94.857 ± 29.9
k_3 = 0.34822 ± 0.0583
k_{-3} = 1.3158 ± 1.05
k_4 = 1261.1 ± 270
k_{-4} = 0.0006229 ± 0.000154
k_5 = 429.27 ± 206
k_{-5} = 0.0087171 ± 0.00339

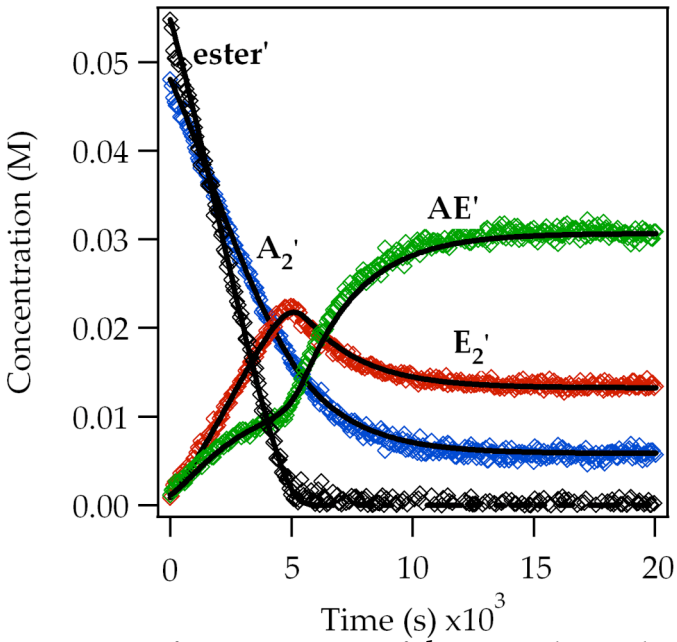

Figure A2.15. Parametric fit to eqs 17-22 of the time-dependent concentrations measured by ^{6}Li NMR spectroscopy using 0.05 M **3** (0.10 *normal*), 0.05 M **12** in 6.1 M THF at -78 °C. Ester = **12**; A_2 = LDA dimer **3**; E_2 = enolate dimer of **12**; AE = enolate mixed dimer . Best-fit values of the rate constants (95% confidence) are as follows:

k_1 = 7.0944e-005 ± 3.87e-006
k_{-1} = 267.46 ± 471
k_2 = 223.44 ± 1.1e+003
k_3 = 0.33594 ± 0.0308
k_{-3} = 0.84648 ± 11.3
k_4 = 910.74 ± 131
k_{-4} = 0.00051948 ± 3.04e-005
k_5 = 451.57 ± 81.1
k_{-5} = 0.0080254 ± 0.000959

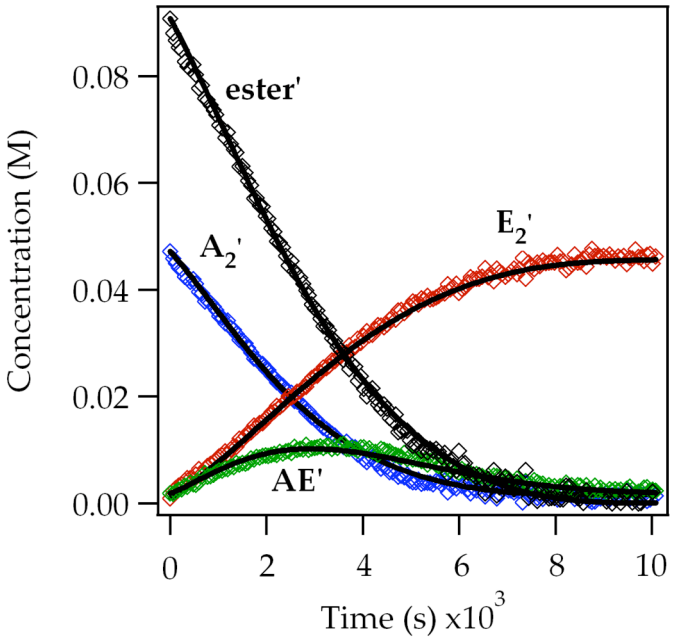

Figure A2.16. Parametric fit to eqs 17-22 of the time-dependent concentrations measured by ^{6}Li NMR spectroscopy using 0.05 M **3** (0.10 *normal*), 0.10 M **12** in 6.1 M THF at -78 °C. Ester = **12**; A_2 = LDA dimer **3**; E_2 = enolate dimer of **12**; AE = enolate mixed dimer. Best-fit values of the rate constants (95% confidence) are as follows:

k_1 = 0.00011944 ± 2.61e-006
k_{-1} = 7415.7 ± 599
k_2 = 962.34 ± 209
k_3 = 0.46237 ± 0.0395
k_{-3} = 18.327 ± 0.467
k_4 = 83.523 ± 4.44
k_{-4} = 0.00054909 ± 7.49e-006
k_5 = 280.11 ± 57.1
k_{-5} = 0.0069795 ± 0.00172

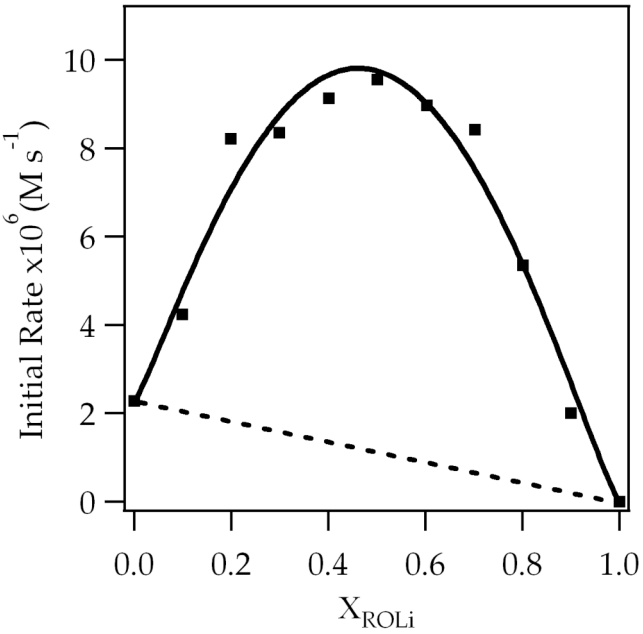

Figure A2.17. Plot of initial rate (y_1) versus X_{ROLi} for the serial injection of ten aliquots of ester **1 (**0.01 M final concentrations) to 0.10 M LDA in 6.1 M THF/hexanes co-solvent at -78 °C. The dashed line depicts the theoretical initial rates in the absence of autocatalysis. The curve depicts an unweighted least squares fit to $y_1 = k[X_{ROLi}]^n[1 - X_{ROLi}]^m + k'[1 - X_{ROLi}]^{1.0}$, $n = 1.15 \pm 0.20$), $m = (1.20 \pm 0.18) \times 10^{-7}$, $k = (4.40 \pm 1.16) \times 10^{-5}$), $k' = (2.25 \pm 6.71) \times 10^{-6}$.

X_{ROLi}	$y_1 \times 10^{-6}$ ($M^{-1} \cdot s^{-1}$)
0.00	2.28
0.10	4.24
0.20	8.22
0.30	8.35
0.40	9.13
0.50	9.56
0.60	8.97
0.70	8.42
0.80	5.35
0.90	2.00
1.00	0.00

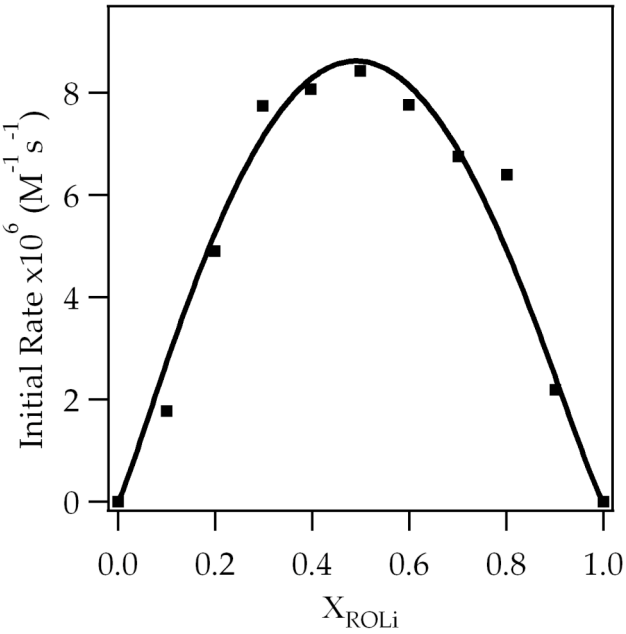

Figure A2.18. Plot of initial rate (y_1) versus X_{ROLi} for the serial injection of ten aliquots of ester **1** (0.01 M final concentrations) to 0.10 M LDA in 6.1 M THF/hexanes co-solvent at -78 °C. The initials rate have been corrected to only include rates effected by autocatalysis. The curve depicts an unweighted least squares fit to $y_1 = k[X_{ROLi}]^n[1 - X_{ROLi}]^m$, $n = 1.15 \pm 0.16$), $m = (1.20 \pm 0.16) \times 10^{-7}$, $k = (4.41 \pm 1.05) \times 10^{-5}$), $k' = (2.25 \pm 6.71) \times 10^{-6}$.

X_{ROLi}	$y_1 \times 10^{-6}$ ($M^{-1} \cdot s^{-1}$)
0.00	0.00
0.10	1.77
0.20	4.90
0.30	7.74
0.40	8.07
0.50	8.42
0.60	7.76
0.70	6.75
0.80	6.39
0.90	2.19
1.00	0.00

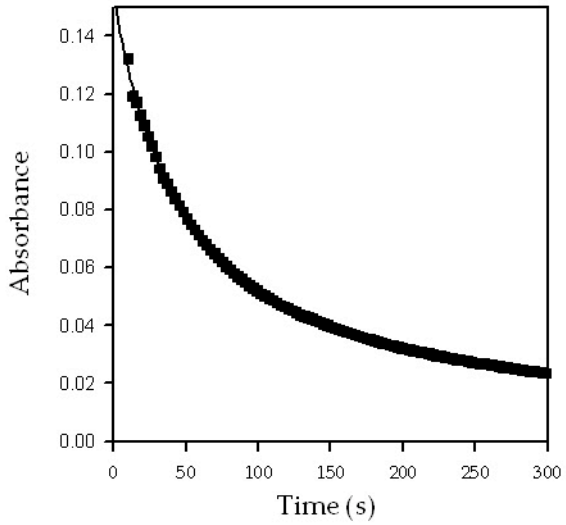

Figure A2.19. Plot showing IR absorbance of ester **1** vs time for the 1,4-addition of LDA (0.10 M) to equimolar ester **1** (0.10 M) in THF (6.10 M) with hexane cosolvent at -78 °C containing 1.0 mol % LiCl. The curve corresponds to a least squares fit to the second order functionm, $f(x) = a/(1 + bx)$.

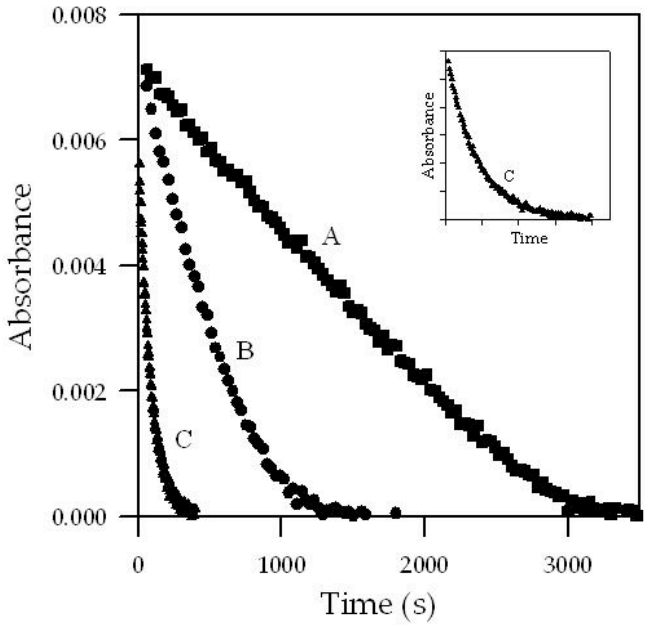

Figure A2.20. Plot of IR absorbance vs time in THF (6.10 M) for the 1,4-addition of LDA (0.10 M) to ester **1** (00M) at -78 °C in the presence of LiCl. (A) no LiCl; (B) 0.01 mol % LiCl; (C) 0.4 mol % LiCl.

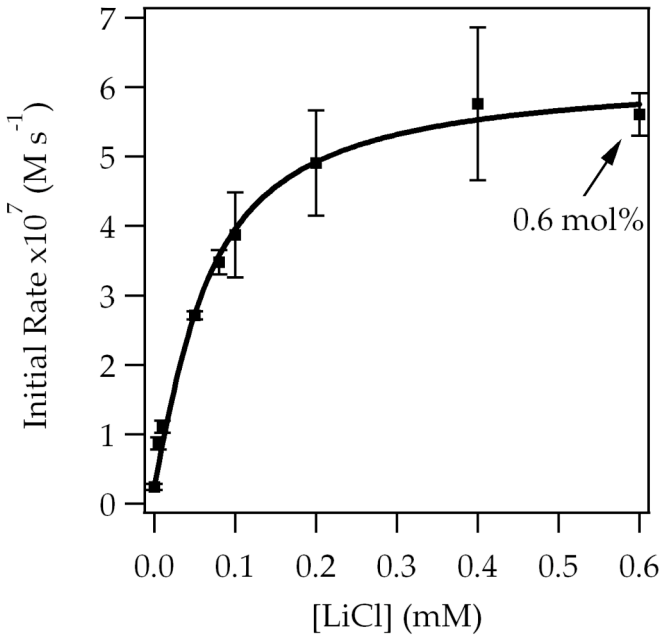

Figure A2.21. Plot of initial rates vs [LiCl] for the 1,4-addition of LDA (0.10 M) to ester **1** (0.004 M) in THF (6.1 M) at -78 °C.

LiCl (mM)	y_1 x 10^{-6} ($M^{-1}.s^{-1}$)	y_2 x 10^{-6} ($M^{-1}.s^{-1}$)	y_3 x 10^{-6} ($M^{-1}.s^{-1}$)	y_3 x 10^{-6} ($M^{-1}.s^{-1}$)
0.0001	1.88	2.22	2.07	3.06
0.005	8.7			
0.01	11.1			
0.05	26.8	2.74		
0.08	33.9	35.7		
0.10	44.9	36.2	34.9	
0.20	49.1	44.3	53.8	
0.40	63.2	52.0		
0.60	57.6	54.5		

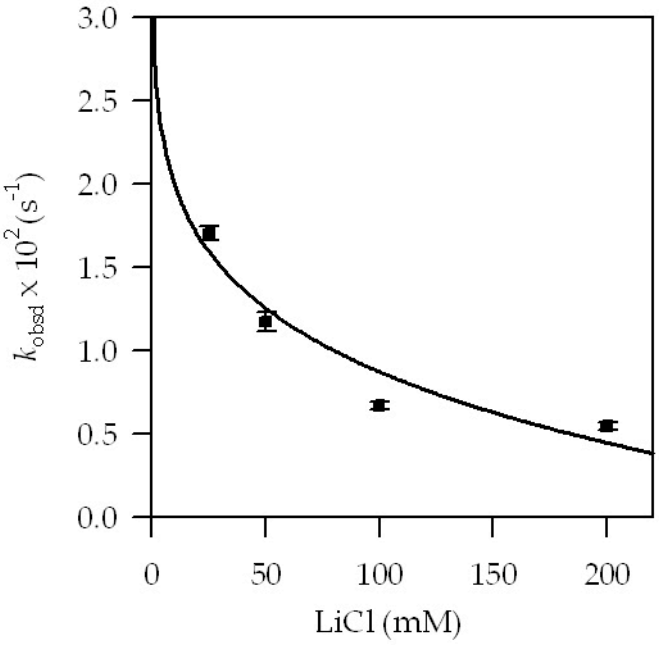

Figure A2.22. Plot of k_{obsd} vs [LiCl] for the 1,4-addition of LDA (0.10 M) to ester **1** (0.004 M) in THF (6.10 M) at -78 °C. The curve depicts an unweighted least squares fit to $y = k[LDA]^n + k'$ (k = (-1.74 ± 0.08) x 10^{-2}, n = (-1.60 ± 0.02), k' = (4.50 ± 0.02) x 10^{-2}.

[LiCl] (%)	$k_{obsd\ 1}$ x 10^2 (s^{-1})	$k_{obsd\ 2}$ x 10^2 (s^{-1})	k_{obsd} (avg) x 10^4 (s^{-1})
25	1.67 ± 0.03	1.73 ± 0.02	1.70 ± 0.01
50	1.21 ± 0.01	1.13 ± 0.04	1.17 ± 0.03
100	0.68 ± 0.02	0.65 ± 0.08	0.67 ± 0.02
200	0.56 ± 0.01	0.53 ± 0.02	0.64 ± 0.02

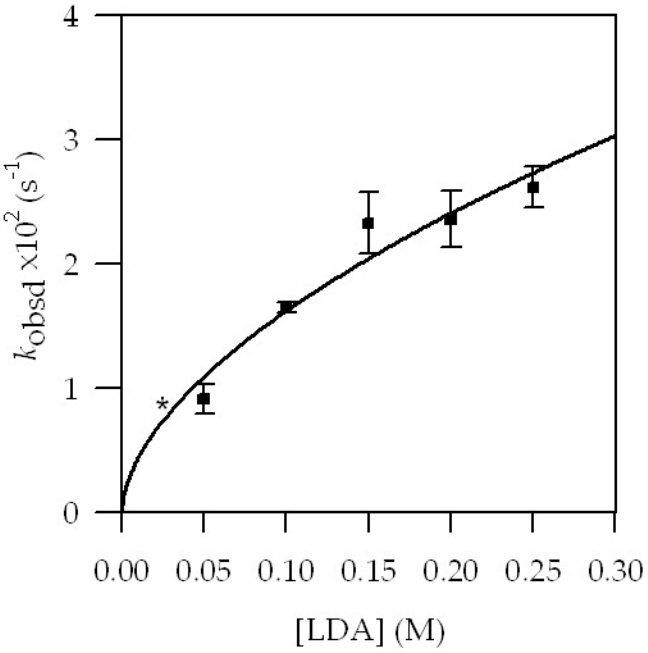

Figure A2.23. Plot of k_{obsd} vs [LDA] for the 1,4-addition of in LDA (0.10 M) ester **1** (0.004 M) with LDA (0.10 M) in [THF] in hexane cosolvent at -78 °C. The curve depicts an unweighted least squares fit to $y = k[LDA]^n + k'$ ($k = (6.0 \pm 0.1) \times 10^{-2}$, $n = 0.57 \pm 0.08$).

[LDA] (M)	$k_{obsd\ 1}$ x 10^2 (s^{-1})	$k_{obsd\ 2}$ x 10^2 (s^{-1})	k_{obsd3} x 10^2 (s^{-1})
0.025	0.83 ± 0.02		
0.05	0.83 ± 0.03	1.01 ± 0.04	9.8 ± 0.04
0.10	1.62 ± 003	1.68 ± 0.03	1.72 ± 0.03
0.15	2.15 ± 0.02	2.50 ± 0.08	
0.20	2.20 ± 0.07	2.52 ± 0.03	
0.25	2.73 ± 0.02	2.50 ± 0.02	

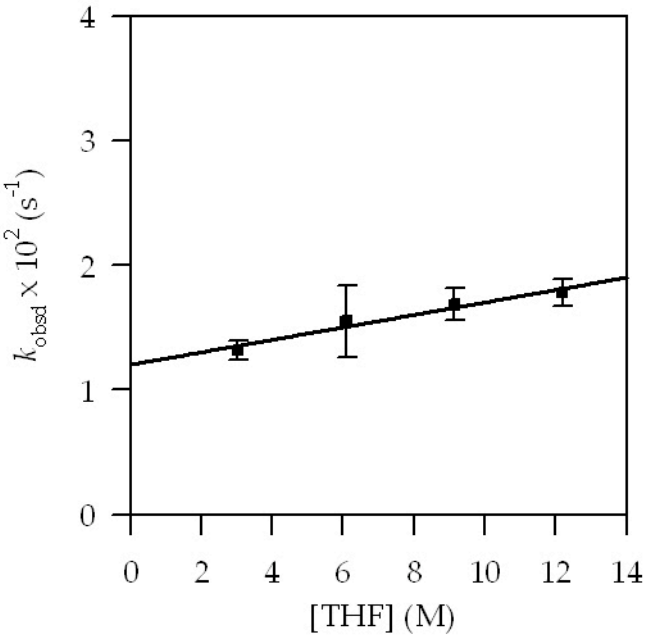

Figure A2.24. Plot of k_{obsd} vs [THF] in hexane cosolvent for the 1,4-addition of [LDA] (0.10 M) to ester **1** (0.004 M) in the presence of 1% LiCl at -78 °C. The curve depicts an unweighted least-squares fit to y = -k[THF] + k' (k = (5.0 $\pm$ 0.01) x 10^{-4}, k' = (1.2 $\pm$ 0.1) x 10^{-2}).

[THF] (M)	y_1 x 10^{-2} (abs.s^{-1})	y_2 x 10^{-2} (abs.s^{-1})
3.01	1.27 $\pm$ 0.02	1.41 $\pm$ 0.01
6.10	1.67 $\pm$ 0.03	1.76 $\pm$ 0.01
9.15	1.96 $\pm$ 0.01	1.95 $\pm$ 0.02
11.20	1.92 $\pm$ 0.02	1.69 $\pm$ 0.03

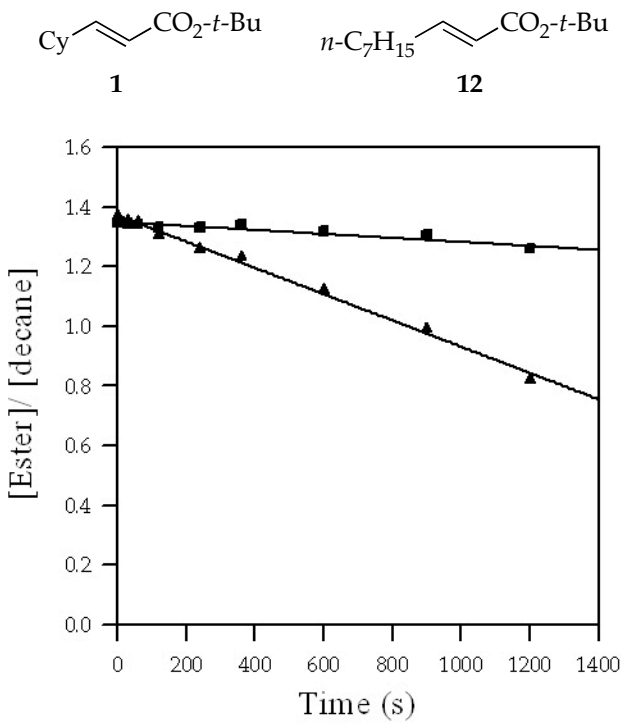

Figure A2.25. Plot of concentration vs time for the uncatalyzed 1,4-addition of a mixture of esters **1** and **12** (0.05 M each) to LDA (0.10 M) in THF (6.10 M) at -78 °C. Results are analyzed by GC relative to a decane internal standard. The slopes correspond to $k_1/k_{12} = 7.1$ (■) Ester **1**; (▲) Ester **12**.

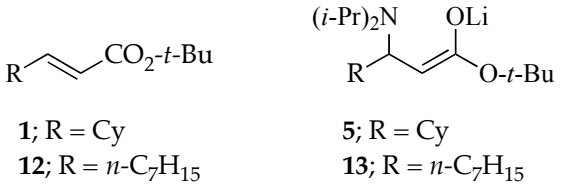

1; R = Cy
12; R = *n*-C_7H_{15}

5; R = Cy
13; R = *n*-C_7H_{15}

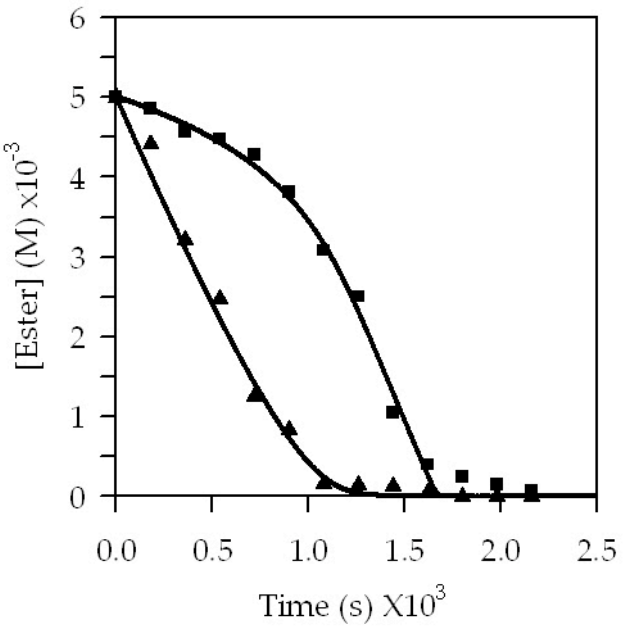

Figure A2.26. Plot of concentration vs time for the uncatalyzed 1,4-addition of a mixture of esters **1** and **12** (0.005 M each) to LDA (0.10 M) in THF (6.10 M) at -78 °C. Results are analyzed by GC relative to a decane internal standard. (■) Ester **1**; (▲) Ester **12**. The curves in correspond to numerical integration to the highly simplified model as follows:

$$\tfrac{1}{2}\,A_2 \rightleftharpoons A$$
$$A + \mathbf{1} \longrightarrow \mathbf{5}$$
$$A + \mathbf{12} \longrightarrow \mathbf{13}$$

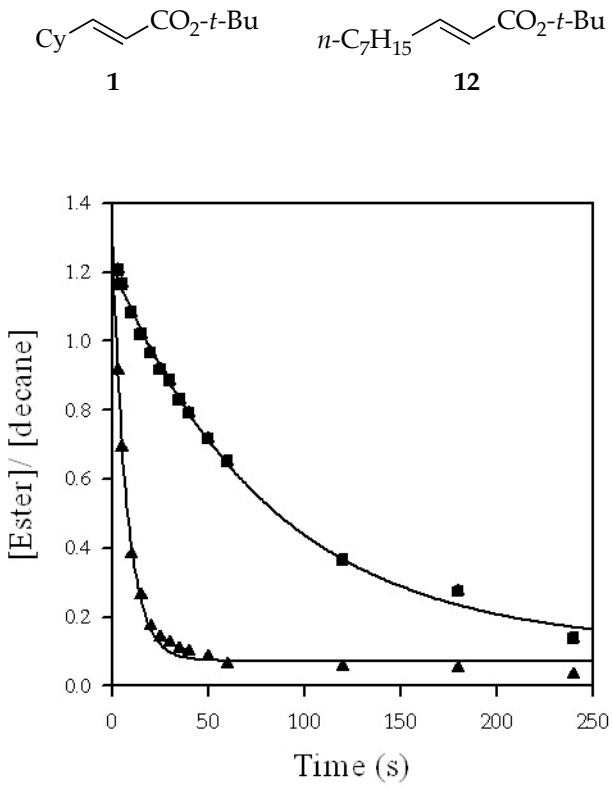

Figure A2.27. Plot of concentration vs time for the LiCl catalyzed (1.0 mol %) 1,4-addition of LDA (0.10 M) to a mixture of esters **1** and **12** (0.05 M each) to LDA in THF (6.10 M) at -78 °C. Results are analyzed by GC relative to a decane internal standard. The rate correspond to $k_1/k_{12} = 6.9$. (■) Ester **1**; (▲) Ester **12**.

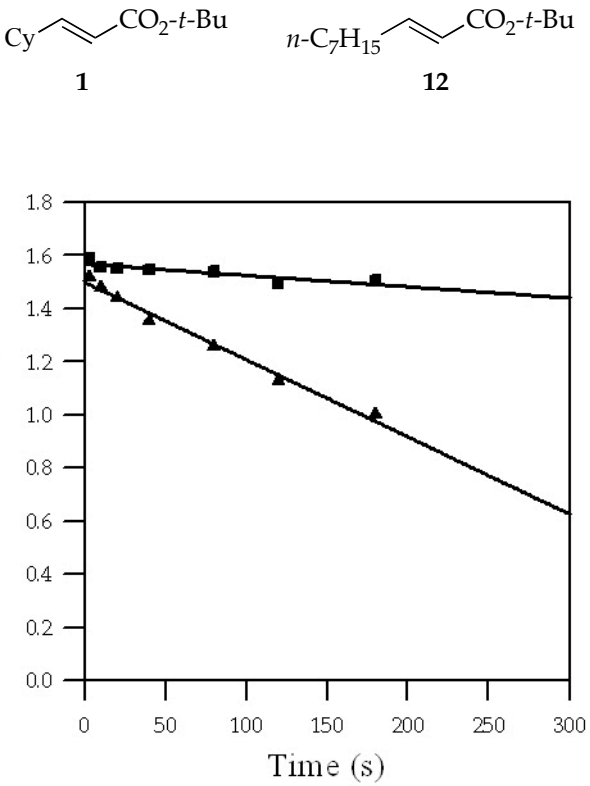

Figure A2.28. Plot of concentration vs time for the 1,4-addition of LDA (0.10 M) to a mixture of esters **1** and **12** (0.05 M each) to LDA (0.10 M) in THF (6.10 M) at -78 ºC in the presence of lithium enolate **5** (50.0 mol %). Results are analyzed by GC relative to a decane internal standard. The slopes correspond to $k_1/k_{12} = 7.1$. (■) Ester **1**; (▲) Ester **12**.

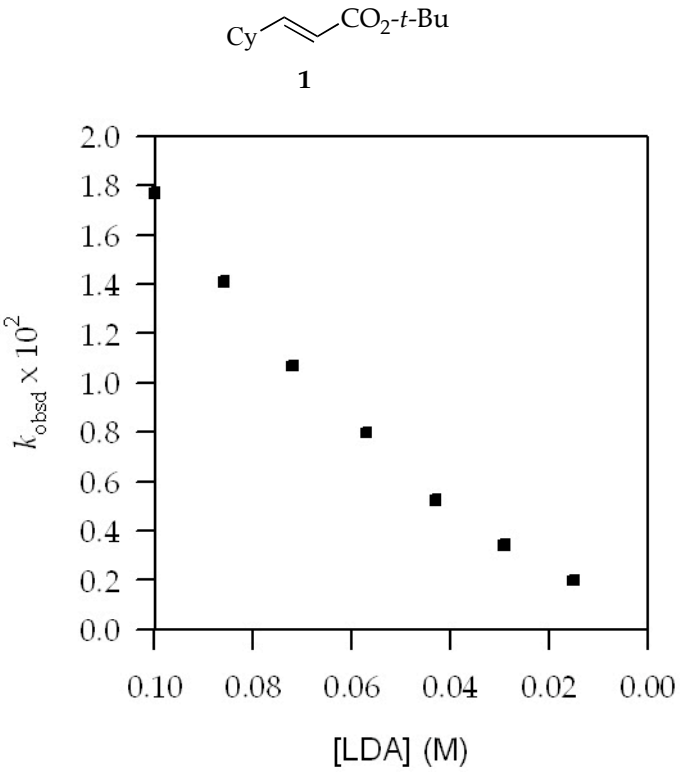

Figure A2.29. Plot of initial rate vs [LDA] in THF (6.10 M) on serially injecting ester **1** and (0.014 M) in LDA (0.10 M) in presence of 1.0% LiCl at -78 °C.

[LDA] (M)	$y_1 \times 10^{-2}$ (abs.s^{-1})
0.10	1.77
0.086	1.41
0.072	1.07
0.057	0.80
0.043	0.53
0.029	0.34
0.015	0.20

$$A_2 + LiCl \underset{k_{-1}}{\overset{k_1}{\rightleftharpoons}} 2A + LiCl$$

$$A + ester \xrightarrow{k_2} product$$

The rate of consumption of ester and its initial rate ($rate_{init}$) are defined as:

$$-\frac{d[\text{ester}]}{dt} = k_2[\text{A}][\text{ester}] \tag{1}$$

Applying the steady-state approximation to monomer A,

$$\frac{d[\text{A}]}{dt} = 2k_1[\text{A}_2][\text{LiCl}_T] - 2k_{-1}[\text{A}]^2[\text{LiCl}_T] - k_2[\text{A}][\text{ester}] = 0 \tag{2}$$

solving for [A] using the quadratic equation,

$$[A] = \frac{1}{4k_{-1}[\text{LiCl}_T]}(\sqrt{k_2^2[\text{ester}]^2 + 16k_1k_{-1}[\text{A}_2][\text{LiCl}_T]^2} - k_2[\text{ester}]) \tag{3}$$

and substituting eq 4 into eq 2 gives:

$$-\frac{d[\text{ester}]}{dt} = \frac{k_2[\text{ester}]}{4k_{-1}[\text{LiCl}_T]}(\sqrt{k_2^2[\text{ester}]^2 + 16k_1k_{-1}[\text{A}_2][\text{LiCl}_T]^2} - k_2[\text{ester}]) \tag{4}$$

where [ester] and $[A_2]$ are evaluated at t=0. To account for the LiCl-free pathway as outline below:

$$A_2 \underset{k_{-1}}{\overset{k_1}{\rightleftharpoons}} 2A$$

$$A + ester \xrightarrow{k_2} product$$

We add a constant c to eq 4 that reflects the initial rate without LiCl. The constant is determined experimentally rather than as an adjustable parameter.

$$-\frac{d[\text{ester}]}{dt} = \frac{k_2[\text{ester}]}{4k_{-1}[\text{LiCl}_T]}(\sqrt{k_2^2[\text{ester}]^2 + 16k_1k_{-1}[\text{A}_2]_0[\text{LiCl}_T]^2} - k_2[\text{ester}]) + \text{c} \tag{5}$$

Figure A2.30. Derivation of expression for fitting LiCl saturation curve (eq 13 in manuscript):

In a serial injection experiment, the amount of [ester] injected remains constant, but the concentration of LDA and ROLi **5** varies with each successive injection. Hence, the rate of consumption of ester **1** and its initial rate ($rate_{init}$) are defined as:

$$-d[\text{ester}]/dt = k[\text{ROLi}]^n[\text{LDA}]^m \quad (1)$$

Writing the concentrations in terms of mole fractions:

$$-d[\text{ester}]/dt = k[X_{\text{ROLi}}]^n[X_{\text{LDA}}]^m \quad (2)$$

where $X_{\text{ArLi}} = \text{N}_{\text{ROLi}}/(\text{N}_{\text{ROLi}} + \text{N}_{\text{LDA}})$ (N stands for normality)

Also, $X_{\text{LDA}} = 1 - X_{\text{ROLi}}$ (3)

Substituting eq 3 into eq 2 gives:

$$-d[\text{ester}]/dt = k[X_{\text{ROLi}}]^n[1 - X_{\text{ROLi}}]^m \quad (4)$$

Eq 4 is used to fit the serial injection curve depicted in Figure 2.10. The initial rates y_i only reflect the effects of autocatalysis. To account for the uncatalyzed rate, we must add the rate term associated with LDA aggregation. It is given by the following expression:

$$-d[\text{ester}]/dt = k'[X_{\text{LDA}}]^{1.0} \quad (5)$$

or,

$$-d[\text{ester}]/dt = k'[1 - X_{\text{ROLi}}]^{1.0} \quad (6)$$

Adding expression 6 to equation 4 gives:

$$-d[\text{ester}]/dt = k[X_{\text{ROLi}}]^n[1 - X_{\text{ROLi}}]^m + k'[1 - X_{\text{ROLi}}]^{1.0} \quad (7)$$

Eq 7 describes the initial rate of the uncatalyzed and autocalyzed pathways combined. It is used to fit the serial injection curve depicted in Figure 2.9.

Figure A2.31. Derivation of expression for fitting incremental addition curves depicted in Figures 2.9 and 2.10:

Table A2.1. Optimized geometry, free energy (G, Hartrees), and cartesian coordinates (X, Y, Z).

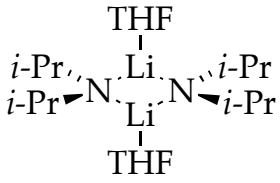

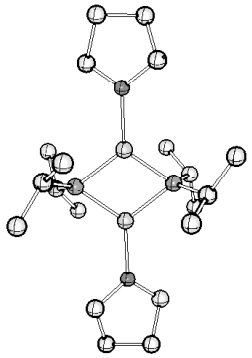

3
G = -1063.135499
(-78 °C)

Atom	X	Y	Z	Atom	X	Y	Z
Li	-1.194627	-0.007825	0.022332	H	-1.500486	-3.820717	-0.761885
N	0.013907	1.643769	0.077205	C	0.932582	-1.814844	-2.212451
C	0.196558	2.410032	1.319032	H	1.876607	-1.339195	-1.919069
C	1.159764	1.707079	2.290512	H	1.147416	-2.498388	-3.043457
H	2.159075	1.604292	1.849772	H	0.264859	-1.033240	-2.596749
H	1.262404	2.264200	3.230548	H	1.002689	-3.335209	-0.721109
H	0.802179	0.701928	2.550069	O	3.182976	-0.015444	-0.127663
C	-1.131524	2.719155	2.048700	C	4.032339	-1.143606	0.199177
H	-1.598978	1.790545	2.404654	C	5.437966	-0.758062	-0.271094
H	-0.983501	3.376104	2.917980	C	5.411742	0.774063	-0.154916
H	-1.838550	3.216969	1.374689	C	3.984087	1.095274	-0.593500
H	0.658344	3.392275	1.104388	H	3.902781	1.157446	-1.686665
Li	1.194600	0.007938	0.022158	H	3.572808	2.009642	-0.160821
N	-0.013962	-1.643687	0.077247	H	6.162143	1.270000	-0.777688
C	-0.196637	-2.409858	1.319127	H	5.571005	1.083108	0.884979
C	1.131405	-2.718766	2.048953	H	5.590704	-1.057380	-1.314703
H	1.598735	-1.790078	2.404863	H	6.219980	-1.226951	0.333343
H	0.983363	-3.375653	2.918275	H	3.991648	-1.300598	1.282899
H	1.838548	-3.216575	1.375059	H	3.630188	-2.031035	-0.296809
C	-1.160039	-1.706940	2.290445	C	-0.277970	2.554246	-1.035528
H	-2.159328	-1.604365	1.849606	C	-0.932408	1.814820	-2.212599
H	-1.262680	-2.263956	3.230543	H	-1.876483	1.339255	-1.919253
H	-0.802631	-0.701703	2.549918	H	-1.147122	2.498323	-3.043671
H	-0.658276	-3.392178	1.104519	H	-0.264714	1.033138	-2.596792
C	0.278101	-2.554233	-1.035377	C	0.961585	3.312183	-1.569417
C	-0.961328	-3.312344	-1.569312	H	1.655983	2.609117	-2.049010
H	-1.655760	-2.609392	-2.049018	H	0.685387	4.074299	-2.312169
H	-0.684990	-4.074495	-2.311978	H	1.500736	3.820562	-0.761989
H	-1.002510	3.335320	-0.721398	H	-6.220074	1.226032	0.334511
O	-3.182976	0.015599	-0.128112	H	-5.592104	1.056795	-1.314054

Table A2.1. (Continued).

C	-3.983928	-1.095127	-0.594129	H	-5.569779	-1.083823	0.885463
C	-5.411404	-0.774615	-0.154519	H	-6.162035	-1.270817	-0.776806
C	-5.438354	0.757507	-0.270589	H	-3.903299	-1.156675	-1.687391
C	-4.032490	1.143719	0.198539	H	-3.572024	-2.009558	-0.162195
H	-3.991063	1.301394	1.282122	H	-3.630993	2.030985	-0.298285

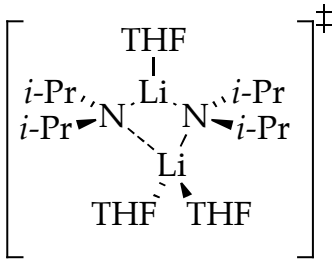

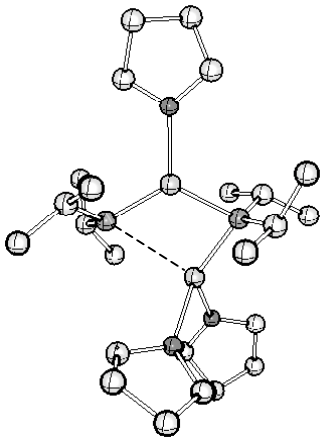

8
G = -1295.456449
(-78 °C)

Atom	X	Y	Z	Atom	X	Y	Z
C	0.636461	1.802019	-2.288673	C	-0.228490	-3.982087	0.385700
N	0.822011	1.650311	-0.845433	H	-1.269985	-3.797777	0.102697
Li	1.509939	-0.037022	-0.014373	H	0.122300	-4.863948	-0.166914
N	0.286781	-1.501106	0.742168	H	-0.216642	-4.238917	1.449715
Li	-1.146230	-0.270797	-0.032281	C	0.690582	-2.553474	-1.453263
O	-2.510661	1.057607	0.794776	H	1.362710	-1.735653	-1.742380
C	-2.337956	2.465455	0.532152	H	1.043009	-3.459209	-1.963223
C	-2.432389	3.108190	1.912554	H	-0.308431	-2.317014	-1.841562
C	-3.519611	2.258037	2.608278	H	1.685699	-3.068606	0.349498
C	-3.489760	0.913150	1.840339	C	0.174180	-1.670666	2.199914
H	-3.182299	0.065610	2.458766	C	1.392000	-2.317572	2.901757
H	-4.466721	0.683652	1.395180	H	2.284188	-1.691893	2.772302
H	-3.319955	2.124170	3.675140	H	1.205622	-2.416944	3.979311
H	-4.503762	2.728962	2.513868	H	1.623810	-3.316002	2.517617
H	-1.472274	3.009721	2.429465	C	-0.077981	-0.320020	2.884625
H	-2.689185	4.170776	1.868346	H	-0.890699	0.233692	2.405983
H	-3.147604	2.816828	-0.128143	H	-0.334522	-0.458221	3.943108
H	-1.372289	2.558508	0.028097	H	0.816931	0.312346	2.839767
O	-2.826029	-1.121251	-1.159407	H	-0.692228	-2.316303	2.459782
C	-3.370205	-2.445604	-0.949735	O	3.539508	-0.424249	-0.080401
C	-4.859373	-2.384226	-1.339020	C	4.465644	0.420610	-0.807038

Table A2.1. (Continued).

C	-5.158347	-0.876746	-1.333203	C	5.845577	0.108709	-0.229752
C	-3.822443	-0.297125	-1.791052	C	5.707807	-1.380081	0.120532
H	-3.714339	-0.353768	-2.883831	C	4.268910	-1.449874	0.635618
H	-3.649180	0.730217	-1.469606	H	3.779447	-2.410189	0.455585
H	-5.991110	-0.597334	-1.985685	H	4.219378	-1.228689	1.708550
H	-5.387610	-0.532409	-0.318163	H	5.826596	-1.996423	-0.778642
H	-5.013832	-2.797044	-2.341993	H	6.432293	-1.723139	0.865379
H	-5.488963	-2.950056	-0.645975	H	6.651578	0.317555	-0.939656
H	-3.223505	-2.695854	0.105007	H	6.026795	0.699619	0.676360
H	-2.809624	-3.164728	-1.555670	H	4.149812	1.457471	-0.677231
C	0.657291	-2.754042	0.069113	H	4.409965	0.168246	-1.872591
H	2.533919	2.936276	-0.843762	C	1.578011	2.774401	-0.291109
C	-0.555892	0.969153	-2.774494	C	1.976020	2.495264	1.167560
H	-1.479919	1.305108	-2.290136	H	2.604451	1.599818	1.261741
H	-0.697773	1.050809	-3.860567	H	2.538744	3.334121	1.596772
H	-0.412035	-0.094191	-2.545512	H	1.079821	2.343049	1.781508
C	1.880444	1.442510	-3.140188	C	0.875046	4.159259	-0.322210
H	2.121643	0.375543	-3.036146	H	0.035927	4.191469	0.384163
H	1.720468	1.649978	-4.208251	H	1.574962	4.957822	-0.038812
H	2.756911	2.019299	-2.824130	H	0.487522	4.405706	-1.316147
H	0.391623	2.848661	-2.556343				

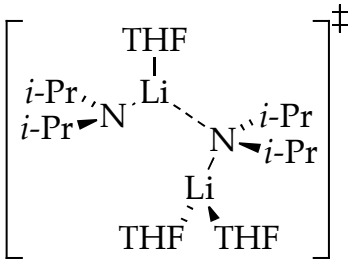

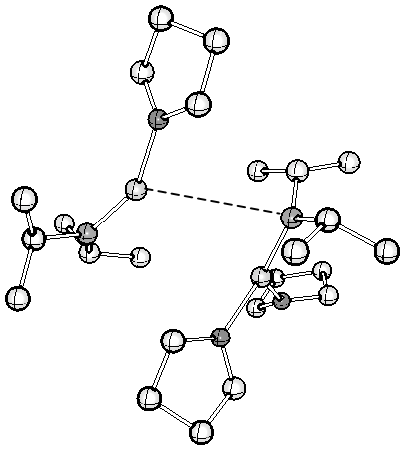

9
G = -1295.449326
(-78 °C)

Atom	X	Y	Z	Atom	X	Y	Z
C	1.998047	-2.440567	1.794156	C	-4.708315	0.542008	2.247373
N	2.597024	-1.667569	0.720492	C	-3.935206	-0.572849	3.006501
Li	2.253942	0.099387	0.331597	C	-3.390356	-1.472232	1.884782

Table A2.1. (Continued).

O	2.798805	1.907549	0.160525	H	-2.396985	-1.882114	2.076383
C	3.596110	2.622805	1.137194	H	-4.082621	-2.298466	1.663307
C	4.004805	3.927200	0.451212	H	-3.111371	-0.144585	3.584534
C	2.814595	4.186622	-0.486461	H	-4.571267	-1.133158	3.698051
C	2.459154	2.777163	-0.955734	H	-4.311158	1.528683	2.500369
H	1.400680	2.626251	-1.174614	H	-5.776931	0.542976	2.481639
H	3.062815	2.473831	-1.820858	H	-5.307965	-0.331767	0.325113
H	1.974986	4.622928	0.066035	H	-4.239966	1.092047	0.139970
H	3.058061	4.851435	-1.320296	C	-1.083484	2.749563	0.267657
H	4.176077	4.735048	1.168690	C	-2.286546	3.702730	0.500577
H	4.925151	3.783779	-0.126933	H	-3.181195	3.138427	0.797732
H	4.438994	1.986329	1.420906	H	-2.067548	4.436533	1.290003
H	2.974619	2.806838	2.022167	H	-2.532406	4.264777	-0.405909
N	-1.245827	1.724573	-0.743670	C	-0.703776	2.106274	1.610442
Li	-1.718222	-0.075010	-0.386750	H	0.210430	1.508748	1.508255
O	-1.343436	-1.812615	-1.241548	H	-0.536428	2.856716	2.393657
C	-2.388815	-2.767475	-1.539990	H	-1.502502	1.436699	1.958447
C	-1.776508	-3.762833	-2.528083	H	-0.242736	3.436500	0.004067
C	-0.293922	-3.742903	-2.126949	C	-1.356089	2.250631	-2.097705
C	-0.073274	-2.269730	-1.792301	C	-0.610623	1.347453	-3.101344
H	0.709032	-2.091370	-1.046473	H	-1.030563	0.332678	-3.075100
H	0.140518	-1.680431	-2.692647	H	-0.696806	1.715443	-4.132732
H	-0.123837	-4.365250	-1.240745	H	0.453204	1.268715	-2.849725
H	0.373953	-4.092912	-2.919160	C	-2.812049	2.416777	-2.609699
H	-2.236843	-4.753100	-2.456690	H	-3.406367	3.045259	-1.940900
H	-1.898301	-3.404771	-3.557259	H	-2.850910	2.859948	-3.615897
H	-3.251434	-2.226191	-1.940535	H	-3.301501	1.432983	-2.660008
H	-2.688886	-3.259844	-0.606650	H	-0.883428	3.254537	-2.162195
O	-3.293908	-0.617086	0.735168	C	3.779414	-2.292483	0.146704
C	-4.463548	0.222651	0.760167	C	4.584309	-1.257681	-0.655042
H	3.842666	-2.764098	2.947767	H	4.923837	-0.438645	-0.007548
H	1.882263	-3.510708	1.517365	H	5.467294	-1.702042	-1.131043
H	4.466308	-2.668062	0.933125	H	3.964659	-0.828124	-1.458429
C	0.581794	-1.921058	2.086352	C	3.475723	-3.505478	-0.766721
H	-0.054602	-2.002832	1.196914	H	2.940900	-3.179989	-1.669081
H	0.107715	-2.475530	2.907521	H	4.395678	-4.016968	-1.083558
H	0.616481	-0.862253	2.384633	H	2.849787	-4.243697	-0.252317
C	2.812960	-2.427484	3.111071	H	2.368762	-3.083373	3.873731
H	2.856045	-1.407383	3.516514				

Table A2.1. (Continued).

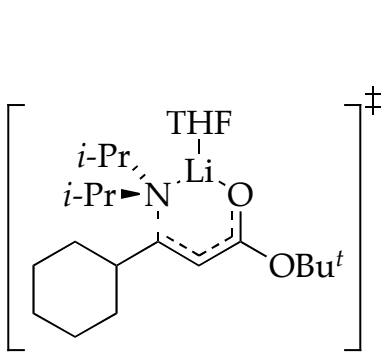

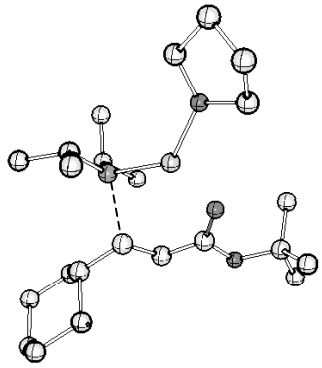

10
G = -1190.331832
(-78 °C)

Atom	X	Y	Z	Atom	X	Y	Z
C	-0.739888	-2.750404	-0.054074	H	1.816202	4.320208	-1.815578
N	-0.507839	-1.460706	0.634981	H	3.494621	4.397447	-1.243583
Li	1.236478	-0.650569	0.121604	H	2.745740	2.822043	-1.603325
O	1.436727	1.089791	-0.524605	C	1.809288	5.140134	0.808286
C	0.510425	1.834540	-0.080053	H	2.732514	5.729816	0.816126
C	-0.834195	1.449058	0.084763	H	1.069146	5.659038	0.190738
C	-1.317812	0.227027	-0.414493	H	1.422855	5.084520	1.831218
H	-0.757954	-0.166002	-1.255995	O	2.953151	-1.535020	-0.114578
C	-2.817526	0.024066	-0.567149	C	3.963712	-0.890801	-0.926256
C	-3.657203	0.304267	0.693171	C	4.486549	-2.001437	-1.831026
C	-5.155660	0.073566	0.436227	C	4.483304	-3.207447	-0.875948
C	-5.666091	0.911626	-0.745099	C	3.245353	-2.950471	0.000407
C	-4.830968	0.657492	-2.008645	H	3.411136	-3.192901	1.055074
C	-3.334031	0.887826	-1.748747	H	2.365059	-3.499102	-0.349308
H	-3.155192	1.946588	-1.519371	H	5.393057	-3.208322	-0.265111
H	-2.753980	0.665307	-2.654587	H	4.428089	-4.168638	-1.394856
H	-5.172642	1.303495	-2.828081	H	5.476142	-1.781417	-2.242299
H	-4.987583	-0.379080	-2.343121	H	3.794947	-2.164528	-2.665760
H	-6.725200	0.695614	-0.937337	H	3.480471	-0.057827	-1.438451
H	-5.606804	1.978497	-0.482600	H	4.755730	-0.498791	-0.272921
H	-5.730853	0.303777	1.342486	C	-0.769432	-1.554279	2.085099
H	-5.326745	-0.992465	0.222829	H	-1.831441	-1.785660	2.287228
H	-3.508567	1.344824	1.013489	C	-0.466773	-0.235374	2.811593
H	-3.314946	-0.331174	1.516830	H	0.583068	0.061548	2.676144
H	-2.990095	-1.020273	-0.848793	H	-1.088359	0.585821	2.456673
H	-1.474617	2.117655	0.648215	H	-0.636929	-0.357407	3.888461
O	0.757371	3.114854	0.317368	C	0.056113	-2.668730	2.774112
C	2.076529	3.734253	0.257379	H	1.130538	-2.504878	2.610589
C	3.070975	2.993969	1.162160	H	-0.123267	-2.656064	3.856145
H	3.279284	1.993371	0.780650	H	-0.189704	-3.672586	2.414776
H	4.011686	3.554557	1.218540	H	0.022975	-3.465229	0.309530
H	2.666812	2.907458	2.177062	C	-0.493957	-2.649278	-1.570931

Table A2.1. (Continued).

C	2.565502	3.817193	-1.194476	H	-0.456261	-3.653590	-2.009848
H	-2.942475	-2.875678	-0.169176	H	-1.286969	-2.100602	-2.089510
H	-2.105152	-4.425380	-0.325859	H	0.460192	-2.155353	-1.798958
H	-2.260608	-3.661368	1.257305	C	-2.091960	-3.459734	0.195228

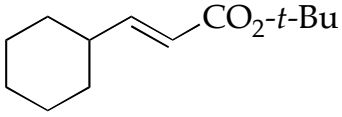

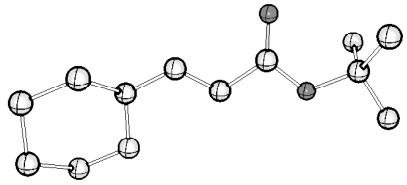

1
G = -658.796394
(-78 °C)

Atom	X	Y	Z	Atom	X	Y	Z
C	2.387451	-0.333797	-0.526491	C	4.702317	-0.895512	0.395076
C	0.933100	-0.711275	-0.481571	C	3.197961	-1.196567	0.474386
C	-0.107160	0.088146	-0.211800	H	2.833266	-0.990483	1.490877
C	-1.489421	-0.451957	-0.204575	H	3.011922	-2.261554	0.284998
O	-1.787466	-1.610305	-0.437212	H	5.241229	-1.491174	1.142719
O	-2.364625	0.535105	0.096694	H	5.081823	-1.210782	-0.588209
C	-3.814444	0.290584	0.166741	H	6.064952	0.797171	0.480805
C	-4.336694	-0.156746	-1.203256	H	4.726809	0.886725	1.621860
H	-3.935840	-1.133711	-1.477121	H	4.366345	2.524655	-0.204991
H	-5.430616	-0.218365	-1.176935	H	4.537311	1.259741	-1.416629
H	-4.055697	0.570718	-1.972777	H	2.306431	1.460041	0.680203
C	-4.124942	-0.729876	1.267745	H	-4.110211	2.407198	-0.232859
H	-3.697023	-0.402702	2.221825	H	0.004102	1.145502	0.004311
H	-5.210428	-0.813995	1.393581	H	0.707380	-1.759291	-0.683160
H	-3.722619	-1.712924	1.018890	C	2.681020	1.160209	-0.309466
C	-4.368542	1.669947	0.534289	C	4.186339	1.458749	-0.393154
H	-5.459421	1.627818	0.621861	C	4.991347	0.599791	0.593233
H	-3.956654	2.009652	1.490213	H	2.135469	1.761658	-1.047548
H	2.748213	-0.604484	-1.534716				

Table A2.1. (Continued).

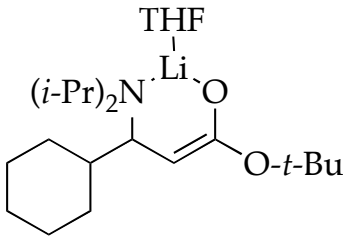

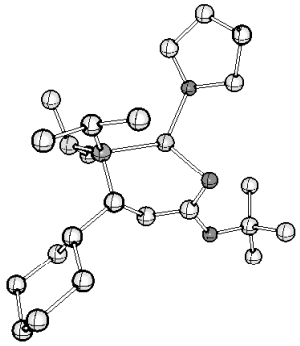

5·THF
G_{B3LYP} = -1190.344333
G_{MP2} = -1186.25046
(-78 °C)

Atom	X	Y	Z	Atom	X	Y	Z
C	-0.546335	-2.466533	-1.001785	H	3.132061	4.603567	-1.401570
N	-0.590506	-1.470430	0.120830	H	2.463374	3.000961	-1.818827
Li	1.212498	-0.410991	0.170977	C	1.570854	5.071326	0.819589
O	1.329604	1.121256	-0.890535	H	2.446197	5.730212	0.790782
C	0.461143	1.699140	-0.134920	H	0.742558	5.570103	0.305764
C	-0.673130	1.093409	0.376637	H	1.281330	4.920263	1.864937
C	-1.283383	-0.131085	-0.260560	O	2.977118	-1.235616	0.369323
H	-1.050138	-0.076215	-1.327332	C	4.054104	-0.609040	-0.378794
C	-2.851254	-0.135503	-0.181494	C	4.819571	-1.771978	-1.001569
C	-3.502115	0.364257	1.129056	C	4.729403	-2.833405	0.106964
C	-5.035662	0.257030	1.072596	C	3.317997	-2.610653	0.667602
C	-5.607318	1.058781	-0.104475	H	3.254710	-2.762917	1.749869
C	-4.960860	0.627656	-1.428007	H	2.578726	-3.255653	0.178610
C	-3.426367	0.679728	-1.363122	H	5.483661	-2.640948	0.878481
H	-3.088526	1.721247	-1.267195	H	4.872639	-3.855231	-0.256214
H	-3.009155	0.308024	-2.309291	H	5.848466	-1.505680	-1.260604
H	-5.322990	1.256206	-2.252281	H	4.314698	-2.117251	-1.911406
H	-5.275505	-0.401076	-1.661137	H	3.590452	0.081666	-1.084574
H	-6.697903	0.942775	-0.156352	H	4.684483	-0.042160	0.318736
H	-5.413293	2.128587	0.062720	C	-1.048403	-2.052477	1.423778
H	-5.468239	0.609491	2.018193	H	-2.148302	-2.076488	1.446959
H	-5.328945	-0.799147	0.971170	C	-0.568750	-1.200224	2.611965
H	-3.239129	1.416059	1.294649	H	0.525130	-1.254112	2.704699
H	-3.126559	-0.188569	1.996754	H	-0.836672	-0.149305	2.511045
H	-3.189688	-1.170221	-0.316388	H	-0.999257	-1.589439	3.542952
H	-1.251596	1.670100	1.085437	C	-0.581905	-3.498155	1.670622
O	0.627184	3.012706	0.264473	H	0.509595	-3.587326	1.604107
C	1.882022	3.727405	0.147254	H	-0.871484	-3.786275	2.687245
C	2.998543	3.005682	0.914799	H	-1.031087	-4.226829	0.990014
H	3.226606	2.046366	0.448085	H	-0.006330	-3.323063	-0.590473
H	3.909842	3.615792	0.925905	C	0.311482	-1.992610	-2.188843
H	2.693114	2.830762	1.953143	H	0.437615	-2.828394	-2.887874
C	2.253264	3.950712	-1.326187	H	-0.136850	-1.165318	-2.745275

Table A2.1. (Continued).

H	1.421657	4.435502	-1.849684	H	1.308796	-1.672796	-1.869639
H	-1.719002	-3.854343	-2.187891	C	-1.896529	-3.003375	-1.518563
H	-2.543302	-3.352657	-0.706708	H	-2.445174	-2.247590	-2.089614

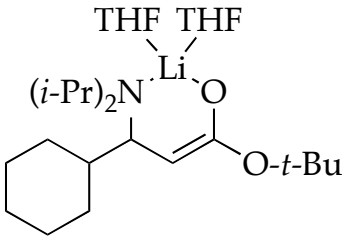

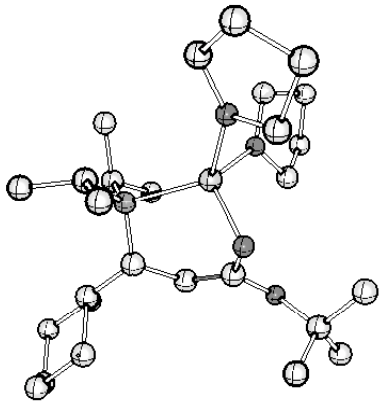

5·(THF)$_2$
G_{B3LYP} = -1422.691459
G_{MP2} = -1417.830597
(-78 °C)

Atom	X	Y	Z	Atom	X	Y	Z
Li	1.151303	-0.438243	-0.052861	C	-3.905727	-0.121155	1.264706
N	-0.809879	-1.490165	0.229151	C	-5.424628	-0.369692	1.271721
C	-0.758339	-2.651128	-0.731470	C	-6.126828	0.367889	0.124947
H	0.108549	-3.231436	-0.398276	C	-5.505123	-0.010929	-1.225532
C	-0.443404	-2.236260	-2.180000	C	-3.984317	0.205231	-1.232016
H	-0.076524	-3.116104	-2.724111	H	-3.759704	1.277980	-1.155161
H	-1.328886	-1.879109	-2.715757	H	-3.572197	-0.124077	-2.195747
H	0.317839	-1.454784	-2.227285	H	-5.969551	0.566168	-2.036251
C	-1.954297	-3.631097	-0.745068	H	-5.722114	-1.069773	-1.434698
H	-2.816208	-3.219032	-1.278383	H	-7.202821	0.148670	0.127712
H	-1.659020	-4.548873	-1.269475	H	-6.026964	1.452650	0.279029
H	-2.283368	-3.918470	0.257967	H	-5.846110	-0.061663	2.237857
C	-1.713655	-0.335314	-0.243696	H	-5.617982	-1.449446	1.179112
C	-1.255316	1.038012	0.177175	H	-3.727623	0.945638	1.451128
C	-0.133641	1.610247	-0.360657	H	-3.454336	-0.662449	2.101595
O	0.737148	1.033031	-1.118180	H	-3.475224	-1.602373	-0.205182
O	0.110568	2.931149	0.055243	C	-1.019587	-1.948457	1.636652
C	0.478396	3.930747	-0.927524	H	-2.053487	-2.310686	1.758906
C	1.973940	3.833985	-1.270816	C	-0.795162	-0.830067	2.667691
H	2.187933	2.867643	-1.729334	H	0.257005	-0.531059	2.679168
H	2.265843	4.638085	-1.958576	H	-1.386623	0.060743	2.467253
H	2.576891	3.932615	-0.359990	H	-1.058627	-1.209395	3.663474

Table A2.1. (Continued).

C	-0.384907	3.802156	-2.190779	C	-0.088684	-3.115025	2.022526
H	-1.448085	3.818868	-1.927937	H	0.960210	-2.858141	1.824975
H	-0.184257	4.636066	-2.873913	H	-0.185083	-3.306308	3.097010
H	-0.170929	2.865985	-2.713255	H	-0.314760	-4.052370	1.507191
C	0.184640	5.257593	-0.216355	O	2.303474	0.099338	1.557045
H	0.462155	6.109249	-0.848413	C	3.389026	-0.635127	2.156942
H	-0.880205	5.334053	0.027104	C	4.122176	0.352839	3.075448
H	0.752913	5.320515	0.718249	C	3.023272	1.376783	3.403169
H	-1.885048	1.656183	0.804044	C	2.262645	1.450629	2.082234
H	-1.549024	-0.379373	-1.321889	H	2.749423	2.123975	1.367644
C	-3.261812	-0.533436	-0.079397	H	1.214324	1.739165	2.164469
H	4.952794	-1.040376	-3.403845	H	3.418768	2.348445	3.714022
H	2.577851	-0.578468	-2.971330	H	2.371532	1.001656	4.201298
H	3.333164	0.402138	-1.701668	H	4.943636	0.839674	2.536732
C	3.132171	-2.779119	-1.164477	H	4.542392	-0.135425	3.959894
H	3.585283	-3.043996	-0.201223	H	2.963917	-1.474831	2.722312
H	2.290166	-3.455272	-1.347825	H	4.023909	-1.035956	1.360509
H	5.004166	-3.454199	-2.103241	O	2.642006	-1.425784	-1.066654
H	3.690958	-3.121664	-3.241474	C	3.243254	-0.609314	-2.098825
H	5.319391	-1.054830	-1.667311	C	4.561032	-1.308150	-2.418018
C	4.160445	-2.788876	-2.308949				

REFERENCES

1. (a) Herrman, J. L.; Kieczykowski, G. R.; Schlessinger, R. H. *Tetrahedron Lett.* **1973**, 2433. (b) Doi, H.; Sakai, T.; Iguchi, M.; Yamada, K.; Tomioka, K. *J. Am. Chem. Soc.* **2003**, *125*, 2886. (c) Uyehara, T.; Asao, N.; Yamamoto, Y. *J. Chem. Soc., Chem. Commun.* **1987**, 1410. (d) Amputch, M. A.; Matamoros, R.; Little, R. D. *Tetrahedron* **1994**, *50*, 5591. (e) Hase, T. A.; Kukkola, P. *Synth. Commun.* **1980**, *10*, 451. (f) Inokuchi, T.; Kawafuchi, H. *J. Org. Chem.* **2007**, *72*, 1472.

2. Bellasoued, M.; Ennigrou, R.; Gaudemar, M. *J. Organomet. Chem.* **1988**, *338*, 149.

3. Davies, S. G.; Smith, A. D.; Price, P. D. *Tetrahedron: Asymmetry* **2005**, *16*, 2833.

4. (a) Bakker, W. I. I.; Wong, P. L.; Snieckus, V. Lithium Diisopropylamide. In *e-EROS*; Paquette, L. A., Ed.; Wiley: New York, 2001. (b) Clayden, J. *Organolithiums: Selectivity for Synthesis*; Baldwin, J. E., Williams, R. M., Eds.; Pergamon Press: New York, 2002.

5. Ma, Y.; Collum, D. B. *J. Am. Chem. Soc.* **2007**, *129*, 14818.

6. For a review summarizing rate studies of LDA-mediated reactions, see: Collum, D. B.; McNeil, A. J.; Ramirez, A. *Angew. Chem., Int. Ed.* **2007**, *46*, 3002.

7. For an attempted comprehensive bibliography of triple ions of lithium salts, see: Ma, Y.; Ramirez, A.; Singh, K. J.; Keresztes, I.; Collum, D. B. *J. Am. Chem. Soc.* **2006**, *128*, 15399.

8. (a) Espenson, J. H. *Chemical Kinetics and Reaction Mechanisms*, 2nd ed.; McGraw-Hill: New York, 1995; Chapter 2, p 44. Atkins, P. W.; Jones, L. L. *Chemical Principles: The Quest for Insight*, 2nd ed.; W H. Freeman: New York, 2002.

9. For other examples of odd linearities that may or may not have origins similar to those described herein, see: (a) Blackmond, D. G.; Ropic, M.; Stefinovic, M. *Org. Process. Res. Dev.* **2006**, *10*, 457. (b) Akao, A.; Nonoyama, N.; Mase, T.; Yasuda, N. *Org. Process. Res. Dev.* **2006**, *10*, 1178. (c) Rowley, J. M.; Lobkovsky, E. B.; Coates, G. W. *J. Am. Chem. Soc.* **2007**, *129*, 4948. (d) Yin, C.-X.; Finke, R. G. *J. Am. Chem. Soc.* **2005**, *127*, 13988.

10. For examples of reactions that are fast relative to the rates of aggregate-aggregate exchanges see: (a) McGarrity, J. F.; Ogle, C. A. *J. Am. Chem. Soc.* **1985**, *107*, 1810. (b) Jones, A. C.; Sanders, A. W.; Bevan, M. J.; Reich, H. J. *J. Am. Chem. Soc.* **2007**, *129*, 3492. (c) Thompson, A.; Corley, E. G.; Huntington, M. F.; Grabowski, E. J. J.; Remenar, J. F.; Collum, D. B. *J. Am. Chem. Soc.* **1998**, *120*, 2028. (d) Jones, A. C.; Sanders, A. W.; Sikorski, W. H.; Jansen, K. L.; Reich, H. J. *J. Am. Chem. Soc.*, **2008**, *130* , 6060. (e) Reference 11.

11. Singh, K. J.; Hoepker, A. C.; Collum, D. B. *J. Am. Chem. Soc.* **2008**, *130*, 18008.

12. Gupta, L.; Hoepker, A. C.; Singh, K. J.; Collum, D. B. *J. Org. Chem.* **2009**, *74*, 2231.

13. For leading references and discussions of mixed aggregation effects, see: (a) Seebach, D. *Angew. Chem., Int. Ed. Engl.* **1988**, *27*, 1624. (b) Tchoubar, B.; Loupy, A. *Salt Effects in Organic and Organometallic Chemistry*; VCH: New York, 1992; Chapters 4, 5, and 7. (c) Briggs, T. F.; Winemiller, M. D.; Xiang, B.; Collum, D. B. *J. Org. Chem.* **2001**, *66*, 6291. (d) Caubère, P. *Chem. Rev.* **1993**, *93*, 2317.

14. Seebach, D. In *Proceedings of the Robert A. Welch Foundation Conferences on Chemistry and Biochemistry*; Wiley: New York, 1984; p 93.

15. Ramirez, A.; Sun, X.; Collum, D. B. *J. Am. Chem. Soc.* **2006**, *128*, 10326 and references cited therein.

16. A. Evans, *Potentiometry and Ion-Selective Electrodes*; Wiley: New York, 1987.

17. Fuji, T. *Anal. Chem.* **1992**, *64*, 775.

18. Kim, Y.-J.; Bernstein, M. P.; Galiano-Roth, A. S.; Romesberg, F. E.; Fuller, D. J.; Harrison, A. T.; Collum, D. B.; Williard, P. G. *J. Org. Chem.* **1991**, *56*, 4435.

19. Kottke, T.; Stalke, D. *Angew. Chem., Int. Ed. Engl.* **1993**, *32*, 580. Rennels, R. A.; Maliakal, A. J.; Collum, D. B. *J. Am. Chem. Soc.* **1998**, *120*, 421.

20. (a) Marck, W.; Huisgen, R. *Chem. Ber.* **1960**, *93*, 608. (b) Gaudemar-Bardone, F.; Gaudemar M. *Synthesis* **1979**, 463. (c) Reetz, M. T.; Maier, W. F. *Liebigs Ann. Chem.* **1980**, 1471. (d) Williard, P. G.; Carpenter, G. B. *J. Am. Chem. Soc.* **1986**, *108*, 462.
Williard, P. G.; Salvino, J. M. *J. Org. Chem.* **1993**, *58*, 1. (e) Morrison, R. C.; Hall, R. W.; Rathman, T. L. Stable Lithium Diisopropylamide and Method of Preparation. U.S. Patent 595,779, June 17, 1986.

21. See: Zhao, P.; Collum, D. B. *J. Am. Chem. Soc.* **2003**, *125*, 14411 and references cited therein.

22. Lucht, B. L.; Collum, D. B. *J. Am. Chem. Soc.* **1996**, *118*, 3529. Waldmüller, D.; Kotsatos, B. J.; Nichols, M. A.; Williard, P. G. *J. Am. Chem. Soc.* **1997**, *119*, 5479. Sato, D.; Kawasaki, H.; Shimada, I.; Arata, Y.; Okamura, K.; Date, T.; Koga, K. *J. Am. Chem. Soc.* **1992**, *114*, 761. Reich, H. J.; Goldenberg, W. S.; Gudmundsson, B. O.; Sanders, A. W.; Kulicke, K. J.; Simon, K.; Guzei, I. A. *J. Am. Chem. Soc.* **2001**, *123*, 8067. Johansson, A.; Davidsson, O. *Chem. Eur. J.* **2001**, *7*, 3461. Aubrecht, K. B.; Lucht, B. L.; Collum, D. B. *Organometallics* **1999**, *18*, 2981.

23. Job, P. *Ann. Chim.* **1928**, *9*, 113. For more recent examples and leading references, see: Huang, C. Y. *Methods Enzymol.* **1982**, *87*, 509. Hubbard, R. D.; Horner, S. R.; Miller, B. L. *J. Am. Chem. Soc.* **2001**, *123*, 5810. Potluri, V.; Maitra, U. *J. Org. Chem.* **2000**, *65*, 7764.

24.(a) Liou, L. R.; McNeil, A. J.; Ramirez, A.; Toombes, G. E. S.; Gruver, J. M.; Collum, D. B. *J. Am. Chem. Soc.* **2008**, *130*, 4859. (b) Gruver, J. M.; Liou, L. R.; McNeil, A. J.; Ramirez, A.; Collum, D. B. *J. Org. Chem.* **2008**, *73*, 7743.

25. Gaussian 03, revision B.04; Frisch, M. J.; Trucks, G. W.; Schlegel, H. B.; Scuseria, G. E.; Robb, M. A.; Cheeseman, J. R.; Montgomery, Jr., J. A.; Vreven, T.; Kudin, K. N.; Burant, J. C.; Millam, J. M.; Iyengar, S. S.; Tomasi, J.; Barone, V.; Mennucci, B.; Cossi, M.; Scalmani, G.; Rega, N.; Petersson, G. A.; Nakatsuji, H.; Hada, M.; Ehara, M.; Toyota, K.; Fukuda, R.; Hasegawa, J.; Ishida, M.; Nakajima, T.; Honda, Y.; Kitao, O.; Nakai, H.; Klene, M.; Li, X.; Knox, J. E.; Hratchian, H. P.; Cross, J. B.; Bakken, V.; Adamo, C.; Jaramillo, J.; Gomperts, R.; Stratmann, R. E.; Yazyev, O.; Austin, A. J.; Cammi, R.; Pomelli, C.; Ochterski, J. W.; Ayala, P. Y.; Morokuma, K.; Voth, G. A.; Salvador, P.; Dannenberg, J. J.; Zakrzewski, V. G.; Dapprich, S.; Daniels, A. D.; Strain, M. C.; Farkas, O.; Malick, D. K.; Rabuck, A. D.; Raghavachari, K.; Foresman, J. B.; Ortiz, J. V.; Cui, Q.; Baboul, A. G.; Clifford, S.; Cioslowski, J.; Stefanov, B. B.; Liu, G.; Liashenko, A.; Piskorz, P.; Komaromi, I.; Martin, R. L.; Fox, D. J.; Keith, T.; Al-Laham, M. A.; Peng, C. Y.; Nanayakkara, A.; Challacombe, M.; Gill, P. M. W.; Johnson, B.; Chen, W.; Wong, M. W.; Gonzalez, C.; and Pople, J. A.; Gaussian, Inc.: Wallingford CT, 2004.

26. (a) Reich, H. J.; Borst, J. P.; Dykstra, R. R.; Green, D. P. *J. Am. Chem. Soc.* **1993**, *115*, 8728. (b) Wong, M. K.; Popov, A. I. *J. Inorg. Nucl. Chem.* **1972**, *34*, 3615. (c) Yakimansky, A. V.; Müller, A. H.; Beylen, M. V. *Macromolecules* **2000**, *33*, 5686. (d) Goralski, P.; Chabanel, M. *Inorg. Chem.* **1987**, *26*, 2169 and references cited therein.

27. Studies of LDA-LiCl at ultralow LiCl concentrations as well as confirmation of LiCl in THF as a dimer will be reported in due course.

28. Galiano-Roth, A. S.; Kim, Y.-J.; Gilchrist, J. H.; Harrison, A. T.; Fuller, D. J.; Collum, D. B. *J. Am. Chem. Soc.* **1991**, *113*, 5053. Also see: Hall, P. L.; Gilchrist, J. H.; Collum, D. B. *J. Am. Chem. Soc.* **1991**, *113*, 9571.

29. Snaith and coworkers underscored the merits of R_3NHX salts as precursors to anhydrous LiX salts. See: Barr, D.; Snaith, R.; Wright, D. S.; Mulvey, R. E.; Wade, K. *J. Am. Chem. Soc.* **1987**, *109*, 7891. Also see: Hall, P. L.; Gilchrist, J. H.; Collum, D. B. *J. Am. Chem. Soc.* **1991**, *113*, 9571.

30. Rein, A. J.; Donahue, S. M.; Pavlosky, M. A. *Curr. Opin. Drug Discovery Dev.* **2000**, *3*, 734.

31. Addition of excess *i*-Pr_2NH to the metalation had no measurable effect on the rates or curvatures.

32. The concentration of LDA, although expressed in units of molarity, refers to the concentration of the monomer unit (normality).

33. We define the idealized rate law as that obtained by rounding the observed reaction orders to the nearest rational order.

34. The rate law provides the stoichiometry of the transition structure relative to that of the reactants. See: Edwards, J. O.; Greene, E. F.; Ross, J. *J. Chem. Educ.* **1968**, *45*, 381.

35. Open dimers were first proposed for the isomerization of oxiranes to allylic alcohols by mixed metal bases. See: Mordini, A.; Rayana, E. B.; Margot, C.; Schlosser, M. *Tetrahedron* **1990**, *46*, 2401. For a bibliography of lithium amide open dimers, see ref 15.

36. (a) Besson, C.; Finney, E. E.; Finke, R. G. *J. Am. Chem. Soc.* **2005,** *127,* 8179. (b) Besson, C.; Finney, E. E.; Finke, R. G. *Chem. Mater.* **2005,** *17,* 4925. (c) Huang, K. T.; Keszler, A.; Patel, N.; Patel, R. P.; Gladwin, M. T.; Kim-Shapiro, D. B.; Hogg, N. *J. Biol. Chem.* **2005**, *280*, 31126. (d) Huang, Z.; Shiva, S.; Kim-Shapiro, D. B.; Patel, R. P.; Ringwood, L. A.; Irby, C. E.; Huang, K. T.; Ho, C.; Hogg, N.; Schechter, A. N.; Gladwin, M. T. *J. Clin. Invest.* **2005**, *115*, 2099. (e) Tanj, S.; Ohno, A.; Sato, I.; Soai, K *Org. Lett.* **2001**, *3*, 287. (f) Barrios-Landeros, F.; Carrow, B. P.; Hartwig, J. F. *J. Am. Chem. Soc.* **2008**, *130*, 5842.

37. (a) Depue, J. S.; Collum, D. B. *J. Am. Chem. Soc.* **1988**, *110*, 5524. (b) McNeil, A. J.; Toombes, G. E. S.; Gruner, S. M.; Lobkovsky, E.; Collum, D. B.; Chandramouli, S. V.; Vanasse, B. J.; Ayers, T. A. *J. Am. Chem. Soc.* **2004**, *126*, 16559. (c) Nudelman, N. S.; Velurtas, S.; Grela, M. A. *J. Phys. Org. Chem.* **2003**, *16*, 669. (d) Alberts, A. H.; Wynberg, H. *J. Am. Chem. Soc.* **1989**, *111,* 7265. (e) Alberts, A. H.; Wynberg, H. *J. Chem. Soc., Chem. Commun.* **1990**, 453.

38. Tetramer-based intermediates have also been implicated in LDA-mediated ortholithiations. See: Ma, Y.; Hoepker, A. C.; Gupta, L.; Collum, D. B., Unpublished work.

39. A four-rung LDA/enolate ladder structure has been characterized crystallographically. See: Williard, P. G.; Hintze, M. J. *J. Am. Chem. Soc.* **1987**, *109*, 5539.

40. (a) Gregory, K.; Schleyer, P. v. R.; Snaith, R. *Adv. Inorg. Chem.* **1991**, *37*, 47. (b) Mulvey, R. E. *Chem. Soc. Rev.* **1991,** *20*, 167. (c) Beswick, M. A.; Wright, D. S. In *Comprehensive Organometallic Chemistry II*; Abels, E. W., Stone, F. G. A., Wilkinson, G., Eds.; Pergamon Press: New York, 1995; Vol. 1, Chapter 1. (d) Mulvey, R. E. *Chem. Soc. Rev*. **1998**, *27,* 339. (e) Rutherford, J. L.; Collum, D. B. *J. Am. Chem. Soc.* **1999**, *121*, 10198.

41. (a) Paté, F.; Gérard, H.; Oulyadi, H.; de la Lande, A.; Harrison-Marchand, A.; Parisel, O.; Maddaluno, J. *Chem. Commun.* **2009**, 319. (b) Arvidsson, P. I.; Ahlberg, P.; Hilmersson, G. *Chem. Eur. J.* **1999**, *5*, 1348.

42. Saturation was also apparent when the observed rate constants from fits to the exponential decays were plotted.

43. Espenson, J. H. *Chemical Kinetics and Reaction Mechanisms*, 2nd ed.; McGraw-Hill: New York, 1995.

44. Frey, P. A.; Hegeman, A. D. *Enzymatic Reaction Mechanisms*; Oxford University Press: New York, 2007; Chapter 2.

45. In fact, addition of 100 mol % causes a 3-fold *inhibition* relative to native LDA containing 1.0 mol % LiCl. Davies noted inhibition by LiCl on the 1,4-additions of chiral lithium amides to unsaturated esters (see: Davies, S. G.; Hermann, G. J.; Sweet, M. J.; Smith, A. D. *Chem. Commun.* **2004**, 1128). LiCl had no measurable effect on the stereoselectivity.

46. Equation 13 would appear to become undefined at $[LiCl_T] = 0$, but this turns out not to be the case. Qualitatively, the $[LiCl_T]^2$ term within the argument of the square root approaches zero at low values of $[LiCl_T]$ faster than the $[LiCl_T]$ term in the denominator. Alternatively, let $a = k_2[\text{ester}]$, $b = 16k_1k_{-1}[A_2S_2]_0$, $d = 4k_{-1}$, and $x = [LiCl_T]^2$. Eq 13 can then be rewritten as

$$\frac{-d[\text{ester}]}{dt} = \frac{a}{dx^{0.5}}[(a^2 + bx)^{0.5} - a] + c = \frac{a}{dx^{0.5}}[a(1 + \frac{b}{a^2}x)^{0.5} - a] + c$$

Applying the Taylor expansion to $[1 + (b/a^2)x]^{0.5}$ for $x \ll 1$ gives

$$\frac{-d[\text{ester}]}{dt} = \frac{a}{dx^{0.5}}[a(1 + \frac{b}{2a^2}x) - a] + c = \frac{bx}{2dx^{0.5}} + c$$

Since x approaches zero faster than $x^{0.5}$, it follows that

$$\lim_{x \to 0}\left(\frac{bx}{2dx^{0.5}} + c\right) = c$$

47. Although the saturation behavior is not sigmoidal, excluding a higher-order dependence on LiCl, the data do not exclude a fractional LiCl dependence.

48. Viciu, M.; Gupta, L.; Collum, D. B. *J. Am. Chem. Soc.* **2010**, *132*, 6361.

49. (a) Carpenter, B. K. *Determination of Organic Reaction Mechanisms*; Wiley: New York, 1984. (b) Whisler, M. C.; MacNeil, S.; Snieckus, V.; Beak, P. *Angew. Chem., Int. Ed.* **2004**, *43*, 2206.

50. Davies, S. G.; Mulvaney, A. W.; Russell, A. J.; Smith, A. D. *Tetrahedron: Asymmetry* **2007**, *18*, 1554.

51. The curves in Figure 2.16 correspond to numerical integration of the following highly simplified model:

$$\tfrac{1}{2}\,A_2 \rightleftharpoons A$$

$$A + \mathbf{1} \longrightarrow \mathbf{5}$$

$$A + \mathbf{12} \longrightarrow \mathbf{13}$$

52. For an explanation of Levenberg-Marquardt nonlinear least-squares optimization, see: Press, W. H.; Flannery, B. P.; Teukolsky, S. A.; Vetterling, V. T. *Numerical Recipes in C*; Cambridge University Press: London, 1988; Chapter 14.4.

53. Brown, P. N.; Byrne, G. D.; Hindmarsh, A. C. *J. Sci. Stat. Comput.* **1989**, *10*, 1038.

54. Given a reaction coordinate $SM \rightarrow I \rightarrow P$ in which *I* builds to appreciable concentrations, the rate of formation of *P* will show an induction period (see ref 43).

55. (a) Sun, X.; Collum, D. B. *J. Am. Chem. Soc.* **2000**, *122*, 2459. (b) See the references cited in ref 6.

56. (a) The principle of detailed balance asserts that individual equilibria within an ensemble of equilibria are maintained.[57b-d] It is particularly useful in understanding the complex equilibria observed in organolithium chemistry. See: (a) Alberty, R. A. *J. Chem. Educ.* **2004**, *81*, 1206-1209. (b) Casado, J.; Lopez-Quintela, M. A.; Lorenzo-Barral, F. M. *J. Chem. Educ.* **1986**, *63*, 450. (c) Hammes, G. G. *Principles of Chemical Kinetics*; Academic Press: New York, 1978; pp 14-15.

57. (a) Cottet, F.; Schlosser, M. *Eur. J. Org. Chem.* **2004**, 3793. (b) Trecourt, F.; Mallet, M.; Marsais, F.; Quéguiner, G. *J. Org. Chem.* **1988**, *53*, 1367. (c) Comins, D. L.; LaMunyon, D. H. *Tetrahedron Lett.* **1988**, *29*, 773. (d) Eaton, P. E.; Cunkle, G. T.; Marchioro, G.; Martin, R. M. *J. Am. Chem. Soc.* **1987**, *109*, 948. (e) Bridges. A. J.; Patt, W. C.; Stickney, T. M. *J. Org. Chem.* **1990**, *55*, 773. (f) Trécourt, F.; Marsais, F.; Güngör, T.; Quéguiner, G. *J. Chem. Soc., Perkin Trans. 1* **1990**, 2409. (g) Gros, P. C.; Fort, Y. *Eur. J. Org. Chem.* **2009**, 4199. (h) Cottet, F.; Marull, M.; Lefebvre, O.; Schlosser, M. *Eur. J. Org. Chem.* **2003**, 1559. (i) Güngör, T.; Marsais, F.; Queguiner, G. *J. Organomet. Chem.* **1981**, *215*, 139.

58. (a) Schlosser, M. *Angew. Chem., Int. Ed.* **2005**, *44*, 376. (b) Schlosser, M.; Rausis, T. *Eur. J. Org. Chem.* **2004**, 1018.

59. *Gaussview*, Version 3.09, Dennington II, R.; Keith, T.; Millam, J.; Eppinett, K.; Hovell, W. L.; Gilliland, R.; Semichem, Inc.; Shawnee Mission, KS, 2003.

CHAPTER 3

REGIOSELECTIVE LITHIUM DIISOPROPYLAMIDE-MEDIATED ORTHOLITHIATION OF 1-CHLORO-3-(TRIFLUOROMETHYL)BENZENE: ROLE OF AUTOCATALYSIS, LITHIUM CHLORIDE CATALYSIS, AND REVERSIBILITY

Regioselective Lithium Diisopropylamide–Mediated Ortholithiation of 1-Chloro-3-(trifluoromethyl)benzene: Role of Autocatalysis, Lithium Chloride Catalysis, and Reversibility

Abstract

Ortholithiation of 1-chloro-3-(trifluoromethyl)benzene with lithium diisopropylamide (LDA) in tetrahydrofuran at –78 °C displays characteristics of reactions in which aggregation events are rate limiting. Metalation with lithium chloride-free LDA involves a rate-limiting deaggregation via dimer-based transition structures. The post-rate-limiting proton transfers are suggested to involve highly solvated triple ions. Autocatalysis by the resulting aryllithiums or catalysis by traces (<100 ppm) of LiCl divert the reaction through di- and trisolvated monomer-based pathways for metalation at the two and six positions, respectively. The regiochemistry is dictated by a combination of kinetically controlled metalations overlayed by an equilibration involving diisopropylamine that is shown to occur by the microscopic reverse of the monomer-based metalations.

Introduction

Equation 1 illustrates lithium amide-mediated ortholithiations of **1** first studied by Schlosser and coworkers.[1] Divergent regioselectivities derived from lithium diisopropylamide (LDA) and lithium 2,2,6,6-tetramethylpiperidide (LiTMP) have been observed for ortholithiations and are often attributed to steric effects.[2] Further experiments, however, show this to be too simplistic. The reactions are extraordinarily sensitive to the source of

LDA: *commercially purchased LDA prepared from styrene and lithium metal is approximately 10-times less reactive than LDA generated using n-BuLi and i-Pr_2NH, and the regioselectivities are similar but not identical.* Monitoring reactions of analytically pure LDA[3] using in situ IR and ^{19}F NMR spectroscopies uncovers additional oddities. Addition of low concentrations of arene **1** affords a linear disappearance of **1** and a slight drift in regioselectivity that continues after the metalation is complete (Figure 3.1A). Ortholithiation using higher substrate concentrations (Figure 3.1B) affords a sigmoidal disappearance of arene **1** and a distribution of regioisomers **2** and **3** that changes markedly over time. Traces of LiCl added to a reaction in progress causes a burst of reactivity that displays upward curvature (Figure 3.2).

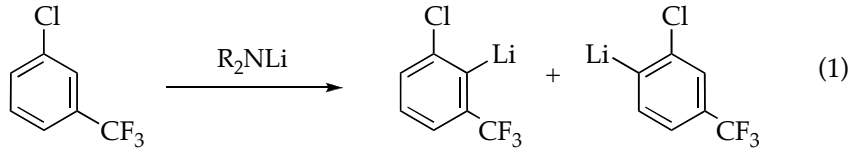

(1)

1 **2** **3**

LDA/THF/-78 °C 1:1.5
LDA/THF/-60 °C >40:1
LiTMP/THF/-78 °C 1:20

(A)

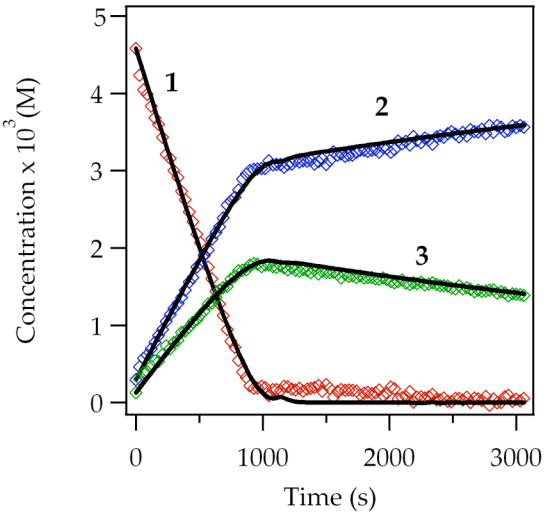

(B)

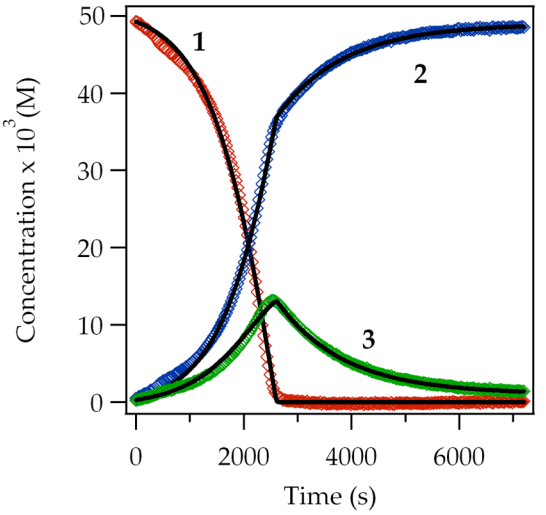

Figure 3.1. Representative plots of concentration versus time monitored by ^{19}F NMR spectroscopy for the ortholithiation of **1** and formation of **2** and **3** by LDA (0.10 M) in THF (12.2 M) at –60 °C: (A) 0.005 M **1**; (B) 0.050 M **1**. The curves represent best-fit numerical integrations as described below.

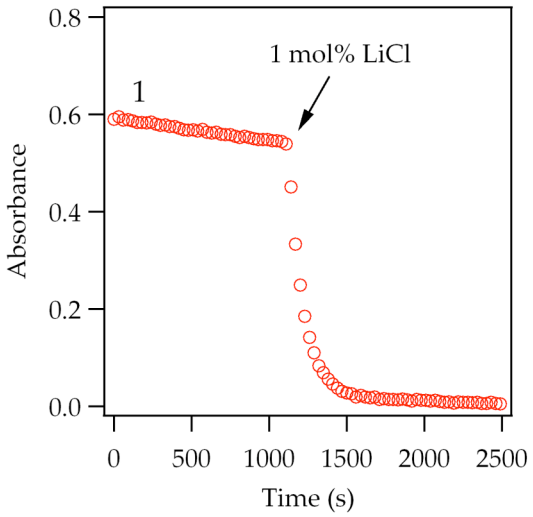

Figure 3.2. Ortholithiation of **1** (0.010 M) with LDA (0.10 M) in THF (12.2 M) at –78 °C monitored by IR spectroscopy (1325 cm^{-1}) with injection of 1.0 mol % LiCl.

We describe herein rate and mechanistic studies of the ortholithiation in eq 1 that support the simplified mechanistic scenario summarized in Scheme 1, studies which culminated in the best-fit numerical integrations displayed in Figure 3.1. The high regioselectivity of the reaction at –60 °C derives from an equilibration of aryllithiums (**2a** and **3a**), which is discussed in detail.[4,5] The really interesting part of this story, however, is what lurks beneath the 2:1 selectivity using LDA in tetrahydrofuran (THF) at –78 °C. The ortholithiation of **1** joins a growing class of LDA-mediated transformations in which the fragmentation of LDA dimer **4** is rate limiting.[3,6,7] Reactions within this class proceed at –78 °C—conditions prevalent in organic chemistry[8]—and are prone to both autocatalysis as well as catalysis by traces of LiCl and other exogenous lithium salts.[8,9] The ortholithiation of **1** introduces two prominent dimensions absent in previous studies: (1) aryllithiums **2a** and **3a** are inequiva-

lent autocatalysts, and (2) the uncatalyzed and catalyzed lithiations proceed via distinctly different fleeting structural forms of LDA (**5** and **6**).

Scheme 1

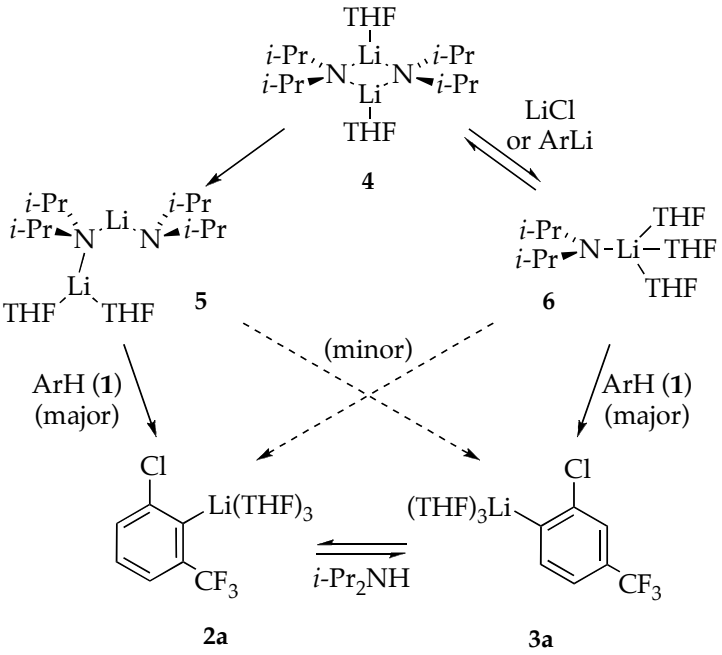

The results section offers a view of *how* the mechanisms were determined. The data are highly interdependent but are necessarily presented linearly. Evidence supporting the conclusions paints a compelling picture when considered collectively. The discussion begins with a summary, which is followed by analyses of rate-limiting deaggregation, LiCl catalysis, autocatalysis, and aryllithium (ArLi) equilibration. The conclusion considers the implications from the divergent perspectives of mechanistic and synthetic organic chemists.

Results

Solution Structures. Structural assignments of LDA and aryllithiums are required to interpret the rate data. Previous studies of [^{6}Li,^{15}N]LDA using ^{6}Li and ^{15}N NMR spectroscopies[10] reveal exclusively disolvated dimer **4**.[11] The ^{13}C NMR spectra of aryllithiums **2** and **3** display 1:1:1 triplets for the lithiated carbons.[12] The triplet corresponding to **2** is further split by ^{19}F–^{13}C coupling, whereas no such coupling is observed for **3**. The ^{19}F{^{1}H}NMR spectra display singlets.[13] Generating **2** and **3** with excess [^{6}Li,^{15}N]LDA shows no ^{6}Li–^{15}N splitting in the ^{6}Li resonances of **2** and **3**, confirming the absence of mixed aggregation.[10] Comparing **1** recovered from quenching metalations using D_2O with authentic samples prepared from the corresponding aryl bromides[14] confirm the assignments. Density functional theory (DFT) computations at the B3LYP/6-31G(d) level[15] with single-point calculations at the MP2 level of theory implicate trisolvated monomers (**2a** and **3a**; Scheme 1) in accord with other monomeric aryllithiums.[16] References to **2a** and **3a** are used instead of **2** and **3** when the structural details need to be specified. Under conditions of LiCl catalysis (≤5.0 mol % LiCl), LiCl has been shown to exist exclusively as an 8:1 mixture of mixed trimer **7** and dimer **8**.[3,17]

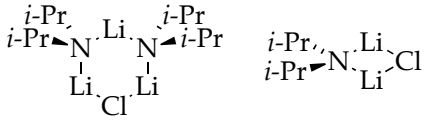

7 **8**

Kinetics: General Protocols. Acceleration of ortholithiations by as little as 0.01 mol % LiCl—*1.0 ppm*—demands preparation of rigorously LiCl-free LDA from lithium metal and isoprene. The solid LDA was subsequently recrystallized from hexanes.[3] Exogenous LiCl was generated in situ from

$Et_3N{\cdot}HCl$.[18] Et_3N is a poor ligand[19] that has no effect on LDA structure or reactivity.

The disappearance of arene **1** is most conveniently followed using in situ IR spectroscopy (1325 cm^{-1}).[20] ^{19}F NMR spectroscopy was used to follow **1** (δ –62.21 ppm), **2** (δ –61.71 ppm), and **3** (δ –60.90 ppm) concurrently. The initial rates of metalation[21] were obtained from the first derivative of a polynomial fit to data from 0–5% conversion.[22] On several occasions the reaction temperature was raised to –65 °C (as noted) to avoid protracted reaction times.

Uncatalyzed Ortholithiation: Rate-Limiting Deaggregation. Let us first examine the mechanism of the uncatalyzed metalation. Monitoring the metalation of **1** at early conversion—measuring the rates before the onset of autocatalysis—reveals a rate-limiting deaggregation of dimer **4**. Thus, a plot of initial rate versus arene **1** concentration shows a clear zeroth-order dependence consistent with the absence of arene **1** in the rate-limiting step (Figure 3.3).[23] The initial rates are independent of THF concentration (Figure 3.4) and display an approximate first-order dependence (1.15 $\pm$ 0.09 order) on LDA concentration (Figure 3.5).[24,25] Isotopic labeling studies (below) confirm post-rate-limiting proton transfer.

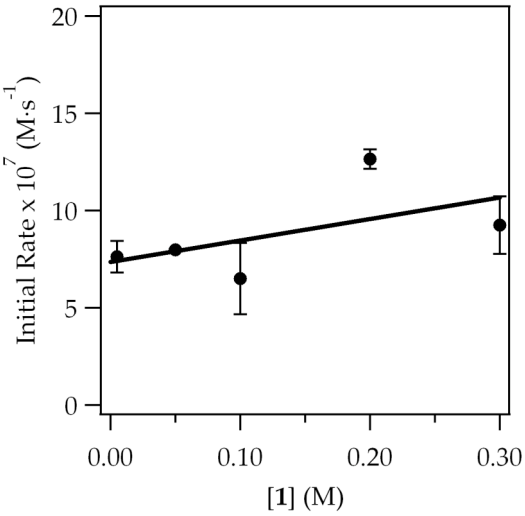

Figure 3.3. Plot of initial rate vs [**1**] (initial arene concentration) for the ortholithiation of **1** with LDA (0.10 M) in THF (12.2 M) at –78 °C measured by IR spectroscopy. The curve depicts an unweighted least-squares fit to y = a[ArH] + b. [a = (9 $\pm$ 1) x 10^{-7}, b = (7 $\pm$ 8) x 10^{-9}]

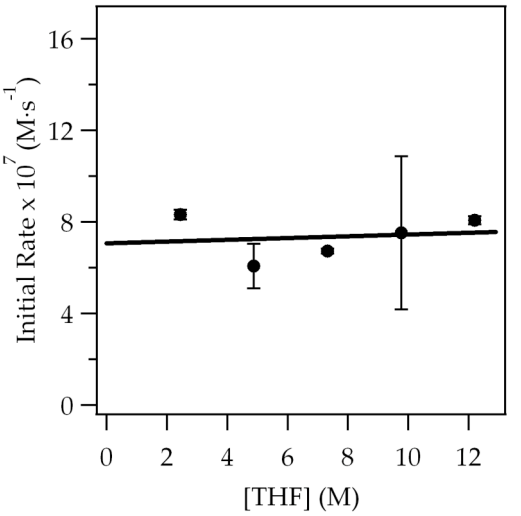

Figure 3.4. Plot of initial rate versus [THF] for the ortholithiation of **1** (0.050 M) by LDA (0.10 M) at –78 °C measured by IR spectroscopy. The curve depicts an unweighted least-squares fit to y = a[THF] + b. [a = (7 $\pm$ 1) x 10^{-7}, b = (3.9 $\pm$ 0.1) x 10^{-9}]

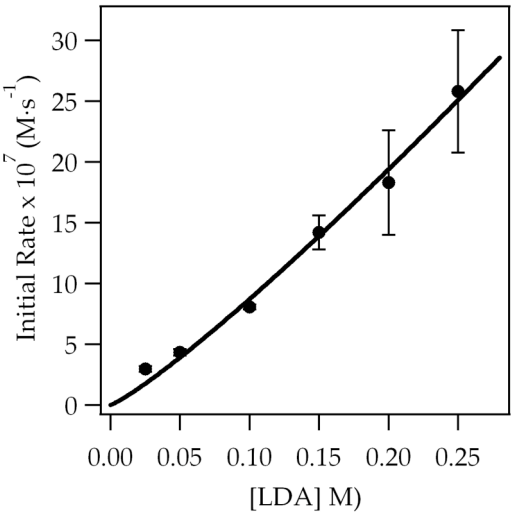

Figure 3.5. Plot of initial rate versus [LDA] in THF (12.2 M) for the ortholithiation of **1** (0.050 M) at –78 °C measured by IR spectroscopy. The curve depicts an unweighted least-squares fit to y = a[LDA]^n. [a = (1.2 $\pm$ 0.2) x 10^{-5}, n = (1.16 $\pm$ 0.09)]

To simplify mechanistic discussions, we introduce the following shorthand: A = an LDA subunit, S = THF, ArH = arene, and ArLi refers to aryllithiums **2** and **3** collectively. By example, A_2S_2 corresponds to disolvated LDA dimer **4**. The rate data are consistent with the idealized[26] rate law in eq 2. The generic mechanism described by eq 3 reduces to eq 4 because the trapping step is efficient (k_2[ArH] >> k_{-1}). Curiously, previous studies of 1,4–additions of LDA to unsaturated esters revealed a rate-limiting deaggregation of dimer **4**,[3] but in those studies the rate-limiting step involved a *tri*solvated-dimer-based transition structure, $[A_2S_3]^‡$. The existence of $[A_2S_3]^‡$ constitutes the first of several observations suggesting that $[A_2S_2]^‡$ is the rate-limiting transition structure en route to only *partial* deaggregation. DFT computations indicate that facile solvent reorganization is followed by the formation of open dimer **5** via a quite reasonable transition structure **9** (eq 5).[27]

$$-d[\mathrm{ArH}]/dt = k[\mathrm{A_2S_2}][\mathrm{S}]^0[\mathrm{ArH}]^0 \quad (2)$$

$$\mathrm{A_2S_2} \underset{k_{-1}}{\overset{k_1}{\rightleftharpoons}} [\mathrm{A_2S_2}^*] \xrightarrow{k_2[\mathrm{ArH}]} \mathrm{ArLi} \quad (3)$$

$$\mathrm{A_2S_2} \xrightarrow{k_2} [\mathrm{A_2S_2}]^{\ddagger} \quad (4)$$

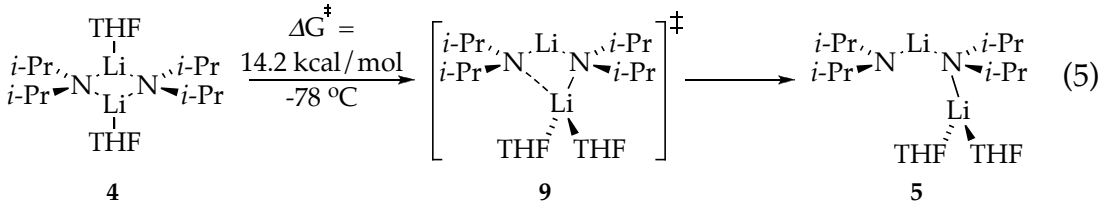

4 9 5 (5)

Uncatalyzed Ortholithiation: Kinetic Isotope Effects. Deuterium labeling studies confirm that the critical proton transfer (still measured at early conversion) is post rate limiting. The analysis was carried out using ^{19}F NMR spectroscopy and is summarized in Scheme 2. By first focusing on the unlabeled substrate (**1**) and monodeuterated substrates (**1**-2-*d* and **1**-6-*d*), we noted that the rates of disappearance of the three isotopomers are indistinguishable ($\pm$5%) despite the suppression of specific pathways. Such equivalent intermolecular isotope effects[28,29] are consistent with post-rate-limiting proton (deuterium) transfers. The ratios of rate constants corresponding to isotopically sensitive (but post-rate-limiting) branch points—$k_{\mathrm{H(2)}}/k_{\mathrm{H(6)}}$, $k_{\mathrm{D(2)}}/k_{\mathrm{H(6)}}$, and $k_{\mathrm{H(2)}}/k_{\mathrm{D(6)}}$—were determined by measuring the respective **2**/**3** ratios at early conversion using ^{19}F NMR spectroscopy. The regioselectivities make intuitive sense: deuteration at C2 (**1**-2-*d*) markedly promotes metalation at C6 (**2**:**3** = 1:18), whereas deuteration at C6 (**1**-6-*d*) promotes metalation at C2 (**2**:**3** = 34:1). The intramolecular isotope effects[28,29] corresponding to $k_{\mathrm{H(2)}}/k_{\mathrm{D(2)}}$ and $k_{\mathrm{H(6)}}/k_{\mathrm{D(6)}}$

were calculated according to eqs 6 and 7 and found to be substantial and inequivalent.[30]

Scheme 2

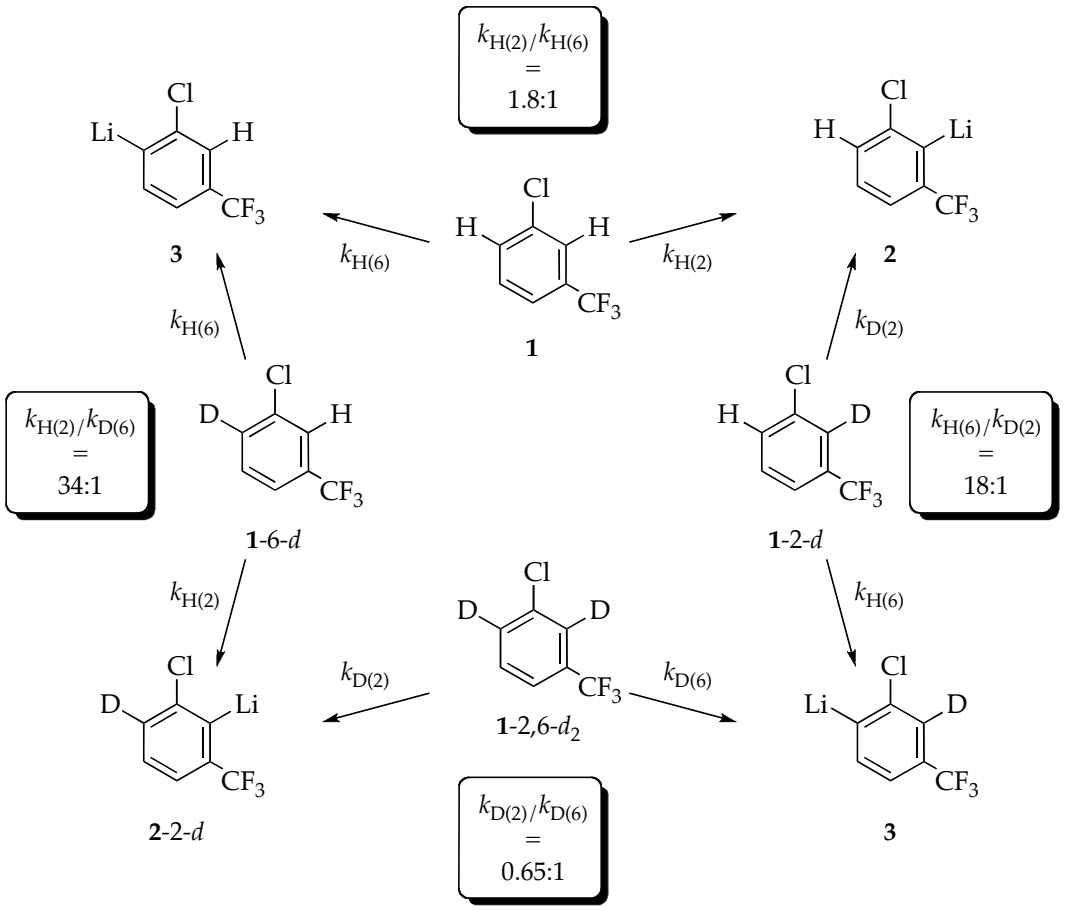

$$k_{H(2)}/k_{D(2)} = (k_{H(2)}/k_{H(6)})(k_{H(6)}/k_{D(2)}) = 31 \quad (6)$$

$$k_{H(6)}/k_{D(6)} = (k_{H(6)}/k_{H(2)})(k_{H(2)}/k_{D(6)}) = 19 \quad (7)$$

The behavior of doubly deuterated arene **1**-2,6-d_2 diverges from that of the other three substrates and offers an interesting window into the mechanism.[31] The curvatures exhibited by the decays are highly dependent on arene concentration. At high concentration (0.10 M) we observe downward curva-

ture characteristic of autocatalysis. As the concentration decreases, the downward curvature gives way to upward curvature that becomes exponential at <0.005 M, which is expected for first-order arene dependencies.

The upward curvature suggests that deuteration causes the metalation to become at least partially rate limiting.[32] Moreover, the initial metalation rate at 0.050 M **1**-2,6-d_2 is approximately threefold slower than that of the other three isotopomers (eq 8), showing that the metalation rate has an attenuated but detectable isotopic sensitivity. To understand the origins of this partial rate limitation we return to eq 3. A rate-limiting deaggregation demands that the fleeting intermediate denoted as A_2S_2* (suggested computationally to be open dimer **5**) be trapped efficiently by ArH (k_2[ArH] >> k_{-1}). The much slower metalations of **1**-2,6-d_2 causes deuterium transfer to become partially rate limiting

(k_2[**1**-2,6-d_2] ≈ k_{-1}.) The appearance of **1**-2,6-d_2 in the rate law would be accompanied by upward curvature and a partial isotope effect as observed.

Several experiments confirm that lithiation of **1**-2,6-d_2 involves only partially rate-limiting deaggregation. A competitive isotope effect measured according to eq 9 plumbs post-rate-limiting behavior akin to measuring an intramolecular isotope effect,[28] except that the competitive isotope effect involves two distinct substrates. If the intermolecular isotope effect obtained using **1** and **1**-2,6-d_2 is simply a small primary kinetic isotope effect, the competitive isotope effect (eq 9) should be comparable. As illustrated in eq 9, the measured value is large and similar to the intramolecular isotope effects summarized in Scheme 2 and eqs 6 and 7. The crudeness of the estimate stems from technical difficulties associated with deconvoluting the IR absorbances corresponding to **1** and **1**-2,6-d_2 combined with measuring initial rates.[33] The

decays of the isotopomers also display a highly revealing biphasic behavior (Figure 3.6) emblematic of post-rate-limiting competition between the two substrates.[3,6c] The different curvatures for **1** (downward) and **1**-2,6-d_2 (upward) also reflect separate stages along the reaction coordinate: ArLi autocatalyst has reached substantial concentrations as **1**-2,6-d_2 begins to react in earnest.

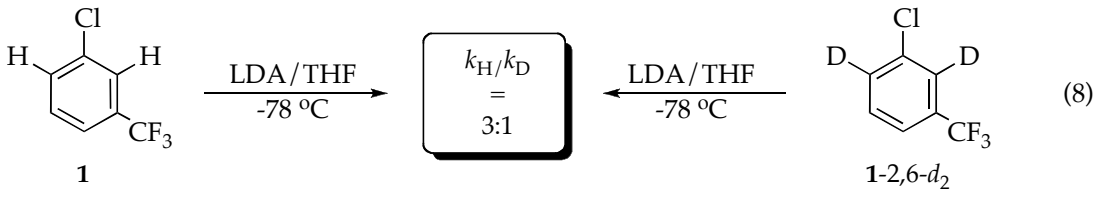

(8)

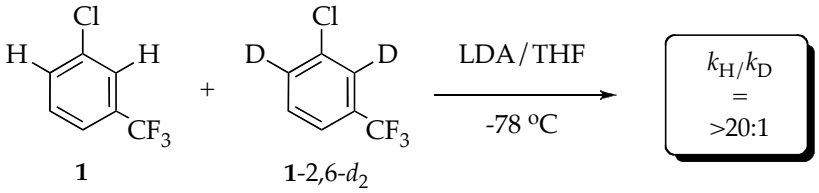

(9)

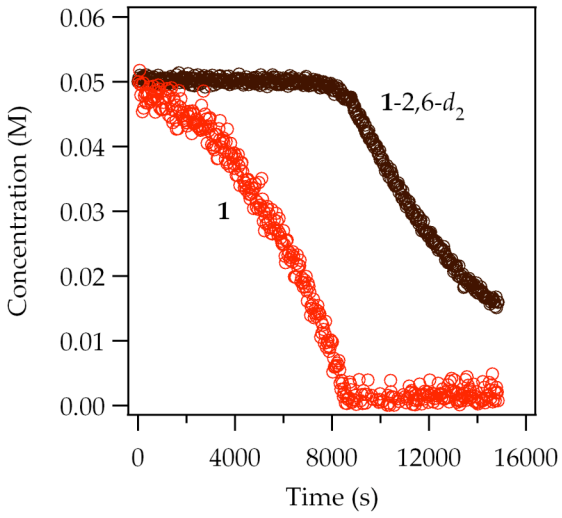

Figure 3.6. Competitive ortholithiation of **1** (0.050 M) and **1**-2,6-d_2 (0.050 M) with LDA (0.10 M) in THF (12.2 M) at –78 °C monitored by IR spectroscopy.

Partial rate limitation leads to a second clear prediction. If k_2[**1**-2,6-d_2] ≈ k_{-1}, then high **1**-2,6-d_2 concentrations should cause k_2[**1**-2,6-d_2] >> k_{-1} and reduce eq 3 to eq 4. In short, high **1**-2,6-d_2 concentration would cause deaggregation to become fully rate limiting and be accompanied by a zeroth-order substrate dependence (saturation kinetics). Indeed, Figure 3.7 shows saturation at high **1**-2,6-d_2 concentration that is accompanied by nearly identical rates of disappearance for **1** and **1**-2,6-d_2. The curve in Figure 3.7 is a simple first-order saturation function, and the concentrations refer to initial concentrations. The inset in Figure 3.7 shows a slightly different view by plotting the intermolecular isotope effect versus **1**-2,6-d_2 concentration, which approaches unity at the high concentration limit.

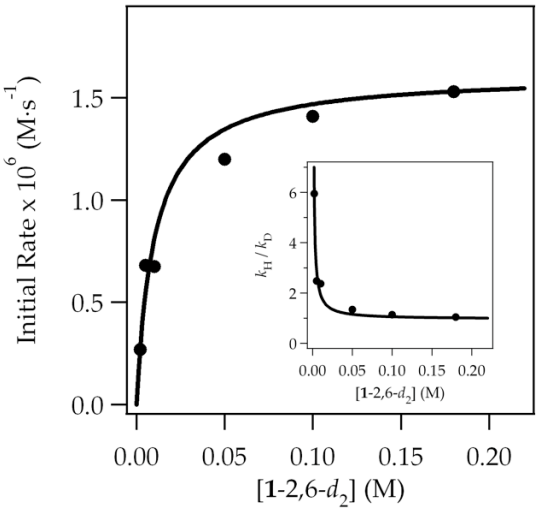

Figure 3.7. Plot of initial rate versus [**1**-2,6-d_2] for the ortholithiation of **1**-2,6-d_2 by 0.10 M LDA in 12.2 M THF at –78 °C measured by IR spectroscopy. The curve depicts an unweighted least-squares fit to a first-order saturation function: $-\Delta[\mathrm{ArH}]/\Delta t\,|_{t=0} = (a[\mathrm{ArH}])/\,(1 + b[\mathrm{ArH}])$ where ArH is **1**-2,4-d_2. The ratio a/b was constrained to 1.6 x10^{-6} M·s^{-1} to ensure saturation at the initial rate of **1** (1.6 x10^{-6} M·s^{-1}). [b = (2.62 ± 0.08) x 10^{-6}]

Uncatalyzed Ortholithiation: Mechanisms of Proton Transfers. The regioselectivity in this reaction provides a glimpse beyond rate-limiting deaggregation, a portion of the reaction coordinate considered largely invisible to kineticists. Monitoring the initial rates of formation of aryllithiums **2** and **3** using ^{19}F NMR spectroscopy affords what one might call a *relative* rate law (eq 10). If, for example, **2** and **3** form via a single (shared) fleeting intermediate, then the regioselectivity—the post-rate-limiting branch—would be independent of LDA and THF concentrations. Indeed, the product ratios are independent of LDA concentration, showing a shared aggregation state. By contrast, although the overall metalation rates are THF-concentration independent, the product ratios show a greater tendency to form **3** at elevated THF concentration (Figure 3.8). A nonlinear least squares fit shows that the metalation to form **3** requires *one* THF ligand beyond what is required for the metalation to form **2**.

$$[\mathbf{2}]/[\mathbf{3}] = c[\mathrm{ArH}]^0[\mathrm{LDA}]^0[\mathrm{THF}]^{-1} \qquad (10)$$

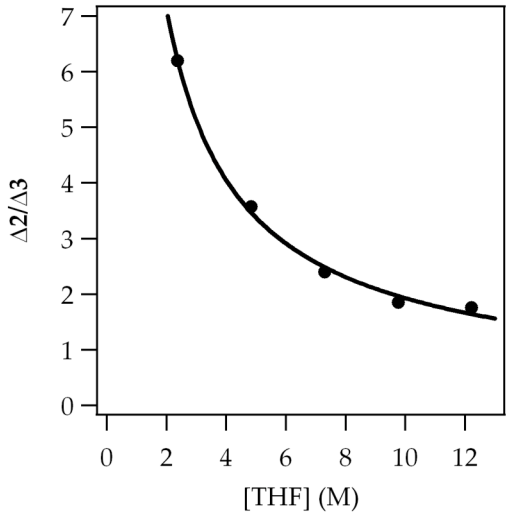

Figure 3.8. Ratio of relative initial rates of formation of **2** and **3**, $(\Delta\mathbf{2}/\Delta t)/(\Delta\mathbf{3}/\Delta t)$, versus [THF] for the ortholithiation of **1** (0.050 M) by LDA (0.10 M) at –65 °C measured by ^{19}F NMR spectroscopy. The elevated temperature was used to shorten the duration of the experiments. The curve depicts an unweighted least-squares fit to $y = a[\text{THF}]^n + b$. ($a = 12.5 \pm 0.8$, $n = -0.8 \pm 0.2$ and $b = 0.1 \pm 0.8$.)

Metalations at the lowest concentrations of **1**-2,6-d_2, conditions in which both the curvatures and isotope effects indicate that the rate limiting step is deuterium transfer, allowed us to probe the events following the deaggregation step. A plot of k_{obsd} vs LDA concentration (Figure 3.9) shows near linearity (0.92 order), indicating that the metalation of **1**-2,6-d_2 is dimer-based as suspected. The corresponding plot of k_{obsd} vs THF concentration affords an altogether unexpected second-order THF dependence (Figure 3.10). Switching from hexane to 2,5-Me_2THF as the cosolvent to maintain a more constant polarity had no effect on the observed rates, again affording a second-order THF dependence. The combined data afford the rate law in eq 11 and the mechanism in eq 12 involving tetrasolvated dimers. We hasten to add that the two terms in eq 11—the second order affiliated with the formation of **2** and the third-order solvent affiliated with formation of **3**—and accompanying tetra-

and pentasolvated terms in eq 12 do *not* derive from the measured solvent order in Figure 3.10 (which clearly approximates two) but rather from the relative solvent order illustrated in Figure 3.8 demanding differential solvation. We estimate from relative contributions of pathways leading to **2** and **3** that the measured solvent order should have measured slightly above two.

Concerned that we might be getting deceived by the LDA order, we examined the influence of LiCl on the metalation rates. If the rate limiting metalation proceeds via a pre-equilibrated monomer-based pathway, then LiCl should have no effect because LiCl serves to catalyze dimer-monomer exchange (vide infra). In the event, addition of LiCl to a metalation of **1**-2,6-d_2 at low concentrations elicited a tenfold acceleration, suggesting that the uncatalyzed and LiCl-catalyzed metalation are indeed different. Triple ions **10** and **11** are computationally viable candidates for the dimer-based reactions. Although the absolute energies of such highly ionized forms are of little value, **10** is 3.5 kcal/mol more stable than **11**.[3,34]

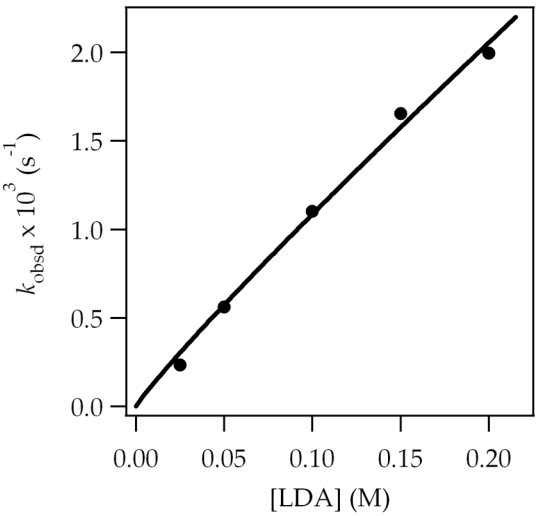

Figure 3.9. Plot of k_{obsd} versus [LDA] in THF (12.2 M) for the ortholithiation of **1**-2,6-d_2 (0.002 M) at –65 °C measured by ^{19}F NMR spectroscopy. The curve depicts an unweighted least-squares fit to y = k[LDA]^n. [k = (9 $\pm$ 1) x 10^{-3}, n = 0.92 $\pm$ 0.06]

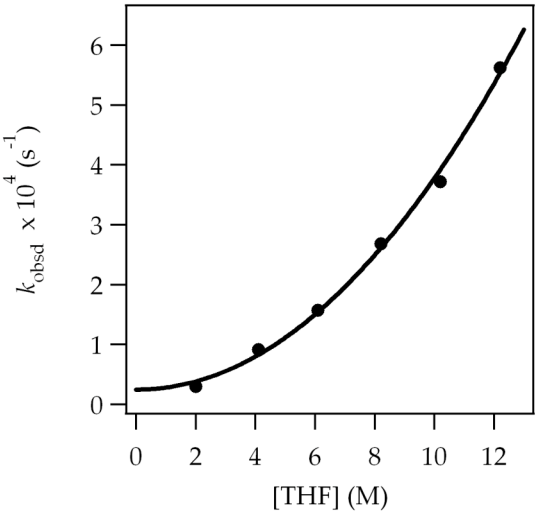

Figure 3.10. Plot of k_{obsd} versus [THF] in hexanes for the ortholithiation of **1**-2,6-d_2 (0.002 M) by LDA (0.050 M) at –65 °C measured by ^{19}F NMR spectroscopy. The curve depicts an unweighted least-squares fit to y = k[THF]^n + c. [k = (3 $\pm$ 1) x 10^{-6}, n = 2.0 $\pm$ 0.2, c = (3 $\pm$ 1) x 10^{-5}]

$$-d[\mathrm{ArH}]/dt = k_{(2)}[\mathrm{ArD}]^1[\mathrm{A_2S_2}][\mathrm{S}]^2 + k_{(3)}[\mathrm{ArD}]^1[\mathrm{A_2S_2}][\mathrm{S}]^3 \qquad (11)$$

$$\mathrm{A_2S_2} \underset{k_{-1}}{\overset{k_1}{\rightleftharpoons}} [\mathrm{A_2S_{4/5}}] \xrightarrow{k_2[\mathrm{ArD}]} \mathrm{ArLi} \qquad (12)$$

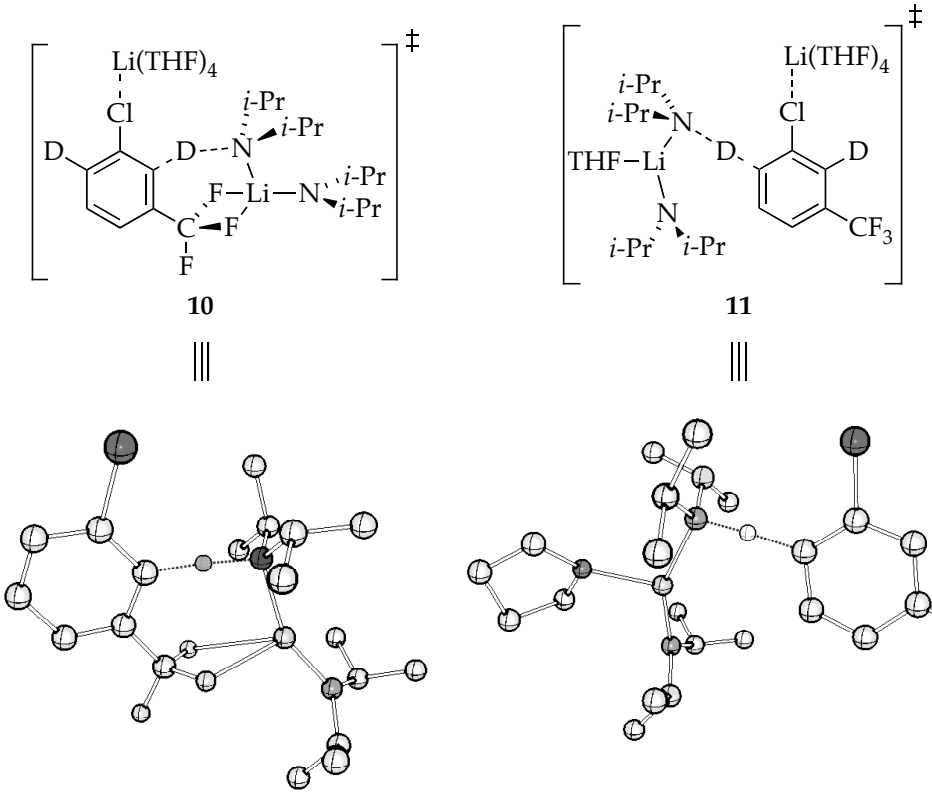

Although the data implicate tetra- and pentasolvated dimers, we also explored various di- and trisolvated-dimer-based transition structures summarized in Figure 3.11. (We include those leading to the unobserved regioisomeric ArLi for comparison.) All are computationally reasonable, displaying absolute activation energies of 13–18 kcal/mol. The origins of the solvent-dependent regioselectivities fall within the error of the computations.[35]

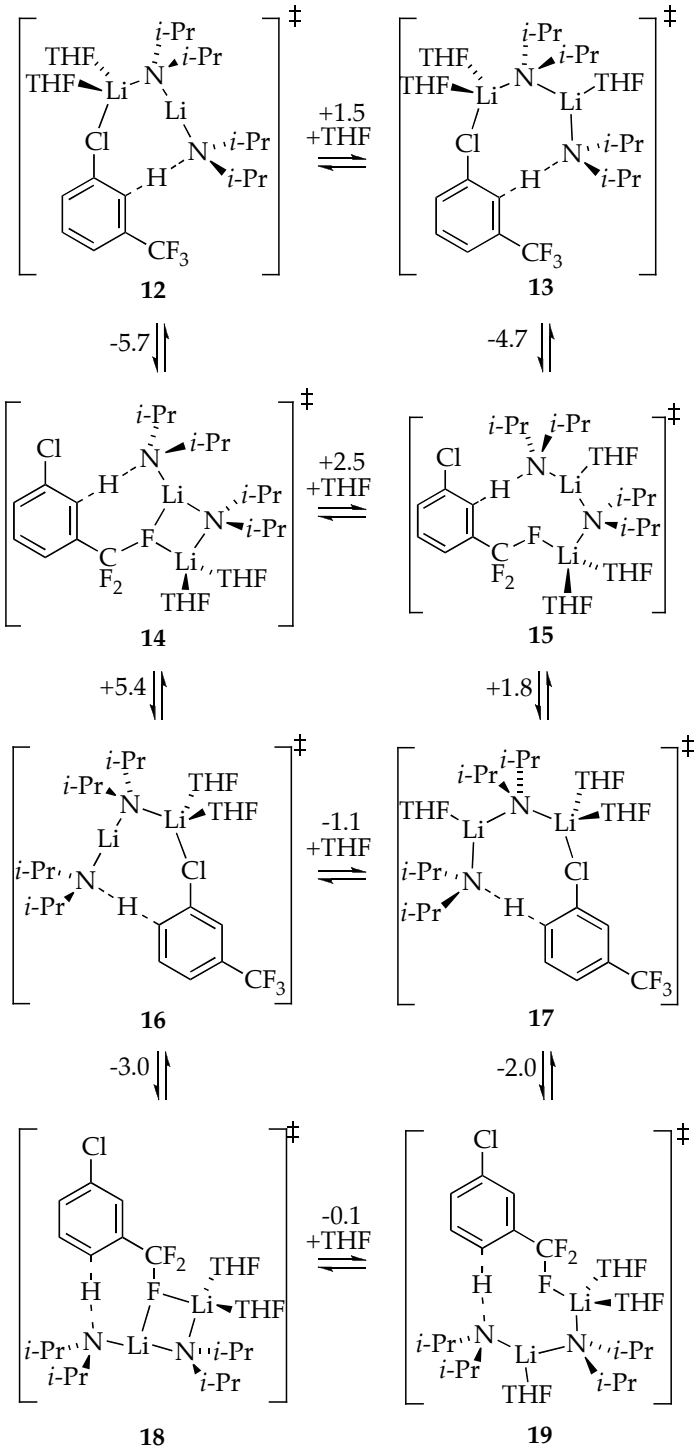

Figure 3.11. DFT computations [MP2/6–31G(d)//B3LYP/6–31G(d)] of dimer-based transition structures for the metalation of **1**. The free energy of activation for the formation of **12** ($\Delta G^{\ddagger}$) is 19.3 kcal/mol calculated at –78 °C. The numbers affiliated with the arrows represent the relative free energies (ΔG).

LiCl Catalysis. Traces of LiCl elicit marked rate accelerations that are accompanied by distinct upward curvatures, suggesting that LiCl catalysis brings arene **1** back into the rate law. Clean first-order decays are observed at >5 mol % LiCl (Figure 3.12). A plot of the initial rates versus LiCl concentration shows second-order saturation kinetics with the onset of saturation at low levels (<2.0 mol % LiCl) as noted in previous studies (Figure 3.13).[3,6] The saturation behavior in Figure 3.13 is *not* Michaelis–Menten kinetics, however, which would require stoichiometric LiCl to attain saturation.[36] It should also not be confused with the saturation kinetics noted for metalations of **1**-2,6-d_2 and shown in Figure 3.7 (although they are related). *LiCl catalyzes a deaggregation.* Analogous LiCl saturation behavior was observed for 1,4-additions of LDA to unsaturated esters, although the sigmoidal curvature evident at low LiCl concentrations (inset in Figure 3.13) that would signify a *second*-order LiCl dependence has not been observed.[3,37]

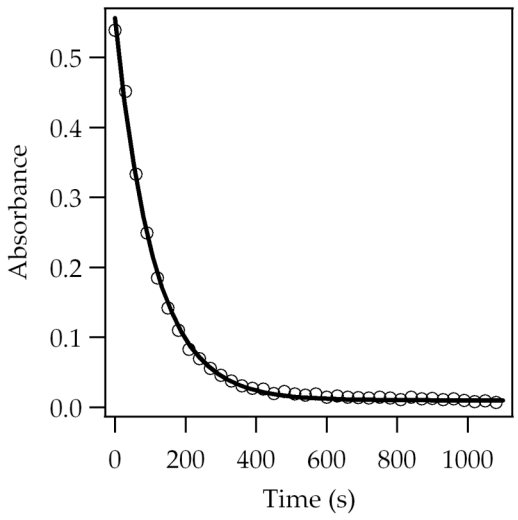

Figure 3.12. Representative plot of the IR absorbance of **1** (0.005 M) versus time for the ortholithiation by LDA (0.10 M) in 12.2 M THF in the presence of 5 mol% LiCl at –78 °C. The curve depicts an unweighted least-squares fit to $y = Ae^{-kt}$.

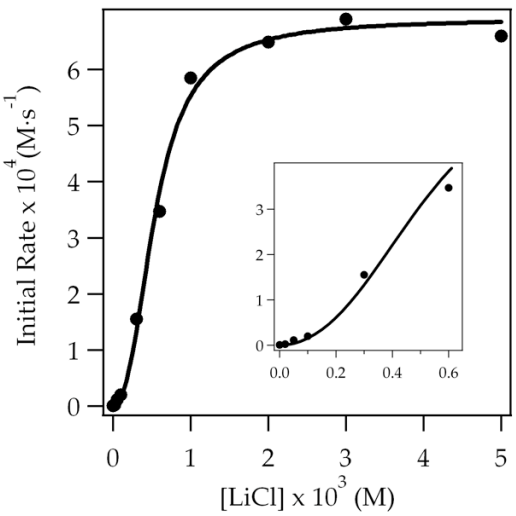

Figure 3.13. Plot of initial rate versus [LiCl] for the ortholithiation of **1** (0.074 M) by 0.10 M LDA in 12.2 M THF at –78 °C measured by IR spectroscopy. The inset is a magnified view of the data at low concentrations. The curve depicts an unweighted least-squares fit to eq 17. [ArH] = 0.074 M, [A_2S_2] = 0.050 M, c = 1.0 x 10^{-8}. [k_1 = (1.5 $\pm$ 0.1) x 10^4, k_{-1} = (3.2 $\pm$ 0.4) x 10^6, k_2 = 0.61 $\pm$ (6 x 10^{-4}), n = 2.0 $\pm$ 0.3]

The details of the deaggregation were examined at full saturation (5.0 mol % LiCl) as follows. Ortholithiation of **1** and **1**-2,6-d_2 reveals large and equivalent standard and competitive isotope effects (eqs 13 and 14) consistent with rate-limiting proton (and deuterium) transfer. Plotting initial rates versus LDA concentration affords a generic half-order dependence implicating a dimer–monomer preequilibrium (Figure 3.14).[23] A plot of initial rates versus THF concentration using *hexanes* as cosolvent (Figure 3.15) shows a high (1.6 $\pm$ 0.3) order in THF. The curvature—a departure from a linear first-order dependence—was traced to medium effects using a now-routine protocol[38] in which the hydrocarbon is replaced with the polar[39] yet weakly coordinating[40] cosolvent, 2,5-dimethyltetrahydrofuran (Me_2THF). Holding the polarity of the medium approximately constant afforded a THF order slightly above unity

(1.1 ± 0.1 order). The mechanism (eqs 15 and 16) and rate law (eq 17) include provisions for second-order saturation by LiCl. The odd mathematical form of eq 17 stems from the quadratic equation required by the deaggregation.[3] The *c* term corresponds to the basal (uncatalyzed) rate. In the limit of full saturation, eq 17 reduces to eq 18.[41]

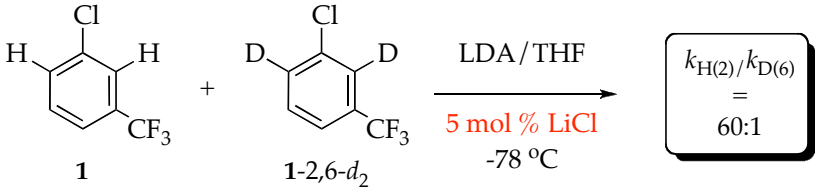

(13)

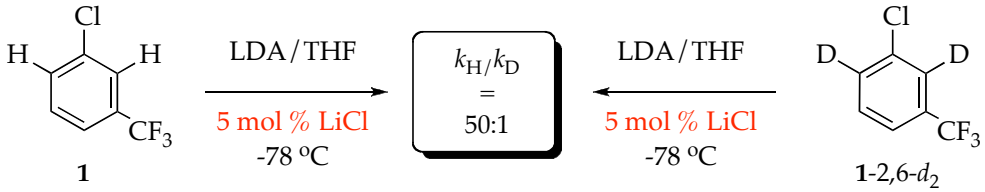

(14)

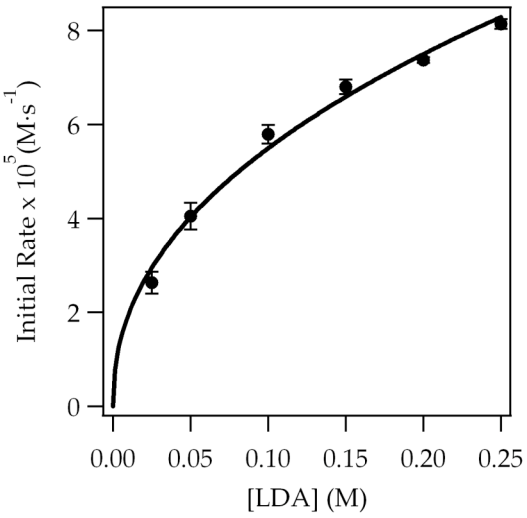

Figure 3.14. Plot of initial rate versus [LDA] in THF (12.2 M) for the ortholithiation of **1** (0.075 M) in the presence of 5 mol% LiCl at –78 °C measured by IR spectroscopy. The curve depicts an unweighted least-squares fit to $y = a[\text{LDA}]^n$. [$a = (154 \pm 9) \times 10^{-6}$, $n = 0.45 \pm 0.03$]

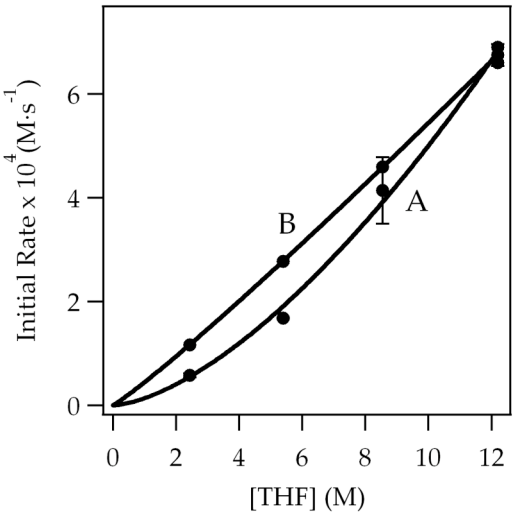

Figure 3.15. Plot of initial rate versus [THF] in hexanes (curve A) and 2,5-dimethyl-tetrahydrofuran (curve B) cosolvent for the ortholithiation of **1** (0.075 M) by LDA (0.10 M) in the presence of 5 mol% LiCl at –78 °C. The data was measured by IR spectroscopy. The curve depicts an unweighted least-squares fit to $y = a[\mathrm{THF}]^n + b$. Curve A: $a = (1.4 \pm 1.0) \times 10^{-5}$, $n = 1.6 \pm 0.3$, $b = (1.6 \pm 1) \times 10^{-5}$. Curve B: $a = (4.44 \pm 2.0) \times 10^{-5}$, $n = 1.1 \pm 0.1$, $b = (0.0 \pm 5) \times 10^{-5}$.

$$\tfrac{1}{2}\,A_2S_2 + S \underset{k_{-1}[\mathrm{LiCl_{total}}]^n}{\overset{k_1[\mathrm{LiCl_{total}}]^n}{\rightleftharpoons}} AS_2 \qquad (15)$$

$$AS_2 + \mathrm{ArH} \xrightarrow{k_2} [AS_2(\mathrm{ArH})]^{\ddagger} \qquad (16)$$

$$-\Delta[\mathrm{ArH}]/\Delta t\big|_{t=0} = \frac{k_2[\mathrm{ArH}]}{4k_{-1}[\mathrm{LiCl}]^n}\left(\sqrt{k_2^2[\mathrm{ArH}]^2 + 16k_1k_{-1}[A_2S_2][\mathrm{LiCl}]^{2n}} - k_2[\mathrm{ArH}]\right) + c \qquad (17)$$

$$-\Delta[\mathrm{ArH}]/\Delta t\,|_{t=0} = (k_1/k_{-1})^{1/2}k_2[\mathrm{ArH}][\mathrm{THF}][\mathrm{LDA}]^{0.5} \qquad (18)$$

Comparing the regioselectivity in neat THF without catalysis (**2**:**3** = 1.8:1) with that derived from LiCl catalysis (**2**:**3** = 0.85:1) shows subtle differences that are mechanistically important. Nonetheless, the regioselectivities under LiCl catalysis are, as noted for the uncatalyzed metalation, independent of LDA concentration and dependent on the THF concentration (Figure 3.16).

In conjunction with the rate law, the results implicate an $[AS_3(ArH)]^‡$ stoichiometry for the formation of **3** and an $[AS_2(ArH)]^‡$ stoichiometry for the formation of **2**. We examined the selectivities using DFT computations (Figure 3.17). All are computationally reasonable, displaying absolute activation energies of 12–15 kcal/mol.[35] Disolvated monomer-based transition structure **21** and the corresponding trisolvate **24** are the most favorable, consistent with both the rate data and THF-dependent regioselectivities.

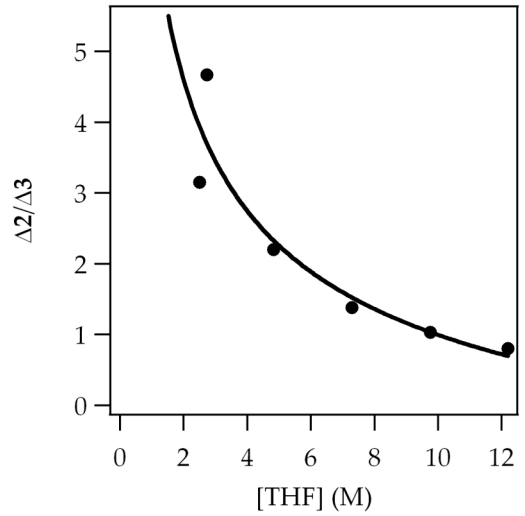

Figure 3.16. Plot of relative initial rate versus [THF] in 2,5-dimethyltetrahydrofuran cosolvent for the ortholithiation of **1** (0.050 M) by LDA (0.10 M) in the presence of 5 mol% LiCl at –78 °C. The concentrations of **2** and **3** were monitored by ^{19}F NMR spectroscopy. The curve depicts an unweighted least-squares fit to $y = a[THF]^n + b$. [$a = 9 \pm 6$, $n = -0.94 \pm 0.21$, $b = 0.0 \pm 0.3$]

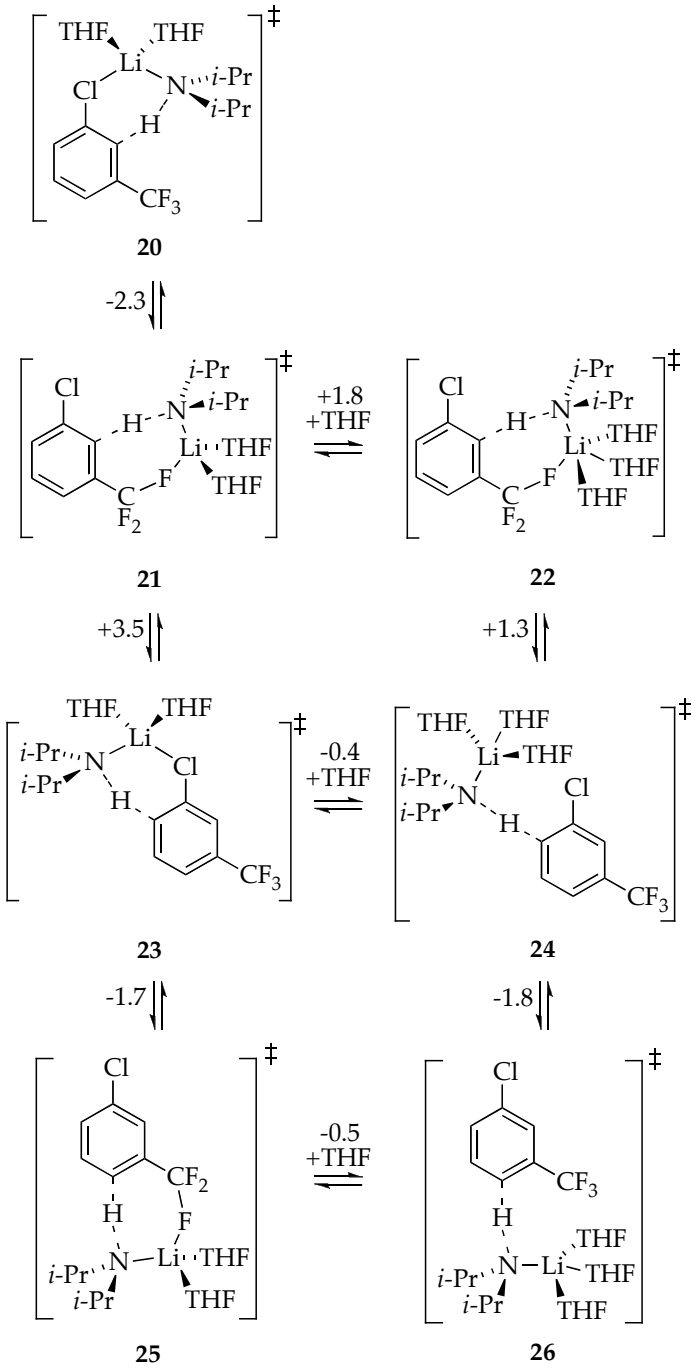

Figure 3.17. DFT computations [MP2/6–31G(d)//B3LYP/6–31G(d)] of monomer-based transition structures for the metalation of **1**. The free energy of activation for the formation of **20** ($\Delta G^{\ddagger}$) is 14.5 kcal/mol calculated at –78 °C. The numbers affiliated with the arrows represent the relative free energies (ΔG).

Autocatalysis. Autocatalysis is easily detected as downward curvature in plots of arene **1** versus time (Figure 3.1B).[42,43] What makes detailed studies so challenging is that (1) **2** and **3** display different autocatalytic activities, (2) autocatalysis diverts dimer-based metalations prevalent in the absence of catalysis to monomer-based metalations, (3) the dimer- and monomer-based metalations display inherently different regioselectivities, and (4) an equilibration pathway superimposed on the autocatalysis converts **3** to **2**.

The task of untangling the role of autocatalysis began with a routine control experiment to confirm its existence. After a kinetic run using 0.10 M LDA and 0.010 M arene **1** in neat THF, the IR baseline was zeroed and a second aliquot of **1** added (Figure 3.18). The loss of arene displays a distinct acceleration accompanied by substantially greater upward curvature (loss of downward curvature). Autocatalysis by ArLi (**2** and **3**) is analogous to the 100-fold more efficient catalysis by LiCl. Of particular note, the regioselectivities for the ArLi- and LiCl-catalyzed metalations are indistinguishable (**2**:**3** = 0.85:1) and different from the 1.8:1 ratio observed for the uncatalyzed metalation. Moreover, plotting the initial rates versus ArLi concentration (Figure 3.19) shows saturation kinetics analogous to that observed for LiCl (Figure 3.13) but at much higher ArLi concentrations. The data shown in Figure 3.13 was generated using regioisomer **2**-6-*d* because it was easily generated in 95% regioisomeric purity from **1**-6-*d* by exploiting the isotope effect to direct the metalation. Comparing the efficacy of catalysis using **2**-6-*d* (generated in situ from **1**-6-*d*) to the catalysis elicited by **3**-2-*d* (generated in situ from **1**-2-*d*), we found that regioisomer **2** is 6-fold more effective than **3** as an autocatalyst.

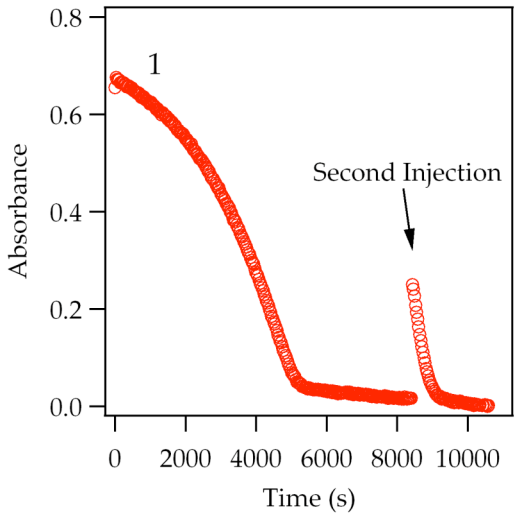

Figure 3.18. Representative plot showing absorbance of arene **1** vs time for the ortholithiation of **1** (0.010 M) with LDA (0.10 M) in THF (12.20 M) at –78 °C. After completion of the reaction a second aliquot of **1** (0.005) was injected.

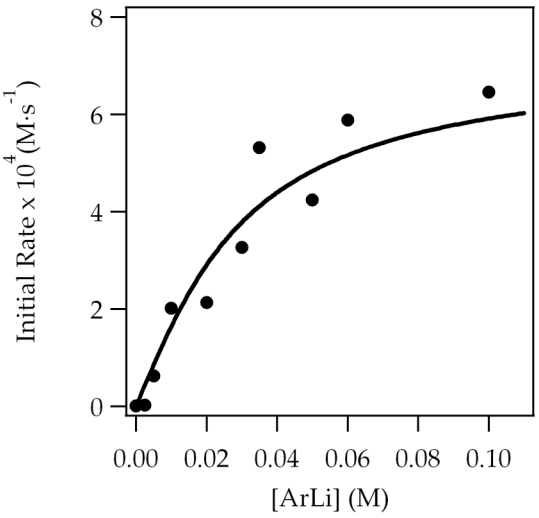

Figure 3.19. Plot of initial rate versus aryllithium [**2**-6-*d*] for the ortholithiation of **1** (0.075 M) by 0.10 M LDA in 12.2 M THF at –78 °C measured by IR spectroscopy. Aryllithium **2** was generated from **1**-6-*d* with one equivalent LDA at –40 °C prior to injection **1**. The curve depicts an unweighted least-squares fit a simple first-order saturation function: $-\Delta[\mathrm{ArH}]/\Delta t\,|_{t=0} = (k_1 k_2[\mathrm{A_2S_2}][\mathrm{ArH}])/(k_{-1} + k_2[\mathrm{ArH}])$ where [ArH] = 0.075 M, $[\mathrm{A_2S_2}]$ = 0.050 M. k_2 was constrained to the same value corresponding to lithium chloride saturation (see Figure 3.13). [k_1 = (0.18 $\pm$ 0.02); k_{-1} = (1.97 $\pm$ 0.01) x 10^9]

Mechanism of Equilibration. Conversion of ArLi **3** to **2** is observed over the course of the metalations and is readily effected through gentle warming. The equilibration is accelerated by added *i*-Pr_2NH, which was anticipated from rate studies of a reaction requiring an analogous equilibration.[5] To study the mechanism in detail, we generated less stable regioisomer **3** from **1** in 20:1 selectivity using LiTMP. Equilibration during the ortholithiation is negligible because the highly hindered *N,N,N′,N′*-tetramethylpiperidine byproduct does not mediate the exchange. Subsequent addition of *i*-Pr_2NH initiates the conversion of **3** to **2**. The decay of ArLi **3** fits a first-order function (Figure 3.20). The pseudo-first-order rate constants show a first-order dependence on *i*-Pr_2NH (Figure 3.21) and a zeroth-order dependence on THF. The idealized[26] rate law (eq 19) in conjunction with the assigned resting state of **3** as trisolvate **3a** is consistent with the generic mechanism in eq 20 and 21. The proton transfer is necessarily *partially* rate limiting in that the fleeting arene partitions to an ≈1:1 mixture of **2** and **3**. It is satisfying that transition structure $[(ArLi)(THF)_3(i\text{-}Pr_2NH)]^{‡}$ for the protonation of **2** is stoichiometrically the same as the transition structure $[(i\text{-}Pr_2NLi)(THF)_3(ArH)]^{‡}$ for metalation because the principle of microscopic reversibility[44] demands that they be the same transition structure.

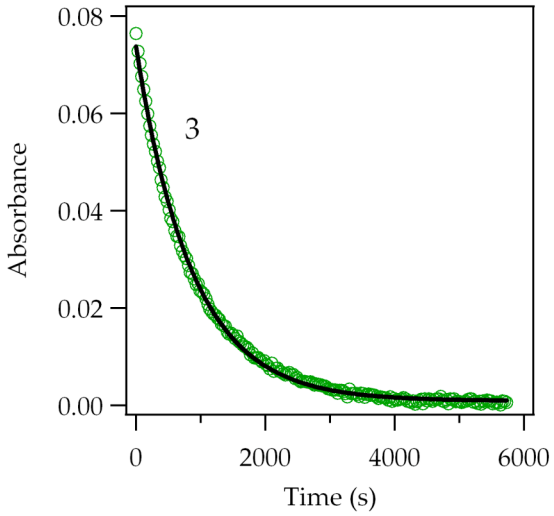

Figure 3.20. Representative plot of absorbance of **3** (0.050 M, 1154 cm^{-1}) versus time for isomerization by *i*-Pr_2NH (0.31 M) in 12.2 M THF at –78 °C. The curve depicts an unweighted least-squares fit to $y = Ae^{-kt}$.

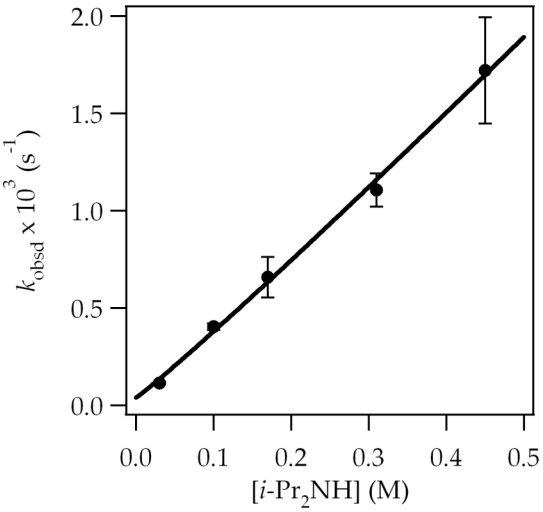

Figure 3.21. Plot of k_{obsd} vs [*i*-Pr_2NH] for the isomerization of **3** (0.050 M) to **2** in 12.2 M THF at –78 °C measured by IR spectrocopy. The curve depicts an unweighted least-squares fit to $y = k[i\text{-}Pr_2NH]^n + c$. [$k = (3.8 \pm 0.3) \times 10^{-3}$, $n = 1.1 \pm 0.1$, $c = (2 \pm 1) \times 10^{-5}$]

$$-d[\mathbf{3}]/dt = k'[\mathbf{3}][i\text{-}Pr_2NH][THF]^0 \quad (19)$$

$$\underset{(\mathbf{3})}{ArLiS_3} + i\text{-}Pr_2NH \longrightarrow [ArLiS_3(i\text{-}Pr_2NH)]^{\ddagger} \longrightarrow ArH + [AS_3] \quad (20)$$

$$ArH + [AS_3] \xrightarrow{fast} \mathbf{2} + \mathbf{3} \quad (21)$$

Mechanistic Hypothesis and Numeric Integrations. Rate and mechanistic studies were pieced together to form the mechanistic hypothesis shown in Scheme 1, which has been reformulated as Scheme 3 and described by the affiliated differential equations in eqs 22-28. (A_2* represents an activated LDA dimer whereas $ArLi_{(2)}$ and $ArLi_{(3)}$ denote aryllithiums **2** and **3**.) We have taken some liberties with the depiction of the model in Scheme 3 to optimize the visual presentation. Although the role of solvent has been elucidated for a number of steps, it is not germane to the numerical fits and has been omitted for clarity. We depict the critical autocatalytic step by affiliating k_2 and k_{-2} with autocatalyst ArLi (either **2** or **3**); it is described numerically in the differential equations based on the equilibrium

$$A_2 + ArLi \rightleftharpoons A + ArLi$$

ArLi generically stands for $ArLi_{(2)}$ and $ArLi_{(3)}$. Because $ArLi_{(3)}$ is 6-times less catalytically active than $ArLi_{(2)}$, its rate contribution is scaled accordingly in the curve fit. (We avoid treating the two autocatalysts separately.) The equilibria in Scheme 3 are unbalanced to minimize clutter. The differential equations, by contrast, are all fully balanced to provide a valid mathematical

description. Representative results from best-fit numerical integrations are illustrated in Figure 3.1.

Scheme 3

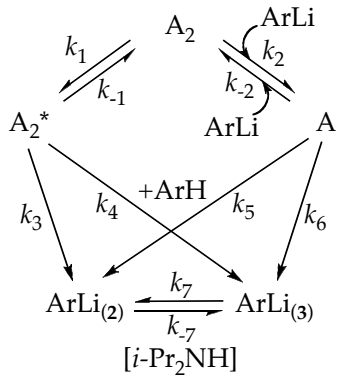

$$d[\mathrm{ArH}]/dt = -k_3[\mathrm{A_2}^*][\mathrm{ArH}] - k_4[\mathrm{A_2}^*][\mathrm{ArH}] - k_5[\mathrm{A}][\mathrm{ArH}] - k_6[\mathrm{A}][\mathrm{ArH}] \quad (22)$$

$$d[\mathrm{A_2}]/dt = -k_1[\mathrm{A_2}] + k_{-1}[\mathrm{A_2}^*] - k_2[\mathrm{A_2}]([\mathrm{ArLi_{(2)}}] + 1/6[\mathrm{ArLi_{(3)}}]) + k_{-2}[\mathrm{A}]^2 ([\mathrm{ArLi_{(2)}}] + 1/6[\mathrm{ArLi_{(3)}}]) + 1/2k_3[\mathrm{A_2}^*][\mathrm{ArH}] + 1/2k_4[\mathrm{A_2}^*][\mathrm{ArH}] \quad (23)$$

$$d[\mathrm{A}]/dt = 2k_2[\mathrm{A_2}]([\mathrm{ArLi_{(2)}}] + 1/6[\mathrm{ArLi_{(3)}}]) - 2k_{-2}[\mathrm{A}]^2([\mathrm{ArLi_{(2)}}] + 1/6[\mathrm{ArLi_{(3)}}]) - k_5[\mathrm{A}][\mathrm{ArH}] - k_6[\mathrm{A}][\mathrm{ArH}] \quad (24)$$

$$d[\mathrm{A_2}^*]/dt = k_1[\mathrm{A_2}] - k_{-1}[\mathrm{A_2}^*] - k_3[\mathrm{A_2}^*][\mathrm{ArH}] - k_4[\mathrm{A_2}^*][\mathrm{ArH}] \quad (25)$$

$$d[\mathrm{ArLi_{(2)}}]/dt = k_3[\mathrm{A_2}^*][\mathrm{ArH}] + k_5[\mathrm{A}][\mathrm{ArH}] - k_7[\mathrm{ArLi_{(2)}}][i\text{-}\mathrm{Pr_2NH}] + k_8[\mathrm{ArLi_{(3)}}][i\text{-}\mathrm{Pr_2NH}] \quad (26)$$

$$d[\mathrm{ArLi_{(3)}}]/dt = k_4[\mathrm{A_2}^*][\mathrm{ArH}] + k_6[\mathrm{A}][\mathrm{ArH}] + k_7[\mathrm{ArLi_{(2)}}][i\text{-}\mathrm{Pr_2NH}] - k_8[\mathrm{ArLi_{(3)}}][i\text{-}\mathrm{Pr_2NH}] \quad (27)$$

$$d[i\text{-}\mathrm{Pr_2NH}]/dt = k_3[\mathrm{A_2}^*][\mathrm{ArH}] + k_4[\mathrm{A_2}^*][\mathrm{ArH}] + k_5[\mathrm{A}][\mathrm{ArH}] + k_6[\mathrm{A}][\mathrm{ArH}] \quad (28)$$

Discussion

Summary. Metalation of arene **1** by LDA in THF at –78 °C (eq 1) joins a growing list of LDA-mediated reactions in which rates of aggregate exchanges dictate reactivity and in which autocatalysis and catalysis by exogenous lithium salts are prominent. The results can be understood in the context of Scheme 1 with amplification in Scheme 4. Under conditions in which lithium salt catalysis is absent—metalations of **1** at early conversion using rigorously LiCl-free LDA—the rate-limiting step involves LDA deaggregation via a disolvated-dimer-based transitions structure. DFT computations are consistent with dimer-based transition structure **9** to form open dimer **5** (eq 5). Open dimers are prominent in many of our discussions of LDA-mediated reactions.[23,27]

Scheme 4

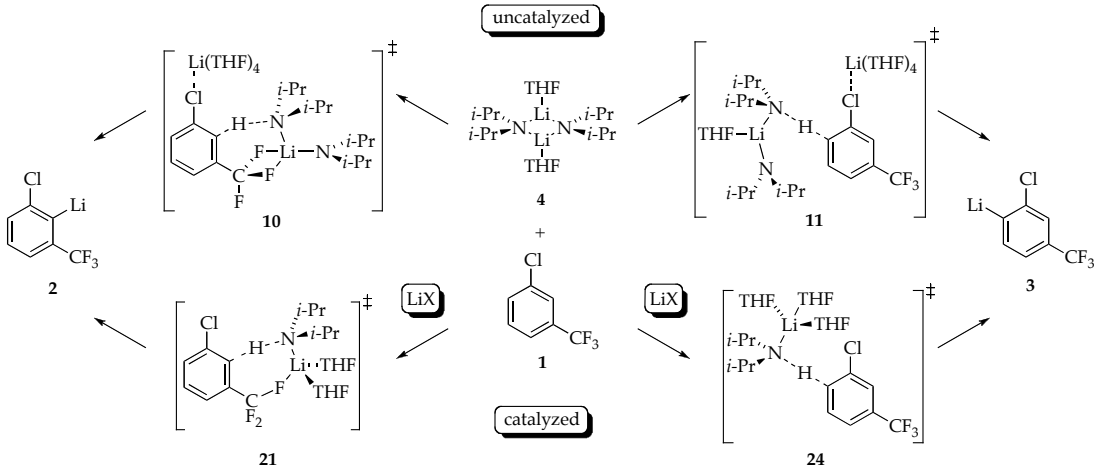

The post-rate-limiting proton transfers manifest a mechanistic bifurcation in which the critical metalation steps proceed via differentially solvated dimers. We seriously considered di- and trisolvated dimers, and DFT computations were supportive (Figure 3.11). Rate studies of **1**-2,6-d_2, however, implicated tetra- and pentasolvated dimers. To explain the high solvent orders we

turned to triple-ion-based transition structures **10** and **11**, which were shown to be computationally viable. The result is that the *rate* of metalation is THF independent but the *regioselectivity* shows a distinct THF dependence.

Lithium salts catalyze the deaggregation of LDA by diverting metalations through monomer-based pathways. LiCl catalysis, for example, causes large (100-fold) accelerations and affords concentration dependencies and isotope effects consistent with di- and trisolvated-monomer-based metalations and rate-limiting proton transfers. Computational studies support di- and trisolvated-monomer-based transition structures **21** and **24** (Scheme 4), but others are plausible as well (Figure 3.17).

In the absence of LiCl, autocatalysis by **2** and **3** that form during the reaction elicit acceleration as the reaction proceeds (Figure 3.1B). Autocatalysis appears to divert the reaction through the same monomer-based pathways as those shown in Scheme 4. This conclusion derives support from regioselectivities that suggest a commonality of intermediate(s) with LiCl-catalyzed metalation. Moreover, **2** is sixfold more autocatalytically active than is isomer **3**. Both pale in comparison with LiCl, however.

Diisopropylamine formed during the reaction slowly equilibrates regioisomers **2** and **3**. Such equilibrations are well known,[4,5] and participation by diisopropylamine has been documented.[4i,j] Detailed studies of such an equilibration appear to have been reported in only one instance.[5] The nearly quantitative formation of **2** at equilibrium restricted rate studies to the unidirectional conversion of **3** to **2**. The conversion is shown to be the microscopic reverse of the monomer-based metalation in Scheme 4, proceeding via trisolvated-monomer-based transition structure **24**. It is *not* a particularly bold assertion

that the protonation of **2** to give **1**, although kinetically invisible to us, involves the microscopic reverse of the metalation via disolvate **21**.

The independent pieces assemble to afford the mechanistic scenario summarized in Scheme 1. Additional insights about the role of solvation as well as steps that follow rate-limiting formation of open dimer **5** are not included in Scheme 1. The mechanism was reduced to the mathematically tractable model summarized in Scheme 3 and described by differential eqs 22-28. Best-fit numerical integrations are illustrated in Figure 3.1. On the one hand, the mechanistic model is not uniquely defined by the data; there are minor mechanistic variants that fit the data equally well. Nonetheless, the quality of the fits show *consistency* with the proposed mechanism.

Regioselectivities. The regioselectivities of the metalations are highly sensitive to reaction conditions as underscored in Figures 1 and 2. A number of underlying factors are at play. In the absence of salt-catalyzed deaggregation, the metalations show a modest bias toward **2** that approaches 7:1 selectivity at low THF concentration (Figure 3.8), a bias that derives from the dimer-based metalations in Scheme 4. Autocatalyzed or LiCl-catalyzed metalations promote the formation of **3**, more so at high THF concentrations, owing to the monomer-based pathways. As the reactions proceed to full conversion, however, the equilibration becomes dominant, obscuring the kinetic selectivity and affording exclusively **2** in the limit of long reaction times.

The kinetically controlled regioselectivity appears to be dominated by steric effects with contributions from an eclectic mix of directing effects. Solvating lithium cations can be sterically very demanding.[10] Not surprisingly, therefore, both dimer- and monomer-based metalations of **1** to form **2** require lower solvation numbers than do the analogous metalations to form regioiso-

mer **3**. Coordinating effects are also complex, however. Computations show viable transition structures with lithiums ligated by trifluoromethyl and chlorine and even with no ligation by substrate whatsoever. A natural tension arises between the tendency to maximally solvate lithium with strongly coordinating solvent and the tendency to coordinate the ortho-directing moieties.[45]

Peering Beyond Rate-Limiting Steps. A rate-limiting LDA deaggregation may seem to constitute an opaque wall that renders the structures of fleeting intermediates and the mechanisms of proton transfers invisible (Scheme 5). This is incorrect. Admittedly, intermolecular isotope effects—the influence of isotopic substitution on the reaction rate—will be unity if the proton transfer occurs after the rate-limiting step. By contrast, intramolecular isotope effects—isotope effects measured by a competition for abstraction between hydrogen and deuterium within the same molecule—will reflect the isotopic sensitivity of the post-rate-limiting metalation in the product distribution.[29] The isotope effects illustrated in Scheme 2 offer excellent examples: isotopically *insensitive* rates are accompanied by large isotopic biases in the regioselectivity. Purists might argue that these are not truly intramolecular isotope effects because they lack an explicit symmetry equivalence of the sites containing hydrogen-deuterium labels.[29] Nonetheless, solving eqs 6 and 7 affords the deconvoluted k_H/k_D values. (As an aside, it would be a mistake to get excited about isotope effects that exceed 30; they are common for ortholithiations using both LDA and *n*-BuLi.[46]

Scheme 5

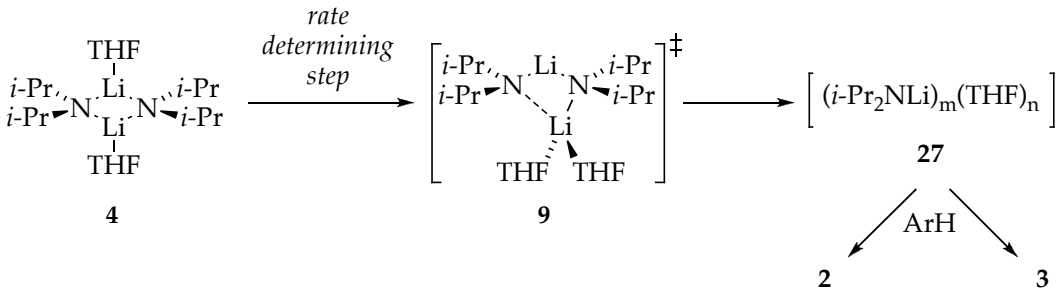

The concept behind intramolecular isotope effects also applies to competitive isotope effects in which two isotopically distinct substrates are competed. In this experiment, comparing **1** and **1**-2,6-d_2 (eq 9) reveals a large competitive isotope effect comparable to the values in Scheme 2, confirming that the post-rate-limiting metalation is isotopically sensitive. Of particular note, the accompanying biphasic kinetics (Figure 3.6), in which the less reactive isotopomer metalates only after the protio form has been consumed, is highly characteristic of a post-rate-limiting branch point.[3]

Details of post-rate-limiting metalations are also reflected in their condition-dependent regioselectivities. We found, for example, that the proportions of **2** and **3** are LDA concentration independent but show a distinct THF dependence—a preference for **3** over **2** at high THF concentration—that corresponds to transition structures differing by a single THF ligand. The relative stoichiometries of the transition structures leading to **2** and **3** are described by eq 10. Being unaware of formal nomenclature, we refer to eq 10 as a *relative rate law*. The information in eq 10 was critical for developing the mechanistic model describing the differentially solvated triple-ion-based transition structures in Scheme 4.

An altogether different strategy to observe post-rate-limiting behavior is simply to shift the rate limiting step. Let us slightly reformulate the mechanistic scenario as Scheme 6. In the most general terms, rate limitation is determined by the relative tendency of intermediate **27** to return to starting material versus proceed to product as described by the critical ratio $(k_2 + k_3)[\mathrm{ArH}]/k_{-1}$. Deaggregation is rate limiting when the metalation by **27** is fast relative to its return to the resting state of LDA—when $(k_2 + k_3)[\mathrm{ArH}]/k_{-1} >> 1$. By contrast, metalation becomes rate limiting when putative intermediate **27** is formed as a fully established equilibrium—$(k_2 + k_3)[\mathrm{ArH}]/k_{-1} << 1$.

Scheme 6

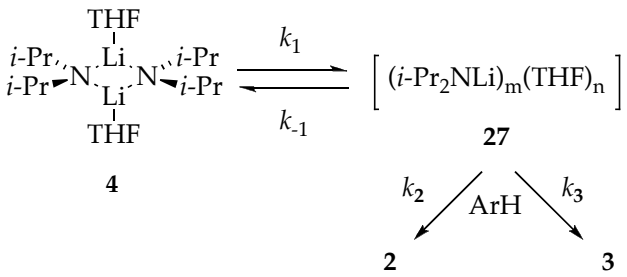

Thus, the metalation can be brought into view by (1) increasing the rate of reaggregation, or (2) decreasing the rate of metalation. As an example of the former, LiCl-catalyzed dimer–monomer exchange causes proton transfer to become rate limiting. LiCl-catalyzed reaggregation—the accelerated back reaction in eq 15—causes the rate limiting step to shift to proton transfer. Standard kinetic methods showed that the LiCl-catalyzed metalations proceed via di- and trisolvated-monomer-based transition structures described computationally as **21** and **24** (Scheme 4).

The alternative strategy of slowing the metalation is achieved using deuteration. As noted above, **1**-2,6-d_2 showed an isotope effect consistent with

a metalation that is partially rate limiting. Partially rate-limiting steps occur when the highest barriers are also of nearly equal energy.[32] Enzymology is rich with examples, presumably because evolutionary pressures relentlessly pushed down barriers in the quest for rate efficiency.[47] Through careful control of arene concentration, the critical $(k_2 + k_3)[\mathrm{ArD}]/k_{-1}$ (such that ArD is **1**-2,6-d_2) could be shifted to produce rate-limiting deaggregation at high ArD concentration and rate-limiting metalation at low concentrations. The two limiting behaviors are seen in the saturation behavior depicted in Figure 3.7. By determining the rate law under conditions of rate-limiting deuterium transfer, we were able to show what we had only suspected throughout the duration of this mechanistic study: metalations of **1** in the absence of salt catalysts occur via dimers, not via monomers. The high order in THF implicating tetra- or higher-solvated dimers caught us completely by surprise. Transition structures **10** and **11** based on triple ions[34] moved to center stage rather abruptly.

Mechanism of LiCl Catalysis. LiCl influences the reaction rate by catalyzing the conversion of LDA dimer **4** to highly reactive LDA monomer,[9] and the quantities of LiCl required to attain full equilibration are stunningly small (<1.0 mol %; 1.0 ppm). Such catalysis has been observed previously, but the second-order saturation behavior evident in Figure 3.13 (see inset) was not observed.[6] Our ongoing struggle to understand the details of LiCl catalysis are acute because LiCl exists exclusively as a mixture of mixed aggregates **7** and **8** at such low concentrations,[3,17] and we do not know the fate of **7** and **8** under the reaction conditions. Let us make the seemingly plausible supposition, however, that the second order derives from a catalyzed deaggregation involving a transition structure of stoichiometry $[(i\text{-}Pr_2NLi)_2(LiCl)_2]^{‡}$ (mixed tetramer).

We envision two fleeting intermediates that account for the catalysis and the accompanying second-order dependence on LiCl concentration. The first is ladder **28**, which has ample precedent in structural lithium amide chemistry.[48,49] The dissociation of LDA monomer from **28** (eq 29) has an energetic appeal because **28** would require dissociation of only one monomer rather than dissociating *two* high energy monomers from a dimer. The remaining three-rung ladder, **29**, could be loosely considered a leaving group.

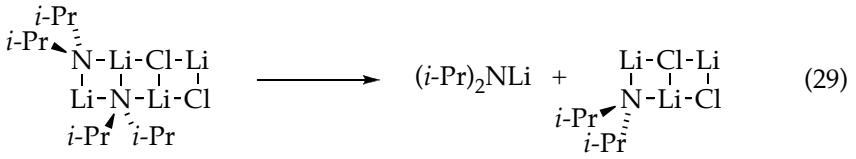

28 **29** (29)

Triple ions offer an even more provocative vehicle for deaggregating LDA dimer (Scheme 7). One could view chloride ion as simply a dipolar ligand, possibly akin to a sterically unhindered hexamethylphosphoramide analogue. Ongoing computational and spectroscopic studies show that LiCl catalyzes subunit exchanges in LDA dimers.[6] Computations archived in supporting information show **30** to be a minimum and transition structure **31** to be only 5 kcal/mol higher energy than **30**. Adduct **30** is structurally similar to a halide adduct tentatively assigned spectroscopically.[50] Moreover, the Li–Cl–Li cationic triple ion fragment is well precedented[51] and is computationally preferred relative to the simple lithium counterion.[52] (The heptasolvation of the $(THF)_3Li–Cl–Li(THF)_4$ counterion is odd, but it is the preferred form computationally.) X–Li–X anionic triple ion fragments analogous to **32** are also well documented.[34] The bridging THF in **31** is an especially provocative struc-

tural feature that finds precedence in the crystallographic literature,[53] and a possible role in deaggregation has been mentioned.[54]

Scheme 7

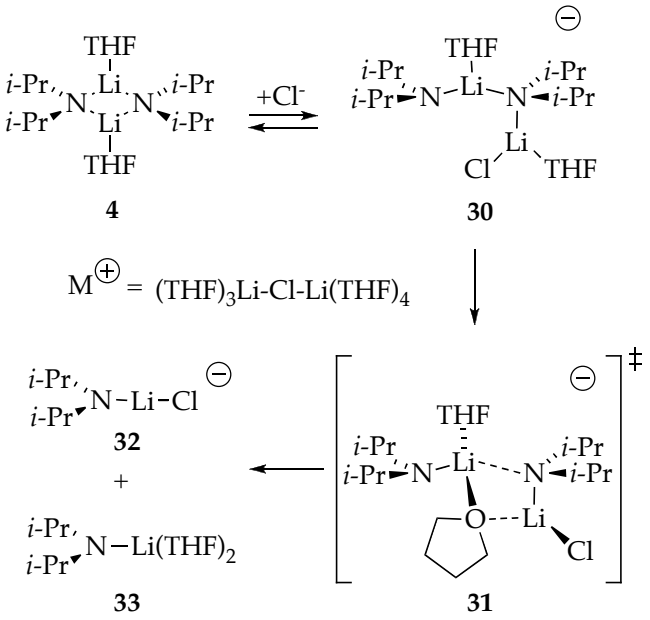

Autocatalysis. Catalysis by aryllithiums is also baffling. Previous studies of carbamate metalations[6a] offer a technically tractable system in which to study the condensation of an aryllithium with LDA dimer, revealing a rate-limiting transition structure of stoichiometry $[(i\text{-Pr}_2\text{NLi})_2(\text{ArLi})]^{‡}$ (mixed trimers). It appeared that reactive LDA-lithiated carbamate mixed dimers interceded. Thus, we cannot say for certain whether the two instances of aryllithium-derived autocatalysis are completely analogous. Moreover, the studies described herein, showing that **2** is sixfold more catalytically active than **3**, underscore the two critical prerequisites to observe autocatalysis: a reaction must be sensitive to catalysis, and a product (or by-product) must be a viable catalyst. Evidence is accruing that failures to observe autocatalysis may trace to one or both requirements. Although details of *how* aryllithiums catalyze

LDA deaggregation remain elusive, we are optimistic that mechanistic descriptions of salt-catalyzed LDA deaggregation will continue to evolve albeit obstinately.

Dimer- versus Monomer-Based Metalations in Review. Throughout this paper we have described uncatalyzed and catalyzed metalations as dimer- and monomer-based, respectively. One could imagine, however, being troubled by the seemingly parallel behavior of the two classes showing an oddly similar THF-dependent regioselectivity. The monomer-based metalations are, to the maximum extent possible within our hands, unassailable. Are we sure, however, that the uncatalyzed metalations proceed via a different intermediate? There is no question that highly solvated tetramers—implicated triple ions—give us pause.

We attribute the uncatalyzed metalations to dimer-based mechanisms based on four lines of reasoning: (1) although not really evidence per se, the computational studies show that the both dimer- and triple-ion-based metalations are highly competent; (2) the regioselectivities for LiCl- and ArLi-catalyzed reactions are indistinguishable, yet the regioselectivity for the uncatalyzed metalations is reversed and differs by an overall factor of >2; (3) competitive isotope effects for metalation to form both **2** and **3** are higher for uncatalyzed than LiCl-catalyzed metalation (although the differences are nearing our limits of distinction); (4) **1**-2,6-d_2 displays a nearly first-order LDA dependence under conditions of rate-limiting deuterium transfer. Point 4 seems to put to rest what had been a persistently circumstantial case for dimer-based metalation. We are unsure, however, how many structurally distinct aggregated forms can be intercepted by reactive substrates; this topic is being actively studied.

Conclusion

We conclude this paper in a somewhat unorthodox way by considering the consequences of the work from two very different perspectives. In the first, we address those interested in mechanistic organolithium chemistry. This viewpoint was most certainly the primary focus of the paper. In the second, we try to imagine what the ortholithiation of **1** might look like to a synthetic chemist peering through a largely empirical lens.

Mechanistic Organolithium Perspective. One could legitimately ask why LDA-mediated reactions in THF at –78 °C are proving so complex compared with their counterparts at elevated temperatures.[23] To answer this question, we offer the ensemble of aggregates en route to LDA monomer in Scheme 8. The structures are not just figments of our imaginations but rather computationally legitimate minima that will be described in the next paper of this series.[6] The computed barriers separating them are, with the exception of the first solvation step,[55] surprisingly high (>10 kcal/mol) relative to dimeric LDA in its resting state **4**, and the barriers are at notably comparable energies.

Scheme 8

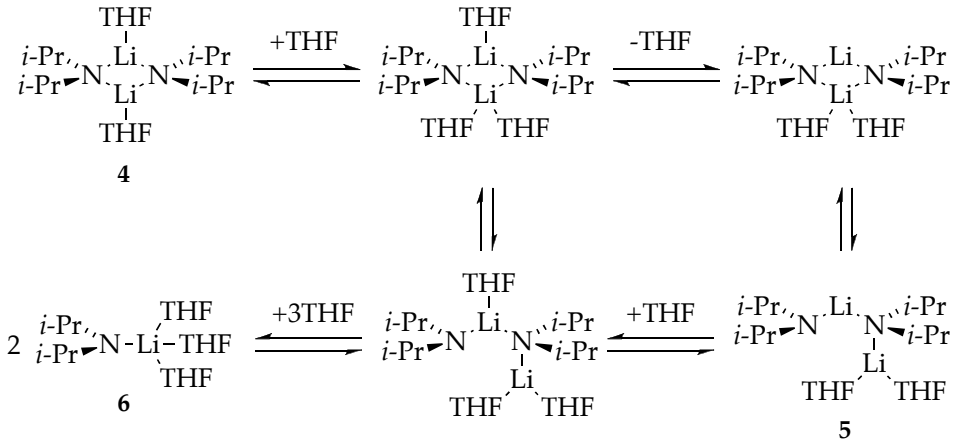

For substrates of relatively low reactivity the equilibria in Scheme 8 are rapid on the time scales of reactions with the substrate. All species are available to react, and 25 years of accumulated rate studies confirm that many do.[23] Now imagine monotonically increasing the reactivity of the substrate; instead of following the kinetics over shorter time scales, we simply reduce the reaction temperatures to monitor the reaction on convenient laboratory time scales. At some level of reactivity—at some temperature required to monitor reaction rates conveniently using standard analytical methods—the rates that substrates react with LDA aggregates become comparable to those at which the aggregates exchange. Through an odd twist of fate, this critical temperature for LDA/THF is at or near –78 °C.

Evidence is accruing that highly reactive substrates can intercept LDA at various stages of deaggregation, rendering aggregation events rate limiting and the conditions decidedly non-equilibrium. Simplistic thinking early on led us to surmise that a rate-limiting deaggregation would be substrate independent and that all substrates above some threshold of reactivity would react at precisely the same rate. We realized, however, that intercepting different fleeting intermediates would necessarily lead to substrate-dependent rates *even if the rates were independent of the substrate concentration*. Substrates also may participate in a critical deaggregation or complexation event but with the key reaction of interest (proton transfer, for example) occurring as a post-rate-limiting step. In this scenario, even substrate concentration dependencies could be affiliated with an aggregation-limiting transformation.

Of course, LiX-catalyzed deaggregation adds a further layer of complexity in the form of a hypersensitivity to LiCl contaminants and accelera-

tions elicited by autocatalysis. The appearance of autocatalysis and its virulence depend on both the catalytic efficacy of the lithium salt being formed *and* on a mechanistic advantage of the catalyzed deaggregation. Enolates, for example, are particularly poor autocatalysts[6] compared with aryllithiums, aryllithiums display autocatalysis that depends on the substituents on the arene (as in **2** and **3**), and the catalytic activity of all salts studied to date pale in comparison with LiCl.[6]

As we gather insights about LDA-mediated reactions under conditions in which aggregates are not at full equilibrium, we are constantly reevaluating published conclusions.[56] Case studies considered in isolation can be fully self-consistent whereas results from different case studies can seem to conflict. As a simple example, LiCl-catalyzed deaggregation is sensitive to the substrate, appearing as a first-order dependence on LiCl concentration in one case[3] and second-order dependencies in others.[6b-d] A fully self-consistent holistic view is beyond our gaze.

Synthetic Chemistry Perspective. Now consider the chemistry from the vantage point of a synthetic chemist who relies less on mechanism and more on empiricism and instinct. Schlosser and coworkers, for example, studied the metalation of **1**, but we can neither retrace their experience nor would we describe them as generic empiricists.[1] Let us assume the hypothetical synthetic chemist is you.

Imagine you metalate **1** and quench the intermediate aryllithiums to form regioisomeric products P_2 and P_3 (Scheme 9). You begin by generating LDA in situ from commercial *n*-BuLi and diisopropylamine and quench the reaction with an efficient electrophile (maybe benzaldehyde).[57] What you could not possibly know is that the metalation is dramatically accelerated by

the LiCl contaminant in the *n*-BuLi. What you *observe* is that the metalation is complete within only a minute or two, and a prompt quench affords regioisomers P_2 and P_3 in an uninspiring 2:1 ratio. As a consummate empiricist, you heed a previous assertion that THF *concentration* is a critical variable[23] and carry out the reaction using 2.0 M THF. Once again, what you would not know is that the regioselectivity under the auspices of LiCl catalysis derives from differentially solvated monomers. You would observe that using low THF concentration in a hydrocarbon cosolvent promotes the formation of regioisomer P_2 (up to 5:1 selectivity for **2**). You might also notice that the metalation is a little slower, requiring delayed quenching to obtain a good yield.

Beneath the surface of the kinetically controlled regioselectivities lurks a diisopropylamine-catalyzed equilibration of **2** and **3**. Such aryllithium equilibrations are well documented.[4,5] Varying the time allowed for the metalation by as little as 10 minutes is sufficient to alter the regioselectivity owing to this equilibration. Frustration caused by erratic selectivities is easy to imagine. You would likely discover, whether through intent or by chance, that the selectivity for **2** improves with protracted metalation at –78 °C or by warming (but below –20 °C to preclude benzyne formation).[58] Product P_2 derived from aryllithium **2** can be isolated in >40:1 selectivity. Diisopropylamine added at the outset would also accelerate the equilibration.

Scheme 9

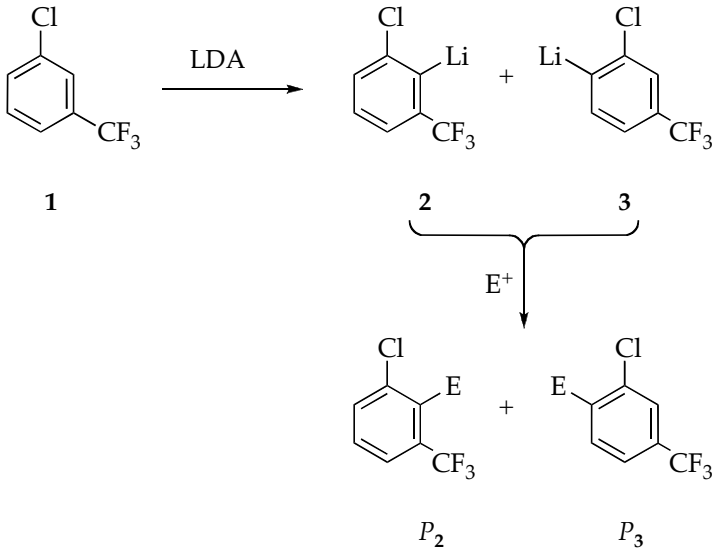

For the sake of discussion, let us assume that you require the more elusive product P_3. Of course, timely quenching with the electrophile is already established as essential to retain maximal (albeit disappointing) selectivity for P_3. You decide to try commercially available LDA as the THF solvate rather than prepare your LDA in situ. (It is certainly more convenient.) Alas, commercial LDA is often uncontaminated by catalytically active LiCl. (Halide-free commercial LDA lists ethyl benzene as a component.) Imagine your surprise when metalation and prompt quenching elevates the selectivity—the dimer-based metalations are, afterall, slightly more selective for **3**—but the isolated yield collapses to <10% owing to low conversion. If you are a pharmaceutical process chemist working on large scale, this result would be an unmitigated disaster. A graduate student might simply titrate the LDA, show that the reported titer is valid, and, once again, isolate a terrible yield of product. A third attempt with protracted stirring reveals that the metalation does occur but slowly. It is now obvious that commercial LDA offers little advantage because

the slight bias toward formation of **3** is eroded by the equilibration of **3** to **2** during protracted reaction times. You could have enjoyed the convenience and greater safety[59] of commercial LDA with the activity of LDA prepared in situ by adding a few mole percent LiCl generated using Et_3NHCl.[18]

By this time, your quest to prepare P_3 via **3** would have led to other bases. Success is achieved: whereas *n*-BuLi gives a 4:1 selectivity favoring **2**, either *sec*-BuLi or LiTMP affords **3** in 20:1 selectivity.[1,60] Possibly not realizing that the hindrance of the tetramethylpiperidine by-product completely suppresses amine-mediated equilibration, you invoke a model based on purely steric effects, declare victory, and move on to the next step. Concerns about the prohibitive cost of tetramethylpiperidine linger, but inspection of the synthesis[61] suggests that it is seriously mispriced.

Experimental Section

Reagents and Solvents. THF and hexane were distilled from blue or purple solutions containing sodium benzophenone ketyl. The hexane contained 1% tetraglyme to dissolve the ketyl. $Et_3N{\cdot}HCl$ was recrystallized from THF/2-propanol.[18] Literature procedures[62] were modified to prepare LDA as a LiCl- and ligand-free solid.[3] Solutions of LDA were titrated using a literature method.[63] Deuterated substrates were prepared as described below.

IR Spectroscopic Analyses. IR spectra were recorded using an in situ IR spectrometer fitted with a 30-bounce, silicon-tipped probe. The spectra were acquired in 16 scans at a gain of 1 and a resolution of 4 cm^{-1}. A representative reaction was carried out as follows: The IR probe was inserted through a nylon adapter and O-ring seal into an oven-dried, cylindrical flask fitted with a magnetic stir bar and a T-joint. The T-joint was capped by a septum for injec-

tions and a nitrogen line. After evacuation under full vacuum, heating, and flushing with nitrogen, the flask was charged with LDA (108 mg, 1.01 mmol) in THF and cooled in a dry ice–acetone bath prepared from fresh acetone. (Preparation of a the same solution but containing 5.0 mol% LiCl (0.005 M) requires the addition of a LiCl stock solution (0.50 mL) prepared from $Et_3N{\cdot}HCl$ (27.5 mg, 0.20 mmol) and LDA (25.0 mg, 0.23 mmol) in 2.0 mL THF.) After recording a background spectrum, we added arene **1** (0.76 mmol) with stirring. For the most rapid reactions, IR spectra were recorded every 3 s over the course of the reaction, monitoring the absorbance at 1325 cm^{-1}.

NMR Spectroscopic Analyses. All NMR tubes were prepared using stock solutions and sealed under partial vacuum. Standard ^{6}Li, ^{13}C, ^{15}N, and ^{19}F NMR spectra were recorded on a 500 MHz spectrometer at 73.57, 125.79, 50.66, and 470.35 MHz (respectively). The ^{6}Li, ^{13}C, and ^{15}N resonances are referenced to 0.30 M [^{6}Li]LiCl/MeOH at –90 °C (0.0 ppm), the CH_2O resonance of THF at –90 °C (67.57 ppm), and neat Me_2NEt at –90 °C (25.7 ppm), respectively.

2-Deutero-1-chloro-3-(trifluoromethyl)benzene (1-2-*d*). Using a method published by Knochel,[14] commercially available 2-bromo-1-chloro-3-(trifluoromethyl)benzene (4.86 g, 18.7 mmol, 1.0 equiv) was added via syringe to a 1.3 M THF solution of isopropylmagnesium chloride–LiCl complex (29.0 mL, 22.3 mmol, 1.2 equiv) in dry THF at 0 °C under argon. After the solution was stirred for 20 minutes, 10 equiv of deuterium oxide (3.7 mL) was added to the solution. The mixture was allowed to warm to room temperature, and the pH was adjusted to 1.0 with 2.0 M aqueous HCl solution to dissolve all salts. Organic and aqueous layers were separated, and the aqueous layer was washed with 3 x 20 mL Et_2O. The organic layers were combined, dried over granular Na_2SO_4 and distilled, and **1**-2-*d* was collected at 135 °C as a colorless

liquid (3.69g, 14.2 mmol) in 76% yield. ^{1}H NMR δ7.52 (m, 2H), 7.43 (m, 1H); ^{13}C NMR δ135.2 (s), 132.6 (q, $^{2}J_{C\text{-}F}$ = 33 Hz), 132.1 (s), 130.2 (s), 125.5 (tq, $^{2}J_{C\text{-}D}$ = 26 Hz, $^{2}J_{C\text{-}F}$ = 4.0 Hz), 123.8 (q, $^{2}J_{C\text{-}F}$ = 272 Hz), 123.4 (q, $^{2}J_{C\text{-}F}$ = 4.0 Hz).

4-Deutero-1-chloro-3-(trifluromethyl)benzene (1-6-*d*). The compound was synthesized as above from commercially available 4-bromo-1-chloro-3-(trifluoromethyl)benzene, and **1**-6-*d* was collected at 135 °C as a colorless liquid (3.9g, 15.0 mmol) in 80% yield. ^{1}H NMR δ7.62 (s, 1H), 7.52 (m, 1H), 7.43 (m, 1H); ^{13}C NMR δ135.0 (s), 132.5 (q, $^{2}J_{C\text{-}F}$ = 33 Hz), 131.9 (t, $^{2}J_{C\text{-}D}$ = 26 Hz), 130.2 (s), 125.8 (q, $^{2}J_{C\text{-}F}$ = 4.0 Hz), 123.6 (q, $^{2}J_{C\text{-}F}$ = 4.0 Hz), 123.5 (q, $^{2}J_{C\text{-}F}$ = 272 Hz).

2,6-Dideutero-1-chloro-3-(trifluoromethyl)benzene (1-2,6-d_2). A 2.5 M solution of *n*-BuLi in hexane (14.8 mL, 37.0 mmol) was added via syringe pump to a solution of dry diisopropylamine (5.7 mL, 40.7 mmol) and $Et_3N{\cdot}HCl$ (0.25 g, 1.85 mmol, 0.050 equiv) in 100 mL of dry THF at –78 °C under argon. After the solution was stirred for 20 minutes, **1** (5.0 mL, 37.0 mmol, 1 equiv) was added to the in situ generated LDA solution. After stirring at –78 °C for 30 min, *d*-MeOH (1.51 mL, 37.0 mmol, 1 equiv) was added. The process of sequential *n*-BuLi and *d*-MeOH addition of 1.0 equiv was repeated three more times. A final amount of *d*-MeOH (15 mL, 10 equiv) was added to fully quench the reaction. After the mixture was allowed to warm to room temperature, the pH was adjusted to 1.0 with 2.0 M HCl solution to dissolve all salts. Organic and aqueous layer were separated, and the aqueous layer was washed with 3 x 20 mL Et_2O. The organic layers were combined and dried over granular Na_2SO_4 and distilled, and **1**-2,6-d_2 was collected at 135 °C as a colorless liquid (3.74 g, 18.2 mmol) in 49% yield. ^{1}H NMR δ7.52 (m, 1H), 7.43 (m, 1H); ^{13}C NMR δ135.3 (s), 132.6 (q, $^{2}J_{C\text{-}F}$ = 33 Hz), 131.9 (t, $^{2}J_{C\text{-}D}$ = 26 Hz),

130.2 (s), 125.8 (tq, $^2J_{C\text{-}D}$ = 26 Hz, $^2J_{C\text{-}F}$ = 4.0 Hz), 123.8 (q, $^2J_{C\text{-}F}$ = 272 Hz), 123.5 (q, $^2J_{C\text{-}F}$ = 4.0 Hz).

Numeric Integrations. The time-dependent concentration plots obtained using IR spectroscopy are fit to a mechanistic model expressed by a set of differential equations. The curve-fitting operation minimizes chi-square in searching for the coefficient values (rate constants). The Levenberg–Marquardt algorithm[64] is used for the chi-square minimization and is a form of nonlinear, least-squares fitting. The fitting procedure implements numeric integration based on the backward differentiation formula[65] to solve the differential equations, yielding functions describing concentration versus time.

APPENDIX THREE

Chart 1

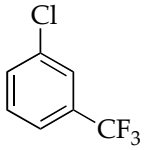

1

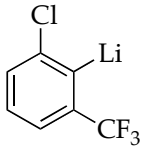

2

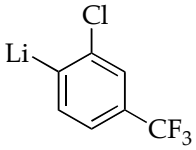

3

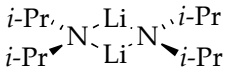

4

Part 1: Experimental Procedures:

Synthesis of deuterated 3-chlorobenzotrifluoride derivatives:

2-Deutero-1-chloro-3-(trifluoromethyl)benzene (1-2-*d*).
Using a method published by Knochel,[ref 14] commercially available 2-bromo-1-chloro-3-(trifluoromethyl)benzene (4.86 g, 18.7 mmol, 1.0 equiv) was added via syringe to a 1.3 M THF solution of isopropylmagnesium chloride–LiCl complex (29.0 mL, 22.3 mmol, 1.2 equiv) in dry THF at 0 °C under argon. After the solution was stirred for 20 minutes, 10 equiv of deuterium oxide (3.7 mL) was added to the solution. The mixture was allowed to warm to room temperature, and the pH was adjusted to 1.0 with 2.0 M aqueous HCl solution to dissolve all salts. Organic and aqueous layers were separated, and the aqueous layer was washed with 3 x 20 mL Et_2O. The organic layers were combined, dried over granular Na_2SO_4 and distilled, and **1**-2-*d* was collected at 135 °C as a colorless liquid (3.69g, 14.2 mmol) in 76% yield. ^{1}H NMR δ7.52 (m, 2H), 7.43 (m, 1H); ^{13}C NMR δ135.2 (s), 132.6 (q, $^2J_{C\text{-}F}$ = 33 Hz), 132.1 (s), 130.2 (s), 125.5 (tq, $^2J_{C\text{-}D}$ = 26 Hz, $^2J_{C\text{-}F}$ = 4.0 Hz), 123.8 (q, $^2J_{C\text{-}F}$ = 272 Hz), 123.4 (q, $^2J_{C\text{-}F}$ = 4.0 Hz).

4-Deutero-1-chloro-3-(trifluromethyl)benzene (1-6-*d*). The compound was synthesized as above from commercially available 4-bromo-1-chloro-3-(trifluoromethyl)benzene, and **1**-6-*d* was collected at 135 °C as a colorless liquid (3.9g, 15.0 mmol) in 80% yield. ^{1}H NMR δ7.62 (s, 1H), 7.52 (m, 1H), 7.43 (m, 1H); ^{13}C NMR δ135.0 (s), 132.5 (q, $^2J_{C\text{-}F}$ = 33 Hz), 131.9 (t, $^2J_{C\text{-}D}$ = 26 Hz), 130.2 (s), 125.8 (q, $^2J_{C\text{-}F}$ = 4.0 Hz), 123.6 (q, $^2J_{C\text{-}F}$ = 4.0 Hz), 123.5 (q, $^2J_{C\text{-}F}$ = 272 Hz).

2,6-Dideutero-1-chloro-3-(trifluoromethyl)benzene (1-2,6-d_2). A 2.5 M solution of *n*-BuLi in hexane (14.8 mL, 37.0 mmol) was added via syringe pump to a solution of dry diisopropylamine (5.7 mL, 40.7 mmol) and $Et_3N{\cdot}HCl$ (0.25 g, 1.85 mmol, 0.050 equiv) in 100 mL of dry THF at –78 °C under argon. After the solution was stirred for 20 minutes, **1** (5.0 mL, 37.0 mmol, 1 equiv) was added to the in situ generated LDA solution. After stirring at –78 °C for 30 min, *d*-MeOH (1.51 mL, 37.0 mmol, 1 equiv) was added. The process of sequential *n*-BuLi and *d*-MeOH addition of 1.0 equiv was repeated three more times. A final amount of *d*-MeOH (15 mL, 10 equiv) was added to fully quench the reaction. After the mixture was allowed to warm to room temperature, the pH was adjusted to 1.0 with 2.0 M HCl solution to dissolve all salts. Organic and aqueous layer were separated, and the aqueous layer was washed with 3 x 20 mL Et_2O. The organic layers were combined and dried over granular Na_2SO_4 and distilled, and **1**-2,6-d_2 was collected at 135 °C as a colorless liquid (3.74 g, 18.2 mmol) in 49% yield. ^{1}H NMR δ7.52 (m, 1H), 7.43 (m, 1H); ^{13}C NMR δ135.3 (s), 132.6 (q, $^2J_{C\text{-}F}$ = 33 Hz), 131.9 (t, $^2J_{C\text{-}D}$ = 26 Hz), 130.2 (s), 125.8 (tq, $^2J_{C\text{-}D}$ = 26 Hz, $^2J_{C\text{-}F}$ = 4.0 Hz), 123.8 (q, $^2J_{C\text{-}F}$ = 272 Hz), 123.5 (q, $^2J_{C\text{-}F}$ = 4.0 Hz).

Part 2: NMR Spectroscopic Studies

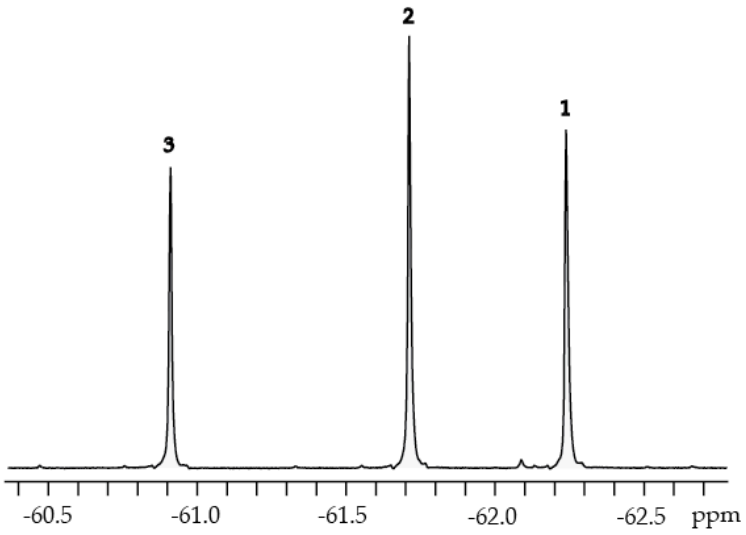

Figure A3.1. ^{19}F NMR spectrum of LDA (0.10 M) with **1** (0.050 M) in 12.2 M THF after aging for 10 minutes at - 90 °C: δ -60.90 (s), -61.70 (s), -62.23 (s).

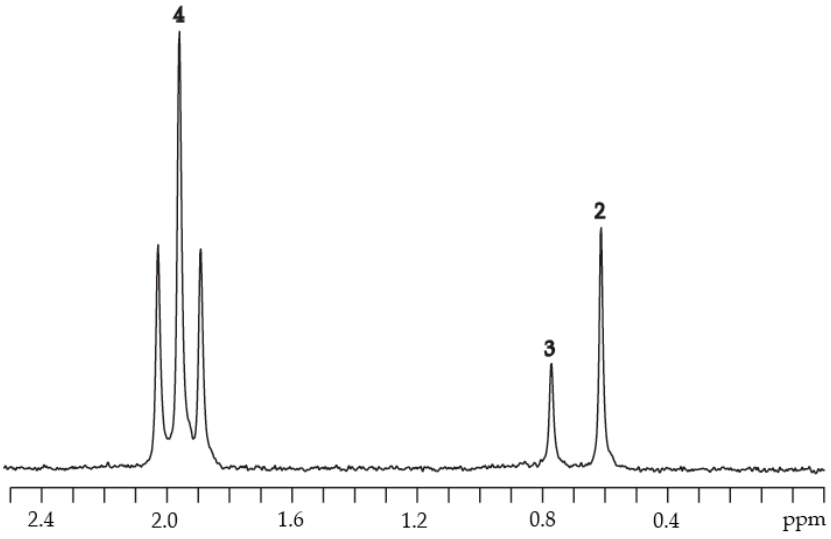

Figure A3.2. ^{6}Li NMR spectrum of [^{6}Li,^{15}N]LDA (0.10 M) and **1** (0.050 M) in neat THF recorded at -90 °C: δ 1.96 (t, $^{2}J_{\text{Li-N}}$ = 5.0 Hz), 0.77 (s), 0.61 (s).

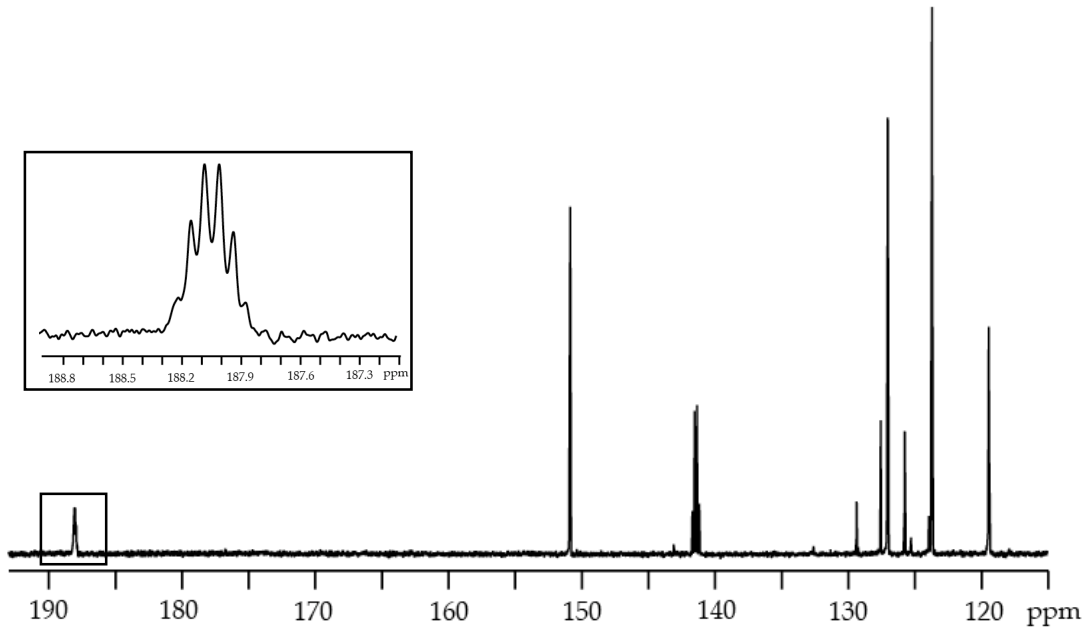

Figure A3.3. $^{13}C\{^{1}H\}$ NMR spectrum of **2** generated from **1** (0.20 M) with [^{6}Li]LDA (0.30 M) in 12.2 M THF-d_8 at -105 °C: δ188.05 (m), 150.87 (s), 141.45 (q, $^{2}J_{C\text{-}F}$ = 26.6 Hz), 127.04 (s), 126.67 (q, $^{2}J_{C\text{-}F}$ = 272.0 Hz), 123.73 (s), 119.45 (q, $^{2}J_{C\text{-}F}$ = 3.9 Hz).

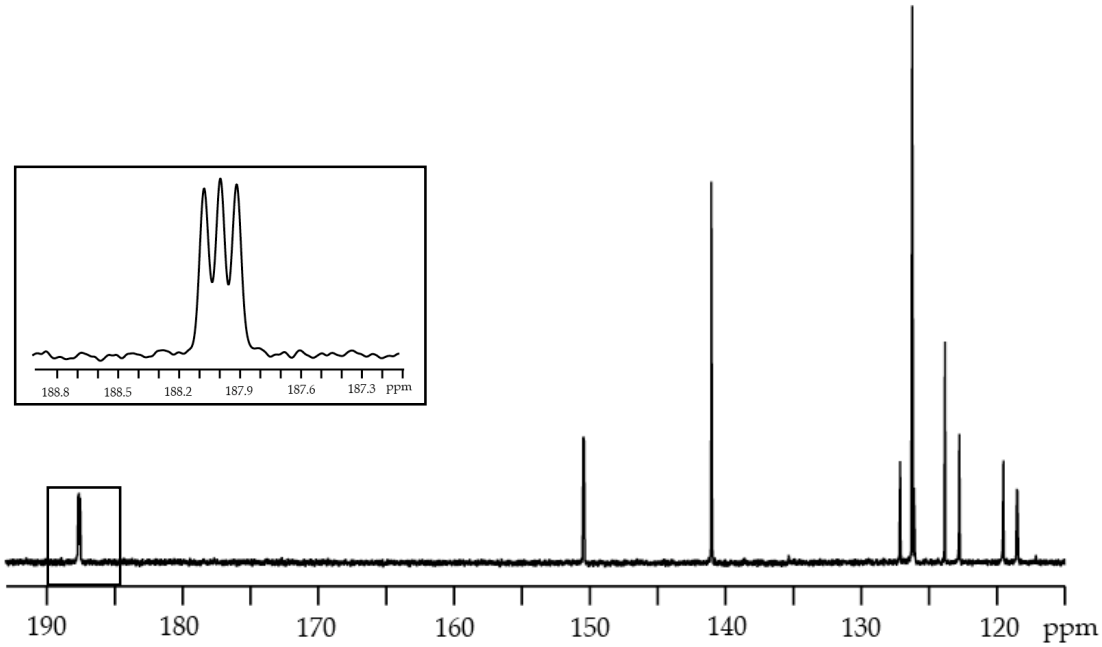

Figure A3.4. $^{13}C\{^{19}F\}$ NMR spectrum of **2** generated from **1** (0.20 M) with [^{6}Li]LDA (0.30 M) in 12.2 M THF-d_8 at -105 °C: δ188.05 (t, $^{2}J_{C\text{-}Li}$ = 11.4 Hz), 150.87 (dm, $^{2}J_{C\text{-}H}$ = 10.8 Hz), 141.45 (d, $^{2}J_{C\text{-}H}$ = 8.6 Hz), 127.04 (dd, $^{2}J_{C\text{-}H}$ = 78.7 Hz, $^{2}J_{C\text{-}H}$ = 6.5 Hz), 126.67 (m), 123.73 (d, $^{2}J_{C\text{-}H}$ = 159.0 Hz), 119.45 (dd, $^{2}J_{C\text{-}H}$ = 155.8 Hz, $^{2}J_{C\text{-}H}$ = 6.2 Hz).

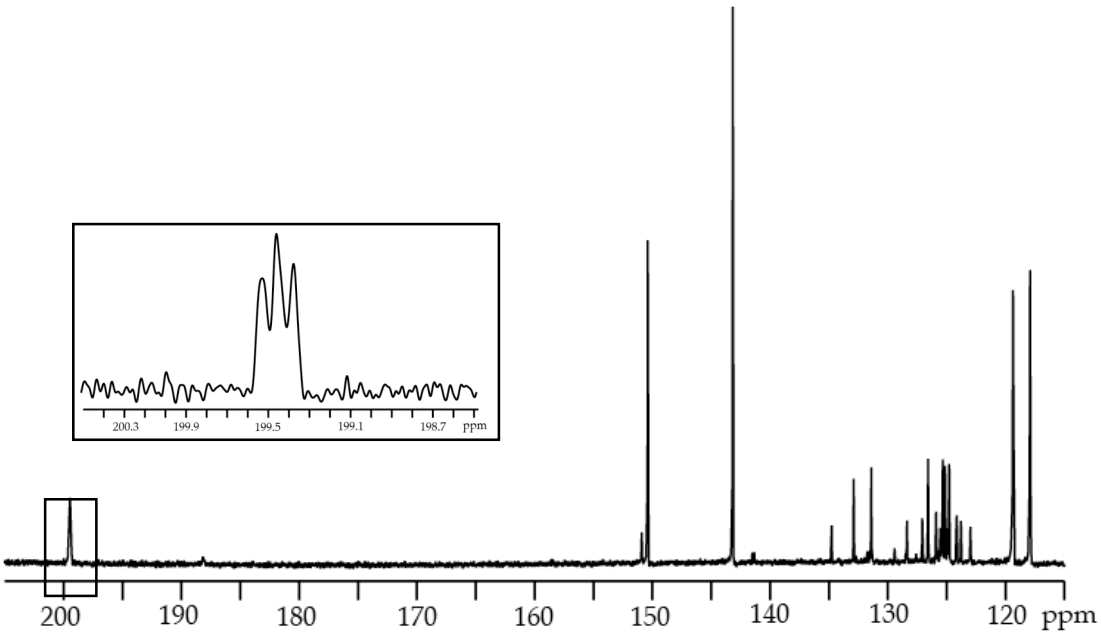

Figure A3.5. $^{13}C\{^{19}F\}$ NMR spectrum of **3** generated from **1** (0.15 M) with [^{6}Li,^{15}N]LiTMP (0.20 M) in 12.2 M THF-d_8 at -90 °C: δ199.52 (t, $^{2}J_{C\text{-}Li}$ = 11.0 Hz), 150.40 (s), 143.17 (s), 125.68 (q, $^{2}J_{C\text{-}F}$ = 270.5 Hz), 125.23 (q, $^{2}J_{C\text{-}F}$ = 30.8 Hz), 119.36 (m), 117.91 (m).

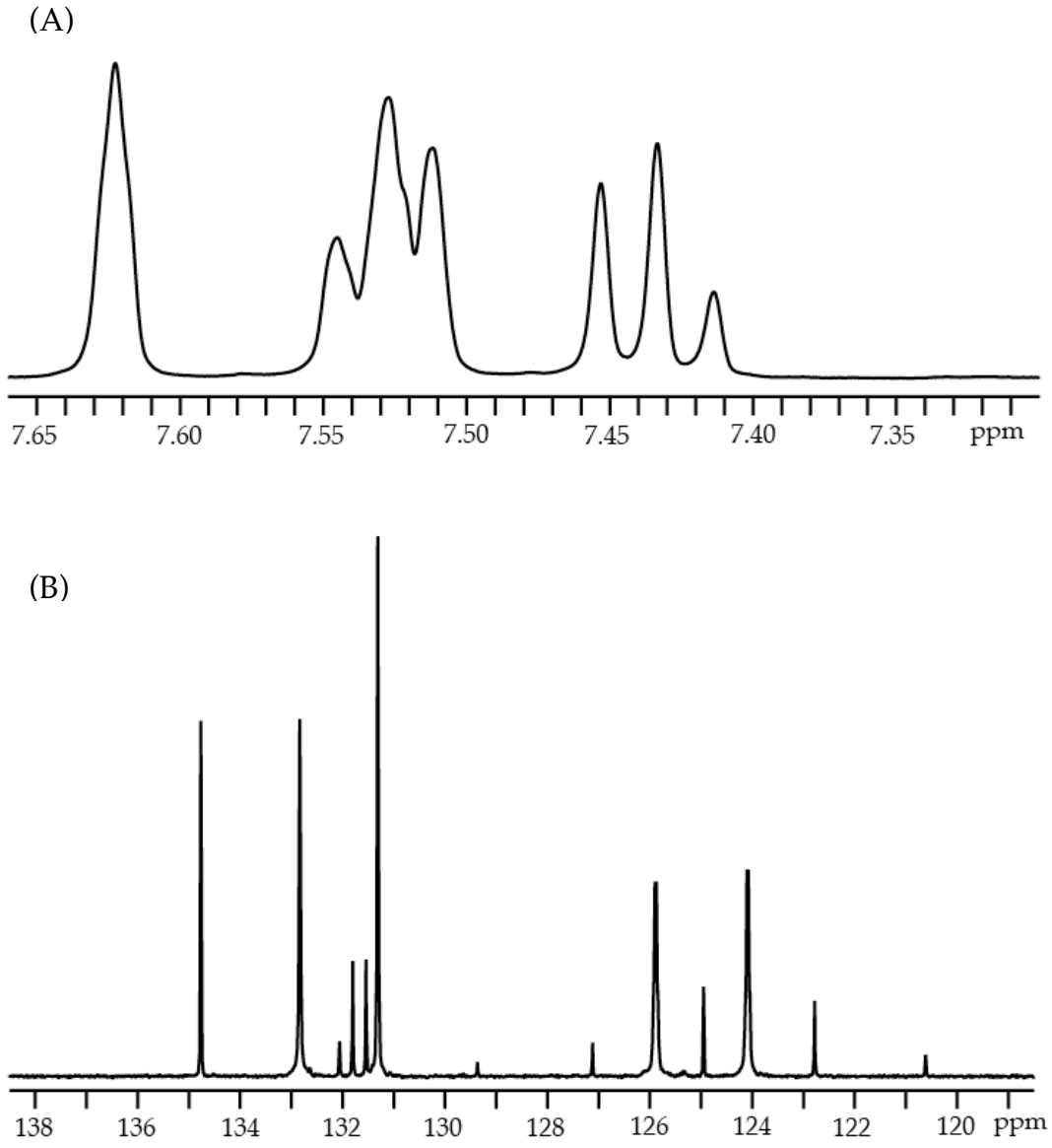

Figure A3.6. ^{1}H and ^{13}C NMR spectra of **1** in $CDCl_3$ and THF-d_8, respectively: (A) ^{1}H NMR δ7.62 (s, 1H), 7.52 (m, 2H), 7.43 (m, 1H); (B) ^{13}C NMR δ134.8 (s), 132.8 (s), 131.7 (q, $^{2}J_{C\text{-}F}$ = 33 Hz), 131.3 (s), 125.9 (q, $^{2}J_{C\text{-}F}$ = 3.8 Hz), 124.1 (q, $^{2}J_{C\text{-}F}$ = 2.5 Hz), 123.9 (q, $^{2}J_{C\text{-}F}$ = 273 Hz).

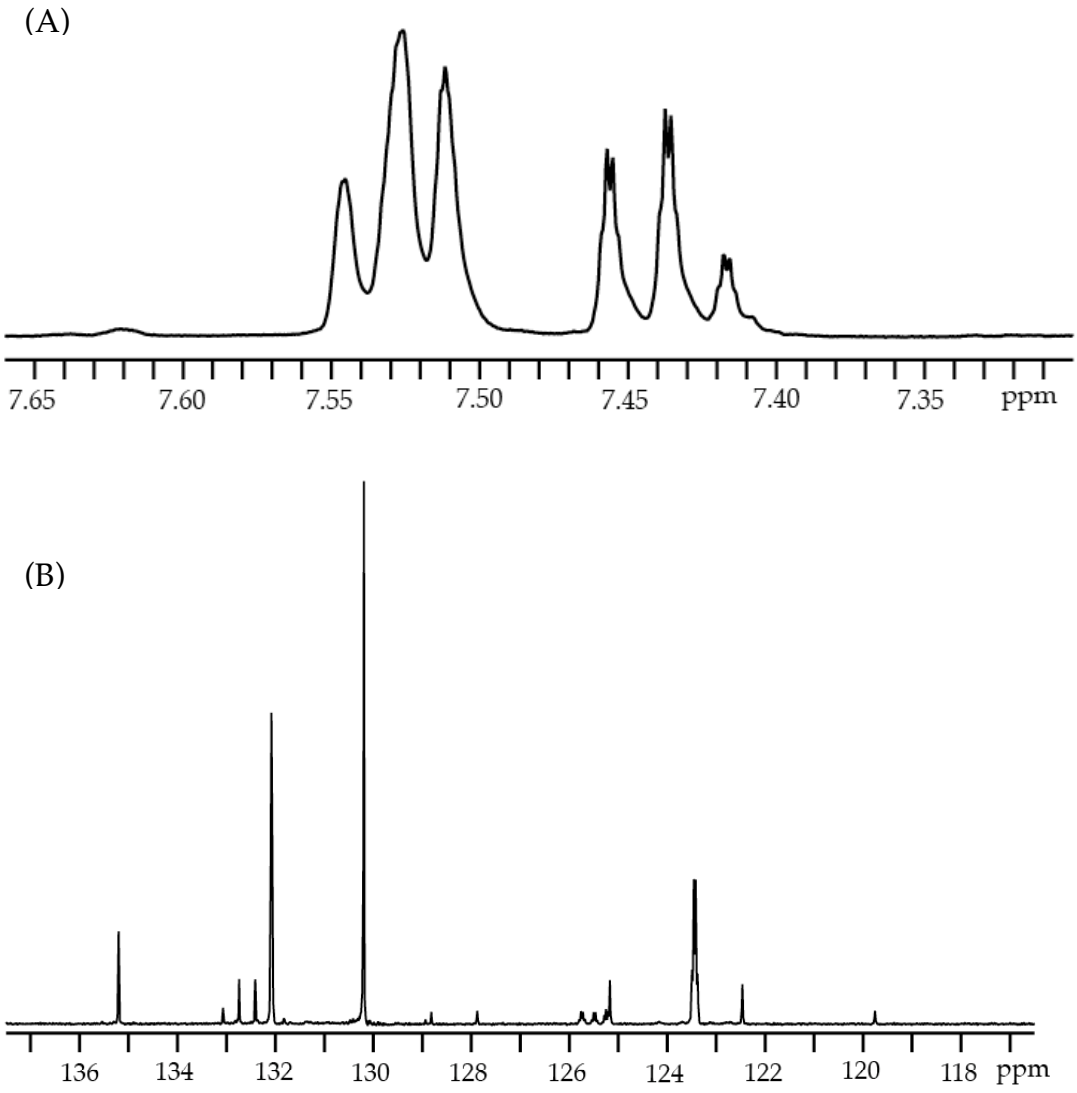

Figure A3.7. ^{1}H and ^{13}C NMR spectra of **1**-2-d_1 in $CDCl_3$. The compound was prepared as described in Part 1 using the Grignard method: (A) ^{1}H NMR δ7.52 (m, 2H), 7.43 (m, 1H); (B) ^{13}C NMR δ135.2 (s), 132.6 (q, $^{2}J_{C\text{-}F}$ = 33 Hz), 132.1 (s), 130.2 (s), 125.5 (tq, $^{2}J_{C\text{-}D}$ = 26 Hz, $^{2}J_{C\text{-}F}$ = 4.0 Hz), 123.8 (q, $^{2}J_{C\text{-}F}$ = 272 Hz), 123.4 (q, $^{2}J_{C\text{-}F}$ = 4.0 Hz).

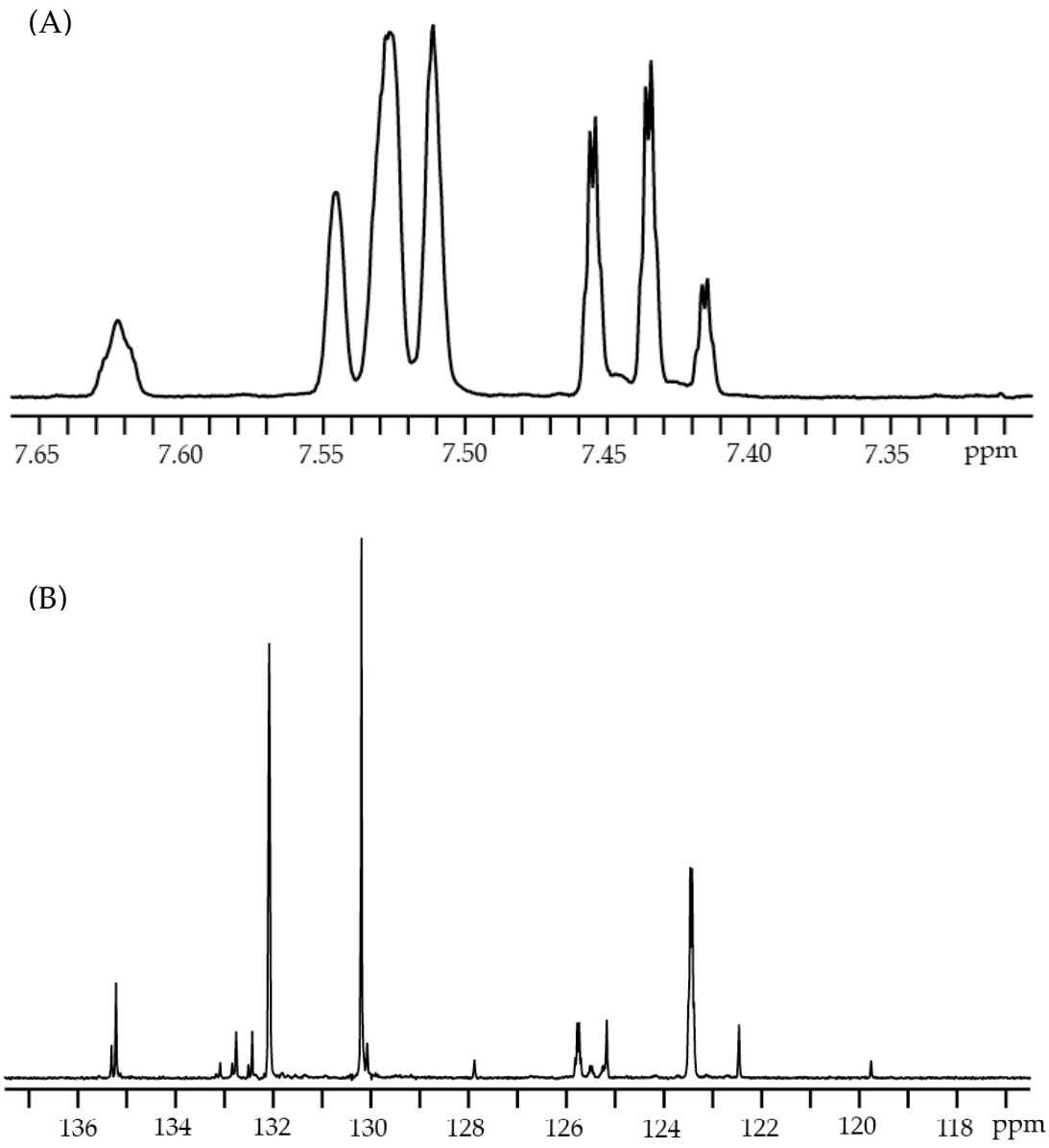

Figure A3.8. ^{1}H and ^{13}C NMR spectra of **1**-2-d_1 in $CDCl_3$. The compound was prepared as described in Part 1 using an LDA-mediated ortholithiation: (A) ^{1}H NMR δ7.62 (s, 0.2 H*), 7.52 (m, 2H), 7.43 (m, 1H); (B) ^{13}C NMR δ135.2 (s), 135.2 (s)*, 132.6 (q, $^{2}J_{C\text{-}F}$ = 33 Hz), 132.1 (s), 130.2 (s), 125.5 (tq, $^{2}J_{C\text{-}D}$ = 26 Hz, $^{2}J_{C\text{-}F}$ = 4.0 Hz), 125.8 (q, $^{2}J_{C\text{-}F}$ = 4.0 Hz)*, 123.8 (q, $^{2}J_{C\text{-}F}$ = 272 Hz), 123.4 (q, $^{2}J_{C\text{-}F}$ = 4.0 Hz).

*proton resonance at position 2 of remaining **1**.

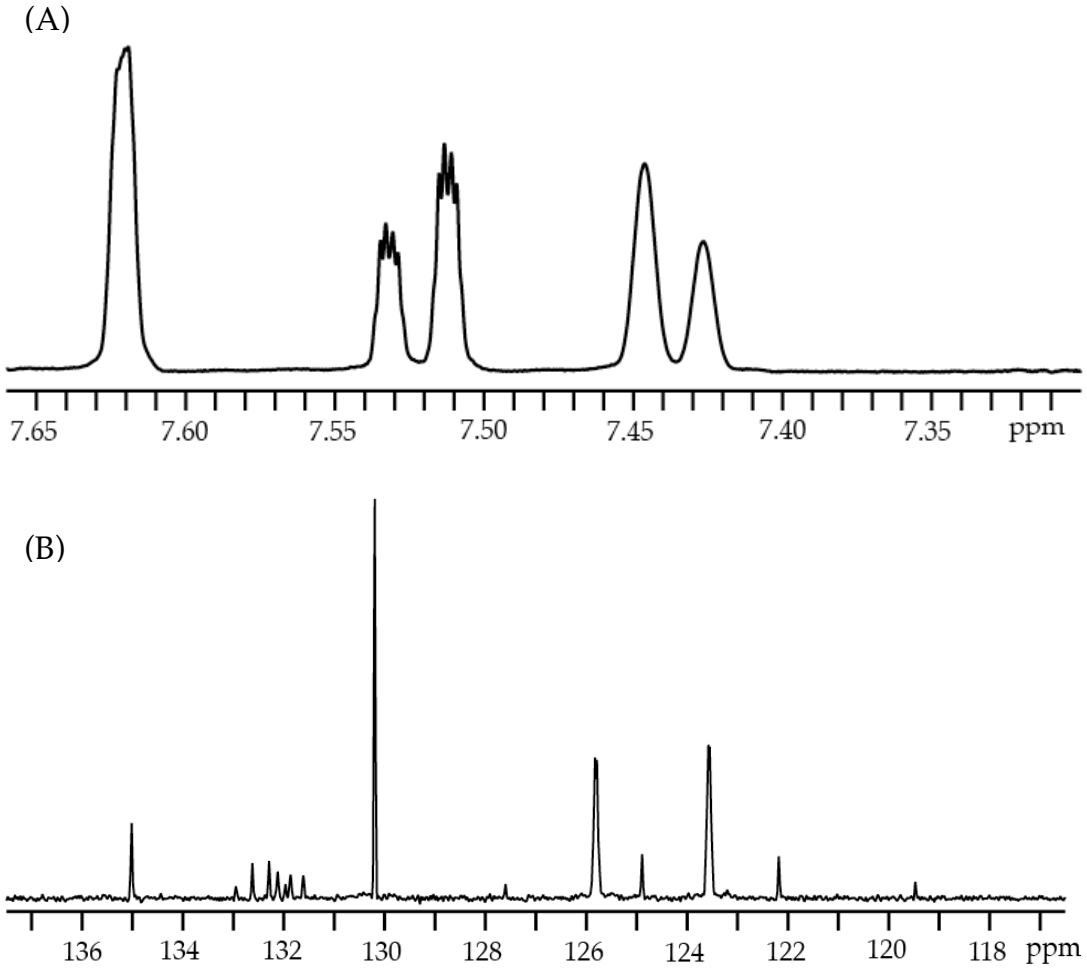

Figure A3.9. ^{1}H and ^{13}C NMR spectra of **1**-6-d_1 in $CDCl_3$. The compound was prepared as described in Part 1 using the Grignard method: (A) ^{1}H NMR δ7.62 (s, 1H), 7.52 (m, 1H), 7.43 (m, 1H); (B) ^{13}C NMR δ135.0 (s), 132.5 (q, $^{2}J_{C\text{-}F}$ = 33 Hz), 131.9 (t, $^{2}J_{C\text{-}D}$ = 26 Hz), 130.2 (s), 125.8 (q, $^{2}J_{C\text{-}F}$ = 4.0 Hz), 123.6 (q, $^{2}J_{C\text{-}F}$ = 4.0 Hz), 123.5 (q, $^{2}J_{C\text{-}F}$ = 272 Hz).

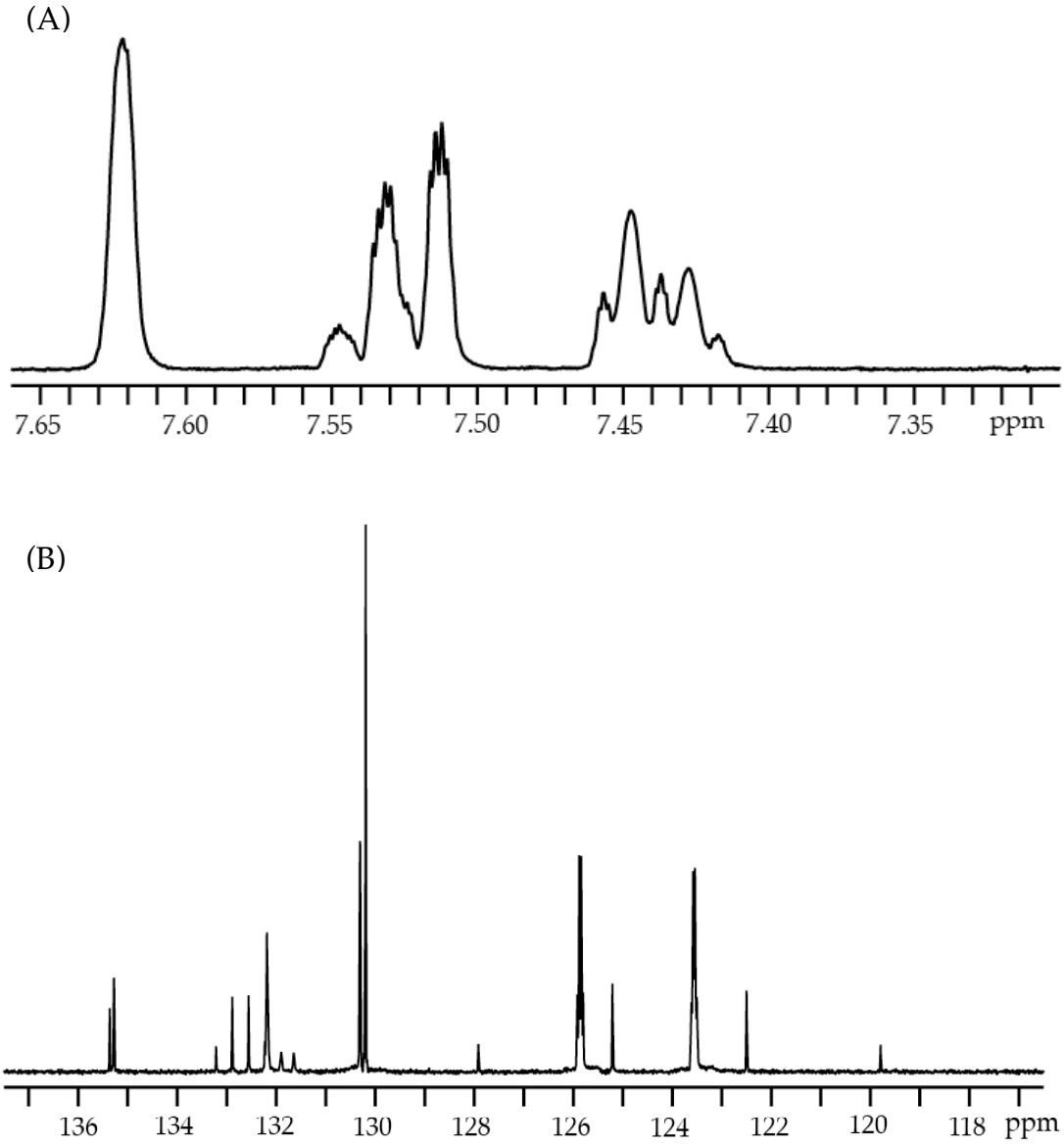

Figure A3.10. ^{1}H and ^{13}C NMR spectra of **1**-6-d_1 in $CDCl_3$. The compound was prepared as described in Part 1 using LiTMP: (A) ^{1}H NMR δ7.62 (s, 1H), 7.52 (m, 2H), 7.43 (m, 1H)*; (B) ^{13}C NMR δ135.4 (s), 135.3 (s)*, 132.7 (q, $^{2}J_{C\text{-}F}$ = 33 Hz), 132.1 (s)*, 131.9 (t, $^{2}J_{C\text{-}D}$ = 26 Hz), 130.3 (s), 130.2 (s)*, 125.9 (q, $^{2}J_{C\text{-}F}$ = 4.0 Hz), 123.9 (q, $^{2}J_{C\text{-}F}$ = 272 Hz), 123.6 (q, $^{2}J_{C\text{-}F}$ = 4.0 Hz).

* additional resonances are due to **1**-2-*d*.

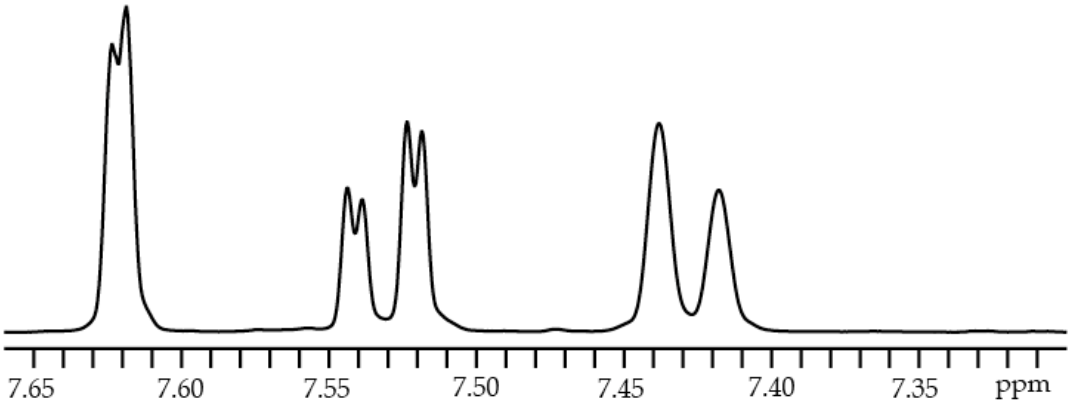

Figure A3.11. ^{1}H NMR spectra of **1-**6-d_1 in $CDCl_3$. The compound was prepared as described in Part 1 using the Grignard method: ^{1}H NMR δ7.62 (s, 1H), 7.52 (m, 1H), 7.43 (m, 1H).

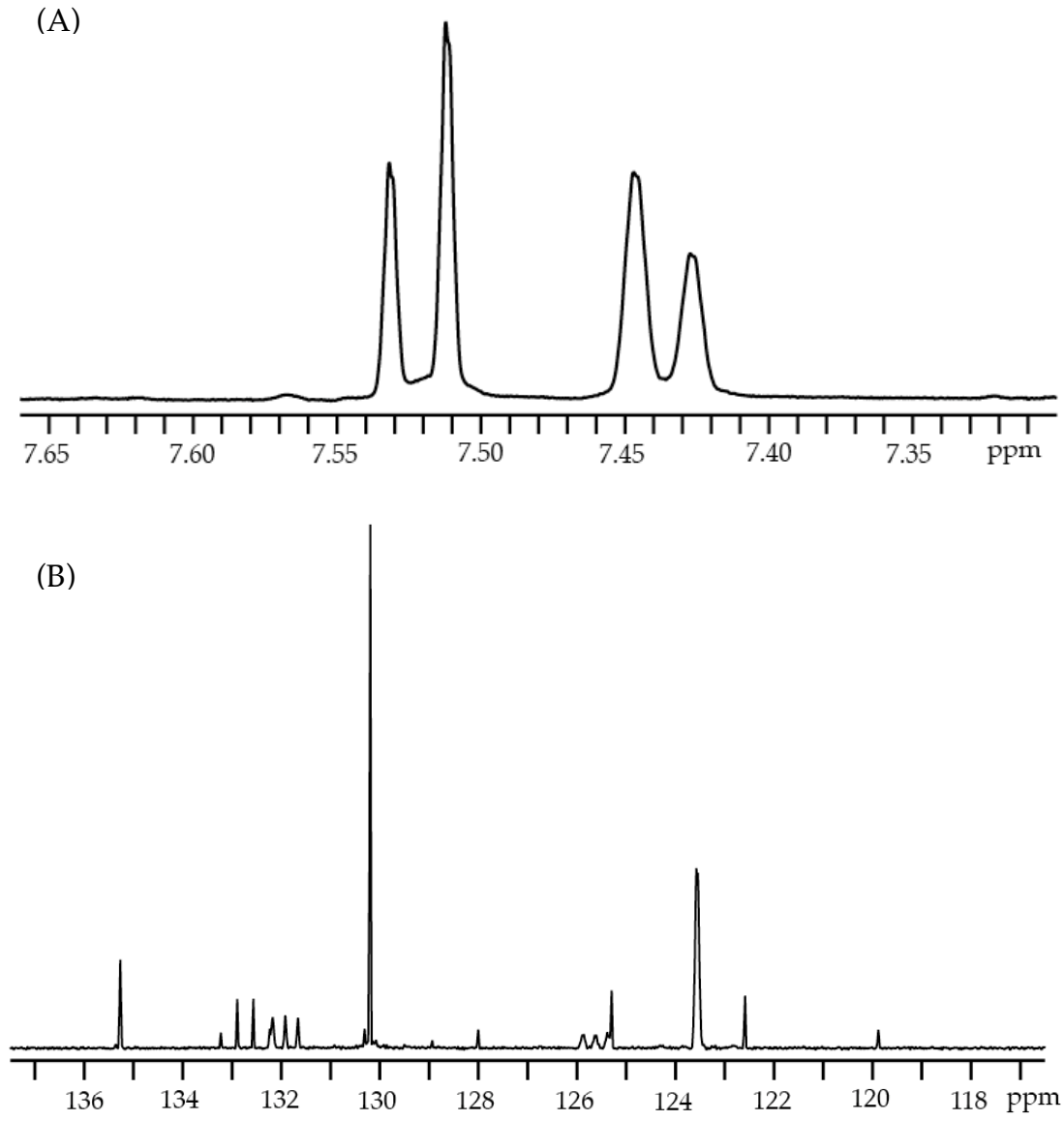

Figure A3.12. ^{1}H and ^{13}C NMR spectra of **1**-2,6-d_2 in $CDCl_3$. The compound was prepared as described in Part 1: (A) ^{1}H NMR δ7.52 (m, 1H), 7.43 (m, 1H); (B) ^{13}C NMR δ135.3 (s), 132.6 (q, $^{2}J_{C\text{-}F}$ = 33 Hz), 131.9 (t, $^{2}J_{C\text{-}D}$ = 26 Hz), 130.2 (s), 125.8 (tq, $^{2}J_{C\text{-}D}$ = 26 Hz, $^{2}J_{C\text{-}F}$ = 4.0 Hz), 123.8 (q, $^{2}J_{C\text{-}F}$ = 272 Hz), 123.5 (q, $^{2}J_{C\text{-}F}$ = 4.0 Hz).

Part 3: Rate Studies

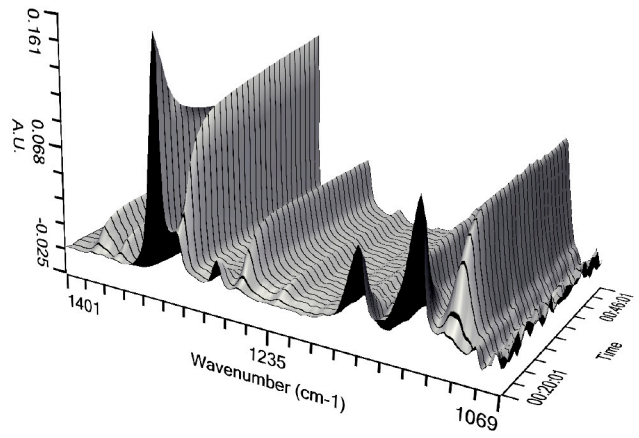

Figure A3.13. Representative in situ IR trace for the ortholithiation of **1** (0.050 M) by LDA (0.10 M) in THF at -78 °C. Compounds **1**, **2**, and **3** exhibit the IR absorptions listed for the four possible isotopomers. The IR spectra were deconvoluted using ConcIRT®. Deconvolution of the product absorbances was not possible.

1: 1428 cm^{-1}, 1325 cm^{-1}, 1276 cm^{-1}, 1171 cm^{-1}, 1131 cm^{-1}
2: 1378 cm^{-1}, 1306 cm^{-1}, 1260 cm^{-1}, 1140 cm^{-1}, 1104 cm^{-1}
3: 1378 cm^{-1}, 1324 cm^{-1}, 1258 cm^{-1}, 1154 cm^{-1}, 1109 cm^{-1}

1-2-d_1: 1325 cm^{-1}, 1215 cm^{-1}, 1170 cm^{-1}, 1132 cm^{-1}
2+3: 1322 cm^{-1}, 1245 cm^{-1}, 1176 cm^{-1}, 1140 cm^{-1}, 1108 cm^{-1}

1-6-d_1: 1401 cm^{-1}, 1326 cm^{-1}, 1173 cm^{-1}, 1131 cm^{-1}
2+3: 1378cm^{-1}, 1329 cm^{-1}, 1299 cm^{-1}, 1260 cm^{-1}, 1146 cm^{-1}, 1121 cm^{-1}, 1104 cm^{-1}

1-2,6-d_2: 1383 cm^{-1}, 1324 cm^{-1}, 1181 cm^{-1}, 1161 cm^{-1}, 1131 cm^{-1}
2+3: 1322 cm^{-1}, 1297 cm^{-1}, 1260 cm^{-1}, 1245 cm^{-1}, 1212 cm^{-1}, 1176 cm^{-1} ,1108 cm^{-1}

Figure A3.14. Time-dependent concentrations measured by ^{19}F NMR spectroscopy using 0.05 M **4** (0.10 N) and **1** in 12.2 M THF at -65 °C. Legend: ArH = **1**; A_2 = LDA dimer **4**; $ArLi_{(2)}$ = **2**; $ArLi_{(2)}$ = **3**. The curves represent a parametric fit to eqs 22-28 in the manuscript. (A) 0.005 M **1**; (B) 0.010 M **1**. (C) 0.020 M **1**. (D) 0.050 M **1**.

Figure A3.14 (continued).

(A)

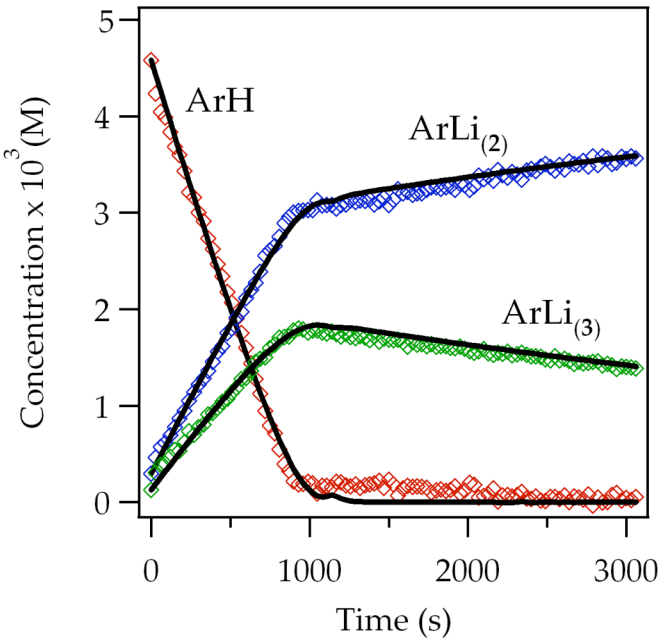

$k_1 = 0.000115 \pm 1e\text{-}006$
$k_{-1} = 1000k_1$
$k_2 = 0$
$k_{-2} = 0$
$k_3 = 220 \pm 20$
$k_4 = 150 \pm 13$
$k_5 = 0$
$k_6 = 0$
$k_7 = 0.0010 \pm 0.0008$
$k_{-7} = 0.30 \pm 0.002$

To simplify the curve fit, it was assumed that the effect of autocatalysis are negligible and the affiliated rate constants (k_2, k_{-2}, k_5, k_6) were set to zero.

Figure A3.14 (continued).

(B)

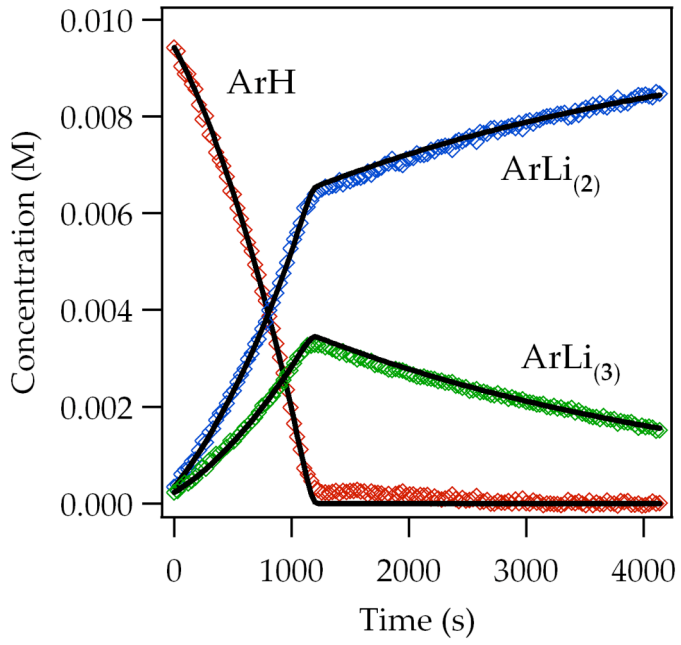

$k_1 = 0.00022 \pm 3e\text{-}005$
$k_{-1} = 1000k_1$
$k_2 = 0.020 \pm 0.0004$
$k_{-2} = 1000k_2$
$k_3 = 9.0 \pm 0.9$
$k_4 = 4.2 \pm 0.5$
$k_5 = 152 \pm 50$
$k_6 = 105 \pm 30$
$k_7 = 0.0001 \pm 0.0004$
$k_{-7} = 0.028 \pm 0.001$

Figure A3.14 (continued).

(C)

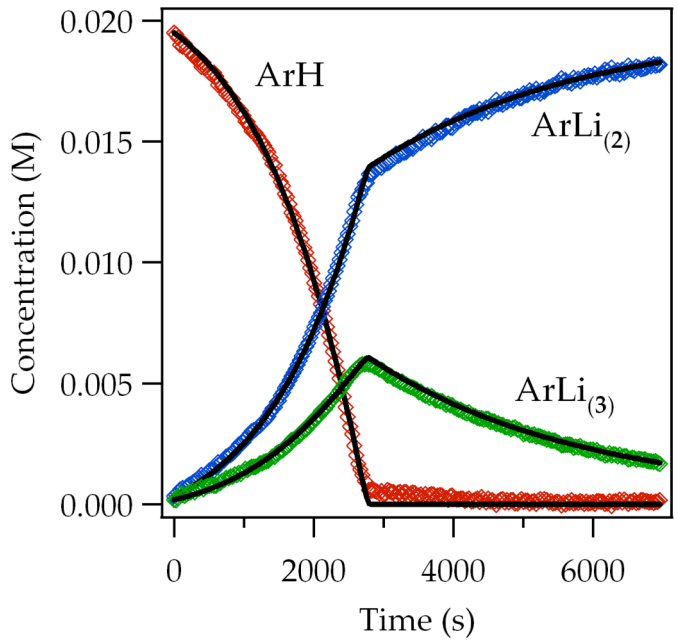

$k_1 = 3.97\text{e-}005 \pm 1\text{e-}006$
$k_{-1} = 1000k_1$
$k_2 = 0.0123 \pm 7\text{e-}005$
$k_{-2} = 1000k_2$
$k_3 = 9.9 \pm 0.9$
$k_4 = 4.5 \pm 0.4$
$k_5 = 150 \pm 20$
$k_6 = 92 \pm 9$
$k_7 = 0.00021 \pm 2\text{e-}005$
$k_{-7} = 0.016 \pm 0.0002$

Figure A3.14 (continued).

(D)

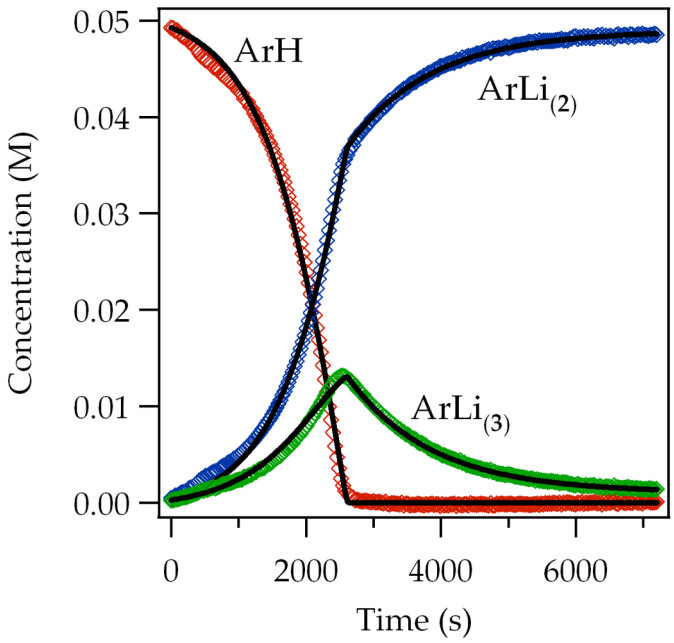

$k_1 = 3.6\text{e-}005 \pm 1\text{e-}006$
$k_{-1} = 1000k_1$
$k_2 = 0.023 \pm 9\text{e-}005$
$k_{-2} = 1000k_2$
$k_3 = 8.4 \pm 1$
$k_4 = 6.1 \pm 0.05$
$k_5 = 160 \pm 4$
$k_6 = 90 \pm 2$
$k_7 = 0.00033 \pm 2\text{e-}005$
$k_{-7} = 0.016 \pm 0.0003$

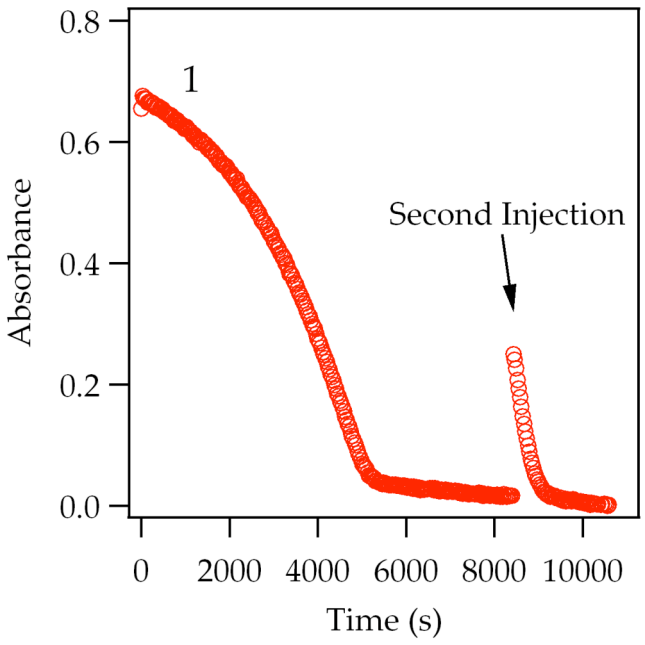

Figure A3.15. Representative plot showing absorbance of arene **1** vs time for the ortholithiation of **1** (0.010 M) with LDA (0.10 M) in THF (12.20 M) at –78 °C. After completion of the reaction a second aliquot of **1** (0.005) was injected.

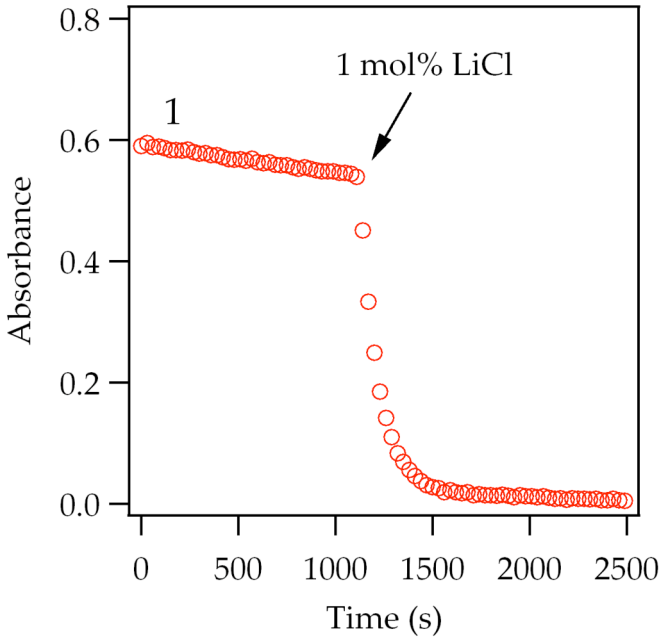

Figure A3.16. Ortholithiation of **1** (0.010 M) with LDA (0.10 M) in THF (12.2 M) at –78 °C monitored by IR spectroscopy (1325 cm^{-1}) with injection of 1.0 mol % LiCl.

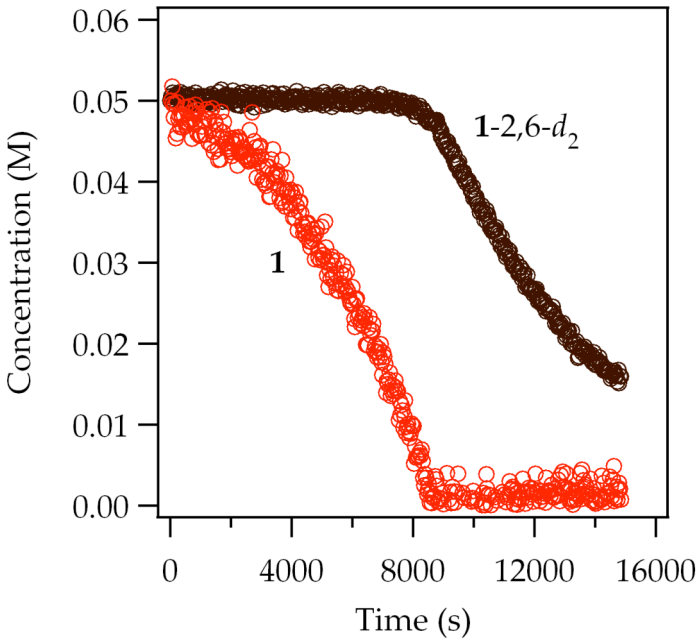

Figure A3.17 Competitive ortholithiation of **1** (0.050 M) and **1**-2,6-d_2 (0.050 M) with LDA (0.10 M) in THF (12.2 M) at –78 °C monitored by IR spectroscopy.

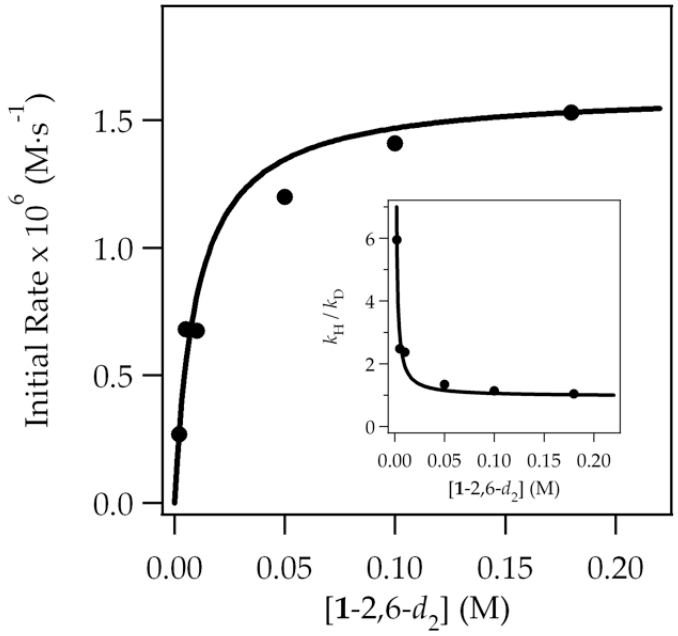

Figure A3.18. Plot of initial rate versus [**1**-2,6-d_2] for the ortholithiation of **1**-2,6-d_2 by 0.10 M LDA in 12.2 M THF at –78 ºC measured by IR spectroscopy. The curve depicts an unweighted least-squares fit to a first-order saturation function: $-\Delta[\mathrm{ArH}]/\Delta t\,|_{t=0} = (a[\mathrm{ArH}])/\,(1 + b[\mathrm{ArH}])$ where ArH is **1**-2,4-d_2. The ratio a/b was constrained to 1.6 x10^{-6} M·s^{-1} to ensure saturation at the initial rate of **1** (1.6 x10^{-6} M·s^{-1}). [b = (2.62 $\pm$ 0.08) x 10^{-6}]

[**1**-2,6-d_2] (M)	-Δ[ArH]/Δt (M·s^{-1})
0.002	2.69 e-7 $\pm$ 2 e-8
0.005	6.46 e-7 $\pm$ 4 e-8
0.010	6.74 e-6 $\pm$ 1 e-7
0.050	1.96 e-6 $\pm$ 3 e-7
0.10	1.41 e-6 $\pm$ 6 e-7
0.18	1.53 e-6 $\pm$ 4 e-7
0.38	2.62 e-6 $\pm$ 2 e-7

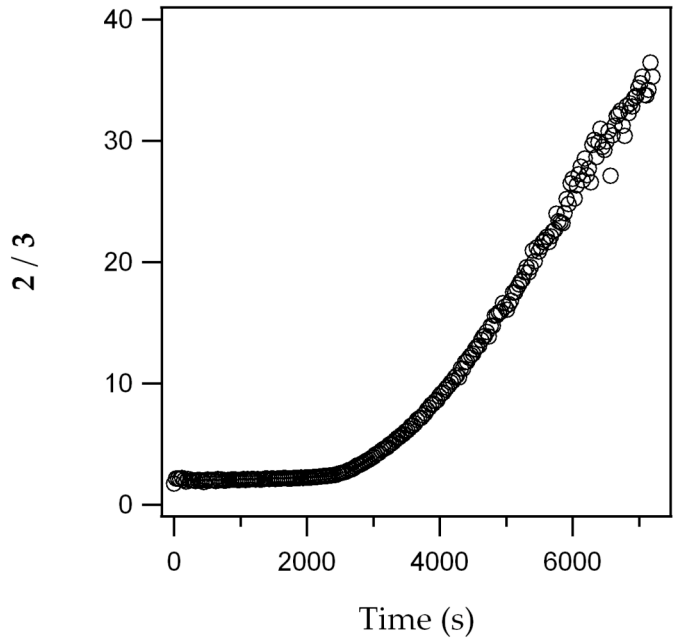

Figure A3.19. Plot of **2/3** versus time for the ortholithiation of **1** by LDA in THF (12.2 M) at -65 ^{o}C measured by ^{19}F NMR spectroscopy.

Table A3.1. Relative initial rates for the formation of **2** and **3** for the ortholithiation of **1**, **1**-2-*d*, **1**-6-*d*, and **1**-2,6-d_2 (0.050 M each) by LDA (0.10 M) in THF (12.2 M) at -78 °C measured by ^{19}F NMR spectroscopy (A) in the absence of LiCl and (B) with 5 mol% LiCl.

No LiCl	(Δ**2**/Δ**3**)
1	1.65
1-2-*d*	0.057
1-6-*d*	34.0
1-2,6-d_2	0.70

5 mol% LiCl	(Δ**2**/Δ**3**)
1	0.78
1-2-*d*	0.016
1-6-*d*	26.0
1-2,6-d_2	0.30

Table A3.2. Table showing the relative initial rates for the formation of **2** and **3** with various lithium salts (0.020 M) for the ortholithiation of **1** (0.050 M) by LDA (0.10 M) in 12.2 M THF at -90 °C measured by ^{19}F NMR spectroscopy.

Lithium salt	$(\Delta\mathbf{2}/\Delta t)/(\Delta\mathbf{3}/\Delta t)$
LiCl	0.78
2	0.84
34	0.72
35	0.73
36	0.49

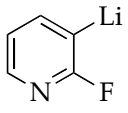

34

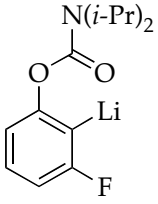

35

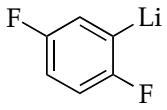

36

Table A3.3. Table showing regioselectivity at equilibrium for the ortholithiation of **1** by *sec*-BuLi (0.11 M) and *n*-BuLi (0.11 M) in 12.2 M THF at -90 °C measured by ^{19}F NMR spectroscopy.

base	[**1**] (M)	(**2**/**3**)
n-BuLi (0.11 M)	0.005	1.2
	0.020	2.4
	0.10	3.8
sec-BuLi (0.11 M)	0.005	0.15
	0.020	0.06
	0.10	0.05

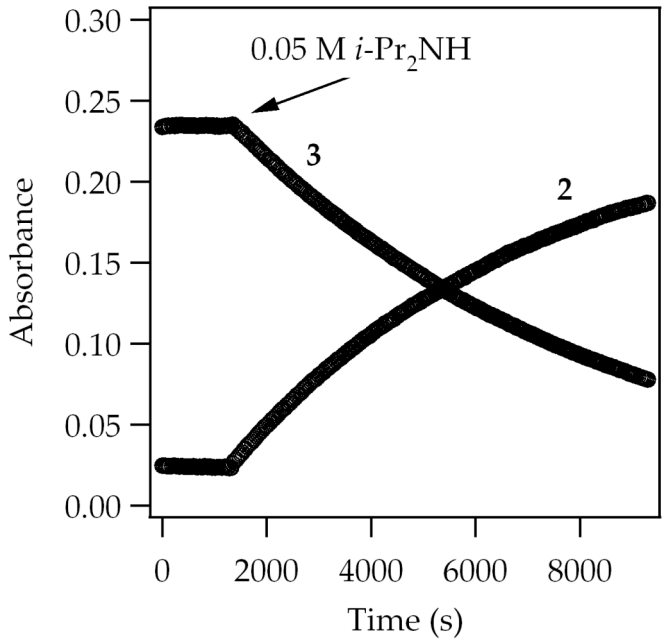

Figure A3.20. Representative IR plot for the equilibration of **3** (1151 cm^{-1}) to **2** (1306 cm^{-1}) was monitored by IR spectroscopy. Aryllithium **3** was generated by addition of LiTMP (0.050 M) to **1** (0.050 M) in 12.2 M THF at -78 °C. After **3** was produced quantitatively and no observable isomerization was detected, *i*-Pr_2NH (0.050 M) was injected.

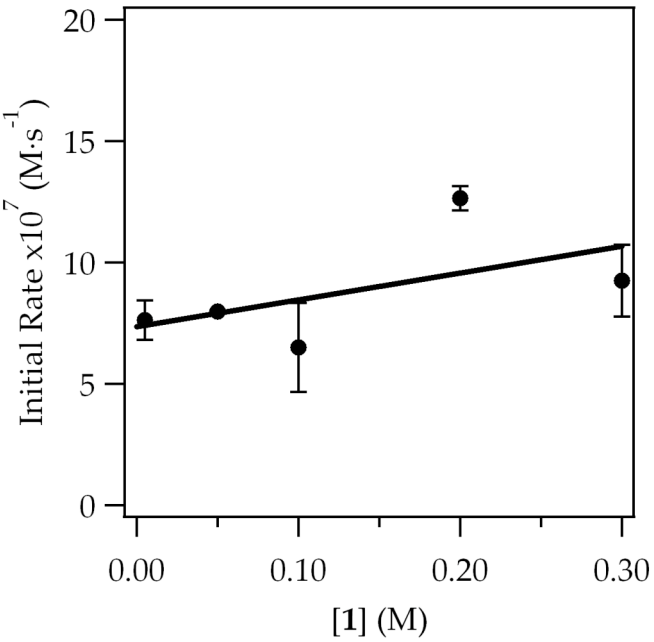

Figure A3.21. Plot of initial rate vs [**1**] (initial arene concentration) for the ortholithiation of **1** with LDA (0.10 M) in THF (12.2 M) at –78 °C measured by IR spectroscopy. The curve depicts an unweighted least-squares fit to y = a[ArH] + b. [a = (9 ± 1) x 10^{-7}, b = (7 ± 8) x 10^{-9}]

[**1**] (M)	y1 ($M \cdot s^{-1}$)	y2 ($M \cdot s^{-1}$)
0.005	7.04 e-7 ± 4 e-9	8.20 e-7 ± 4 e-9
0.050	8.00 e-7 ± 2 e-8	7.94 e-7 ± 2 e-8
0.10	7.78 e-7 ± 2 e-8	5.21 e-7 ± 1 e-8
0.20	1.32 e-6 ± 6 e-8	1.23 e-6 ± 6 e-8
0.30	8.22 e-7 ± 1 e-7	1.03 e-6 ± 1 e-7

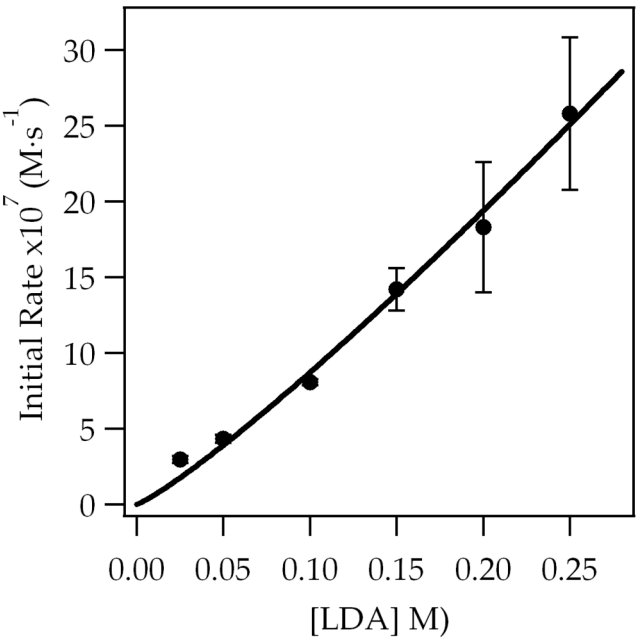

Figure A3.22. Plot of initial rate versus [LDA] in THF (12.2 M) for the ortholithiation of **1** (0.050 M) at –78 °C measured by IR spectroscopy. The curve depicts an unweighted least-squares fit to $y = a[\text{LDA}]^n$. [$a = (1.2 \pm 0.2) \times 10^{-5}$, $n = (1.16 \pm 0.09)$]

[LDA] (M)	y1 ($M \cdot s^{-1}$)	y2 ($M \cdot s^{-1}$)
0.025	3.14 e-7 ± 4 e-8	2.81 e-7 ± 5 e-8
0.05	4.51 e-7 ± 6 e-8	4.13 e-6 ± 8 e-8
0.10	7.94 e-7 ± 3 e-8	8.20 e-7 ± 3 e-8
0.15	1.52 e-6 ± 3 e-7	1.32 e-6 ± 8 e-8
0.20	1.81 e-6 ± 2 e-7	1.20 e-6 ± 5 e-8
0.25	2.33 e-6 ± 3 e-7	2.37 e-6 ± 4 e-8

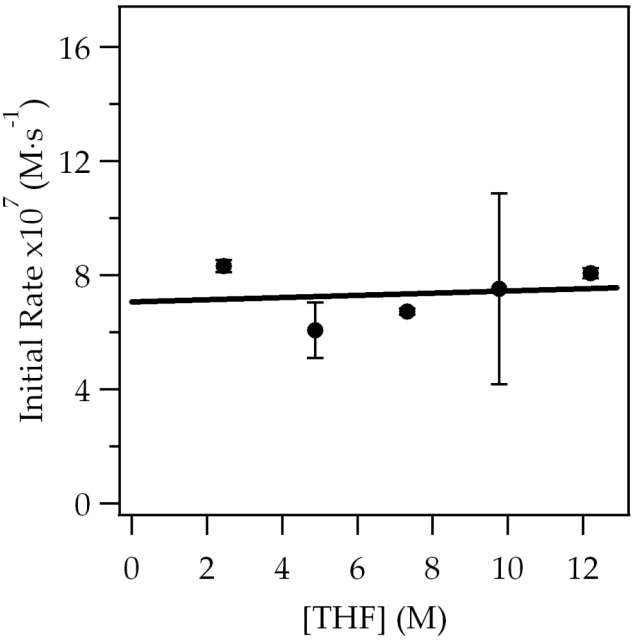

Figure A3.23. Plot of initial rate versus [THF] for the ortholithiation of **1** (0.050 M) by LDA (0.10 M) at –78 °C measured by IR spectroscopy. The curve depicts an unweighted least-squares fit to y = a[THF] + b. [a = (7 ± 1) x 10^{-7}, b = (3.9 ± 0.1) x 10^{-9}]

[THF] (M)	y1 ($M \cdot s^{-1}$)	y2 ($M \cdot s^{-1}$)
2.44	8.18 e-7 ± 4 e-8	8.47 e-7 ± 5 e-8
4.88	5.39 e-7 ± 6 e-8	6.76 e-7 ± 4 e-8
7.32	6.65 e-7 ± 3 e-8	6.81 e-7 ± 3 e-8
9.77	9.89 e-7 ± 3 e-8	5.16 e-7 ± 1 e-8
12.2	7.94 e-7 ± 2 e-8	8.20 e-7 ± 5 e-8

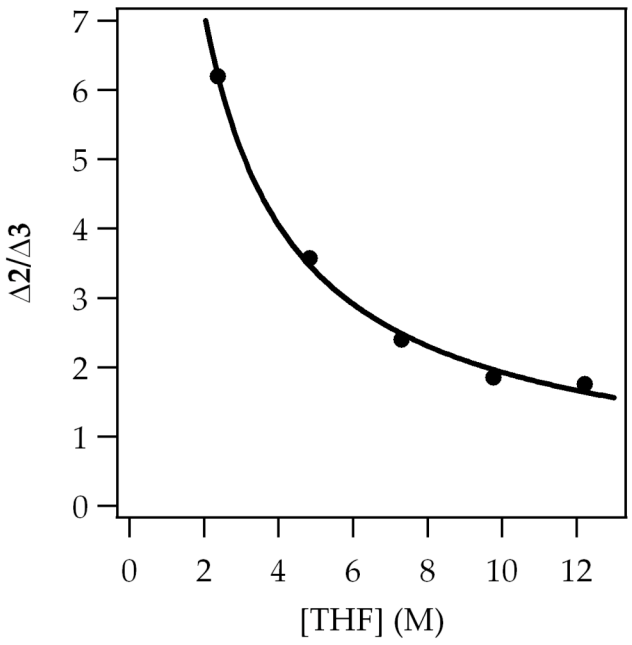

Figure A3.24. Ratio of relative initial rates of formation of **2** and **3**, $(\Delta\mathbf{2}/\Delta t)/(\Delta\mathbf{3}/\Delta t)$, versus [THF] for the ortholithiation of **1** (0.050 M) by LDA (0.10 M) at –65 °C measured by ^{19}F NMR. The elevated temperature was used to shorten the duration of the experiments. The curve depicts an unweighted least-squares fit to $y = a[\mathrm{THF}]^n + b$. [$a = 12.5 \pm 0.8$, $n = -0.8 \pm 0.2$ and $b = 0.1 \pm 0.8$]

[THF] (M)	$(\Delta\mathbf{2}/\Delta t)/(\Delta\mathbf{3}/\Delta t)$
2.37	6.20
4.83	3.57
7.30	2.40
9.76	1.85
12.21	1.76

Table A3.4. Table of relative initial rate versus [LDA] for the ortholithiation of **1** (0.050 M) by LDA (0.10 M) at -65 °C measured by ^{19}F NMR. The relative initial rate is defined as $(\Delta \mathbf{2}/\Delta t)/(\Delta \mathbf{3}/\Delta t)$.

[LDA] (M)	$(\Delta \mathbf{2}/\Delta t)/(\Delta \mathbf{3}/\Delta t)$
0.020	1.74
0.10	1.76
0.20	1.71

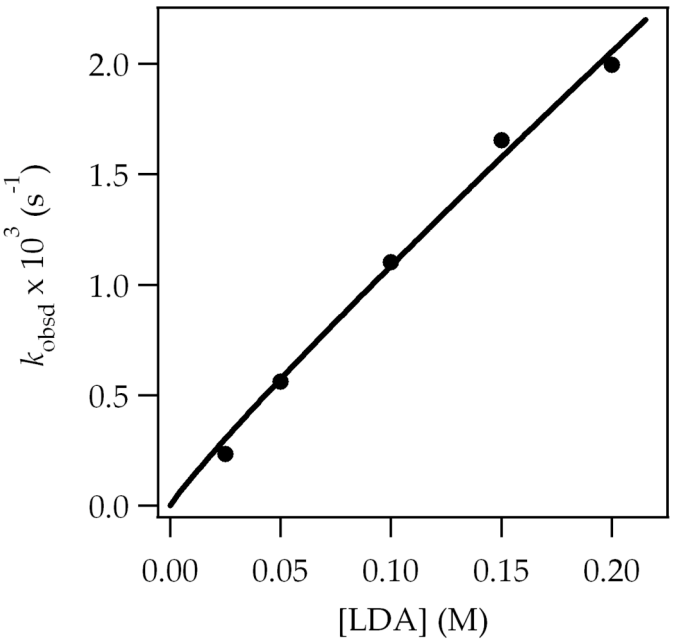

Figure A3.25. Plot of k_{obsd} versus [LDA] in THF (12.2 M) for the ortholithiation of **1**-2,6-d_2 (0.002 M) at –65 °C measured by ^{19}F NMR spectroscopy. The curve depicts an unweighted least-squares fit to y = k[LDA]^n. [k = (9 $\pm$ 1) x 10^{-3}, n = 0.92 $\pm$ 0.06]

[LDA] (M)	y (s^{-1})
0.025	0.23 e-3 ± 2 e-6
0.050	0.58 e-3 ± 5 e-6
0.10	1.10 e-3 ± 5 e-6
0.15	1.68 e-3 ± 3 e-5
0.20	1.95 e-3 ± 2 e-5

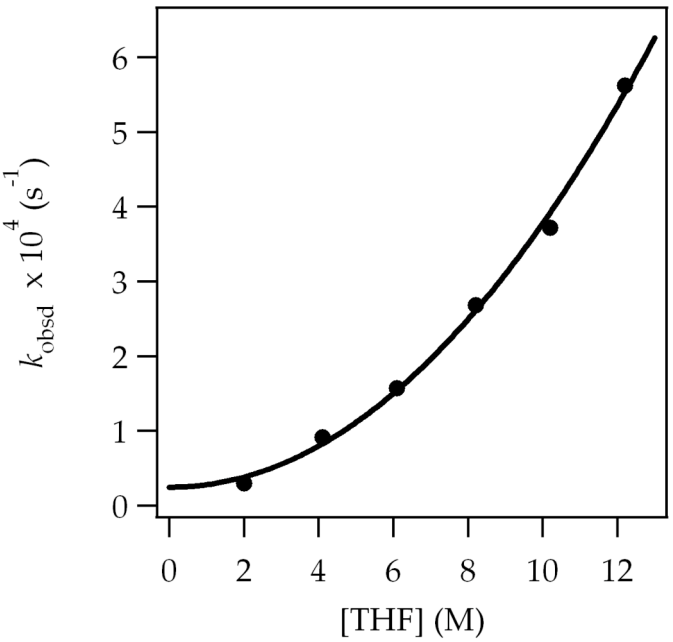

Figure A3.26. Plot of k_{obsd} versus [THF] in hexanes for the ortholithiation of **1**-2,6-d_2 (0.002 M) by LDA (0.050 M) at –65 °C measured by ^{19}F NMR spectroscopy. The rates are not affected by medium effects as measured by the use of 2,6-dimethyltetra-hydrofuran as a cosolvent. The curve depicts an unweighted least-squares fit to y = k[THF]^n + c. [k = (3 ± 1) x 10^{-6}, n = 2.0 ± 0.2, c = (3 ± 1) x 10^{-5}]

[THF] (M)	y (s^{-1})
2.1	2.97 e-5 ± 5 e-7
4.1	9.15 e-5 ± 5 e-7
6.1	1.57 e-4 ± 7 e-7
8.2	2.68 e-4 ± 8 e-7
10.2	3.72 e-4 ± 1 e-6
12.2	5.62 e-4 ± 5 e-6

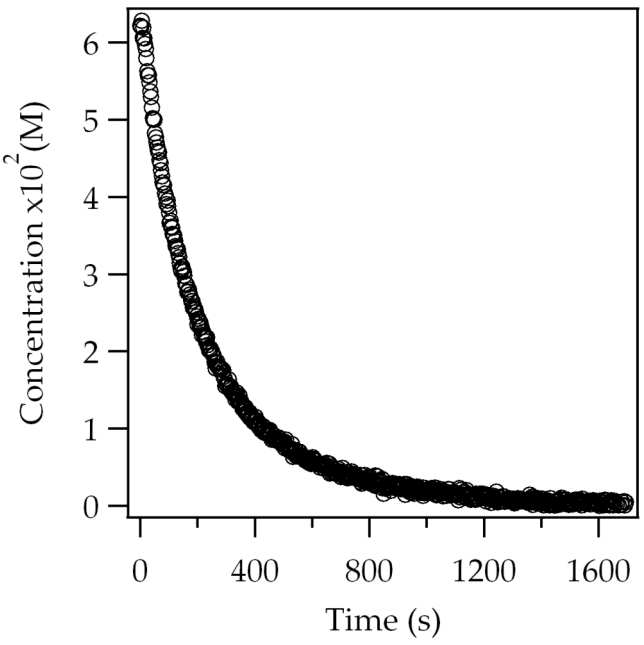

Figure A3.27. Representative plot of **1** (0.005 M) versus time for the ortholithiation by LDA (0.10 M) in 12.2 M THF in the presence of 5 mol% LiCl at -90 ºC.

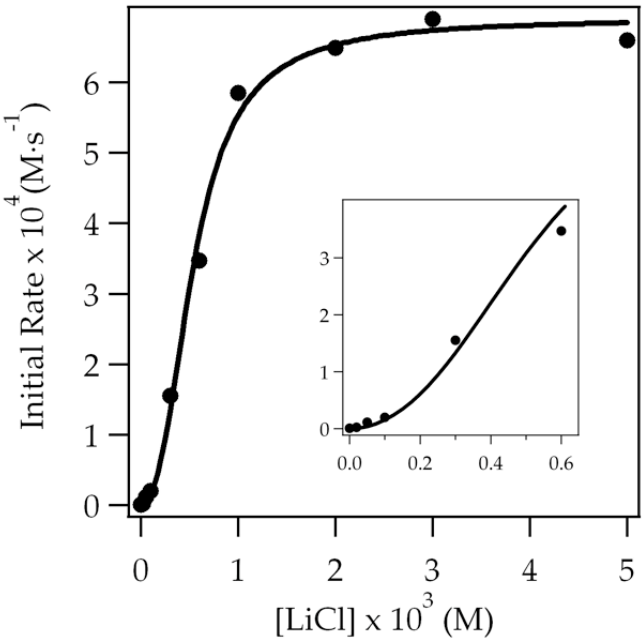

Figure A3.28. Plot of initial rate versus [LiCl] for the ortholithiation of **1** (0.074 M) by 0.10 M LDA in 12.2 M THF at –78 °C measured by IR spectroscopy. The inset is a magnified view of the data at low concentrations. The curve depicts an unweighted least-squares fit to eq 17. [ArH] = 0.074 M, $[A_2S_2]$ = 0.050 M, c = 1.0 x 10^{-8}. [k_1 = (1.5 $\pm$ 0.1) x 10^4, k_{-1} = (3.2 $\pm$ 0.4) x 10^6, k_2 = 0.61 $\pm$ (6 x 10^{-4}), n = 2.0 $\pm$ 0.3]

[LiCl] (mM)	(Δ[**1**]/Δt) (abs·s^{-1})
0.0	6.08 e-7 ± 4 e-7
0.02	2.37 e-6 ± 2 e-7
0.05	1.15 e-5 ± 9 e-7
0.10	1.99 e-5 ± 5 e-7
0.30	1.55 e-4 ± 4 e-6
0.60	3.47 e-4 ± 2 e-5
1.0	6.08 e-4 ± 1 e-5
2.0	6.49 e-4 ± 2 e-5
3.0	6.90 e-4 ± 2 e-5
5.0	6.602 e-4 ± 2 e-5

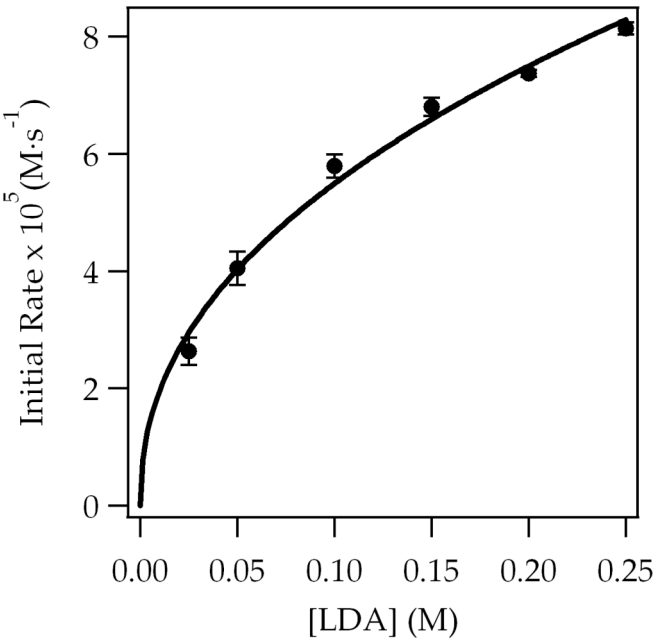

Figure A3.29. Plot of initial rate versus [LDA] in THF (12.2 M) for the ortholithiation of **1** (0.075 M) in the presence of 5 mol% LiCl at –78 °C measured by IR spectroscopy. The curve depicts an unweighted least-squares fit to $y = a[\text{LDA}]^n$. [$a = (154 \pm 9) \times 10^{-6}$, $n = 0.45 \pm 0.03$]

[LDA] (M)	y1 ($M \cdot s^{-1}$)	y2 ($M \cdot s^{-1}$)
0.025	2.60 e-5± 9 e-7	2.47 e-5 ± 8 e-7
0.050	5.35 e-5 ± 8 e-7	3.65 e-5 ± 9 e-7
0.10	6.08 e-5 ± 4 e-7	5.51 e-5 ± 3 e-7
0.15	6.58 e-5 ± 6 e-7	7.02 e-5 ± 2 e-6
0.20	7.28 e-5 ± 1 e-6	7.46 e-5 ± 1 e-6
0.25	8.29 e-5 ± 1 e-6	7.99 e-5 ± 1 e-6

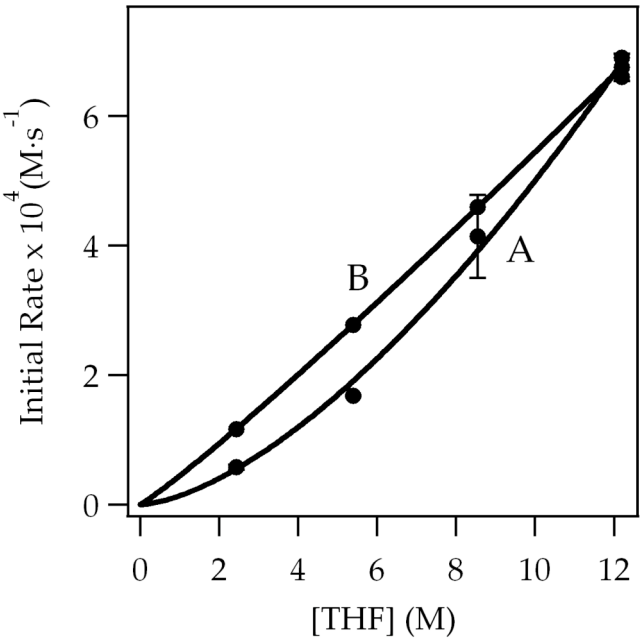

Figure A3.30. Plot of initial rate versus [THF] in hexanes (curve A) and 2,5-dimethyl-tetrahydrofuran (curve B) cosolvent for the ortholithiation of **1** (0.075 M) by LDA (0.10 M) in the presence of 5 mol% LiCl at –78 °C. The data was measured by IR spectroscopy. The curve depicts an unweighted least-squares fit to $y = a[THF]^n + b$. Curve A: $a = (1.4 \pm 1.0) \times 10^{-5}$, $n = 1.6 \pm 0.3$, $b = (1.6 \pm 1) \times 10^{-5}$. Curve B: $a = (4.44 \pm 2.0) \times 10^{-5}$, $n = 1.1 \pm 0.1$, $b = (0.0 \pm 5) \times 10^{-5}$.

[THF] (M)	y1 ($M \cdot s^{-1}$)	y2 ($M \cdot s^{-1}$)
2.44	6.08 e-5 ± 8 e-7	5.5 e-5 ± 7 e-7
5.39	1.68 e-4 ± 3 e-6	1.67 e-4 ± 2 e-6
8.54	3.69 e-4 ± 1 e-5	3.40 e-4 ± 7 e-6
12.2	6.08 e-4 ± 4 e-6	5.51 e-4 ± 3 e-6

[Me_2-THF] (M)	y ($M \cdot s^{-1}$)
2.44	1.17 e-4 ± 4 e-6
5.39	2.77 e-4 ± 8 e-6
8.54	4.59 e-4 ± 2 e-5

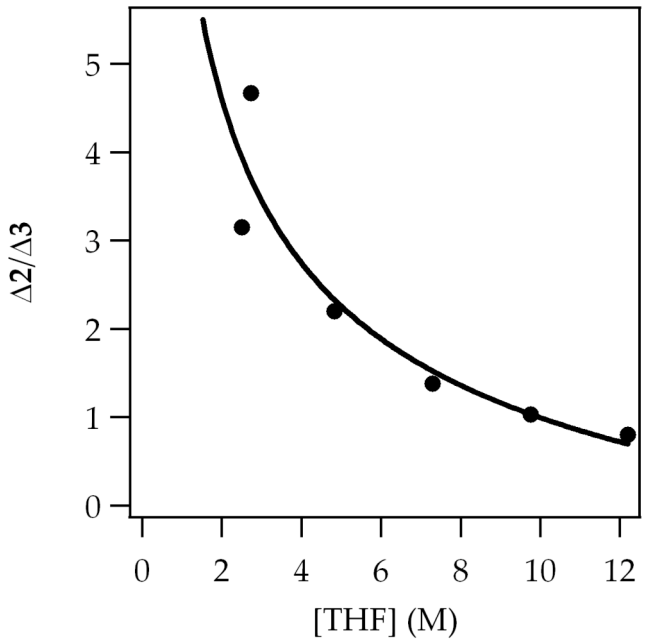

Figure A3.31. Plot of relative initial rate versus [THF] in 2,5-dimethyltetrahydrofuran cosolvent for the ortholithiation of **1** (0.050 M) by LDA (0.10 M) in the presence of 5 mol% LiCl at –78 °C. The concentrations of **2** and **3** were monitored by ^{19}F NMR spectroscopy. The curve depicts an unweighted least-squares fit to $y = a[\text{THF}]^n + b$. [$a = 9 \pm 6$, $n = -0.94 \pm 0.21$, $b = 0.0 \pm 0.3$]

[THF] (M)	y1	y2
2.50	3.15	4.30
4.83	2.20	/
7.30	1.38	/
9.76	1.03	/
12.2	0.78	/

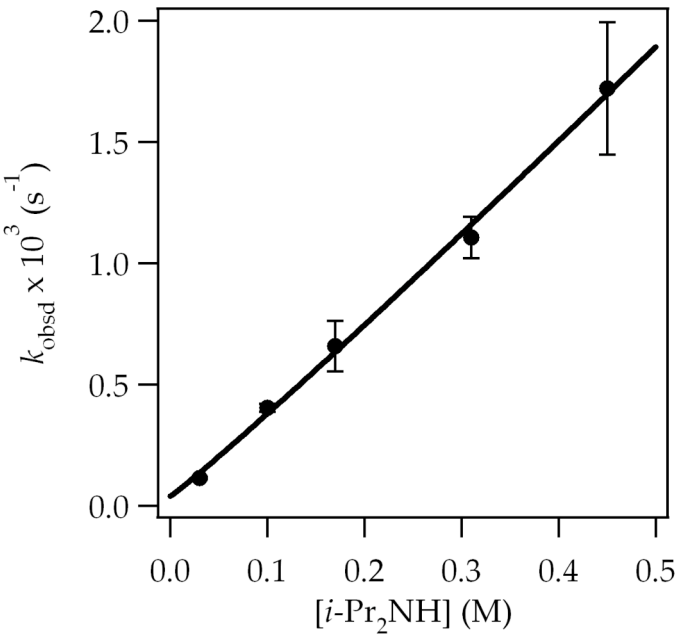

Figure A3.32. Plot of k_{obsd} vs [i-Pr_2NH] for the isomerization of **3** (0.050 M) to **2** in 12.2 M THF at –78 °C measured by IR spectrocopy. The curve depicts an unweighted least-squares fit to $y = k[i\text{-}Pr_2NH]^n + c$. [$k = (3.8 \pm 0.3) \times 10^{-3}$, $n = 1.1 \pm 0.1$, $c = (2 \pm 1) \times 10^{-5}$]

[i-Pr_2NH] (M)	y1 (s^{-1})	y2 (s^{-1})
0.030	1.12 e-4 ± 4 e-6	1.18 e-4± 1 e-6
0.10	3.92 e-4 ± 3 e-6	4.15 e-4± 3 e-6
0.17	7.33 e-4 ± 5 e-6	5.86 e-4 ± 3 e-6
0.31	1.17 e-3 ± 7 e-6	1.05 e-3 ± 8 e-6
0.45	1.91 e-3± 2 e-5	1.53 e-3 ± 1 e-5

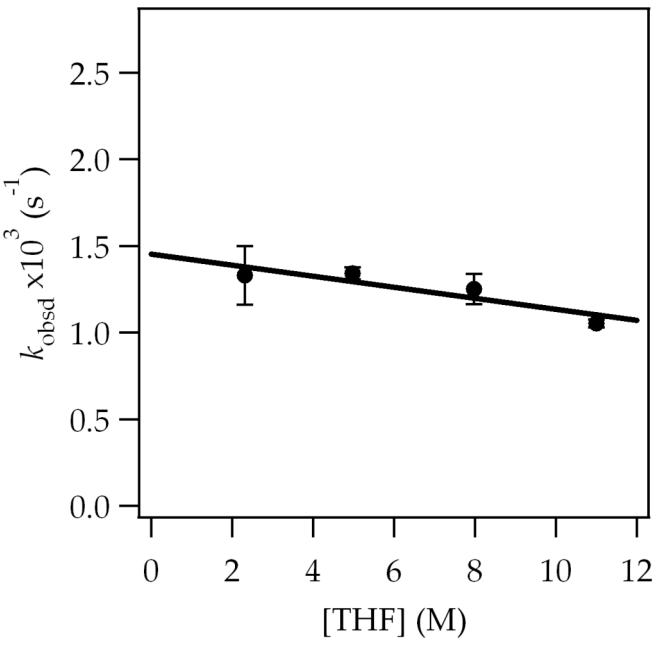

Figure A3.33. Plot of k_{obsd} versus [THF] for the isomerization of **3** (0.050 M) to **2** in 12.2 M THF at –78 °C measured by IR spectroscopy. The curve depicts an unweighted least-squares fit to y = *a*[THF]+b. [*a*= (1.45 $\pm$ 0.08) x 10^{-3}, *b* = (3.2 $\pm$ 1.1) x 10^{-5}]

[THF] (M)	y1 (s^{-1})	y2 (s^{-1})
2.31	1.21 e-3 ± 3 e-5	1.44 e-3 ± 2 e-5
4.97	1.32 e-3 ± 1 e-5	1.37 e-3 ± 2 e-5
7.98	1.31 e-3 ± 7 e-6	1.19 e-3 ± 1 e-5
11.0	1.04 e-3 ± 9 e-6	1.07 e-3 ± 8 e-6

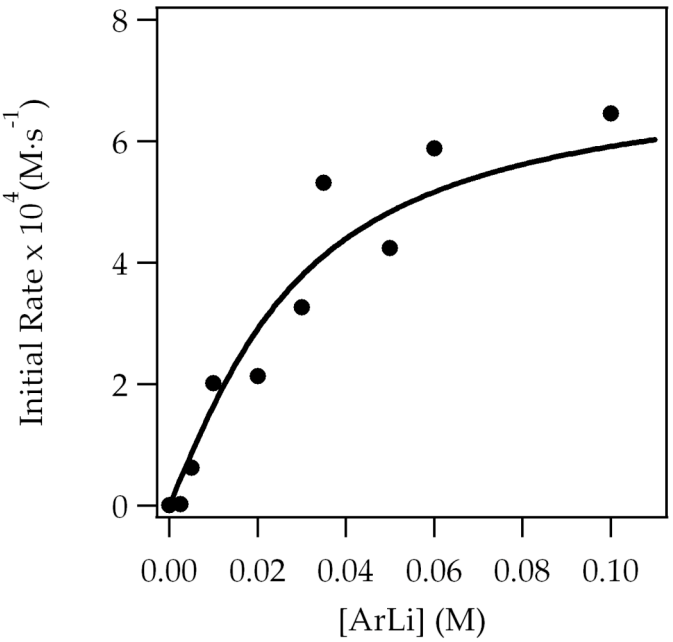

Figure A3.34. Plot of initial rate versus aryllithium **2**-6-*d* for the ortholithiation of **1** (0.075 M) by 0.10 M LDA in 12.2 M THF at –78 °C measured by IR spectroscopy. Aryllithium **2** was generated from **1**-6-*d* with one equivalent LDA at –40 °C prior to injection **1**. The curve depicts an unweighted least-squares fit a simple first-order saturation function: $-\Delta[ArH]/\Delta t\,|_{t=0} = (k_1k_2[A_2S_2][ArH])/(k_{-1} + k_2[ArH])$ where [ArH] = 0.075 M, $[A_2S_2]$ = 0.050 M. k_2 was constrained to the same value corresponding to lithium chloride saturation (see Figure A3.13). [k_1 = (0.18 $\pm$ 0.02); k_{-1} = (1.97 $\pm$ 0.01) x 10^9]

[**2**-6-*d*] (M)	y ($M \cdot s^{-1}$)
0.0	0.006 e-4 $\pm$ 1 e-7
0.0025	0.026 e-4 $\pm$ 2 e-7
0.005	0.623 e-4 $\pm$ 7 e-7
0.010	2.02 e-4 $\pm$ 3 e-6
0.020	2.13 e-4 $\pm$ 4 e-6
0.030	3.27 e-4 $\pm$ 7 e-6
0.035	5.32 e-4 $\pm$ 8 e-6
0.050	4.24 e-4 $\pm$ 8 e-6
0.060	5.88 e-4 $\pm$ 1 e-5
0.10	6.46 e-4 $\pm$ 1 e-5

Derivation. Derivation of 2nd-order LiCl saturation curve (eq 17 in manuscript):

$$A_2S_2 + 2S \underset{k_{-1}[LiCl]^n}{\overset{k_1[LiCl]^n}{\rightleftharpoons}} 2AS_2$$

$$AS_2 + ArH \xrightarrow{k_2} \text{product}$$

The initial rate of consumption of ArH is defined as:

$$-\Delta[ArH]/\Delta t\big|_{t=0} = k_2[AS_2]_0[ArH]_0 \quad (1)$$

Applying the steady-state approximation to monomer AS_2 gives

$$\frac{d[AS_2]}{dt} = 2k_1[A_2S_2][LiCl]^n - 2k_{-1}[AS_2]^2[LiCl]^n - k_2[AS_2][ArH] = 0 \quad (2)$$

solving for $[AS_2]$ using the quadratic equation gives

$$[AS_2] = \frac{1}{4k_{-1}[LiCl]^n}\left(\sqrt{k_2^2[ArH]^2 + 16k_1k_{-1}[A_2S_2][LiCl]^{2n}} - k_2[ArH]\right) \quad (3)$$

Substituting eq 3 into eq 1 gives

$$-\Delta[ArH]/\Delta t\big|_{t=0} = \frac{k_2[ArH]}{4k_{-1}[LiCl]^n}\left(\sqrt{k_2^2[ArH]^2 + 16k_1k_{-1}[A_2S_2][LiCl]^{2n}} - k_2[ArH]\right) \quad (4)$$

where [ArH] and $[A_2S_2]$ are evaluated at t=0. To account for the LiCl-free pathway, we add a constant c to eq 4 that reflects the initial rate without LiCl. The constant is determined experimentally rather than as an adjustable parameter.

$$-\Delta[ArH]/\Delta t\big|_{t=0} = \frac{k_2[ArH]}{4k_{-1}[LiCl]^n}\left(\sqrt{k_2^2[ArH]^2 + 16k_1k_{-1}[A_2S_2][LiCl]^{2n}} - k_2[ArH]\right) + c \quad (5)$$

Figure A3.35. Plot of the equilibrium constant (K_{eq}) versus total concentration of lithium titer LiX_T (=LDA+LiCl) assuming (A) monomeric lithium chloride and (B) dimeric lithium chloride. Amounts of LDA-LiCl mixed dimer AX and mixed trimer A_2X and lithium chloride X_n are measured by ^{6}Li NMR for solutions of 2:1 ratios of LiCl to LDA in 12.2 M THF at -78 ^{o}C.

Figure A3.35 (continued).

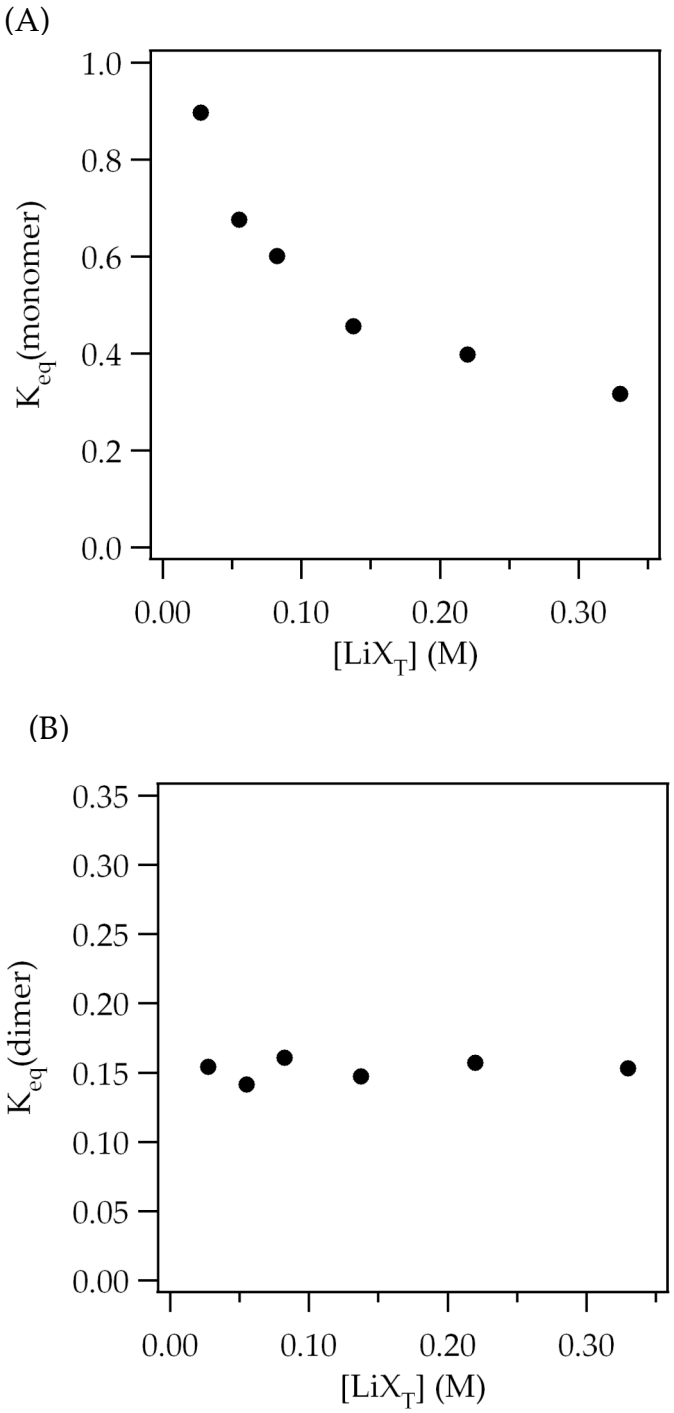

Figure A3.35 (continued).

$K_{equ}(\text{monomer}) = [AX]^2/([X][A_2X])$

$K_{equ}(\text{dimer}) = [AX]^2/([X_2]^{0.5}[A_2X])$

where values of AX, X_n and A_2X are expressed in units of molarity.

$[LiX_T]$ (M)*	K_{equ} (monomer)	K_{equ}(dimer)
0.023	0.90	0.15
0.055	0.68	0.14
0.083	0.60	0.16
0.14	0.46	0.16
0.22	0.40	0.16
0.33	0.32	0.15

*The concentration of LiX_T, although expressed in units of molarity, refers to concentration of monomer unit (normality).

Part 4: Computational Studies

A

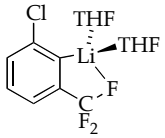

B

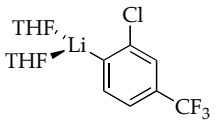

C

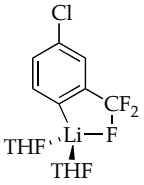

D

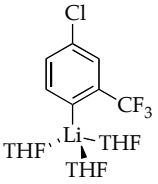

E

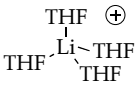

F

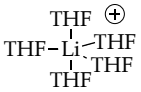

G

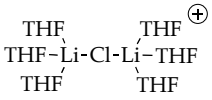

H

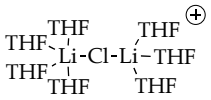

I

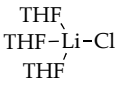

J

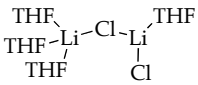

K

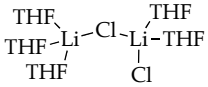

L

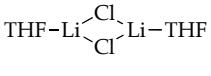

M

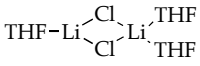

N

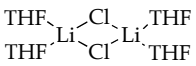

O

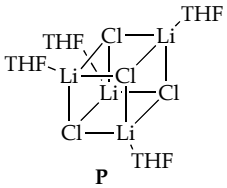

P

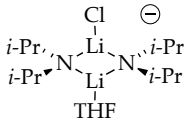

Q

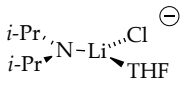

R

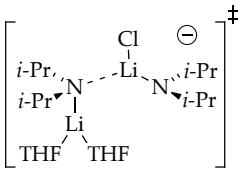

S

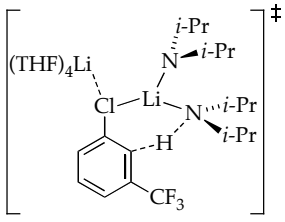

T

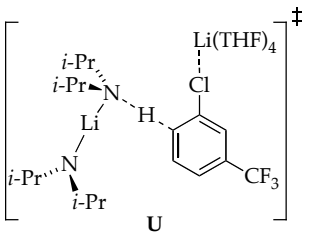

U

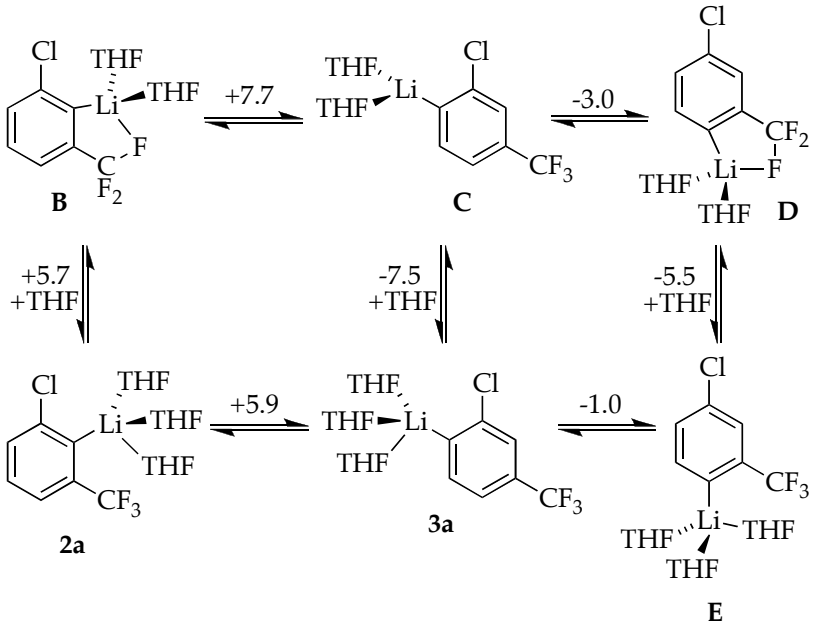

Figure A3.36. Relative free energies for the solvation (Δ*G*, kcal/mol) of **2**, **3**, and 4-lithio-1-chloro-3-(trifluoromethyl)benzene at -78 °C calculated at the MP2 level of theory with the 6-31G(d) basis set. Relative free energies are given in kcal/mol.

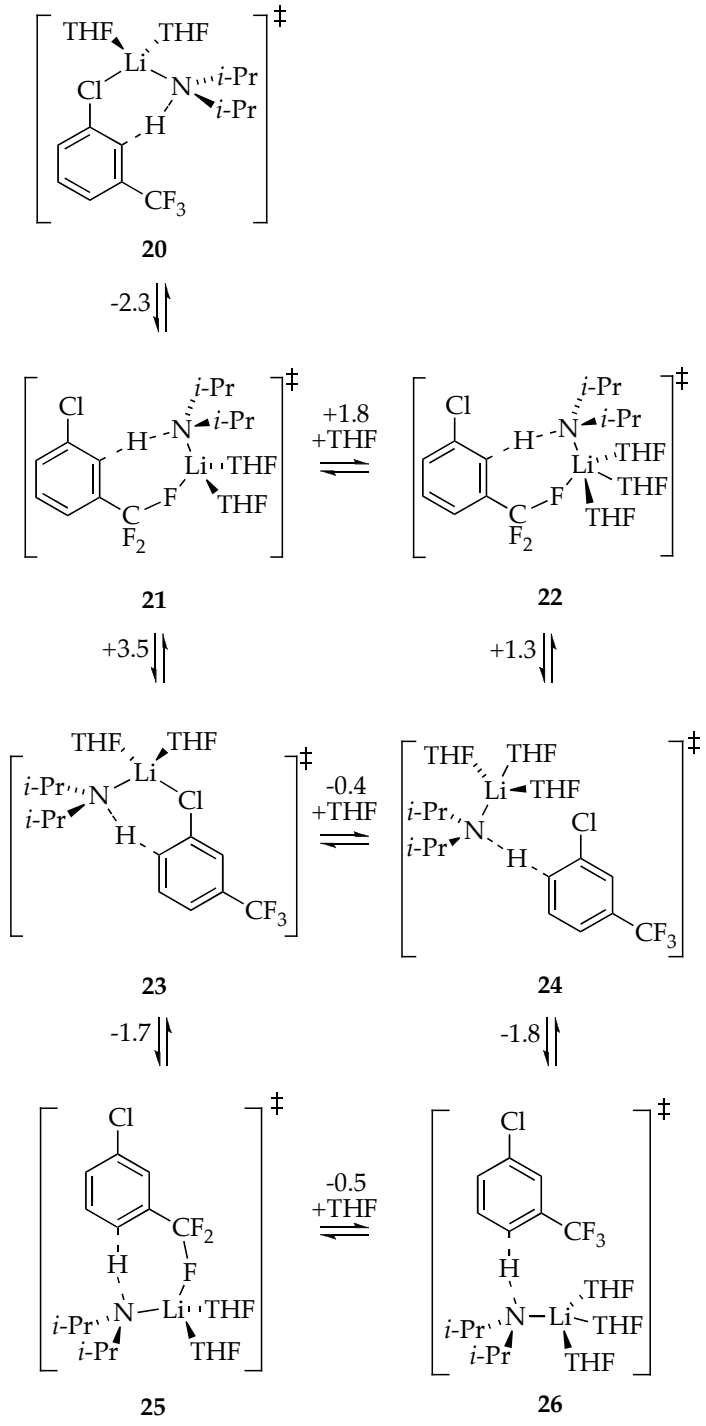

Figure A3.37. DFT computations [MP2/6–31G(d)//B3LYP/6–31G(d)] of monomer-based transition structures for the metalation of **1**. The free energy of activation for the formation of **18** ($\Delta G^{\ddagger}$) is 14.5 kcal/mol calculated at –78 °C. The numbers affiliated with the arrows represent the relative free energies (ΔG).

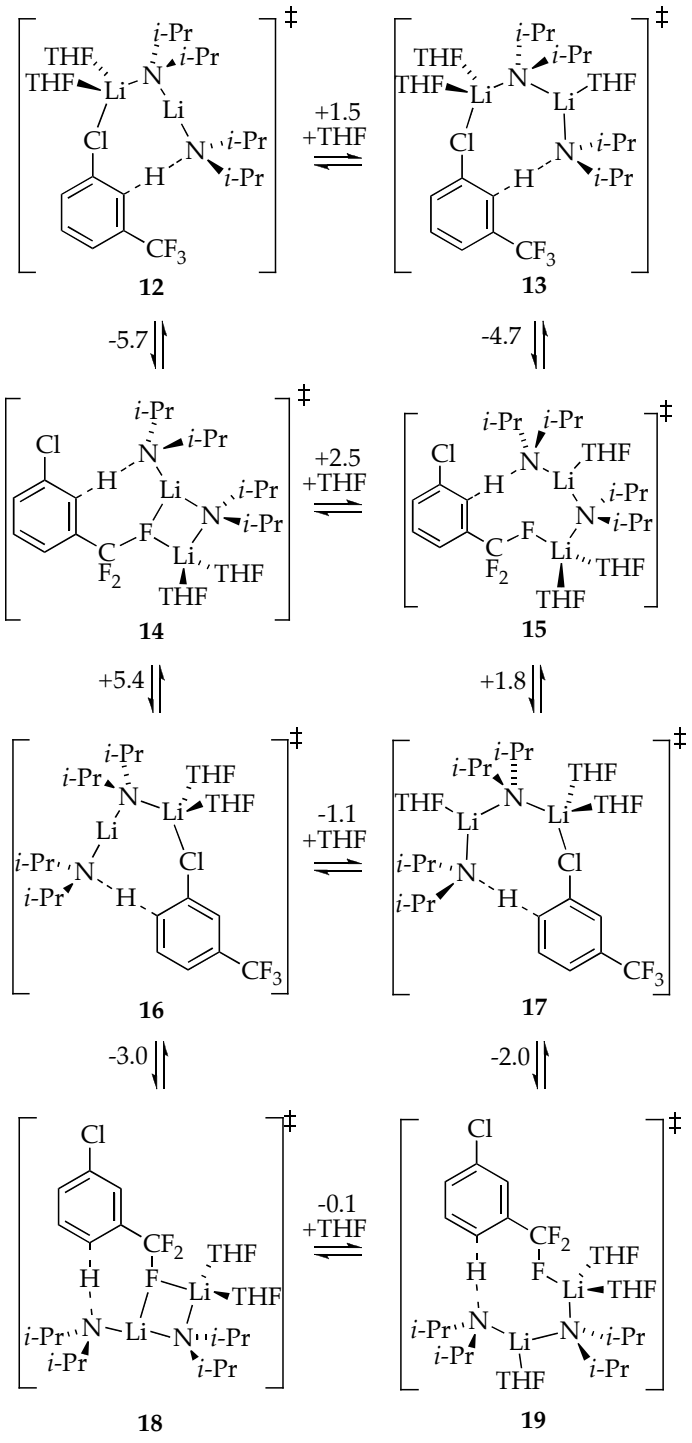

Figure A3.38. DFT computations [MP2/6–31G(d)//B3LYP/6–31G(d)] of dimer-based transition structures for the metalation of **1**. The free energy of activation for the formation of **12** ($\Delta G^{\ddagger}$) is 19.3 kcal/mol calculated at –78 °C. The numbers affiliated with the arrows represent the relative free energies (ΔG).

(A)

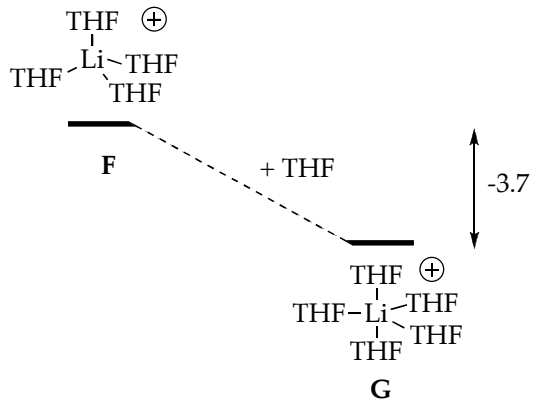

(B)

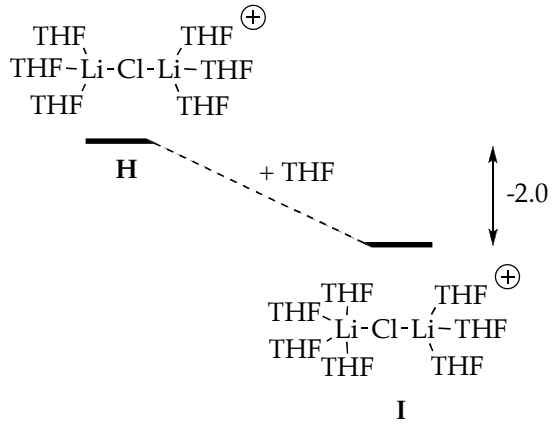

(C)

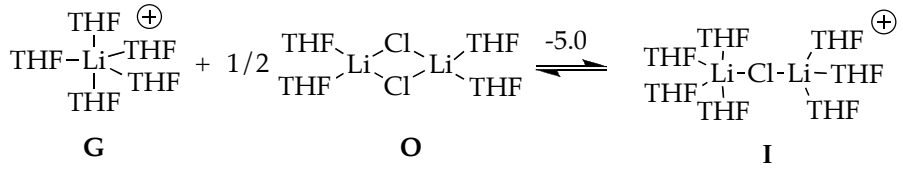

Figure A3.39. Relative free energies (ΔG, kcal/mol) at -78 °C for the solvation of (A) THF-tetrasolvated lithium ion and (B) THF-hexasolvated LiCl triple ion. (C) Relative free energy (ΔG, kcal/mol) at -78 °C showing the relative propensity of the lithium ion to exist in the triple-ion form rather than the simple ion pair.

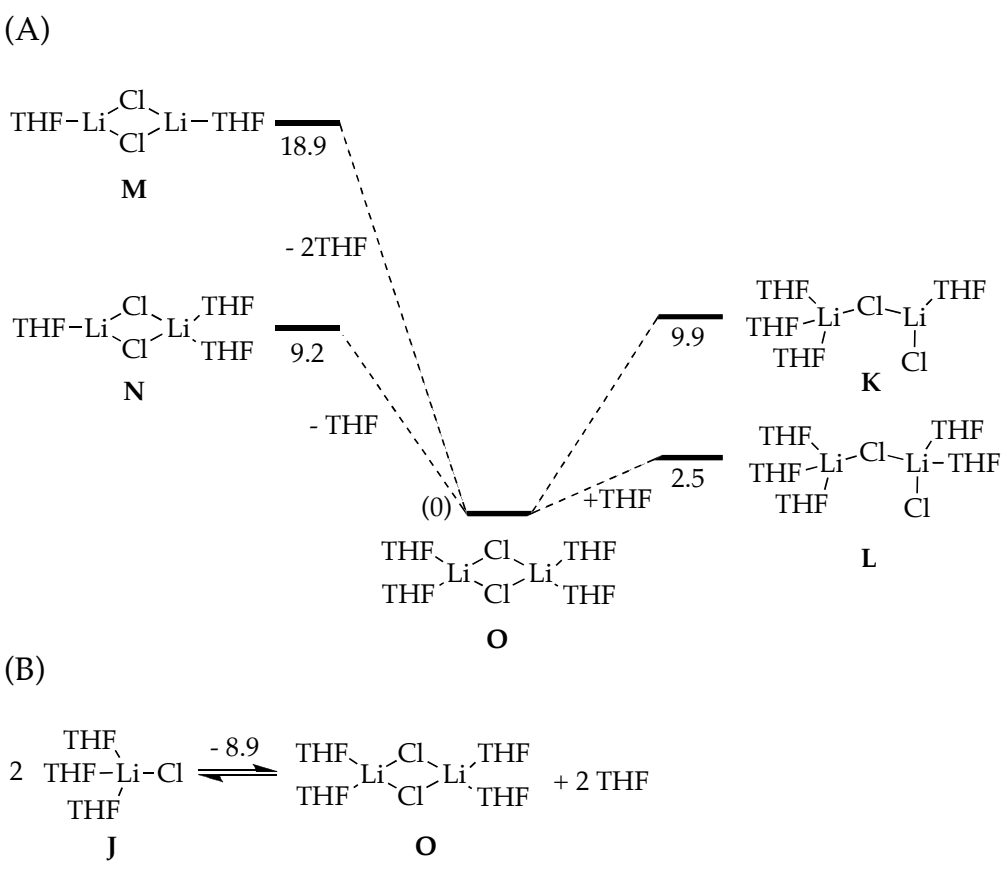

Figure A3.40. Relative free energies (ΔG, kcal/mol) at -78 °C of (A) dimeric LiCl and relative free energy of monomeric and dimeric LiCl at -78 °C. Tetra-solvated monomeric LiCl failed to minimize.

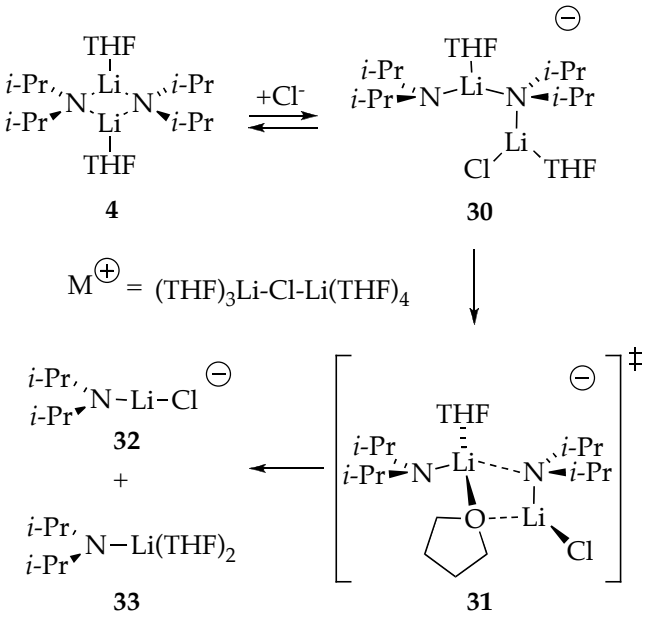

Figure A3.41. Reaction scheme showing lithium chloride deaggregating THF-disolvated closed dimer. The free energy of **31** is + 5.0 kcal/mol at -78 °C relative to chloride-solvated opendimer **30**. The left side of the equation could, in principle, be balanced by the inclusion of LDA-LiCl mixed aggregates. Because a comparison in free energies of neutral and ionic/charge-separated species results in large errors in DFT, the equation was not balanced. The negatively charged triple ions all have the counterion $(THF)_3Li\text{-}Cl\text{-}Li(THF)_3$.

Table A3.5. Optimized geometries at B3LYP level of theory with 6-31G(d) basis set for the serial solvation of **2**, **3**, and 4-lithio-1-chloro-3-(trifluoromethyl)benzene at -78 °C with free energies (Hartrees) and cartesian coordinates (X, Y, Z) (Note: G_{MP2} includes single point MP2 corrections to B3LYP/6-31G(d) optimized structures).

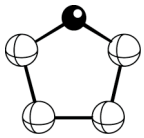

A
G = -232.349385
G_{MP2} = -231.669937

Atom	X	Y	Z
C	-0.77676	0.78926	-0.12614
C	-1.13241	-0.69941	0.08086
O	-0.00028	-1.43271	-0.37154
C	1.13192	-0.69999	0.08156
C	0.77743	0.78860	-0.12707
H	-1.99954	-1.03544	-0.49441
H	-1.32099	-0.90818	1.14790
H	1.99943	-1.03711	-0.49250
H	1.31917	-0.90803	1.14900
H	1.16400	1.14893	-1.08517
H	1.20108	1.42138	0.65905
H	-1.16426	1.15158	-1.08311
H	-1.19880	1.42112	0.66158

Table A3.5 (Continued).

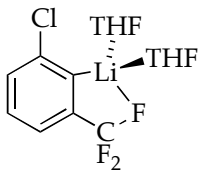

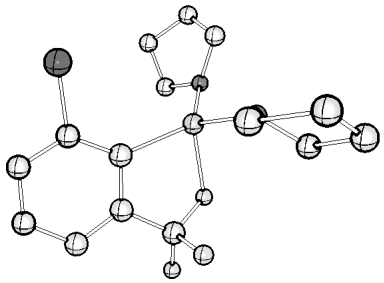

B
G = -1500.483215
G_{MP2} = -1496.753504

Atom	X	Y	Z	Atom	X	Y	Z
C	0.171979	-0.561478	0.062389	H	5.498146	-3.424722	-1.329519
C	0.115382	-0.096682	1.487325	H	3.920372	-4.197710	-1.491305
C	1.349549	0.202902	2.104120	H	2.756084	-2.150808	-1.356020
C	1.200229	0.563148	3.436685	H	4.317262	-1.364466	-1.710260
C	-0.002228	0.636029	4.139933	O	3.958476	1.725702	0.304060
C	-1.185051	0.324860	3.462701	C	5.375893	1.748285	0.611941
C	-1.134155	-0.046403	2.121014	C	5.683633	3.171821	1.090353
H	-2.047243	-0.284615	1.582034	C	4.329084	3.632441	1.652367
H	-2.137281	0.377840	3.983600	C	3.349609	2.992331	0.673148
H	-0.024323	0.929828	5.185307	H	3.222735	3.595648	-0.235417
Cl	2.685533	0.995259	4.385639	H	2.370730	2.769833	1.104270
Li	2.892118	0.159067	0.718571	H	4.227816	4.721024	1.693493
O	3.847390	-1.497348	0.282465	H	4.167290	3.228522	2.657484
C	3.803669	-2.061661	-1.044191	H	5.983391	3.804271	0.246470
C	4.480416	-3.444418	-0.929722	H	6.488348	3.191965	1.831025
C	4.488085	-3.736530	0.596515	H	5.567031	1.005192	1.395041
C	3.638868	-2.604887	1.186698	H	5.929358	1.461708	-0.287793
H	3.940943	-2.275017	2.182116	F	1.221839	0.027145	-0.631663
H	2.571142	-2.856052	1.202110	F	0.404427	-1.900989	-0.058579
H	5.507792	-3.692138	0.990997	F	-0.937557	-0.302515	-0.654913
H	4.077820	-4.720544	0.840800				

Table A3.5 (Continued).

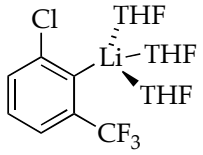

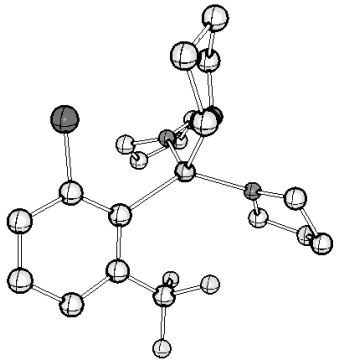

2a
G = -1732.830143
G_{MP2} = -1728.332611

Atom	X	Y	Z	Atom	X	Y	Z
C	0.017822	2.843992	-0.388654	C	2.239799	-1.363506	3.560118
C	-1.339085	2.265150	-0.112398	C	1.021688	-0.478445	3.941691
C	-1.397940	0.868650	0.120209	C	-0.071618	-0.931617	2.966786
C	-2.694989	0.456009	0.397622	H	-0.773197	-0.154462	2.664612
C	-3.840393	1.253842	0.451419	H	-0.631199	-1.794293	3.355846
C	-3.699465	2.619132	0.206201	H	1.249998	0.579629	3.780988
C	-2.435315	3.135009	-0.077081	H	0.719272	-0.601434	4.985878
H	-2.309189	4.196535	-0.266188	H	3.137326	-0.755203	3.413316
H	-4.568006	3.271566	0.238257	H	2.469974	-2.104778	4.331560
H	-4.812554	0.826152	0.678373	H	1.519471	-3.100741	2.427504
Cl	-3.003377	-1.311472	0.745665	H	2.542349	-2.019728	1.446948
Li	0.294935	-0.475574	0.001013	O	-0.078641	-1.957407	-1.352658
O	2.278988	-0.225409	-0.588333	C	-0.179857	-3.331650	-0.920970
C	2.539633	-0.262144	-2.011693	C	-0.943451	-4.054940	-2.031449
C	3.553526	0.850425	-2.277492	C	-1.896257	-2.954620	-2.524227
C	4.359282	0.863739	-0.970271	C	-1.027127	-1.698915	-2.418904
C	3.268432	0.603024	0.071072	H	-1.586584	-0.797235	-2.158990
H	2.785441	1.529006	0.390784	H	-0.459627	-1.518768	-3.342173
H	3.632086	0.065460	0.952954	H	-2.757408	-2.869420	-1.854493
H	4.883574	1.807524	-0.792949	H	-2.261923	-3.122807	-3.541809
H	5.101158	0.055935	-0.967418	H	-1.463148	-4.946458	-1.667350
H	3.033423	1.804155	-2.411581	H	-0.258691	-4.360681	-2.831823
H	4.164434	0.657529	-3.164648	H	0.834566	-3.712121	-0.764133
H	2.941893	-1.250880	-2.269129	H	-0.724981	-3.362613	0.029905
H	1.592795	-0.122323	-2.536255	F	0.865438	2.702856	0.677114
O	0.650776	-1.330273	1.787958	F	0.650378	2.227029	-1.432185
C	1.800123	-2.052723	2.246807	F	0.007908	4.163940	-0.684460

Table A3.5 (Continued).

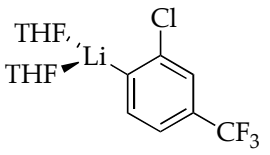

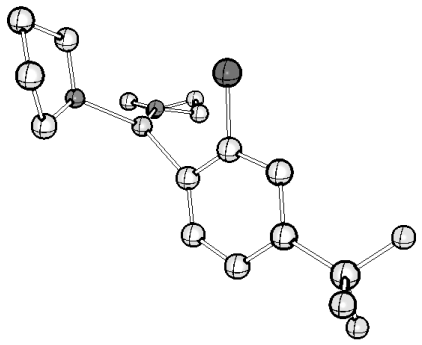

C
G = -1500.472097
G_{MP2} = -1496.741357

Atom	X	Y	Z	Atom	X	Y	Z
C	4.228498	-1.630255	-0.619511	C	1.726562	2.794350	-1.282569
O	2.877050	-1.419008	-0.152078	H	2.273506	3.163010	-2.160724
Li	1.656774	0.036753	-0.472780	H	0.794132	2.322429	-1.600537
C	-0.387058	-0.159538	-0.721856	H	1.332794	4.859306	-0.663125
C	-1.331327	-0.362525	-1.756929	H	0.738244	3.613785	0.455994
C	-2.709566	-0.442054	-1.545263	H	3.662707	4.390870	-0.063380
C	-3.220465	-0.320538	-0.248363	H	2.867534	4.244894	1.513379
C	-2.346981	-0.119577	0.824270	H	2.862492	1.837671	1.405926
C	-0.990575	-0.050571	0.523365	H	4.299277	2.122366	0.387380
Cl	0.112580	0.211146	1.974581	C	2.318401	-2.659529	0.362600
H	-2.720957	-0.029876	1.838178	C	3.513197	-3.597898	0.523913
C	-4.701189	-0.338895	-0.013961	C	4.432626	-3.147281	-0.622400
F	-5.260594	0.889051	-0.171340	H	5.480238	-3.425803	-0.475640
F	-5.019486	-0.745436	1.238368	H	4.095696	-3.576706	-1.572904
F	-5.344397	-1.161715	-0.877106	H	4.000738	-3.437602	1.492707
H	-3.391136	-0.605959	-2.375710	H	3.225457	-4.651031	0.457744
H	-0.977859	-0.468811	-2.783991	H	1.796768	-2.427836	1.293819
O	2.525862	1.767909	-0.635611	H	1.591270	-3.037927	-0.364923
C	3.231104	2.333916	0.501043	H	4.328027	-1.171807	-1.608279
C	2.906349	3.833029	0.500916	H	4.919705	-1.130360	0.071226
C	1.552788	3.880923	-0.226001				

Table A3.5 (Continued).

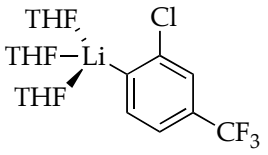

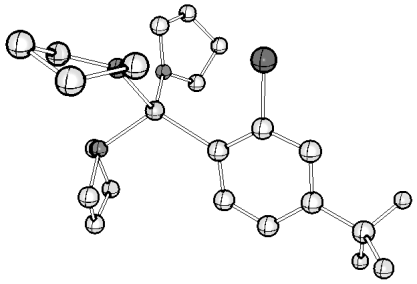

3a
G = -1732.822222
G_{MP2} = -1728.323065

Atom	X	Y	Z	Atom	X	Y	Z
Li	1.414884	0.079137	-0.074857	H	3.065675	0.909809	-2.390627
C	-0.709391	0.224189	-0.043682	O	2.344193	-0.242844	1.673865
C	-1.493806	1.330662	-0.459511	C	3.692392	0.178926	1.980854
C	-2.889252	1.368287	-0.432017	C	3.711550	0.529382	3.480924
C	-3.597033	0.254816	0.030979	C	2.221032	0.718350	3.812610
C	-2.896048	-0.877654	0.451294	C	1.564848	-0.304181	2.889933
C	-1.504453	-0.834355	0.387809	H	0.530871	-0.087316	2.618419
Cl	-0.689662	-2.378199	0.934688	H	1.618589	-1.318988	3.306587
H	-3.424713	-1.755922	0.804637	H	1.888821	1.730167	3.551711
C	-5.091590	0.299065	0.130641	H	1.990859	0.544727	4.868053
F	-5.513104	0.911761	1.267810	H	4.316411	1.416610	3.690630
F	-5.650470	0.986124	-0.896275	H	4.125264	-0.301156	4.063899
F	-5.646735	-0.936050	0.133017	H	4.386823	-0.632869	1.733197
H	-3.430971	2.247137	-0.772589	H	3.915908	1.037010	1.340102
H	-0.990801	2.223434	-0.838908	O	2.131888	-1.265583	-1.401593
O	2.421217	1.782679	-0.660842	C	2.851694	-2.422939	-0.909231
C	2.988107	1.915474	-1.974400	C	2.574105	-3.546315	-1.910744
C	2.024005	2.847823	-2.704661	C	1.166981	-3.187725	-2.413561
C	1.637106	3.852043	-1.597125	C	1.224704	-1.661353	-2.465205
C	1.864475	3.062714	-0.284414	H	0.264836	-1.174952	-2.276726
H	0.943138	2.857213	0.264747	H	1.635955	-1.303294	-3.419225
H	2.569229	3.578240	0.380806	H	0.409504	-3.508812	-1.691711
H	0.603402	4.194373	-1.694800	H	0.930859	-3.628130	-3.387003
H	2.282726	4.735886	-1.630316	H	2.627633	-4.535689	-1.446701
H	1.146265	2.284418	-3.038205	H	3.297606	-3.516848	-2.734490
H	2.475993	3.329335	-3.577137	H	3.911276	-2.157321	-0.832934
H	3.994653	2.356166	-1.901175	H	2.471644	-2.665045	0.089263

Table A3.5 (Continued).

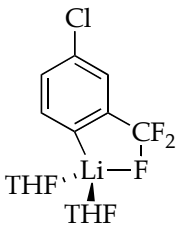

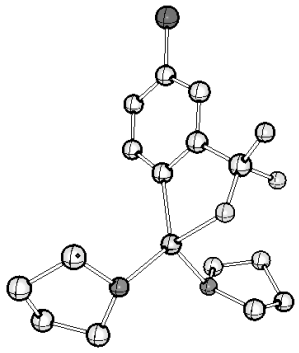

D
G = -1500.475537
G_{MP2} = -1496.746032

Atom	X	Y	Z	Atom	X	Y	Z
C	0.928658	-1.012816	1.482744	O	-2.299268	-1.328246	-0.680100
C	1.584391	-0.172928	0.426750	C	-1.748621	-1.930597	-1.881721
C	2.986545	-0.101788	0.456051	C	-1.412668	-3.363833	-1.483259
C	3.615938	0.617026	-0.550917	C	-2.559332	-3.697790	-0.515193
C	2.873361	1.242314	-1.552503	C	-2.772809	-2.368023	0.219323
C	1.478800	1.138183	-1.527622	H	-2.179853	-2.309365	1.137511
C	0.752596	0.430434	-0.543355	H	-3.822383	-2.168200	0.458139
Li	-1.228053	0.161675	0.028393	H	-2.318014	-4.512283	0.173744
O	-2.414558	1.597610	0.591841	H	-3.460506	-3.980430	-1.071828
C	-3.685001	1.862119	-0.032705	H	-0.450699	-3.388534	-0.961525
C	-3.498856	3.212694	-0.718366	H	-1.363035	-4.038487	-2.343076
C	-2.636748	3.968272	0.309662	H	-2.509025	-1.894967	-2.673993
C	-1.771916	2.857531	0.935483	H	-0.883206	-1.330569	-2.172890
H	-1.711113	2.932259	2.026135	H	0.939113	1.647314	-2.329082
H	-0.759119	2.816629	0.524806	H	3.384723	1.801577	-2.331573
H	-3.274602	4.434364	1.068871	Cl	5.380289	0.744753	-0.557808
H	-2.028154	4.755727	-0.143374	H	3.570370	-0.582161	1.234878
H	-4.447118	3.713763	-0.934719	F	0.748409	-2.312037	1.110809
H	-2.954283	3.082178	-1.660493	F	1.581797	-1.044088	2.659751
H	-3.894406	1.028414	-0.707441	F	-0.357376	-0.565965	1.776938
H	-4.470327	1.906035	0.735823				

Table A3.5 (Continued).

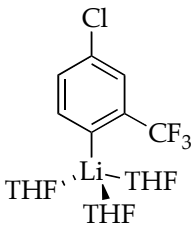

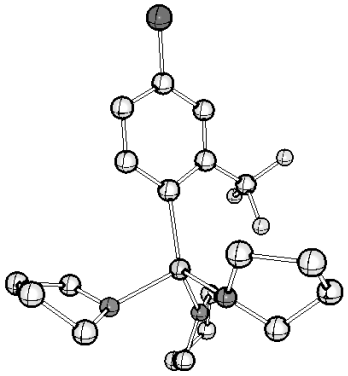

E
G = -1732.822473
G_{MP2} = -1728.324732

Atom	X	Y	Z	Atom	X	Y	Z
C	1.362083	-2.061318	-0.542082	H	-3.815293	0.580027	-0.655885
C	1.977997	-0.694734	-0.435157	H	-5.302976	-0.890849	-2.460373
C	3.378274	-0.638230	-0.530033	H	-3.931275	0.076652	-3.036293
C	3.986268	0.609180	-0.493216	H	-3.904220	-2.900539	-2.296116
C	3.222304	1.766658	-0.363672	H	-3.287784	-2.175582	-3.789894
C	1.831116	1.646140	-0.273308	H	-1.365095	-1.231360	-2.655703
C	1.120742	0.422996	-0.307311	H	-1.598911	-2.650666	-1.622697
Li	-0.960239	0.210810	0.114260	O	-1.928390	2.047014	-0.115734
O	-1.354895	-0.144046	2.097916	C	-1.524996	2.835676	-1.262682
C	-2.088741	-1.329699	2.470324	C	-1.350574	4.285558	-0.762185
C	-1.105062	-2.175068	3.275626	C	-1.355003	4.140185	0.771972
C	-0.315992	-1.095270	4.033898	C	-2.263027	2.929105	0.968110
C	-0.239095	0.048075	3.011722	H	-3.325098	3.213216	0.902376
H	0.676666	0.023419	2.415019	H	-2.101834	2.373935	1.894106
H	-0.334565	1.037540	3.472793	H	-1.721366	5.034631	1.285153
H	0.676477	-1.430380	4.348593	H	-0.349388	3.915794	1.143642
H	-0.864984	-0.780107	4.929205	H	-2.190166	4.909926	-1.087546
H	-0.446829	-2.726833	2.597989	H	-0.431570	4.741953	-1.140217
H	-1.605641	-2.888677	3.937337	H	-0.597561	2.394446	-1.636408
H	-2.959992	-1.040867	3.076924	H	-2.296382	2.757478	-2.038772
H	-2.435120	-1.800202	1.547502	H	1.277616	2.582621	-0.165647
O	-2.388145	-0.878552	-0.888548	H	3.711285	2.737032	-0.330954
C	-2.079722	-1.751213	-2.009238	Cl	5.749590	0.726110	-0.602319
C	-3.413297	-2.014102	-2.715206	H	3.980293	-1.536152	-0.623468
C	-4.220763	-0.751240	-2.378001	F	1.016705	-2.388769	-1.820074
C	-3.771254	-0.471722	-0.944651	F	2.170004	-3.059502	-0.108244
H	-4.351139	-1.067219	-0.224349	F	0.201784	-2.178032	0.180739

Table A3.6. Optimized geometries of reactants and monomer-based transition structures at B3LYP level of theory with 6-31G(d) basis set for the ortholithiation of **1** at -78 °C with free energies (Hartrees), and cartesian coordinates (X,Y,Z). (Note: G_{MP2} includes single point MP2 corrections to B3LYP/6-31G(d) optimized structures).

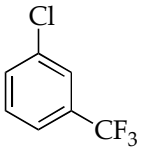

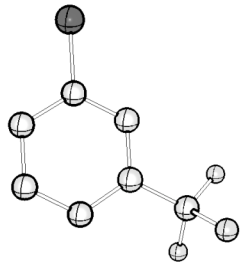

1
G = -1028.806251
G_{MP2} = -1026.746114

Atom	X	Y	Y
C	-2.022802	-0.354078	-0.001457
C	-0.643328	0.251689	-0.033108
C	-0.495501	1.640876	-0.019701
C	0.783061	2.195416	0.003163
C	1.912125	1.375235	0.012535
C	1.743556	-0.009039	-0.002061
C	0.475114	-0.584206	-0.024773
H	0.360420	-1.661422	-0.043478
Cl	3.156784	-1.051435	0.002466
H	2.910210	1.799814	0.027779
H	0.905815	3.274380	0.009824
H	-1.372674	2.278709	-0.035400
F	-2.913870	0.401844	-0.679607
F	-2.486544	-0.467172	1.264392
F	-2.042081	-1.591612	-0.541256

Table A3.6 (Continued).

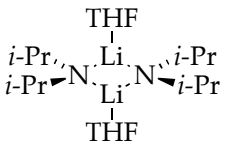

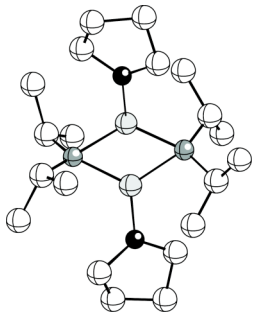

4
G = -1063.135499
G_{MP2} = -1059.937725

Atom	X	Y	Z	Atom	X	Y	Z
Li	-1.19464	-0.00774	0.01421	H	1.83816	-3.21720	1.36630
O	-3.18299	0.01572	-0.13583	H	-2.15959	-1.60468	1.84082
C	-3.98409	-1.09503	-0.60154	H	-1.26327	-2.26497	3.22164
C	-5.41144	-0.77445	-0.16155	H	-0.80287	-0.70251	2.54173
C	-5.43839	0.75767	-0.27769	H	-0.65863	-3.39245	1.09537
C	-4.03238	1.14387	0.19102	H	-1.65573	-2.60864	-2.05785
N	-0.01403	-1.64369	0.06875	H	-0.68498	-4.07367	-2.32132
C	-0.19692	-2.41025	1.31036	H	-1.50052	-3.82045	-0.77116
C	-1.16039	-1.70758	2.28179	H	1.87669	-1.33857	-1.92728
C	1.13099	-2.71953	2.04026	H	1.14764	-2.49745	-3.05209
Li	1.19465	0.00783	0.01436	H	0.26500	-1.03245	-2.60504
N	0.01400	1.64376	0.06872	H	1.00263	-3.33501	-0.73003
C	0.19652	2.41040	1.31033	H	3.90323	1.15737	-1.69393
C	1.15952	1.70771	2.28220	H	3.57283	2.00952	-0.16815
C	-1.13164	2.71990	2.03968	H	6.16235	1.26993	-0.78433
C	-0.27768	2.55391	-1.04433	H	5.57076	1.08298	0.87817
C	-0.93195	1.81412	-2.22127	H	5.59112	-1.05745	-1.32156
C	0.96199	3.31164	-1.57823	H	6.21990	-1.22706	0.32667
O	3.18302	-0.01557	-0.13517	H	3.99129	-1.30081	1.27554
C	4.03229	-1.14374	0.19184	H	3.63030	-2.03115	-0.30431
C	5.43806	-0.75816	-0.27799	H	-1.87605	1.33861	-1.92791
C	5.41178	0.77396	-0.16178	H	-1.14658	2.49738	-3.05257
C	3.98424	1.09517	-0.60075	H	-0.26417	1.03236	-2.60515
C	0.27810	-2.55390	-1.04412	H	1.65649	2.60840	-2.05742
C	0.93270	-1.81416	-2.22091	H	0.68595	4.07349	-2.32131
C	-0.96133	-3.31179	-1.57838	H	1.50097	3.82031	-0.77087
H	2.15887	1.60463	1.84163	H	-1.00225	3.33509	-0.73054
H	1.26211	2.26520	3.22203	H	-3.99064	1.30159	1.27458
H	0.80177	0.70272	2.54212	H	-3.63100	2.03110	-0.30596
H	-1.59922	1.79146	2.39591	H	-6.21992	1.22625	0.32760
H	-0.98370	3.37716	2.90874	H	-5.59242	1.05690	-1.32113
H	-1.83853	3.21752	1.36538	H	-5.56953	-1.08360	0.87850
H	0.65842	3.39254	1.09542	H	-6.16225	-1.27067	-0.78359
H	1.59838	-1.79101	2.39653	H	-3.90377	-1.15665	-1.69482
H	0.98277	-3.37667	2.90936	H	-3.57208	-2.00943	-0.16966

Table A3.6 (Continued).

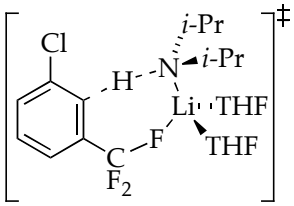

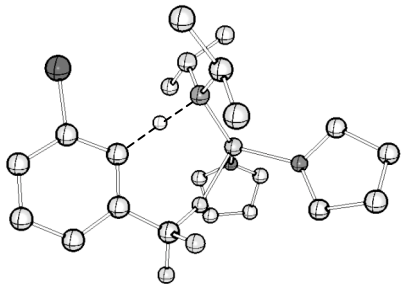

21
G = -1792.691253
G_{MP2} = -1787.893790
$\Delta G^{‡}$ = 20.2 kcal/mol
$\Delta G_{MP2}^{‡}$ = 12.2 kcal/mol

Atom	X	Y	Z	Atom	X	Y	Z
C	0.547744	-1.751918	-1.431940	H	-1.619713	-4.202638	2.584304
C	1.964405	-1.475261	-1.021925	H	-1.437177	-3.604604	0.927775
C	2.923706	-2.416344	-1.426851	H	-0.017417	-1.998246	2.042620
C	4.262518	-2.197764	-1.117503	H	-1.015858	-2.037437	3.519128
C	4.623060	-1.053991	-0.405722	C	0.742327	2.131285	1.792377
C	3.624101	-0.155589	-0.028813	H	1.718436	2.642057	1.764642
C	2.266898	-0.295004	-0.308794	C	-0.276591	3.144338	2.350397
H	1.326341	0.696764	0.079079	H	-0.353782	4.042927	1.728836
N	0.390341	1.615552	0.453824	H	-1.277707	2.692910	2.413298
Li	-1.103124	0.283914	0.467077	H	0.009120	3.467961	3.359714
O	-2.847194	0.610487	-0.496225	C	0.897395	0.969109	2.783267
C	-3.488886	1.911085	-0.441893	H	1.590898	0.213976	2.400179
C	-4.600047	1.865473	-1.491818	H	1.291875	1.331159	3.740465
C	-4.007071	0.916670	-2.545317	H	-0.069056	0.490221	2.983151
C	-3.277833	-0.111185	-1.679342	C	0.332044	2.678199	-0.573894
H	-2.393687	-0.542051	-2.154087	H	-0.511294	3.362000	-0.355683
H	-3.945853	-0.923962	-1.364703	C	1.589631	3.568433	-0.678707
H	-3.293175	1.451098	-3.181716	H	1.467784	4.301860	-1.486362
H	-4.762027	0.456601	-3.189432	H	1.782435	4.128377	0.241805
H	-4.836742	2.857264	-1.887555	H	2.478764	2.966028	-0.892299
H	-5.517050	1.441355	-1.065739	C	0.050600	2.063432	-1.952503
H	-3.852805	2.066679	0.578156	H	0.875388	1.420638	-2.274281
H	-2.739515	2.676798	-0.670628	H	-0.861358	1.457514	-1.941615
O	-1.804050	-0.993815	1.904336	H	-0.076582	2.850272	-2.706549
C	-1.034761	-2.096153	2.421358	Cl	4.191448	1.272307	0.900050
C	-1.782143	-3.340208	1.931366	H	5.660658	-0.865356	-0.146496
C	-3.264505	-2.879528	1.898408	H	5.021564	-2.913280	-1.421135
C	-3.183580	-1.347925	2.101138	H	2.629517	-3.308398	-1.971130
H	-3.482056	-1.066075	3.120584	F	0.292116	-3.061369	-1.649381
H	-3.765474	-0.766819	1.384753	F	0.153045	-1.097745	-2.551959
H	-3.857771	-3.345953	2.690659	F	-0.373417	-1.373305	-0.462774
H	-3.734112	-3.134009	0.943808				

Table A3.6 (Continued).

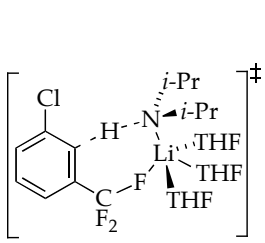

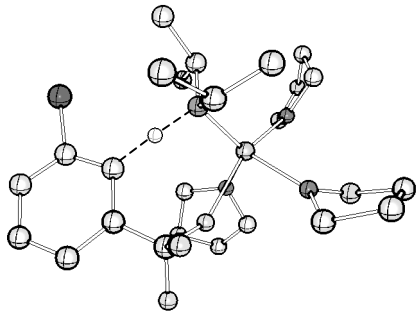

22
G = -2025.024264
G_{MP2} = -2019.460718
$\Delta G^{‡}$ = 30.4 kcal/mol
$\Delta G_{MP2}^{‡}$ = 14.0 kcal/mol

Atom	X	Y	Z	Atom	X	Y	Z
C	1.894567	-2.056084	-0.592524	H	1.526579	-2.207951	2.576220
C	2.970506	-1.087248	-0.191325	H	1.128542	0.113056	2.024400
C	4.241742	-1.635777	0.032121	H	0.230658	0.392432	3.542001
C	5.297999	-0.796993	0.372383	O	-3.039261	0.926147	0.722114
C	5.067082	0.571809	0.490684	C	-3.387435	1.211770	2.098918
C	3.780958	1.060984	0.254389	C	-4.507042	2.263921	2.057430
C	2.672201	0.292301	-0.099803	C	-4.316279	2.906956	0.674542
Cl	3.618310	2.838758	0.452326	C	-3.872641	1.707562	-0.157534
H	5.870767	1.249749	0.762072	H	-3.278140	1.965389	-1.035224
H	6.290448	-1.201862	0.549969	H	-4.736913	1.104709	-0.477696
H	4.401597	-2.705974	-0.053431	H	-3.518792	3.657685	0.701734
F	2.123392	-3.316399	-0.139251	H	-5.224101	3.379304	0.287384
F	1.737821	-2.165915	-1.938693	H	-4.431127	2.979635	2.881212
F	0.664066	-1.715135	-0.103897	H	-5.491290	1.784811	2.119385
Li	-1.103446	-0.018679	0.127261	H	-3.698532	0.281455	2.586927
O	-2.172304	-1.633827	-0.749242	H	-2.489259	1.580910	2.601529
C	-3.516352	-2.027136	-0.436960	N	0.170999	1.237104	-0.919056
C	-4.171417	-2.342441	-1.793923	C	-0.216503	2.629055	-0.621107
C	-2.963814	-2.692178	-2.708130	H	-1.287487	2.773661	-0.868298
C	-1.746701	-2.545084	-1.779040	C	-0.091250	2.862394	0.894121
H	-0.860088	-2.128007	-2.252077	H	-0.649041	2.108346	1.459372
H	-1.479780	-3.506357	-1.315774	H	0.954844	2.820127	1.210527
H	-2.895017	-1.990418	-3.543957	H	-0.486467	3.848422	1.170835
H	-3.029592	-3.701287	-3.125579	C	0.523187	3.765405	-1.366015
H	-4.707189	-1.469190	-2.177863	H	0.257137	3.799566	-2.426614
H	-4.891093	-3.162534	-1.711411	H	0.247308	4.737720	-0.935200
H	-3.489558	-2.922726	0.203452	H	1.607667	3.654620	-1.287473
H	-3.973012	-1.206492	0.115016	C	0.157464	0.835950	-2.343790
O	-0.791772	-0.658660	2.067490	H	0.254144	-0.257341	-2.319368
C	0.449891	-0.336804	2.750683	C	-1.166305	1.127239	-3.077552
C	0.952657	-1.657858	3.329322	H	-1.149504	0.700233	-4.089029
C	-0.361622	-2.387390	3.646568	H	-2.019087	0.690114	-2.543001
C	-1.250710	-1.968535	2.472242	H	-1.349309	2.202962	-3.185743

Table A3.6 (Continued).

H	-2.311795	-1.897236	2.735137	C	1.354255	1.297692	-3.215186
H	-1.144990	-2.649350	1.620721	H	1.382920	0.713329	-4.145369
H	-0.779998	-2.028100	4.594453	H	1.299741	2.353039	-3.495115
H	-0.251091	-3.473827	3.714990	H	2.299350	1.135743	-2.689473
H	1.589725	-1.511824	4.206616	H	1.415445	0.841583	-0.453604

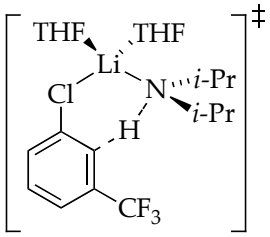

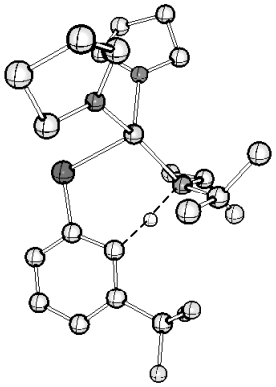

20
G = -1792.687140
G_{MP2} = -1787.890107
$\Delta G^{‡}$ = 22.7 kcal/mol
$\Delta G_{MP2}{}^{‡}$ = 14.5 kcal/mol

Atom	X	Y	Z	Atom	X	Y	Z
C	3.479230	-2.218775	-0.393569	H	4.518384	3.116270	2.579946
O	2.999478	-0.885316	-0.689354	H	2.511843	4.762001	1.718754
Li	1.313725	-0.041099	0.004941	H	3.598642	4.064870	0.501901
N	-0.196507	-1.149082	0.696694	H	1.462015	3.216000	-0.314552
C	-0.389619	-1.078667	2.156223	H	0.835341	3.028322	1.341132
H	-1.341898	-1.549451	2.449065	C	3.742283	-0.322021	-1.798089
C	0.719332	-1.789126	2.958159	C	4.642055	-1.448157	-2.317347
H	0.784215	-2.856056	2.718321	C	4.850587	-2.307602	-1.060690
H	1.701353	-1.339496	2.746681	H	5.139965	-3.338414	-1.284713
H	0.538463	-1.705300	4.037802	H	5.621335	-1.868108	-0.416339
C	-0.484696	0.387823	2.601039	H	4.124289	-2.026252	-3.091045
H	-1.285296	0.907689	2.068472	H	5.574860	-1.069565	-2.745301
H	-0.694654	0.453183	3.675925	H	3.029203	0.043079	-2.542922
H	0.457596	0.917094	2.410346	H	4.325616	0.528242	-1.423565
C	-0.224505	-2.528131	0.162652	H	3.499349	-2.334134	0.693125
H	0.669329	-3.081709	0.510790	H	2.777248	-2.949682	-0.811623
C	-1.442651	-3.378489	0.582772	C	-3.437435	0.546428	-0.495085
H	-1.398682	-4.363669	0.100759	C	-4.223218	1.399041	-1.279664
H	-1.475392	-3.549593	1.663904	C	-3.628127	2.162034	-2.283358
H	-2.381062	-2.897772	0.291714	C	-2.253761	2.065449	-2.494916
C	-0.147037	-2.491040	-1.372708	C	-1.538478	1.194877	-1.675907
H	-1.027939	-1.999135	-1.798232	C	-2.042811	0.403810	-0.663191
H	0.737054	-1.944365	-1.720108	Cl	0.263812	1.141837	-2.037840

Table A3.6 (Continued).

H	-0.097957	-3.508098	-1.781297	H	-1.762036	2.646681	-3.269254
O	2.234445	1.615295	0.729682	H	-4.227459	2.828791	-2.897022
C	1.734404	2.975449	0.714586	H	-5.291907	1.470665	-1.106013
C	2.869272	3.823845	1.284377	C	-4.144560	-0.297623	0.535928
C	3.484261	2.870514	2.321018	F	-3.450122	-0.410314	1.690587
C	3.367008	1.510400	1.624488	F	-4.362677	-1.564912	0.091579
H	3.186662	0.684131	2.319223	F	-5.364027	0.198725	0.864650
H	4.256478	1.277642	1.026511	H	-1.176942	-0.419911	0.071609
H	2.892392	2.880135	3.243337				

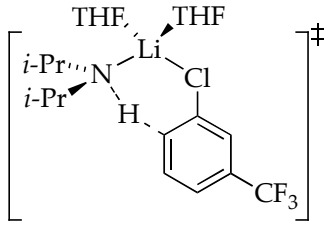

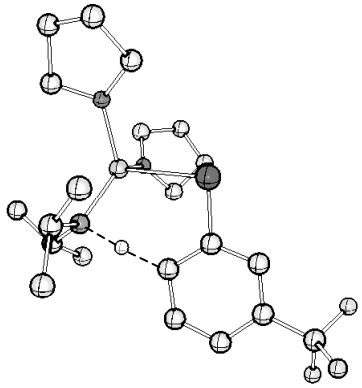

23
G = -1792.686523
G_{MP2} = -1787.888105
$\Delta G^{‡}$ = 23.1 kcal/mol
$\Delta G_{MP2}{}^{‡}$ = 15.7 kcal/mol

Atom	X	Y	Z	Atom	X	Y	Z
C	4.548756	-0.324498	-0.770219	H	2.327883	4.614006	0.576521
O	3.332471	0.449856	-0.936476	H	-0.106306	4.363551	1.990944
Li	1.703537	0.047088	0.181556	H	0.138061	3.709961	0.360225
N	1.149821	-1.810359	0.725085	H	-0.377417	1.655127	1.551745
C	1.473961	-2.202789	2.110056	H	0.499070	2.207716	3.005120
H	1.102926	-3.220765	2.320304	C	3.307758	1.066048	-2.249334
C	2.993125	-2.225986	2.374908	C	4.425592	0.389082	-3.042702
H	3.520664	-2.869606	1.661689	C	5.449517	0.064330	-1.943960
H	3.410789	-1.212726	2.290904	H	6.139694	-0.738275	-2.219155
H	3.217744	-2.598086	3.383586	H	6.042294	0.953129	-1.697503
C	0.792147	-1.274964	3.125859	H	4.058036	-0.532337	-3.508204
H	-0.294336	-1.267263	2.996584	H	4.824713	1.033662	-3.831187
H	1.013346	-1.599465	4.150094	H	2.312311	0.917692	-2.675316
H	1.154855	-0.246187	3.017237	H	3.487507	2.142744	-2.132455
C	1.320427	-2.933974	-0.221680	H	4.972734	-0.085053	0.209141
H	2.305222	-3.406313	-0.055485	H	4.285613	-1.387874	-0.788786
C	0.259357	-4.049220	-0.073989	C	-2.561586	-1.482525	0.968015
H	0.477466	-4.884750	-0.751719	C	-3.864004	-1.071913	0.683547

Table A3.6 (Continued).

H	0.226800	-4.455087	0.942563	C	-4.078229	-0.039595	-0.237665
H	-0.738307	-3.666431	-0.315661	C	-2.989213	0.570463	-0.865250
C	1.306960	-2.426267	-1.670597	C	-1.722994	0.103341	-0.526681
H	0.350117	-1.949788	-1.909737	C	-1.424574	-0.903484	0.368523
H	2.100926	-1.690383	-1.841922	Cl	-0.331664	0.960654	-1.375104
H	1.454356	-3.253822	-2.375538	H	-3.136445	1.375044	-1.577256
O	1.668402	1.657810	1.372684	C	-5.476277	0.371613	-0.596472
C	0.465850	2.248209	1.906611	F	-6.311780	0.306098	0.467187
C	0.505941	3.684437	1.390487	F	-5.531856	1.638364	-1.072852
C	2.014399	4.027844	1.445039	F	-6.013106	-0.424858	-1.554153
C	2.711497	2.645016	1.492700	H	-4.714385	-1.538655	1.172955
H	3.237897	2.494358	2.444672	H	-2.423388	-2.290982	1.687356
H	3.408731	2.467708	0.672002	H	-0.104959	-1.399607	0.609165
H	2.257958	4.610130	2.339152				

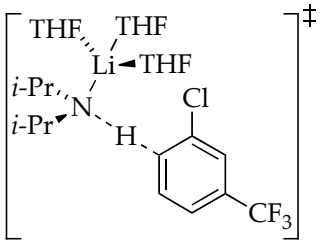

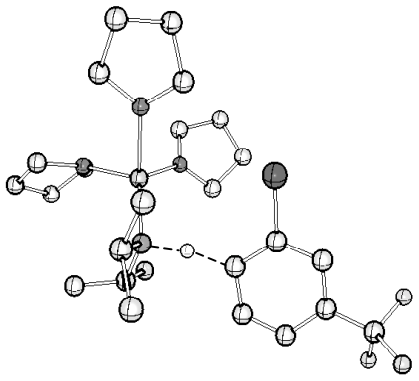

24
G = -2025.025028
G_{MP2} = -2019.458608
$\Delta G^{‡}$ = 30.0 kcal/mol
$\Delta G_{MP2}^{‡}$ = 15.3 kcal/mol

Atom	X	Y	Z	Atom	X	Y	Z
Li	1.859866	-0.091191	0.010361	C	4.873500	-2.289455	2.016501
N	0.605071	-1.545310	-0.771106	C	4.259025	-0.890996	1.943776
C	0.598268	-2.821929	-0.021326	H	5.004113	-0.111003	2.166087
H	-0.297909	-3.413326	-0.282334	H	3.388997	-0.744583	2.585906
C	1.804971	-3.738063	-0.296356	H	5.603040	-2.383992	2.826239
H	1.866938	-4.044064	-1.345619	H	4.085508	-3.030822	2.178639
H	2.739433	-3.229342	-0.035360	H	6.585565	-2.298318	0.638404
H	1.736163	-4.652875	0.306677	H	5.333745	-3.470074	0.220756
C	0.500611	-2.544274	1.484777	H	4.287339	-1.787122	-1.121852
H	-0.386134	-1.949409	1.718088	H	5.524138	-0.622957	-0.586044
H	0.435982	-3.483179	2.049032	O	1.345027	0.951877	1.698270
H	1.383134	-1.998222	1.843482	C	2.138571	1.967932	2.330260
C	0.685346	-1.751244	-2.237075	C	1.151192	3.060156	2.796754
H	1.654917	-2.217645	-2.491796	C	-0.239133	2.375658	2.708530

Table A3.6 (Continued).

C	-0.410986	-2.664552	-2.831254	C	0.091117	0.908653	2.411495
H	-0.292445	-2.739964	-3.919600	H	-0.633708	0.408698	1.768598
H	-0.369418	-3.682935	-2.430203	H	0.225390	0.326940	3.335583
H	-1.408550	-2.262821	-2.624072	H	-0.825918	2.794359	1.887351
C	0.649104	-0.396229	-2.955342	H	-0.820636	2.482231	3.628835
H	-0.293307	0.126406	-2.761327	H	1.196789	3.941830	2.150438
H	1.466992	0.249737	-2.618973	H	1.388123	3.389426	3.813116
H	4.032885	0.850155	-2.256263	H	2.672501	1.531401	3.187258
C	3.887886	1.738878	-1.633315	H	2.870467	2.306750	1.594616
O	2.613618	1.634694	-0.958800	C	-2.862419	-1.721783	0.104666
C	1.799790	2.791220	-1.270366	C	-4.233111	-1.549406	0.299276
C	2.792777	3.868998	-1.695537	C	-4.798815	-0.283956	0.116151
C	3.841922	3.037762	-2.450351	C	-3.985175	0.786375	-0.261031
H	3.498553	2.835809	-3.471082	C	-2.624738	0.540711	-0.437416
H	4.820434	3.522915	-2.513512	C	-1.984638	-0.680738	-0.273342
H	2.330709	4.644201	-2.313675	Cl	-1.654363	2.001911	-0.911055
H	3.239164	4.351645	-0.817435	H	-4.404221	1.776677	-0.402223
H	1.106112	2.535636	-2.079368	C	-6.277231	-0.083330	0.267067
H	1.215572	3.029564	-0.380152	F	-6.807474	-0.900342	1.209156
H	4.674039	1.761548	-0.869330	F	-6.589227	1.187471	0.619184
H	0.747064	-0.530611	-4.039907	F	-6.952238	-0.338490	-0.882574
O	3.812203	-0.763333	0.585602	H	-4.862218	-2.383074	0.598821
C	4.807943	-1.384646	-0.250110	H	-2.455592	-2.721354	0.256602
C	5.504103	-2.464533	0.614154	H	-0.600274	-1.040914	-0.535784

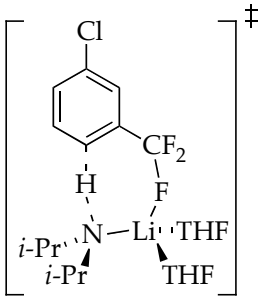

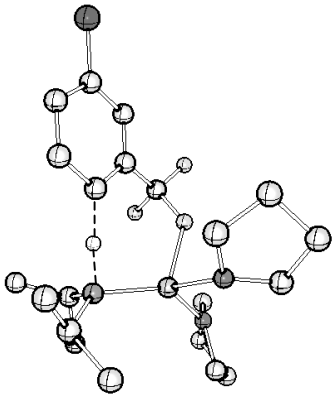

25
G = -1792.689753
G_{MP2} = -1787.890791
$\Delta G^{‡}$ = 21.1 kcal/mol
$\Delta G_{MP2}^{‡}$ = 14.0 kcal/mol

Atom	X	Y	Z	Atom	X	Y	Z
C	1.009448	-0.601446	-1.699157	H	1.208483	-3.581788	2.830537
C	2.113782	-0.072290	-0.835471	H	0.967471	-3.275082	1.098909
C	3.421763	-0.460759	-1.165118	H	0.768205	-1.009541	1.967823
C	4.465995	0.033170	-0.393768	H	-0.076997	-1.583686	3.434476

Table A3.6 (Continued).

C	4.217682	0.890961	0.675835	C	-1.109307	2.306452	2.036829
C	2.897032	1.250185	0.960978	H	-1.359123	3.373586	1.939071
C	1.785976	0.793410	0.228839	C	-2.353440	1.631257	2.649442
H	0.463742	1.302074	0.559530	H	-3.216296	1.731787	1.980029
N	-0.769510	1.744743	0.712389	H	-2.174466	0.560960	2.816220
Li	-1.366694	-0.128080	0.336673	H	-2.623424	2.079015	3.615762
O	-2.966953	-0.663162	-0.744886	C	0.066640	2.232386	3.027349
C	-4.333537	-0.554919	-0.275256	H	0.912551	2.828121	2.670249
C	-5.221999	-0.732287	-1.511923	H	-0.222805	2.612507	4.015617
C	-4.306974	-0.246743	-2.647408	H	0.414225	1.200064	3.154876
C	-2.943073	-0.758047	-2.191220	C	-0.932617	2.697220	-0.406132
H	-2.096743	-0.171392	-2.551922	H	-0.595762	2.150460	-1.297449
H	-2.791279	-1.808449	-2.473662	C	-2.394439	3.108454	-0.662220
H	-4.304348	0.847803	-2.699203	H	-2.477807	3.744765	-1.553363
H	-4.592265	-0.636416	-3.628938	H	-3.023371	2.223159	-0.813704
H	-6.154694	-0.166238	-1.434883	H	-2.809596	3.673579	0.181744
H	-5.477977	-1.788663	-1.654239	C	-0.030887	3.948464	-0.313974
H	-4.498618	-1.319395	0.490607	H	-0.115977	4.557729	-1.223122
H	-4.458896	0.432965	0.181996	H	-0.301382	4.590568	0.533212
O	-1.183312	-1.606045	1.669418	H	1.017443	3.655284	-0.198787
C	0.081129	-1.761478	2.362114	H	2.737127	1.922865	1.803531
C	0.501112	-3.201824	2.087718	H	5.045775	1.267610	1.269918
C	-0.851462	-3.932164	2.110142	Cl	6.124604	-0.440781	-0.773771
C	-1.803254	-2.901758	1.483730	H	3.625812	-1.130277	-1.993239
H	-2.789785	-2.890275	1.960285	F	1.368605	-1.629247	-2.493087
H	-1.936385	-3.058458	0.408035	F	0.442099	0.329993	-2.507842
H	-1.147284	-4.150240	3.142702	F	-0.052833	-1.089716	-0.938652
H	-0.843300	-4.875741	1.556751				

Table A3.6 (Continued).

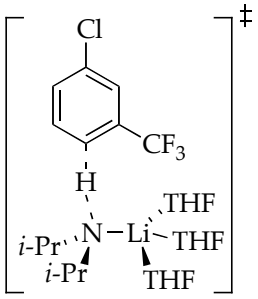

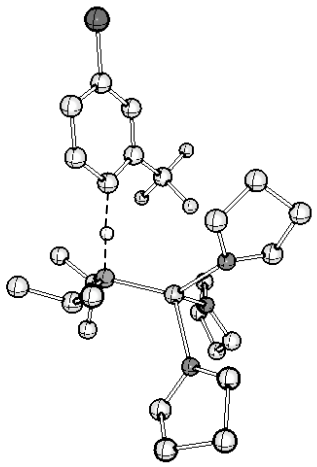

26
G = -2025.02701
G_{MP2} = -2019.461570
$\Delta G^{‡}$ = 28.7 kcal/mol
$\Delta G_{MP2}{}^{‡}$ = 13.5 kcal/mol

Atom	X	Y	Z	Atom	X	Y	Z
C	2.099262	-1.624323	-0.721682	H	1.728408	-1.635521	2.639896
C	2.891387	-0.407130	-0.340558	H	0.931180	0.500589	1.876597
C	4.250683	-0.583469	-0.043147	H	-0.013717	0.767339	3.371211
C	4.997620	0.536319	0.302979	O	-3.336708	0.752425	0.863634
C	4.410773	1.798412	0.348970	C	-3.649895	0.807927	2.276546
C	3.052332	1.920404	0.037999	C	-4.943238	1.620522	2.395066
C	2.227421	0.837168	-0.316901	C	-4.864250	2.538287	1.165905
H	2.626619	2.924127	0.079406	C	-4.238956	1.609291	0.127020
H	5.008667	2.663988	0.621231	H	-3.660107	2.125822	-0.640170
Cl	6.712246	0.349289	0.693571	H	-5.002565	0.987743	-0.363178
H	4.717189	-1.561609	-0.076280	H	-4.200686	3.388156	1.361791
F	2.763043	-2.790248	-0.537732	H	-5.836562	2.927797	0.850114
F	1.697469	-1.616813	-2.022139	H	-5.004878	2.165527	3.341648
F	0.942830	-1.734096	0.009690	H	-5.819724	0.965199	2.325066
Li	-1.419150	0.008313	0.143985	H	-3.746023	-0.215273	2.652190
O	-2.204758	-1.785105	-0.607560	H	-2.814120	1.289450	2.795368
C	-3.561247	-2.215728	-0.420267	N	-0.404284	1.334372	-1.073042
C	-4.023051	-2.724452	-1.799195	C	-0.732472	2.752432	-0.842172
C	-2.692621	-3.067307	-2.526597	H	-1.785416	2.942256	-1.123002
C	-1.614383	-2.774363	-1.471536	C	-0.623908	3.046192	0.664366
H	-0.686024	-2.367798	-1.866484	H	-1.270943	2.379339	1.244319
H	-1.383490	-3.671163	-0.877174	H	0.404555	2.909717	1.016126
H	-2.554730	-2.423415	-3.399701	H	-0.918920	4.079824	0.884455
H	-2.651662	-4.105984	-2.867416	C	0.096426	3.806203	-1.615832
H	-4.570040	-1.945794	-2.338717	H	-0.126307	3.799240	-2.686191
H	-4.686197	-3.589474	-1.703332	H	-0.130368	4.815084	-1.245618
H	-3.580048	-3.026828	0.324323	H	1.171381	3.633948	-1.496570
H	-4.119268	-1.364251	-0.032044	C	-0.545449	0.834256	-2.462252

Table A3.6 (Continued).

O	-0.833885	-0.572395	2.010383	H	-0.501673	-0.258986	-2.363539
C	0.332406	0.015233	2.649334	C	-1.905601	1.147890	-3.111824
C	1.049314	-1.142090	3.342118	H	-1.997488	0.632809	-4.076751
C	-0.116992	-2.072549	3.707426	H	-2.736686	0.820647	-2.474594
C	-1.036157	-1.919802	2.493561	H	-2.031565	2.219727	-3.306811
H	-2.097625	-2.044297	2.733689	C	0.600082	1.177656	-3.446961
H	-0.771695	-2.620659	1.695055	H	0.527176	0.538301	-4.337302
H	-0.618276	-1.721483	4.617617	H	0.568805	2.216004	-3.789440
H	0.188500	-3.110990	3.867403	H	1.573966	0.999982	-2.984742
H	1.629976	-0.812777	4.208739	H	0.835446	1.089365	-0.702770

Table A3.7. Optimized geometries of reactants and dimer-based transition structures at B3LYP level of theory with 6-31G(d) basis set for the ortholithiation of **1** at -78 °C with free energies (Hartrees), and cartesian coordinates (X,Y,Z). (Note: G_{MP2} includes single point MP2 corrections to B3LYP/6-31G(d) optimized structures).

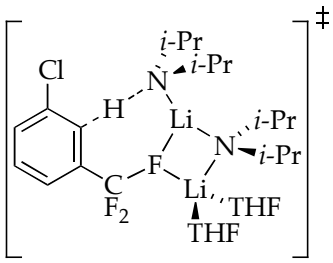

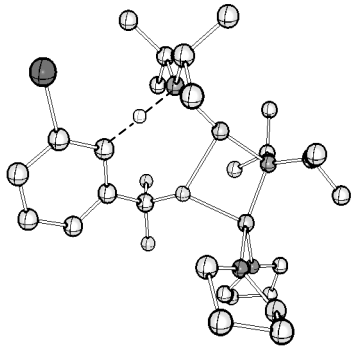

14
G = -2091.909073
G_{MP2} = -2085.993661
$\Delta G^{‡}$ = 20.5 kcal/mol
$\Delta G_{MP2}^{‡}$ = 13.5 kcal/mol

Atom	X	Y	Z	Atom	X	Y	Z
C	-0.494484	-1.372784	-1.460317	O	1.927643	-1.290283	1.636969
F	0.489120	-2.297221	-1.620070	C	3.033433	-1.608191	2.510313
F	0.029259	-0.476610	-0.521918	C	2.393771	-2.028433	3.831237
Li	2.126407	0.098417	0.192018	C	1.126970	-2.750103	3.347737
N	1.606287	2.037170	0.167737	C	0.708676	-1.916085	2.131731
Li	-0.380619	1.652531	0.033998	H	0.006426	-1.120169	2.397139
N	-2.375370	1.599570	0.003300	H	0.273559	-2.513373	1.327355
C	-2.970577	1.868175	1.327903	H	0.339126	-2.794696	4.104729
H	-4.057690	1.687000	1.307707	H	1.365036	-3.777197	3.047637
C	-2.402239	0.883271	2.360986	H	2.132108	-1.143940	4.423212
H	-2.871924	1.035144	3.340532	H	3.051996	-2.662026	4.433080
H	-2.582193	-0.152017	2.057262	H	3.620109	-2.425235	2.068148
H	-1.320543	1.020262	2.493280	H	3.668335	-0.721700	2.587517
C	-2.772410	3.316095	1.817351	O	3.799721	-0.641004	-0.629558
H	-3.257759	4.043129	1.157598	C	3.878567	-1.938047	-1.268409
H	-3.195486	3.450394	2.821483	C	4.939968	-1.782738	-2.354522
H	-1.705165	3.574144	1.863307	C	5.930789	-0.816860	-1.686677
C	-2.959430	2.429743	-1.075846	C	5.005236	0.122657	-0.905178
H	-2.697099	3.491957	-0.912913	H	4.718776	1.002948	-1.489758
C	-2.345013	2.031310	-2.424913	H	5.428065	0.457995	0.045476
H	-2.591653	0.996123	-2.682063	H	6.557204	-0.276444	-2.402034
H	-2.719697	2.678784	-3.226904	H	6.592314	-1.362870	-1.004030
H	-1.252626	2.124411	-2.417305	H	4.502085	-1.328818	-3.250913
C	-4.497161	2.376493	-1.196356	H	5.390893	-2.737859	-2.639268
H	-4.843263	1.353309	-1.376492	H	2.183997	2.414203	-3.201461
H	-4.998162	2.741833	-0.294269	C	1.210468	4.069403	-1.296293

Table A3.7 (Continued).

H	-4.831103	3.004996	-2.031869	H	1.242491	4.734589	-0.426874
F	-0.551499	-0.672911	-2.609251	H	1.609099	4.628699	-2.153599
C	2.098689	2.725271	1.374759	H	0.155064	3.848672	-1.506865
H	1.940544	3.817070	1.300177	H	4.174471	-2.687808	-0.521796
C	3.614125	2.537193	1.629098	H	2.884783	-2.185258	-1.644262
H	4.210351	2.818882	0.754210	C	-1.801784	-1.962503	-1.027212
H	3.961060	3.147619	2.473769	C	-2.788439	-1.109918	-0.489550
H	3.839315	1.486485	1.865946	C	-3.971448	-1.771176	-0.168160
C	1.326439	2.266274	2.617311	C	-4.207100	-3.134302	-0.356701
H	0.272283	2.555649	2.557003	C	-3.195237	-3.923966	-0.901341
H	1.371619	1.173112	2.721417	C	-1.978763	-3.338675	-1.239321
H	1.738207	2.706916	3.534028	H	-1.183038	-3.943041	-1.663115
C	2.009733	2.767011	-1.050284	H	-3.356840	-4.986802	-1.057780
H	3.073509	3.072627	-0.990521	H	-5.162989	-3.570158	-0.081580
C	1.895048	1.870642	-2.293543	Cl	-5.328434	-0.855247	0.560090
H	2.539768	0.987223	-2.212319	H	-2.602969	0.262955	-0.270294
H	0.869402	1.513885	-2.441531				

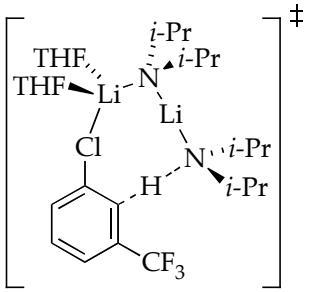

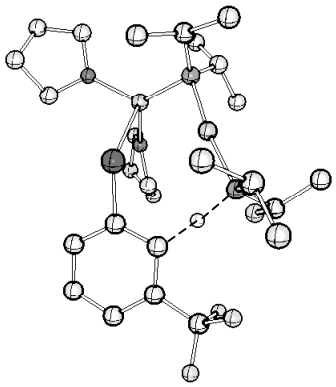

12
G = -2091.897802
G_{MP2} = -2085.98452
$\Delta G^{‡}$ = 27.6 kcal/mol
$\Delta G_{MP2}{}^{‡}$ = 19.3 kcal/mol

Atom	X	Y	Z	Atom	X	Y	Z
N	1.999882	1.967933	0.292844	H	-2.006141	1.319855	-2.783326
Li	2.393813	0.005958	0.226267	H	-1.996502	3.031866	-3.249239
O	1.876794	-1.403614	1.532529	H	-0.633496	2.351113	-2.358615
C	2.838468	-1.990841	2.440064	C	-3.949484	2.755344	-1.400180
C	2.130009	-3.190306	3.068961	H	-4.335502	1.779798	-1.708974
C	0.672916	-2.705600	3.116011	H	-4.511130	3.069885	-0.514833
C	0.545806	-1.928840	1.805210	H	-4.164302	3.478610	-2.197201
H	-0.151513	-1.090605	1.858422	C	2.476053	2.474924	1.595181
H	0.254959	-2.574510	0.970386	H	2.489231	3.579876	1.600571

Table A3.7 (Continued).

H	0.519308	-2.040661	3.973686	C	3.922290	2.036056	1.936826
H	-0.053537	-3.520186	3.184149	H	4.616452	2.277394	1.123969
H	2.536068	-3.444096	4.052544	H	4.293716	2.530006	2.845030
H	2.221296	-4.072032	2.423538	H	3.970149	0.950491	2.112450
H	3.731126	-2.249836	1.864128	C	1.543668	2.053933	2.736502
H	3.110967	-1.243741	3.197000	H	0.554182	2.510022	2.626990
O	3.962426	-0.906608	-0.604941	H	1.414930	0.963067	2.752464
C	3.817780	-2.113446	-1.394704	H	1.941816	2.356820	3.713275
C	4.964724	-2.074696	-2.402336	C	2.558299	2.795555	-0.796605
C	6.074936	-1.388981	-1.591077	H	3.621620	3.030485	-0.593064
C	5.293783	-0.352739	-0.777696	C	2.539401	2.057055	-2.143505
H	5.199640	0.600654	-1.308889	H	3.095569	1.113306	-2.092886
H	5.718072	-0.162368	0.211804	H	1.516714	1.818925	-2.458437
H	6.845736	-0.927912	-2.215095	H	2.987364	2.670976	-2.934790
H	6.564014	-2.111589	-0.927285	C	1.845742	4.158745	-0.963195
H	4.688650	-1.464517	-3.269917	H	1.817461	4.716189	-0.020715
H	5.240878	-3.071229	-2.759031	H	2.350415	4.791211	-1.706288
H	3.894618	-2.983632	-0.728887	H	0.808538	4.018558	-1.297582
H	2.823581	-2.100484	-1.847310	C	-3.520024	-1.705945	-0.620448
Li	0.006074	1.758639	0.020637	C	-2.383980	-0.877317	-0.758275
N	-1.989861	1.783907	-0.058426	C	-1.324124	-1.511712	-1.377664
C	-2.680302	2.027993	1.224028	C	-1.300482	-2.817097	-1.866318
H	-3.766758	1.876248	1.113219	C	-2.455638	-3.582046	-1.715566
C	-2.214764	1.001378	2.267370	C	-3.567798	-3.025831	-1.084699
H	-2.751790	1.140894	3.213782	H	-4.469128	-3.616138	-0.957575
H	-2.401251	-0.020346	1.928727	H	-2.486507	-4.602128	-2.088123
H	-1.143634	1.109169	2.479346	H	-0.418379	-3.221791	-2.354123
C	-2.485373	3.453202	1.777495	Cl	0.236863	-0.584345	-1.614589
H	-2.894620	4.216432	1.107294	C	-4.725974	-1.191432	0.128081
H	-2.986271	3.565384	2.747761	F	-5.042404	0.081621	-0.189604
H	-1.418635	3.675801	1.920685	F	-4.526437	-1.215071	1.473900
C	-2.428956	2.696583	-1.140883	F	-5.835914	-1.937207	-0.100601
H	-2.118190	3.730613	-0.899390	H	-2.256870	0.457281	-0.405062
C	-1.725368	2.326357	-2.454603				

Table A3.7 (Continued).

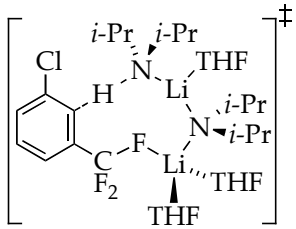

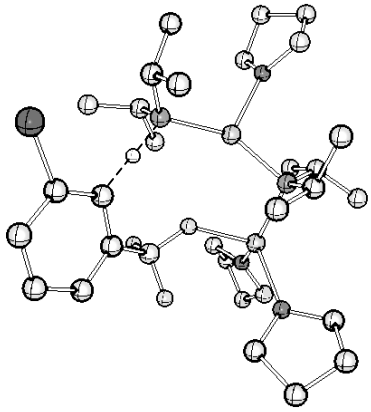

15
G = -2324.240665
G_{MP2} = -2317.559550
$\Delta G^{‡}$ = 31.7 kcal/mol
$\Delta G_{MP2}{}^{‡}$ = 16.0 kcal/mol

Atom	X	Y	Z	Atom	X	Y	Z
Li	1.994601	-0.544030	-0.065503	H	-3.484859	-3.537886	-1.771787
F	0.644657	0.935800	0.488421	H	-1.888819	-4.320632	-1.689205
C	0.859981	2.199555	0.991710	C	0.765266	-1.566299	-2.432405
F	2.191240	2.427839	0.816594	H	1.756674	-1.861889	-2.837219
F	0.687042	2.093326	2.334931	C	-0.256440	-2.360746	-3.278874
C	-0.013184	3.242832	0.367087	H	-0.129041	-2.146174	-4.347973
C	-1.362772	2.939181	0.074619	H	-0.142550	-3.442540	-3.148690
C	-2.068977	4.054919	-0.383251	H	-1.286821	-2.095926	-3.007036
C	-1.536888	5.333201	-0.569032	C	0.619885	-0.069986	-2.751894
C	-0.194972	5.559456	-0.274555	H	-0.339265	0.326068	-2.403127
C	0.574600	4.507102	0.206987	H	1.413356	0.517803	-2.278283
H	1.618224	4.666417	0.459000	H	0.679130	0.106872	-3.833395
H	0.238812	6.545808	-0.413229	C	0.897956	-3.197151	-0.609384
H	-2.166429	6.138380	-0.935536	H	0.098729	-3.845001	-1.017738
Cl	-3.815363	3.939417	-0.775100	C	2.224149	-3.829618	-1.094811
N	0.689488	-1.787428	-0.977426	H	2.299101	-4.875781	-0.769555
Li	-1.220812	-1.168606	-0.283536	C	0.830802	-3.356328	0.916150
N	-2.529984	0.373599	0.287851	H	-0.088926	-2.921575	1.321434
C	-3.677405	0.480357	-0.647531	H	0.856065	-4.414648	1.206395
H	-4.253842	1.393717	-0.442848	H	1.681173	-2.856185	1.394406
C	-4.692276	-0.678932	-0.591396	O	2.916818	-0.715793	1.742340
H	-5.242133	-0.710414	0.355798	C	4.324221	-1.031646	1.847398
H	-5.437160	-0.563087	-1.389377	C	4.675386	-0.881779	3.328550
H	-4.190295	-1.643067	-0.723125	C	3.352752	-1.265203	4.009267
C	-3.148748	0.618600	-2.079893	C	2.321028	-0.648679	3.065381
H	-2.415792	1.427529	-2.153005	H	2.122978	0.400193	3.302952
H	-2.668254	-0.310359	-2.418654	H	1.371296	-1.187939	3.034923
H	-3.964399	0.839361	-2.779246	H	3.262545	-0.881432	5.029669
C	-2.981412	0.223088	1.688775	H	3.241902	-2.355464	4.042837

Table A3.7 (Continued).

H	-3.690646	-0.619602	1.759864	H	4.934430	0.158744	3.557046
C	-1.804344	-0.138248	2.605559	H	5.517139	-1.515490	3.623329
H	-1.283460	-1.040401	2.255265	H	2.315848	-3.823647	-2.186286
H	-1.075144	0.672409	2.656318	H	3.087962	-3.289864	-0.679950
H	-2.155003	-0.338150	3.626483	H	4.476615	-2.062932	1.501193
C	-3.719955	1.450392	2.271560	H	4.873797	-0.355126	1.189213
H	-4.600079	1.715832	1.677451	O	3.686692	0.133556	-1.110013
H	-4.060458	1.246782	3.295670	C	4.056213	1.514624	-1.370505
H	-3.064235	2.327256	2.298503	C	5.127709	1.474583	-2.468249
O	-2.385961	-3.153647	-0.054410	C	4.853650	0.130770	-3.161131
C	-2.778307	-4.058303	-1.112214	C	4.437969	-0.741726	-1.981113
C	-3.435067	-5.258280	-0.424518	H	5.315322	-1.124852	-1.439278
C	-4.027355	-4.617807	0.839285	H	3.791551	-1.578738	-2.247414
C	-2.953389	-3.591186	1.199977	H	5.722462	-0.267308	-3.693679
H	-2.158912	-4.042927	1.809825	H	4.024122	0.221858	-3.871239
H	-3.343420	-2.714031	1.721018	H	6.131875	1.476370	-2.028229
H	-4.209759	-5.334067	1.646271	H	5.056264	2.332037	-3.143519
H	-4.973018	-4.114651	0.607257	H	3.155706	2.047429	-1.691120
H	-2.680282	-6.006665	-0.155221	H	4.411339	1.964575	-0.439484
H	-4.183087	-5.743257	-1.058891	H	-1.922346	1.634804	0.199905

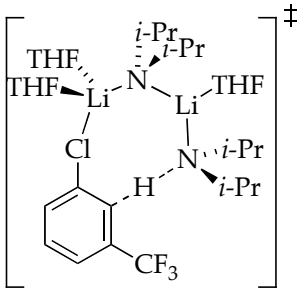

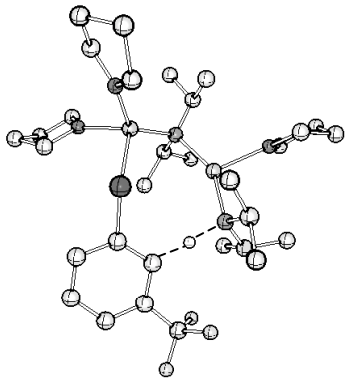

13
G = -2324.230678
G_{MP2} = -2317.552005
$\Delta G^{‡}$ = 37.9 kcal/mol
$\Delta G_{MP2}^{‡}$ = 20.8 kcal/mol

Atom	X	Y	Z	Atom	X	Y	Z
C	3.382045	1.015891	-0.332080	H	-2.824007	3.851274	0.707015
N	2.203611	0.714380	0.519915	H	-2.979647	2.124380	1.081464
Li	0.466508	1.561708	-0.285372	O	0.762616	3.802775	-0.250152
N	-1.467645	1.287755	-1.107929	C	0.909357	4.662765	-1.404321
Li	-2.300505	-0.239856	-0.118292	C	1.043327	6.089375	-0.860769
O	-3.362212	-0.245306	1.649267	C	1.668112	5.852625	0.522379

Table A3.7 (Continued).

C	-4.808641	-0.261167	1.648793	C	0.974175	4.563144	0.958891
C	-5.224051	-0.355642	3.117705	H	0.001053	4.773516	1.423908
C	-4.083964	0.398676	3.818722	H	1.568107	3.951605	1.642021
C	-2.867045	-0.026970	2.996743	H	1.499326	6.676832	1.222208
H	-2.434472	-0.965087	3.362064	H	2.748716	5.693058	0.434254
H	-2.078319	0.727470	2.950170	H	0.056278	6.555766	-0.758598
H	-3.979937	0.142099	4.876989	H	1.652637	6.725287	-1.509948
H	-4.239462	1.481250	3.743809	H	1.808610	4.354006	-1.951999
H	-5.248020	-1.402108	3.444099	H	0.039869	4.525147	-2.051455
H	-6.210810	0.080385	3.299810	C	2.424610	1.096429	1.930643
H	-5.168500	0.669126	1.189416	H	2.690656	2.167437	1.984048
H	-5.138542	-1.104106	1.037062	C	1.133342	0.944261	2.746173
O	-3.480779	-1.670937	-0.990813	H	0.302690	1.501902	2.290771
C	-3.374890	-3.073395	-0.637457	H	0.828863	-0.103216	2.816850
C	-4.399248	-3.797184	-1.511847	H	1.271693	1.329124	3.764953
C	-4.400443	-2.931468	-2.780956	C	3.565079	0.340891	2.649418
C	-4.258453	-1.522321	-2.204670	H	4.526140	0.478600	2.145146
H	-5.234512	-1.093509	-1.941698	H	3.675968	0.703938	3.680055
H	-3.733044	-0.826667	-2.862162	H	3.364127	-0.734557	2.684921
H	-5.305232	-3.045685	-3.385119	H	4.213176	0.337549	-0.092412
H	-3.536424	-3.175483	-3.409464	F	4.581298	-1.794996	-1.393960
H	-5.388935	-3.785889	-1.039343	C	4.493295	-2.519192	-0.249989
H	-4.123450	-4.839348	-1.697486	C	3.089793	-3.012270	0.016731
H	-2.352703	-3.409100	-0.845831	C	2.066169	-2.093321	0.365132
H	-3.559688	-3.167187	0.436019	C	0.855957	-2.723445	0.601520
C	-1.350071	0.893230	-2.522863	C	0.585221	-4.089242	0.511509
H	-2.350715	0.741381	-2.979435	C	1.625161	-4.935918	0.142877
C	-0.652996	1.921690	-3.442865	C	2.884607	-4.392601	-0.099257
H	-0.614449	1.557672	-4.477950	H	3.708888	-5.042845	-0.369363
H	-1.180926	2.881738	-3.454464	H	1.459276	-6.006471	0.060248
H	0.378172	2.107971	-3.117040	H	-0.402745	-4.479821	0.737154
C	-0.626343	-0.457457	-2.635639	Cl	-0.579216	-1.746297	1.159745
H	0.382998	-0.407330	-2.214374	F	4.964073	-1.734696	0.747833
H	-1.165192	-1.247464	-2.099931	F	5.385926	-3.534073	-0.383462
H	-0.534730	-0.768905	-3.683952	C	3.953573	2.441885	-0.203936
C	-2.246084	2.525410	-0.933232	H	4.395615	2.633292	0.779744
H	-1.741190	3.392634	-1.401998	H	4.747186	2.592799	-0.946984
C	-3.670943	2.501740	-1.537875	H	3.171998	3.189021	-0.378421
H	-3.660654	2.374077	-2.625417	C	3.017802	0.757772	-1.799140
H	-4.260998	1.676637	-1.111525	H	2.590950	-0.239401	-1.931586
H	-4.202933	3.438562	-1.325401	H	2.288241	1.496354	-2.160452
C	-2.363433	2.865819	0.559729	H	3.902779	0.829497	-2.443124
H	-1.380127	2.881815	1.040951	H	2.144451	-0.690918	0.462667

Table A3.7 (Continued).

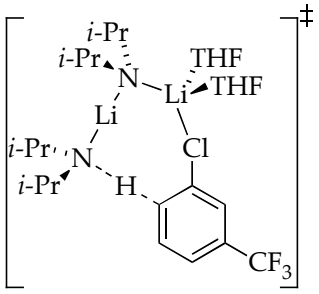

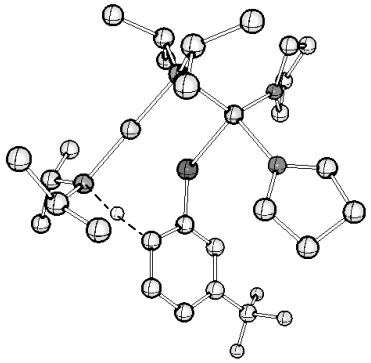

16
G = -2091.89831
G_{MP2} = -2085.985027
$\Delta G^{‡}$ = 27.3 kcal/mol
$\Delta G_{MP2}^{‡}$ = 18.9 kcal/mol

Atom	X	Y	Z	Atom	X	Y	Z
N	2.930733	0.326087	0.398201	H	-1.558793	3.972213	-2.169631
Li	1.560061	-1.178484	0.276513	H	-1.367006	5.337343	-1.059285
O	0.129324	-1.712758	1.596862	H	-0.750023	5.456579	-2.711446
C	-0.205904	-3.100920	1.844125	C	3.565880	0.266455	1.730843
C	-1.227502	-3.092615	2.982977	H	4.520511	0.820851	1.729356
C	-1.934002	-1.744388	2.774811	C	3.917654	-1.171843	2.180741
C	-0.775189	-0.849021	2.341747	H	4.524985	-1.685116	1.426702
H	-0.235773	-0.448656	3.208665	C	2.694202	0.931408	2.800643
H	-1.070069	-0.025208	1.689868	H	2.578849	2.003303	2.606245
H	-2.422448	-1.372207	3.680169	H	1.693835	0.481707	2.823638
H	-2.690745	-1.814435	1.986384	H	3.128835	0.820808	3.802197
H	-0.720002	-3.113990	3.954621	C	3.969294	0.282391	-0.652070
H	-1.905322	-3.949987	2.935052	H	4.717909	-0.503877	-0.423229
H	-0.634230	-3.523239	0.927451	C	3.373425	-0.076079	-2.021716
H	0.714343	-3.641601	2.083750	H	2.871536	-1.049967	-2.001233
O	1.918988	-2.982739	-0.593910	H	2.637033	0.670394	-2.343631
C	1.089818	-3.632234	-1.589161	H	4.154310	-0.113732	-2.791341
C	2.062350	-4.389520	-2.489395	C	4.768955	1.599889	-0.796824
C	3.137369	-4.831133	-1.484575	H	5.199803	1.923393	0.156382
C	3.219496	-3.628997	-0.537844	H	5.595029	1.492350	-1.512847
H	3.970382	-2.900526	-0.861281	H	4.119646	2.409476	-1.158797
H	3.424102	-3.906255	0.499988	C	-3.076702	2.075887	0.074746
H	4.101082	-5.054667	-1.950895	C	-1.797884	1.732307	-0.408240
H	2.807597	-5.726004	-0.944029	C	-1.733266	0.460588	-0.945175
H	2.488569	-3.715944	-3.241549	C	-2.770603	-0.462237	-1.022647
H	1.585618	-5.225700	-3.009126	C	-4.008739	-0.076256	-0.500779
H	0.397592	-4.319358	-1.083698	C	-4.165549	1.202308	0.044937
H	0.511767	-2.858358	-2.097725	H	-5.132094	1.503323	0.438570
H	4.487155	-1.176444	3.120201	C	-5.121387	-1.078504	-0.445809
H	3.004454	-1.762241	2.348069	F	-6.340362	-0.500079	-0.410802

Table A3.7 (Continued).

Li	1.667132	1.835339	0.003959	H	1.145995	5.064040	-1.229988
N	0.405417	3.383759	-0.174600	C	1.110411	3.400049	-2.557750
C	0.282812	4.241352	1.023235	H	0.525680	2.499725	-2.778071
H	-0.413202	5.076385	0.825685	H	1.158140	3.999135	-3.475665
C	-0.304165	3.458578	2.206704	H	2.136254	3.093302	-2.315198
H	-0.348247	4.090461	3.102083	C	-0.878472	4.773529	-1.861881
H	-1.314769	3.100297	1.993468	F	-5.103041	-1.926379	-1.500826
H	0.315303	2.586706	2.451583	F	-5.033753	-1.861129	0.669047
C	1.624980	4.878498	1.436542	H	-2.636839	-1.442629	-1.467851
H	2.076758	5.443643	0.614211	Cl	-0.132556	-0.110390	-1.621528
H	1.493781	5.569194	2.280172	H	-3.229755	3.069028	0.498586
H	2.343943	4.107012	1.743107	H	-0.682222	2.606036	-0.292946
C	0.483967	4.200981	-1.409481				

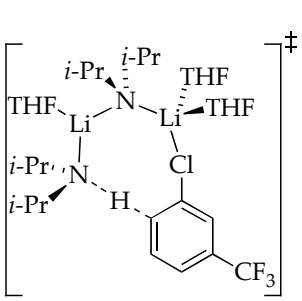

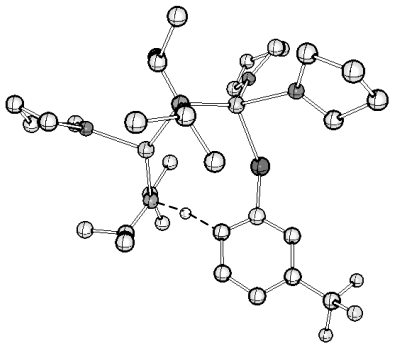

17
G = -2324.23695
G_{MP2} = -2317.556712
$\Delta G^{‡}$ = 34.0 kcal/mol
$\Delta G_{MP2}^{‡}$ = 17.8 kcal/mol

Atom	X	Y	Z	Atom	X	Y	Z
N	1.718676	1.115895	-1.084696	H	-0.555634	-3.224665	2.672606
Li	0.233451	1.974734	-0.017449	O	4.184641	-1.235028	-0.394244
O	0.384983	3.018609	1.752338	C	4.995955	-1.435919	-1.575260
C	0.113239	4.436696	1.831944	C	6.429202	-1.635428	-1.074709
C	-0.080454	4.735645	3.318099	C	6.203164	-2.263451	0.308698
C	0.878482	3.726987	3.968301	C	4.960642	-1.516404	0.792523
C	0.714169	2.500498	3.068461	H	5.227409	-0.565963	1.274209
H	-0.107632	1.856609	3.398378	H	4.335880	-2.097177	1.474934
H	1.619892	1.895944	2.979818	H	7.054050	-2.141639	0.985766
H	0.636777	3.509046	5.012614	H	4.626168	-2.324537	-2.102693
H	1.908673	4.100128	3.927894	H	4.878471	-0.566276	-2.225867
H	-1.114452	4.529580	3.618657	C	1.241288	0.970393	-2.471708
H	0.147476	5.776186	3.567973	H	1.089238	1.959488	-2.952449
H	0.973508	4.984588	1.423014	C	2.195084	0.212454	-3.423994
H	-0.762531	4.644328	1.214051	H	1.771669	0.151907	-4.435005

Table A3.7 (Continued).

O	-1.154623	3.238722	-0.915194	H	3.169481	0.706473	-3.508044
C	-2.598566	3.072184	-0.858175	H	2.366571	-0.814509	-3.075094
C	-3.178680	4.056785	-1.878860	C	-0.131857	0.282754	-2.484098
C	-2.033968	4.193044	-2.893790	H	-0.093396	-0.702163	-2.007314
C	-0.808940	4.150428	-1.983953	H	-0.879504	0.873845	-1.944403
H	-0.596154	5.140096	-1.554686	H	-0.496862	0.146291	-3.510029
H	0.093465	3.772996	-2.467418	C	2.989937	1.855370	-1.001442
H	-2.084697	5.111698	-3.485856	H	3.808524	1.310987	-1.513865
H	-2.024934	3.340078	-3.581812	C	2.982465	3.269729	-1.629063
H	-3.387126	5.025110	-1.408396	H	2.762678	3.249259	-2.701812
H	-4.109238	3.689313	-2.320794	H	2.229149	3.906449	-1.142877
H	-2.830490	2.032605	-1.110702	H	3.959217	3.756527	-1.507384
H	-2.929163	3.259770	0.167178	C	3.426764	1.988624	0.464440
Li	2.077962	-0.810087	-0.314074	H	3.444205	1.014052	0.964258
N	1.154304	-2.455745	0.545580	H	4.432357	2.422038	0.540325
C	1.271972	-3.723131	-0.210526	H	2.736571	2.637040	1.016542
H	0.496509	-4.439930	0.119647	C	-2.373948	-0.963684	0.631578
C	2.621263	-4.450756	-0.056546	H	0.755753	-3.660827	3.789424
H	2.800434	-4.796120	0.967037	C	-1.571984	-2.040002	0.298949
H	2.652427	-5.334953	-0.705982	C	-2.305231	-3.143465	-0.192692
H	3.445370	-3.786618	-0.342152	C	-3.692713	-3.147119	-0.336559
C	1.014593	-3.460153	-1.700035	C	-4.426740	-2.011615	0.020937
H	0.060905	-2.949418	-1.857038	C	-3.760081	-0.890382	0.519034
H	1.809979	-2.837213	-2.131793	H	-4.312358	-0.006471	0.818959
H	0.992723	-4.400895	-2.264467	C	-5.911403	-1.972529	-0.183989
C	1.437818	-2.626922	1.985696	F	-6.243930	-1.619530	-1.453101
H	2.451828	-3.044336	2.119025	F	-6.520272	-1.078175	0.632005
C	1.439373	-1.259720	2.681094	F	-6.488218	-3.176509	0.039037
H	2.180381	-0.584881	2.230815	H	-4.209498	-4.025238	-0.714058
H	0.459117	-0.780406	2.604695	H	-1.767733	-4.048166	-0.473714
H	1.689598	-1.360824	3.744933	Cl	-1.606619	0.548624	1.320147
C	0.477534	-3.582693	2.730429	H	-0.150161	-2.166926	0.444391
H	0.503420	-4.594135	2.310769				

Table A3.7 (Continued).

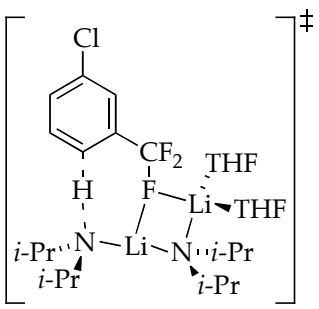

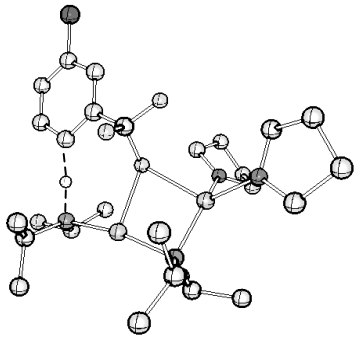

18
G = -2091.906847
G_{MP2} = -2085.989806
$\Delta G^{‡}$ = 21.9 kcal/mol
$\Delta G_{MP2}^{‡}$ = 15.9 kcal/mol

Atom	X	Y	Z	Atom	X	Y	Z
C	-1.016912	-1.025891	-1.186328	C	2.651738	-1.665946	2.780365
F	-0.440688	-2.259098	-1.190432	C	1.891826	-2.055811	4.046670
F	-0.181076	-0.261089	-0.360827	C	0.634859	-2.720392	3.465214
Li	2.050968	-0.260269	0.151503	C	0.344196	-1.854693	2.237722
N	2.181464	1.725892	-0.166606	H	-0.302917	-1.005350	2.476976
Li	0.193359	1.958297	-0.113946	H	-0.094896	-2.408446	1.405567
N	-1.678389	2.564426	0.185278	H	-0.207022	-2.740360	4.162856
C	-1.971104	2.934364	1.587532	H	0.852203	-3.752933	3.167297
H	-1.322845	3.775691	1.894393	H	1.623327	-1.160419	4.618857
C	-3.420897	3.382675	1.871380	H	2.473146	-2.716468	4.696469
H	-3.541093	3.619955	2.935973	H	3.253497	-2.501641	2.397547
H	-3.699815	4.276967	1.305335	H	3.299547	-0.794232	2.904745
H	-4.134946	2.589254	1.622308	O	3.252352	-1.582775	-0.724780
C	-1.632751	1.748474	2.505776	C	2.916185	-2.983080	-0.896148
H	-0.598477	1.414261	2.364208	C	3.910773	-3.522001	-1.924979
H	-1.747062	2.027403	3.560283	C	5.151630	-2.657064	-1.655289
H	-2.294243	0.899695	2.301417	C	4.528808	-1.294388	-1.352498
C	-2.129575	3.558299	-0.807609	H	4.344465	-0.719183	-2.266945
H	-3.224967	3.693354	-0.750192	H	5.112794	-0.680105	-0.663133
C	-1.495074	4.948693	-0.624743	H	5.844646	-2.617696	-2.500583
H	-0.400164	4.884884	-0.689491	H	5.699228	-3.033579	-0.783085
H	-1.839407	5.639421	-1.405157	H	3.539177	-3.351372	-2.941902
H	-1.745103	5.395047	0.343668	H	4.093227	-4.593844	-1.805011
C	-1.835252	3.031491	-2.219859	H	3.022832	-3.487263	0.072779
H	-0.753220	2.971113	-2.404677	H	1.873664	-3.045329	-1.213793
H	-2.262207	2.035126	-2.367372	C	-2.441153	-1.024142	-0.728364
H	-2.254824	3.701254	-2.980379	C	-3.018788	0.194628	-0.325377
F	-0.833325	-0.513835	-2.419423	C	-4.387799	0.104182	-0.012451
C	2.930290	2.404520	0.905031	C	-5.125554	-1.080425	-0.082714

Table A3.7 (Continued).

H	3.074396	3.475501	0.675093	C	-4.481990	-2.251860	-0.480418
C	4.348897	1.834382	1.145714	C	-3.134424	-2.243569	-0.813672
H	4.953021	1.852813	0.231862	H	2.477726	1.362541	-3.563755
H	4.890587	2.410671	1.907565	C	2.626946	3.517317	-1.921571
H	4.297415	0.790997	1.491488	H	3.149972	4.184010	-1.228707
C	2.139843	2.364423	2.219509	H	3.063643	3.675042	-2.916531
H	1.197439	2.918409	2.133054	H	1.576666	3.835900	-1.960512
H	1.897297	1.330903	2.502876	O	1.634657	-1.333325	1.807861
H	2.709190	2.812542	3.043342	H	-2.647337	-3.158633	-1.132628
C	2.731592	2.032963	-1.501182	Cl	-5.385820	-3.767997	-0.563470
H	3.811241	1.782193	-1.554863	H	-6.182816	-1.103718	0.167009
C	2.041894	1.176758	-2.574369	H	-4.920166	1.002230	0.303591
H	2.135024	0.104715	-2.364904	H	-2.308937	1.443608	-0.085067
H	0.972041	1.406265	-2.644811				

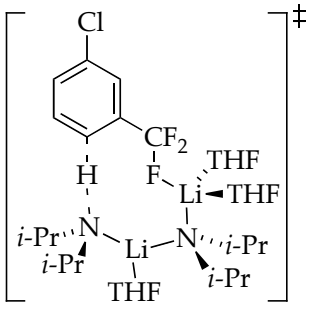

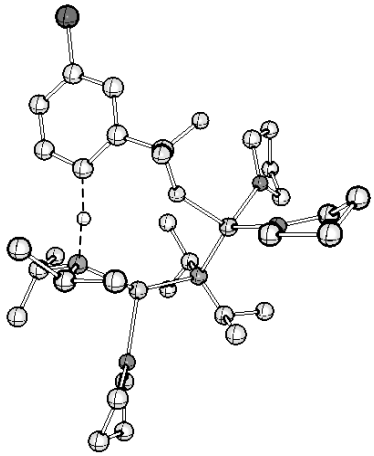

19
G = -2324.242208
G_{MP2} = -2317.55991
$\Delta G^{‡}$ = 30.7 kcal/mol
$\Delta G_{MP2}^{‡}$ = 15.8 kcal/mol

Atom	X	Y	Z	Atom	X	Y	Z
Li	-0.272486	1.933725	-0.045018	H	6.705227	0.601706	-0.476194
F	-1.066358	0.176203	0.617594	H	7.252240	-0.838950	-1.354867
C	-2.210185	-0.412128	1.124240	H	4.979452	-1.470722	-1.924707
F	-3.176513	0.539150	1.036513	H	4.802161	0.301060	-1.938842
F	-1.968428	-0.564587	2.453434	C	1.103494	1.282301	-2.458562
C	-2.545381	-1.690166	0.423256	H	0.840322	2.273557	-2.883972
C	-1.497930	-2.560571	0.063241	C	2.250223	0.761981	-3.356466
C	-1.941231	-3.761348	-0.529386	H	1.938406	0.729697	-4.408586
C	-3.284543	-4.075305	-0.752849	H	3.138515	1.400940	-3.300042
C	-4.262924	-3.159519	-0.370157	H	2.547514	-0.255093	-3.067925
C	-3.910732	-1.956671	0.224928	C	-0.134376	0.396818	-2.669456
H	-4.678396	-1.250680	0.522986	H	0.016192	-0.608991	-2.263962

Table A3.7 (Continued).

Cl	-5.970584	-3.525672	-0.646504	H	-1.015857	0.819219	-2.176339
H	-3.574640	-5.014147	-1.216642	H	3.482898	1.919477	-1.211730
H	-1.205990	-4.501911	-0.841668	C	2.379802	3.736995	-1.269331
N	1.417860	1.380141	-1.022053	H	2.251418	3.778989	-2.356398
Li	1.950534	-0.540460	-0.320384	H	1.506997	4.220568	-0.807015
N	1.269358	-2.400283	0.344700	H	3.262775	4.341872	-1.023984
C	1.638588	-3.543957	-0.521899	C	2.814269	2.352699	0.759648
H	1.017842	-4.425980	-0.276228	H	2.954753	1.351740	1.181369
C	3.102729	-4.009700	-0.406448	H	3.718177	2.936270	0.977291
H	3.335644	-4.429816	0.577746	H	1.974285	2.824693	1.282829
H	3.310164	-4.791755	-1.147936	O	-0.481151	2.889014	1.746045
H	3.785374	-3.172114	-0.589669	C	-0.948764	4.249934	1.865862
C	1.338061	-3.194278	-1.984989	C	-1.431921	4.388238	3.308443
H	0.305088	-2.858328	-2.109055	C	-0.450877	3.471730	4.055185
H	2.002553	-2.395967	-2.343417	C	-0.262457	2.318608	3.065115
H	1.492980	-4.064877	-2.634857	H	-0.993882	1.520462	3.215013
C	1.581786	-2.651007	1.768363	H	0.740877	1.884809	3.087856
H	2.651928	-2.898580	1.873859	H	-0.829461	3.127310	5.021877
C	1.355820	-1.377971	2.595445	H	0.498589	3.991864	4.227904
H	1.941751	-0.534994	2.204491	H	-2.457357	4.012440	3.404861
H	0.303412	-1.086874	2.596157	H	-1.412036	5.424273	3.659753
H	1.661965	-1.533261	3.638028	H	-0.114002	4.933546	1.656256
H	-0.368966	0.296472	-3.736858	H	-1.726563	4.400102	1.114708
C	2.544804	2.288272	-0.750770	O	-1.765508	3.020126	-1.043126
C	0.802288	-3.822090	2.409975	C	-3.153287	2.619612	-1.214364
H	0.989009	-4.768623	1.891350	C	-3.710642	3.473258	-2.362431
H	1.103330	-3.957795	3.456971	C	-2.444148	3.877364	-3.132665
H	-0.276129	-3.635881	2.384074	C	-1.440821	4.055138	-1.998011
O	4.151666	-0.633512	-0.213738	H	-1.552106	5.038884	-1.518209
C	5.076733	-0.557356	-1.322771	H	-0.399660	3.918918	-2.292555
C	6.469342	-0.445536	-0.699518	H	-2.571326	4.785865	-3.728880
C	6.299726	-1.245704	0.599583	H	-2.119439	3.069271	-3.797421
C	4.875464	-0.872254	1.015378	H	-4.217348	4.363404	-1.971641
H	4.863162	0.048316	1.614007	H	-4.429664	2.919669	-2.972870
H	4.359807	-1.660711	1.567962	H	-3.165839	1.551367	-1.449150
H	7.037705	-0.992967	1.366904	H	-3.681644	2.771678	-0.269241
H	6.370613	-2.320977	0.398758	H	-0.053390	-2.377066	0.243261

Table A3.8. Optimized geometries at the B3LYP level of theory with 6-31G(d) basis set of lithium ions, LiCl aggregates, LiCl triple ions, LiCl-LDA mixed aggregates and LiCl-LDA triple ions at -78 °C with free energies (Hartrees) and cartesian coordinates (X, Y, Z). Single point MP2 energies are included.

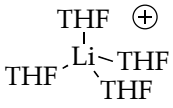

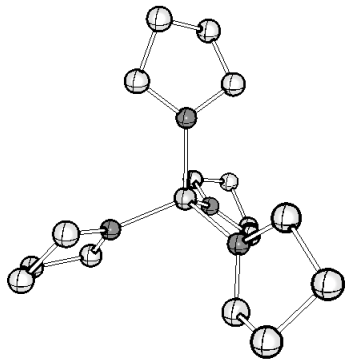

F
G = -936.852895
G_{MP2} = -933.704189

Atom	X	Y	Z	Atom	X	Y	Z
Li	-0.006449	0.001038	-0.009157	O	1.191545	1.220605	-0.970730
O	-1.077777	-1.026060	-1.295317	C	2.297282	1.933630	-0.357946
C	-0.989910	-2.462953	-1.508784	C	3.270383	2.229150	-1.496696
C	-2.132747	-2.816892	-2.464896	C	2.314055	2.442198	-2.680370
C	-3.164470	-1.715775	-2.173973	C	1.225143	1.399943	-2.415227
C	-2.268061	-0.502979	-1.939270	H	1.461585	0.432429	-2.872967
H	-2.697261	0.253434	-1.276585	H	0.230932	1.713191	-2.746231
H	-1.979832	-0.025559	-2.884933	H	2.793140	2.300813	-3.652757
H	-3.737433	-1.950673	-1.269413	H	1.893118	3.453407	-2.654471
H	-3.871172	-1.560270	-2.993477	H	3.923574	1.367847	-1.678120
H	-2.518079	-3.825188	-2.292093	H	3.901818	3.097306	-1.290120
H	-1.795718	-2.758029	-3.505587	H	1.915196	2.857533	0.095229
H	0.000191	-2.692371	-1.913886	H	2.708844	1.297860	0.430975
H	-1.097298	-2.956151	-0.535998	O	-1.236654	1.033713	1.121026
O	1.102928	-1.230097	1.050946	C	-2.269354	0.461832	1.968338
C	2.270584	-1.905345	0.513630	C	-3.249489	1.600110	2.249196
C	3.181542	-2.153074	1.713094	C	-2.324461	2.827204	2.240319
C	2.162391	-2.403646	2.835346	C	-1.344388	2.484692	1.118917
C	1.044761	-1.414890	2.493348	H	-0.344441	2.901385	1.265602
H	1.200174	-0.438633	2.967237	H	-1.719882	2.801928	0.138394
H	0.047388	-1.780647	2.754423	H	-1.797773	2.917682	3.196897
H	2.571312	-2.234846	3.834979	H	-2.854323	3.765320	2.055151
H	1.791464	-3.433513	2.791200	H	-3.780163	1.466271	3.195494
H	3.784018	-1.263155	1.929201	H	-3.995082	1.673546	1.449237
H	3.861908	-2.993687	1.553117	H	-2.712408	-0.385399	1.436410
H	1.951993	-2.846493	0.047474	H	-1.800550	0.096006	2.889973
H	2.704206	-1.258975	-0.254455				

Table A3.8 (Continued).

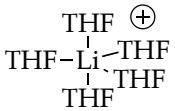

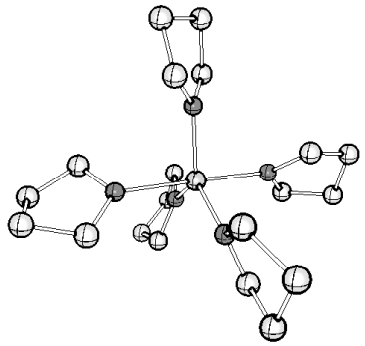

G
G = -1169.19433
G_{MP2} = -1165.279988

Atom	X	Y	Z	Atom	X	Y	Z
Li	-0.014627	-0.019310	0.032833	H	2.105502	-0.957041	-2.234215
O	2.092823	0.695684	0.132841	H	0.663926	-3.478052	-3.212980
C	2.753883	1.717327	-0.651421	H	2.365339	-3.046867	-3.454857
C	4.237583	1.343169	-0.673616	H	1.749754	-4.765441	-1.422854
C	4.405092	0.626669	0.674675	H	2.876275	-3.441408	-1.085768
C	3.081276	-0.129150	0.790943	H	1.191834	-2.915250	0.565714
H	2.752971	-0.297026	1.820427	H	-0.114956	-3.561982	-0.454225
H	3.127996	-1.099454	0.278859	O	-2.115883	-0.713223	-0.140070
H	4.505837	1.355452	1.487182	C	-3.179621	0.074960	0.441072
H	5.272077	-0.038927	0.707813	C	-4.441255	-0.278173	-0.346681
H	4.886478	2.216016	-0.786043	C	-4.185718	-1.750183	-0.702432
H	4.450674	0.655895	-1.500977	C	-2.677566	-1.761326	-0.966708
H	2.292211	1.745489	-1.642609	H	-2.447815	-1.539982	-2.017034
H	2.596879	2.690064	-0.167155	H	-2.200587	-2.708729	-0.701558
O	-0.548295	1.758109	-0.848809	H	-4.762716	-2.095358	-1.564723
C	-1.097509	1.827082	-2.189010	H	-4.431662	-2.396007	0.148270
C	-1.699024	3.227667	-2.326913	H	-4.511216	0.331022	-1.255740
C	-0.819185	4.054007	-1.375803	H	-5.355116	-0.124672	0.233821
C	-0.581281	3.068705	-0.232604	H	-3.283391	-0.190291	1.502072
H	-1.401543	3.096851	0.497594	H	-2.893467	1.127458	0.371156
H	0.363099	3.217591	0.296537	O	-0.091440	-0.129446	2.047041
H	-1.297287	4.977527	-1.038237	C	0.201893	0.968188	2.949462
H	0.128387	4.318498	-1.858858	C	0.128708	0.379635	4.359114
H	-2.740856	3.234994	-1.986586	C	-0.916305	-0.734379	4.188719
H	-1.679043	3.588960	-3.358567	C	-0.582145	-1.269212	2.796904
H	-0.281315	1.665354	-2.904968	H	-1.435814	-1.680961	2.253769
H	-1.827311	1.020153	-2.297534	H	0.210474	-2.028087	2.841133
O	0.605380	-1.690607	-1.000315	H	-1.929559	-0.316465	4.207965
C	0.837295	-3.017614	-0.464154	H	-0.853785	-1.507708	4.959104
C	1.852666	-3.677268	-1.399304	H	-0.151947	1.125820	5.107325
C	1.535138	-3.006661	-2.744517	H	1.096342	-0.044823	4.650576
C	1.204232	-1.577657	-2.314267	H	1.182132	1.371763	2.683251
H	0.488597	-1.076111	-2.972997	H	-0.553139	1.750803	2.801162

Table A3.8 (Continued).

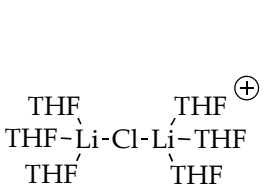

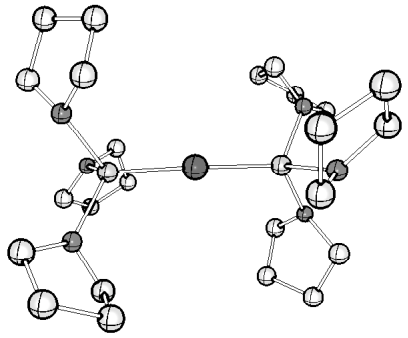

H
G = -1869.437502
G_{MP2} = -1864.094163

Atom	X	Y	Z	Atom	X	Y	Z
Li	-2.309220	-0.063071	0.051572	H	3.036500	1.015043	3.617927
Cl	0.012786	-0.023900	-0.007906	C	2.262868	-1.029499	3.735624
Li	2.335520	0.048590	-0.000622	H	2.072138	-0.908774	4.807453
O	3.149071	1.702927	-0.861548	H	1.412497	-1.558142	3.285558
C	2.366301	2.446946	-1.821620	C	3.586950	-1.767082	3.437391
H	1.483590	1.841057	-2.054531	H	3.422549	-2.831862	3.236283
H	2.963246	2.602161	-2.733440	H	4.283140	-1.689678	4.279391
C	2.054281	3.761185	-1.114723	C	4.152774	-1.035445	2.195016
H	1.794890	4.563710	-1.814073	H	5.106958	-0.538178	2.416750
H	1.209975	3.606363	-0.430090	H	4.275863	-1.682953	1.322802
C	3.353220	4.039094	-0.335377	O	-3.085002	-1.736989	0.880236
H	3.170429	4.572586	0.604578	C	-2.265737	-2.607969	1.685614
H	4.040095	4.645874	-0.936147	H	-2.790685	-2.833373	2.627471
C	3.945651	2.634694	-0.090420	H	-1.336514	-2.066652	1.895995
H	4.991066	2.564337	-0.419304	C	-2.089919	-3.854046	0.822363
H	3.880854	2.309829	0.951728	H	-1.823587	-4.739340	1.409954
O	3.216265	-1.472276	-0.995455	H	-1.293480	-3.667156	0.091131
C	2.464359	-2.672411	-1.272767	C	-3.459873	-3.984079	0.122383
H	1.511609	-2.580290	-0.740264	H	-4.100361	-4.705349	0.641629
H	3.020046	-3.546215	-0.898137	H	-3.358514	-4.315835	-0.917188
C	2.341280	-2.688856	-2.792904	C	-4.063773	-2.561261	0.210162
H	2.119705	-3.685522	-3.190081	H	-4.244062	-2.097682	-0.762927
H	1.535741	-2.005521	-3.091009	H	-4.995709	-2.553080	0.791901
C	3.713717	-2.152687	-3.245024	O	-3.212861	0.011927	-1.763012
H	3.649752	-1.569698	-4.170498	C	-4.264640	0.946391	-2.090622
H	4.412308	-2.978693	-3.418018	H	-4.422767	1.557544	-1.198333
C	4.185048	-1.288071	-2.053636	H	-5.183112	0.384755	-2.309705
H	5.175021	-1.594994	-1.689712	C	-3.777216	1.747250	-3.322812
H	4.205060	-0.215596	-2.268545	H	-3.690540	2.816719	-3.099139
O	3.178629	-0.035980	1.826804	H	-4.479596	1.635727	-4.155856
C	2.443873	0.305665	3.018969	H	-5.012534	1.357490	2.102851
C	-2.406847	1.119842	-3.658811	C	-3.394006	2.211976	3.334972

Table A3.8 (Continued).

H	-1.592483	1.699062	-3.204040	H	-4.159776	2.950827	3.596139
H	-2.223242	1.042881	-4.735956	H	-3.084148	1.708900	4.258502
C	-2.476172	-0.243451	-2.975481	C	-2.210576	2.884884	2.613229
H	-3.023966	-0.980068	-3.584072	H	-1.276888	2.337404	2.798228
H	-1.502555	-0.651274	-2.681317	H	-2.069610	3.931404	2.905781
O	-3.209282	1.432874	1.068675	C	-2.586296	2.732023	1.143437
C	-3.941940	1.208371	2.296495	H	-3.306341	3.501084	0.822175
H	-3.774697	0.162620	2.569849	H	-1.728533	2.717724	0.458942
H	1.509872	0.779916	2.696561				

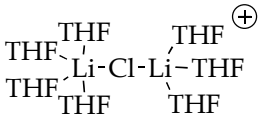

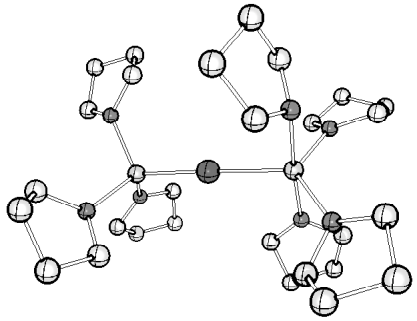

I
G = -2101.774411
G_{MP2} = -2095.667218

Atom	X	Y	Z	Atom	X	Y	Z
Li	2.092644	-0.204286	0.158816	C	-2.657925	4.258283	-0.147982
Cl	-0.389978	-0.130696	-0.001816	C	-2.534004	2.970481	0.664104
Li	-2.704165	0.088780	-0.123903	H	-2.977136	3.081723	1.662926
O	-3.635244	-0.787110	1.398964	H	-1.513522	2.593050	0.764508
C	-4.856790	-0.239895	1.965413	H	-2.532860	5.154421	0.466367
C	-4.876390	-0.667542	3.440073	H	-1.905056	4.281760	-0.944769
C	-3.390760	-0.927738	3.739468	H	-4.823775	4.409719	-0.003605
C	-2.905703	-1.514472	2.417461	H	-4.221913	4.736302	-1.636818
H	-3.151723	-2.582650	2.339627	H	-3.775104	2.388965	-2.048381
H	-1.842735	-1.370802	2.212122	H	-5.160524	2.214269	-0.946338
H	-3.236004	-1.605563	4.583846	O	-3.481095	-0.694049	-1.761838
H	-2.866939	0.011524	3.952783	C	-2.702904	-0.744402	-2.989600
H	-5.454988	-1.589265	3.565834	C	-3.192056	-1.981378	-3.757181
H	-5.319670	0.096058	4.085149	C	-3.798180	-2.856266	-2.647440
H	-4.815717	0.847003	1.842404	C	-4.407162	-1.805395	-1.724363
H	-5.709732	-0.625636	1.397058	H	-4.498934	-2.113886	-0.680864
O	-3.294253	1.978277	-0.071594	H	-5.387492	-1.470110	-2.089787
C	-4.151774	2.625407	-1.046260	H	-3.014809	-3.414147	-2.121445
C	-4.068128	4.123784	-0.744097	H	-4.538586	-3.570430	-3.018770
H	-2.382470	-2.476106	-4.301047	H	5.214521	-1.050874	-1.182708
H	-3.963413	-1.704348	-4.484205	H	4.129033	-2.445845	-0.992925
H	-2.861986	0.188439	-3.541069	O	3.019001	0.289475	1.898603

Table A3.8 (Continued).

H	-1.649044	-0.811571	-2.701628	C	4.371926	-0.005140	2.315054
O	2.043238	-2.288081	0.724449	C	4.742508	1.081342	3.326973
C	1.655365	-2.597688	2.080387	C	3.380727	1.406836	3.960021
C	1.103974	-4.021412	2.035302	C	2.438090	1.298137	2.760715
C	0.425508	-4.043545	0.657749	H	2.374600	2.236588	2.197757
C	1.377556	-3.194108	-0.190198	H	1.424837	0.977913	3.019022
H	0.854491	-2.598012	-0.942064	H	3.347170	2.394018	4.429540
H	2.143905	-3.809956	-0.678282	H	3.124835	0.660245	4.720637
H	-0.556737	-3.561242	0.711544	H	5.146087	1.962439	2.814405
H	0.293510	-5.051769	0.254205	H	5.488195	0.740683	4.050641
H	0.418074	-4.232916	2.861193	H	4.391868	-1.004335	2.768853
H	1.920825	-4.751356	2.076610	H	5.012154	-0.014355	1.427663
H	2.535301	-2.485672	2.719007	O	2.302456	1.948061	-0.472769
H	0.888317	-1.880301	2.400473	C	3.621237	2.498703	-0.682438
O	3.194293	-0.676031	-1.497003	C	3.429912	3.835076	-1.418757
C	4.338761	-1.560070	-1.599918	C	2.045548	3.666983	-2.065274
C	4.497749	-1.886988	-3.092697	C	1.311603	2.847459	-1.005877
C	3.087576	-1.629910	-3.649295	H	0.486423	2.237988	-1.378222
C	2.634593	-0.440566	-2.806546	H	0.932113	3.495508	-0.200764
H	1.551679	-0.351469	-2.689107	H	2.120321	3.101027	-3.001534
H	3.026785	0.505202	-3.206563	H	1.553413	4.619765	-2.282553
H	2.436978	-2.493385	-3.468939	H	4.226810	4.029920	-2.142073
H	3.081300	-1.414467	-4.721643	H	3.415006	4.668268	-0.707048
H	4.846634	-2.910052	-3.257696	H	4.116452	2.620068	0.287857
H	5.218973	-1.208177	-3.561203	H	4.192154	1.773998	-1.273130

Table A3.8 (Continued).

THF
THF–Li–Cl
THF

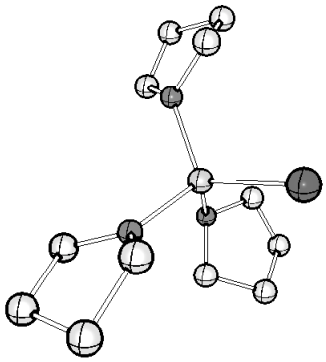

J
G = -1164.913673
G_{MP2} = -1161.942118

* Tetrasolvated lithium chloride monomer fails to minimize.

Atom	X	Y	Z	Atom	X	Y	Z
Li	-0.030161	-0.109586	0.290648	H	-1.942805	-1.419516	1.805276
Cl	-0.124011	0.560351	2.423159	H	-4.470547	-2.142028	0.967611
O	-0.291182	1.484173	-0.918817	H	-3.901650	-0.485490	0.682078
C	-1.392889	2.318883	-0.453211	H	-3.860424	-2.842244	-1.276024
C	-0.835540	3.743276	-0.337165	H	-4.380131	-1.187066	-1.613696
C	0.667081	3.495044	-0.131166	H	-2.104221	-0.444894	-1.880131
C	0.904132	2.290474	-1.037109	H	-1.750163	-2.173243	-2.097146
H	1.748831	1.665628	-0.736625	O	1.758263	-0.888047	-0.121882
H	1.031328	2.589627	-2.087939	C	2.582283	-1.311417	0.985451
H	0.864680	3.217351	0.908989	C	4.001180	-1.175372	0.442750
H	1.288981	4.354509	-0.400889	C	3.841807	-1.662279	-1.013739
H	-1.294269	4.292374	0.489891	C	2.359491	-1.355775	-1.343280
H	-1.009692	4.308156	-1.261123	H	1.826883	-2.248225	-1.695881
H	-2.214187	2.234546	-1.173382	H	2.237482	-0.563376	-2.088232
H	-1.704012	1.929553	0.520848	H	4.032340	-2.738446	-1.082692
O	-1.457624	-1.409572	-0.183798	H	4.529898	-1.162106	-1.701458
C	-2.200144	-1.434678	-1.422696	H	4.731065	-1.761580	1.008992
C	-3.655910	-1.788389	-1.056036	H	4.310243	-0.124508	0.471487
C	-3.707652	-1.541562	0.462941	H	2.323739	-0.671722	1.830451
C	-2.289801	-1.905836	0.891116	H	2.347324	-2.356082	1.238760
H	-2.161906	-2.995069	0.974030				

Table A3.8 (Continued).

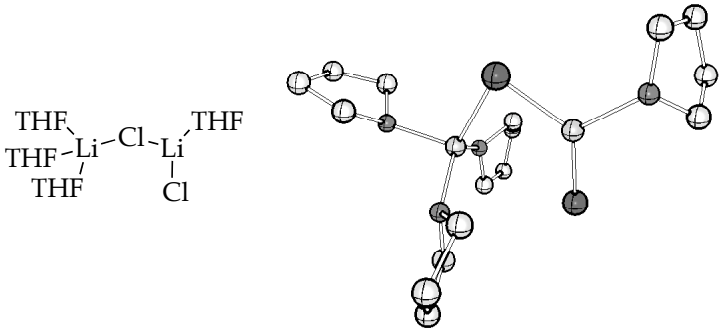

K
G = -1865.131896
G_{MP2} = -1860.742824

Atom	X	Y	Z	Atom	X	Y	Z
Li	-1.157373	-0.069142	-0.069344	H	-3.694448	1.053497	-1.611361
Cl	0.402606	-0.278979	-1.812373	H	-2.595701	0.176338	-2.709544
Li	1.964071	0.577751	-0.393609	O	-1.567693	1.847739	0.296200
Cl	1.697598	1.043337	1.752870	C	-1.878844	2.346929	1.614055
O	3.761042	0.629470	-1.073347	C	-2.085910	3.871714	1.451128
C	4.880917	0.703529	-0.170100	C	-1.556492	4.171604	0.024199
C	5.514841	-0.685741	-0.260085	C	-0.803722	2.890919	-0.344469
C	5.283833	-1.088491	-1.739917	H	0.213947	2.885326	0.066203
C	4.197943	-0.102735	-2.237356	H	-0.770212	2.663377	-1.411185
H	3.311700	-0.578941	-2.660997	H	-0.910581	5.053869	-0.011968
H	4.605100	0.608219	-2.967955	H	-2.388435	4.333671	-0.669329
H	4.955415	-2.128183	-1.824869	H	-1.523245	4.417124	2.214382
H	6.198461	-0.983857	-2.331880	H	-3.138314	4.153273	1.551830
H	4.990238	-1.371450	0.413184	H	-2.769692	1.814289	1.957468
H	6.572662	-0.681691	0.019314	H	-1.034947	2.128122	2.278009
H	5.569898	1.488653	-0.514837	O	-0.916072	-1.460161	1.336256
H	4.481177	0.967135	0.810840	C	0.221637	-2.345658	1.259536
O	-2.909575	-0.674767	-0.845469	C	-0.019566	-3.335278	2.398209
C	-3.406119	0.066480	-1.976913	C	-0.624125	-2.437791	3.504460
C	-4.573595	-0.771405	-2.540769	C	-1.129365	-1.188660	2.740675
C	-4.352828	-2.183256	-1.930095	H	-0.556416	-0.296799	3.013773
C	-2.996933	-2.060305	-1.221655	H	-2.199044	-1.000009	2.868753
H	-2.163481	-2.302240	-1.896294	H	0.136161	-2.149602	4.236302
H	-2.903659	-2.649675	-0.308178	H	-1.429103	-2.945340	4.044210
H	-4.346607	-2.975008	-2.685105	H	0.898566	-3.838852	2.715674
H	-5.140744	-2.417205	-1.207371	H	-0.737156	-4.101897	2.085255
H	-4.551619	-0.786110	-3.634484	H	0.227815	-2.780907	0.258510
H	-5.541177	-0.361942	-2.236263	H	1.138222	-1.762471	1.413782

Table A3.8 (Continued).

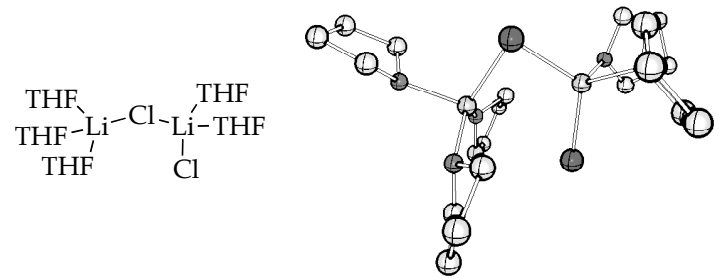

L
G = -2097.482363
G_{MP2} = -2092.324568

Atom	X	Y	Z	Atom	X	Y	Z
Li	-1.645970	-0.147008	-0.040343	H	-2.625812	-1.494039	-2.536674
Cl	-0.091724	0.105549	-1.764153	H	-3.570044	-2.349706	-1.286694
Li	1.683314	0.007390	-0.207878	H	-4.648472	-1.507463	-3.786670
Cl	1.131884	0.172049	2.018032	H	-5.649012	-1.752078	-2.352998
O	2.797808	-1.647805	-0.462347	H	-5.081447	0.839031	-3.586160
C	3.532934	-1.814784	-1.697075	H	-5.954933	0.540331	-2.079238
C	4.885199	-2.443860	-1.315640	H	-4.027911	1.625590	-1.101731
C	5.014032	-2.099065	0.178284	H	-2.975906	1.108417	-2.449710
C	3.561482	-2.183418	0.638831	O	-1.623844	-1.952134	0.820954
H	3.311028	-1.589154	1.519984	C	-1.890570	-2.145614	2.223347
H	3.262481	-3.227938	0.813949	C	-1.700593	-3.657417	2.474700
H	5.391446	-1.078183	0.309177	C	-0.878693	-4.138677	1.247128
H	5.672762	-2.782291	0.723377	C	-0.522643	-2.835871	0.519330
H	5.708272	-2.054143	-1.922238	H	-0.456681	-2.916681	-0.566715
H	4.856532	-3.531410	-1.450647	H	0.400020	-2.389038	0.905381
H	2.944887	-2.439346	-2.377254	H	-1.488116	-4.783888	0.605868
H	3.651113	-0.823470	-2.145946	H	0.015960	-4.700668	1.532090
O	2.980903	1.487922	-0.722441	H	-2.661318	-4.178068	2.531228
C	3.589086	2.272286	0.330466	H	-1.174474	-3.830615	3.418129
C	3.223537	3.749900	0.045643	H	-1.173550	-1.550427	2.801165
C	2.345541	3.681222	-1.224372	H	-2.906387	-1.788991	2.412607
C	2.761823	2.351791	-1.849809	O	-2.066262	1.533927	0.966136
H	3.696076	2.452572	-2.424655	C	-1.243758	2.691534	0.713200
H	1.993736	1.884265	-2.468171	C	-1.905238	3.793620	1.543406
H	2.497591	4.532301	-1.895678	C	-2.405981	3.032352	2.797454
H	1.284379	3.637239	-0.960090	C	-2.332101	1.541848	2.385093
H	4.126248	4.343490	-0.134208	H	-3.267332	0.996516	2.538178
H	2.692543	4.204980	0.886565	H	-1.511212	1.027591	2.896485
H	3.185013	1.891255	1.270708	H	-3.422584	3.332867	3.068138
H	4.676016	2.116412	0.307812	H	-1.764110	3.219263	3.663411
O	-3.419588	-0.326545	-1.019539	H	-2.747802	4.227577	0.994050
C	-3.812606	0.815436	-1.800408	H	-1.209741	4.602331	1.788033
C	-5.023540	0.335818	-2.616295	H	-0.222043	2.478893	1.050303
C	-4.793529	-1.195902	-2.747904	H	-1.246275	2.860674	-0.365399
C	-3.525685	-1.454070	-1.908567				

Table A3.8 (Continued).

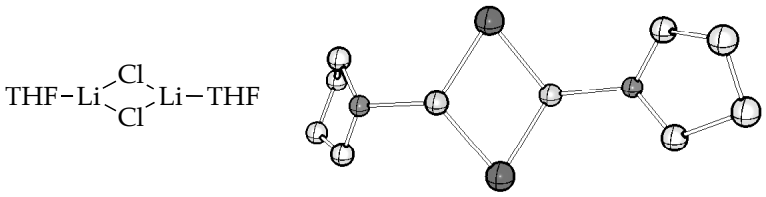

M
G = -1400.432963
G_{MP2} = -1397.58876

Atom	X	Y	Z	Atom	X	Y	Z
Li	1.224110	0.056448	0.583724	H	-3.288569	1.815396	0.242365
Cl	-0.000071	1.876521	-0.000606	H	-4.147110	1.720238	-1.312896
Li	-1.224402	0.056560	-0.585074	O	3.114196	0.007075	0.737816
Cl	-0.000216	-1.771825	-0.000681	C	3.828251	-1.199145	0.369709
O	-3.114591	0.006934	-0.738054	C	4.735454	-0.765170	-0.776506
C	-3.910617	1.177484	-0.392669	C	5.160538	0.644126	-0.327247
C	-5.160087	0.644226	0.328488	C	3.910614	1.177530	0.393033
C	-4.734737	-0.765017	0.777665	H	3.289078	1.815532	-0.242408
C	-3.828352	-1.199229	-0.369104	H	4.146524	1.720236	1.313440
H	-4.406690	-1.551196	-1.233802	H	5.459273	1.286858	-1.160093
H	-3.079620	-1.949348	-0.104241	H	6.005729	0.580776	0.367289
H	-5.581491	-1.441894	0.924423	H	4.164149	-0.721081	-1.710744
H	-4.162781	-0.720783	1.711499	H	5.582288	-1.442100	-0.922561
H	-6.005723	0.580789	-0.365500	H	4.405994	-1.550881	1.234903
H	-5.458268	1.287081	1.161437	H	3.079750	-1.949374	0.104494

Table A3.8 (Continued).

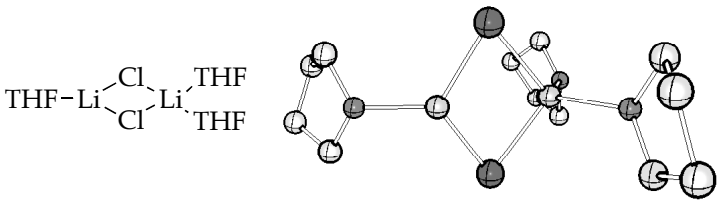

N
G = -1632.79084
G_{MP2} = -1629.174087

Atom	X	Y	Z	Atom	X	Y	Z
Li	-1.263759	0.257486	-0.059976	H	-2.520828	-1.421331	1.882389
Cl	0.121472	-0.564014	-1.831186	H	-4.220699	-0.938594	1.639370
Li	1.211897	-1.051697	0.075573	H	-3.247450	-3.650454	1.360859
Cl	0.083053	-0.270455	1.851823	H	-4.812599	-3.050037	0.802190
O	3.064641	-1.492822	0.088890	H	-2.212313	-3.253565	-0.793013
C	3.880562	-1.220161	1.262295	H	-3.860028	-3.622497	-1.344036
C	5.194280	-0.606732	0.738930	H	-4.422917	-1.219940	-1.404551
C	4.855791	-0.210999	-0.710601	H	-2.726570	-1.207424	-1.985669
C	3.853177	-1.289784	-1.106463	O	-1.511893	2.204156	-0.211716
H	4.353428	-2.230753	-1.373937	C	-0.886485	2.948570	-1.279686
H	3.160525	-1.008265	-1.902861	C	0.054274	3.916847	-0.569347
H	5.733163	-0.188094	-1.363779	C	-0.769698	4.302819	0.671314
H	4.376209	0.773901	-0.744160	C	-1.533308	3.007104	0.998699
H	5.996513	-1.352778	0.749976	H	-2.576251	3.190608	1.279062
H	5.521250	0.242244	1.345846	H	-1.048099	2.418595	1.782791
H	3.306177	-0.541019	1.898644	H	-1.467420	5.111604	0.425230
H	4.039767	-2.158363	1.803567	H	-0.151812	4.637322	1.509696
O	-2.957146	-0.741652	-0.002565	H	0.326175	4.776261	-1.190075
C	-3.383956	-1.486822	-1.160074	H	0.972849	3.395566	-0.276736
C	-3.260956	-2.944672	-0.728085	H	-0.391052	2.224541	-1.929840
C	-3.730451	-2.891080	0.739410	H	-1.659779	3.484115	-1.849317
C	-3.365629	-1.458504	1.190920				

Table A3.8 (Continued).

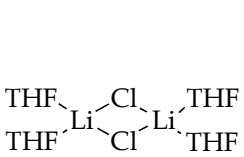

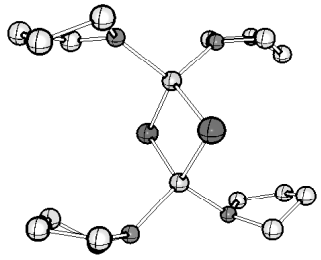

O
G = -1865.144982
G_{MP2} = -1860.758608

Atom	X	Y	Z	Atom	X	Y	Z
Li	0.032551	-1.524063	0.022267	H	2.632291	3.481070	1.528251
Cl	0.079285	-0.094857	1.893780	H	2.302701	1.731682	1.694753
Li	-0.041459	1.384887	0.065541	O	-1.513441	-2.762613	0.060842
Cl	-0.100281	-0.046379	-1.805635	C	-2.066179	-3.166078	-1.204530
O	-1.659752	2.524905	0.169501	C	-3.333512	-2.325918	-1.339722
C	-2.376416	2.652219	1.413201	C	-3.864923	-2.283411	0.110839
C	-3.765679	2.101625	1.105821	C	-2.610703	-2.552404	0.978849
C	-4.003681	2.618518	-0.324504	H	-2.732094	-3.451559	1.596123
C	-2.588487	2.636821	-0.938565	H	-2.322910	-1.717389	1.620997
H	-2.383153	3.567264	-1.480506	H	-4.619770	-3.059602	0.275947
H	-2.392551	1.791142	-1.603086	H	-4.327693	-1.320905	0.348419
H	-4.424670	3.629912	-0.296153	H	-4.053071	-2.753356	-2.045043
H	-4.691954	1.989197	-0.896468	H	-3.056496	-1.325203	-1.685044
H	-4.525293	2.440538	1.817065	H	-1.313754	-2.962190	-1.969036
H	-3.738314	1.006362	1.125248	H	-2.286305	-4.244108	-1.181877
H	-1.821863	2.085588	2.164097	O	1.651191	-2.660923	-0.054328
H	-2.419129	3.711881	1.705779	C	2.671173	-2.457932	-1.062610
O	1.527444	2.591616	0.002541	C	4.007685	-2.278070	-0.305880
C	2.574811	2.522423	0.992288	C	3.582414	-2.178369	1.173112
C	3.846763	2.259184	0.190187	C	2.290921	-2.990889	1.192357
C	3.602142	3.105054	-1.070741	H	1.603337	-2.713556	1.993774
C	2.083347	2.979900	-1.280405	H	2.488310	-4.072656	1.230171
H	1.816923	2.197699	-1.997660	H	3.355183	-1.143100	1.447866
H	1.620684	3.922653	-1.592162	H	4.339516	-2.563932	1.863002
H	4.167602	2.756690	-1.940112	H	4.555139	-1.393266	-0.644712
H	3.882381	4.148390	-0.884606	H	4.657643	-3.146144	-0.461540
H	3.914083	1.195248	-0.065491	H	2.691494	-3.330680	-1.726498
H	4.755287	2.542671	0.730585	H	2.368509	-1.581724	-1.640600

Table A3.8 (Continued).

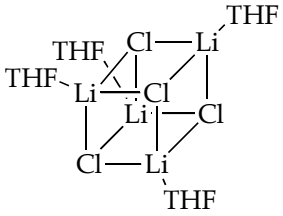

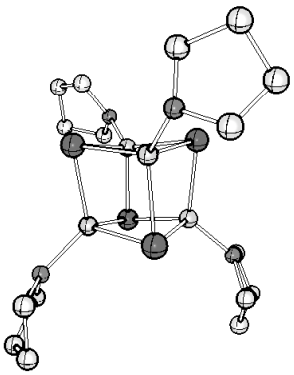

P
G = -2800.897208
G_{MP2} = -2795.229129

Atom	X	Y	Z	Atom	X	Y	Z
Li	0.485646	-1.117847	1.156965	H	-0.196529	5.228972	0.561741
Cl	0.679319	-1.786881	-1.135521	H	-0.567354	6.169025	2.023413
Li	-1.567669	-0.957524	-1.052778	H	-1.265891	4.138158	3.223286
Cl	-1.849460	-0.735402	1.347813	H	0.116353	3.516848	2.272921
Li	-1.090489	1.441055	0.757779	O	-2.991248	-2.074226	-1.726702
Cl	-1.269625	1.320005	-1.639666	C	-4.344334	-1.621542	-1.442615
Li	0.977393	0.617485	-1.283952	C	-5.123633	-2.865044	-0.990229
Cl	1.298108	1.159241	1.029019	C	-4.009715	-3.798675	-0.487551
O	2.434591	1.073452	-2.456532	C	-2.885996	-3.495776	-1.473753
C	3.632758	1.742328	-1.983476	H	-3.017893	-4.036094	-2.421140
C	4.757499	1.317201	-2.937334	H	-1.880078	-3.687199	-1.092226
C	4.245887	-0.024125	-3.488524	H	-4.298593	-4.854236	-0.488966
C	2.744957	0.232546	-3.592756	H	-3.701231	-3.518105	0.525205
H	2.129559	-0.666429	-3.512577	H	-5.649713	-3.320839	-1.837331
H	2.487169	0.770672	-4.514664	H	-5.863920	-2.627077	-0.221037
H	4.439325	-0.834717	-2.776539	H	-4.279589	-0.867601	-0.651393
H	4.694145	-0.294812	-4.449222	H	-4.749612	-1.159153	-2.347543
H	5.721559	1.235187	-2.426708	O	1.493622	-2.188849	2.400605
H	4.868132	2.043389	-3.751053	C	1.919193	-1.604663	3.661087
H	3.450504	2.821312	-1.984784	C	3.217816	-2.328010	4.044208
H	3.809717	1.418301	-0.952784	C	3.744758	-2.821407	2.686244
O	-1.728986	3.122218	1.464646	C	2.449878	-3.181011	1.962129
C	-0.859803	4.002432	2.210897	H	2.089146	-4.177176	2.252705
C	-0.871817	5.307517	1.421220	H	2.503291	-3.124811	0.872523
C	-2.337082	5.381336	0.957817	H	4.428481	-3.671499	2.771465
C	-2.705147	3.905492	0.724565	H	4.262341	-2.013168	2.156761
H	-2.625896	3.608908	-0.325190	H	3.006439	-3.180105	4.700741
H	-3.705203	3.654362	1.092923	H	3.918120	-1.668011	4.564384
H	-2.470544	5.984293	0.055064	H	2.072108	-0.533747	3.491745
H	-2.962401	5.815243	1.746510	H	1.116457	-1.740164	4.392060

Table A3.8 (Continued).

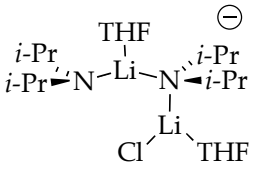

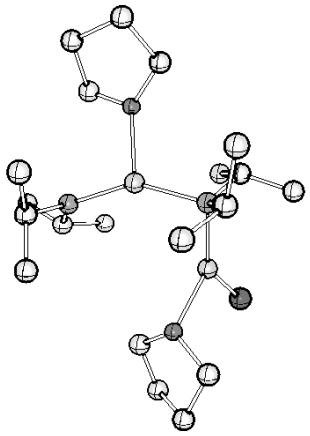

30
G = -1523.430812
G_{MP2} = -1519.042557

Atom	X	Y	Z	Atom	X	Y	Z
Li	-1.940275	-0.992163	-0.318219	C	5.174999	-1.255140	0.360461
N	1.156792	2.004180	-0.145390	C	5.219053	0.244615	-0.049563
C	1.289829	2.886835	0.997919	C	3.962379	0.422358	-0.919395
C	2.294392	2.314662	2.012573	H	4.195119	0.249910	-1.983654
H	3.293617	2.240091	1.566968	H	3.419929	1.364548	-0.799458
H	2.365379	2.936852	2.916131	H	6.132778	0.507410	-0.593525
H	1.993946	1.306189	2.327266	H	5.161012	0.885795	0.835539
C	-0.049175	3.187729	1.724494	H	6.036387	-1.820516	-0.011918
H	-0.468398	2.265796	2.144919	H	5.157497	-1.360883	1.449957
H	0.073592	3.919851	2.539079	H	3.288781	-2.444035	0.374292
H	-0.785022	3.598185	1.022445	H	4.041705	-2.254569	-1.229297
H	1.696742	3.882452	0.710269	C	0.628430	2.690489	-1.309036
Li	1.052586	0.029062	-0.011853	C	0.159704	1.676320	-2.361837
N	-0.125715	-1.648400	0.324822	H	-0.628301	1.025306	-1.964818
C	-0.224951	-2.051587	1.733329	H	-0.233244	2.168274	-3.261772
C	1.029559	-2.749189	2.316646	H	0.995368	1.033726	-2.672994
H	1.902050	-2.083975	2.246401	C	1.633547	3.663380	-1.987775
H	0.879999	-2.999083	3.376630	H	2.476701	3.100643	-2.411466
H	1.271565	-3.680462	1.792390	H	1.163412	4.237498	-2.801422
C	-0.539049	-0.834165	2.615821	H	2.040993	4.384950	-1.269797
H	-1.404036	-0.279657	2.241575	H	-0.264891	3.314034	-1.066650
H	-0.739181	-1.140680	3.652244	O	-3.058000	0.398904	0.709225
H	0.309959	-0.138645	2.633850	C	-3.324410	1.572571	-0.096280
H	-1.057746	-2.772197	1.896784	C	-4.839922	1.603017	-0.293694
C	0.244166	-2.767818	-0.558210	C	-5.346399	0.962663	1.007899
C	-0.731112	-3.970489	-0.532694	C	-4.294309	-0.123154	1.248939
H	-1.730421	-3.662561	-0.865404	H	-4.542073	-1.042513	0.706729
H	-0.380955	-4.768366	-1.203513	H	-4.130495	-0.348393	2.308418
H	-0.821259	-4.405059	0.470381	H	-6.355435	0.546398	0.920769
C	0.376071	-2.270481	-2.006656	H	-5.345380	1.693865	1.826646
H	1.119861	-1.468541	-2.081315	H	-5.103853	0.973537	-1.148869

Table A3.8 (Continued).

H	0.696982	-3.085479	-2.670234	H	-5.220803	2.617088	-0.457297
H	-0.583576	-1.895822	-2.383233	H	-2.953074	2.451523	0.445200
H	1.238809	-3.182141	-0.288835	H	-2.775198	1.472268	-1.035186
O	3.060628	-0.595886	-0.464355	Cl	-3.477198	-1.529859	-1.898789
C	3.855205	-1.762667	-0.261202				

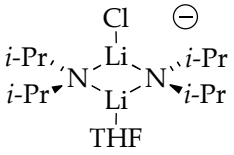

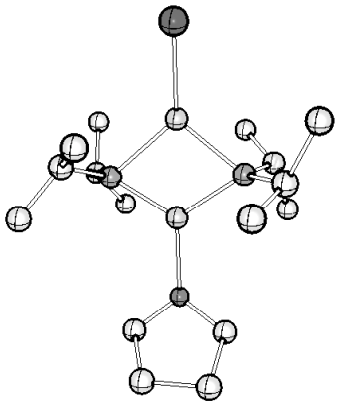

Q
G = -1291.089569
G_{MP2} = -1287.473699

Atom	X	Y	Z	Atom	X	Y	Z
Li	-1.875668	-0.000879	-0.247326	C	-1.996111	-1.704697	2.117327
N	-0.491629	1.698042	0.121140	H	-2.897181	-1.469112	1.538476
C	-0.628084	2.625046	-1.002131	H	-2.293234	-2.308381	2.987036
C	-0.894549	1.891635	-2.322853	H	-1.585141	-0.762903	2.503539
H	-1.826115	1.315320	-2.279414	H	-1.469770	-3.373992	0.924549
H	-0.979356	2.600920	-3.157977	O	2.515510	-0.050533	0.584129
H	-0.064790	1.210299	-2.556016	C	3.341578	-1.216145	0.465095
C	0.603561	3.549626	-1.197487	C	4.376419	-0.885166	-0.635967
H	1.465430	2.957696	-1.539123	C	4.280252	0.658223	-0.788348
H	0.417175	4.333488	-1.948144	C	3.373819	1.076756	0.378259
H	0.886265	4.049070	-0.262680	H	2.731823	1.935102	0.176698
H	-1.495567	3.300162	-0.848528	H	3.959897	1.262549	1.292627
Li	0.515878	0.013858	0.272285	H	3.806752	0.921526	-1.739231
N	-0.564517	-1.645555	0.081369	H	5.256619	1.152310	-0.750814
C	-0.265472	-2.520464	-1.052414	H	4.128242	-1.387592	-1.575229
C	-1.519517	-3.144125	-1.714833	H	5.380107	-1.209709	-0.341801
H	-2.174246	-2.353383	-2.099431	H	3.835740	-1.406557	1.429386
H	-1.247083	-3.820167	-2.540658	H	2.681495	-2.052824	0.234728
H	-2.106479	-3.725052	-0.995115	C	-0.706469	2.414487	1.384142
C	0.520149	-1.768507	-2.138741	C	0.121469	1.810355	2.532699
H	1.451553	-1.341452	-1.742734	H	1.195835	1.892206	2.326476
H	0.782567	-2.430554	-2.975069	H	-0.083252	2.313659	3.488171
H	-0.080005	-0.946162	-2.544136	H	-0.111027	0.746573	2.674519

Table A3.8 (Continued).

H	0.380894	-3.374883	-0.741055	C	-2.195290	2.491091	1.796988
C	-0.968075	-2.441569	1.244436	H	-2.585459	1.495037	2.039616
C	0.232738	-2.890795	2.114752	H	-2.346962	3.140770	2.673927
H	0.726438	-2.017059	2.563248	H	-2.804636	2.878125	0.973802
H	-0.068943	-3.565943	2.931145	H	-0.361631	3.465183	1.300349
H	0.975731	-3.421010	1.504936	Cl	-4.011287	0.018832	-0.951594

i-Pr, ⊖
i-Pr N–Li–Cl

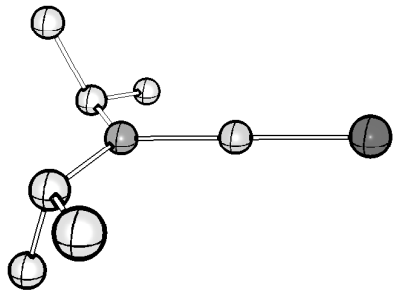

32
G = -759.521337
G_{MP2} = -757.793267

Atom	X	Y	Z	Atom	X	Y	Z
C	1.291509	1.197901	0.158166	H	-0.438698	-2.519497	-0.190255
N	0.500585	-0.000009	-0.000101	H	2.164322	-1.040352	-0.834253
Li	-1.380691	-0.000102	-0.000067	C	0.446290	2.306271	0.806056
Cl	-3.567016	-0.000282	-0.000042	H	0.095684	1.990739	1.795905
C	1.291932	-1.197657	-0.158029	H	1.006538	3.246021	0.914576
C	1.883062	-1.725703	1.176791	H	-0.439509	2.519247	0.189403
H	1.068497	-2.024639	1.850050	C	1.883128	1.726049	-1.176386
H	2.549293	-2.591136	1.028364	H	1.068801	2.024642	-1.850087
H	2.462081	-0.944277	1.683857	H	2.548970	2.591734	-1.027691
C	0.447381	-2.306257	-0.806414	H	2.462687	0.944795	-1.683095
H	0.097218	-1.990786	-1.796438	H	2.163596	1.040886	0.834845
H	1.007960	-3.245842	-0.914655				

Table A3.8 (Continued).

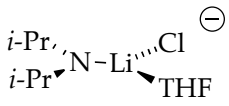

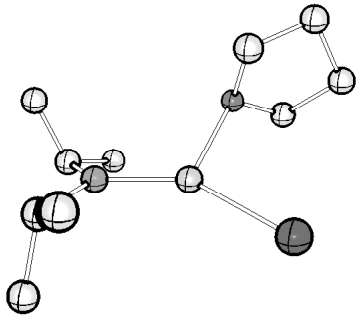

R
G = -991.864401
G_{MP2} = -989.363875

Atom	X	Y	Z	Atom	X	Y	Z
C	2.263088	-1.415273	-0.455439	C	3.600589	1.457332	-0.464303
N	1.733926	-0.147812	-0.011409	H	2.963089	2.162704	-1.012523
Li	-0.013959	0.522737	-0.373476	H	4.433269	2.019020	-0.008485
Cl	-1.282097	2.391671	-0.757805	H	4.030797	0.759430	-1.193685
O	-1.629948	-0.839192	-0.085256	C	2.109799	1.706726	1.550924
C	-2.755784	-0.685464	-0.977602	H	1.611429	1.181815	2.375702
C	-3.910009	-0.160191	-0.119181	H	2.852490	2.398371	1.976203
C	-3.573133	-0.733747	1.265841	H	1.352004	2.305640	1.027764
C	-2.047130	-0.618914	1.277477	H	3.473580	0.101576	1.191656
H	-1.544618	-1.359762	1.906632	C	1.384566	-2.014976	-1.566745
H	-1.734583	0.387549	1.584254	H	1.356419	-1.340673	-2.432034
H	-3.883213	-1.784747	1.339564	H	1.750724	-2.997292	-1.901077
H	-4.038278	-0.181089	2.089293	H	0.356669	-2.142450	-1.203159
H	-4.891550	-0.471449	-0.494640	C	2.407350	-2.455141	0.690613
H	-3.861281	0.932870	-0.096623	H	1.414954	-2.709109	1.087030
H	-2.472047	0.018624	-1.763562	H	2.899899	-3.385738	0.361194
H	-2.981529	-1.669414	-1.414851	H	2.998419	-2.039717	1.516049
C	2.748924	0.693995	0.585798	H	3.283434	-1.310639	-0.893966

Table A3.8 (Continued).

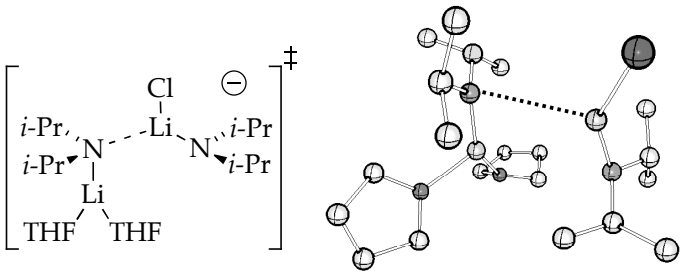

S
G = -1523.406885
G_{MP2} = -1519.015314
$\Delta G^{‡}$ = 20.1 kcal/mol*
$\Delta G_{MP2}^{‡}$ = 17.7 kcal/mol*

* Activation barrier is measured relative to the ground state energy of open disolvated triple ion **30**.

Atom	X	Y	Z	Atom	X	Y	Z
C	1.776906	2.538051	0.232587	H	0.317279	0.559410	4.132115
N	1.227796	1.397912	0.953630	H	-0.602377	0.361838	2.619612
Li	1.171507	-0.333737	0.205339	H	0.656643	2.497901	2.684432
O	2.861143	-0.986656	-0.777676	C	1.259722	3.931913	0.659149
C	4.069983	-0.224680	-0.561744	H	1.552952	4.185500	1.684987
C	4.628696	0.039880	-1.958796	H	1.680283	4.707280	0.002944
C	4.242732	-1.250069	-2.702069	H	0.166452	3.976498	0.588718
C	2.876355	-1.591502	-2.088965	C	1.492798	2.371187	-1.270152
H	2.709029	-2.668654	-1.982884	H	0.420814	2.491623	-1.466647
H	2.048721	-1.168413	-2.669927	H	2.032160	3.119730	-1.868126
H	4.969277	-2.043825	-2.488112	H	1.793532	1.376492	-1.626697
H	4.189466	-1.126622	-3.788305	H	2.894817	2.603403	0.324985
H	5.707275	0.227739	-1.952048	Li	-2.055355	1.533886	-0.220696
H	4.130176	0.906867	-2.405022	N	-2.753862	-0.223038	-0.697244
H	3.788068	0.667078	0.000134	C	-2.635554	-0.696075	-2.063530
H	4.768912	-0.827262	0.037735	C	-1.201724	-0.451214	-2.563165
O	0.522265	-2.198400	0.472971	H	-0.474681	-0.940094	-1.902114
C	1.289193	-3.150901	1.217106	H	-1.053454	-0.839319	-3.581058
C	0.372771	-3.638338	2.365435	H	-0.975042	0.623379	-2.578056
C	-1.033352	-3.113844	1.967299	C	-3.621841	-0.052501	-3.072290
C	-0.852830	-2.646399	0.520852	H	-3.485571	1.036591	-3.088161
H	-1.493153	-1.803580	0.208507	H	-3.470193	-0.441444	-4.090788
H	-0.968312	-3.485116	-0.184202	H	-4.664486	-0.250115	-2.798266
H	-1.318655	-2.265130	2.595911	H	-2.796847	-1.798092	-2.151067
H	-1.811714	-3.877723	2.059259	C	-4.061381	-0.451493	-0.099042
H	0.690487	-3.229995	3.329577	C	-4.480442	-1.940574	0.030269
H	0.398882	-4.730718	2.444580	H	-3.804611	-2.480382	0.707613
H	1.570587	-3.984649	0.555303	H	-5.500771	-2.032044	0.430915

Table A3.8 (Continued).

H	2.201612	-2.652643	1.553672	H	-4.461490	-2.454486	-0.938331
C	1.190306	1.571874	2.394059	C	-4.104179	0.197540	1.293993
C	2.589746	1.661021	3.058152	H	-3.942765	1.281275	1.230549
H	3.185798	2.470682	2.620304	H	-5.073796	0.036714	1.785606
H	2.523933	1.845859	4.141265	H	-3.321779	-0.229227	1.937884
H	3.141706	0.721412	2.903560	H	-4.881168	0.030995	-0.677561
C	0.405496	0.424573	3.045471	Cl	-2.547082	3.683872	-0.173796
H	0.908724	-0.539371	2.873054				

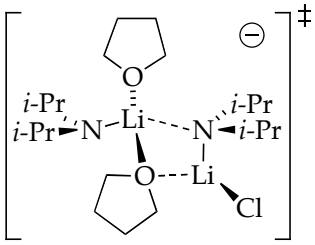

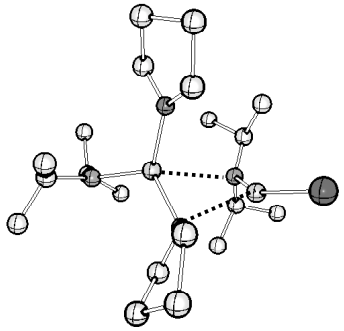

31
G = -1523.421283
G_{MP2} = -1519.035557
$\Delta G^{‡}$ = 11.1 kcal/mol*
$\Delta G_{MP2}^{‡}$ = 5.0 kcal/mol*

* Activation barrier is measured relative to the ground state energy of open disolvated triple ion **30**.

Atom	X	Y	Z	Atom	X	Y	Z
C	2.482956	2.180137	-1.350140	Li	-0.612649	0.201313	0.011151
N	2.154939	1.281835	-0.249863	N	-2.379643	0.965791	-0.310221
Li	2.263919	-0.620748	-0.502218	C	-2.602859	2.404053	-0.346994
O	0.045637	-1.327991	-1.345638	H	-3.534722	2.655735	-0.897405
C	-0.076458	-2.766982	-1.166597	C	-2.775486	3.030891	1.062547
C	-0.280434	-3.331638	-2.568903	H	-3.553723	2.502639	1.628135
C	-1.108305	-2.224515	-3.237533	H	-1.836793	2.955094	1.626506
C	-0.486540	-0.954025	-2.654489	H	-3.060607	4.094308	1.018350
H	-1.202433	-0.142065	-2.491751	C	-1.469275	3.124587	-1.090531
H	0.348173	-0.600611	-3.265948	H	-1.440655	2.808223	-2.139949
H	-2.162311	-2.306106	-2.946064	H	-1.590481	4.217332	-1.062742
H	-1.056745	-2.239736	-4.331563	H	-0.496707	2.884108	-0.643852
H	-0.783022	-4.304910	-2.555522	C	-3.640138	0.254535	-0.221829
H	0.688135	-3.451020	-3.068589	H	-4.338361	0.737787	0.502428
H	0.838403	-3.111027	-0.680430	C	-3.448836	-1.183764	0.283604
H	-0.949513	-2.966201	-0.531994	H	-2.793021	-1.741017	-0.397754

Table A3.8 (Continued).

Cl	3.254689	-2.596275	-0.175605	H	-2.981755	-1.196634	1.273866
C	2.577607	1.842529	1.030518	H	-4.404002	-1.724303	0.341283
H	3.554006	2.362034	0.941275	C	-4.422235	0.193172	-1.564238
C	1.600979	2.900993	1.600239	H	-5.419870	-0.259455	-1.445023
H	1.407359	3.694654	0.869494	H	-4.562225	1.194696	-1.986551
H	0.635957	2.437972	1.843960	H	-3.861237	-0.400590	-2.298903
H	1.994996	3.376651	2.512417	O	-0.359192	-0.755229	1.848781
C	2.794089	0.734357	2.071422	C	0.134696	-2.058289	2.240259
H	3.572163	0.034531	1.744831	C	0.130224	-2.053697	3.769824
H	3.085970	1.146555	3.048101	C	-1.061601	-1.134978	4.081771
H	1.867346	0.165494	2.207605	C	-0.932323	-0.073116	2.987116
H	2.138052	3.219206	-1.150685	H	-0.248329	0.729151	3.291587
C	1.780268	1.743725	-2.640625	H	-1.875965	0.372248	2.664005
H	2.005729	2.425282	-3.472336	H	-1.028714	-0.701943	5.087017
H	2.122004	0.741174	-2.939629	H	-2.005821	-1.683872	3.976740
H	0.696172	1.711637	-2.504260	H	1.060240	-1.615838	4.150274
C	4.002780	2.285335	-1.652535	H	0.029502	-3.060431	4.188557
H	4.210184	3.024332	-2.441979	H	-0.550317	-2.821670	1.847580
H	4.576890	2.581675	-0.767970	H	1.123345	-2.207645	1.796360
H	4.385910	1.310045	-1.982880				

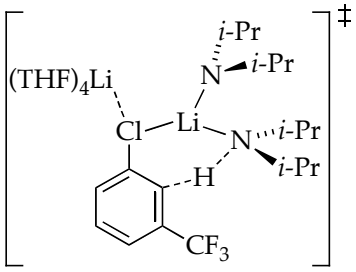

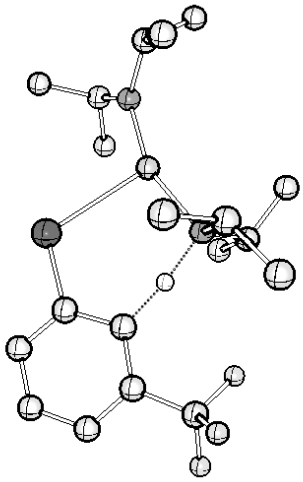

T
G = -1619.659781
G_{MP2} = -1615.331737
(calculation does not include $Li(THF)_4^+$ ion)

Atom	X	Y	Z	Atom	X	Y	Z
C	0.060727	-2.013382	1.167439	H	-0.915399	-0.443616	-2.495034
N	-0.036174	-1.226121	-0.071550	C	1.218349	-2.983723	-1.433805
Li	-1.707462	-0.067164	-0.020452	H	2.162376	-2.431522	-1.397084
N	-3.552859	0.327947	0.131311	H	1.238369	-3.731041	-0.632587
C	-4.095204	1.416629	0.918751	H	1.175650	-3.528023	-2.387563
H	-5.055978	1.133218	1.404776	H	1.004486	-2.587070	1.204265

Table A3.8 (Continued).

C	-4.407368	2.683730	0.078473	C	0.091485	-1.054973	2.368470
H	-5.058987	2.436946	-0.768500	H	0.213472	-1.610414	3.308028
H	-4.909466	3.467255	0.669196	H	0.919874	-0.345726	2.282386
H	-3.476469	3.099543	-0.328392	H	-0.843684	-0.483336	2.440480
C	-3.141338	1.794138	2.063789	C	-1.084795	-3.030409	1.351646
H	-2.994939	0.941370	2.737410	H	-1.101846	-3.778627	0.550628
H	-2.159458	2.085142	1.665815	H	-0.977324	-3.569979	2.303351
H	-3.521182	2.641386	2.652734	H	-2.056194	-2.518885	1.354936
C	-4.587742	-0.405942	-0.567135	C	3.291126	0.718573	0.097751
H	-5.366062	0.273544	-0.983767	C	1.902657	0.754527	-0.143459
C	-4.003343	-1.163167	-1.769471	C	1.425317	2.019499	-0.462357
H	-3.555811	-0.463682	-2.485591	C	2.195910	3.177849	-0.559558
H	-3.217202	-1.857344	-1.439632	C	3.566343	3.081656	-0.318796
H	-4.766672	-1.756103	-2.293402	C	4.118940	1.846678	0.012733
C	-5.349869	-1.411470	0.337709	H	5.183125	1.762296	0.211005
H	-5.743236	-0.911400	1.230739	H	4.194963	3.966458	-0.384331
H	-6.199421	-1.883204	-0.182440	H	1.738284	4.129902	-0.814111
H	-4.667644	-2.203458	0.673919	Cl	-0.337279	2.234272	-0.780352
C	0.007080	-2.032124	-1.303359	C	3.949297	-0.599173	0.414392
H	-0.892742	-2.674476	-1.371487	F	4.198993	-1.333516	-0.706825
C	-0.036352	-1.097241	-2.523273	F	3.211518	-1.381926	1.228569
H	0.852100	-0.456622	-2.558012	F	5.159104	-0.444687	1.024159
H	-0.077327	-1.675303	-3.455883	H	0.999858	-0.290017	-0.095613

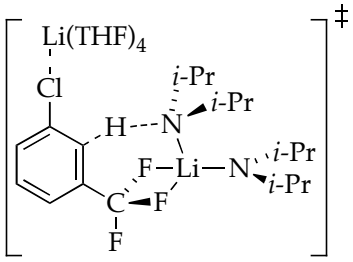

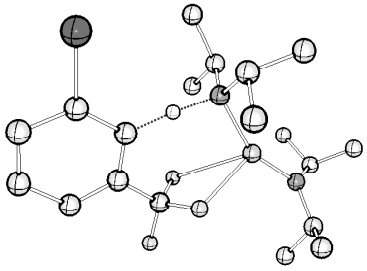

10
G = -1619.663984
G_{MP2} = -1615.334181
(calculation does not include $Li(THF)_4^+$ ion)

Atom	X	Y	Z	Atom	X	Y	Z
C	-0.623252	-2.109718	-0.480839	H	-0.364569	1.711072	3.401139
F	-0.458024	-3.452268	-0.551905	H	-1.054472	0.463649	2.343218
F	0.189831	-1.682943	0.535875	H	0.706325	0.632872	2.492852
Li	1.411741	0.170956	0.045232	C	0.924972	3.184480	1.465743
N	3.261093	-0.259004	0.112426	H	0.916098	3.978749	0.710491
C	3.838386	-1.290861	0.952814	H	0.865331	3.667211	2.451492

Table A3.8 (Continued).

H	4.902063	-1.069534	1.190858	H	1.889112	2.664158	1.395079
C	3.838565	-2.687060	0.274940	C	-0.209207	2.317601	-1.187305
H	4.320493	-2.633762	-0.708956	H	0.729236	2.903834	-1.244051
H	4.369169	-3.449433	0.869354	C	-0.255561	1.454033	-2.457256
H	2.805774	-3.025803	0.121794	H	-1.182816	0.871624	-2.501386
C	3.120917	-1.383814	2.309998	H	-0.205813	2.083865	-3.355422
H	3.187074	-0.426978	2.840961	H	0.582978	0.752354	-2.493663
H	2.058474	-1.620534	2.170637	C	-1.359022	3.349810	-1.246257
H	3.550474	-2.169705	2.948736	H	-2.334927	2.852368	-1.242648
C	4.249076	0.304742	-0.783815	H	-1.338391	4.041442	-0.396862
H	4.939825	-0.477469	-1.175539	H	-1.282506	3.952476	-2.162145
C	3.582940	0.930726	-2.017938	H	-1.299906	0.584830	-0.003008
H	3.027023	0.170204	-2.579416	C	-2.314774	-0.336636	0.003766
H	2.873943	1.714166	-1.715201	C	-2.054642	-1.696388	-0.262701
H	4.316964	1.394410	-2.692495	C	-3.046996	-2.681124	-0.326532
C	5.155864	1.367298	-0.106347	C	-4.376581	-2.320443	-0.113606
H	5.622363	0.959563	0.798623	C	-4.690992	-0.992601	0.173274
H	5.963735	1.718252	-0.769529	C	-3.655886	-0.056789	0.225705
H	4.551645	2.233802	0.193515	Cl	-4.156628	1.622618	0.645010
N	-0.190897	1.449348	0.002600	H	-5.718547	-0.691031	0.357528
C	-0.237362	2.187692	1.275468	H	-5.163904	-3.068838	-0.160200
H	-1.175893	2.768305	1.364828	H	-2.785688	-3.714229	-0.532627
C	-0.240126	1.187735	2.443709	F	-0.088752	-1.595207	-1.615185

Table A3.8 (Continued).

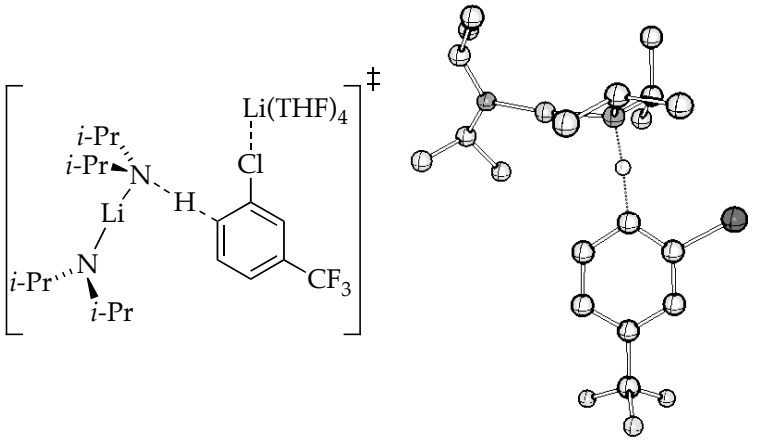

U
G = -1619.663694
G_{MP2} = -1615.330688
(calculation does not include $Li(THF)_4^+$ ion)

Atom	X	Y	Z	Atom	X	Y	Z
C	-1.491079	2.499118	-0.899219	H	-1.398463	1.463873	3.632376
N	-1.312434	1.558857	0.221351	C	-0.456644	3.319443	1.843229
Li	-2.421028	-0.085776	-0.009103	H	-0.602546	4.154984	1.149673
N	-3.621630	-1.507209	-0.131038	H	-0.597487	3.706558	2.861701
C	-3.255168	-2.812076	-0.641670	H	0.580905	2.983609	1.741416
H	-4.047469	-3.237901	-1.297238	H	-0.710953	3.282074	-0.883118
C	-1.993698	-2.708565	-1.512869	C	-2.853692	3.216284	-0.900957
H	-1.668635	-3.689194	-1.886922	H	-2.991488	3.849841	-0.017517
H	-2.170647	-2.050817	-2.372224	H	-2.951111	3.859551	-1.786027
H	-1.157860	-2.289052	-0.933454	H	-3.673661	2.485156	-0.921093
C	-3.016996	-3.864767	0.471998	C	-1.309179	1.728001	-2.215432
H	-3.885347	-3.933828	1.137867	H	-0.344618	1.211499	-2.232218
H	-2.829663	-4.869950	0.062694	H	-2.102809	0.977793	-2.345074
H	-2.152292	-3.572660	1.082947	H	-1.349521	2.407323	-3.076743
C	-5.005028	-1.426700	0.286292	C	2.440158	1.137860	-0.377292
H	-5.322224	-2.331207	0.852999	C	1.251915	0.562516	0.051401
C	-6.000571	-1.297023	-0.896404	C	1.390320	-0.767333	0.497556
H	-5.831247	-0.348440	-1.423553	C	2.604289	-1.455939	0.510045
H	-5.858055	-2.108076	-1.620415	C	3.761264	-0.809165	0.061773
H	-7.050341	-1.328173	-0.563961	C	3.685366	0.512249	-0.389897
C	-5.205225	-0.238303	1.239631	H	4.572447	1.025911	-0.745511
H	-4.591473	-0.358792	2.140354	C	5.086094	-1.500409	0.126554
H	-4.903544	0.698752	0.748016	F	5.696676	-1.351502	1.335133
H	-6.254590	-0.125535	1.545706	F	5.965880	-1.031762	-0.794851
C	-1.440032	2.161748	1.561969	F	4.982804	-2.838812	-0.073628
H	-2.458513	2.568374	1.696724	H	2.659640	-2.485556	0.854063
C	-1.262449	1.061083	2.620226	H	0.502443	-1.294143	0.854087
H	-1.993437	0.254177	2.481238	Cl	2.431352	2.842865	-0.990819
H	-0.260197	0.622368	2.560244	H	-0.074787	1.129106	0.120510

Table A3.8 (Continued).

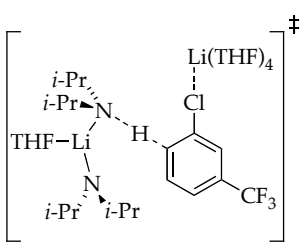

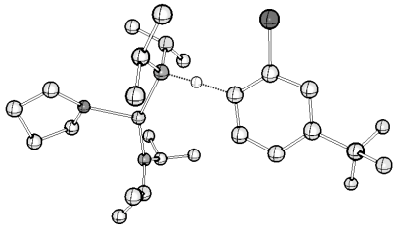

11
G = -1851.998595
G_{MP2} = -1846.899014
(calculation does not include $Li(THF)_4^+$ ion)

Atom	X	Y	Z	Atom	X	Y	Z
C	-0.829428	-2.469154	1.290779	H	-4.594894	-2.480053	-0.640760
N	-0.759814	-1.628579	0.081532	C	-0.953930	-2.384617	-1.169939
Li	-1.975610	0.104943	0.186621	H	-1.976424	-2.804391	-1.204669
N	-2.162551	2.050643	0.503606	C	-0.830849	-1.424285	-2.362146
C	-1.953124	2.656795	1.810281	H	-1.565892	-0.613635	-2.300901
H	-2.284559	3.717552	1.821540	H	0.164891	-0.968012	-2.390697
C	-2.795426	1.956601	2.890913	H	-0.991095	-1.951749	-3.312155
H	-2.594438	2.360600	3.893408	C	0.005820	-3.578931	-1.381833
H	-3.866584	2.068374	2.683546	H	-0.097380	-4.333702	-0.594936
H	-2.573633	0.881499	2.920214	H	-0.205549	-4.072726	-2.340796
C	-0.466377	2.681698	2.247796	H	1.049918	-3.250477	-1.386235
H	0.153445	3.155423	1.477593	H	-0.041829	-3.244903	1.271781
H	-0.314793	3.236839	3.187648	C	-2.172738	-3.202006	1.475348
H	-0.090707	1.660617	2.387246	H	-2.367987	-3.917241	0.667341
C	-1.958607	3.016839	-0.559612	H	-2.179609	-3.765468	2.418776
H	-1.050382	3.641166	-0.389892	H	-3.001639	-2.483224	1.496056
C	-3.129319	4.026191	-0.725851	C	-0.538975	-1.600777	2.521723
H	-4.033206	3.502550	-1.067633	H	0.407249	-1.065201	2.402344
H	-3.368991	4.516144	0.224927	H	-1.331134	-0.857471	2.677850
H	-2.895427	4.816666	-1.456679	H	-0.474829	-2.216634	3.428611
C	-1.737648	2.313548	-1.906271	C	3.047543	-1.303666	0.285050
H	-0.835747	1.691850	-1.884153	C	1.833431	-0.682858	0.025547
H	-2.593624	1.661385	-2.135916	C	1.957265	0.658221	-0.392939
H	-1.636456	3.030098	-2.733145	C	3.182499	1.307805	-0.548799
O	-3.992719	-0.545694	-0.170834	C	4.366532	0.612249	-0.278532
C	-4.548071	-1.488146	-1.105888	C	4.304700	-0.717545	0.149048
C	-5.941813	-0.954728	-1.498454	H	5.211930	-1.267850	0.375870
C	-5.881854	0.519572	-1.061338	C	5.695072	1.260820	-0.501507
C	-4.986121	0.442930	0.171303	F	6.145488	1.112259	-1.779416
H	-5.554774	0.103368	1.052308	F	6.667718	0.747648	0.295460

Table A3.8 (Continued).

H	-4.416913	1.349404	0.406066	F	5.666383	2.598431	-0.273479
H	-6.868225	0.944961	-0.847196	H	3.226131	2.346951	-0.864826
H	-5.401839	1.134919	-1.831780	H	1.047190	1.226387	-0.588260
H	-6.725918	-1.481967	-0.941411	Cl	3.070187	-3.020286	0.874006
H	-6.148983	-1.084505	-2.566113	H	0.497549	-1.204643	0.070433
H	-3.870689	-1.546135	-1.963828				

REFERENCES

1. Mongin, F.; Desponds, O.; Schlosser, M. *Tetrahedron Lett.* **1995**, *37*, 2767.

2. (a) Queguiner, G.; Marsais, F.; Snieckus, Epsztajn, J. *Adv. Heterocycl. Chem.* **1991**, *52*, 187. (b) Mongin, F.; Queguiner, G. *Tetrahedron* **2001**, *57*, 5897. (c) Mongin, F.; Queguiner, G. *Tetrahedron* **2001**, *57*, 4059. (d) Merino, P. *Progr Heterocycl. Chem.* **1999**, *11*, 21. (e) Clayden, J. In *The Chemistry of Organolithium Compounds*; Rappoport, Z.; Marek, I., Eds.; Wiley: New York, 2004, Vol. 1, p 495. (f) Caubere, P. In *Reviews of Heteroatom Chemistry*; MYU: Tokyo, *vol. 4*, (1991); pp. 78-139. (g) Caubere, P. *Chem. Rev.* **1993**, *93*, 2317. (h) Marsais, F.; Queguiner, G. *Tetrahedron* **1983**, *39*, 2009. (i) Collins, I. *Perkin 1* **2000**, 2845. (i) Schlosser, M.; Mongin, F. *Chem. Soc. Rev.* **2007**, *36*, 1161. (j) Hartung, C. G.; Snieckus, V. In *Modern Arene Chemistry*, Astruc, D. (Ed.), Wiley-VCH: Weinheim, 2002; Chapter 10. (k) Snieckus, V. *Chem. Rev.* **1990**, *90*, 879. (l) Taylor, C. M.; Watson, A. J. *Curr. Org. Chem.* **2004**, *8*, 623. (m) Bakker, W. I. I.; Wong, P. L.; Snieckus, V. Lithium Diisopropylamide. In *e-EROS*; Paquette, L. A., Ed.; John Wiley: New York, 2001.

3. Ma, Y.; Hoepker, A. C.; Gupta, L.; Faggin; M. F.; Collum, D. B. *J. Am. Chem. Soc.*, **2010**, *132*, 15610.

4. (a) Cottet, F.; Schlosser, M. *Eur. J. Org. Chem.* **2004**, 3793. (b) Trecourt, F.; Mallet, M.; Marsais, F.; Quéguiner, G. *J. Org. Chem* **1988**, *53*, 1367. (c) Comins, D. L.; LaMunyon, D. H. *Tetrahedron Lett.* **1988**, *29*, 773. (d) Eaton, P. E.; Cunkle, G. T.; Marchioro, G.; Martin, R. M. *J. Am. Chem. Soc.* **1987**, *109*, 948. (e) Bridges.

A. J.; Patt, W. C.; Stickney, T. M. *J. Org. Chem.* **1990**, *55*, 773. (f) Trécourt, F.; Marsais, F.; Güngör, T.; Quéguiner, G. *J. Chem. Soc., Perkin Trans. 1* **1990**, 2409. (g) Gros, P. C.; Fort, Y. *Eur. J. Org. Chem.* **2009**, 4199. (h) Cottet, F.; Marull, M.; Lefebvre, O.; Schlosser, M. *Eur. J. Org. Chem.* **2003**, 1559. (i) Güngör, T.; Marsais, F.; Quéguiner, G. *J. Organomet. Chem.* **1981**, *215*, 139. (j) Fukuda, T.; Ohta, T.; Sudo, E.; Iwao, M. *Org. Lett.* **2010**, *12*, 2734.

5. Viciu, M.; Gupta, L.; Collum, D. B. *J. Am. Chem. Soc.* **2010**, *132*, 6361.

6. (a) Singh, K. J.; Hoepker, A. C.; Collum, D. B. *J. Am. Chem. Soc.* **2008**, *130*, 18008. (b) Gupta, L.; Hoepker, A. C.; Singh, K. J.; Collum, D. B. *J. Org. Chem.* **2009**, *74*, 2231. (c) Gupta, L. Rate Studies of Organolithium-Mediated Reactions: Reaction of Lithium Diisopropyamide with Fluoropyridines and Reaction of Lithium Diethamide with an Alkyl Bromide and an Alkyl Sulfonate. Ph.D. Thesis, Cornell University, Ithaca, NY, August 2010. (d) Hoepker, A. C. Aggregation Dynamics of Lithium Diisopropylamide and Their Influence on Reactivity. Ph.D. Thesis, Cornell University, Ithaca, NY, August 2011.

7. For examples of reactions that are fast relative to the rates of aggregate-aggregate exchanges see: (a) McGarrity, J. F.; Ogle, C. A. *J. Am. Chem. Soc.* **1985**, *107*, 1810. (b) Jones, A. C.; Sanders, A. W.; Bevan, M. J.; Reich, H. J. *J. Am. Chem. Soc.* **2007**, *129*, 3492. (c) Thompson, A.; Corley, E. G.; Huntington, M. F.; Grabowski, E. J. J.; Remenar, J. F.; Collum, D. B. *J. Am. Chem. Soc.* **1998**, *120*, 2028. (d) Jones, A. C.; Sanders, A. W.; Sikorski, W. H.; Jansen, K. L.; Reich, H. J. *J. Am. Chem. Soc.*, **2008**, *130* , 6060.

8. A survey of approximately 500 total syntheses revealed LDA to be the most commonly used reagent. Reich, H. J., unpublished.

9. (a) Seebach, D. In *Proceedings of the Robert A. Welch Foundation Conferences on Chemistry and Biochemistry*; Wiley: New York, 1984; p 93. (b) Seebach, D. *Angew. Chem., Int. Ed. Engl.* **1988**, *27*, 1624. (c) Tchoubar, B.; Loupy, A. *Salt Effects in Organic and Organometallic Chemistry*; VCH: New York, 1992; Chapters 4, 5, and 7. (d) Caubère, P. *Chem. Rev.* **1993**, *93*, 2317.

10. (a) Collum, D. B. *Acc. Chem. Res.* **1993**, *26*, 227. (b) Lucht, B. L.; Collum, D. B. *Acc. Chem. Res.* **1999**, *32*, 1035.

11. (a) Kim, Y.-J.; Bernstein, M. P.; Galiano-Roth, A. S.; Romesberg, F. E.; Fuller, D. J.; Harrison, A. T.; Collum, D. B.; Williard, P. G. *J. Org. Chem.* **1991**, *56*, 4435. (b) Collum, D. B. *Acc. Chem. Res.* **1993**, *26*, 227.

12. ^{6}Li is spin one. For a review of ^{6}Li NMR spectroscopy, see: Günther, H. *J. Brazil. Chem.* **1999**, *10*, 241.

13. (a) Espinet, P.; Albeniz, A. C.; Casares, J. A.; Martinez-Ilarduya, J. M. *Coor. Chem. Rev.* **2008**, *252*, 2180. (b) Gakh, Y. G.; Gakh, A. A.; Gronenborn, A. M. *Magn. Reson. Chem.* **2000**, *38*, 551. (c) McGill, C. A.; Nordon, A.; Littlejohn, D. *J. Process Analyt. Chem.* **2001**, *6*, 36. (d) Espinet, P.; Albeniz, A. C.; Casares, J. A.; Martinez-Ilarduya, J. M. *Coor. Chem. Rev.* **2008**, *252*, 2180.

14. Krasovskiy, A.; Knochel, P. *Angew. Chem., Int. Ed.* **2004**, *43*, 3333.

15. *Gaussian 03*; revision B.04; Frisch, M. J.; Trucks, G. W.; Schlegel, H. B.; Scuseria, G. E.; Robb, M. A.; Cheeseman, J. R.; Montgomery, Jr., J. A.; Vreven, T.; Kudin, K. N.; Burant, J. C.; Millam, J. M.; Iyengar, S. S.; Tomasi, J.; Barone, V.; Mennucci, B.; Cossi, M.; Scalmani, G.; Rega, N.; Petersson, G. A.; Nakatsuji, H.; Hada, M.; Ehara, M.; Toyota, K.; Fukuda, R.; Hasegawa, J.; Ishida, M.; Nakajima, T.; Honda, Y.; Kitao, O.; Nakai, H.; Klene, M.; Li, X.; Knox, J. E.; Hratchian, H. P.; Cross, J. B.; Bakken, V.; Adamo, C.; Jaramillo, J.; Gomperts, R.; Stratmann, R. E.; Yazyev, O.; Austin, A. J.; Cammi, R.; Pomelli, C.; Ochterski, J. W.; Ayala, P. Y.; Morokuma, K.; Voth, G. A.; Salvador, P.; Dannenberg, J. J.; Zakrzewski, V. G.; Dapprich, S.; Daniels, A. D.; Strain, M. C.; Farkas, O.; Malick, D. K.; Rabuck, A. D.; Raghavachari, K.; Foresman, J. B.; Ortiz, J. V.; Cui, Q.; Baboul, A. G.; Clifford, S.; Cioslowski, J.; Stefanov, B. B.; Liu, G.; Liashenko, A.; Piskorz, P.; Komaromi, I.; Martin, R. L.; Fox, D. J.; Keith, T.; Al-Laham, M. A.; Peng, C. Y.; Nanayakkara, A.; Challacombe, M.; Gill, P. M. W.; Johnson, B.; Chen, W.; Wong, M. W.; Gonzalez, C.; and Pople, J. A.; Gaussian, Inc., Wallingford CT, 2004.

16. (a) Ramirez, A.; Candler, J.; Bashore, C. G.; Wirtz, M. C.; Coe, J. W.; Collum, D. B. *J. Am. Chem. Soc.* **2004**, *126*, 14700. (b) Riggs, J. C.; Ramirez, A.; Cremeens, M. E.; Bashore, C. G.; Candler, J.; Wirtz, M. C.; Coe, J. W.; Collum, D. B. *J. Am. Chem. Soc.* **2008**, *130*, 3406. (c) Kottke, T.; Sung, K.; Lagow, R. J. *Angew. Chem., Int. Ed. Engl.* **1995**, *34*, 1517. (d) Reich, H. J.; Green, D. P.; Medina, M. A.; Goldenberg, W. S.; Gudmundsson, B. Ö.; Dykstra, R. R.; Phillips, N. H. *J. Am. Chem. Soc.* **1998**, *120*, 7201. (e) Bonasia, P. J.; Arnold, J. *J. Organomet. Chem.* **1993**, *449*, 147. (f) ref 6a.

17. Galiano-Roth, A. S.; Kim, Y.-J.; Gilchrist, J. H.; Harrison, A. T.; Fuller, D. J.; Collum, D. B. *J. Am. Chem. Soc.* **1991**, *113*, 5053.

18. Snaith and coworkers underscored the merits of R_3NHX salts as precursors to anhydrous LiX salts. See: Barr, D.; Snaith, R.; Wright, D. S.; Mulvey, R. E.; Wade, K. *J. Am. Chem. Soc.* **1987**, *109*, 7891. Also see: Hall, P. L.; Gilchrist, J. H.; Collum, D. B. *J. Am. Chem. Soc.* **1991**, *113*, 9571.

19. Zhao, P.; Collum, D. B. *J. Am. Chem. Soc.* **2003**, *125*, 14411 and references cited therein.

20. Rein, A. J.; Donahue, S. M.; Pavlosky, M. A. *Curr. Opin. Drug Discovery Dev.* **2000**, *3*, 734.

21. (a) Espenson, J. H. *Chemical Kinetics and Reaction Mechanisms*, 2nd ed.; McGraw-Hill: New York, 1995; Chapter 2, p 44. (b) Atkins, P. W.; Jones, L. L. *Chemical Principles: The Quest for Insight*, 2nd ed.; W H. Freeman: New York, 2002. (c) Rae, M.; Berberan-Santos, M. N. *J. Chem. Educ.*, **2004**, *81*, 436.

22. Determining initial rates (slopes) of a curved decay can be strongly dependent on the percent conversion, requiring a compromise between adequate sample size and loss of linearity. This problem is avoided by fitting a significant part of the decay—a portion that includes some curvature—to a third-order polynomial (at^2+bt+c), making sure not to include too much curvature. The parameter b represents the rate at time zero. (One may verify this by tak-

ing the first derivative with respect to t and setting $t = 0$. Initial rate = $f'(0)$ = b). The experimental observable (NMR intensity, IR absorbance etc.) is converted to concentration to ensure a valid comparison between initial rates of varying concentrations.

23. For a review of rate studies of LDA-mediated reactions see: Collum, D. B.; McNeil, A. J.; Ramirez, A. *Angew. Chem., Int. Ed.* **2007**, *46*, 3002.

24. The concentration of LDA, although expressed in units of molarity, refers to the concentration of the monomer unit (normality). The concentration of THF is expressed as total concentration of free (uncoordinated) ligand.

25. The minor deviation above first order has the appearance of experimental error. A forthcoming study, however, describes experimental evidence of LDA-tetramer-based reactivities.

26. We define the idealized rate law as that obtained by rounding the observed reaction orders to the nearest rational order.

27. Open dimers were first proposed for the isomerization of oxiranes to allylic alcohols by mixed metal bases. See: Mordini, A.; Rayana, E. B.; Margot, C.; Schlosser, M. *Tetrahedron* **1990**, *46*, 2401. For a bibliography of lithium amide open dimers, see Ramirez, A.; Sun, X.; Collum, D. B. *J. Am. Chem. Soc.* **2006**, *128*, 10326 and references cited therein.

28. Competitive and intramolecular isotope effects can be used to examine post-rate-limiting proton transfer. They differ in that the intramolecular isotope effect demands a symmetry-equivalent choice of H versus D within the same molecule whereas the competitive isotope effect requires an exchange mechanism to establish the choice of H versus D.

29. (a) Carpenter, B. K. *Determination of Organic Reaction Mechanisms*; Wiley: New York, 1984. (b) Whisler, M. C.; MacNeil, S.; Snieckus, V.; Beak, P. *Angew. Chem., Int. Ed.* **2004**, *43*, 2206.

30. The calculated isotope effects in eqs 6 and 7 derive from the regioselectivities derived from **1**, **1**-2-d_1, and **1**-6-d_1. If the isotope effects are calculated using **1**-2,6-d_2 instead of **1**, the isotope effects are calculated as follows:

$$k_{H(2)}/k_{D(2)} = (k_{H(2)}/k_{D(6)})(k_{D(6)}/k_{D(2)}) = 50$$

$$k_{H(6)}/k_{D(6)} = (k_{H(6)}/k_{D(2)})(k_{D(2)}/k_{D(6)}) = 12$$

31. The method used to prepare **1**-2,4-d_2 involves initial metalation by LDA and quenching with MeOD (1.0 equiv) followed by alternating pulses of *n*-BuLi *without intermediate workups* may have a general utility for exhaustive deuteration of the acidic sites on arenes.

32. (a) Stegelmann, C.; Andreasen, A.; Campbell, C. T. *J. Am. Chem. Soc.* **2009**, *131*, 8077. (b) Maniscalco, S. J.; Tally, J. F.; Fisher, H. F. *Archives Biochem. Biophys.* **2004**, *425* 165.

33. (a) Isotopic perturbation is insufficient to resolve the resonances of **1** and **1**-2,6-d_2 by ^{19}F NMR spectroscopy.[33b-d] The IR absorbances of **1** (1428 cm^{-1}) and **1**-2,6-d_2 (1384 cm^{-1}) could be monitored, but with some error introduced by absorbances of the aryllithiums. (b) Hindermann, D. K.; Cornwell, C. D. *J. Chem. Phys.* **1968**, *48*, 4148. (c) Forsyth, D. A.; Yang, J.-R. *J. Am. Chem. Soc.* **1986**, *108,* 2157. (d) Lambert, J. B.; Greifenstein, L. G. *J. Am. Chem. Soc.* **1973**, *95*, 6150.

34. For an attempted comprehensive bibliography of anionic triple ions of lithium salts (X-Li-X$^-$), see: Ma, Y.; Ramirez, A.; Singh, K. J.; Keresztes, I.; Collum, D. B. *J. Am. Chem. Soc.* **2006**, *128*, 15399.

35. The computations use the Gaussian standard state of 1.0 atm. If the THF concentration is corrected to neat THF (approximately 12 M), each solvation step benefits from approximately 2.0 kcal/mol of additional stabilization at -78 °C (195 K). Pratt, L. M.; Merry, S.; Nguyen, S. C.; Quan, P.; Thanh, B. T. *Tetrahedron* **2006**, *62*, 10821.

36. Frey, P. A.; Hegeman, A. D. *Enzymatic Reaction Mechanisms*; Oxford University Press: New York, 2007; Chapter 2.

37. LDA-mediated ortholithiations of 2-fluoropyridines also show a second-order catalysis by LiCl.[6]

38. (a) Ma, Y.; Collum, D. B. *J. Am. Chem. Soc.* **2007**, *129*, 14818. (b) Depue, J. S.; Collum, D. B. *J. Am. Chem. Soc.* **1988**, *110*, 5524. (c) Galiano-Roth, A. S.; Collum, D. B. *J. Am. Chem. Soc.* **1989**, *111*, 6772.

39. Laurence, C.; Nicolet, P.; Dalati, M.T.; Abboud, J.-L. M.; Notario, R. *J. Phys. Chem.* **1994**, *98*, 5807.

40. (a) Lucht, B. L.; Collum, D. B. *J. Am. Chem. Soc.* **1994**, *116*, 6009. (b) Remenar, J. F.; Lucht, B. L.; Collum, D. B. *J. Am. Chem. Soc.* **1997**, *119*, 5567.

41. Equation 15 appear to become undefined at $[LiCl_T] = 0$, but this is not the case as described previously.[3]

42. (a) Besson, C.; Finney, E. E.; Finke, R. G. *J. Am. Chem. Soc.* **2005,** *127,* 8179. (b) Besson, C.; Finney, E. E.; Finke, R. G. *Chem. Mater.* **2005,** *17,* 4925. (c) Huang, K. T.; Keszler, A.; Patel, N.; Patel, R. P.; Gladwin, M. T.; Kim-Shapiro, D. B.; Hogg, N. *J. Biol. Chem.* **2005**, *280,* 31126. (d) Huang, Z.; Shiva, S.; Kim-Shapiro, D. B.; Patel, R. P.; Ringwood, L. A.; Irby, C. E.; Huang, K. T.; Ho, C.; Hogg, N.; Schechter, A. N.; Gladwin, M. T. *J. Clin. Invest.* **2005**, *115*, 2099. (e) Tanj, S.; Ohno, A.; Sato, I.; Soai, K *Org. Lett.* **2001**, *3*, 287. (f) Barrios-Landeros, F.; Carrow, B. P.; Hartwig, J. F. *J. Am. Chem. Soc.* **2008**, *130*, 5842.

43. (a) Depue, J. S.; Collum, D. B. *J. Am. Chem. Soc.* **1988**, *110*, 5524. (b) McNeil, A. J.; Toombes, G. E. S.; Gruner, S. M.; Lobkovsky, E.; Collum, D. B.; Chandramouli, S. V.; Vanasse, B. J.; Ayers, T. A. *J. Am. Chem. Soc.* **2004**, *126*, 16559. (c) Nudelman, N. S.; Velurtas, S.; Grela, M. A. *J. Phys. Org. Chem.* **2003**, *16*, 669. (d) Alberts, A. H.; Wynberg, H. *J. Am. Chem. Soc.* **1989**, *111,* 7265. (e) Alberts, A. H.; Wynberg, H. *J. Chem. Soc., Chem. Commun.* **1990**, 453.

44. The principle of microscopic reversibility seems to have been the source of frequent controversies and must be applied with caution. It is not obvious to us, for example, that following authors, all warning of the risks, would agree with each other's assertions: (a) Blackmond, D. G. *Angew. Chem., Int. Ed.* **2009**, *48*, 2648. (b) Krupka, R. M.; Kaplan, H.; Laidler, K. J. *J. Chem. Soc., Faraday Trans. 62*, **1966**, 2754. (c) Chandrasekhar, S. *Res. Chem. Intermed.* **1992**, *17*, 173. (d) Burwell, R. L.; Pearson, R. G. *J. Phys. Chem.* **1966**, *70*, 300.

45. For a discussion of the mechanistic basis of cooperative substituent effects in ortholithiation, see: Chadwick, S. T.; Ramirez, A.; Gupta, L.; and Collum, D. B. *J. Am. Chem. Soc.* **2007**, *129*, 2259.

46. (a) Chadwick, S. T.; Rennels, R. A.; Rutherford, J. L.; Collum, D. B. *J. Am. Chem. Soc.* **2000,** *122,* 8640. (b) Anderson, D. R.; Faibish, N. C.; Beak, P. *J. Am. Chem. Soc.* **1999,** *121,* 7553. (c) Singh, K. J.; Collum, D. B. *J. Am. Chem. Soc.* **2006**, *128*, 13753. (d) Meyers, A. I.; Mihelich, E. D. *J. Org. Chem.* **1975**, *40*, 3158. (e) Ramirez, A.; Sun, X.; Collum, D. B. *J. Am. Chem. Soc.* **2006**, *128*, 10326. (f) Sun, X.; Collum, D. B. *J. Am. Chem. Soc.* **2000**, *122*, 2452. (g) Ma, Y.; Breslin, S.; Keresztes, I.; Lobkovsky, E.; Collum, D. B. *J. Org. Chem.* **2008**, *73*, 9610.

47. (a) Ruszczycky, M. W.; Anderson, V. E. *J. Theoretical Biol.* **2006**, *243*, 328. (b) Ray, W. J., Jr. *Biochemistry* **1983**, *22*, 4625.

48. (a) Gregory, K.; Schleyer, P. v. R.; Snaith, R. *Adv. Inorg. Chem.* **1991**, *37*, 47. (b) Mulvey, R. E. *Chem. Soc. Rev.* **1991,** *20*, 167. (c) Beswick, M. A.; Wright, D. S. In *Comprehensive Organometallic Chemistry II*; Abels, E. W., Stone, F. G. A., Wil-

kinson, G., Eds.; Pergamon Press: New York, 1995; Vol. 1, Chapter 1. (d) Mulvey, R. E. *Chem. Soc. Rev*. **1998**, *27,* 339. (e) Rutherford, J. L.; Collum, D. B. *J. Am. Chem. Soc.* **1999**, *121*, 10198.

49. A four-rung LDA/LiX ladder has been characterized: Williard, P. G.; Hintze, M. J. *J. Am. Chem. Soc.* **1987**, *109*, 5539.

50. Romesberg, F. E.; Collum, D. B. *J. Am. Chem. Soc.* **1994**, *116*, 9198.

51. (a) Evans, W. J.; Broomhall-Dillard, R. N. R.; Ziller, J. W. *J. Organomet. Chem.* **1998**, *569*, 89. (b) Klingebiel, U.; Tecklenburg, B.; Noltemeyer, M.; Schmidt-Baese, D.; Herbst-Irmer, R. *Z. Naturforsch., B: Chem. Sci.* **1998**, *53*, 355.

52. The most stable lithium cation [+Li(THF)$_5$] and most stable triple ion {[(THF)$_4$LiClLi(THF)$_3$]+} are related as follows:

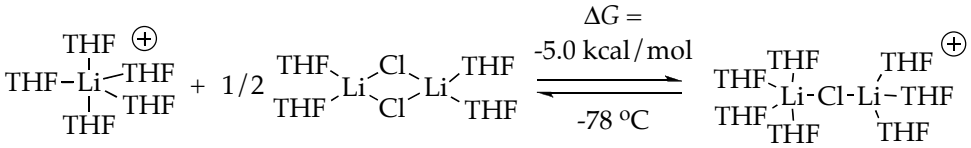

For related computations, see: Yakimansky, A. V.; Müller, A. H. E.; Van Beylen, M. *Macromolecules* **2000**, *33*, 5686.

53. Representative examples of structurally characterized bridging THF ligands: (a) Pratt, L. M.; Merry, A.; Nguyen, S. C.; Quanb, P.; Thanh, B. T. *Tetrahedron* **2006**, *62*, 10821. (b) Clegg, W.; Liddle, S. T.; Mulvey, R. E.; Robertson, A. *Chem.Commun.* **1999**, 511. (c) Boche, G.; Boie, C.; Bosold, F.; Harms, K.;

Marsch, M. *Angew. Chem., Int. Ed.* **1994**, *33*, 115. (d) Daniele, S.; Drost, C.; Gehrhus, B. Hawkins, S. M.; Hitchcock, P. B.; Lappert, M. F.; Merle, P. G.; Bott, S. G. *J. Chem.Soc., Dalton Trans.* **2001**, 3179. (e) Chivers, T.; Fedorchuk, C.; Parvez, M. *Inorg.Chem.* **2004**, *43*, 2643. (f) Briand, G. G.; Chivers, T.; Parvez, M. *J. Chem. Soc., Dalton Trans.* **2002**, 3785.

54. Clegg, W.; Horsburgh, L.; Mackenzie, F. M.; Mulvey, R. E. *J. Chem. Soc., Chem. Commun.* **1995**, 2011.

55. THF exchange on LDA is too fast to monitor by NMR spectroscopy, but it is calculated to occur with activation barriers of <4 kcal/mol.[6d]

56. During the the following carbamate metalation[6a]

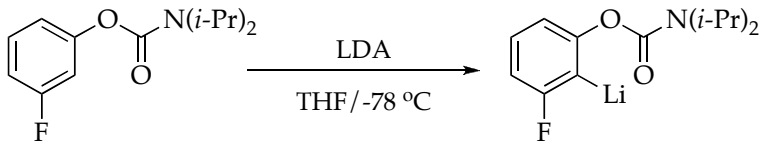

two concerns lingered: the metalation displayed an unexpectedly small isotope effect (k_H/k_D = 3–4), and a plot of rate versus concentration showed a first order arene dependence but with a downward curvature that looks suspiciously like an incomplete version of the saturation curve in Figure 3.7. Indeed, we have now found a large competitive isotope effect (k_H/k_D > 30), suggesting that the first order dependence does *not* involve proton transfer and that deuterium transfer is partially rate limiting.

57. Trapping experiments can be unreliable measures of the rates because they generate catalytically active lithium salts. Trimethylchlorosilane, for example, generates LiCl, rendering LiCl-sensitive arene lithiations nearly instantaneous. We chose benzaldehyde for our hypothetical example because alkoxides are not active deaggregation catalysts.[6]

58. Warming to -20 °C in the presence of spiro[2.4]hepta-4,6-diene shows no evidence of trapping products. We do, however, see evidence of *n*-BuLi adducts if metalations with *n*-BuLi are allowed to inadvertently warm. Leading reference to benzyne formation: Riggs, J. C.; Ramirez, A.; Cremeens, M. E.; Bashore, C. G.; Candler, J.; Wirtz, M. C.; Coe, J. W.; Collum, D. B. *J. Am. Chem. Soc.* **2008**, *130*, 3406.

59. Kopach, M. E.; Kobierski, M. E.; Coffey, D. S.; Alt, C. A.; Zhang, T.; Borghese, A.; Trankle, W. G.; Roberts, D. J. *Org. Process Res. Dev.* **2010**, *14*, 1229.

60. The observed selectivities for the metalation of **1** by *n*-BuLi and *sec*-BuLi show approximately threefold higher proportions of **2** relative to **3** as the arene concentration goes from 0.05 equiv of **1** to 1.0 equiv of **1**. This result appears to be a kinetic consequence of mixed aggregates favoring formation of **3**. For references to structures and reactivities of *n*-BuLi/RLi ensembles, see: Chase, P. A.; Lutz, M.; Spek, A. L.; Gossage, R. A.; van Koten, G. *Dalt. Trans.* **2008**, 5783.

61. (a) Guareschi, I. *Atti della Reale Accademia delle Scienze di Torino* **1894**, *29*, 680. (b) Leonard, N. J.; Nommensen, E. W. *J. Am. Chem. Soc.* **1949**, *71*, 2808. (c) Hall, P. L.; Gilchrist, J. H.; Harrison, A. T.; Fuller, D. J.; Collum, D. B. *J. Am. Chem. Soc.* **1991**, *113*, 9575.

62. (a) Marck, W.; Huisgen, R. *Chem. Ber.* **1960**, *93*, 608. (b) Gaudemar-Bardone, F.; Gaudemar M. *Synthesis* **1979**, 463. (c) Reetz, M. T.; Maier, W. F. *Liebigs Ann. Chem.* **1980**, 1471. (d) Williard, P. G.; Carpenter, G. B. *J. Am. Chem. Soc.* **1986**, *108*, 462.
Williard, P. G.; Salvino, J. M. *J. Org. Chem.* **1993**, *58*, 1. (e) Morrison, R. C.; Hall, R. W.; Rathman, T. L. Stable Lithium Diisopropylamide and Method of Preparation. U.S. Patent 595,779, June 17, 1986.

63. Kofron, W. G.; Baclawski, L. M. *J. Org. Chem.* **1976**, *41*, 1879.

64. For an explanation of Levenberg-Marquardt nonlinear least-squares optimization, see: Press, W. H.; Flannery, B. P.; Teukolsky, S. A.; Vetterling, V. T. *Numerical Recipes in C*; Cambridge University Press: London, 1988; Chapter 14.4.

65. Brown, P. N.; Byrne, G. D.; Hindmarsh, A. C. *J. Sci. Stat. Comput.* **1989**, *10*, 1038.

CHAPTER 4

COMPUTATIONAL STUDIES OF LITHIUM DIISOPROPYLAMIDE DEAGGREGATION

Computational Studies of Lithium Diisopropylamide Deaggregation

Abstract

Density functional theory computations (MP2/6–31G*//B3LYP/6–31G*) on the deaggregation of lithium diisopropylamide (LDA) dimer solvated by two tetrahydrofuran ligands to give the corresponding trisolvated monomer show seven structurally distinct minima. The barriers to exchange are comparable to those expected from experimental studies showing rate-limiting deaggregations. The role of conformational isomerism in deaggregation and the extent that deaggregation rates dictate LDA reactivity under synthetically important conditions are considered.

Introduction

Lithium diisopropylamide (LDA) is prominent in organic synthesis.[1] In a comprehensive survey of reagents used in approximately 500 natural product syntheses, LDA came out number one.[2] This prevalence is one of the two reasons why we have focused on understanding the structure-reactivity relationships in LDA-mediated reactions. The other is that LDA offers a highly tractable template with which to study the influence of aggregation and solvation on organolithium reaction mechanism.[3] The numerous synthetic applications of LDA combine with its complex coordination chemistry to produce considerable mechanistic variations.

To understand the source of the complexity—if not the complexity itself—we present Scheme 1, which summarizes the deaggregation of disolvated LDA dimer **1** to trisolvated monomer **6**. For many reactions, typically those that are conveniently monitored between 0 °C and –60 °C, the

aggregate equilibrations proceed very quickly compared to the rate of reaction being studied. Under conditions of fully established equilibria, all aggregates are available to react with the substrate, and studies have shown that many do.[3] During the course of our research we began to believe that a coherent picture of reactivity had emerged, which prompted us to summarize the results in a review.[3]

Scheme 1

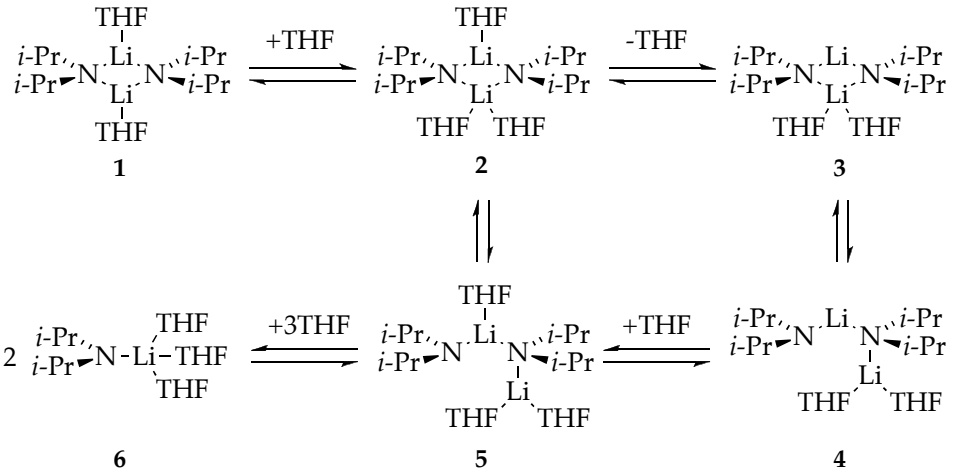

Recent rate studies, however, began to uncover aberrant behaviors that failed to follow conventional patterns. For example, during studies of imine metalations in which the relative reactivities spanned an approximate 60,000-fold range, the most reactive imine required that the reaction temperature be reduced to –78 °C (eq 1).[4] This was the first time that we had investigated the kinetics of an LDA-mediated metalation at -78 ^{0}C, and something odd happened: the loss of imine failed to follow a normal (first-order) decay, instead displaying a persistent linearity over the first two half lives. We noted but largely ignored this observation.[4] Soon thereafter, odd substrate decays

began appearing in disparate reactions including a host of ortholithiations[5,6,7] (such as eqs 2 and 3)[8] and even 1,4-additions of LDA to unsaturated esters (eq 4).[9] *All* shared two common traits: they were carried out using LDA in tetrahydrofuran (THF) at –78 °C, and they displayed hypersensitivities to traces of LiCl (as little as 1.0 ppm).

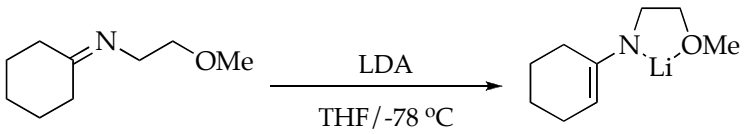

(1)

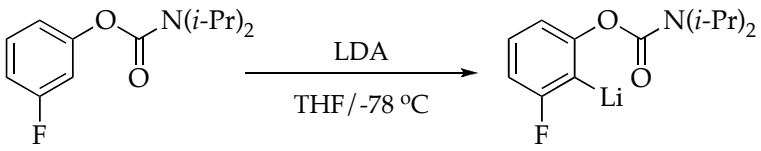

(2)

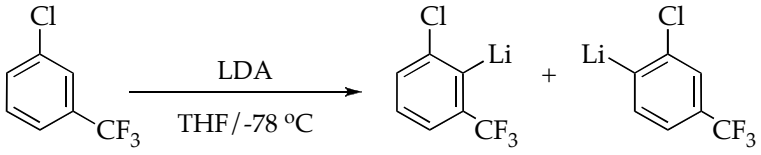

(3)

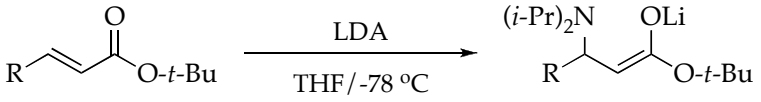

(4)

Mechanistic studies indicated that LDA aggregate exchanges were dictating the reaction rate,[10] causing the emerging mechanistic picture to be quite vexing. The odd linear decays observed for ortholithiations of aryl carbamates (eq 2)—apparent zeroth-order substrate dependencies consistent with rate-limiting deaggregation of LDA dimer—were traced instead to virulent autocatalysis and the intervention of highly reactive mixed aggregates.[6] Unusual time-dependent changes in the concentration of LDA-

ArLi mixed dimers attested to non-equilibrium conditions. The ortholithiation in eq 3 was found to be both autocatalyzed[11,12] and LiCl catalyzed, but the rate-limiting step of the uncatalyzed metalation involved rate-limiting deaggregation—a true zeroth-order substrate dependence—via a disolvated-dimer-based transition structure. Post-rate-limiting lithiation was shown to occur via a fleeting dimer-based rather than a monomer-based intermediate. Both autocatalysis and LiCl catalysis, by contrast, were shown to divert the reaction through a monomer-based mechanism. Seemingly analogous linear decays for 1,4-additions of LDA to unsaturated esters (eq 4) also involved a rate-limiting deaggregation of LDA, but it was found to occur via a *trisolvated*-dimer-based transition structure rather than via a disolvated dimer seen for ortholithiation.[9] Different substrates were reacting via different rate-limiting deaggregations! The post-rate-limiting 1,4-additions were shown to proceed via an LDA-monomer-based pathway. Highly muted autocatalysis and dramatic catalysis by LiCl were traced explicitly to catalyzed deaggregation to the same LDA monomer.[13]

Although in isolation the case studies seemed logical, considered together they were painting a chaotic mechanistic picture. We began to realize that a complete understanding of LDA-mediated reactions under these highly prevalent conditions—LDA/THF/–78 °C—demanded a greater understanding of LDA deaggregation. Although aggregation dynamics have received some attention, detailed analyses of organolithium deaggregations seem to be absent.[14] In this paper computational studies show that the intermediates in Scheme 1 are not just figments of our imagination but rather legitimate minima en route from the resting state of LDA (**1**)[15] to fleeting trisolvated monomer **6**. Moreover, conformational effects on the stabilities of

1–6 as well as on the activation barriers to exchange are surprising in both detail and implication.[16]

Results

General. All structures were computed using diisopropylamido groups and THF ligands without structural approximations. Density functional theory (DFT) and MP2 calculations were performed with the Gaussian 09 package using Gaussview 5.0 and WebMO as a graphical user interface.[17] Geometry optimizations and frequency calculations were performed at the B3LYP/6–31G(d) level of theory. Free energies were calculated from an MP2-derived single-point energy [6–31G(d) basis set] and a B3LYP-derived thermal correction [6–31G(d)] at 195 K (–78 °C) and 1 atm.[18] (MP2 corrections seem to provide superior correlations of theory and experiment, especially for the most highly solvated forms of LDA.)[19] Transition structures were confirmed by the existence of a single imaginary frequency, and intrinsic reaction coordinate (IRC) calculations[20] confirm the connection with specific minima. The energy surface describing LDA deaggregation is summarized in Scheme 2.

Minima. Moving from left to right in Scheme 2 corresponds to the stepwise conversion of known disolvated dimer **1**[15] (and related less symmetric cyclic dimers) through open dimers to give monomers as indicated in grey scale along the reaction coordinate (*x* axis). The key minima in Scheme 2 correspond to structures **1–6** in Scheme 1. Bridged dimer **7** and disolvated monomer **8** are also valid minima. The shaded regions correspond to conformational ensembles of di- and trisolvated open dimers **4** and **5**.[21] Energy levels inside the shaded region correspond to specific conformers. The lines

illustrate connections between transition structures and specific conformational isomers of minima. Minima **2** and **3** are linked directly because the transformation is computed to be barrierless.

Scheme 2

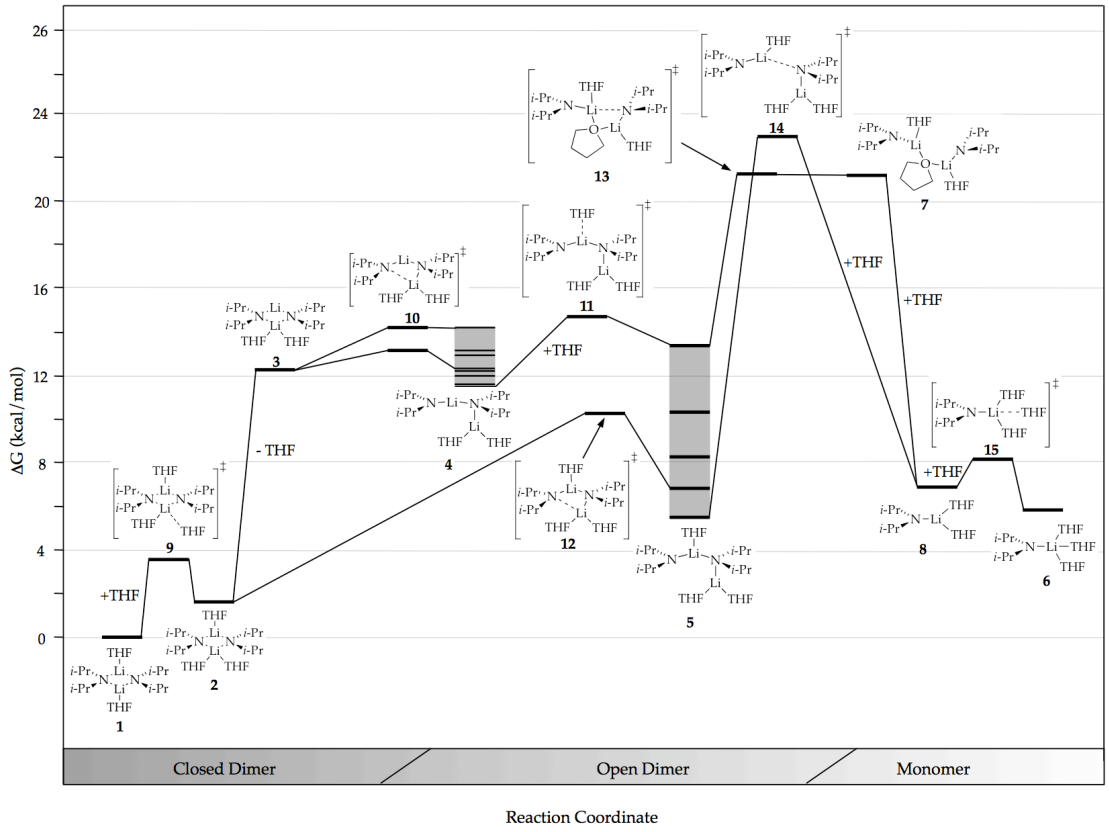

The steric demands and chirality of the isopropyl group render the potential energy surface of LDA aggregation and solvation rich in detail. Diisopropylamido moieties display two conformational minima corresponding to mirror images (eq 5).[22] Consequently, LDA dimers can exist as both homochiral and heterochiral (meso) diastereomers. A number of comparisons, however, show that in the open dimers and open dimer-based transition structures, the two diisopropylamido moieties do not communicate, resulting in comparable energies. The energies in Scheme 2 derive from the homochiral form. In the cyclic dimers (**1**, **2**, and **3**), the homochiral form is preferred over the heterochiral (meso) form by ≈1 kcal/mol. The computed structure of **1** matches the crystal structure.[15a]

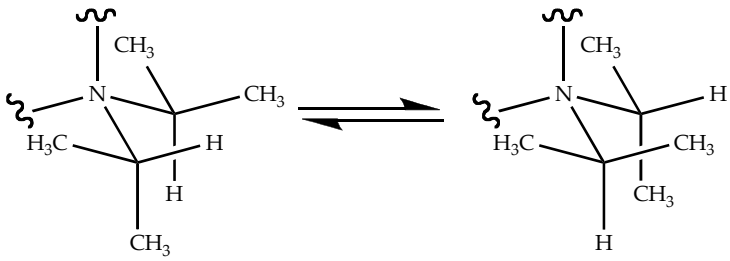

(5)

Two spatial relationships are prominent in open dimers. By sighting along the axis defined by the two nitrogen atoms (dashed line in Scheme 3), we loosely define a pseudo dihedral angle (ω_{CC}) to describe conformational isomerism arising from the rotational orientations of the two diisopropylamido moieties. These orientations are most easily envisioned by imagining rotation about the N–Li bond of the terminal diisopropylamido group. We define a second, standard dihedral angle (ω_{LiO}) that describes the THF orientations as defined by rotation about the N–Li bond to the terminal lithium. The open dimers are organized by dihedral angles ω_{CC} and ω_{LiO} in

supporting information. Other minor conformational adjustments, such as the rotations about the individual THF ligands, coincide with these primary conformational changes.

Scheme 3

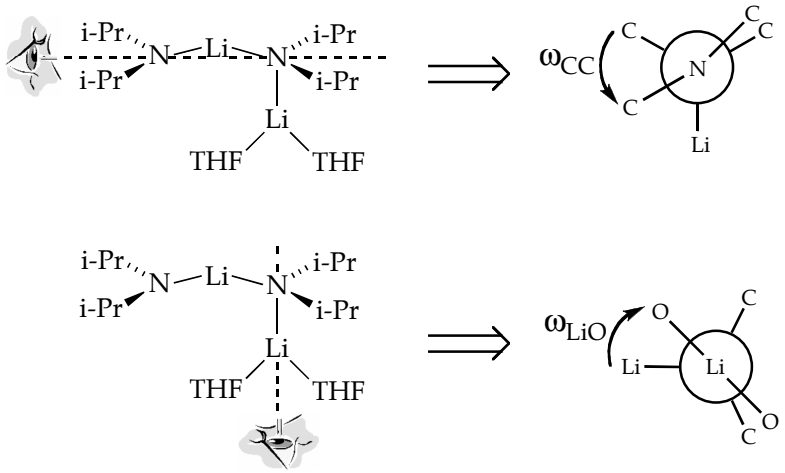

We sampled the conformers of disolvated open dimers **4** by incrementally varying ω_{CC}. Structures **4a**–**4e** (Scheme 4) are representative of the eight conformers available through a 180° rotation, and they span a 5-6 kcal/mol range. (The three omitted do not include any exceptional structural features.) All conformers fall within an approximate 90° rotation. The conversion of **4e** to **4a** to complete the cycle requires an approximate 90° rotation of the diisopropylamido group, yet *no* minima are detectable. Changes in ω_{CC} are accompanied by changes in ω_{LiO} corresponding to seemingly fluid rotations about the THF-bearing N–Li bond that loosely approximate three orientations. We can find no simple (predictable) relationship between ω_{CC} and ω_{LiO}.

Scheme 4

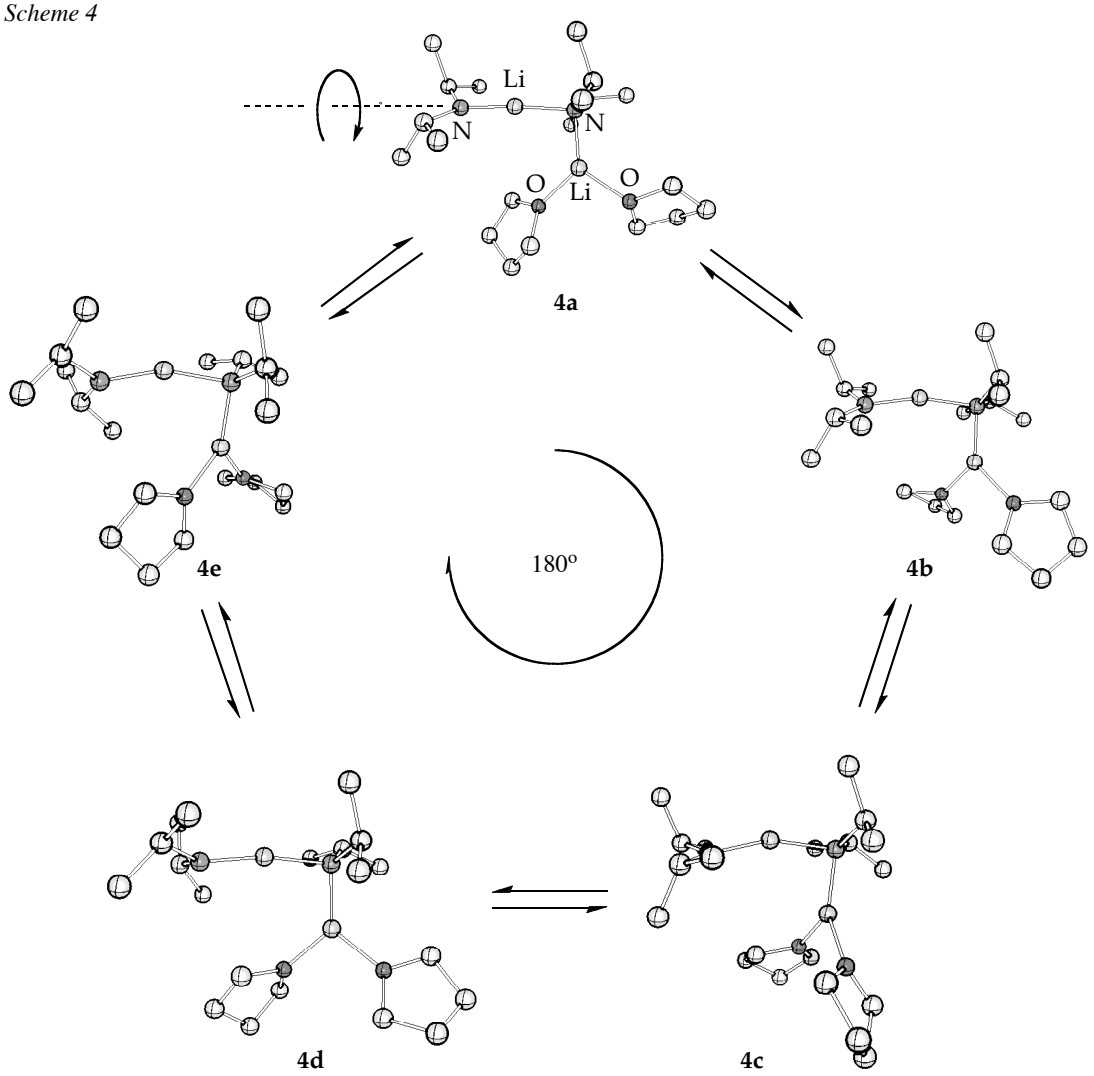

Analogous conformers are observed for trisolvated open dimers (Scheme 5), yet gearing arising from the high steric demands seems to allow for fewer minima at larger increments of ω_{CC}. The relative energies of the five conformers span an 8 kcal/mol range. All show a reduction of the N–Li–N angle to ≈165° owing to solvation of the internal lithium. The conformers fit into three groups: (1) **5a** is unique in that the THF ligand on the interior lithium is orthogonal relative to the orientation in the other four conformers. Conformers **5b** and **5c** show evidence of diisopropylamido distortion and

reduction of the Li–N–Li angle when compared with the disolvates that we attribute to buttressing. Conformers **5d** and **5e** seem most akin to the disolvated dimers in Scheme 4.

Scheme 5

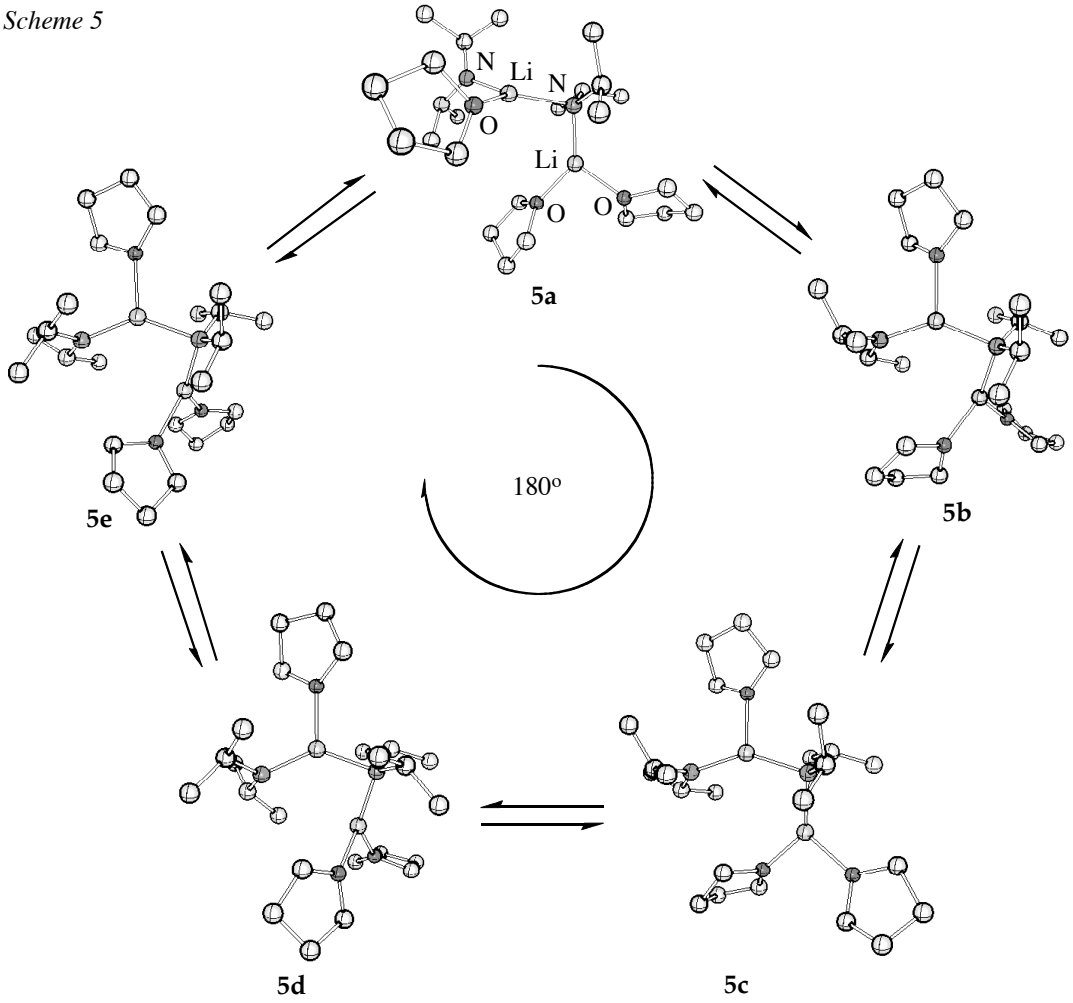

Transition Structures. Transition structures **9–15** connect select minima; dashed lines indicate bonds being cleaved. The transition structures are described by two fundamentally different imaginary vibrational modes: (1) Li–O stretching during THF dissociation/association, and (2) N–Li stretching during lithium amide bond formation/cleavage. Both modes are characterized

by low absolute values in imaginary frequencies ranging from 18 to 49 cm^{-1}. The protocols required for locating transition structures are instructive. The standard method for locating transition structures was to perform a relaxed potential energy scan by incrementally stretching the bond of interest. For example, incrementally increasing the Li–O distance from 2.0 Å by steps of 0.1 Å raised the energy continuously until it dropped at 2.8 Å. Geometries were optimized at each point along the surface with the reaction coordinate describing the Li–O distance. The optimized geometry with $r_{Li–O}$ = 2.8 Å was a good initial guess for a transition state optimization.

It became evident that only specific conformers could exit the trisolvated open dimer ensemble (Scheme 2). Whereas one conformer of **5** led to THF dissociation (**11**), another led to closed dimer-formation (**12**), and two others led to fragmentation (**13** and **14**). The importance of sampling conformational space cannot be overstated. Transition structure **11** proved particularly difficult to locate but offered interesting insights. Incrementally stretching the Li–O bond afforded no saddle points starting from any of the four lowest-energy trisolvated open dimer conformers akin to **5**. Only by scanning from the highest-energy conformer could **11** finally be located. Incidentally, the highest-energy conformer connecting to **11** was not located by a rational sampling of all trisolvated open dimer conformers. A reverse IRC calculation from **13** led to this new geometry, which allowed us to locate **11**. In other words, we got lucky. The strategy of palpating forward and backward along the reaction coordinate using output geometries as the input for a new search was an important strategy for locating transition structures.

Transition structures corresponding to N–Li stretching (**10**, **12**, and **13**) were located using the scanning protocol. Again, the conformational geometry

proved critical. Attempts to find transition structures describing the interconversion of conformers within the open dimer ensembles were unsuccessful, presumably owing to exceedingly low absolute values in the imaginary frequency. Casual inspection of the minima, however, suggests that their interconversion occurs via low energy barriers.

Discussion

The experimental background presented in the introduction paints a chaotic mechanistic picture of a delicate balance between rate-limiting aggregation events and rate-limiting reaction with substrates. DFT computational studies of LDA deaggregation afforded the series of minima that are illustrated in Scheme 1 and delineated in full detail with the accompanying transition structures in Scheme 2. Although interpreting the computed energies too literally would be a mistake, they do point to some provocative insights. The overall picture shows a series of fleeting intermediates and transition structures computed to be within an energy range commensurate with the activation energies of LDA-mediated metalations.

LDA Deaggregation: An Overview. The deaggregation of LDA dimer **1** is depicted moving from left to right along the reaction coordinate (*x* axis) of Scheme 2. Solvent exchanges interconverting closed dimers **1**–**3** are all facile, although asymmetric disolvate **3** is more than 12 kcal/mol less stable than dimer **1**. The N–Li bond scission affords either disolvated open dimer **4** from asymmetric disolvated dimer **3** or trisolvated open dimer **5** from **2**. Trisolvate **5** appears to be more easily accessed, but we do not take such subtle energetic distinctions too seriously. Curiously, once open dimer **4** is formed, conversion

to trisolvate **5** is a relatively unfavorable process. We elaborate on this finding in detail below.

The highest barriers in the conversion of LDA dimer **1** to monomer **6** result from the second N–Li bond scission. The direct cleavage of **5** via transition structure **14** is quite unfavorable. We suspected that the requisite extrusion of a monosolvated monomer fragment to be highly destabilizing. Consequently, we considered alternative transition structures in which one of the two THF ligands on the terminal lithium of **5** bridges the two lithiums (via **13**) to afford **7**. Computations show transition structure **13** to be preferred slightly over **14**. Dimer **7** is held together by a single bridging THF ligand and has exclusively three-coordinate lithiums. The role of bridging THFs has been mentioned previously in the context of deaggregations,[23] and they are prevalent in the crystallographic literature.[24] We were drawn to both the idea of such a neighboring-group-assisted scission as well as the symmetry of the resulting fleeting intermediate, **13**. Once extruded, disolvated LDA monomer **8** undergoes a facile solvation to give trisolvated monomer **6** as the most stable form.

Conformers and Portals. Both the cyclic dimers as well as the various transition structures are conformationally rigid, affording a single conformer (or two trivially different variants of **10**). We could have missed a few, of course, but the cyclic dimers and transition structures are clearly *not* conformationally promiscuous. By contrast, open dimers **4** and **5** display inordinate conformational diversity. Rotation about the terminal diisopropylamido moiety in **4** by 180° (see ω_{CC} in Scheme 3) afford eight conformers spanning a 5–6 kcal/mol range; five of these conformers are illustrated in Scheme 4 and discussed in the results section. The analogous

survey of the more congested (highly geared) trisolvate **5** uncovered only five conformers spanning an 8 kcal/mol range (Scheme 5). An intriguing consequence of the conformationally variable open dimers and conformationally rigid transition structures is a notion we refer to as portals. In the most general sense, we find that the transition structures are flanked by a *single* conformer—a so-called portal—within the ensemble of conformers.

The specific example illustrated in Scheme 6 is instructive. The sequence begins with open dimer **4** in its most stable conformer (**4a**). IRC calculations confirm the conversion of conformer **4a** via transition structure **11** to give trisolvated open dimer as conformer **5a**. A particularly interesting point is noted by returning to Scheme 2. Conformer **4a** is the *lowest* energy conformer of **4**, whereas trisolvate **5a** is the *highest* energy conformer of **5**—*8 kcal/mol above the most stable conformer*. Even casual inspection of **5a** reveals an odd looking orthogonal orientation of the THF ligand on the internal lithium when compared with the four other trisolvates illustrated in Scheme 5. To complete the deaggregation, **5a** is converted to dimer **7** via transition structure **13** involving N–Li bond scission with assistance by a bridging THF ligand. Dimer **7** is held together by a single bridging THF ligand, rendering it labile to solvent-assisted fragmentation to give monomer.

Scheme 6

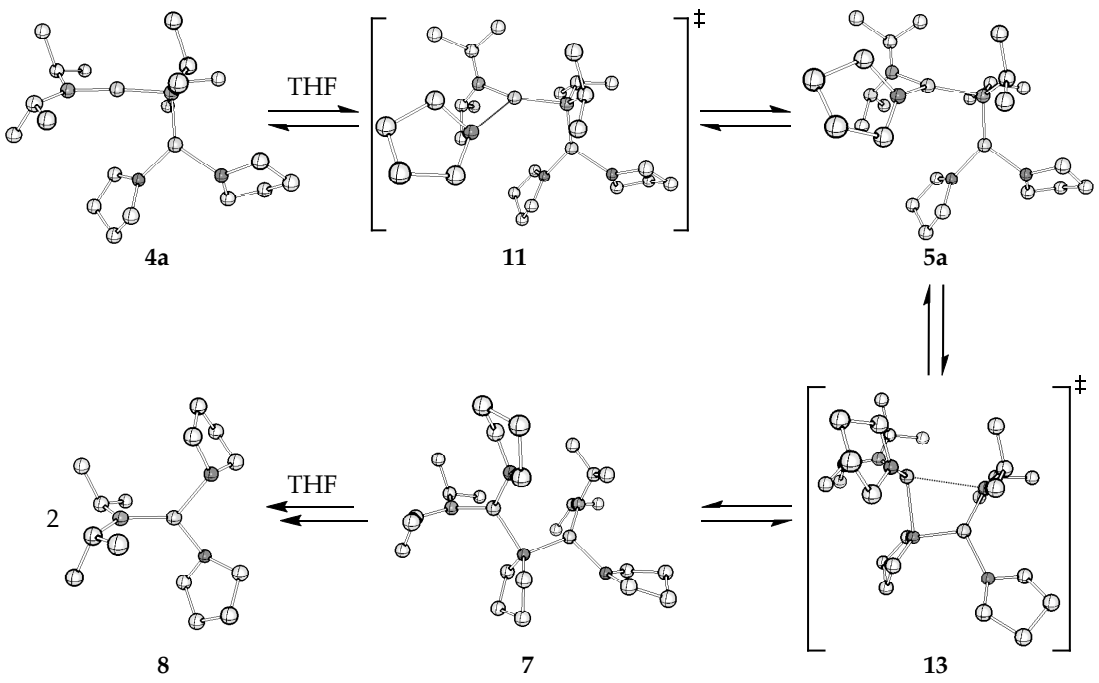

The conformational effects may be more than just idle curiosities; they may dictate reactivity. IRC calculations show that the transition structures represent specific transitions between two *unique* conformers of two minima. The conversion of the lowest energy conformer of open dimer **4a** via transition structure **11** may be an extreme example, but the principle is general. Transition structure **11** was the only legitimate transition structure for the conversion of **4** to **5** that we could detect. If this is the case, the calculations suggest that the most expedient conversion of **4** to **5** is to return to starting dimer **1** (Scheme 7). One should be cautious in interpreting the notion of conformational portals too liberally, however. We suspect, for example, that basis set superposition errors may be preventing the detection of other transition structures connecting the ensembles of **4** and **5**. (We would not be surprised if some were barrierless.)

Scheme 7

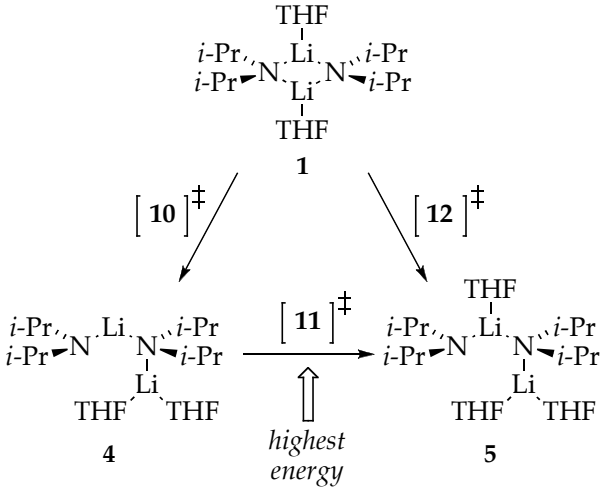

Rate-Limiting Deaggregations and Substrate Dependencies. The unequal receptivity of conformers of **4** to incoming ligands may be an important determinant of reactivity; precoordinating substrates, for example, may manifest a preference for particular conformers. Under conditions in which the subsequent reaction is fast on the time scale of substrate complexation (vide infra), coordination of substrate would be rate limiting and could be product determining.

Mechanistic studies of LDA-mediated reactions in THF at –78 °C have focused on the role of rate-limiting deaggregation as well as ways in which salts catalyze and autocatalyze the deaggregation to form monomers. Throughout these studies, however, we have noted some odd behaviors including (1) rate-limiting deaggregations that proceed through transition structures of distinctly different stoichiometries (di- versus trisolvated dimers),[8,9,25a] (2) substrate-concentration-dependent rate-limiting deaggregations,[25a,d] (3) reactions following post-rate-limiting steps that involve dimers and others that involve monomers,[25a] (4) reactions that are faster than

those limited by aggregation and display substrate dependencies,[25e] and (5) reactions in which proton transfers are *mechanistically* different than the corresponding deuterium transfers.[25a,b] The computations serve as a pedagogically useful template with which to understand these seemingly disparate experimental observations.

Let us simplify the discussion by focusing on three structurally distinct forms of LDA (Scheme 8) and consider several discrete categories of reactivity:

(1) For the preponderance of LDA-mediated reactions studied to date, the barriers to reactions with an electrophile, E^+, are measurably higher than the barriers to solvent and aggregate exchanges, which ensures that **1**, **4**, and **6** are at full equilibrium on the time scales of the reaction. Although one cannot say a priori which of the three will be the key intermediate from which the reaction occurs, the historical record suggests that reaction out of monomers is most likely.[3] Importantly, the *rates* that aggregation and solvation events occur do *not* dictate reaction rates.

Scheme 8

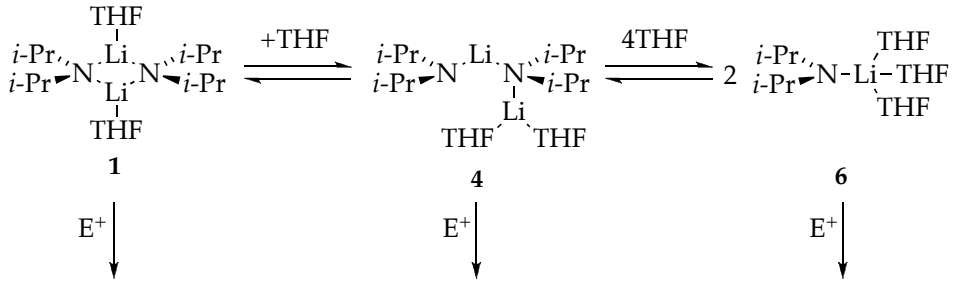

(2) Imagine that the reactivity of E^+ is systematically increased with a commensurate decrease in reaction temperature to allow us to monitor the rates conveniently. At some level of reactivity—at some affiliated reaction

temperature—the barrier to the formation of **6** is predicted to become higher than the barrier to reaction of E^+ with **1** or **4**. Through a bizarre twist of fate, that temperature is found experimentally to be approximately –78 °C, the most prevalent temperature reported by synthetic chemists. The reaction rate has become aggregation limited. Provided that monomer is the preferred pathway, then the rate-limiting transition structure is one of the trisolvated dimers **11**-**14**, which coincides nicely with rate studies of the 1,4-additions to unsaturated esters.[9] LiCl-catalyzed deaggregation (facile dimer-monomer equilibration) reduces the barrier to exchange, causing the reaction to become dependent once again on the structure and concentration of E^+. This theme recurs for ortholithiations and 1,4-additions.

(3) With increasing reactivity of E^+, reaction via **4** becomes more viable. (In fact, reactions via all intermediates would be predicted to become more viable.) Even if monomers are extraordinarily reactive, reaction via dimer **4** will be observed if the barrier to deaggregation is too high. Fleeting dimer **4** could be formed reversibly, and the reaction would *still* be aggregation limited to the extent that access to monomer has been precluded. In such a scenario, the reaction with E^+ would be rate limiting and manifest a seemingly normal first-order substrate dependence. This scenario was noted during ortholithiations (eq 3).

(4) Increasing the reactivity of the substrate in part 3 could cause **4** to be trapped efficiently on the time scales that **4** returns to cyclic dimer **1**. If so, the formation of dimer **4** becomes rate limiting. The reaction will display a zeroth-order in substrate, zeroth order in THF, and first order in LDA, all consistent with disolvated dimer **10** being the rate-limiting transition structure. The reaction would also, at least in principle, show no isotope effect. (We say more

about isotope effects below.) Comparison of the two limiting scenarios in parts 3 and 4 shows that open dimer **4** can be cleanly rate limiting, partially rate limiting, or not rate limiting, all depending on the choice of substrate.[26]

(5) The most reactive substrates, may find that the barrier to reaction with one of the closed dimers (**1**–**3**) may be lower than the barrier to partial scission to form **4** or **5** and even lower than the free energies of **4** and **5.** Given the putative facile solvent exchange, these reactions would be faster than those that are aggregation limited. They would also exhibit first-order dependencies on E^+ and LDA concentrations as well as standard kinetic isotope effects. We have not documented uncontestable examples of facile reactions via closed dimers because the half-lives are quite short at –78 °C.[27] We have, however, obtained some hints of this behavior from ortholithiations, imine lithiations, and enolizations.[25c]

In a survey of the influence of catalytic quantities of LiCl on the rate of ortholithiation, we may have inadvertently scanned through the behaviors covered by parts 1–5. We offer a highly stylized graphic in Figure 4.1 to aid the description. We found that the least reactive substrates and the most reactive substrates were *not* catalyzed by LiCl, whereas substrates of intermediate reactivity displayed the properties of aggregate-limiting behavior consistent with the descriptions in parts 2–4.[7] These findings baffled us at the time but make sense in retrospect. Of course, the least reactive substrates lithiate under conditions of full aggregate equilibration (part 1), which eliminates the need for LiCl catalysis in the deaggregation. The most reactive substrates do not benefit from deaggregation because the free energy of formation of monomer is higher than the dimer-based transition structure (part 5). It is only those of

intermediate reactivity for which catalysis of monomer formation can reduce the barrier of a beneficial (possibly mandatory) deaggregation (parts 2-4).

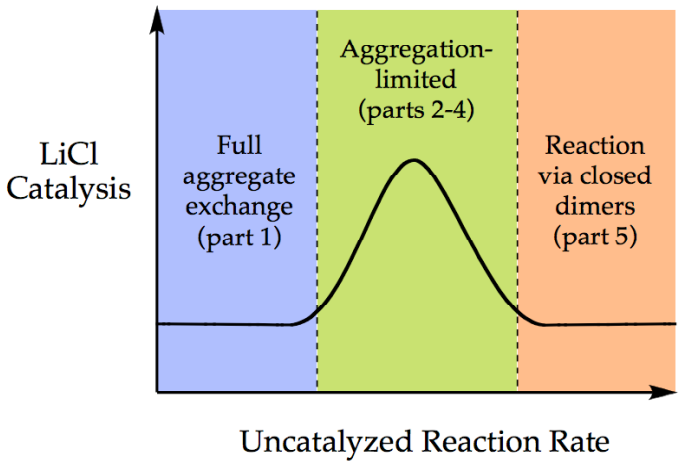

Figure 4.1. Artist's rendition of the influence of lithium chloride on metalation rate plotted (*y* axis) versus the rate of the corresponding uncatalyzed metalation.

We close with some comments about kinetic isotope effects. Of course, a reaction in which proton transfer is rate limiting would manifest a primary kinetic isotope effect. In theory, a zeroth-order substrate dependence arising from a rate-limiting deaggregation also would afford an isotope effect of unity. In practice, we have found that large kinetic isotope effects—k_H/k_D above 30 is commonplace for ortholithiations—can cause the rate-limiting step to shift from deaggregation to deuterium transfer. This shift in rate limitation is, although complicating at times, quite logical.[25b]

Conclusion

We are struggling to understand a mechanistically complex subset of LDA chemistry in which aggregation events dictate reactivity. DFT computations describing the deaggregation of LDA dimer **1** to monomer **6**

offer a number of potentially interesting qualitative and semi-quantitative insights. The computed barriers for partial and total scission are comparable to the barriers gleaned from a growing body of experimentally derived examples of aggregation-limited reactions of LDA in THF at –78 °C. Although conformational isomerism of key intermediates (especially the most conformationally flexible open dimers) was expected, the number of minima and the range of their computed energies were certainly not. The most interesting aspect is that conformationally rigid transition structures serve as portals connecting specific conformers of open dimer intermediates. The conformational restrictions contribute to experimentally important activation barriers. The summaries in Schemes 1 and 2 offer excellent structural supports for discussions of seemingly disparate, sometimes paradoxical experimental observations.

The complexity is exacerbated by lithium salt-catalyzed dimer-monomer exhange.[7] We have had some success examining the mechanism of catalysis, but the details of the underlying LDA–LiX interactions are still elusive. We also have unpublished data suggesting conversions of cyclic dimers to open dimers are catalyzed, and that LDA-derived *tetramers* are central to some reactions.[25] Tetramer intermediates significantly change the plotline and add to the growing demand for a detailed experimental investigation of the solution dynamics of LDA in THF.

Of course, the experimental and computational conclusions apply only to reactions in THF solution. What happens when reactions are carried out in inferior ligands such as diethyl ether or *tert*-butyl methyl ether? Are rate-limiting deaggregations and salt-catalyzed deaggregations more or less prominent? We may have only scratched the surface.

APPENDIX FOUR

Scheme 9

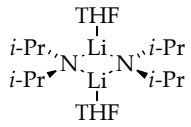

1

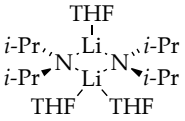

2

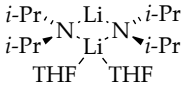

3

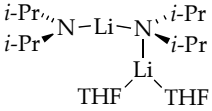

4

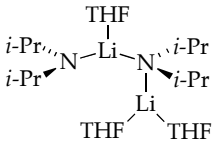

5

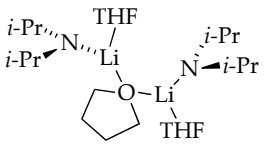

7

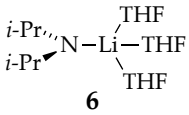

6

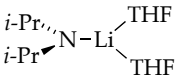

8

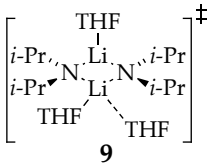

9

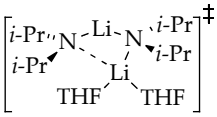

10

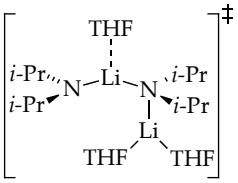

11

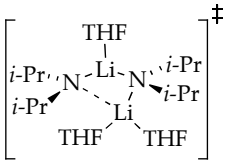

12

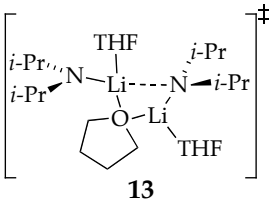

13

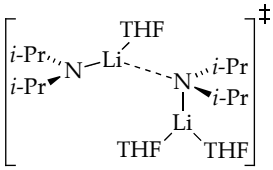

14

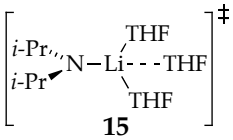

15

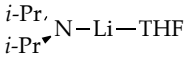

16

Table A4.1. Optimized geometries at the B3LYP level of theory with 6-31G(d) basis set of THF disolvated and trisolvated LDA aggregates including closed and open dimers as well as monomers at -78 °C with free energies (Hartrees) and cartesian coordinates (X, Y, Z). Single point MP2 energies are included. $\Delta G^{\ddagger}$ and ΔG (when reported) is the difference in free energy relative to disolvated LDA dimer **1**.

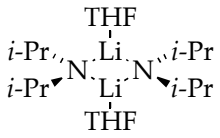

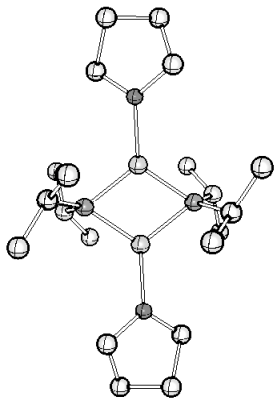

1
G = -1063.135499
G_{MP2} = -1059.343827

Atom	X	Y	Z	Atom	X	Y	Z
Li	-1.194627	-0.007825	0.022332	C	4.032339	-1.143606	0.199177
N	0.013907	1.643769	0.077205	C	5.437966	-0.758062	-0.271094
C	0.196558	2.410032	1.319032	C	5.411742	0.774063	-0.154916
C	1.159764	1.707079	2.290512	C	3.984087	1.095274	-0.593500
H	2.159075	1.604292	1.849772	H	3.902781	1.157446	-1.686665
H	1.262404	2.264200	3.230548	H	3.572808	2.009642	-0.160821
H	0.802179	0.701928	2.550069	H	6.162143	1.270000	-0.777688
C	-1.131524	2.719155	2.048700	H	5.571005	1.083108	0.884979
H	-1.598978	1.790545	2.404654	H	5.590704	-1.057380	-1.314703
H	-0.983501	3.376104	2.917980	H	6.219980	-1.226951	0.333343
H	-1.838550	3.216969	1.374689	H	3.991648	-1.300598	1.282899
H	0.658344	3.392275	1.104388	H	3.630188	-2.031035	-0.296809
Li	1.194600	0.007938	0.022158	C	-0.277970	2.554246	-1.035528
N	-0.013962	-1.643687	0.077247	C	-0.932408	1.814820	-2.212599
C	-0.196637	-2.409858	1.319127	H	-1.876483	1.339255	-1.919253
C	1.131405	-2.718766	2.048953	H	-1.147122	2.498323	-3.043671
H	1.598735	-1.790078	2.404863	H	-0.264714	1.033138	-2.596792
H	0.983363	-3.375653	2.918275	C	0.961585	3.312183	-1.569417
H	1.838548	-3.216575	1.375059	H	1.655983	2.609117	-2.049010
C	-1.160039	-1.706940	2.290445	H	0.685387	4.074299	-2.312169
H	-2.159328	-1.604365	1.849606	H	1.500736	3.820562	-0.761989
H	-1.262680	-2.263956	3.230543	H	-1.002510	3.335320	-0.721398
H	-0.802631	-0.701703	2.549918	O	-3.182976	0.015599	-0.128112
H	-0.658276	-3.392178	1.104519	C	-3.983928	-1.095127	-0.594129
C	0.278101	-2.554233	-1.035377	C	-5.411404	-0.774615	-0.154519

Table A4.1 (continued).

C	-0.961328	-3.312344	-1.569312	C	-5.438354	0.757507	-0.270589
H	-1.655760	-2.609392	-2.049018	C	-4.032490	1.143719	0.198539
H	-0.684990	-4.074495	-2.311978	H	-3.991063	1.301394	1.282122
H	-1.500486	-3.820717	-0.761885	H	-3.630993	2.030985	-0.298285
C	0.932582	-1.814844	-2.212451	H	-6.220074	1.226032	0.334511
H	1.876607	-1.339195	-1.919069	H	-5.592104	1.056795	-1.314054
H	1.147416	-2.498388	-3.043457	H	-5.569779	-1.083823	0.885463
H	0.264859	-1.033240	-2.596749	H	-6.162035	-1.270817	-0.776806
H	1.002689	-3.335209	-0.721109	H	-3.903299	-1.156675	-1.687391
O	3.182976	-0.015444	-0.127663	H	-3.572024	-2.009558	-0.162195

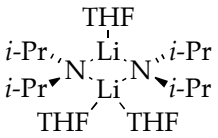

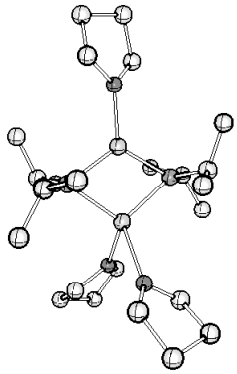

2
G = -1295.468552
G_{MP2} = -1290.911118
ΔG = 10.2 kcal/mol
ΔG_{MP2} = 1.6 kcal/mol

Atom	X	Y	Z	Atom	X	Y	Z
Li	0.818515	-0.011749	0.004258	H	-6.633962	-0.029432	1.356314
N	-0.496059	-1.437484	0.988166	H	-6.620794	0.423336	-1.339571
C	-0.681340	-2.820306	0.515699	H	-5.838785	1.620894	-0.288742
C	-0.333526	-2.984896	-0.967682	H	-3.951622	1.036081	-1.700686
H	0.670807	-2.607385	-1.178994	H	-4.495241	-0.657976	-1.834598
H	-0.381100	-4.040340	-1.266183	C	-0.453127	-1.446768	2.457559
H	-1.040201	-2.437207	-1.601717	C	-0.775698	-0.071705	3.052081
C	-2.113477	-3.378256	0.727230	H	-1.767842	0.274567	2.733930
H	-2.829240	-2.817093	0.111600	H	-0.768881	-0.099513	4.149612
H	-2.178574	-4.438251	0.443040	H	-0.043473	0.678653	2.735678
H	-2.434446	-3.302876	1.772178	C	0.891450	-1.938843	3.048504
H	-0.007660	-3.513315	1.059369	H	1.700346	-1.247902	2.782079
Li	-1.642109	-0.068981	0.010468	H	0.851865	-2.012142	4.144778
N	-0.569511	1.360057	-0.965104	H	1.158485	-2.930282	2.665912
C	-0.549529	1.365185	-2.434744	H	-1.219905	-2.131912	2.868840
C	0.748338	1.941691	-3.054151	O	2.485894	1.082386	1.028619
H	1.608142	1.312977	-2.792467	C	3.164391	1.956383	0.097963
H	0.684827	1.994694	-4.150329	C	3.776576	3.069184	0.948373
H	0.952920	2.955213	-2.691895	C	4.115724	2.319506	2.245463

Table A4.1 (continued).

C	-0.786821	-0.033966	-3.012818	C	2.934390	1.352405	2.374768
H	-1.748285	-0.444678	-2.678085	H	2.105362	1.801073	2.936113
H	-0.797335	-0.016146	-4.110432	H	3.200641	0.404757	2.851643
H	-0.000717	-0.729344	-2.700209	H	4.214220	2.974542	3.116342
H	-1.367862	1.992878	-2.839386	H	5.055614	1.766125	2.130254
C	-0.791028	2.733856	-0.483994	H	3.035753	3.853730	1.140987
C	-2.229862	3.269764	-0.707945	H	4.647250	3.530557	0.472262
H	-2.944776	2.684342	-0.113865	H	3.937435	1.380593	-0.428505
H	-2.316965	4.321898	-0.401935	H	2.426359	2.301410	-0.629022
H	-2.536145	3.213526	-1.758343	O	2.525183	-1.005662	-1.041557
C	-0.470385	2.886557	1.006609	C	3.282317	-1.819904	-0.116349
H	0.538433	2.528638	1.229448	C	3.958762	-2.894665	-0.967381
H	-0.545946	3.936783	1.317484	C	4.206898	-2.142148	-2.283001
H	-1.175044	2.315104	1.621929	C	2.948149	-1.276745	-2.395801
H	-0.123400	3.447978	-1.007964	H	2.141299	-1.808150	-2.915950
O	-3.634504	-0.116304	-0.021547	H	3.119497	-0.324230	-2.904790
C	-4.443741	0.217064	-1.172605	H	4.337341	-2.801529	-3.146378
C	-5.818902	0.572918	-0.610332	H	5.100957	-1.512412	-2.199075
C	-5.914867	-0.365209	0.603246	H	3.277713	-3.737798	-1.130865
C	-4.476736	-0.361501	1.130763	H	4.873836	-3.279474	-0.506742
H	-4.170055	-1.307364	1.583443	H	4.020134	-1.183456	0.389667
H	-4.313695	0.447729	1.853649	H	2.585845	-2.211297	0.628166
H	-6.203684	-1.373366	0.283550				

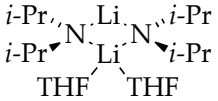

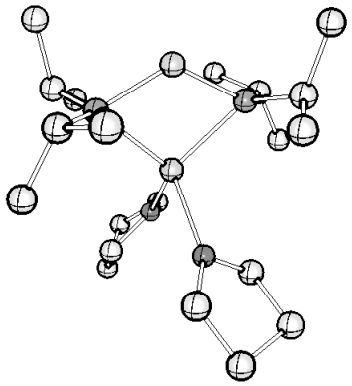

3
G = -1063.113999
G_{MP2} = -1059.324336
ΔG = 13.5 kcal/mol
ΔG_{MP2} = 12.2 kcal/mol

Closed dimer **3** connects directly to closed trisolvated LDA dimer **2**.

Atom	X	Y	Z	Atom	X	Y	Z
C	-1.953915	-0.136916	-2.517778	H	1.626270	-2.544548	-0.586163
N	-2.024230	0.029074	-1.058690	C	-0.811157	-4.348437	1.104056
Li	-1.904250	-1.470243	0.151949	H	-1.307975	-4.297854	2.079484
N	-0.336937	-1.879002	1.223499	H	-0.356528	-5.345170	1.011557

Table A4.1 (continued).

Li	0.023702	-0.044634	0.021905	H	-1.588008	-4.266697	0.327871
O	1.937212	0.002412	-0.935458	H	1.040154	-3.438806	1.661016
C	3.051478	0.059134	-0.011461	C	-0.332962	-1.675119	2.680124
C	4.311359	0.093857	-0.878408	C	-1.404666	-0.675490	3.126741
C	3.875639	-0.724117	-2.102568	H	-1.258839	0.300245	2.649954
C	2.415969	-0.296308	-2.267214	H	-1.382290	-0.520484	4.213066
H	2.327547	0.607633	-2.883771	H	-2.409658	-1.031852	2.862883
H	1.779764	-1.073852	-2.696120	C	1.043445	-1.230583	3.229173
H	4.472169	-0.522808	-2.997389	H	1.832068	-1.931995	2.933756
H	3.936390	-1.796686	-1.885488	H	1.048663	-1.170851	4.326877
H	4.550863	1.123294	-1.171472	H	1.311355	-0.243640	2.831314
H	5.181985	-0.323826	-0.363958	H	-0.572185	-2.622209	3.201357
H	3.019242	-0.832546	0.625842	C	-3.088752	0.997500	-0.744366
H	2.919149	0.943055	0.616290	C	-4.514070	0.402510	-0.866118
O	0.533347	1.911470	0.805633	H	-4.680047	-0.065430	-1.842203
C	0.624702	2.553275	2.098409	H	-5.290539	1.168621	-0.730117
C	1.041869	3.999220	1.820894	H	-4.666849	-0.368949	-0.096396
C	0.405735	4.255187	0.446469	C	-2.944352	1.598084	0.658044
C	0.599648	2.905915	-0.246046	H	-3.091831	0.834575	1.431541
H	-0.170929	2.664029	-0.981030	H	-3.696816	2.378452	0.829139
H	1.582995	2.837443	-0.729150	H	-1.950937	2.031508	0.803168
H	-0.661551	4.479883	0.554799	H	-3.052024	1.852986	-1.448053
H	0.873507	5.077643	-0.103036	C	-1.152640	0.980795	-3.227019
H	0.695842	4.687833	2.597396	H	-1.547843	1.970952	-2.971523
H	2.133776	4.079722	1.757312	H	-1.194285	0.884196	-4.321275
H	1.342965	1.999593	2.709298	H	-0.099009	0.951393	-2.922220
H	-0.356735	2.503763	2.585670	C	-1.380139	-1.501148	-2.913505
C	0.228801	-3.212084	0.943667	H	-0.361634	-1.624260	-2.529032
C	0.864046	-3.317289	-0.447193	H	-1.338342	-1.621800	-4.003570
H	0.113681	-3.198088	-1.236892	H	-1.993914	-2.317879	-2.509925
H	1.332200	-4.299540	-0.592136	H	-2.966705	-0.101901	-2.960703

Table A4.1 (continued).

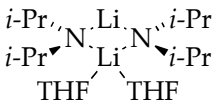

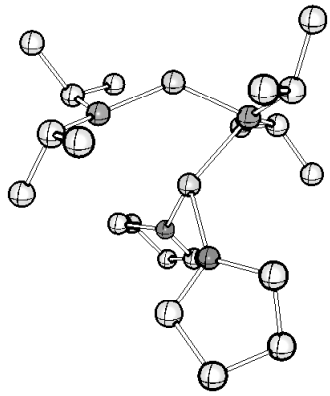

3*
G = -1063.113625
G_{MP2} = -1059.323335
ΔG = 13.7 kcal/mol
ΔG_{MP2} = 12.9 kcal/mol

Closed dimer **3*** connects directly to transition structure **10** and **10a**. It exhibits an elongated N-Li bond length of 2.68 Å.

Atom	X	Y	Z	Atom	X	Y	Z
C	3.426237	-0.427821	-0.283587	H	-2.661415	2.227511	2.055561
N	2.226054	0.127897	-0.915322	C	0.350575	0.833835	3.114525
Li	1.622508	1.564067	0.162849	H	1.399906	1.148709	3.125096
N	-0.120884	1.964397	0.951106	H	0.021573	0.722985	4.155878
Li	-0.308638	0.088012	-0.026578	H	0.302686	-0.155569	2.641993
O	-0.435677	-1.839014	0.776563	H	-0.369744	2.810313	2.890739
C	-1.427480	-2.393495	1.670724	C	-0.573651	3.252629	0.397904
C	-0.770552	-3.607574	2.364697	C	0.193298	4.481126	0.948483
C	0.721078	-3.459980	2.008874	H	1.250494	4.434272	0.647165
C	0.649111	-2.783968	0.644914	H	-0.224473	5.420037	0.560314
H	0.409599	-3.509949	-0.146342	H	0.163629	4.537239	2.041060
H	1.525170	-2.211688	0.345647	C	-0.455869	3.277272	-1.130674
H	1.249539	-4.417625	1.980439	H	-0.995206	2.447081	-1.594742
H	1.231265	-2.806526	2.725127	H	-0.848607	4.216070	-1.540265
H	-1.168115	-4.543856	1.957822	H	0.593485	3.205378	-1.449677
H	-0.952249	-3.611655	3.443179	H	-1.643687	3.431267	0.629471
H	-1.706714	-1.606125	2.374813	C	2.159612	-0.196302	-2.339912
H	-2.316943	-2.678012	1.094615	C	1.150637	0.694894	-3.071796
O	-1.945706	-0.146384	-1.199861	H	1.434036	1.749754	-2.993796
C	-3.115434	0.695441	-1.166654	H	1.097255	0.436583	-4.137536
C	-4.284619	-0.280737	-1.244579	H	0.142190	0.585246	-2.652190
C	-3.753779	-1.321543	-2.247285	C	1.828766	-1.679860	-2.638426
C	-2.235334	-1.333774	-1.977165	H	0.815883	-1.926301	-2.292731
H	-1.644960	-1.309614	-2.899047	H	1.881039	-1.893326	-3.714952
H	-1.914173	-2.191116	-1.379561	H	2.526662	-2.360345	-2.137266
H	-3.957711	-0.996249	-3.273208	H	3.128948	-0.005421	-2.836253
H	-4.204737	-2.309712	-2.117551	C	3.413416	-0.137804	1.225285

Table A4.1 (continued).

H	-5.213721	0.195143	-1.572192	H	2.504388	-0.515331	1.704285
H	-4.459972	-0.736800	-0.263184	H	4.276106	-0.589712	1.728883
H	-3.064186	1.283288	-0.249321	H	3.475144	0.946261	1.422098
H	-3.106721	1.376591	-2.029427	C	4.770895	0.091372	-0.849943
C	-0.516658	1.851211	2.362504	H	4.824409	1.184522	-0.749851
C	-2.012372	1.500443	2.557003	H	5.620395	-0.346518	-0.308723
H	-2.236536	0.510462	2.137138	H	4.902658	-0.151739	-1.908484
H	-2.294660	1.490013	3.618957	H	3.474068	-1.536848	-0.376266

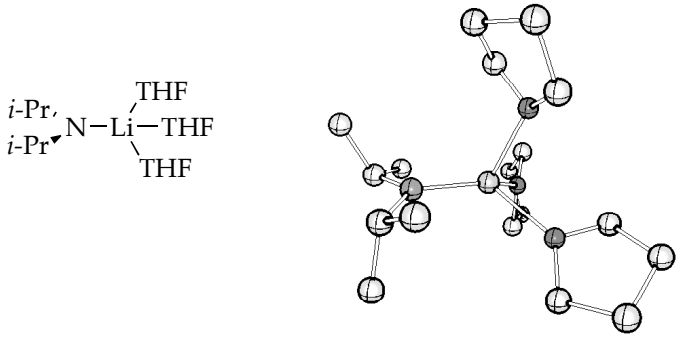

6
G = -996.24738
G_{MP2} = -992.802383
ΔG = 12.2 kcal/mol
ΔG_{MP2} = 5.8 kcal/mol

Atom	X	Y	Z	Atom	X	Y	Z
C	-2.739984	0.909518	-1.265496	H	-1.164003	-0.061722	3.517775
N	-1.657323	-0.052568	-1.154433	H	-1.896622	0.279295	1.916956
C	-1.833533	-1.127095	-2.118529	H	-2.678094	-1.975074	1.671695
C	-1.279404	-0.780699	-3.525233	H	-2.920155	-1.771196	3.423456
H	-1.500475	-1.558866	-4.272078	H	-1.314059	-3.818242	2.559507
H	-1.711966	0.159844	-3.885794	H	-0.772838	-2.826939	3.923665
H	-0.190164	-0.642603	-3.483088	H	0.143583	-2.681738	1.022488
C	-1.204481	-2.440764	-1.624950	H	1.081057	-2.355465	2.501384
H	-1.709997	-2.788133	-0.715974	O	1.871871	-0.709018	-0.552973
H	-1.266529	-3.237106	-2.379369	C	2.489283	-1.097627	-1.787877
H	-0.142900	-2.297138	-1.380678	C	3.558661	-2.138193	-1.398840
H	-2.908210	-1.358249	-2.274109	C	3.830863	-1.844085	0.103413
Li	-0.069969	0.062572	-0.073571	C	2.938360	-0.626724	0.400442
O	0.880063	1.846911	0.485875	H	3.490644	0.314030	0.252452
C	1.460351	2.620597	-0.588337	H	2.490727	-0.615830	1.394391
C	1.777282	3.998424	0.003775	H	4.884658	-1.633801	0.310038
C	0.725578	4.123070	1.117527	H	3.535931	-2.696723	0.722644
C	0.645506	2.685461	1.632607	H	4.456600	-2.037535	-2.015796
H	-0.329595	2.424533	2.052500	H	3.178441	-3.154965	-1.532813
H	1.417625	2.484515	2.388915	H	1.705986	-1.476784	-2.444306
H	-0.239679	4.428258	0.699122	H	2.948247	-0.214339	-2.257791
H	1.003569	4.835580	1.900171	C	-4.049821	0.450617	-0.570435

Table A4.1 (continued).

H	1.713385	4.795602	-0.742728	H	-4.349988	-0.545010	-0.916340
H	2.787745	4.014067	0.429880	H	-3.902409	0.392804	0.516912
H	2.345055	2.090753	-0.954720	H	-4.888193	1.136771	-0.764863
H	0.729062	2.679175	-1.401782	C	-2.345377	2.283546	-0.706302
O	-0.159110	-0.817466	1.856247	H	-1.501094	2.701072	-1.266193
C	0.104092	-2.232042	2.018931	H	-3.178941	2.996739	-0.756210
C	-1.046965	-2.801306	2.862318	H	-2.045679	2.200196	0.348272
C	-2.172958	-1.783175	2.623895	H	-3.014878	1.090871	-2.328091
C	-1.393665	-0.476156	2.524600				

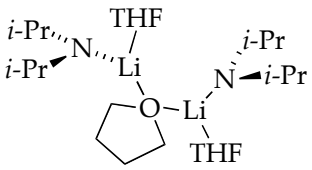

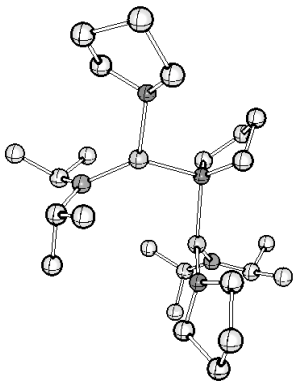

7
G = -1295.446719
G_{MP2} = -1290.87978
ΔG = 23.9 kcal/mol
ΔG_{MP2} = 21.3 kcal/mol

Atom	X	Y	Z	Atom	X	Y	Z
C	2.060864	2.473439	-1.765852	C	-2.872929	0.960920	3.788161
N	1.938336	1.736632	-0.518589	C	-2.324099	1.384782	2.427604
Li	1.666746	-0.093941	-0.328202	H	-1.717318	2.294926	2.495470
O	3.237978	-1.345800	-0.034622	H	-3.082897	1.506078	1.650810
C	3.589374	-2.136218	1.124778	H	-3.146158	1.818281	4.410162
C	5.119425	-2.179862	1.164918	H	-3.761352	0.330992	3.663868
C	5.497553	-0.846775	0.502354	H	-0.938489	0.806404	4.773116
C	4.434981	-0.712918	-0.584887	H	-2.011643	-0.554668	5.151680
H	4.716913	-1.251370	-1.498758	H	-1.702852	-1.533320	2.958475
H	4.155462	0.317456	-0.820885	H	-0.101572	-0.768174	3.158069
H	6.512432	-0.841251	0.094159	C	0.075689	-2.586535	0.229869
H	5.413126	-0.022341	1.219755	C	0.504599	-3.629904	-0.793413
H	5.493707	-3.022512	0.571943	C	-0.270112	-3.174859	-2.041317
H	5.502936	-2.285730	2.184161	C	-0.258102	-1.646279	-1.937283
H	3.179860	-1.646274	2.018399	H	-1.218996	-1.181162	-2.180231
H	3.133264	-3.126487	1.024322	H	0.550104	-1.187435	-2.512525
O	0.007401	-1.337172	-0.510561	H	-1.299604	-3.547548	-2.006612
Li	-1.611807	-0.069541	0.069348	H	0.183595	-3.522430	-2.973783
N	-3.174186	-0.025054	-0.966557	H	0.256338	-4.648356	-0.479254

Table A4.1 (continued).

C	-3.527313	1.070667	-1.859809	H	1.585600	-3.567676	-0.961834
H	-4.114750	0.710258	-2.730236	H	0.775197	-2.441391	1.056252
C	-4.397493	2.162424	-1.187185	H	-0.917260	-2.813430	0.638018
H	-5.274739	1.724311	-0.696746	C	2.016163	2.565761	0.670624
H	-3.814351	2.693578	-0.421969	H	2.951685	3.165963	0.704738
H	-4.759736	2.906484	-1.911496	C	0.861805	3.585447	0.829213
C	-2.265583	1.725732	-2.439141	H	0.813339	4.274971	-0.020151
H	-1.709267	1.020355	-3.067548	H	-0.100355	3.058058	0.880410
H	-2.505146	2.605109	-3.050741	H	0.978314	4.192452	1.738427
H	-1.593069	2.062382	-1.635816	C	2.052008	1.668183	1.918960
C	-4.274882	-0.955291	-0.784461	H	2.900785	0.972044	1.874004
H	-5.244242	-0.424991	-0.669011	H	2.146006	2.252481	2.843173
C	-4.093876	-1.773038	0.504024	H	1.121142	1.084822	1.990682
H	-3.150031	-2.340578	0.467930	H	1.315564	3.292955	-1.842635
H	-4.060303	-1.116952	1.382144	C	1.768897	1.540379	-2.949217
H	-4.902107	-2.501669	0.647883	H	1.870267	2.056600	-3.911983
C	-4.471224	-1.932931	-1.971481	H	2.472434	0.692167	-2.956357
H	-5.376224	-2.547765	-1.857816	H	0.748359	1.146591	-2.885680
H	-4.556982	-1.388900	-2.918618	C	3.440043	3.144053	-1.986967
H	-3.608445	-2.609428	-2.053606	H	3.457615	3.727329	-2.917960
O	-1.454974	0.292328	2.006830	H	3.695376	3.826798	-1.169071
C	-1.179952	-0.581986	3.122820	H	4.233699	2.386024	-2.046569
C	-1.707892	0.141566	4.364230				

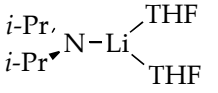

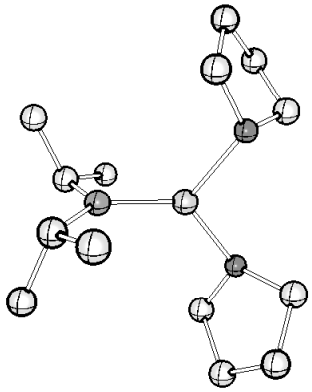

8
G = -763.908312
G_{MP2} = -761.230838
ΔG = 5.5 kcal/mol
ΔG_{MP2} = 6.9 kcal/mol

Atom	X	Y	Z	Atom	X	Y	Z
C	-0.620691	2.385888	1.043481	H	-2.159107	-3.421673	-0.578605
N	-0.000631	1.591937	0.000014	H	-1.272626	-2.846301	0.860673
C	0.618888	2.386186	-1.043542	O	1.413260	-1.477861	0.659195
C	1.958906	3.042469	-0.624112	C	1.991867	-2.560094	-0.087797
H	2.355466	3.708145	-1.404656	C	3.307953	-1.991594	-0.615089

Table A4.1 (continued).

H	1.839859	3.638157	0.287930	C	3.786793	-1.111163	0.560966
H	2.712370	2.268506	-0.419421	C	2.490139	-0.769455	1.331869
C	0.857626	1.520629	-2.290915	H	2.217027	0.288157	1.297255
H	-0.089459	1.131338	-2.684603	H	2.532154	-1.106389	2.374607
H	1.358477	2.078589	-3.092423	H	4.299814	-0.210688	0.212422
H	1.501093	0.660998	-2.042337	H	4.482660	-1.662153	1.202033
H	-0.035053	3.221869	-1.375085	H	3.116481	-1.379208	-1.502798
Li	0.000334	-0.275582	0.000230	H	4.026839	-2.770770	-0.886072
O	-1.412130	-1.478631	-0.658939	H	2.160979	-3.420565	0.577053
C	-1.990341	-2.561735	0.087030	H	1.274211	-2.844220	-0.861655
C	-3.306667	-1.994177	0.614791	C	-1.961165	3.041178	0.623983
C	-3.785699	-1.112530	-0.560323	H	-1.842537	3.636894	-0.288095
C	-2.489268	-0.770669	-1.331575	H	-2.714076	2.266665	0.419339
H	-2.216392	0.287008	-1.297272	H	-2.358211	3.706623	1.404479
H	-2.531435	-1.107918	-2.374215	C	-0.858789	1.520300	2.290956
H	-4.482160	-1.662589	-1.201538	H	0.088586	1.131673	2.684605
H	-4.298113	-0.212135	-0.210681	H	-1.359952	2.078004	3.092448
H	-4.025346	-2.773862	0.884855	H	-1.501704	0.660225	2.042491
H	-3.115447	-1.382724	1.503193	H	0.032667	3.222071	1.374904

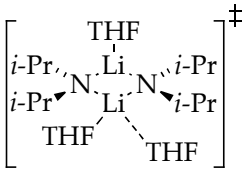

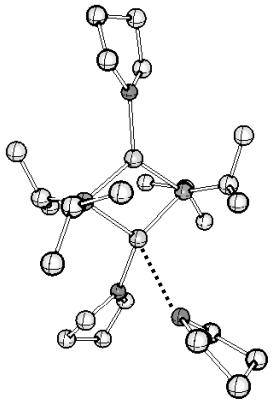

9
G = -1295.468162
G_{MP2} = -1290.908076
$\Delta G^{\ddagger}$ = 10.5 kcal/mol
$\Delta G_{MP2}^{\ddagger}$ = 3.5 kcal/mol

Atom	X	Y	Z	Atom	X	Y	Z
Li	0.681480	0.174041	0.198217	H	-6.631217	0.059755	-1.619163
N	-0.650842	1.368723	-0.958075	H	-6.770071	-0.433149	1.065940
C	-0.938767	2.761153	-0.577105	H	-6.161678	-1.719020	0.008376
C	-0.663346	3.032749	0.906930	H	-4.225903	-1.499955	1.435073
H	0.355904	2.745297	1.183795	H	-4.533239	0.233211	1.709227
H	-0.797575	4.096906	1.140974	C	-0.544731	1.287888	-2.423535
H	-1.355590	2.471288	1.544509	C	-0.730664	-0.144414	-2.936266
C	-2.391874	3.214364	-0.873839	H	-1.689943	-0.567886	-2.609649
H	-3.096699	2.649672	-0.248082	H	-0.710022	-0.179365	-4.033299

Table A4.1 (continued).

H	-2.532809	4.283622	-0.661489	H	0.068692	-0.797100	-2.570578
H	-2.666221	3.054004	-1.922528	C	0.786970	1.833965	-2.996524
H	-0.287308	3.463185	-1.136671	H	1.628277	1.216570	-2.657203
Li	-1.724383	-0.070755	-0.000344	H	0.782861	1.833420	-4.095957
N	-0.531551	-1.302068	1.121228	H	0.972584	2.864897	-2.674726
C	-0.647017	-1.243656	2.585838	H	-1.342650	1.884192	-2.908822
C	0.628763	-1.684037	3.347349	O	2.869745	-0.936722	-1.124503
H	1.449806	-0.984337	3.151559	C	3.646135	-1.609009	-0.114353
H	0.459550	-1.714046	4.433175	C	4.301360	-2.806484	-0.808790
H	0.962629	-2.681657	3.042535	C	4.482928	-2.279165	-2.240544
C	-1.039932	0.154922	3.073005	C	3.212464	-1.444092	-2.428652
H	-1.991785	0.478955	2.632228	H	2.381898	-2.058750	-2.801380
H	-1.154220	0.178190	4.164337	H	3.342521	-0.594757	-3.106795
H	-0.278638	0.896762	2.805154	H	4.578523	-3.072333	-2.988383
H	-1.449885	-1.918335	2.944964	H	5.374728	-1.643781	-2.304044
C	-0.559356	-2.714548	0.701516	H	3.623949	-3.668220	-0.803150
C	-1.961356	-3.372294	0.776530	H	5.239433	-3.107718	-0.332332
H	-2.642349	-2.891319	0.061205	H	4.402336	-0.913004	0.276971
H	-1.916617	-4.443437	0.534001	H	2.974543	-1.888190	0.702699
H	-2.402796	-3.285389	1.775919	O	2.310950	1.198885	0.992677
C	-0.022406	-2.916933	-0.719466	C	2.960308	2.126151	0.088817
H	0.953883	-2.438124	-0.844310	C	3.681185	3.129572	0.986558
H	0.080833	-3.985963	-0.948159	C	4.092236	2.247765	2.175315
H	-0.704652	-2.493358	-1.464754	C	2.890901	1.305847	2.311764
H	0.092201	-3.326237	1.355116	H	2.131583	1.710716	2.992017
O	-3.695500	-0.248253	-0.125193	H	3.166313	0.305138	2.656035
C	-4.582901	-0.577518	0.971529	H	4.283356	2.811919	3.093112
C	-5.980318	-0.695019	0.355576	H	4.998851	1.680668	1.932152
C	-5.891438	0.266420	-0.839975	H	2.991284	3.916355	1.313278
C	-4.459151	0.037755	-1.320048	H	4.529780	3.605499	0.485646
H	-4.006561	0.904257	-1.805901	H	3.658247	1.564619	-0.543377
H	-4.395675	-0.826311	-1.995116	H	2.185844	2.562806	-0.543316
H	-6.022365	1.303826	-0.510155				

Table A4.1 (continued).

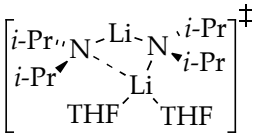

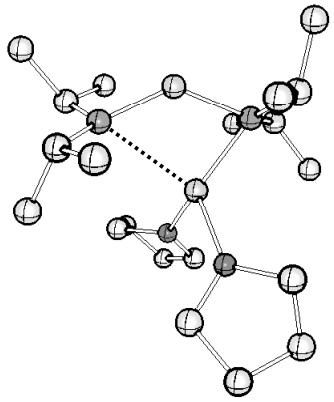

10
G = -1063.11353
G_{MP2} = -1059.322919
$\Delta G^{‡}$ = 13.8 kcal/mol
$\Delta G_{MP2}^{‡}$ = 13.1 kcal/mol

Transition structure **10** connects to disolvated open dimer **4c**.

Atom	X	Y	Z	Atom	X	Y	Z
C	3.446563	-0.423810	-0.280640	H	-2.665936	2.229715	2.058056
N	2.247606	0.128915	-0.915718	C	0.349554	0.840271	3.112913
Li	1.616388	1.551906	0.160785	H	1.398733	1.155763	3.119717
N	-0.130638	1.959457	0.945956	H	0.023489	0.731862	4.155437
Li	-0.345875	0.092097	-0.015986	H	0.301189	-0.150198	2.642720
O	-0.448614	-1.831852	0.780804	H	-0.370224	2.816627	2.881838
C	-1.428123	-2.395050	1.683140	C	-0.580114	3.247231	0.388882
C	-0.754268	-3.602106	2.372894	C	0.198732	4.473355	0.927604
C	0.733578	-3.437862	2.008894	H	1.253275	4.418245	0.618410
C	0.647121	-2.764097	0.644674	H	-0.215706	5.413285	0.538325
H	0.411732	-3.493468	-0.144622	H	0.177765	4.534429	2.020174
H	1.515524	-2.182214	0.340657	C	-0.473836	3.262751	-1.140678
H	1.272562	-4.389543	1.978358	H	-1.021486	2.432959	-1.595876
H	1.240249	-2.778204	2.721934	H	-0.864278	4.201437	-1.552746
H	-1.143765	-4.542450	1.967570	H	0.572572	3.182626	-1.466611
H	-0.930274	-3.608585	3.452318	H	-1.647150	3.433114	0.628054
H	-1.709353	-1.609734	2.388899	C	2.179843	-0.200228	-2.338395
H	-2.319206	-2.688258	1.113945	C	1.167526	0.686922	-3.070420
O	-1.969798	-0.145738	-1.197590	H	1.449027	1.742545	-2.995587
C	-3.145041	0.688736	-1.165455	H	1.111467	0.425970	-4.135382
C	-4.307908	-0.294759	-1.245322	H	0.160324	0.576212	-2.647576
C	-3.769036	-1.332298	-2.247173	C	1.850478	-1.684993	-2.633228
C	-2.251272	-1.336136	-1.973725	H	0.836675	-1.930867	-2.289332
H	-1.658676	-1.310038	-2.894126	H	1.905126	-1.901531	-3.709037
H	-1.926840	-2.190580	-1.373780	H	2.547513	-2.363777	-2.128538
H	-3.972466	-1.007863	-3.273467	H	3.147976	-0.008867	-2.837275
H	-4.214682	-2.323006	-2.118615	C	3.434129	-0.120826	1.225742

Table A4.1 (continued).

H	-5.239281	0.175554	-1.574507	H	2.524711	-0.493758	1.708025
H	-4.482188	-0.751972	-0.264266	H	4.296205	-0.569217	1.733548
H	-3.098885	1.276561	-0.247723	H	3.496507	0.965015	1.412098
H	-3.139229	1.370401	-2.027781	C	4.792337	0.087357	-0.851507
C	-0.520374	1.854576	2.359886	H	4.849560	1.180918	-0.758841
C	-2.015580	1.506161	2.562919	H	5.640806	-0.349924	-0.308135
H	-2.242463	0.512722	2.152344	H	4.922077	-0.163469	-1.908572
H	-2.293703	1.504407	3.626005	H	3.491860	-1.533894	-0.363855

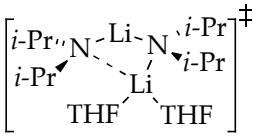

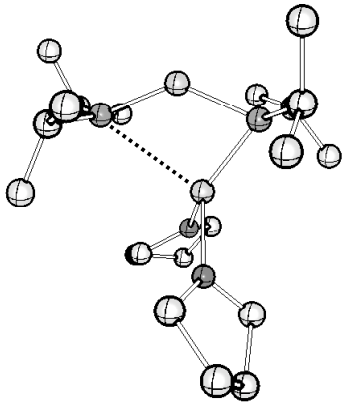

10*
G = -1063.113154
G_{MP2} = -1059.321215
$\Delta G^{‡}$ = 14.0 kcal/mol
$\Delta G_{MP2}^{‡}$ = 14.2 kcal/mol

10* is akin to **10** with an activation barrier of 1.1 kcal/mol higher. **10*** connects to disolvated open dimer **4b**.

Atom	X	Y	Z	Atom	X	Y	Z
C	-2.114283	-0.542780	-2.472623	H	2.288305	-2.294138	-0.238505
N	-2.200964	-0.293521	-1.035316	C	-0.282290	-4.291674	0.977752
Li	-1.638272	-1.556364	0.252300	H	-0.890476	-4.324505	1.889516
N	0.024066	-1.819164	1.300307	H	0.233957	-5.257738	0.884766
Li	0.388083	-0.083821	0.240418	H	-0.965282	-4.200001	0.119441
O	2.072738	0.239915	-0.892168	H	1.428184	-3.325858	1.817244
C	3.261165	0.603800	-0.151312	C	-0.082042	-1.666733	2.761898
C	4.348374	0.831190	-1.202036	C	-1.281619	-0.802666	3.166746
C	3.948491	-0.174272	-2.292622	H	-1.231794	0.189120	2.702926
C	2.420294	-0.099491	-2.256453	H	-1.326207	-0.659566	4.253863
H	2.035877	0.686941	-2.917066	H	-2.226593	-1.269035	2.856821
H	1.930307	-1.041724	-2.512055	C	1.206916	-1.100943	3.402358
H	4.352575	0.071261	-3.279127	H	2.080060	-1.698413	3.115893
H	4.289488	-1.181344	-2.026476	H	1.154758	-1.091156	4.500409
H	4.301338	1.856250	-1.588800	H	1.382371	-0.071455	3.061788
H	5.353639	0.663265	-0.804409	H	-0.249800	-2.653205	3.235094

Table A4.1 (continued).

H	3.519155	-0.220532	0.526153	C	-3.281174	0.647639	-0.736740
H	3.024419	1.488129	0.445189	C	-4.700528	0.049387	-0.904190
O	0.413563	1.897745	0.836375	H	-4.854287	-0.369084	-1.904205
C	0.398198	2.619552	2.090225	H	-5.481463	0.805705	-0.740931
C	0.459327	4.101778	1.717075	H	-4.851788	-0.761377	-0.177794
C	-0.281521	4.120853	0.370978	C	-3.164962	1.195338	0.690502
C	0.185116	2.813361	-0.268107	H	-3.311295	0.394958	1.427899
H	-0.547405	2.350766	-0.933274	H	-3.927226	1.959798	0.888526
H	1.130614	2.942119	-0.810068	H	-2.176396	1.631489	0.864879
H	-1.365189	4.102015	0.530863	H	-3.240444	1.530761	-1.409910
H	-0.041695	4.993317	-0.244035	C	-1.408090	0.587957	-3.260248
H	-0.001326	4.739965	2.476895	H	-1.881734	1.558209	-3.070316
H	1.499505	4.424370	1.587253	H	-1.438966	0.414754	-4.345536
H	1.246394	2.280725	2.691934	H	-0.355687	0.663269	-2.956243
H	-0.528199	2.378040	2.624589	C	-1.411238	-1.873215	-2.764648
C	0.702231	-3.098732	1.014834	H	-0.385898	-1.861259	-2.373766
C	1.519298	-3.072058	-0.281924	H	-1.349072	-2.075484	-3.841551
H	0.879417	-2.871123	-1.149099	H	-1.944631	-2.709598	-2.293709
H	2.012532	-4.036740	-0.457922	H	-3.121579	-0.633572	-2.922681

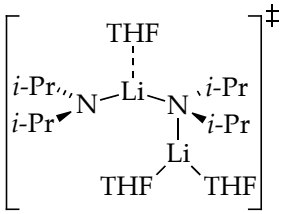

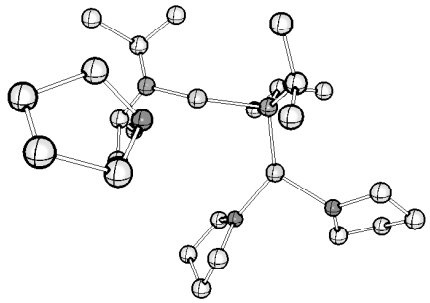

11
G = -1295.456439
G_{MP2} = -1290.890247
$\Delta G^{‡}$ = 17.8 kcal/mol
$\Delta G_{MP2}^{‡}$ = 14.7 kcal/mol

Atom	X	Y	Z	Atom	X	Y	Z
C	-0.892566	-2.419404	-1.171013	H	4.082729	1.184968	-1.847740
N	-0.661285	-1.593854	0.029333	C	2.346574	2.003749	-0.933718
Li	-1.814919	-0.025294	0.022911	H	1.262974	1.823752	-0.862909
O	-3.729470	0.035294	0.562338	H	2.752197	1.946280	0.080913
C	-4.727749	0.741847	-0.207108	H	2.495344	3.023821	-1.315207
C	-5.932414	-0.194667	-0.258306	C	2.520846	1.191731	-3.303075
C	-5.871909	-0.856281	1.127320	H	2.816626	2.184339	-3.675030
C	-4.364051	-1.001906	1.363528	H	2.941291	0.446233	-3.986676
H	-3.978733	-1.966338	1.021414	H	1.426275	1.110980	-3.366576
H	-4.073704	-0.856112	2.407565	C	-0.750886	-2.356191	1.283959

Table A4.1 (continued).

H	-6.389191	-1.818975	1.167454	H	-1.698301	-2.929760	1.339500
H	-6.320960	-0.200304	1.882042	C	0.378222	-3.391448	1.487088
H	-5.798705	-0.942172	-1.048598	H	0.429639	-4.101444	0.654900
H	-6.869810	0.337804	-0.444135	H	1.353965	-2.891741	1.561007
H	-4.973144	1.685623	0.299059	H	0.228394	-3.971018	2.408242
H	-4.298662	0.970105	-1.186013	C	-0.763976	-1.393273	2.482179
O	-1.589021	1.844997	-0.556654	H	-1.600147	-0.680470	2.418432
C	-1.476342	2.917015	0.410886	H	-0.877820	-1.938783	3.427914
C	-1.703213	4.202564	-0.383087	H	0.168873	-0.821274	2.527910
C	-1.086167	3.844935	-1.744583	H	-0.132781	-3.219912	-1.264654
C	-1.467237	2.371316	-1.905894	C	-0.747897	-1.546458	-2.427117
H	-0.717068	1.782594	-2.438196	H	-0.863831	-2.142970	-3.340596
H	-2.437661	2.252980	-2.405557	H	-1.527143	-0.766208	-2.452204
H	0.002752	3.950036	-1.708963	H	0.232464	-1.055697	-2.461154
H	-1.463874	4.461034	-2.565605	C	-2.262164	-3.136624	-1.227060
H	-1.233547	5.070368	0.088934	H	-2.359090	-3.718538	-2.152697
H	-2.775845	4.407225	-0.484256	H	-2.408046	-3.830281	-0.392011
H	-2.219145	2.740308	1.194682	H	-3.082696	-2.403348	-1.204725
H	-0.473163	2.886529	0.853010	O	2.130157	0.351341	2.166802
Li	1.230999	-0.793283	-0.235581	C	1.976652	1.475563	3.044284
N	2.722385	-0.381693	-1.341487	C	3.306087	1.626723	3.796645
C	3.590441	-1.391590	-1.925789	C	4.308659	1.044417	2.787290
H	3.653697	-1.295202	-3.032095	C	3.503519	-0.099089	2.169231
C	5.055745	-1.343674	-1.420719	H	3.578883	-1.011831	2.779350
H	5.489329	-0.343616	-1.535680	H	3.761520	-0.327781	1.131310
H	5.099997	-1.607279	-0.355208	H	5.240265	0.703397	3.249435
H	5.698771	-2.046413	-1.970431	H	4.559820	1.789356	2.022935
C	3.028077	-2.795087	-1.659973	H	3.297539	1.026287	4.714299
H	2.036078	-2.913361	-2.110738	H	3.514965	2.664923	4.074283
H	3.681524	-3.579503	-2.063530	H	1.759210	2.370434	2.441960
H	2.932611	-2.970391	-0.578165	H	1.123748	1.293825	3.709797
C	2.995467	0.950668	-1.845601				

Table A4.1 (Continued).

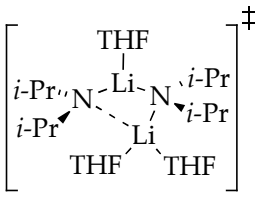

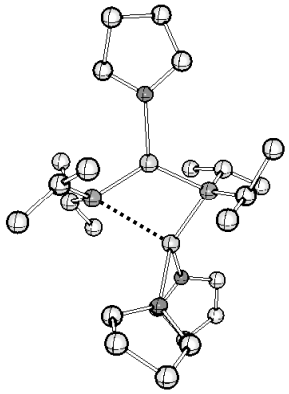

12
G = -1295.456449
G_{MP2} = -1290.897348
$\Delta G^{‡}$ = 17.8 kcal/mol
$\Delta G_{MP2}{}^{‡}$ = 10.3 kcal/mol

Atom	X	Y	Z	Atom	X	Y	Z
C	0.636461	1.802019	-2.288673	C	1.392000	-2.317572	2.901757
N	0.822011	1.650311	-0.845433	H	2.284188	-1.691893	2.772302
Li	1.509939	-0.037022	-0.014373	H	1.205622	-2.416944	3.979311
N	0.286781	-1.501106	0.742168	H	1.623810	-3.316002	2.517617
Li	-1.146230	-0.270797	-0.032281	C	-0.077981	-0.320020	2.884625
O	-2.510661	1.057607	0.794776	H	-0.890699	0.233692	2.405983
C	-2.337956	2.465455	0.532152	H	-0.334522	-0.458221	3.943108
C	-2.432389	3.108190	1.912554	H	0.816931	0.312346	2.839767
C	-3.519611	2.258037	2.608278	H	-0.692228	-2.316303	2.459782
C	-3.489760	0.913150	1.840339	O	3.539508	-0.424249	-0.080401
H	-3.182299	0.065610	2.458766	C	4.465644	0.420610	-0.807038
H	-4.466721	0.683652	1.395180	C	5.845577	0.108709	-0.229752
H	-3.319955	2.124170	3.675140	C	5.707807	-1.380081	0.120532
H	-4.503762	2.728962	2.513868	C	4.268910	-1.449874	0.635618
H	-1.472274	3.009721	2.429465	H	3.779447	-2.410189	0.455585
H	-2.689185	4.170776	1.868346	H	4.219378	-1.228689	1.708550
H	-3.147604	2.816828	-0.128143	H	5.826596	-1.996423	-0.778642
H	-1.372289	2.558508	0.028097	H	6.432293	-1.723139	0.865379
O	-2.826029	-1.121251	-1.159407	H	6.651578	0.317555	-0.939656
C	-3.370205	-2.445604	-0.949735	H	6.026795	0.699619	0.676360
C	-4.859373	-2.384226	-1.339020	H	4.149812	1.457471	-0.677231
C	-5.158347	-0.876746	-1.333203	H	4.409965	0.168246	-1.872591
C	-3.822443	-0.297125	-1.791052	C	1.578011	2.774401	-0.291109
H	-3.714339	-0.353768	-2.883831	C	1.976020	2.495264	1.167560
H	-3.649180	0.730217	-1.469606	H	2.604451	1.599818	1.261741
H	-5.991110	-0.597334	-1.985685	H	2.538744	3.334121	1.596772
H	-5.387610	-0.532409	-0.318163	H	1.079821	2.343049	1.781508
H	-5.013832	-2.797044	-2.341993	C	0.875046	4.159259	-0.322210
H	-5.488963	-2.950056	-0.645975	H	0.035927	4.191469	0.384163
H	-3.223505	-2.695854	0.105007	H	1.574962	4.957822	-0.038812
H	-2.809624	-3.164728	-1.555670	H	0.487522	4.405706	-1.316147

Table A4.1 (Continued).

C	0.657291	-2.754042	0.069113	H	2.533919	2.936276	-0.843762
C	-0.228490	-3.982087	0.385700	C	-0.555892	0.969153	-2.774494
H	-1.269985	-3.797777	0.102697	H	-1.479919	1.305108	-2.290136
H	0.122300	-4.863948	-0.166914	H	-0.697773	1.050809	-3.860567
H	-0.216642	-4.238917	1.449715	H	-0.412035	-0.094191	-2.545512
C	0.690582	-2.553474	-1.453263	C	1.880444	1.442510	-3.140188
H	1.362710	-1.735653	-1.742380	H	2.121643	0.375543	-3.036146
H	1.043009	-3.459209	-1.963223	H	1.720468	1.649978	-4.208251
H	-0.308431	-2.317014	-1.841562	H	2.756911	2.019299	-2.824130
H	1.685699	-3.068606	0.349498	H	0.391623	2.848661	-2.556343
C	0.174180	-1.670666	2.199914				

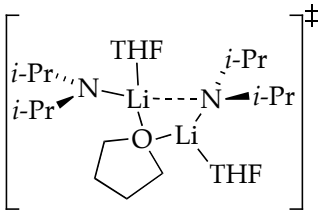

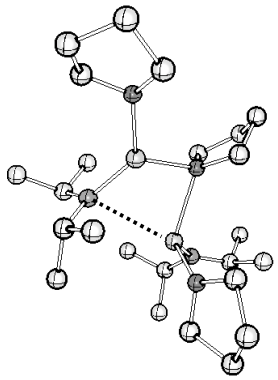

13
G = -1295.443878
G_{MP2} = -1290.879859
$\Delta G^{‡}$ = 25.7 kcal/mol
$\Delta G_{MP2}{}^{‡}$ = 21.2 kcal/mol

13 connects with trisolvated open dimer **5a** and **7**.

Atom	X	Y	Z	Atom	X	Y	Z
C	1.323554	2.622040	-1.440307	C	-3.012289	-0.033052	3.811668
N	1.335446	1.768721	-0.254470	C	-2.491226	0.754934	2.609980
Li	1.732490	-0.056325	-0.368838	H	-2.054362	1.714114	2.912435
O	3.543874	-0.882754	-0.243906	H	-3.229163	0.922319	1.822343
C	4.062073	-1.902955	0.641902	H	-3.427126	0.618789	4.586220
C	5.572265	-1.663028	0.730819	H	-3.794879	-0.735034	3.501547
C	5.676126	-0.149143	0.487613	H	-1.106800	-0.141595	4.859219
C	4.592355	0.078021	-0.562663	H	-1.981233	-1.685767	4.863315
H	4.958868	-0.133474	-1.575284	H	-1.492323	-2.077211	2.520885
H	4.130293	1.067240	-0.539900	H	-0.005613	-1.208559	2.993359
H	6.664578	0.164337	0.139710	C	0.488202	-2.757957	-0.013584
H	5.443362	0.405901	1.403717	C	0.731434	-3.767642	-1.130455
H	6.094360	-2.213674	-0.060215	C	-0.167780	-3.214308	-2.247300
H	5.985395	-1.979227	1.693118	C	-0.028934	-1.699086	-2.088230
H	3.579212	-1.789143	1.621524	H	-0.955520	-1.140680	-2.261225
H	3.804052	-2.885023	0.232957	H	0.780918	-1.294252	-2.703052
O	0.343476	-1.476376	-0.676978	H	-1.206550	-3.521568	-2.086704

Table A4.1 (Continued).

Li	-1.293114	0.191871	-0.001682	H	0.132838	-3.548313	-3.244556
N	-2.923400	0.103986	-0.998597	H	0.473582	-4.788342	-0.831721
C	-3.492009	1.285101	-1.641593	H	1.784568	-3.753485	-1.436961
H	-4.131638	1.004834	-2.503402	H	1.309129	-2.674586	0.703880
C	-4.400008	2.121808	-0.703619	H	-0.436467	-2.980388	0.530738
H	-5.160785	1.492494	-0.226038	C	1.488262	2.500248	0.995318
H	-3.799264	2.587984	0.089807	H	2.394529	3.141252	0.986715
H	-4.925333	2.924292	-1.242310	C	0.314420	3.447140	1.336509
C	-2.391519	2.188224	-2.208780	H	0.158350	4.192408	0.548721
H	-1.832506	1.671576	-2.996512	H	-0.618245	2.877053	1.437949
H	-2.800644	3.116303	-2.630021	H	0.491423	3.991789	2.274818
H	-1.678546	2.470267	-1.422054	C	1.694764	1.511463	2.153077
C	-3.894920	-0.978674	-0.970880	H	2.573486	0.875803	1.968793
H	-4.908306	-0.607225	-0.702797	H	1.856357	2.029398	3.107140
C	-3.547424	-2.023948	0.099388	H	0.812450	0.869177	2.262069
H	-2.544185	-2.437859	-0.079332	H	0.422601	3.268166	-1.479917
H	-3.550460	-1.576807	1.099142	C	1.264443	1.743099	-2.696782
H	-4.254588	-2.863774	0.094268	H	1.193402	2.344081	-3.611540
C	-4.072361	-1.703423	-2.331460	H	2.172654	1.123886	-2.780027
H	-4.894361	-2.434254	-2.305038	H	0.392426	1.082651	-2.665794
H	-4.290364	-0.990590	-3.134022	C	2.524745	3.589064	-1.579468
H	-3.152337	-2.237295	-2.606238	H	2.452718	4.164915	-2.511441
O	-1.431897	-0.061762	2.035417	H	2.576958	4.309467	-0.756517
C	-1.096785	-1.138797	2.931537	H	3.474113	3.034828	-1.597653
C	-1.758571	-0.795071	4.267754				

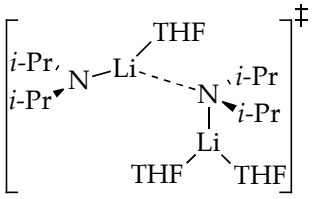

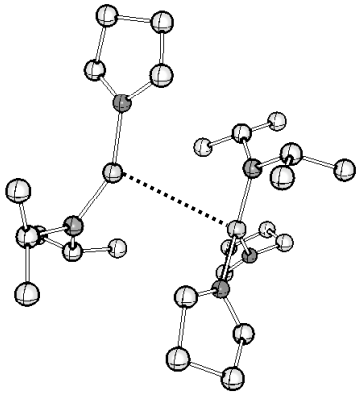

14
G = -1295.449326
G_{MP2} = -1290.877105
$\Delta G^{\ddagger}$ = 22.3 kcal/mol
$\Delta G_{MP2}{}^{\ddagger}$ = 23.0 kcal/mol

Atom	X	Y	Z	Atom	X	Y	Z
C	1.998047	-2.440567	1.794156	H	-5.307965	-0.331767	0.325113
N	2.597024	-1.667569	0.720492	H	-4.239966	1.092047	0.139970
Li	2.253942	0.099387	0.331597	C	-1.083484	2.749563	0.267657
O	2.798805	1.907549	0.160525	C	-2.286546	3.702730	0.500577

Table A4.1 (continued).

C	3.596110	2.622805	1.137194	H	-3.181195	3.138427	0.797732
C	4.004805	3.927200	0.451212	H	-2.067548	4.436533	1.290003
C	2.814595	4.186622	-0.486461	H	-2.532406	4.264777	-0.405909
C	2.459154	2.777163	-0.955734	C	-0.703776	2.106274	1.610442
H	1.400680	2.626251	-1.174614	H	0.210430	1.508748	1.508255
H	3.062815	2.473831	-1.820858	H	-0.536428	2.856716	2.393657
H	1.974986	4.622928	0.066035	H	-1.502502	1.436699	1.958447
H	3.058061	4.851435	-1.320296	H	-0.242736	3.436500	0.004067
H	4.176077	4.735048	1.168690	C	-1.356089	2.250631	-2.097705
H	4.925151	3.783779	-0.126933	C	-0.610623	1.347453	-3.101344
H	4.438994	1.986329	1.420906	H	-1.030563	0.332678	-3.075100
H	2.974619	2.806838	2.022167	H	-0.696806	1.715443	-4.132732
N	-1.245827	1.724573	-0.743670	H	0.453204	1.268715	-2.849725
Li	-1.718222	-0.075010	-0.386750	C	-2.812049	2.416777	-2.609699
O	-1.343436	-1.812615	-1.241548	H	-3.406367	3.045259	-1.940900
C	-2.388815	-2.767475	-1.539990	H	-2.850910	2.859948	-3.615897
C	-1.776508	-3.762833	-2.528083	H	-3.301501	1.432983	-2.660008
C	-0.293922	-3.742903	-2.126949	H	-0.883428	3.254537	-2.162195
C	-0.073274	-2.269730	-1.792301	C	3.779414	-2.292483	0.146704
H	0.709032	-2.091370	-1.046473	C	4.584309	-1.257681	-0.655042
H	0.140518	-1.680431	-2.692647	H	4.923837	-0.438645	-0.007548
H	-0.123837	-4.365250	-1.240745	H	5.467294	-1.702042	-1.131043
H	0.373953	-4.092912	-2.919160	H	3.964659	-0.828124	-1.458429
H	-2.236843	-4.753100	-2.456690	C	3.475723	-3.505478	-0.766721
H	-1.898301	-3.404771	-3.557259	H	2.940900	-3.179989	-1.669081
H	-3.251434	-2.226191	-1.940535	H	4.395678	-4.016968	-1.083558
H	-2.688886	-3.259844	-0.606650	H	2.849787	-4.243697	-0.252317
O	-3.293908	-0.617086	0.735168	H	4.466308	-2.668062	0.933125
C	-4.463548	0.222651	0.760167	C	0.581794	-1.921058	2.086352
C	-4.708315	0.542008	2.247373	H	-0.054602	-2.002832	1.196914
C	-3.935206	-0.572849	3.006501	H	0.107715	-2.475530	2.907521
C	-3.390356	-1.472232	1.884782	H	0.616481	-0.862253	2.384633
H	-2.396985	-1.882114	2.076383	C	2.812960	-2.427484	3.111071
H	-4.082621	-2.298466	1.663307	H	2.856045	-1.407383	3.516514
H	-3.111371	-0.144585	3.584534	H	2.368762	-3.083373	3.873731
H	-4.571267	-1.133158	3.698051	H	3.842666	-2.764098	2.947767
H	-4.311158	1.528683	2.500369	H	1.882263	-3.510708	1.517365
H	-5.776931	0.542976	2.481639				

Table A4.1 (continued).

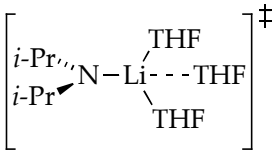

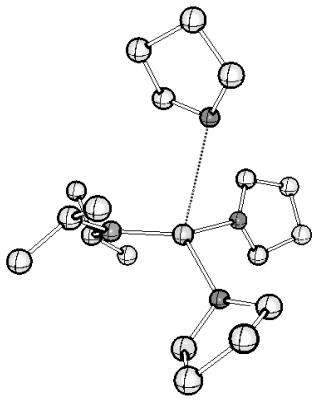

15
G = -1296.24815
G_{MP2} = -992.798680
$\Delta G^{‡}$ = 11.5 kcal/mol
$\Delta G_{MP2}^{‡}$ = 8.2 kcal/mol

Atom	X	Y	Z	Atom	X	Y	Z
C	-0.151278	-1.488130	2.681120	H	3.534626	0.770454	0.435262
N	-0.164812	-1.467352	1.228815	H	2.341117	-0.557186	0.535425
C	0.289774	-2.702771	0.617291	H	3.556732	-1.859054	-1.133666
C	-0.554367	-3.958282	0.954354	H	4.926531	-1.075433	-0.323320
H	-0.157509	-4.852688	0.453927	H	4.609788	-0.661881	-3.012863
H	-0.569410	-4.166906	2.029467	H	4.967456	0.732112	-1.979283
H	-1.594842	-3.815643	0.630561	H	2.254370	-0.132925	-3.084187
C	0.323031	-2.542990	-0.911898	H	2.881816	1.518747	-2.882406
H	0.907172	-1.660955	-1.201427	O	-2.248196	0.188575	-0.846609
H	0.759633	-3.422584	-1.402999	C	-3.234348	-0.822364	-0.532791
H	-0.694912	-2.416193	-1.305210	C	-3.575297	-1.523313	-1.869268
H	1.332811	-2.964970	0.914553	C	-2.810512	-0.703413	-2.939124
Li	-0.558478	0.108232	0.258241	C	-2.469075	0.594479	-2.202232
O	-0.419617	2.091348	0.531713	H	-3.303905	1.311694	-2.244023
C	-1.528275	2.884759	0.977565	H	-1.559794	1.089559	-2.552220
C	-1.155259	4.308241	0.559893	H	-3.399667	-0.527226	-3.844342
C	0.382221	4.333202	0.751116	H	-1.888303	-1.216883	-3.227861
C	0.778601	2.837743	0.830021	H	-4.654711	-1.508309	-2.050148
H	1.123496	2.569130	1.837427	H	-3.255768	-2.568918	-1.866618
H	1.524773	2.524932	0.099640	H	-2.768500	-1.466245	0.217071
H	0.661562	4.855185	1.671561	H	-4.117147	-0.330150	-0.102241
H	0.880672	4.842997	-0.078311	C	1.263601	-1.519934	3.312832
H	-1.671536	5.068479	1.153794	H	1.849168	-2.368466	2.940322
H	-1.415432	4.466219	-0.492012	H	1.812534	-0.600820	3.063866
H	-2.424665	2.485055	0.501138	H	1.220519	-1.606365	4.408092
H	-1.631164	2.797571	2.069851	C	-0.910680	-0.270606	3.230384
O	2.194327	0.607162	-1.151787	H	-1.945986	-0.265476	2.865314
C	2.848085	0.520148	-2.429637	H	-0.934774	-0.264849	4.327737
C	4.242371	-0.068381	-2.169853	H	-0.428900	0.662616	2.904118
C	4.010089	-0.891063	-0.892353	H	-0.680027	-2.374855	3.090282
C	3.012848	-0.013937	-0.135625				

Table A4.1 (continued).

i-Pr, *i*-Pr N−Li—THF

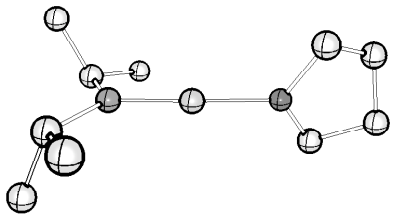

16
G = -531.551232
G_{MP2} = -529.642356
ΔG = 10.4 kcal/mol
ΔG_{MP2} = 18.5 kcal/mol

Atom	X	Y	Z	Atom	X	Y	Z
C	-2.542016	-1.124853	0.250648	H	2.348220	0.847909	1.782018
N	-1.666846	0.004061	0.002239	H	2.953005	-0.829438	1.799181
C	-2.347484	1.254768	-0.269229	H	4.171030	1.585096	0.352865
C	-3.002258	1.892262	0.979568	H	5.025029	0.361788	1.312920
H	-3.563807	2.803268	0.727864	H	4.984644	0.062548	-1.400140
H	-3.699608	1.197636	1.460887	H	4.637452	-1.356151	-0.396787
H	-2.230547	2.152542	1.716673	H	2.572887	-1.309176	-1.639343
C	-1.354616	2.254059	-0.882670	H	2.633325	0.462262	-1.824460
H	-0.942280	1.862185	-1.821529	C	-3.253018	-1.653647	-1.017922
H	-1.817755	3.226836	-1.089789	H	-3.822425	-0.860096	-1.514469
H	-0.519867	2.436123	-0.185054	H	-2.510845	-2.028944	-1.735526
H	-3.159095	1.129283	-1.016311	H	-3.954099	-2.467622	-0.784649
Li	0.132813	-0.150494	0.030515	C	-1.733812	-2.265670	0.887470
O	2.027530	-0.218284	0.039331	H	-1.294202	-1.943228	1.840256
C	2.852175	-0.372488	-1.148827	H	-2.347080	-3.155729	1.075181
C	4.299749	-0.345252	-0.651568	H	-0.916615	-2.574689	0.213877
C	4.198913	0.521169	0.614276	H	-3.344540	-0.873878	0.975655
C	2.856769	0.079785	1.193057				

Table A4.2. Optimized geometries of THF disolvated LDA open dimers at the B3LYP level of theory with a 6-31G(d) basis set at -78 °C with free energies (Hartrees) and cartesian coordinates (X, Y, Z). Single point MP2 energies are included. A representative image is shown in Table 2a. The geometries of the open dimers are categorized most conveniently by two pseudo-dihedral angles ω_C and ω_O as shown in Table 2b. ω_C is defined by a dihedral angle spanning atoms C-N-N-C and ω_O is defined by a dihedral angle spanning atoms O-Li-N-Li. Although the direction of the arrow is irrelevant for the measure of the dihedral angle, it indicates the sign of the angle (clockwise = minus , counter-clockwise = plus). The caption below the energy values indicates the connectivity of transition states and ground states. Structure **4i** and **4j** represent the meso stereoisomer in contrast to the homochiral form.

a)

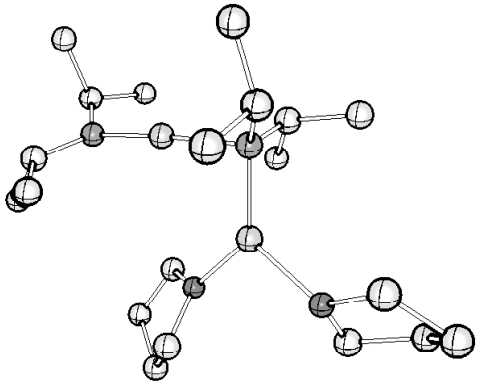

b)

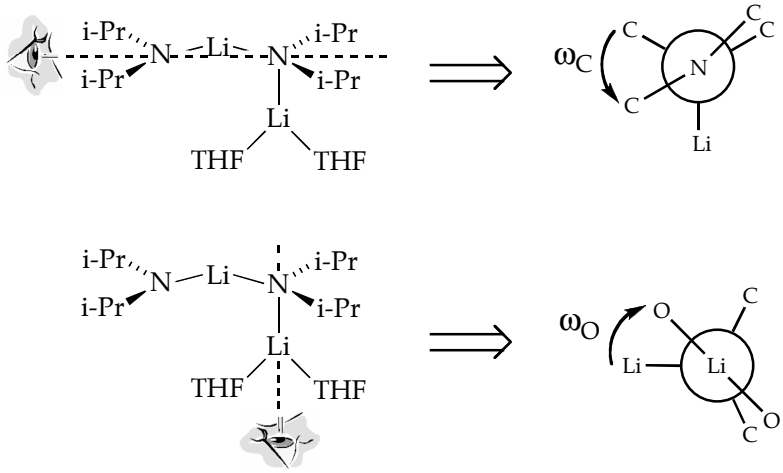

Table A4.2 (continued).

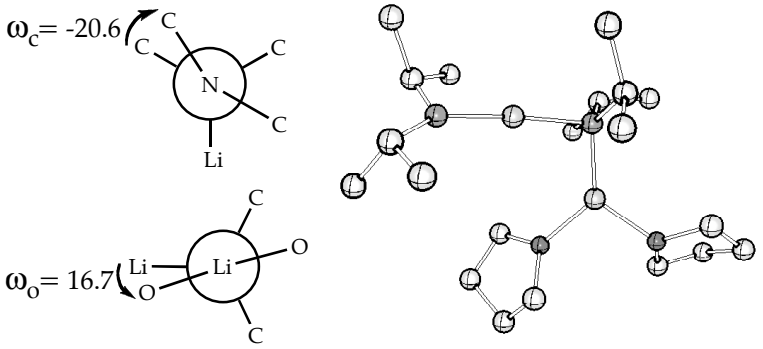

4a
G = -1063.121401
G_{MP2} = 1059.32551
ΔG = 8.8 kcal/mol
ΔG_{MP2} = 11.5 kcal/mol
4a → 11

Atom	X	Y	Z	Atom	X	Y	Z
C	-0.562689	-2.265881	-1.273584	H	4.429804	-2.626589	0.038385
N	-0.399930	-1.595055	0.026309	H	5.865412	-2.071460	-0.860057
Li	-1.310697	0.120142	0.137474	C	3.541530	-1.160201	-2.099251
O	-3.235353	0.436506	0.443202	H	3.007426	-0.359350	-2.624624
C	-4.029225	1.203369	-0.492261	H	4.283446	-1.588171	-2.785653
C	-5.252234	0.337764	-0.784390	H	2.818445	-1.958504	-1.868778
C	-5.491255	-0.335016	0.576788	C	3.716840	0.761867	1.113708
C	-4.065631	-0.570460	1.089302	H	4.616486	0.320037	1.592664
H	-3.676453	-1.552632	0.804545	C	2.693137	0.953929	2.242040
H	-3.969694	-0.450763	2.172290	H	1.750785	1.353316	1.835476
H	-6.060372	-1.265821	0.502436	H	2.472772	-0.002082	2.732897
H	-6.035840	0.341466	1.245451	H	3.048490	1.655288	3.008069
H	-5.013673	-0.411132	-1.548190	C	4.164044	2.153674	0.598371
H	-6.106823	0.924543	-1.133515	H	4.655911	2.742686	1.385944
H	-4.312377	2.156872	-0.026069	H	4.869370	2.063067	-0.234927
H	-3.407765	1.411239	-1.367486	H	3.297195	2.722807	0.236351
O	-0.603464	1.905058	-0.151897	C	-0.574569	-2.487002	1.182124
C	-0.887718	3.024742	0.712892	H	-1.566770	-2.981261	1.165061
C	-0.618184	4.254224	-0.148305	C	0.466186	-3.625332	1.276162
C	0.617291	3.806938	-0.948377	H	0.448645	-4.264177	0.386312
C	0.392800	2.299835	-1.150099	H	1.483281	-3.219260	1.373752
H	1.299551	1.703356	-0.994149	H	0.276594	-4.267165	2.146480
H	-0.034153	2.068828	-2.131333	C	-0.536210	-1.659692	2.476371
H	1.528283	3.979679	-0.366358	H	-1.317795	-0.885770	2.483629
H	0.723834	4.335881	-1.899723	H	-0.694106	-2.290369	3.359538
H	-0.441733	5.154365	0.448084	H	0.431381	-1.155963	2.598075
H	-1.468903	4.443972	-0.813861	H	0.236789	-3.015070	-1.451066
H	-1.921894	2.924299	1.052963	C	-0.428671	-1.226974	-2.397830
H	-0.220070	2.991558	1.584643	H	-0.461499	-1.699860	-3.386492
Li	1.486537	-0.889513	0.111808	H	-1.254526	-0.498132	-2.358481
N	3.172123	-0.107185	0.086603	H	0.514166	-0.673167	-2.325483

Table A4.2 (continued).

C	4.190495	-0.630117	-0.812129	C	-1.894589	-3.025529	-1.460779
H	4.899759	0.161283	-1.133400	H	-1.956928	-3.462767	-2.465456
C	5.055888	-1.752377	-0.187374	H	-2.012275	-3.843485	-0.742401
H	5.517601	-1.424477	0.750723	H	-2.747525	-2.342387	-1.335210

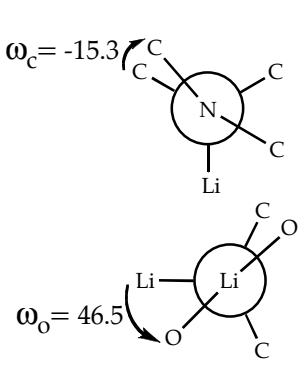

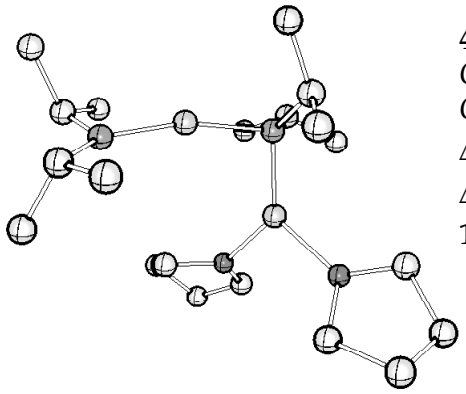

4b
G = -1063.120567
G_{MP2} = -1059.324222
ΔG = 9.4 kcal/mol
ΔG_{MP2} = 12.3 kcal/mol
10* → 4b

Atom	X	Y	Z	Atom	X	Y	Z
C	-3.052490	0.079073	-2.158608	H	2.480688	-2.296775	2.332048
N	-2.945568	-0.124926	-0.720981	C	-0.467076	-0.570685	2.989759
Li	-1.543941	-1.024750	0.143024	H	-1.536162	-0.712774	2.800384
N	0.251114	-1.606019	0.853742	H	-0.320001	-0.557325	4.077030
Li	1.235801	-0.018706	0.231005	H	-0.193171	0.420631	2.602895
O	0.746132	1.874179	0.396741	H	-0.010142	-2.630984	2.706565
C	1.465056	2.741014	1.310151	C	0.602097	-2.901437	0.243918
C	0.579732	3.979316	1.519237	C	-0.525862	-3.954211	0.350965
C	-0.820583	3.464856	1.146782	H	-1.401156	-3.645811	-0.238879
C	-0.511370	2.501696	0.008121	H	-0.203484	-4.936334	-0.021137
H	-0.352900	3.039937	-0.936650	H	-0.852687	-4.085587	1.388644
H	-1.258434	1.712654	-0.146766	C	0.985729	-2.726549	-1.232741
H	-1.504770	4.262418	0.843482	H	1.846204	-2.054726	-1.344385
H	-1.274645	2.924216	1.985142	H	1.246700	-3.686816	-1.694665
H	0.881149	4.784619	0.839599	H	0.153716	-2.301596	-1.806981
H	0.644888	4.361643	2.542135	H	1.485886	-3.342484	0.745710
H	1.622399	2.187715	2.243586	C	-4.211554	0.114840	-0.041276
H	2.442809	2.980993	0.878117	C	-3.992554	0.291960	1.467274
O	3.060112	0.161525	-0.492913	H	-3.292671	1.111561	1.671056
C	4.209960	-0.672552	-0.196333	H	-4.932675	0.502023	1.993042
C	5.348351	-0.117265	-1.052956	H	-3.577986	-0.627920	1.906788
C	4.595854	0.409884	-2.284547	C	-5.262910	-1.002688	-0.256006
C	3.321536	0.980604	-1.660701	H	-4.910551	-1.941016	0.193988
H	2.449117	0.929572	-2.318409	H	-6.231398	-0.745580	0.197185

Table A4.2 (continued).

H	3.456106	2.019450	-1.335358	H	-5.438147	-1.191223	-1.320794
H	4.351985	-0.413525	-2.965457	H	-4.688975	1.054739	-0.391114
H	5.155782	1.162553	-2.846951	C	-1.874966	-0.581017	-2.886707
H	6.094418	-0.879276	-1.295504	H	-1.871606	-1.664476	-2.716602
H	5.856113	0.703808	-0.533334	H	-1.910229	-0.405705	-3.969723
H	4.396996	-0.620543	0.879055	H	-0.920311	-0.173223	-2.518753
H	3.965428	-1.707566	-0.462237	C	-3.135448	1.566455	-2.590858
C	0.372303	-1.667534	2.321564	H	-2.185214	2.081009	-2.395670
C	1.834522	-1.559252	2.821673	H	-3.355834	1.664062	-3.663593
H	2.243499	-0.558275	2.610279	H	-3.922070	2.098321	-2.044152
H	1.910107	-1.720007	3.905767	H	-3.965078	-0.400070	-2.569689

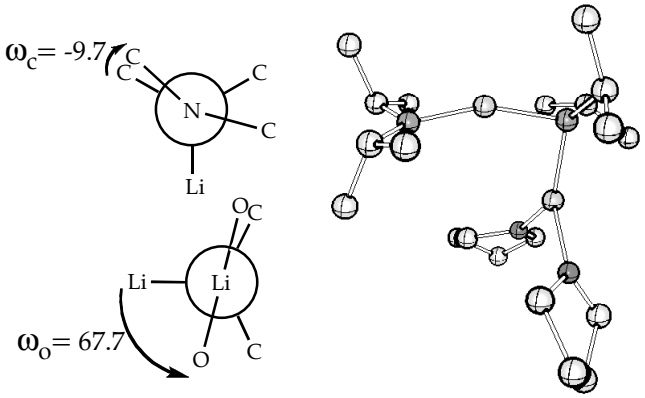

4c
G = -1063.117200
G_{MP2} = -1059.321171
ΔG = 11.5 kcal/mol
ΔG_{MP2} = 14.2 kcal/mol
10 → 4c

Atom	X	Y	Z	Atom	X	Y	Z
C	2.312152	-0.161294	-2.482859	H	-1.900783	2.835830	-0.424085
N	2.515584	-0.208852	-1.041866	C	1.187960	4.004118	0.664634
Li	1.635958	0.949284	0.145295	H	1.785507	3.928480	1.580629
N	0.112899	1.786433	1.172560	H	0.995469	5.070093	0.479790
Li	-1.117424	0.373718	0.532673	H	1.800655	3.627229	-0.167216
O	-2.653178	0.295854	-0.732762	H	-0.732427	3.698528	1.556720
C	-3.926632	-0.238159	-0.298309	C	0.274847	1.700904	2.636886
C	-4.648684	-0.682271	-1.572127	C	1.193659	0.538959	3.036660
C	-4.095205	0.301761	-2.614177	H	0.854046	-0.403284	2.588639
C	-2.638050	0.444745	-2.176175	H	1.227577	0.402467	4.125206
H	-2.005201	-0.343419	-2.602072	H	2.221219	0.716450	2.696566
H	-2.197519	1.415981	-2.409752	C	-1.076840	1.589816	3.381838
H	-4.185854	-0.060114	-3.642283	H	-1.754520	2.396813	3.079173
H	-4.612436	1.265678	-2.544225	H	-0.957535	1.644442	4.473106
H	-4.370717	-1.710401	-1.831954	H	-1.570635	0.633016	3.152913
H	-5.736806	-0.639920	-1.468954	H	0.757464	2.617844	3.021652

Table A4.2 (continued).

H	-4.476274	0.555603	0.223627	C	3.732940	-0.934788	-0.701255
H	-3.731315	-1.055580	0.401508	C	5.027491	-0.119463	-0.945020
O	-1.039289	-1.556339	1.032475	H	5.068598	0.266478	-1.969588
C	-1.444373	-2.273759	2.222769	H	5.932108	-0.723462	-0.781906
C	-1.112099	-3.744469	1.958454	H	5.062259	0.742450	-0.264335
C	0.093068	-3.638492	1.011276	C	3.713012	-1.394168	0.762509
C	-0.277842	-2.435135	0.148796	H	3.643509	-0.530515	1.438569
H	0.579191	-1.868331	-0.235813	H	4.626805	-1.940974	1.028070
H	-0.928124	-2.727251	-0.686963	H	2.853107	-2.044872	0.960440
H	1.010173	-3.433665	1.575008	H	3.833551	-1.858466	-1.310023
H	0.255142	-4.540990	0.414949	C	1.729564	-1.468510	-3.078741
H	-0.894450	-4.290114	2.881371	H	2.320434	-2.339724	-2.773866
H	-1.949584	-4.244784	1.457771	H	1.712249	-1.447689	-4.178265
H	-2.511033	-2.091526	2.393234	H	0.699489	-1.623535	-2.727221
H	-0.881914	-1.878277	3.076262	C	1.397751	1.008767	-2.866172
C	-0.121170	3.191209	0.785983	H	0.425980	0.910166	-2.359730
C	-0.913459	3.302786	-0.522786	H	1.201814	1.044818	-3.945846
H	-0.379797	2.809994	-1.345394	H	1.840824	1.966155	-2.565450
H	-1.061018	4.351405	-0.810250	H	3.266975	0.013440	-3.019569

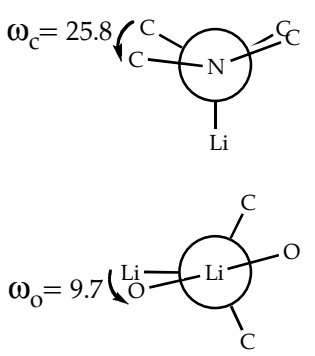

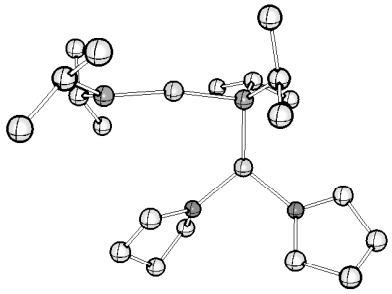

4d
G = -1063.119115
G_{MP2} = -1059.323269
ΔG = 10.3 kcal/mol
ΔG_{MP2} = 12.9 kcal/mol

Atom	X	Y	Z	Atom	X	Y	Z
C	-3.746713	-0.163010	-1.560314	H	2.620118	-3.018853	1.441428
N	-3.055397	-0.105518	-0.278875	C	-0.427054	-1.847975	2.638457
Li	-1.467832	-1.067975	0.023677	H	-1.483278	-1.908333	2.347104
N	0.401932	-1.772920	0.312692	H	-0.330151	-2.334846	3.616547
Li	1.292315	-0.014437	0.310747	H	-0.176278	-0.785324	2.772456
O	0.525152	1.769805	0.346420	H	0.135943	-3.540163	1.478991
C	0.694816	2.698195	1.436838	C	0.890564	-2.585542	-0.813480
C	0.357206	4.061651	0.840733	C	-0.059042	-3.732837	-1.227449
C	-0.807812	3.709701	-0.100265	H	-1.006998	-3.332891	-1.609487

Table A4.2 (continued).

C	-0.457220	2.302019	-0.604817	H	0.385228	-4.356459	-2.015083
H	0.033635	2.322417	-1.585075	H	-0.290732	-4.388947	-0.381680
H	-1.321944	1.624122	-0.627675	C	1.153128	-1.688083	-2.034550
H	-0.923184	4.423250	-0.921108	H	1.936214	-0.944128	-1.830158
H	-1.750455	3.685725	0.456362	H	1.479560	-2.273192	-2.902742
H	1.213381	4.450482	0.276268	H	0.241590	-1.149367	-2.325661
H	0.087635	4.797722	1.604081	H	1.860006	-3.065397	-0.566875
H	0.006248	2.436207	2.251115	C	-3.962714	0.301903	0.787274
H	1.724390	2.605056	1.796192	C	-3.210010	0.985134	1.939757
O	3.225110	0.406603	0.126052	H	-2.719531	1.902616	1.593691
C	4.279895	-0.596033	0.139272	H	-3.883765	1.248208	2.765917
C	5.512152	0.079163	-0.472973	H	-2.435106	0.322291	2.347365
C	4.889744	1.156952	-1.373895	C	-4.800485	-0.872609	1.350784
C	3.693871	1.604686	-0.537877	H	-4.144842	-1.597266	1.853773
H	2.862263	2.010886	-1.117558	H	-5.559335	-0.538184	2.074152
H	3.989242	2.342165	0.220726	H	-5.318547	-1.401410	0.542649
H	4.550313	0.720463	-2.320350	H	-4.696061	1.049576	0.421441
H	5.573441	1.979984	-1.601288	C	-3.010632	-1.084644	-2.541637
H	6.141815	-0.629400	-1.018374	H	-2.962928	-2.109185	-2.151797
H	6.124995	0.543989	0.307934	H	-3.500133	-1.116660	-3.523616
H	4.429821	-0.924913	1.170323	H	-1.981396	-0.730201	-2.703501
H	3.936518	-1.449091	-0.455213	C	-3.941854	1.224071	-2.224768
C	0.487874	-2.498141	1.592189	H	-2.971580	1.647226	-2.519840
C	1.920081	-2.591517	2.168203	H	-4.571720	1.164843	-3.124452
H	2.288223	-1.593202	2.449235	H	-4.417830	1.929223	-1.533621
H	1.954654	-3.221795	3.067013	H	-4.765496	-0.590721	-1.448275

Table A4.2 (continued).

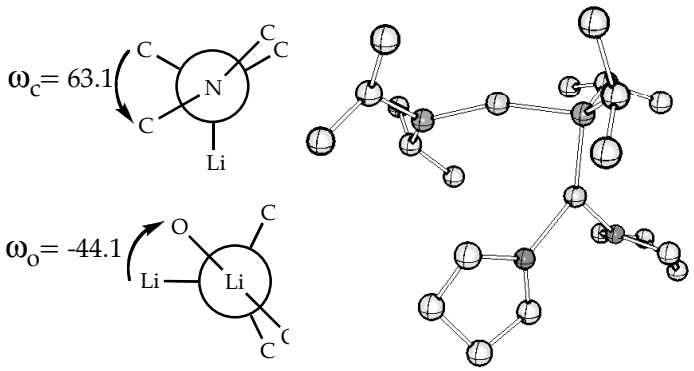

4e
G = -1063.119655
G_{MP2} = -1059.324365
ΔG = 9.9 kcal/mol
ΔG_{MP2} = 12.2 kcal/mol

Atom	X	Y	Z	Atom	X	Y	Z
C	-2.736853	0.672998	2.001700	H	2.699703	-3.290804	-0.747489
N	-2.802689	-0.114503	0.781804	C	0.488986	-2.563597	1.835718
Li	-1.462388	-1.241467	0.136308	H	-0.597666	-2.527788	1.989104
N	0.328772	-1.864973	-0.535642	H	0.894099	-3.311227	2.528734
Li	1.102309	-0.040092	-0.436232	H	0.896129	-1.585898	2.130607
O	0.425706	1.732392	-0.963894	H	0.399134	-3.876387	0.165656
C	-0.948053	2.033114	-1.364257	C	0.276527	-2.373699	-1.918641
C	-1.119561	3.523792	-1.089621	C	-0.896327	-3.345079	-2.185476
C	0.284926	4.070938	-1.385128	H	-1.859543	-2.822746	-2.112420
C	1.186819	2.957396	-0.845334	H	-0.833646	-3.787952	-3.188853
H	1.429125	3.113615	0.213115	H	-0.906863	-4.169306	-1.463597
H	2.121058	2.846899	-1.404948	C	0.200682	-1.213778	-2.921971
H	0.489469	5.034436	-0.908211	H	1.089980	-0.569149	-2.866709
H	0.428291	4.190188	-2.465594	H	0.127308	-1.579222	-3.953417
H	-1.387934	3.688630	-0.039836	H	-0.681238	-0.589031	-2.729285
H	-1.897836	3.972312	-1.713619	H	1.199560	-2.933372	-2.163815
H	-1.047430	1.809135	-2.434080	C	-4.150539	-0.198882	0.237229
H	-1.614671	1.386081	-0.779463	C	-4.249468	-1.368636	-0.752261
O	2.914101	0.484991	0.215997	H	-4.012031	-2.319245	-0.256749
C	3.241011	0.781669	1.595618	H	-5.251925	-1.454453	-1.190532
C	4.718256	0.421262	1.751078	H	-3.543457	-1.227366	-1.585121
C	5.273285	0.738216	0.353269	C	-4.631419	1.094934	-0.467453
C	4.125304	0.297755	-0.558565	H	-4.038899	1.281441	-1.373834
H	4.200013	-0.761998	-0.827837	H	-5.688262	1.029806	-0.763108
H	4.041923	0.892088	-1.473972	H	-4.527240	1.967380	0.187972
H	6.204776	0.211062	0.128404	H	-4.900013	-0.407363	1.028135
H	5.457778	1.813802	0.249324	C	-1.280115	1.040903	2.328259
H	4.829047	-0.645574	1.975249	H	-0.816751	1.592640	1.501431
H	5.203574	0.990865	2.548738	H	-1.211155	1.655853	3.235120
H	3.062592	1.849377	1.777274	H	-0.688589	0.131372	2.503865
H	2.573089	0.198157	2.234838	C	-3.353042	-0.026185	3.239471

Table A4.2 (continued).

C	0.854556	-2.891206	0.381346	H	-2.785913	-0.936111	3.477596
C	2.384188	-3.099601	0.284486	H	-3.347276	0.627193	4.124201
H	2.911010	-2.204067	0.638779	H	-4.391768	-0.321954	3.056753
H	2.715702	-3.951798	0.893337	H	-3.279033	1.638548	1.897268

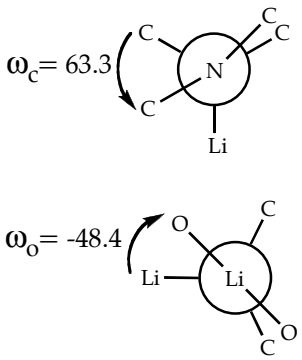

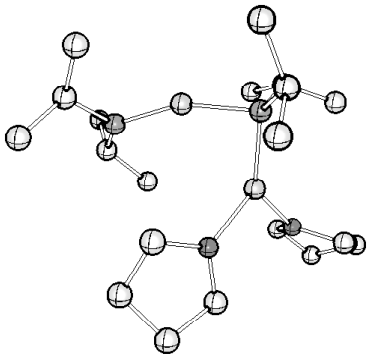

4f
G = -1063.120314
G_{MP2} = -1059.325333
ΔG = 9.5 kcal/mol
ΔG_{MP2} = 11.6 kcal/mol

Atom	X	Y	Z	Atom	X	Y	Z
C	-2.573179	0.747003	2.056481	H	2.667385	-3.326237	-0.814948
N	-2.720673	-0.065884	0.860757	C	0.519841	-2.584895	1.817128
Li	-1.451567	-1.247665	0.169199	H	-0.562935	-2.545081	1.995585
N	0.304397	-1.903488	-0.558130	H	0.938342	-3.330948	2.503943
Li	1.072551	-0.074862	-0.492683	H	0.937020	-1.607698	2.098031
O	0.411867	1.676606	-1.107095	H	0.390488	-3.908274	0.157752
C	1.201913	2.888719	-1.105183	C	0.202052	-2.437410	-1.928926
C	0.290083	3.991327	-1.652616	C	-1.002453	-3.382995	-2.142581
C	-1.106175	3.486090	-1.258521	H	-1.949165	-2.832264	-2.060123
C	-0.971690	1.981050	-1.465294	H	-0.977180	-3.852972	-3.135231
H	-1.120727	1.707222	-2.517765	H	-1.016953	-4.187431	-1.398761
H	-1.621880	1.373664	-0.822231	C	0.130001	-1.299098	-2.956539
H	-1.908256	3.917424	-1.864227	H	1.034609	-0.674599	-2.934624
H	-1.316961	3.708033	-0.206058	H	0.024445	-1.686239	-3.977311
H	0.378214	4.054557	-2.743571	H	-0.732964	-0.650175	-2.758752
H	0.534707	4.973183	-1.235939	H	1.103578	-3.026329	-2.184527
H	1.512793	3.096750	-0.074116	C	-4.101236	-0.154088	0.406006
H	2.097681	2.727079	-1.713662	C	-4.268368	-1.343808	-0.550427
O	2.847890	0.477261	0.225551	H	-4.005656	-2.286144	-0.051517
C	4.101837	0.257038	-0.466713	H	-5.296941	-1.432350	-0.922512
C	5.175012	0.222065	0.622949	H	-3.616117	-1.224153	-1.429307
C	4.582949	1.154222	1.691911	C	-4.620197	1.126936	-0.294715
C	3.093191	0.820894	1.612714	H	-4.085780	1.289943	-1.240851

Table A4.2 (continued).

H	2.435325	1.653585	1.876933	H	-5.694089	1.062231	-0.520776
H	2.836464	-0.043225	2.237209	H	-4.469614	2.012867	0.332899
H	4.756870	2.203604	1.426551	H	-4.798910	-0.342084	1.247970
H	4.993787	0.982585	2.690827	C	-1.099312	1.129947	2.270119
H	6.151634	0.548875	0.254599	H	-0.702980	1.674067	1.404431
H	5.281431	-0.793985	1.019347	H	-0.968714	1.757019	3.161937
H	4.020374	-0.676308	-1.030703	H	-0.489682	0.226429	2.413003
H	4.261065	1.086552	-1.167860	C	-3.095299	0.069288	3.348057
C	0.850722	-2.921766	0.356325	H	-2.507843	-0.833716	3.561948
C	2.377689	-3.129758	0.223626	H	-3.030633	0.739120	4.218076
H	2.911588	-2.231780	0.560734	H	-4.142731	-0.233932	3.244544
H	2.725458	-3.978213	0.828735	H	-3.127919	1.707048	1.971934

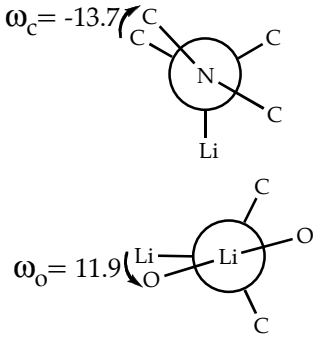

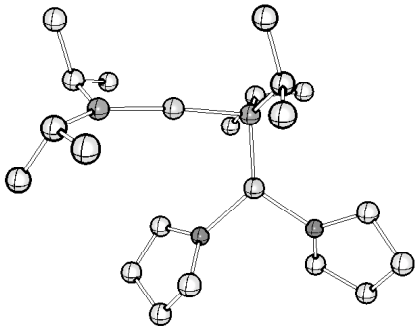

4g
G = -1063.121261
G_{MP2} = -1059.324248
ΔG = 8.9 kcal/mol
ΔG_{MP2} = 12.3 kcal/mol

Atom	X	Y	Z	Atom	X	Y	Z
C	4.239235	-0.301231	-0.707950	H	-1.651012	-4.123563	-0.809332
N	3.152230	0.059435	0.190363	C	-0.206983	-1.437550	-2.479179
Li	1.535220	-0.859754	0.128198	H	0.675276	-0.795547	-2.377779
N	-0.288367	-1.704288	-0.043741	H	-0.134737	-1.950044	-3.445801
Li	-1.327303	-0.063266	-0.093525	H	-1.097487	-0.789644	-2.522360
O	-3.277589	0.114987	0.052386	H	0.553352	-3.121993	-1.418478
C	-4.106565	1.029949	-0.692724	C	-0.479893	-2.556700	1.138443
C	-5.492619	1.010064	-0.004726	C	0.638560	-3.599124	1.362795
C	-5.395597	-0.162767	1.005802	H	1.609192	-3.106245	1.517270
C	-4.151450	-0.921015	0.541589	H	0.434511	-4.221364	2.244116
H	-4.379870	-1.620367	-0.274909	H	0.741346	-4.270123	0.502875
H	-3.618164	-1.456963	1.328106	C	-0.608789	-1.675380	2.390945
H	-6.288504	-0.794220	1.010083	H	-1.447484	-0.968566	2.302894
H	-5.244240	0.215034	2.021871	H	-0.784414	-2.279624	3.289205
H	-6.284527	0.844634	-0.740999	H	0.302105	-1.087549	2.560695
H	-5.707074	1.955416	0.501038	H	-1.424592	-3.131954	1.071108
H	-3.610703	2.002076	-0.675963	C	3.595759	0.905832	1.283971

Table A4.2 (continued).

H	-4.171032	0.685641	-1.733758	C	2.583067	0.868134	2.436938
O	-0.701246	1.771197	-0.315600	H	2.499876	-0.145390	2.848067
C	-0.909435	2.840205	0.626381	H	2.859726	1.546795	3.254380
C	-0.747835	4.107892	-0.206616	H	1.587482	1.172576	2.077326
C	0.419885	3.730202	-1.139807	C	3.842938	2.381916	0.879667
C	0.311137	2.197639	-1.282267	H	2.895203	2.862741	0.600683
H	1.253600	1.685779	-1.050902	H	4.291045	2.963412	1.698610
H	-0.048615	1.883190	-2.265787	H	4.516160	2.449899	0.017973
H	1.376950	3.997922	-0.681612	H	4.556476	0.549971	1.711910
H	0.361195	4.238105	-2.106587	C	3.684339	-0.779817	-2.057327
H	-0.537725	4.990021	0.405443	H	3.088601	0.007048	-2.535570
H	-1.662544	4.298846	-0.780285	H	4.485152	-1.073648	-2.748060
H	-1.902831	2.705086	1.063882	H	3.038494	-1.661109	-1.920469
H	-0.156141	2.783999	1.423735	C	5.178140	-1.393343	-0.137939
C	-0.316613	-2.439636	-1.318945	H	4.622792	-2.332041	-0.005501
C	-1.564804	-3.320160	-1.548106	H	6.034297	-1.588274	-0.800263
H	-2.480137	-2.713394	-1.492195	H	5.577682	-1.104077	0.840559
H	-1.530695	-3.791042	-2.538773	H	4.887043	0.571453	-0.936778

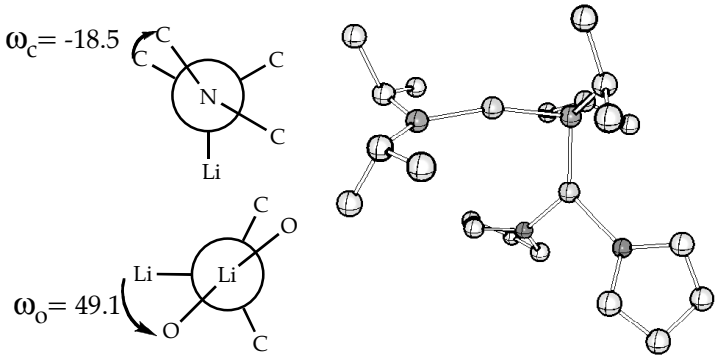

4h
G = -1063.119726
G_{MP2} = -1059.322855
ΔG = 9.9 kcal/mol
ΔG_{MP2} = 13.2 kcal/mol

Atom	X	Y	Z	Atom	X	Y	Z
C	3.068149	-0.324413	-2.138269	H	-2.357427	2.554031	2.174782
N	2.962459	-0.054140	-0.711733	C	0.406735	0.583922	2.932637
Li	1.617746	0.962670	0.107801	H	1.487757	0.621136	2.761031
N	-0.151934	1.665676	0.770461	H	0.239906	0.603136	4.016936
Li	-1.201055	0.142133	0.105035	H	0.044641	-0.382140	2.555674
O	-0.853890	-1.780161	0.340838	H	0.137695	2.674133	2.627359
C	-1.730396	-2.660724	1.065267	C	-0.372442	2.984898	0.148964
C	-0.828077	-3.422781	2.052990	C	0.842126	3.933352	0.282297
C	0.593589	-3.297266	1.437018	H	1.699861	3.548776	-0.288632
C	0.375579	-2.521850	0.130257	H	0.616532	4.939521	-0.096834

Table A4.2 (continued).

H	0.222902	-3.202345	-0.719576	H	1.156053	4.036882	1.327130
H	1.169284	-1.805393	-0.114320	C	-0.734198	2.839854	-1.336265
H	1.057482	-4.269675	1.249408	H	-1.651003	2.251815	-1.467757
H	1.254595	-2.737367	2.104437	H	-0.891850	3.818321	-1.806542
H	-1.150903	-4.462673	2.159230	H	0.067987	2.335703	-1.888805
H	-0.863496	-2.962487	3.044469	H	-1.224836	3.504246	0.628666
H	-2.499406	-2.046722	1.540544	C	4.209105	-0.325851	-0.008766
H	-2.215027	-3.347815	0.355871	C	3.967090	-0.419153	1.503922
O	-3.004993	0.036645	-0.692646	H	3.231203	-1.197983	1.738021
C	-4.099119	0.964568	-0.569730	H	4.891502	-0.642030	2.051724
C	-5.345452	0.115094	-0.837062	H	3.586651	0.537865	1.893051
C	-4.842134	-0.964966	-1.833628	C	5.317277	0.726419	-0.263604
C	-3.306710	-0.792683	-1.833751	H	5.009531	1.700752	0.140449
H	-2.959386	-0.284629	-2.743462	H	6.268256	0.441994	0.209721
H	-2.746567	-1.720937	-1.711380	H	5.509452	0.857494	-1.334063
H	-5.248441	-0.816497	-2.838120	H	4.640926	-1.304185	-0.308531
H	-5.131841	-1.967352	-1.506765	C	1.929942	0.364191	-2.901798
H	-6.168813	0.711741	-1.239607	H	1.983256	1.452518	-2.777549
H	-5.691169	-0.348890	0.091868	H	1.960425	0.141335	-3.976146
H	-4.047444	1.401482	0.428702	H	0.953436	0.023242	-2.522734
H	-3.983708	1.762695	-1.316569	C	3.077529	-1.830993	-2.506124
C	-0.313373	1.744431	2.233533	H	2.103231	-2.288546	-2.289488
C	-1.794629	1.763888	2.685222	H	3.292295	-1.985346	-3.573273
H	-2.280349	0.801235	2.458542	H	3.837331	-2.376753	-1.935610
H	-1.893169	1.933155	3.766170	H	4.006422	0.089897	-2.561827

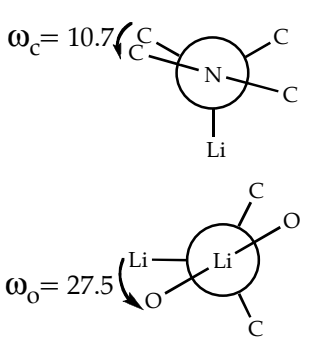

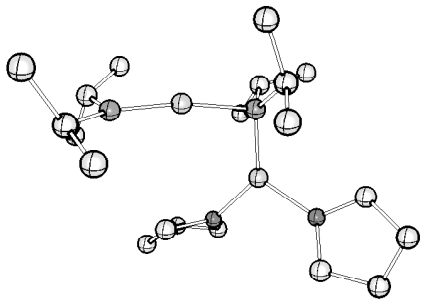

4i
G = -1063.120663
G_{MP2} = -1059.324724
ΔG = 9.3 kcal/mol
ΔG_{MP2} = 12.0 kcal/mol
(example of heterochiral form))

Atom	X	Y	Z	Atom	X	Y	Z
C	-3.529909	-0.237119	-1.835938	H	1.881984	-1.523996	-1.686577
N	-3.028684	-0.331829	-0.474045	C	-0.167800	-3.834433	-0.074133
Li	-1.403610	-1.045648	0.077089	H	-0.347463	-4.159861	0.956593

Table A4.2 (continued).

N	0.488343	-1.491439	0.641564	H	0.176936	-4.708934	-0.641587
Li	1.323260	0.202957	0.166197	H	-1.135112	-3.525424	-0.496962
O	3.227788	0.455816	-0.240753	H	1.818488	-3.110452	0.221333
C	4.213830	-0.569054	0.046023	C	0.401374	-1.729990	2.093750
C	5.205626	-0.505431	-1.113321	C	0.238115	-0.382069	2.814858
C	5.210112	0.995806	-1.441874	H	1.169775	0.202326	2.755687
C	3.742463	1.381364	-1.232192	H	0.008035	-0.519069	3.878077
H	3.154648	1.261791	-2.150428	H	-0.566069	0.217538	2.371812
H	3.606282	2.400223	-0.859520	C	1.603167	-2.470365	2.719178
H	5.555140	1.217220	-2.455893	H	1.706232	-3.493386	2.343820
H	5.853324	1.537625	-0.738763	H	1.492032	-2.532508	3.808994
H	4.833816	-1.085171	-1.966050	H	2.539528	-1.936555	2.503476
H	6.191948	-0.891783	-0.840879	H	-0.492425	-2.334502	2.359092
H	4.696530	-0.333872	1.003431	C	-4.044664	0.012198	0.510276
H	3.684813	-1.519635	0.138555	C	-3.748983	-0.660416	1.859545
O	0.638650	2.034834	0.046550	H	-3.739250	-1.752013	1.752736
C	0.998813	3.031507	1.025187	H	-4.491179	-0.395034	2.623812
C	-0.299600	3.773888	1.324983	H	-2.767338	-0.345846	2.244720
C	-0.963950	3.814801	-0.061137	C	-4.204796	1.538639	0.724306
C	-0.552811	2.474284	-0.685151	H	-3.296554	1.952289	1.185319
H	-0.285733	2.564526	-1.743386	H	-5.056474	1.781147	1.376650
H	-1.320818	1.699500	-0.568290	H	-4.361808	2.051218	-0.232301
H	-0.573492	4.656699	-0.644483	H	-5.044295	-0.354552	0.204014
H	-2.051298	3.913680	-0.006354	C	-2.372432	-0.236263	-2.844617
H	-0.127594	4.766364	1.752359	H	-1.682759	0.596117	-2.662608
H	-0.909484	3.195300	2.027662	H	-2.734560	-0.159761	-3.877746
H	1.429467	2.515135	1.887753	H	-1.802991	-1.173687	-2.768380
H	1.757407	3.705889	0.600995	C	-4.505718	-1.376945	-2.223582
C	0.860890	-2.681785	-0.135765	H	-3.979604	-2.340669	-2.199684
C	1.095167	-2.286039	-1.601749	H	-4.922362	-1.233827	-3.231344
H	0.183124	-1.874889	-2.053513	H	-5.348161	-1.442398	-1.526415
H	1.401563	-3.149138	-2.205161	H	-4.085688	0.712663	-2.001332

Table A4.2 (continued).

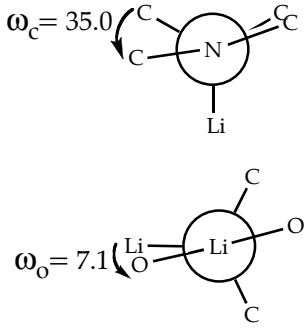

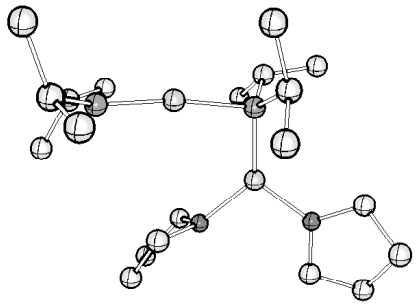

4j
G = -1063.12036
G_{MP2} = -1059.324244
ΔG = 9.5 kcal/mol
ΔG_{MP2} = 12.3 kcal/mol
(example of heterochiral form))

Atom	X	Y	Z	Atom	X	Y	Z
C	-3.822883	-0.419648	-1.400362	H	1.768704	-1.078627	-1.925176
N	-3.079414	-0.194724	-0.167119	C	-0.230629	-3.715896	-0.822635
Li	-1.423501	-0.997980	0.185830	H	-0.333991	-4.299482	0.098911
N	0.494753	-1.636388	0.432405	H	0.061938	-4.408902	-1.622504
Li	1.378233	0.086923	0.223731	H	-1.223220	-3.316078	-1.073411
O	3.284970	0.433162	-0.021492	H	1.776748	-3.076749	-0.488672
C	4.280447	-0.622899	-0.045559	C	0.545412	-2.242670	1.774726
C	5.385514	-0.113282	-0.968939	C	0.394887	-1.136430	2.829624
C	5.345386	1.399993	-0.705116	H	1.263171	-0.458931	2.808914
C	3.845295	1.661546	-0.551559	H	0.329424	-1.552043	3.842238
H	3.368124	1.870826	-1.516521	H	-0.506374	-0.537219	2.659974
H	3.607677	2.474751	0.138957	C	1.821653	-3.051316	2.094275
H	5.789128	1.993207	-1.509838	H	1.933718	-3.928284	1.448707
H	5.874098	1.639167	0.224921	H	1.798980	-3.411290	3.130518
H	5.140019	-0.327452	-2.015675	H	2.717468	-2.426309	1.972529
H	6.355745	-0.566482	-0.746499	H	-0.299735	-2.945156	1.938907
H	4.647012	-0.780803	0.976266	C	-3.918676	0.412652	0.855019
H	3.790783	-1.536379	-0.389881	C	-3.341363	0.176009	2.256617
O	0.582813	1.876776	0.069088	H	-3.248088	-0.897348	2.464333
C	0.206246	2.654966	1.224164	H	-3.965738	0.624623	3.040061
C	-0.282713	4.010505	0.675985	H	-2.341835	0.628564	2.341997
C	-0.561939	3.737657	-0.827436	C	-4.144609	1.933988	0.656459
C	-0.370561	2.223272	-0.972830	H	-3.199581	2.479746	0.787256
H	0.073891	1.919676	-1.924373	H	-4.872997	2.340130	1.373318
H	-1.301901	1.663369	-0.804563	H	-4.516753	2.150089	-0.351344
H	0.150274	4.282481	-1.455150	H	-4.931425	-0.040223	0.867120
H	-1.570461	4.037574	-1.124993	C	-2.873787	-0.596200	-2.593633
H	0.478721	4.786282	0.798850	H	-2.231173	0.283282	-2.721465
H	-1.179946	4.339822	1.207192	H	-3.423842	-0.757863	-3.529587
H	-0.593258	2.132962	1.763567	H	-2.227006	-1.472407	-2.445222
H	1.085656	2.726644	1.870035	C	-4.770280	-1.643844	-1.337054

Table A4.2 (continued).

C	0.801132	-2.578349	-0.654485	H	-4.183805	-2.564907	-1.216386
C	0.947097	-1.808172	-1.977300	H	-5.381338	-1.740044	-2.246627
H	0.028261	-1.262998	-2.226582	H	-5.455850	-1.574388	-0.485089
H	1.166359	-2.484405	-2.812448	H	-4.465192	0.451733	-1.648788

Table A4.3. Optimized geometries of THF trisolvated LDA open dimers at the B3LYP level of theory with 6-31G(d) basis set at -78 °C with free energies (Hartrees) and cartesian coordinates (X, Y, Z). Single point MP2 energies are included. A representative image is shown below. Dihedral angles ω_C and ω_O are included as described in Table 2. The connectivity of transition states and ground states is indicated beneath the energy values. Comments on geometry are included where deemed appropriate.

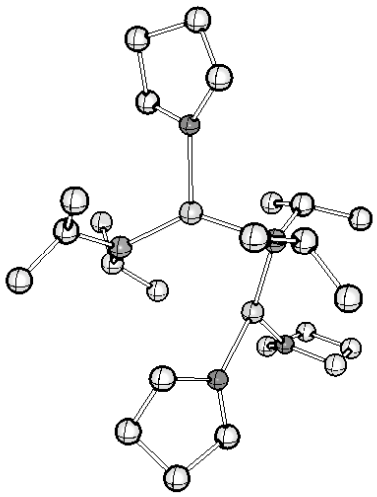

Table A4.3 (continued).

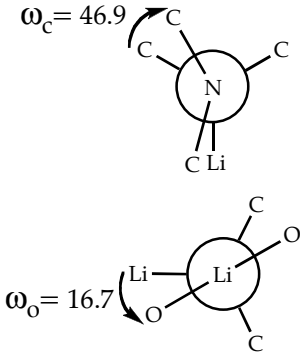

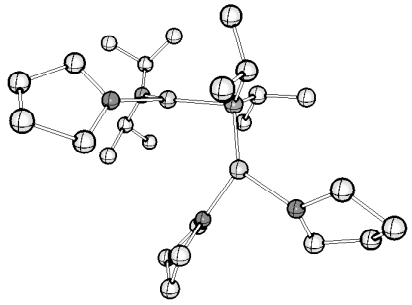

5a
G = -1295.455989
G_{MP2} = -1290.892445
ΔG = 18.1 kcal/mol
ΔG_{MP2} = 13.3 kcal/mol
11 → 5a → 13

Atom	X	Y	Z	Atom	X	Y	Z
C	-0.681747	-2.299236	-1.269863	C	3.836154	0.987902	3.081800
N	-0.542337	-1.581315	0.010766	C	3.296494	-0.181790	2.254925
Li	-1.737316	-0.049876	0.023742	H	3.301533	-1.118334	2.828357
O	-3.700877	-0.067842	0.401335	H	3.801023	-0.327885	1.296348
C	-4.630134	0.562804	-0.510872	H	4.610742	0.675618	3.788869
C	-5.801092	-0.410199	-0.639506	H	4.265467	1.754330	2.426057
C	-5.847995	-1.034253	0.763636	H	2.321276	0.912078	4.646042
C	-4.363737	-1.144192	1.122223	H	2.650657	2.564261	4.088833
H	-3.926028	-2.090800	0.791229	H	1.500577	2.182873	1.983897
H	-4.161739	-1.014588	2.188740	H	0.506336	1.164840	3.061471
H	-6.350752	-2.005217	0.787057	C	-1.780247	2.881565	0.633442
H	-6.366823	-0.366796	1.461683	C	-1.929160	4.203730	-0.121517
H	-5.578694	-1.175246	-1.391967	C	-1.033205	3.974970	-1.348855
H	-6.730932	0.090892	-0.924097	C	-1.286723	2.501703	-1.663930
H	-4.949334	1.524497	-0.086969	H	-0.435103	1.993970	-2.119809
H	-4.107317	0.751217	-1.452586	H	-2.169258	2.370246	-2.304329
O	-1.553972	1.873037	-0.381742	H	0.020397	4.128942	-1.092360
Li	1.389419	-0.645826	-0.016374	H	-1.279396	4.627209	-2.191647
N	2.878329	-0.228701	-1.194989	H	-1.624725	5.062330	0.484027
C	3.754425	-1.232399	-1.779363	H	-2.970804	4.356688	-0.428215
H	3.830934	-1.124280	-2.884370	H	-2.668595	2.595396	1.204922
C	5.214729	-1.179277	-1.257084	H	-0.914244	2.896029	1.306030
H	5.637419	-0.172016	-1.347399	C	-0.698948	-2.464036	1.175645
H	5.249756	-1.462817	-0.196012	H	-1.628574	-3.064373	1.103570
H	5.873193	-1.864488	-1.811322	C	0.443067	-3.488612	1.362634
C	3.202071	-2.643177	-1.535136	H	0.572467	-4.114201	0.473360
H	2.221707	-2.769192	-2.006842	H	1.396034	-2.975573	1.549363
H	3.873678	-3.417386	-1.929038	H	0.247141	-4.156655	2.212671
H	3.084582	-2.827401	-0.457077	C	-0.835940	-1.635307	2.462681

Table A4.3 (continued).

C	3.140482	1.091305	-1.736714	H	-1.676164	-0.927204	2.399977
H	4.229507	1.298677	-1.822793	H	-1.019477	-2.279586	3.332203
C	2.591261	2.181375	-0.802495	H	0.078553	-1.063778	2.645328
H	1.521087	2.011752	-0.607475	H	0.099350	-3.075213	-1.385813
H	3.109168	2.163116	0.162372	C	-0.478166	-1.316406	-2.431250
H	2.700690	3.186374	-1.234095	H	-0.535849	-1.826977	-3.400734
C	2.571159	1.319659	-3.163088	H	-1.264317	-0.541632	-2.431145
H	2.880056	2.288704	-3.583920	H	0.497568	-0.822214	-2.358892
H	2.910351	0.537308	-3.850796	C	-2.028954	-3.033812	-1.477931
H	1.472789	1.285353	-3.149446	H	-2.056334	-3.523880	-2.459793
O	1.914860	0.149780	1.950430	H	-2.208554	-3.809120	-0.725350
C	1.517619	1.325880	2.671704	H	-2.868064	-2.322411	-1.435257
C	2.568371	1.520798	3.767981				

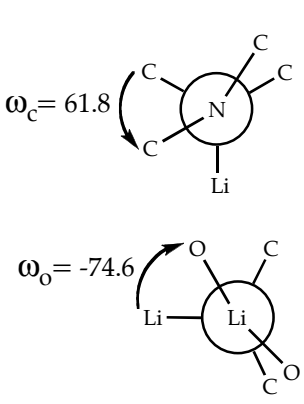

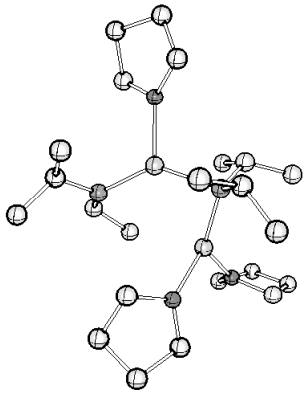

5b
G = -1295.464704
G_{MP2} = -1290.904916
$\Delta G^{\ddagger}$ = 12.2 kcal/mol
$\Delta G_{MP2}{}^{\ddagger}$ = 5.5 kcal/mol
5b → **14**
(geometry akin to **4**)

Atom	X	Y	Z	Atom	X	Y	Z
C	-0.915659	1.893773	2.086103	H	0.297605	2.434192	-0.678429
N	-1.442740	1.663085	0.750524	H	0.984858	2.653581	-2.330595
Li	-1.409317	-0.106153	-0.103283	H	1.909821	4.030927	0.248068
O	-3.200214	-1.152075	0.009106	H	1.581972	4.799225	-1.316040
C	-4.120889	-0.827099	1.079410	H	4.171297	4.123534	-0.731034
C	-5.507468	-1.203883	0.556493	H	3.535807	3.747169	-2.340189
C	-5.188165	-2.397050	-0.357487	H	4.079941	1.504216	-1.731045
C	-3.859653	-1.966750	-0.983939	H	3.925082	1.844944	0.008376
H	-3.200390	-2.800969	-1.238567	O	3.234056	-0.790045	0.647088
H	-4.022254	-1.360298	-1.885307	C	4.258464	-1.558999	-0.009762
H	-5.054318	-3.308609	0.237246	C	4.750051	-2.589672	1.030853
H	-5.960058	-2.591526	-1.108424	C	4.170070	-2.075305	2.375830
H	-6.205958	-1.447859	1.362658	C	3.629927	-0.684636	2.024831

Table A4.3 (continued).

H	-5.933889	-0.379285	-0.026978	H	2.753888	-0.377977	2.597835
H	-3.994318	0.230577	1.315366	H	4.409299	0.086620	2.121394
H	-3.851607	-1.420450	1.963457	H	3.352513	-2.719686	2.712091
C	-2.512963	2.591249	0.408105	H	4.917451	-2.035459	3.173589
C	-3.140284	2.206898	-0.941800	H	4.379160	-3.592255	0.802051
H	-3.526504	1.181373	-0.924945	H	5.843030	-2.636312	1.045116
H	-3.969127	2.876766	-1.204960	H	5.069539	-0.883759	-0.317124
H	-2.391700	2.270047	-1.742532	H	3.809252	-2.002013	-0.900406
C	-2.098184	4.084604	0.324714	C	-0.106312	-2.678801	-0.293255
H	-1.371258	4.237198	-0.484348	C	0.940462	-3.753429	-0.674938
H	-2.967684	4.725472	0.122336	H	1.944728	-3.447964	-0.351333
H	-1.642804	4.441830	1.254549	H	0.708823	-4.716300	-0.198047
H	-3.348497	2.565541	1.149093	H	0.971246	-3.924793	-1.755613
C	0.451191	1.209587	2.247713	C	-0.156833	-2.573927	1.237448
H	1.172034	1.611750	1.525172	H	-0.944917	-1.889518	1.570900
H	0.862258	1.353157	3.256605	H	-0.352229	-3.552387	1.694210
H	0.354849	0.127508	2.082273	H	0.800028	-2.208667	1.634791
C	-1.843117	1.423185	3.236877	H	-1.083775	-3.108808	-0.606421
H	-1.960210	0.330893	3.211776	C	-0.026881	-1.416343	-2.367599
H	-1.447844	1.700544	4.225231	C	-0.885853	-0.265141	-2.922368
H	-2.840497	1.869092	3.147325	H	-0.477021	0.705250	-2.615358
H	-0.728425	2.970124	2.280740	H	-0.927525	-0.275954	-4.019833
N	0.075805	-1.355492	-0.898410	H	-1.916822	-0.323532	-2.553953
Li	1.534677	-0.188477	-0.278696	C	1.337903	-1.399430	-3.101379
O	2.139438	1.551517	-0.988125	H	1.989448	-2.206173	-2.750011
C	3.496739	2.048597	-0.979506	H	1.221235	-1.510545	-4.189119
C	3.406642	3.554539	-1.268881	H	1.852941	-0.444754	-2.922522
C	1.970687	3.895183	-0.838133	H	-0.532797	-2.354141	-2.668222
C	1.210217	2.641853	-1.255048				

Table A4.3 (continued).

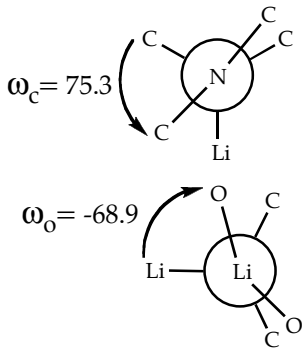

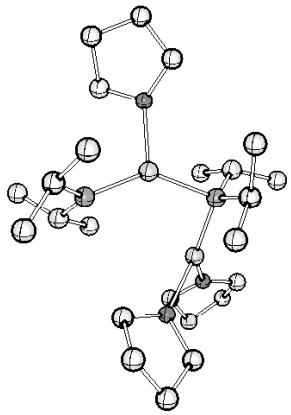

5c
G = -1295.463115
G_{MP2} = -1290.902852
$\Delta G^{\ddagger}$ = 13.7 kcal/mol
$\Delta G_{MP2}{}^{\ddagger}$ = 6.8 kcal/mol
12 → **5c**
(geometry akin to **4**)

Atom	X	Y	Z	Atom	X	Y	Z
C	0.898529	2.043246	-1.964721	C	1.540648	-1.407695	3.108066
N	1.477419	1.642439	-0.695006	H	2.229730	-0.654568	2.702943
Li	1.394719	-0.134025	0.109705	H	1.572665	-1.335040	4.203618
N	-0.040172	-1.336370	1.117720	H	1.923739	-2.396780	2.834891
Li	-1.608175	-0.447628	0.337012	C	-0.373866	0.205858	3.017908
O	-2.454766	1.353267	0.504322	H	-1.441755	0.341601	2.807519
C	-1.717823	2.597663	0.344702	H	-0.228477	0.349584	4.095831
C	-2.108973	3.422782	1.563883	H	0.173904	0.997222	2.491322
C	-3.597267	3.064613	1.725907	H	-0.530787	-1.906875	3.118180
C	-3.653825	1.593286	1.274636	O	3.161618	-1.216474	-0.341585
H	-3.651262	0.899755	2.123831	C	3.897380	-0.693132	-1.471511
H	-4.531217	1.375650	0.653998	C	5.365715	-0.799730	-1.070386
H	-3.965072	3.195232	2.747970	C	5.373829	-2.118149	-0.280218
H	-4.211356	3.689661	1.067594	C	4.015235	-2.085626	0.436738
H	-1.532877	3.102110	2.438779	H	3.546458	-3.072253	0.510954
H	-1.941842	4.493608	1.415953	H	4.096275	-1.665754	1.445335
H	-2.046919	3.083437	-0.584493	H	5.426077	-2.970500	-0.967937
H	-0.655916	2.336648	0.259858	H	6.209736	-2.201496	0.421223
O	-3.178342	-1.209090	-0.705634	H	6.039756	-0.808101	-1.932567
C	-3.962795	-2.408741	-0.487846	H	5.644565	0.040749	-0.424073
C	-4.933546	-2.503768	-1.671459	H	3.523801	0.318545	-1.636781
C	-5.068109	-1.037898	-2.112357	H	3.684419	-1.310443	-2.357245
C	-3.651846	-0.516081	-1.885004	C	2.405523	2.617628	-0.139960
H	-2.993504	-0.756859	-2.729864	C	3.032477	2.066678	1.150389
H	-3.588530	0.554360	-1.681206	H	3.523168	1.102834	0.966725
H	-5.393877	-0.926492	-3.150740	H	3.782606	2.754301	1.561909
H	-5.780491	-0.505121	-1.470951	H	2.263229	1.914676	1.919880
H	-4.496175	-3.102868	-2.478306	C	1.805055	4.012444	0.167403
H	-5.885745	-2.962404	-1.389494	H	1.032357	3.936332	0.944625
H	-4.490490	-2.299341	0.467257	H	2.576455	4.707672	0.526621

Table A4.3 (continued).

H	-3.283853	-3.262004	-0.416939	H	1.345966	4.464191	-0.719377
C	0.198782	-2.718093	0.674371	H	3.262761	2.815185	-0.823277
C	-0.694873	-3.789855	1.342783	C	-0.030683	0.934247	-2.479426
H	-1.757555	-3.536542	1.227767	H	-0.813720	0.711401	-1.743422
H	-0.526334	-4.777919	0.894361	H	-0.524847	1.217678	-3.418139
H	-0.496989	-3.884080	2.415653	H	0.534699	0.009990	-2.659470
C	0.041211	-2.809834	-0.851369	C	1.904592	2.389832	-3.093279
H	0.724441	-2.122125	-1.362011	H	2.524393	1.518957	-3.345959
H	0.260492	-3.822769	-1.212267	H	1.379549	2.706589	-4.005033
H	-0.982359	-2.558281	-1.159874	H	2.577115	3.204770	-2.805202
H	1.239829	-3.036863	0.885463	H	0.255109	2.951408	-1.873819
C	0.106329	-1.182645	2.574487				

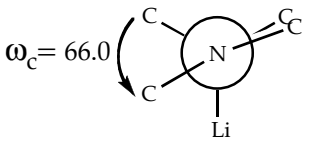

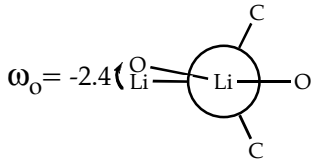

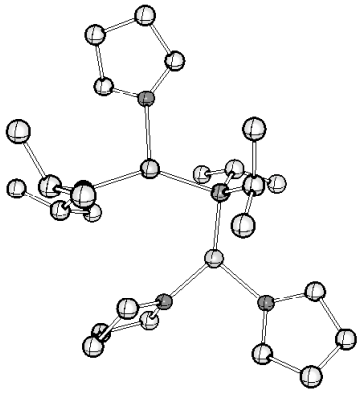

5d
G = -1295.458203
G_{MP2} = -1290.897229
ΔG = 16.7 kcal/mol
ΔG_{MP2} = 10.3 kcal/mol
(distorted diisopropyl-amido geometry)

Atom	X	Y	Z	Atom	X	Y	Z
C	1.965915	2.558584	-0.629722	C	0.419086	-3.005458	1.767022
N	1.946855	1.526908	0.388941	H	1.249523	-2.328689	2.009196
Li	1.315998	-0.306774	0.066784	H	0.120529	-3.518731	2.691123
N	-0.462082	-1.517097	-0.101833	H	0.794215	-3.770130	1.078514
Li	-1.914866	-0.209557	-0.355474	C	-1.306298	-1.236472	2.196275
O	-3.894148	-0.624685	-0.297971	H	-2.254568	-0.781294	1.874403
C	-4.890382	0.365885	0.042944	H	-1.502574	-1.733809	3.154243
C	-5.826328	-0.334604	1.022902	H	-0.587536	-0.430223	2.377332
C	-5.867953	-1.757170	0.443501	H	-1.564992	-2.983571	1.006196
C	-4.435414	-1.956154	-0.071657	O	3.048988	-1.477754	-0.419943
H	-3.793418	-2.451713	0.662602	C	4.192904	-0.727564	-0.865849
H	-4.389394	-2.515965	-1.009034	C	5.395889	-1.412829	-0.201561
H	-6.149190	-2.515628	1.179623	C	4.915173	-2.875198	0.010947
H	-6.586098	-1.808399	-0.382981	C	3.450440	-2.851878	-0.473545
H	-5.389336	-0.338215	2.028266	H	3.371335	-3.214574	-1.509794

Table A4.3 (continued).

H	-6.810574	0.139985	1.077616	H	2.765949	-3.423624	0.152645
H	-5.423802	0.671209	-0.868414	H	5.508741	-3.599976	-0.555183
H	-4.363492	1.229637	0.450941	H	4.973011	-3.155579	1.067059
O	-2.046593	1.742062	-0.413040	H	6.294080	-1.349273	-0.823649
C	-2.420150	2.598901	-1.515577	H	5.619944	-0.935889	0.757294
C	-1.765952	3.953746	-1.235165	H	4.014666	0.304053	-0.563115
C	-1.711212	3.984545	0.300301	H	4.257108	-0.790792	-1.964169
C	-1.414071	2.526626	0.649565	C	2.403399	2.004139	1.687756
H	-0.344612	2.280668	0.652403	C	3.908042	1.761486	1.989001
H	-1.862048	2.210639	1.597524	H	4.553501	2.180983	1.212585
H	-0.939908	4.658145	0.683010	H	4.209261	2.200867	2.951923
H	-2.677955	4.298516	0.713979	H	4.105630	0.681710	2.039221
H	-0.752589	3.978627	-1.646705	C	1.601477	1.353304	2.831220
H	-2.335603	4.783347	-1.664996	H	1.701802	0.258987	2.788775
H	-3.515884	2.674404	-1.544384	H	1.957614	1.673705	3.819803
H	-2.075856	2.135426	-2.445449	H	0.535457	1.594596	2.759021
C	-0.221610	-2.429224	-1.230844	H	2.238168	3.100445	1.779147
C	-1.433667	-3.292579	-1.656487	C	1.406818	1.999395	-1.947266
H	-2.244048	-2.655687	-2.039336	H	0.420601	1.546183	-1.791771
H	-1.155869	-3.992811	-2.455542	H	1.312363	2.779249	-2.714816
H	-1.833187	-3.887960	-0.828482	H	2.071194	1.222980	-2.349344
C	0.245659	-1.629014	-2.454992	C	3.325628	3.241439	-0.937316
H	1.189444	-1.109572	-2.262975	H	4.068491	2.509942	-1.282617
H	0.396209	-2.282521	-3.323572	H	3.210530	4.002993	-1.722546
H	-0.504134	-0.874394	-2.735368	H	3.733150	3.745308	-0.055398
H	0.589773	-3.148509	-1.003318	H	1.300839	3.418065	-0.345512
C	-0.765600	-2.226543	1.149878				

Table A4.3 (continued).

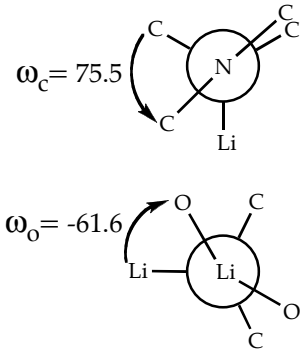

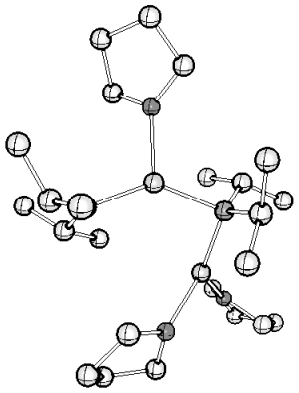

5e
G = -1295.461125
G_{MP2} = -1290.900545
ΔG = 14.9 kcal/mol
ΔG_{MP2} = 8.3 kcal/mol
(distorted diisopropyl-amido geometry)

Atom	X	Y	Z	Atom	X	Y	Z
C	1.063602	2.382851	-1.371190	C	1.230290	-2.201977	2.806660
N	1.651651	1.659754	-0.263044	H	1.984574	-1.418184	2.651615
Li	1.373630	-0.219289	0.182878	H	1.200541	-2.431178	3.880548
N	-0.211854	-1.473457	0.844015	H	1.568444	-3.106754	2.290319
Li	-1.660635	-0.227094	0.356211	C	-0.585209	-0.502201	3.090433
O	-3.412935	-0.789480	-0.518473	H	-1.616133	-0.206361	2.852917
C	-4.478871	-1.269065	0.338866	H	-0.540106	-0.692682	4.169995
C	-5.436816	-2.038532	-0.575195	H	0.068955	0.350291	2.874048
C	-5.233070	-1.337222	-1.927686	H	-0.858801	-2.543734	2.577758
C	-3.732809	-1.047009	-1.906111	O	3.093866	-1.308096	-0.376745
H	-3.149479	-1.909484	-2.250432	C	3.779387	-0.862617	-1.559840
H	-3.439399	-0.168451	-2.487891	C	5.261954	-1.182828	-1.306837
H	-5.526039	-1.952970	-2.782945	C	5.218970	-2.339459	-0.269247
H	-5.805157	-0.402713	-1.967217	C	3.713288	-2.549023	-0.017011
H	-5.137528	-3.090475	-0.643201	H	3.311950	-3.354311	-0.651051
H	-6.470098	-2.001240	-0.218317	H	3.457874	-2.758680	1.021919
H	-4.963883	-0.400101	0.800832	H	5.693806	-3.254552	-0.636670
H	-4.035371	-1.887320	1.124735	H	5.729041	-2.050433	0.654566
O	-2.250754	1.611036	0.849502	H	5.775953	-1.465418	-2.230767
C	-3.400880	2.312855	0.347949	H	5.775406	-0.310013	-0.893344
C	-2.860215	3.663694	-0.110487	H	3.543015	0.195107	-1.673955
C	-1.827806	3.974689	0.986901	H	3.396330	-1.423287	-2.427572
C	-1.301801	2.585023	1.393344	C	2.542353	2.483620	0.545919
H	-0.324377	2.336838	0.963791	C	4.047212	2.413015	0.165214
H	-1.268079	2.457877	2.480087	H	4.214098	2.634249	-0.892200
H	-1.021782	4.622867	0.633839	H	4.650969	3.117480	0.756828
H	-2.313940	4.471013	1.834931	H	4.428481	1.401886	0.360461
H	-2.366788	3.558202	-1.082699	C	2.439280	2.108380	2.038358
H	-3.641740	4.425055	-0.197338	H	2.686769	1.046199	2.180995
H	-4.142160	2.433927	1.153201	H	3.136919	2.688335	2.657635

Table A4.3 (continued).

H	-3.836582	1.702025	-0.444745	H	1.428038	2.268877	2.425445
C	-0.143747	-2.714545	0.057826	H	2.251037	3.554831	0.471870
C	-1.356364	-3.663875	0.224260	C	0.005809	1.511935	-2.068766
H	-2.271387	-3.177005	-0.136933	H	-0.782855	1.221392	-1.363461
H	-1.215209	-4.591721	-0.346702	H	-0.470290	2.040448	-2.905346
H	-1.517377	-3.948244	1.269502	H	0.462333	0.596602	-2.467610
C	0.017867	-2.389268	-1.435065	C	2.029340	2.920105	-2.462082
H	0.947605	-1.844082	-1.626586	H	2.596913	2.098118	-2.919564
H	0.036108	-3.303304	-2.042417	H	1.477023	3.439230	-3.259284
H	-0.814385	-1.769442	-1.795295	H	2.745843	3.634980	-2.046605
H	0.744980	-3.317755	0.333735	H	0.524436	3.298516	-1.013325
C	-0.153013	-1.739722	2.291049				

REFERENCES

1. (a) Bakker, W. I. I.; Wong, P. L.; Snieckus, V. Lithium Diisopropylamide. In *e-EROS*; Paquette, L. A., Ed.; Wiley: New York, 2001. (b) Clayden, J. *Organolithiums: Selectivity for Synthesis*; Baldwin, J. E., Williams, R. M., Eds.; Pergamon Press: New York, 2002. (c) Hartung, C. G.; Snieckus, V. in *Modern Arene Chemistry*, Astruc, D. (Ed.), Wiley-VCH, Weinheim, 2002; Chapter 10.

2. The database compiled by H. J. Reich and coworkers currently resides at http://www.chem.wisc.edu/areas/reich/syntheses/syntheses.htm.

3. Collum, D. B.; McNeil, A. J.; Ramirez, A. *Angew. Chem., Int. Ed.* **2007**, *46*, 3002.

4. Liao, S.; Collum, D. B. *J. Am. Chem. Soc.* **2003**, *125*, 15114.

5. Singh, K. J.; Collum, D. B. *J. Am. Chem. Soc.* **2006**, *128*, 13753.

6. Singh, K. J.; Hoepker, A. C.; Collum, D. B. *J. Am. Chem. Soc.* **2008**, *130*, 18008.

7. Gupta, L.; Hoepker, A. C.; Singh, K. J.; Collum, D. B. *J. Org. Chem.* **2009**, *74*, 2231.

8. Hoepker, A. C.; Gupta, L.; Ma, Y.; Faggin, M. F.; Collum, D. B., submitted for publication.

9. Ma, Y.; Hoepker, A. C.; Gupta, L.; Faggin; M. F.; Collum, D. B. *J. Am. Chem. Soc.*, **2010**, *132*, 15610.

10. For examples of reactions that are fast relative to the rates of aggregate-aggregate exchanges see: (a) McGarrity, J. F.; Ogle, C. A. *J. Am. Chem. Soc.* **1985**, *107*, 1810. (b) Jones, A. C.; Sanders, A. W.; Bevan, M. J.; Reich, H. J. *J. Am. Chem. Soc.* **2007**, *129*, 3492. (c) Thompson, A.; Corley, E. G.; Huntington, M. F.; Grabowski, E. J. J.; Remenar, J. F.; Collum, D. B. *J. Am. Chem. Soc*. **1998**, *120*, 2028. (d) Jones, A. C.; Sanders, A. W.; Sikorski, W. H.; Jansen, K. L.; Reich, H. J. *J. Am. Chem. Soc.*, **2008**, *130* , 6060. (e) (c) Schlosser, M.; Mongin, F. *Chem. Soc. Rev.* **2007**, *36*, 1161.

11. (a) Besson, C.; Finney, E. E.; Finke, R. G. *J. Am. Chem. Soc.* **2005,** *127,* 8179. (b) Besson, C.; Finney, E. E.; Finke, R. G. *Chem. Mater.* **2005,** *17,* 4925. (c) Huang, K. T.; Keszler, A.; Patel, N.; Patel, R. P.; Gladwin, M. T.; Kim-Shapiro, D. B.; Hogg, N. *J. Biol. Chem.* **2005**, *280*, 31126. (d) Huang, Z.; Shiva, S.; Kim-Shapiro, D. B.; Patel, R. P.; Ringwood, L. A.; Irby, C. E.; Huang, K. T.; Ho, C.; Hogg, N.; Schechter, A. N.; Gladwin, M. T. *J. Clin. Invest.* **2005**, *115*, 2099. (e) Tanj, S.; Ohno, A.; Sato, I.; Soai, K *Org. Lett.* **2001**, *3*, 287. (f) Barrios-Landeros, F.; Carrow, B. P.; Hartwig, J. F. *J. Am. Chem. Soc.* **2008**, *130*, 5842.

12. (a) Depue, J. S.; Collum, D. B. *J. Am. Chem. Soc.* **1988**, *110*, 5524. (b) McNeil, A. J.; Toombes, G. E. S.; Gruner, S. M.; Lobkovsky, E.; Collum, D. B.; Chandramouli, S. V.; Vanasse, B. J.; Ayers, T. A. *J. Am. Chem. Soc.* **2004**, *126*, 16559. (c) Nudelman, N. S.; Velurtas, S.; Grela, M. A. *J. Phys. Org. Chem.* **2003**,

16, 669. (d) Alberts, A. H.; Wynberg, H. *J. Am. Chem. Soc.* **1989**, *111*, 7265. (e) Alberts, A. H.; Wynberg, H. *J. Chem. Soc., Chem. Commun.* **1990**, 453.

13. (a) Seebach, D. In *Proceedings of the Robert A. Welch Foundation Conferences on Chemistry and Biochemistry*; Wiley: New York, 1984; p 93. (b) Seebach, D. *Angew. Chem., Int. Ed. Engl.* **1988**, *27*, 1624. (c) Tchoubar, B.; Loupy, A. *Salt Effects in Organic and Organometallic Chemistry*; VCH: New York, 1992; Chapters 4, 5, and 7. (d) Caubère, P. *Chem. Rev.* **1993**, *93*, 2317.

14. For representative examples, see: (a) Arvidsson, P. I.; Ahlberg, P.; Hilmersson, G. *Chem. Eur. J.* **1999**, *5*, 1348. (b) Fraenkel, G.; Henrichs, M.; Hewitt, J. M.; Su, B. M.; Geckle, M. J. *J. Am. Chem. Soc.* **1980**, *102*, 3345. (c) Heinzer, J.; Oth, J. F. M.; Seebach, D. *Helv. Chim. Acta* **1985**, *68*, 1848. (d) Hilmersson, G.; Arvidsson, P. I.; Davidsson, Ö; Håkansson, M. *Organometallics* **1997**, *16*, 3352. (e) Hilmersson, G.; Davidsson, O. *Organometallics* **1995**, *14*, 912. (f) Fraenkel, G.; Fraenkel, A. M. Geckle, M. J.; Schloss, F. *J. Am. Chem. Soc.* **1979**, *101*, 4745. (g) Fraenkel, G.; Chow, A.; Winchester, W. R. *J. Am. Chem. Soc.* **1990**, *112*, 6190.

15. (a) Williard, P. G.; Salvino, J. M. *J. Org. Chem.* **1993**, *58*, 1. (b) Kim, Y.-J.; Bernstein, M. P.; Galiano-Roth, A. S.; Romesberg, F. E.; Fuller, D. J.; Harrison, A. T.; Collum, D. B.; Williard, P. G. *J. Org. Chem.* **1991**, *56*, 4435.

16. (a) Pratt, L. M. *THEOCHEM* **2007**, *811*, 191. (b) Pratt, L. M. *Bull. Chem. Soc. Jpn.* **2005**, *78*, 890. (c) Pratt, L. M.; Newman, A.; Cyr, J. S.; Johnson, H.; Miles, B.; Lattier, A.; Austin, E.; Henderson, S.; Hershey, B.; Lin, M.; Balamraju, Y.;

Sammonds, L.; Cheramie, J.; Karnes, J.; Hymel, E.; Woodford, B.; Carter, C. *J. Org. Chem.* **2003**, *68*, 6387. (d) Armstrong, D. R.; Carstairs, A.; Henderson, K. W. *Organometallics* **1999**, *18*, 3589. (e) Romesberg, F. E.; Collum, D. B. *J. Am. Chem. Soc.* **1995**, *117*, 2166. (f) Romesberg, F. E.; Collum, D. B. *J. Am. Chem. Soc.* **1994**, *116*, 9187. (g) Bernstein, M. P.; Romesberg, F. E.; Fuller, D. J.; Harrison, A. T.; Williard, P. G.; Liu, Q. Y.; Collum, D. B. *J. Am. Chem. Soc.* **1992**, *114*, 5100. Romesberg, F. E.; Collum, D. B. *J. Am. Chem. Soc.* **1992**, *114*, 2112. (h) Also see references 5,9, and 19.

17. *Gaussian 03*; revision B.04; Frisch, M. J.; Trucks, G. W.; Schlegel, H. B.; Scuseria, G. E.; Robb, M. A.; Cheeseman, J. R.; Montgomery, Jr., J. A.; Vreven, T.; Kudin, K. N.; Burant, J. C.; Millam, J. M.; Iyengar, S. S.; Tomasi, J.; Barone, V.; Mennucci, B.; Cossi, M.; Scalmani, G.; Rega, N.; Petersson, G. A.; Nakatsuji, H.; Hada, M.; Ehara, M.; Toyota, K.; Fukuda, R.; Hasegawa, J.; Ishida, M.; Nakajima, T.; Honda, Y.; Kitao, O.; Nakai, H.; Klene, M.; Li, X.; Knox, J. E.; Hratchian, H. P.; Cross, J. B.; Bakken, V.; Adamo, C.; Jaramillo, J.; Gomperts, R.; Stratmann, R. E.; Yazyev, O.; Austin, A. J.; Cammi, R.; Pomelli, C.; Ochterski, J. W.; Ayala, P. Y.; Morokuma, K.; Voth, G. A.; Salvador, P.; Dannenberg, J. J.; Zakrzewski, V. G.; Dapprich, S.; Daniels, A. D.; Strain, M. C.; Farkas, O.; Malick, D. K.; Rabuck, A. D.; Raghavachari, K.; Foresman, J. B.; Ortiz, J. V.; Cui, Q.; Baboul, A. G.; Clifford, S.; Cioslowski, J.; Stefanov, B. B.; Liu, G.; Liashenko, A.; Piskorz, P.; Komaromi, I.; Martin, R. L.; Fox, D. J.; Keith, T.; Al-Laham, M. A.; Peng, C. Y.; Nanayakkara, A.; Challacombe, M.; Gill, P. M. W.; Johnson, B.; Chen, W.; Wong, M. W.; Gonzalez, C.; and Pople, J. A.; Gaussian, Inc.: Wallingford, CT, 2004.

18. The computations use the Gaussian standard state of 1.0 atm. If the THF concentration is corrected to neat THF (approximately 13 M), each solvation step benefits from approximately 2.0 kcal/mol of additional stabilization at -78 °C (195 K). Pratt, L. M.; Merry, S.; Nguyen, S. C.; Quan, P.; Thanh, B. T. *Tetrahedron* **2006**, *62*, 10821.

19. The benefits of MP2 corrections in the context of higher solvates were specifically pointed out by an anonymous referee: Viciu, M.; Gupta, L.; Collum, D. B. *J. Am. Chem. Soc.* **2010**, *132*, 6361.

20. For a discussion of intrinisic reaction coordinate (IRC) calculations, see: Foresman, J. B.; Frisch, A. E. *Exploring Chemistry with Electronic Structure Methods,* 2nd ed.; Gaussian, Inc.: Pittsburgh, 1993.

21. (a) Open dimers were first proposed for the isomerization of oxiranes to allylic alcohols by mixed metal bases. See: Mordini, A.; Rayana, E. B.; Margot, C.; Schlosser, M. *Tetrahedron* **1990**, *46*, 2401. (b) For a bibliography of lithium amide open dimers, see Ramirez, A.; Sun, X.; Collum, D. B. *J. Am. Chem. Soc.* **2006**, *128*, 10326 and references cited therein.

22. For leading references to conformational studies of diisopropylamino fragments, see: (a) Stewart, W. E.; Siddall, T. H., III. *Chem. Rev.* **1970**, *70*, 517. (b) Lidén, A.; Roussel, C.; Liljefors, T.; Chanon, M.; Carter, R. E.; Metzger, J.; Sandström, J. *J. Am. Chem. Soc.* **1976**, *98*, 2853.

23. Clegg, W.; Horsburgh, L.; Mackenzie, F. M.; Mulvey, R. E. *J. Chem. Soc., Chem. Commun.* **1995**, 2011.

24. Representative examples of structurally characterized bridging THF ligands: (a) Pratt, L. M.; Merry, A.; Nguyen, S. C.; Quanb, P.; Thanh, B. T. *Tetrahedron* **2006**, *62*, 10821. (b) Clegg, W.; Liddle, S. T.; Mulvey, R. E.; Robertson, A. *Chem.Commun.* **1999**, 511. (c) Boche, G.; Boie, C.; Bosold, F.; Harms, K.; Marsch, M. *Angew. Chem., Int. Ed.* **1994**, *33*, 115. (d) Daniele, S.; Drost, C.; Gehrhus, B. Hawkins, S. M.; Hitchcock, P. B.; Lappert, M. F.; Merle, P. G.; Bott, S. G. *J. Chem.Soc., Dalton Trans.* **2001**, 3179. (e) Chivers, T.; Fedorchuk, C.; Parvez, M. *Inorg.Chem.* **2004**, *43*, 2643. (f) Briand, G. G.; Chivers, T.; Parvez, M. *J. Chem. Soc., Dalton Trans.* **2002**, 3785.

25. (a) Gupta, L. Rate Studies of Organolithium-Mediated Reactions: Reaction of Lithium Diisopropyamide with Fluoropyridines and Reaction of Lithium Diethylamide with an Alkyl Bromide and an Alkyl Sulfonate. Ph.D. Thesis, Cornell University, Ithaca, NY, August 2010. (b) Hoepker, A. C. Aggregation Dynamics of Lithium Diisopropylamide and Their Influence on Reactivity. Ph.D. Thesis, Cornell University, Ithaca, NY, February 2011. (c) Zhou, B.; Ma, Y.; Liang, J.; Bruneau, A., unpublished.

26. (a) Stegelmann, C.; Andreasen, A.; Campbell, C. T. *J. Am. Chem. Soc.* **2009**, *131*, 8077. (b) Maniscalco, S. J.; Tally, J. F.; Fisher, H. F. *Archives Biochem. Biophys.* **2004**, *425* 165. (c) Ruszczycky, M. W.; Anderson, V. E. *J. Theoretical Biol.* **2006**, *243*, 328. (d) Ray, W. J., Jr. *Biochemistry* **1983**, *22*, 4625.

27. Exceedingly fast LDA-mediated reactions are observable by Reich and coworkers using rapid-injection NMR spectroscopy. For leading references to the method, see: Jones, A. C.; Sanders, A. W.; Sikorski, W. H.; Jansen, K. L.; Reich, H. J. *J. Am. Chem. Soc.* **2008**, *130*, 6060.